Proceedings of the I·R·E

A Journal of Communications and Electronic Engineering

(Including the WAVES AND ELECTRONS Section)

October, 1947

Volume 35 Number 10

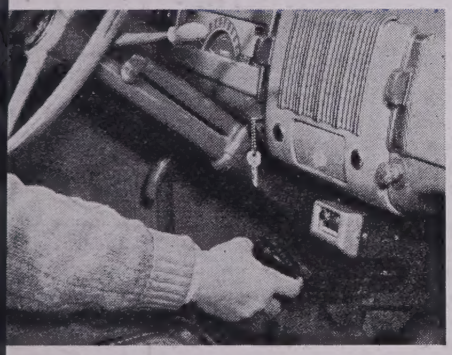

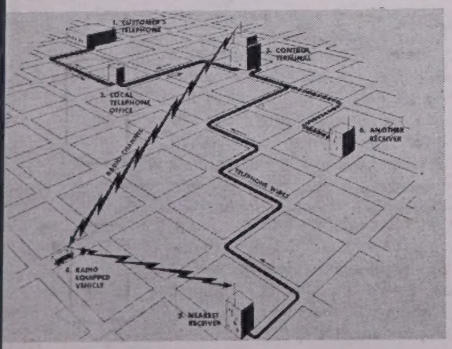

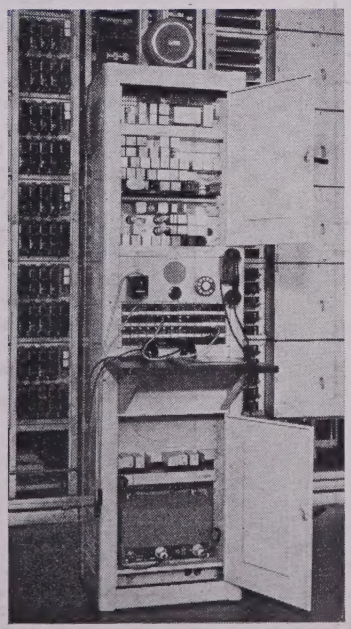

I.R.E. St. Louis Section and Southwestern Bell Telephone Co.

TELEPHONE SERVICE TAKES TO THE ROAD

ile telephone service with selective calling to moving vehicles, inaugurated in St. Louis, ouri, is now available in some 50 cities, and is being extended nationally over major way routes as well.

PROCEEDINGS OF THE I.R.E.

Waves and Electrons Section

TABLE OF CONTENTS FOLLOWS PAGE 32A

The Institute of Radio Engineers

ENGINEERING DEVELOPMENT

Since its inception, the designs of the UTC Engineering Department have set the standard for the transformer field.

1933 — **Hum Balanced Coil Structure:** Used by UTC in practically all high fidelity designs. . . . Hum balanced transformers are now accepted as standard practice in the transformer field.

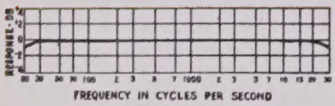

1934 — **Linear Standard Audio Units:** Flat from 20 to 20,000 cycles . . . A goal for others to shoot at.

1935 — **Ultra-Compact Audio Units:** A complete series of light weight audio and power components for aircraft and portable applications. Ultra-Compact Audio units are hum balanced . . . weigh approximately six ounces . . . high fidelity response.

1936 — **Tri-Alloy Shielding:** The combination of Linear Standard frequency response and internal tri-alloy magnetic shielding is a difficult one to approach. Used by G.E., RCA, Western Electric, Westinghouse, Raytheon, Collins, Gates, etc.

1937 — **Ouncer Audio Units:** Extremely compact audio units for portable application were a problem until the development of the UTC Ouncer series. Fifteen types for practically all applications . . . range 40 to 15,000 cycles.

1938 — **Universal Equalizers:** The UTC Universal Equalizers, Attenuators, and Sound Effects Filters fill a specific need of the broadcast and recording field. Almost any type of audio equipment can be equalized to high fidelity standards.

1939 — **Plug-In Audio Units:** These units are a modification of our Ouncer series, incorporating a simple octal base structure. Fifteen standard items cover all applications.

1940 — **Sub-Ouncer Units:** A series of ½ ounce miniature units with non-corrosive—long life construction for hearing aid, miniature radio, and similar applications. Five types cover practically all miniature requirements.

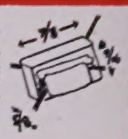

1941 — **Hermetic Seal Pioneering:** Realizing the essentiality of hermetic sealing for many applications, UTC pioneered a large number of the terminals and structures for hermetic transformers . . . now available for commercial use.

1942 — **Toroidal Wound High Q Coils:** UTC type HQA and HQB Coils afford a maximum in Q . . . stability . . . and dependability with a minimum of hum pickup. Standardized types available for all audio requirements.

1943 — **Variable Inductors:** The type VIC high Q variable inductor revolutionizes the approach to tuned audio circuits. Variation of +90% to −50% of mean inductance permits tuning any type of filter or equalizer to precise frequency characteristic.

1944 — **Standardized Filters:** UTC type HPI, LPI, and BPI (low pass, high pass, and band pass) Filters are standardized to effect minimum cost and good delivery time. Available for frequencies throughout the entire audio range.

1945 — **Sub-Audio and Supersonic Transformers:** Embody new design and constructional principles, for special frequency ranges. ½ to 60 cycles for geophysical, brain wave applications . . . 8 to 50,000 cycles for laboratory service, 200 to 200,000 cycles for supersonic applications.

1946 — **Commercial Grade:** (Now catalogued) This group of transformers covers every audio and power requirement of commercial communication equipment. The conservative design and rugged construction of these units, assure professional appearance and permanent dependability.

1947 — **New Items:** The UTC Research Laboratory is developing new items and improving standard designs in 1947. While some of these developments will be described in our advertisements, many are applied to customers' problems. *Write for new catalogue*

United Transformer Corp.

PROCEEDINGS OF THE I.R.E.

(Including the WAVES AND ELECTRONS Section)

Published Monthly by

The Institute of Radio Engineers, Inc.

VOLUME 35 — *October, 1947* — NUMBER 10

PROCEEDINGS OF THE I.R.E.

(Table of Contents continued on page 1002)

Changes of address (with advance notice of fifteen days) and communications regarding subscriptions and payments should be mailed to the Secretary of the Institute, at 450 Ahnaip St., Menasha, Wisconsin, or 1 East 79 Street, New York 21, N. Y.

TABLE OF CONTENTS (Continued)

INSTITUTE NEWS AND RADIO NOTES

SECTION

WAVES AND ELECTRONS

SECTION

A Message to the I.R.E. Membership from Its Board of Directors

The proposed Constitutional Amendments, recently submitted to the voting membership of the Institute, have been approved by a favorable vote of almost ten-to-one. The significance of a vote of these proportions is indeed great, since so high a favorable percentage of voters may be regarded as unusually close to unanimity of opinion.

In the light of the vote of approval of the Institute membership, the Board of Directors desires first to express its deep appreciation of the confidence shown by the membership in the administration of the Institute, as evidenced by the willingness of the membership to grant broad fiscal and other powers to the administrative group of the I.R.E.

The Board is fully conscious that, with that grant of authority, there comes an added responsibility. The Board accordingly accepts this responsibility in a spirit of respect for the membership and its views, and loyalty to the aims and ideals of the Institute. It will endeavor to exercise its newly allotted powers in a spirit of calm and judicial detachment with equitable treatment for all, and in the determination to benefit to the utmost the membership and the Institute. The Board will endeavor to maintain those standards of impartiality, of high scientific and professional purpose, and of effective administration for which the Institute has always stood.

It will be encouraging to the membership and the Board alike that the Board of Directors will soon include a group of Regional Directors, selected specifically to represent the Regions from which they come and whose memberships have elected them. The newly constituted Board will therefore represent the Institute membership even more broadly than in the past. Democratic administration, and the carrying out of the will of the entire Institute membership, will thus be furthered by the Regional Plan now being put into operation.

The Board of Directors will continue to be animated by those purposes which have been outlined in this notice of appreciation to the membership. The Board again thanks the membership for their support, and assures them in turn of unremitting service toward their common aims: the welfare, usefulness, and expansion of the worthy activities of the Institute.

For the Board of Directors:

WALTER R. G. BAKER, *President*

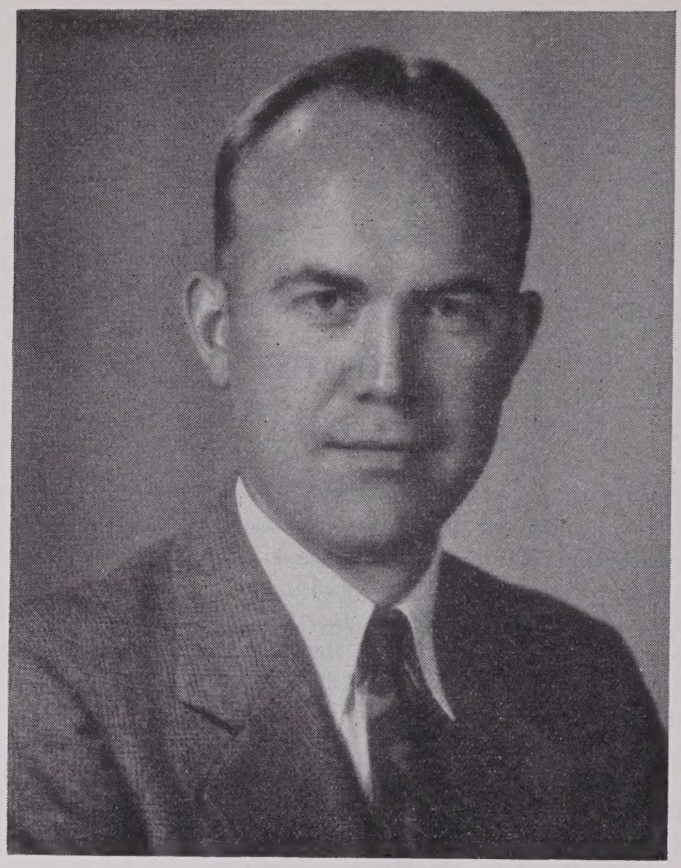

Murray G. Crosby

Board of Directors, 1947–1949

Murray G. Crosby was born at Elroy, Wis., on September 17, 1903. He studied electrical engineering at the University of Wisconsin, receiving the B.S. degree in 1927 and a professional electrical engineering degree in 1943. From 1925 to 1944 he was research engineer for the Radio Corporation of America in the communications division of RCA Laboratories, where he specialized in frequency and phase modulation, and point-to-point reception. He has written a considerable number of technical articles in those fields and has been issued numerous patents.

Mr. Crosby received the Modern Pioneer Award from the National Association of Manufacturers in 1940, for contributions which improved the American standard of living. In 1943 and 1944 he served as expert technical consultant to the Secretary of War and received official commendation for his work. He also served on Panel Number 1 of the Radio Technical Planning Board. In 1945 he became a member of the firm of Paul Godley Company, consulting radio engineers.

Mr. Crosby joined The Institute of Radio Engineers as an Associate in 1925, was transferred to Member in 1938, to Senior Member in 1943, and was awarded a Fellowship that same year for his "contributions to the development of high-frequency radio communications, including a careful study of frequency modulation." He was Vice-Chairman of the New York Section of the I.R.E. in 1943. In 1944 and 1945 he served on the Papers Procurement Committee, and in 1945 and 1946 on the Admissions Committee. At present he is Chairman of the Papers Review Committee, Chairman of the Modulations Systems Committee, member of the Board of Editors, and member of the Editorial Administrative Committee. He is a Fellow of the Radio Club of America, and a member of the American Institute of Electrical Engineers.

New Low-Coefficient Synthetic Piezoelectric Crystals for Use in Filters and Oscillators*

W. P. MASON†, FELLOW, I.R.E.

Summary—Two crystals of the monoclinic sphenoidal class have been found which have modes of vibration with zero temperature coefficients of frequency, high electromechanical coupling constants, and high Q's or low dissipation. These properties make it appear probable that such crystals may have a considerable use in filters and oscillators as a substitute for quartz, which is difficult to obtain in large sizes. These crystals are ethylene diamine tartrate (EDT) having the chemical formula $C_6H_{14}N_2O_6$, and di-potassium tartrate (DKT) having the formula $K_2C_4H_4O_6-1/2\ H_2O$.

The paper describes the properties of EDT, since this crystal has been found more advantageous than DKT. The 13 elastic constants, the 8 piezoelectric constants, and the 4 dielectric constants have been measured over a temperature range, and from these measurements the regions of low temperature coefficients and high electromechanical coupling have been located. Six low-temperature-coefficient cuts have been discovered and the properties of these cuts are given. These cuts are being applied in the crystal channel filters of the long-distance telephone system, and may be applied to the control of oscillators.

I. Introduction

DURING the last 10 years or more, the properties of synthetic crystals have been investigated at Bell Telephone Laboratories with the aim of applying such crystals in the telephone plant. This program has resulted in a number of publications on the properties of synthetic crystals[1–9] and has produced crystals of use in the war. This search has recently resulted in two crystals of the monoclinic sphenoidal class which have cuts having zero temperature coefficients within useful temperature ranges, high Q's, little or no water of crystallization, and a high electromechanical coupling. These crystals are a suitable substitute for quartz for use in electrical wave filters. The requirements for such crystals are: (1) a rather high degree of frequency and inductance stability over a temperature range from 55° F. to 110° F.; (2) a good chemical stability against atmospheric humidity conditions; (3) a low mechanical dissipation; and (4) a long-time stability against structure changes which would produce a change or aging in frequency or other electrical properties.

During the war, quartz crystal plates to the number of 30,000,000 per year were used in the communication equipment of the services to provide oscillator control of high-frequency stability. As the war progressed it became difficult to obtain large-size crystals, and toward the end of the war most manufacturers were using crystal bars whose original weights were under 100 grams. With the end of the war it has become difficult to obtain natural crystals of sufficient size to supply blanks, which may run in size up to two inches long, for use in filters. With these synthetic crystals it is possible to grow crystals of large size and, hence, meet the filter-crystal supply problem.

These crystals are ethylene diamine tartrate ($C_6H_{14}NO$) and di-potassium tartrate ($K_2C_4H_4O_6-1/2H_2O$). The first has been given the designation EDT and the second DKT. EDT has no water of crystallization and hence will not dehydrate. DKT has one molecule of water of crystallization for each two of potassium tartrate, but this is tightly bound and tests show that no dehydration takes place up to 80° C. Of these two crystals DKT is the more stable with temperature, but it is harder to grow and requires more careful handling than does EDT. Accordingly, the first commercial application has been made using the EDT crystal. It is the purpose of the present paper to describe the properties and useful cuts obtained with these two crystals.

II. Properties of Ethylene Diamine Tartrate (EDT) Crystals

Monoclinic crystals are characterized by having two crystallographic axes a and c, not at right angles to each other, and a third axis b, that is perpendicular to the other two. The c axis is along the shortest distance of the unit cell, while the b axis is the axis of two-fold symmetry. In measuring the properties of a crystal, the calculations come out much more simply for a right-angled system of co-ordinates. As shown in Fig. 1, the method chosen[10] for relating the right-angled X, Y, Z systems of axes to the a, b, c crystallographic axes of the crystallographer is to make Z coincide with

* Decimal classification: R214.1×R386.5. Original manuscript received by the Institute, March 27, 1947; revised manuscript received, July 8, 1947.

† Bell Telephone Laboratories, Murray Hill, N. J.

[1] W. P. Mason, "Dynamic measurement of the properties of rochelle salt," *Phys. Rev.*, vol. 55, pp. 775–789; April, 1939.

[2] A. N. Holden and W. P. Mason, "The elastic, dielectric and piezoelectric constants of heavy water rochelle salt," *Phys. Rev.*, vol. 57, pp. 54–56; January 1, 1940.

[3] W. P. Mason, "Location of hysteresis phenomena in rochelle salt crystals," *Phys. Rev.*, vol. 58, pp. 744–756; October 13, 1940.

[4] W. L. Bond, "The mathematics of the physical properties of crystals," *Bell Sys. Tech. Jour.*, vol. 22, pp. 1–73; January, 1943.

[5] W. L. Bond, "A mineral survey of piezoelectric materials," *Bell Sys. Tech. Jour.*, vol. 22, pp. 145–152; July, 1943.

[6] W. P. Mason, "The elastic, piezoelectric and dielectric constants of KDP and ADP," *Phys. Rev.*, vol. 69, pp. 173, 195; March, 1946.

[7] W. P. Mason, "Elastic, piezoelectric and dielectric properties of sodium chlorate and sodium bromate," *Phys. Rev.*, vol. 70, pp. 529–538; October 1, 1946.

[8] W. P. Mason, "Properties of monoclinic crystals," *Phys. Rev.*, vol. 70, pp. 705–728; November 1, 1946.

[9] W. P. Mason, "First and second order piezoelectric equations expressed in tensor form," *Bell. Sys. Tech. Jour.*, vol. 26, pp. 80–138; January, 1947.

[10] This system of relating rectangular axes to crystallographic axes has been recommended as a proposed standard by a committee on piezoelectric crystals of The Institute of Radio Engineers, under the chairmanship of W. G. Cady. This committee also has recommended the symbols and nomenclature used in this paper.

c, Y with b, and to have the X axis lie in the plane perpendicular to the b axis, and at an angle of 51′ above the a axis for DKT. For EDT the angle between X and a is much larger, i.e. 15°30′.

The X, Y, Z axes form a right-handed system of axes. Since $b = Y$ is a binary axis, it is necessary to have a

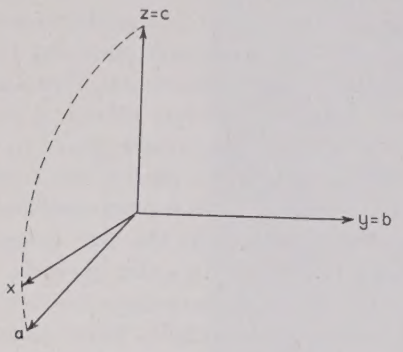

Fig. 1—Relation between rectangular axes and the crystallographic axes for a monoclinic crystal.

convention for specifying which end of the axis is positive. This can be done by locating the two optic axes of the crystal. A monoclinic crystal is a biaxial crystal, and the plane that contains these two axes must be either perpendicular or parallel to the b or Y crystallographic axis. As shown by Fig. 2 (for DKT) for these two crystals the optic axes lie in a plane parallel

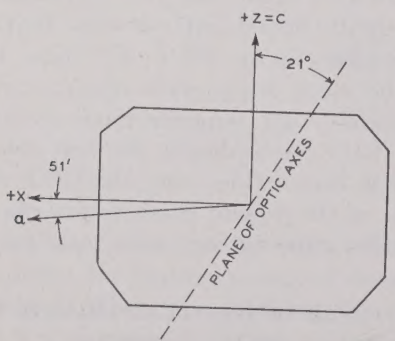

Fig. 2—Use of optic axes in specifying the positive directions of the crystallographic axes.

to the b axis and at an angle of 21° in a clockwise direction from the c or Z crystallographic axis for DKT, and at an angle of 25° for EDT. Since $+X$ lies at a counterclockwise angle of 90° from c, and $+b = +Y$ makes a right-handed system of co-ordinates with the X and Z axes, the measurement determines the positive direction of all three axes.

DKT has two cleavage planes lying along planes determined by the three crystallographic axes. EDT has one cleavage plane which is the 001 plane, i.e., the plane containing the a and b crystallographic axes.

Since not all directions in the crystal are equivalent, useful cuts occur at definite orientations with respect to the crystallographic axes. The quickest method for finding the locations of these cuts is by determining the values and temperature coefficients of the fundamental elastic, piezoelectric, and dielectric constants of the crystal. From these fundamental constants, the properties of a cut at any other orientation can be calculated by applying well-known mathematical formulas for transferring from the set of crystallographic X, Y, Z axes to a rotated X', Y', Z' system of axes. Also, if the fundamental constants are known, the location can be calculated of all crystal cuts having such desirable properties as low temperature coefficients and high electromechanical couplings.

For plated, nonferroelectric-type crystals such as these, the most useful method of expressing the piezoelectric constants is that originally due to Voigt.[11] Voigt expressed the six strains S_1 to S_6 in terms of the six stresses T_1 to T_6, and the three electric fields E_x, E_y, E_z. The strains S_1, S_2, S_3 are the elongation per unit length along the X, Y, Z axes, respectively, while the strains S_4, S_5 and S_6 represent the shearing strains around the axes X, Y, and Z, respectively. The stresses T_1, T_2, T_3 similarly represent the stresses tending to produce elongations along the X, Y, Z axes, respectively, while T_4, T_5, T_6 represent the shearing stresses tending to produce shearing strains around the X, Y, Z axes, respectively. The fields E_x, E_y, E_z are the potential gradients (or the potentials divided by the distance over which they are applied) existing along the X, Y and Z axes, respectively. This relation, shown by (1), is Voigt's method of expressing the inverse piezoelectric effect. For a monoclinic sphenoidal crystal, these equations take the form[12]

$$\begin{aligned}
S_1 &= s_{11}^E T_1 + s_{12}^E T_2 + s_{13}^E T_3 + s_{15}^E T_5 + d_{21} E_y \\
S_2 &= s_{12}^E T_1 + s_{22}^E T_2 + s_{23}^E T_3 + s_{25}^E T_5 + d_{24} E_y \\
S_3 &= s_{13}^E T_1 + s_{23}^E T_2 + s_{33}^E T_3 + s_{35}^E T_5 + d_{23} E_y \\
S_4 &= s_{44}^E T_4 + s_{46}^E T_6 + d_{14} E_x + d_{34} E_z \\
S_5 &= s_{15}^E T_1 + s_{25}^E T_2 + s_{35}^E T_3 + s_{55}^E T_5 + d_{25} E_y \\
S_6 &= s_{46}^E T_4 + s_{66}^E T_6 + d_{16} E_x + d_{36} E_z.
\end{aligned} \tag{1}$$

The s_{11}^E to s_{66}^E are the 13 elastic compliances of the crystal, which are the ratios of the strains to the appropriate stress when all other stresses and the field are held constant, and d_{14} to d_{36} are the eight piezoelectric constants, which are the ratios of the strains to the appropriate applied field when all the stresses are held constant. The superscript E indicates that the fields are held constant for the compliance measurements.

The direct piezoelectric equations express the polarizations generated in the medium along the three axes in

[11] W. Voigt, "Lehrbuch der kristall physik," *Leipzig B. Teubner*, pp. 801–848; October, 1910.

[12] The constants and methods of measuring the properties of the monoclinic crystals have been discussed in the paper referenced in footnote 8. This paper describes the properties of the DKT crystal.

terms of the applied stresses and the applied fields. These become

$$P_x = \eta_{11}{}^T E_X + \eta_{13}{}^T E_Z + d_{14}T_4 + d_{16}T_6$$
$$P_y = \eta_{22}{}^T E_Y + d_{21}T_1 + d_{22}T_2 + d_{23}T_3 + d_{25}T_5 \qquad (2)$$
$$P_z = \eta_{13}{}^T E_X + \eta_{33}{}^T E_Z + d_{34}T_4 + d_{36}T_6$$

where $\eta_{11}{}^T$, etc., are the dielectric susceptibilities measured at constant stress T, and P_x, P_y, P_z are the polarizations along the three axes.

As discussed in a former paper[12], all of these constants can be measured by measuring the resonant frequency, antiresonant frequency, and the capacitance at low frequencies of 18 oriented cuts. This process is further described and illustrated for the DKT crystal and all the constants measured over a temperature range. We can apply the same process to the EDT crystal

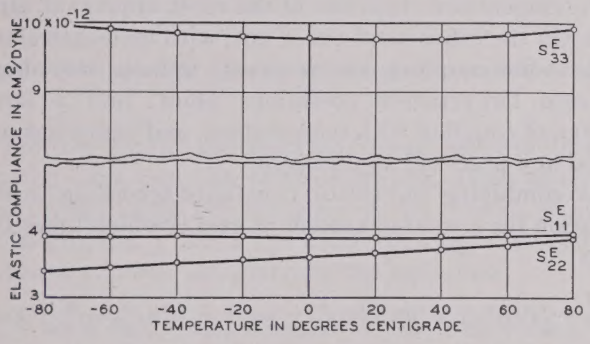

Fig. 3—Longitudinal elastic compliances for EDT crystals.

and the resulting constants expressed in c.g.s. units are shown by Figs. 3, 4, 5, 6, and 7. Fig. 3 shows the longitudinal elastic compliances, Fig. 4 the shear elastic compliances, Fig. 5 the cross-coupling elastic compliances, Fig. 6 the eight piezoelectric constants, and Fig. 7 the four dielectric constants, all plotted as a function of temperature. In deriving the elastic constants as a function of temperature, use has to be made of the temperature expansion coefficient in the various directions in order to eliminate the change in length and the change in density. Measurements[13] of the expansion coefficient in the X, Z plane are shown by Fig. 8. The coefficient along the Y axis is $+20.3$ = parts per million per degree centigrade. From these values the four temperature coefficients become

$$\alpha_{11} = 0; \quad \alpha_{22} = +20.3 \times 10^{-6}; \quad \alpha_{33} = 80 \times 10^{-6};$$
$$\alpha_{13} = -32 \times 10^{-6}.$$

This crystal has a rather remarkable temperature expansion characteristic, since it has a very high positive expansion in one direction (+90 parts in 10^6 per °C) and a small negative coefficient (−12 parts in 10^6 per °C.) in a direction perpendicular to the large coeffi-

[13] These measurements were made by Miss E. J. Armstrong.

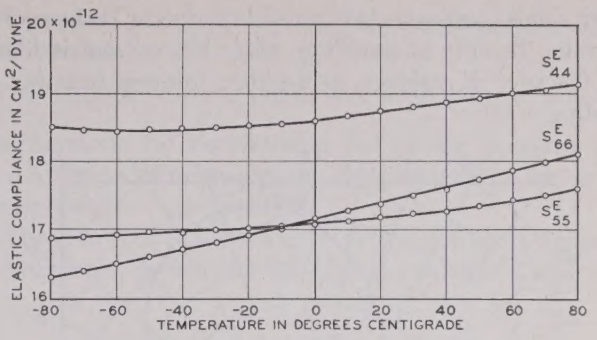

Fig. 4—Shear elastic compliances for EDT crystals.

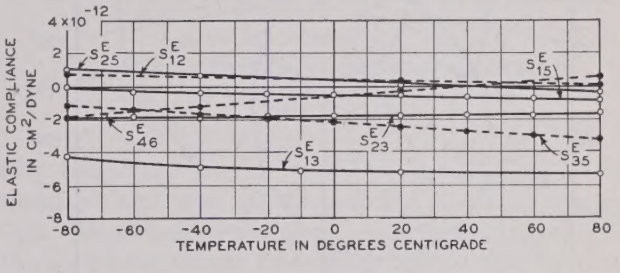

Fig. 5—Cross-coupling elastic compliances for EDT crystals.

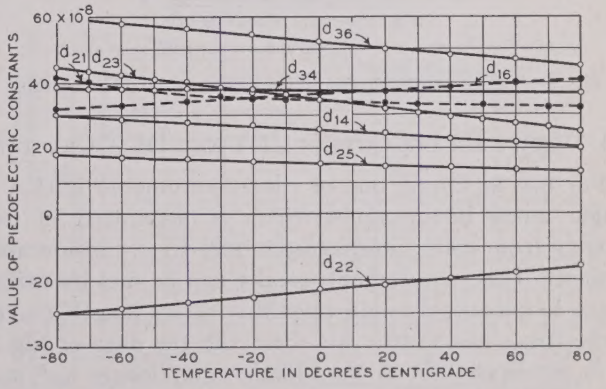

Fig. 6—Eight piezoelectric moduli for EDT crystals.

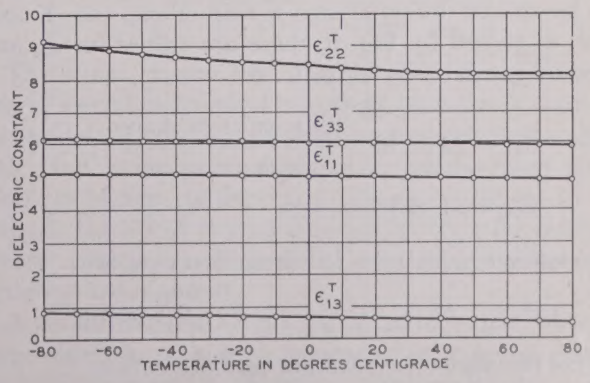

Fig. 7—Four dielectric constants for EDT crystals.

cient. This temperature expansion property is the source of some trouble in handling, since the crystal is likely to fracture if subject to sudden uneven heating or cooling.

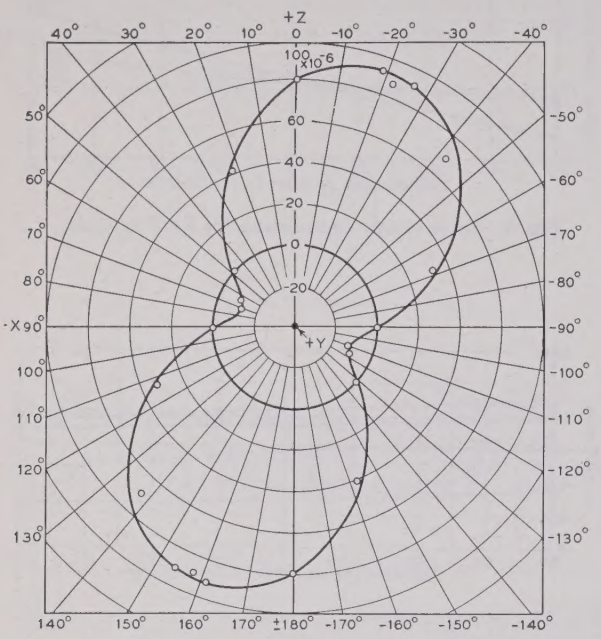

Fig. 8—Temperature expansion coefficients for EDT crystals.

III. Useful Filter Cuts in EDT and DKT Crystals

For use in filters, one of the requirements is that a single mode be obtained which is separated in frequency from other interfering modes by a considerable amount. This requirement usually can be met by utilizing a longitudinal-mode crystal with its length two to three times the width. By observing the data of Fig.3, it is noted that both the elastic compliances s_{11}^E and s_{33}^E of EDT have minimum points at 20°C., and hence crystals cut with their lengths along either the X axis or the Z axis will have zero temperature-frequency values of about 20°C. Furthermore, these two modes can be driven by applying a field along the Y axis since, as shown by Fig. 6, there are values for d_{21} and d_{23} equal respectively at 20°C. to

$$d_{21} = 34 \times 10^{-8} \frac{\text{c.g.s. units of charge}}{\text{dyne per sq. cm.}};$$

$$d_{23} = 31 \times 10^{-8}.$$

The elastic compliances for these two cuts are

$$s_{11}^E = 3.88 \times 10^{-12}; \qquad s_{33}^E = 9.8 \times 10^{-12}$$

and the free dielectric constant for both cuts is

$$\epsilon_{22}^T = 8.22.$$

It has been shown that the electromechanical coupling factor k and the ratio of capacitances r for a longitudinal crystal are given by the formulas[12]

$$k = d_{21}\sqrt{\frac{4\pi}{\epsilon_{22}^T s^E}}; \qquad r = \frac{\pi^2}{8}\left(\frac{1-k^2}{k^2}\right).$$

Hence, for these two crystals, Y cut, length along X, and Y cut, length along Z, the constants are, respectively

$$k = 0.215; \qquad r = 25.5 \text{ length along } X;$$

$$k = 0.126; \qquad r = 76.5 \text{ length along } Z.$$

The first cut, the Y cut with its length along X, has a high coupling and low ratio of capacitance, a relatively small change of frequency about the point of zero temperature coefficient, and a small change of coupling with temperature. It is one of the most important filter cuts. On the other hand the Y cut, with its length along Z, has a low coupling, a large change in frequency about its zero temperature coefficient point, and a large change of coupling with temperature, and hence has not found any practical applications.

By combining the elastic constants according to the equation for a rotated system of axes,[12] which takes the form

$$\begin{aligned} s_{22}^E{}_t^1 = {} & l_2^4 s_{11}^E + l_2^2 m_2^2 (2s_{12}^E + s_{66}^E) + l_2^2 n_2^2 (2s_{13}^E + s_{55}^E) \\ & + 2l_2^3 n_2 s_{15}^E + m_2^4 s_{22}^E + m_2^2 n_2^2 (2s_{23}^E + s_{44}^E) \\ & + 2n_2^3 l_2 s_{35}^E + n_2^4 s_{33}^E + m_2^2 l_2 n_2 (2s_{25}^E + s_{46}^E), \end{aligned}$$

where the directions cosines l_1 to n_3 for the rotated system are related to the crystallographic axes X, Y, Z by the relation

	x	y	z
x'	l_1	m_1	n_1
y'	l_2	m_2	n_2,
z'	l_3	m_3	n_3,

it can be shown that there is another region for which zero-temperature-coefficient crystals can be obtained. This region, as shown by Fig. 9, is obtained by starting with a crystal whose thickness is along Y and whose length is along Z, rotating the direction of the length by a counterclockwise angle of 45° about the thickness then rotating the crystal about its width by a counterclockwise angle of 63°. According to a system of notation proposed by W. L. Bond[14] and adopted by the committee on piezoelectric crystals of The Institute of Radio Engineers, this crystal is designated as the ($YZtw$, 45° 63°) crystal. The first letter indicates the direction of the thickness before rotation; the second letter represents the direction of the length before rotation; the

[14] W. L. Bond, "Crystal rotation systems," unpublished.

third letter and the first number represent, respectively, the axis of the first rotation and the value of the angle measured in a counterclockwise direction; and the fourth letter and second number represent, respectively, the second axis of rotation and the angle of rotation measured in a counterclockwise direction.

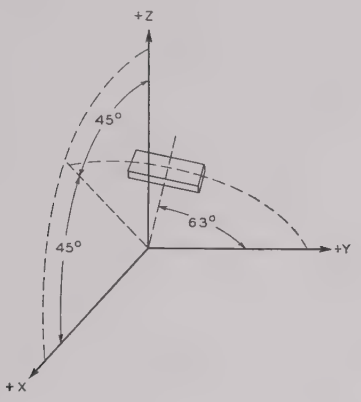

Fig. 9—Orientation for "*A*"-cut zero-temperature-coefficient crystal.

For this crystal, the direction cosines between the new rotated axes and the crystallographic axes, assuming that x' lies along the thickness of the crystal, y' along its length, and z' along the width (in a right handed coordinate system), are given by the equations

$$l_1 = \sin\phi \sin\theta; \quad m_1 = \cos\theta; \quad n_1 = \sin\theta \cos\phi$$

$$l_2 = \sin\phi \cos\theta; \quad m_2 = \sin\theta; \quad n_2 = -\cos\theta \cos\phi$$

$$l_3 = -\cos\phi; \quad m_3 = 0; \quad n_3 = +\sin\phi.$$

With these values, the piezoelectric constants of the rotated crystals become

$$d_{12}' = \cos^3\theta[d_{21}\sin^2\phi + d_{23}\cos^2\phi + d_{23}\sin\phi\cos\phi] + \sin^2\theta\cos\theta[d_{22} - [(d_{14} + d_{36})\sin\phi\cos\phi + d_{16}\sin^2\phi + d_{34}\cos^2\phi]],$$

while the elastic and dielectric constants are given by

$$s_{22}'^E = s_{11}^E\sin^4\phi\cos^4\theta + (2s_{12}^E + s_{66}^E)\sin^2\theta\cos^2\theta\sin^2\phi + (2s_{13}^E + s_{55}^E)\cos^4\theta\sin^2\phi\cos^2\phi + 2s_{15}^E\cos^4\theta\sin^3\phi\cos\phi + s_{22}^E\sin^4\theta + (2s_{23}^E + s_{44}^E)\sin^2\theta\cos^2\theta\cos^2\phi + 2s_{35}^E\cos^4\theta\cos^3\phi\sin\phi + s_{33}^E\cos^4\theta\cos^4\phi + (2s_{25}^E + s_{46}^E)\sin^2\theta\cos^2\theta\sin\phi\cos\phi$$

$$\epsilon_{11}^{T'} = \epsilon_{11}^T\sin^2\theta\sin^2\phi + 2\epsilon_{13}^T\sin^2\theta\sin\phi\cos\phi + \epsilon_{22}^T\cos^2\theta + \epsilon_{33}^T\sin^2\theta\cos^2\phi.$$

With these equations the constants for the (*YZtw*, 45°, 63°) crystal, which has been given the designation "*A*" cut, become

$$d_{12}' = -30.1 \times 10^{-8}; \quad s_{22}^E = 5.5 \times 10^{-12}; \quad \epsilon_{11}'^T = 6.58.$$

Furthermore, by determining the elastic constant s_{22}^E as a function of temperature, we find that the variation is very small.

The characteristics of a crystal that the filter designer is interested in are the change in resonant frequency

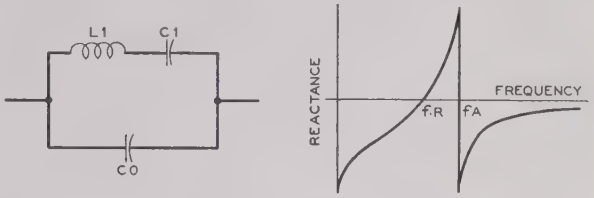

Fig. 10—Impedance and equivalent electrical circuit of a piezoelectric crystal.

with temperature, the ratio of capacitances in the equivalent circuit of the crystal, and the dielectric constant. All the elements of the equivalent circuit (Fig. 10) can be calculated from these values. Fig. 11 shows these values as a function of temperature for temperatures from −80°C to +80°C. Similar quantities for the *Y*-cut crystal are shown by Fig. 12.

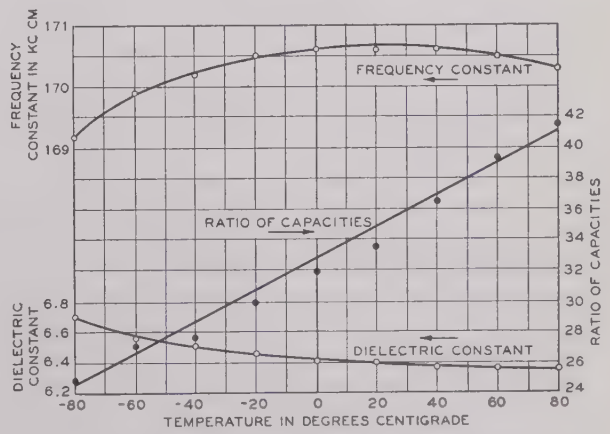

Fig. 11—Frequency constant, ratio of capacitances, and dielectric constant for the "*A*"-cut crystal.

The *A*-cut crystal has a higher ratio of capacitances (lower electromechanical coupling) than the *Y*, but has a considerably flatter temperature-frequency characteristic, and hence is most useful in narrow-band filters where a higher stability and a lower coupling are required. The *Y*-cut crystal is better for wide-band filters, where a high coupling and a moderate temperature stability are required.

A monoclinic crystal has the advantage that, with the large number of elastic constants existing, a greater probability exists of balancing the temperature coefficients of one constant against those of the other con-

stants and obtaining a zero temperature coefficient of frequency, but has the disadvantage that, with the large number of cross-coupling elastic constants, the chances of obtaining disturbing interfering modes is also larger.

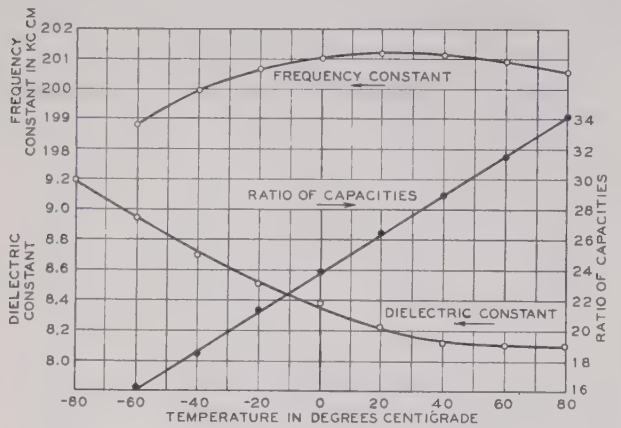

Fig. 12—Frequency constant, ratio of capacitances, and dielectric constant for the Y-cut EDT crystal.

This is illustrated by Fig. 13, which shows the frequency spectrum of a Y-cut EDT crystal plotted as a ratio of width to length. The lower solid line represents the resonant frequency of the main mode, and the numbers

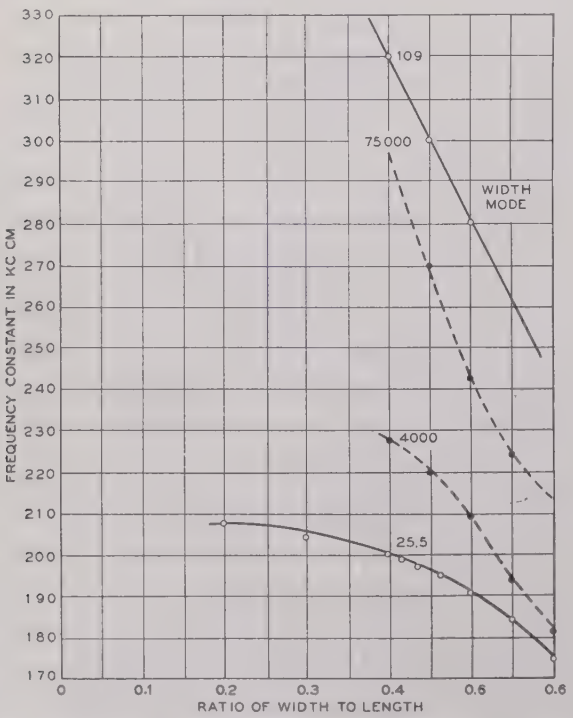

Fig. 13—Frequency spectrum for a Y-cut crystal as a function of the ratio of width to length.

on the figure are the ratios of capacitance at 25°C. The top solid line is the coupled width mode, which is a relatively strong resonance. The first dotted line above the main mode is the second flexure, which is coupled to the main longitudinal mode through the shear coupling, as in quartz. This becomes so strong at low ratios of width to length that it makes the crystal unusable for ratios of width to length less than 0.31 and greater than 0.5. The second dotted line represents another mode that causes a small interfering effect. In addition to these modes, there exists a coupling to a thickness flexure which makes certain ratios of thickness to length unusable.

With all these limitations the constants of the elements in the equivalent circuit for a crystal shown by Fig. 10 cannot be obtained by varying the width and thickness over wide ranges, as can be done with quartz crystals. To get all of these variations it has been found necessary to employ more complicated orientations which vary the fundamental constants of the crystal without changing the temperature stability. Since most of the crystals require a coupling greater than can be obtained in the A cut but less than in the Y cut, we look for modifications in orientations surrounding the Y cut.

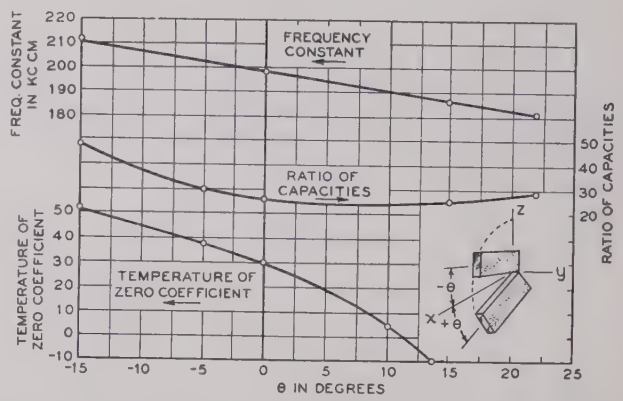

Fig. 14—Effect on the frequency constant, temperature of zero coefficient, and ratio of capacitances of rotating the Y-cut crystal about its thickness, for a plate of $w/l=0.4$.

The simplest orientation to employ is a rotation about the thickness, causing the length to vary from the X direction by $\pm\theta°$. The effect of this rotation is to change the constants of the crystal, as shown by Fig. 14. The top curve shows the frequency constant, at 25°C., of a crystal whose ratio of width to length is 0.4. This increases for negative angles and decreases for positive. The second curve shows the ratio of capacitances as a function of angle, and the bottom curve shows the temperature for which the temperature coefficient becomes zero. This increases for negative angles and decreases for positive angles.

Rotations about the width and rotations about the length are also possible. As shown by Fig. 15, which shows the principal filter orientations so far found useful, an orientation of $\pm 10°$ about the width was found, and this has very similar characteristics to the Y-cut crystal. A rotation around the length has also been tried, and by rotating $\pm 20°$ about the length and $-5°$ about the resulting thickness, an orientation having a zero

temperature coefficient, relative freedom from unwanted modes of motion, and a relative inductance in the equivalent circuit of Fig. 10, about 50 per cent larger than that for the Y cut has been found. This is shown

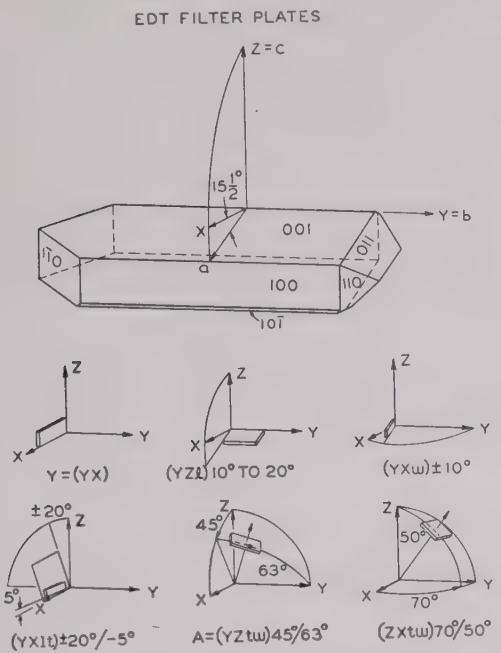

Fig. 15—Zero-temperature-coefficient cuts for EDT crystals.

on Fig. 15 as the ($YXlt \pm 20°$, $-5°$) crystal, and it appears likely that this cut may be used for the higher-channel band-pass filters.

Some interesting cuts for DKT crystals have also been found as discussed in a former paper.[12] Fig. 16

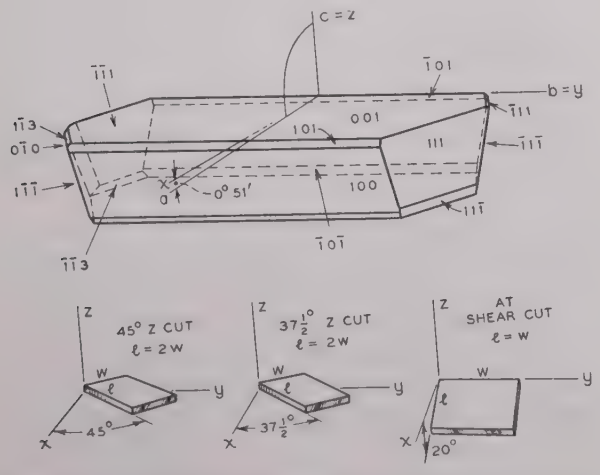

Fig. 16—Zero-temperature-coefficient cuts of DKT crystals.

shows two longitudinal cuts, Z cuts with their lengths, respectively 45° and 37.5° from X, and one face shear cut, all of which have zero temperature coefficients of frequency around room temperature. Fig. 17 shows how the resonant frequency and ratio of capacitances vary over a wide temperature range. Comparing this to the data of Fig. 12, we see that the DKT crystal has a higher coupling (lower ratio of capacitances r) than does the Y-cut EDT crystal, and a frequency variation that is only about a third that for the EDT crystal. It appears likely that, when growing and processing methods are further investigated, this crystal may have uses in apparatus for which a large electromechanical coupling and a low temperature coefficient are required.

The higher coupling existing for EDT and DKT crystals than for quartz also opens up interesting possibilities. With this coupling, band-pass filters having channel bandwidths of 3300 cycles are possible at frequencies as low as 20 kilocycles. Also, with the high coupling, it may be possible to dispense with coils entirely in the high-frequency carrier range for voice

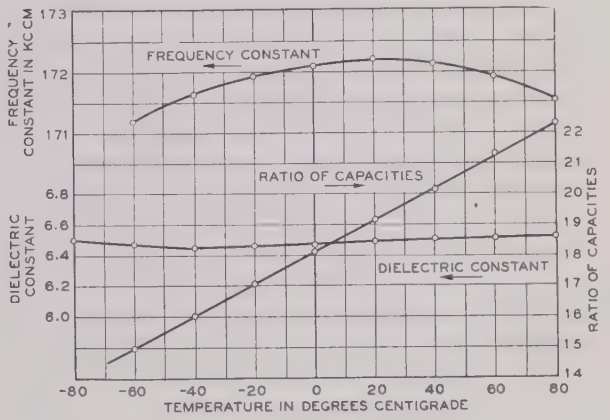

Fig. 17—Frequency constant, ratio of capacitances and dielectric constant for a 45° Z-cut DKT crystal.

channels, and thus reduce the size and cost of such filters. Wider-band filters in the ordinary carrier range are also possible, such as are used, for example, when a broadcasting program channel is transmitted over a carrier system.

IV. Application of EDT Crystals in the Control of High-Frequency Oscillators

A high-frequency shear mode has also been found in EDT crystals which has a zero temperature coefficient at room temperature. This crystal (YXl 10° to 20°) as shown by Fig. 15 has as its major plane the 0, 0, 1 crystallographic plane, i.e., the plane determined by the a and b crystallographic axes. Fig. 18 shows a measurement of a crystal having the dimension l along $Y = 1.737$ cm.; w along $a = 9.22$ cm.; $t = 0.874$ mm. The resonance frequency f_R shown by the curve has a frequency that is given by the equation for a crystal 1 mm. thick:

$$f_R = f_0[1 - a_2(T - T_0)^2]$$
$$= 904{,}000[1 - 1.21 \times 10^{-6}(T - 10°)^2]$$

where T is the temperature in degrees centigrade.

This is a rather large curvature constant a_2 compared to what can be obtained with a quartz crystal. For example, the curvature constant a_2 for BT quartz, which is the cut most widely used for high-frequency oscillators, is

$$a_2 = .042 \times 10^{-6}.$$

Hence, for a given temperature range on either side of zero temperature coefficient, the EDT crystal would have around 29 times as much frequency change as the quartz crystal. Another way of expressing the relation is that, for a given frequency tolerance, the EDT crystal could cover only $1/\sqrt{29}=0.185$ times the temperature range covered by the quartz crystal. This larger curvature appears to be possessed by all synthetic crystals so far examined.

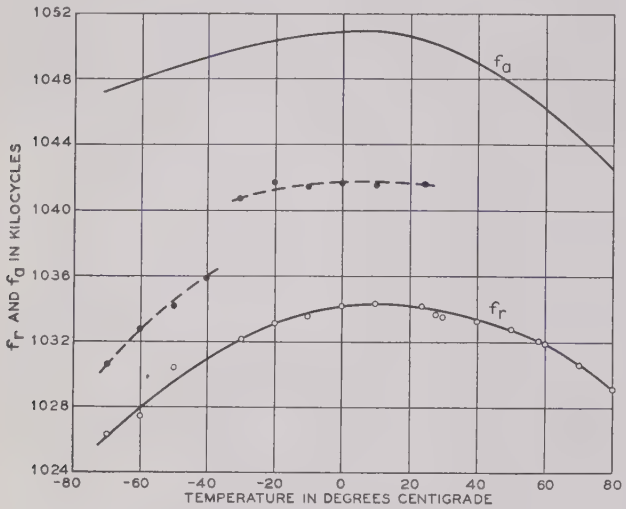

Fig. 18—Frequency spectrum of a thickness-shear EDT crystal.

However, for the very wide temperature range required for military application (−50°C. to +90°C.), a quartz crystal may not give all the accuracy required, and hence a moderate temperature control is often required. If a temperature control is used, it requires one only five times as good to hold the frequency of an EDT crystal to the same variation as a quartz crystal. For example, an accuracy of 0.01 per cent in frequency could be met by holding the temperature constant to ±9°C., and this is easily held by even a snap-switch thermostat. Hence, it appears entirely possible that EDT thickness vibrating crystals may have uses in controlling oscillators.

For a temperature-controlled crystal, it is desirable to have the temperature of zero coefficient up around 70 to 90°C. in order that the thermostat will operate under all ambient conditions. This can be obtained with an EDT crystal by increasing the rotation angle about Y. Fig. 19 shows measured values of this temperature in degrees centigrade as a function of the angle of rotation of the normal from Z. The ratio of capacitances curve and the frequency constant plotted in kilocycle millimeters are also shown. For high angles of rotation the coupling gets quite large, and hence there is a large separation between resonant and antiresonant frequencies. This property of the crystal might be of considerable use in a frequency-modulated oscillator, for it would allow a wide percentage swing of the resonant frequency. By temperature-controlling the crystal, the average frequency can be held quite constant and the frequency swing made quite large, so that these crystals may have applications in frequency-modulated oscillators.

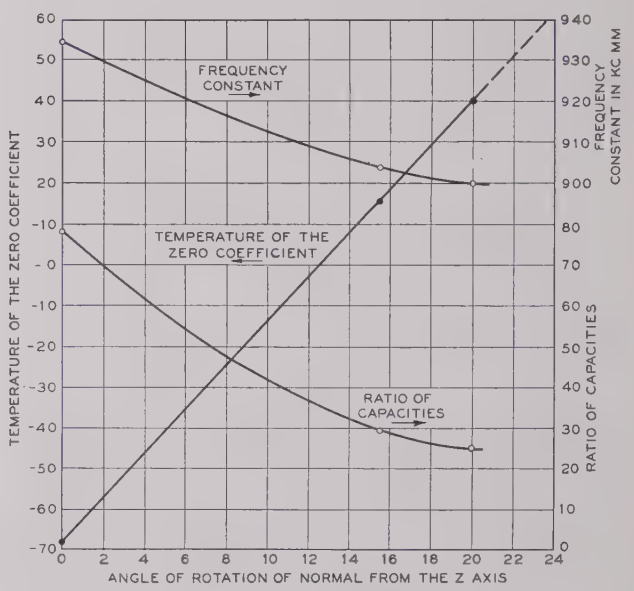

Fig. 19—Effect of angle of rotation on the frequency constant, ratio of capacitances, and temperature of zero coefficient for a thickness-vibrating EDT crystal.

The thickness of the crystal can be lapped down easily to one-third of a millimeter, which will give a frequency of about 2.7 megacycles. On account of the large electromechanical coupling, the third and fifth harmonics are strongly driven, and thus it should be possible to reach frequencies as high as 13.5 megacycles. Hence, for certain purposes the use of EDT crystals to control oscillators appears to be a distinct possibility. However, for any very high degree of frequency stability, the quartz crystal is still much to be preferred.

Variation of Bandwidth with Modulation Index in Frequency Modulation*

MURLAN S. CORRINGTON†

Summary—**Equations are derived for the carrier and side-frequency amplitudes which are obtained when a carrier wave is frequency-modulated by a complex audio signal. The bandwidth occupied by such a frequency-modulated wave is defined as the distance between the two frequencies beyond which none of the side frequencies is greater than 1 per cent of the carrier amplitude obtained when the modulation is removed.**

Curves are given to show the amount this bandwidth exceeds the extremes of deviation for a range of modulation indexes from 0.1 to 10,000, for sinusoidal, square, rectangular, and triangular modulation. For more precise definitions of bandwidth, curves are also given for side-frequency amplitude limits of 0.1 per cent and 0.01 per cent of the carrier-wave amplitude. For complex modulation the total bandwidth can be estimated by computing the bandwidth that would be required by each audio-frequency component, if it were on separately, and adding the results.

Introduction

IF A CARRIER wave is frequency-modulated with a sinusoidal audio voltage, an infinite number of side frequencies is produced. The carrier amplitude is reduced when the modulating voltage is applied, and may even become zero. If the deviation is increased, additional side frequencies are produced in both sidebands, and the distribution of the intensities of the previous ones is changed. For a single audio tone, the distance between side frequencies is always equal to the audio frequency. When two or more modulating tones are used simultaneously, side frequencies are produced which are separated from the carrier by all possible combination frequencies which can be obtained from sums and differences of harmonics of the modulating frequencies.[1,2] Thus, if there are two audio tones of frequencies μ_1 and μ_2, the side frequencies are separated from the carrier by $\pm r\mu_1 \pm s\mu_2$ where r and s are positive integers or zero.

Although, theoretically, an infinite number of side frequencies is produced, in practice the ones separated from the carrier by a frequency greater than the deviation decrease rapidly toward zero, so the bandwidth always exceeds the total frequency excursion, but nevertheless is limited. For large modulation indexes and a sinusoidal modulating voltage, the bandwidth approaches, and is only slightly greater than, the total frequency excursion.

To show how the bandwidth changes with modulation index, exact mathematical expressions for the spectrum will now be obtained.

The Spectrum of a Carrier Wave which is Frequency-Modulated with a Sinusoidal Signal

When a carrier wave is frequency-modulated with a single audio tone, the equation for the voltage is

$$e = E \sin\left(\omega t + \frac{D}{\mu} \sin 2\pi\mu t\right) \qquad (1)$$

where

E = amplitude of the wave
ω = angular frequency of the carrier, radians per second
D = deviation, cycles per second
μ = audio frequency, cycles per second
t = time in seconds
D/μ = modulation index.

This expression can be expanded in a spectrum consisting of a carrier and side frequencies, in accord with the result[3]

$$e = E \sum_{n=-\infty}^{\infty} J_n(D/\mu) \sin(\omega t + 2\pi n\mu t) \qquad (2)$$

where $J_n(D/\mu)$ is a Bessel function of the first kind of order n and argument D/μ.

Graphs of the Bessel Functions

To plot the spectrum of a frequency-modulated wave for a given modulation index D/μ, use a table of Bessel

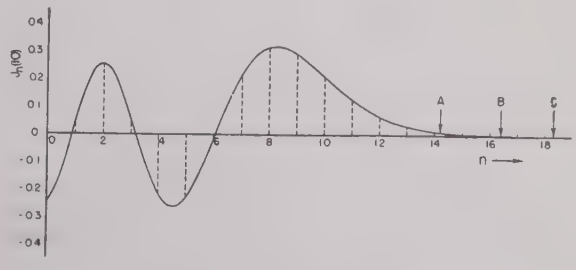

Fig. 1—Graph of $J_n(10)$.

functions[4,5] to obtain the amplitudes of the carrier and the side frequencies in the upper sideband. The odd-order side frequencies in the lower sideband will have

* Decimal classification: R14812. Original manuscript received by the Institute, May 27, 1946; revised manuscript received, February 5, 1947.

† RCA Victor Division, Radio Corporation of America, Camden, N. J.

[1] Murray G. Crosby, "Carrier and side-frequency relations with multitone frequency or phase modulation," *RCA Rev.*, vol. 3, pp. 103–106; July, 1938.

[2] M. Kulp, "Spektra und Klirrfaktoren frequenz- und amplituden-modulierter Schwingungen," Part I. *Elek. Nach.-Tech.*, vol. 19, pp. 72–84; May, 1942.

[3] A. Bloch, "Modulation theory," *Jour. I.E.E.*, (London), Part III, vol. 91, pp. 31–42; March, 1944.

[4] E. Jahnke and F. Emde, "Tables of functions with formulae and curves," Dover Publications, New York, N. Y., 1943, p. 171.

[5] August Hund, "Frequency Modulation," McGraw-Hill Book Co., New York, N. Y., 1942; Table VI, p. 352.

signs opposite to those in the upper sideband, and the even-order side frequencies will have the same sign. Fig. 1 is a graph of $J_n(10)$. If the ordinates are drawn for each integer, as shown by the dotted lines, the side frequencies in the upper sideband will be proportional to these ordinates and the carrier will be proportional to the ordinate at $n=0$.

If the modulation index is increased to 1000, the part of the curve for n nearly equal to the modulation index is similar, but is reduced in amplitude.[6] Fig. 2 shows the variation of the side frequencies near the

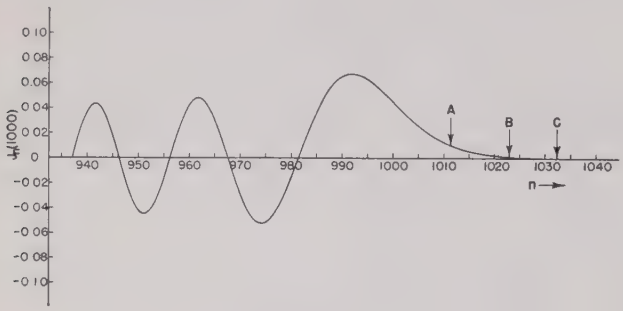

Fig. 2—Graph of $J_n(1000)$.

upper edge of the band. The curve oscillates with gradually increasing amplitude and slowly increasing period all the way from the origin to the last maximum, which is also the absolute maximum, and then decreases rapidly toward zero. The maximum energy occurs at a point in the band just inside the frequencies which correspond to the ends of the swings. When the deviation increases and the modulating frequency remains constant, the total energy of the spectrum is spread over a greater bandwidth, and the average amplitude of the side frequencies must decrease uniformly to maintain constant total energy in the modulated carrier wave.

The absolute maximum value of the Bessel function, for positive values of m, is shown by Fig. 3. For a given

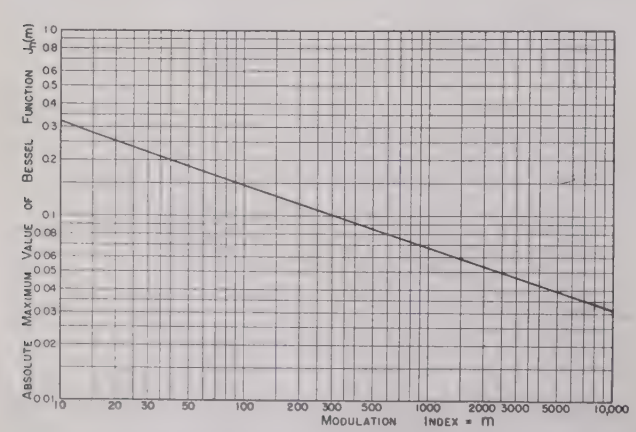

Fig. 3—Absolute maximum value of Bessel function $J_n(m)$.

modulation index, this maximum occurs for a value of the order n slightly less than the modulation index m. For example, for a modulation index of 1000 the maximum occurs at $n=991.91$ and equals 0.06756. If the modulation index is 10, the maximum occurs at $n=8.23$ and equals 0.3210. The curve of Fig. 3 shows this maximum value for a range of modulation indexes from 10 to 10,000. It was computed from the formulas of Meissel[7] which state that the Bessel function $J_n(k)$ reaches its absolute maximum

$$J_n(k) = \frac{0.6748\ 8509\ 6430}{\sqrt[3]{k}} + \frac{0.0727\ 6309\ 8182}{k} + \frac{0.0199\ 5975\ 0328}{\sqrt[3]{k^5}} + \cdots \quad (3)$$

for the value

$$n = k - 0.8086\ 1651\ 7466\sqrt[3]{k} - \frac{0.0606\ 4998\ 7910}{\sqrt[3]{k}} - \frac{0.0316\ 7351\ 0263}{k} - \cdots . \quad (4)$$

A family of curves for modulation indexes from one to twenty is shown by Fig. 4. The vertical scale represents the amplitude of the given side frequency for each modulation index. The curve of Fig. 1 can be obtained by cutting a section through the surface for a modulation index of 10. Contour line A is for the constant value of the Bessel function $J_n(D/\mu)=0.01$. Similarly, the contour B corresponds to $J_n(D/\mu)=0.001$, and contour C is drawn for $J_n(D/\mu)=0.0001$.

Curve D is shown for the order of the Bessel function equal to the argument. If the bandwidth of a frequency-modulated carrier wave were just equal to twice the deviation, the side frequencies would not extend beyond curve D. It is evident that for a given modulation index the bandwidth extends beyond curve D (say to curve A), but that the intensities of the side frequencies beyond curve D are decreasing rapidly.

Curve E is drawn along the top of the first crest and gives the absolute maximum value of the envelope of the side frequencies for each modulation index. This curve is also given by Fig. 3. The curves F, G, H, I, J, and K show where the surface goes through zero, i.e., the zeros of the Bessel functions.

Definition of Bandwidth

Theoretically, there is an infinite number of side frequencies in the spectrum of a frequency-modulated carrier wave, but the amplitudes decrease very rapidly beyond the last maximum. Point A on Fig. 1 corresponds to the value $J_n(10)=0.01$ and will be defined as the edge of the band. Point B is shown for $J_n(10)=0.001$, and point C for $J_n(10)=0.0001$. These latter two points can be used for a more precise definition of bandwidth, but point A is to be taken as the usual limit for practical purposes.

[6] Murlan S. Corrington, "Tables of Bessel functions $J_n(1000)$," *Jour. Math. Phys.* (M.I.T.), vol. 24, pp. 144–147; November, 1945.

[7] E. Meissel, "Beitrag zur Theorie der Bessel'schen Functionen," *Astronom. Nach.*, vol. 128, cols. 435–438; 1891.

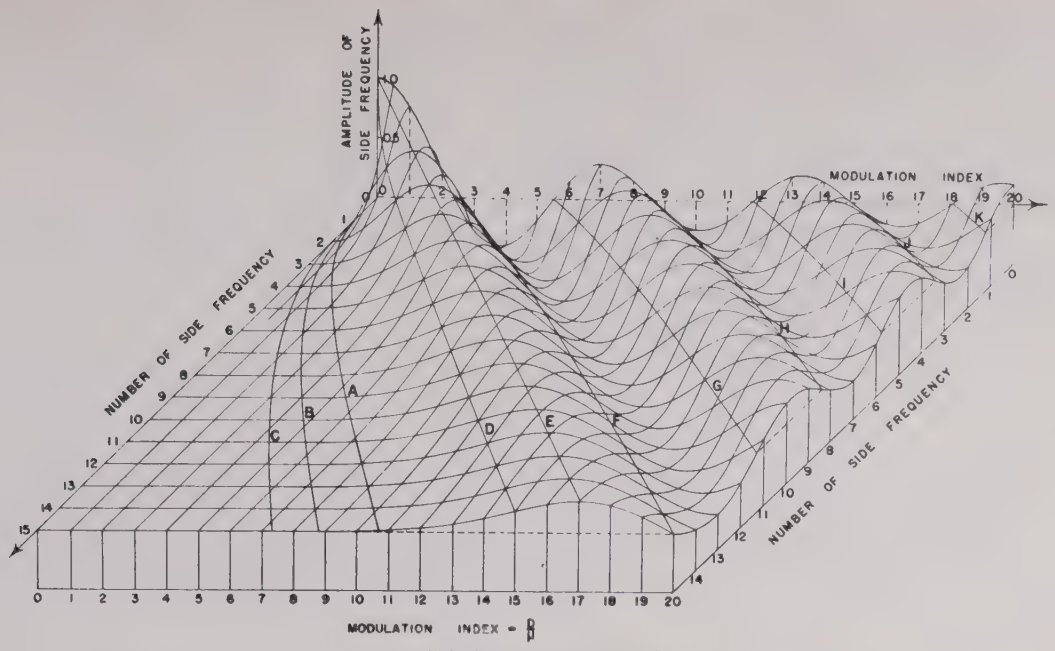

Fig. 4—Side-frequency amplitudes.

The curves of Fig. 5 show the variation of the bandwidth as the modulation index is changed.[8]

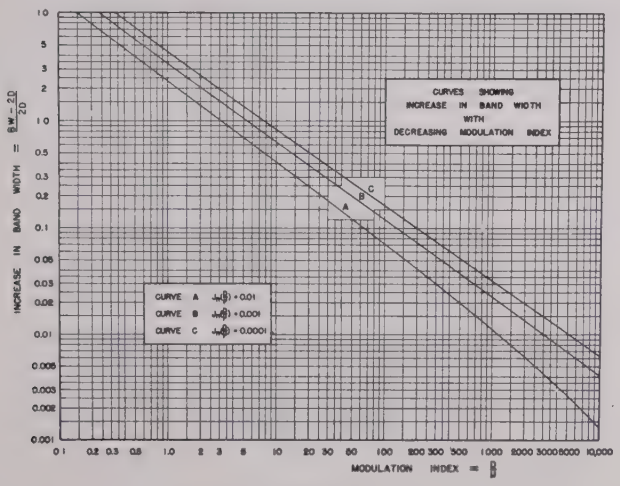

Fig. 5—Variation of bandwidth with modulation index.

Example: Let the deviation be ±50 kilocycles and the audio frequency be 5 kilocycles. Find the bandwidth. The modulation index is 50/5 = 10. From curve A of Fig. 5, the increase in bandwidth is approximately 0.42 or 42 per cent, so the bandwidth is approximately 2(50)(1+0.42) = 142 kilocycles.

[8] A rather simple method for computing the argument for $J_n(x) = 0.01,\ 0.001,\ 0.0001$ is to use the approximate formula

$$J_\nu(\nu \operatorname{sech} \alpha) = \frac{\tanh \alpha}{\pi\sqrt{3}} \exp\left\{\nu(\tanh \alpha + \tfrac{1}{3}\tanh^3 \alpha - \alpha)\right\} K_{1/3}\left(\frac{\nu}{3}\tanh^3 \alpha\right)$$

given in G. N. Watson, "A treatise on the theory of Bessel functions," The Macmillan Company, New York, N. Y., Second Edition, 1944, p. 250, where $K_{1/3}(x)$ is a modified Bessel function of the second kind of order $\frac{1}{3}$ and argument x. A series of values of α was chosen and the corresponding Bessel functions computed. These values were plotted on semilog paper and the arguments corresponding to the ordinates 0.01, 0.001, and 0.0001 were read off. The curves of Fig. 5 were obtained directly from these readings.

Bandwidth Required for Complex Modulation

If several modulating tones are present simultaneously, the carrier wave can be expressed as

$$e = E \sin\left\{\omega t + \sum_{s=1}^{S} \frac{D_s}{\mu_s} \sin(2\pi\mu_s t + \epsilon_s)\right\} \tag{5}$$

where E is the amplitude of the wave, ω is the carrier angular frequency, D_s is the deviation corresponding to the audio frequency μ_s, t is the time, and ϵ_s is the phase angle corresponding to μ_s. This modulated carrier wave can be represented by a spectrum[3,9–11]

$$e = E \sum_{k_s=-\infty}^{\infty} \left\{\prod_{s=1}^{S} J_{k_s}(m_s)\right\} \sin\left(\omega t + \sum_{s=1}^{S} k_s\theta_s\right) \tag{6}$$

where

$$m_s = D_s/\mu_s \quad \text{and} \quad \theta_s = 2\pi\mu_s t + \epsilon_s.$$

In the case of two-tone modulation this becomes[1]

$$E \sin\left\{\omega t + D_1/\mu_1 \sin 2\pi\mu_1 t + D_2/\mu_2 \sin 2\pi\mu_2 t\right\}$$

$$= E \sum_{m=-\infty}^{\infty} \sum_{n=-\infty}^{\infty} J_m(D_1/\mu_1) J_n(D_2/\mu_2) \sin(\omega + 2\pi m\mu_1 + 2\pi n\mu_2)t. \tag{7}$$

This result shows that the spectrum is now much more complicated than for a single modulating tone,

[9] E. C. Cherry and R. S. Rivlin, "Non-linear distortion, with particular reference to the theory of frequency modulated waves, Part I," *Phil. Mag.*, vol. 32, pp. 265–281; October, 1941.

[10] A. S. Gladwin, "Energy distribution in the spectrum of a frequency modulated wave, Part I," *Phil. Mag.*, vol. 35, pp. 787–802; December, 1944.

[11] K. R. Sturley, "Frequency modulation," *Jour. I.E.E.* (London), vol. 92, Part III, pp. 197–218, September, 1945.

and that side frequencies will be produced at spacings from the carrier given by all the possible combinations $\pm m\mu_1 \pm n\mu_2$. The amplitude of each side frequency will be proportional to the product of the two Bessel functions. Just as the maximum deviation occurs when D_1 and D_2 are in phase, the maximum bandwidth is given approximately by the sum of the two bandwidths that would be obtained with the two modulating tones used one at a time.

The graph of Fig. 6 shows the spectrum obtained when two tones are present simultaneously, in accord with (7). The side frequencies are no longer symmetrical

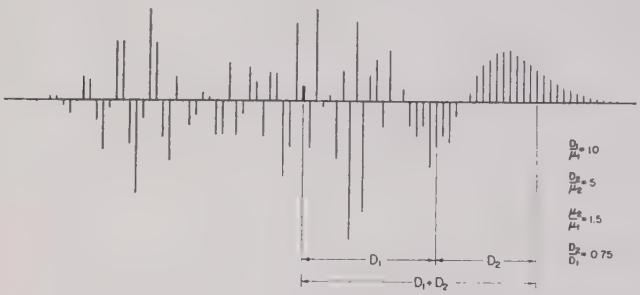

Fig. 6—Spectrum for complex modulation.

about the carrier and, when they are separated from the carrier by a frequency greater than D_1+D_2, decrease rapidly toward zero. The upper sideband contains 57.9 per cent of the power, the lower sideband 42.0 per cent, and the carrier 0.1 per cent.

General Method for Computing Side-Frequency Amplitudes

If the modulating signal is given, the variations of the phase angle will be proportional to the integral of the signal. This integration can be done directly, or by numerical integration, and the constant of integration should be chosen so the average value of the phase angle, over a complete cycle, is zero. If the phase angle is $S(t)$ the frequency-modulated carrier wave can be expressed as

$$e = E \sin \{\omega t + S(t)\}$$
$$= E \sin \omega t \cos S(t) + E \cos \omega t \sin S(t). \quad (8)$$

Expand in the Fourier series

$$\cos S(t) = \sum_{n=0}^{\infty} \{a_n \sin n\theta + b_n \cos n\theta\} \quad (9)$$

$$\sin S(t) = \sum_{n=0}^{\infty} \{c_n \sin n\theta + d_n \cos n\theta\} \quad (10)$$

where $\theta = 2\pi\mu t$ and μ is the repetition rate of the signal in cycles per second. This expansion can be done by direct integration of the integrals for the Fourier coefficients or by one of the numerical methods for harmonic analysis.[12,13]

Then

$$e = E \sin \omega t \sum_{n=0}^{\infty} \{a_n \sin n\theta + b_n \cos n\theta\}$$
$$+ E \cos \omega t \sum_{n=0}^{\infty} \{c_n \sin n\theta + d_n \cos n\theta\}$$
$$= E \sum_{n=0}^{\infty} \{\tfrac{1}{2}(a_n + d_n) \cos (\omega - 2\pi n\mu)t$$
$$- \tfrac{1}{2}(a_n - d_n) \cos (\omega + 2\pi n\mu)t$$
$$+ \tfrac{1}{2}(b_n - c_n) \sin (\omega - 2\pi n\mu)t$$
$$+ \tfrac{1}{2}(b_n + c_n) \sin (\omega + 2\pi n\mu)t\} \quad (11)$$

which gives the side-frequency amplitudes directly.

The results of numerical computation can be checked by taking the sum of the squares of the carrier and each of the side-frequency amplitudes; they should add up to E^2.

The Spectrum of a Carrier Wave which is Frequency-Modulated with a Rectangular Signal

When the signal is a rectangular or square wave, as in frequency-modulated telegraphy, or in television video and synchronizing signals, the carrier wave can be analyzed into a spectrum in a similar manner. If the

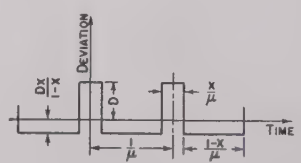

Fig. 7—Modulating signal.

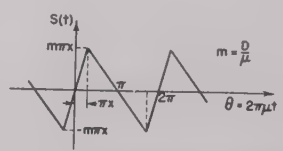

Fig. 8—Variation of phase angle.

modulating signal is as shown by Fig. 7, the phase angle $S(t)$ will be 2π times the integral of this curve, as shown by Fig. 8, where $m = D/\mu$. The equation for the frequency-modulated wave becomes

$$e = E \sin \{\omega t + S(t)\}$$
$$= E \sin \omega t \cos S(t) + E \cos \omega t \sin S(t). \quad (12)$$

Since cos $S(t)$ is symmetrical about the origin, it can be expanded in a cosine series. Similarly, sin $S(t)$ is

[12] C. Runge and H. König, "Vorlesungen Über Numerisches Rechnen," Julius Springer, Berlin, 1924, pp. 211–231.

[13] R. P. G. Denman, "36 and 72 ordinate schedules for general harmonic analysis," *Electronics*, vol. 15, pp. 44–47, September, 1942. In addition to the corrections listed in vol. 16, pp. 214–215, April, 1943, change the correction in column one, p. 215, from "Column for B_{11} and B_{25}, line for $\alpha=20°$, for Δ_3, read Δ_2," to read " . . . for Δ_2, read $-\Delta_2$."

skew symmetric about the origin and can be expanded in a sine series. From Fig. 8,

$$\begin{aligned}\cos S(t) &= \cos m\theta && 0 \leqq \theta \leqq \pi x \\ &= \cos \frac{mx(\pi-\theta)}{1-x} && \pi x \leqq \theta \leqq \pi \\ &= \sum_{n=0}^{\infty} b_n \cos 2\pi n\mu t && (13)\end{aligned}$$

where

$$b_n = \frac{2}{\pi}\int_0^{\pi x} \cos m\theta \cos n\theta d\theta + \frac{2}{\pi}\int_{\pi x}^{\pi} \cos\frac{mx}{1-x}(\pi-\theta)\cos n\theta d\theta \quad (14)$$

$$b_0 = \frac{1}{\pi m x}\sin \pi m x. \quad (15)$$

Similarly,

$$\begin{aligned}\sin S(t) &= \sin m\theta && 0 \leqq \theta \leqq \pi x \\ &= \sin \frac{mx(\pi-\theta)}{1-x} && \pi x \leqq \theta \leqq \pi \\ &= \sum_{n=0}^{\infty} c_n \sin 2\pi n\mu t && (16)\end{aligned}$$

where

$$c_n = \frac{2}{\pi}\int_0^{\pi x} \sin m\theta \sin n\theta d\theta + \frac{2}{\pi}\int_{\pi x}^{\pi} \sin\frac{mx}{1-x}(\pi-\theta)\sin n\theta d\theta. \quad (17)$$

When these results are substituted into (11), the spectrum is given by

$$e = \sum_{n=-\infty}^{\infty} \frac{mE}{\pi(m-n)(mx-nx+n)} \sin \pi x(m-n) \cdot \sin(\omega + 2\pi n\mu)t \quad (18)$$

where

E = amplitude of the wave
m = modulation index $= D/\mu$
D = maximum frequency deviation, cycles per second
μ = repetition rate, cycles per second
x = fraction of the time the frequency is at the extreme deviation D
ω = angular frequency of the carrier, radians per second
t = time in seconds.

When $n=0$, the carrier amplitude is given by

$$\text{Carrier} = \frac{E}{\pi m x}\sin m\pi x \sin \omega t. \quad (19)$$

The side frequencies adjacent to the carrier are given by $n = \pm 1$ and are separated from the carrier by an amount equal to the audio frequency. They are given by:

First upper side frequency

$$= \frac{mE}{\pi(m-1)(mx-x+1)} \sin \pi x(m-1) \sin(\omega+2\pi\mu)t. \quad (20)$$

First lower side frequency

$$= \frac{mE}{\pi(m+1)(mx+x-1)} \sin \pi x(m+1) \sin(\omega-2\pi\mu)t. \quad (21)$$

The other side frequencies can be determined by assigning appropriate values to n in (18).

The indeterminate cases must be evaluated separately:

Case I $\quad m=n, \quad \frac{1}{2}(b_n+c_n) = x \quad (22)$

Case II $\quad \frac{mx}{1-x} = -n, \quad \frac{1}{2}(b_n+c_n) = \frac{1}{\pi(m-n)}\sin \pi x(m-n) + (-)^n(1-x) \quad (23)$

Case III $\quad m=-n, \quad \frac{1}{2}(b_n-c_n) = x \quad (24)$

Case IV $\quad \frac{mx}{1-x} = n, \quad \frac{1}{2}(b_n-c_n) = \frac{1}{\pi(m+n)}\sin \pi x(m+n) + (-)^n(1-x). \quad (25)$

The case of square-wave modulation is obtained by setting $x=\frac{1}{2}$. This gives the result

$$\begin{aligned} e &= \sum_{n=-\infty}^{\infty} \frac{2mE}{\pi(m^2-n^2)} \sin(m-n)\frac{\pi}{2} \sin(\omega+2\pi n\mu)t \\ &= \frac{2E}{\pi m}\sin m\frac{\pi}{2}\sin \omega t \\ &\quad + \frac{2mE}{\pi(m^2-1^2)}\cos\frac{m\pi}{2}\{\sin(\omega-2\pi\mu)t - \sin(\omega+2\pi\mu)t\} \\ &\quad - \frac{2mE}{\pi(m^2-2^2)}\sin\frac{m\pi}{2}\{\sin(\omega-4\pi\mu)t + \sin(\omega+4\pi\mu)t\} \\ &\quad - \frac{2mE}{\pi(m^2-3^2)}\cos\frac{m\pi}{2}\{\sin(\omega-6\pi\mu)t - \sin(\omega+6\pi\mu)t\} \\ &\quad + \cdots . \end{aligned} \quad (26)$$

This result, for $x=\frac{1}{2}$, agrees with that previously obtained by van der Pol.[14]

The limits for the amplitudes of the side frequencies can be determined from the coefficients of (18). Thus, if $m = D/\mu = 5$, and if $x=\frac{1}{4}$, the limit of the amplitudes becomes

$$\text{Amplitude limit} = \frac{m}{\pi(m-n)(mx-nx+n)} = \frac{20}{\pi(5-n)(5+3n)}. \quad (27)$$

[14] Balth. van der Pol, "Frequency modulation," PROC. I.R.E., vol. 18, pp. 1194–1205; July, 1930.

This curve is shown by Fig. 9. Actually, most of the side-frequency amplitudes will be less than this because of the first sinusoidal term of (18). As shown by

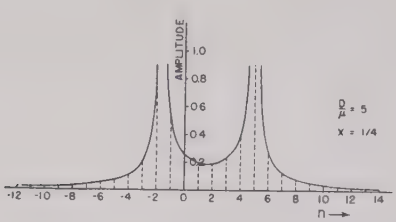

Fig. 9—Limits for side-frequency amplitudes.

Fig. 10, the amplitudes oscillate within the limits of the curve of Fig. 9. It may be easily seen that most of the

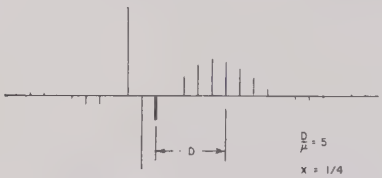

Fig. 10—Spectrum for rectangular modulation.

energy of the spectrum is concentrated about the frequencies that correspond to the two limits of the deviation.

Bandwidth Required for Rectangular Modulation

Equation 18 shows that there is an infinite number of side frequencies in the spectrum of a frequency-modulated wave with rectangular modulation. As shown by Figs. 9 and 10, the amplitudes of these side frequencies decrease uniformly beyond the limits of the deviations. If the edges of the band are defined as the points corresponding to a limiting amplitude of $0.01E$, the bandwidth can be computed directly from (18). For the case of square-wave modulation, $x=0.5$, and the increase in bandwidth with decreasing modulation index will be as shown by Fig. 11. If a more strict definition of bandwidth is required, curve B shows the width for the limiting amplitude $0.001E$. Curve A is an accurate enough limit for most practical cases.

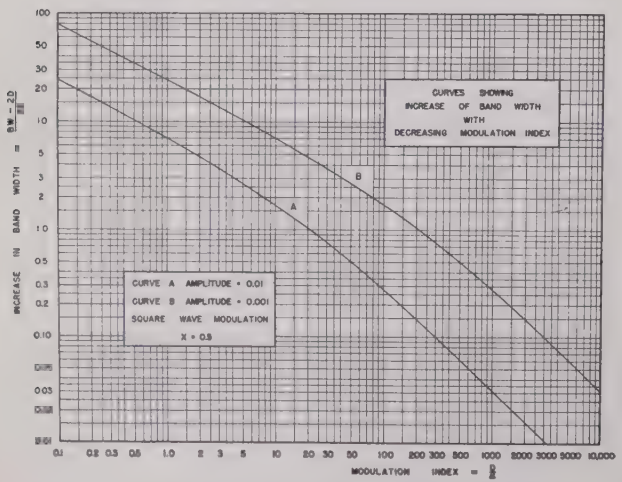

Fig. 11—Variation of bandwidth with modulation index.

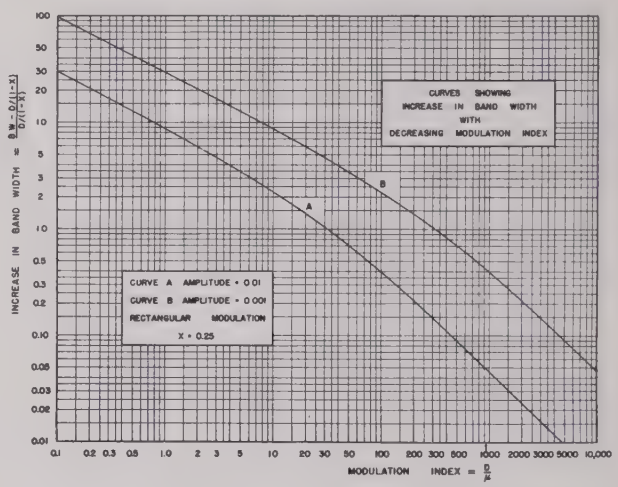

Fig. 12—Variation of bandwidth with modulation index.

If the maximum deviation is for one-fourth the time, $x=0.25$, the curves of Fig. 12 show the corresponding limits of the bandwidth. Other sets of curves, for other values of x, can be computed from (18).

It will be noted that the band does not end as abruptly with rectangular modulation as it did with sinusoidal modulation. The curves of Figs. 11 and 12 are much farther apart than the corresponding curves of Fig. 5.

The Spectrum of a Carrier Wave which is Frequency-Modulated with a Triangular Signal

When a uniformly spaced series of parallel bars, each one unit wide, is scanned at a uniform rate with a

Fig. 13—Scanning of picture element.

rectangular aperture of unit width, as shown by Fig. 13, the resulting signal is proportional to the area of the bar covered by the aperture. The signal will have a tri-

angular wave form, as shown by Fig. 14. During the time the aperture is between the bars, the output will be constant. As the aperture starts to cover a bar, the

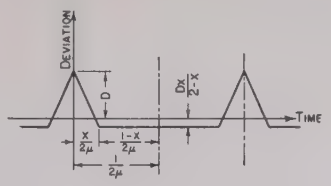

Fig. 14—Modulating signal.

output increases linearly until the aperture covers the entire bar. As the aperture moves on, the signal decreases linearly until it reaches the previous constant value, and remains constant until the next bar is reached. If this wave form is used to modulate the frequency of a carrier wave, the variation of the phase

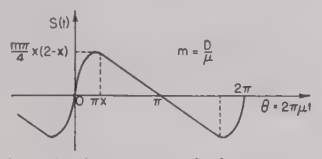

Fig. 15—Variation of phase angle.

angle will be 2π times the integral of this curve of Fig. 14, as shown by Fig. 15. The equation for this frequency-modulated wave becomes

$$e = E \sin \{\omega t + S(t)\}$$
$$= E \sin \omega t \cos S(t) + E \cos \omega t \sin S(t) \quad (28)$$

$$S(t) = \frac{D}{\mu}\left\{\frac{\pi x(2-x)\theta - \theta^2}{\pi x(2-x)}\right\} \qquad 0 \leqq \theta \leqq \pi x \quad (29)$$

$$= \frac{D}{\mu}\left\{\frac{x(\pi - \theta)}{2-x}\right\} \qquad \pi x \leqq \theta \leqq \pi. \quad (30)$$

When $S(t)$ is expanded in a Fourier series[15] and (11) is used, the

amplitude of the nth side frequency

$$= \frac{1}{\sqrt{2\pi\alpha}} \cos \frac{\beta^2}{4\alpha}\left[\operatorname{sgn} \gamma\, C\left\{\frac{\gamma^2}{4\alpha}\right\} - \operatorname{sgn} \beta\, C\left\{\frac{\beta^2}{4\alpha}\right\}\right]$$
$$+ \frac{1}{\sqrt{2\pi\alpha}} \sin \frac{\beta^2}{4\alpha}\left[\operatorname{sgn} \gamma\, S\left\{\frac{\gamma^2}{4\alpha}\right\} - \operatorname{sgn} \beta\, S\left\{\frac{\beta^2}{4\alpha}\right\}\right]$$
$$- \frac{1}{\pi\gamma} \sin (\pi\gamma x + \epsilon) \quad (31)$$

and the

amplitude of carrier

$$= \frac{2}{\sqrt{2\pi\alpha}} \cos \frac{\beta^2}{4\alpha}\left[C\left\{\frac{\alpha\pi^2x^4}{4}\right\} + C\left\{\frac{\beta^2}{4\alpha}\right\}\right]$$
$$+ \frac{2}{\sqrt{2\pi\alpha}} \sin \frac{\beta^2}{4\alpha}\left[S\left\{\frac{\alpha\pi^2x^4}{4}\right\} + S\left\{\frac{\beta^2}{4\alpha}\right\}\right]$$
$$+ \frac{2}{\epsilon} \sin (\pi\gamma x + \epsilon) \quad (32)$$

where

$$\alpha = \frac{m}{\pi x(2-x)} \qquad \gamma = \frac{mx}{2-x} + n$$

$$\beta = n - m \qquad \epsilon = \frac{-\pi m x}{2-x}.$$

sgn β means the algebraic sign of β, and the C and S functions are the Fresnel integrals

$$C(z) = \frac{1}{\sqrt{2\pi}} \int_0^z \frac{\cos t\, dt}{\sqrt{t}} = \frac{1}{2} \int_0^z J_{-1/2}(t)\, dt \quad (33)$$

$$S(z) = \frac{1}{\sqrt{2\pi}} \int_0^z \frac{\sin t\, dt}{\sqrt{t}} = \frac{1}{2} \int_0^z J_{1/2}(t)\, dt. \quad (34)$$

These integrals are tabulated over a considerable range.[16,17]

The vertical lines of Fig. 16 show the spectrum for triangular modulation with a modulation index of 10. The dotted line is the Bessel function $J_n(10)$; it gives the amplitudes of the side frequencies for the corresponding sine-wave signal. During triangular modula-

[15] The integrals can be evaluated by the following process:

$$\int_0^{\pi x} \cos (\alpha\theta^2 + \beta\theta)\, d\theta = \int_0^{\pi x} \cos \{\alpha(\theta + \beta/2\alpha)^2 - \beta^2/4\alpha\}\, d\theta$$
$$= \cos \frac{\beta^2}{4\alpha} \int_0^{\pi x} \cos \{\alpha(\theta + \beta/2\alpha)^2\}\, d\theta$$
$$+ \sin \frac{\beta^2}{4\alpha} \int_0^{\pi x} \sin \{\alpha(\theta + \beta/2\alpha)^2\}\, d\theta.$$

Let

$$\sqrt{\alpha}(\theta + \beta/2\alpha) = \pm\sqrt{v} \quad \text{and} \quad \sqrt{\alpha}\, d\theta = \pm \frac{dv}{2\sqrt{v}}.$$

Then

$$\int_0^{\pi x} \cos \{\alpha(\theta + \beta/2\alpha)^2\}\, d\theta = \sqrt{\frac{\pi}{2\alpha}} \int_{v_1}^{v_2} \frac{\cos v\, dv}{\sqrt{2\pi v}}$$

where

$$v_1 = \operatorname{sgn} \beta \frac{\beta^2}{4\alpha}; \qquad v_2 = \operatorname{sgn} \gamma \frac{\gamma^2}{4\alpha}.$$

The same transformation can be used on the second integral.

[16] See Table V, pp. 744–745, of footnote reference 8. Tables of $C(x)$ and $S(x)$, $x=0.02(0.02)1.00$; 7D, and $x=0.5(0.5)50.0$; 6D. For list of errors, see J. W. Wrench, Jr., "Mathematical tables—Errata," Mathematical Tables and other Aids to Computation, vol. 1, pp. 366–367; January, 1945.

[17] J. R. Airey, Sec'y., "Fresnel's Integrals, $S(x)$ and $C(x)$," British Association for the Advancement of Science, Report of the Ninety-fourth Meeting, 1926, pp. 273–275. Tables of $C(x)$ and $S(x)$, $x=0.0(0.1)20.0$; 6D.

tion, $x=1$, the frequency varies linearly from one extreme of the frequency excursion to the other, while for sinusoidal modulation the frequency is near the extremes of frequency a greater portion of the time. As might be expected, more of the energy in the spectrum is near the ends of the swing for sine-wave modulation than for triangular modulation.

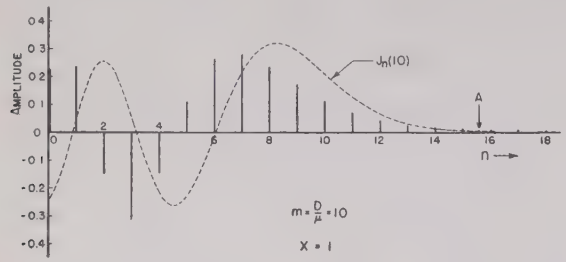

Fig. 16—Spectrum for triangular modulation.

Bandwidth Required for Triangular Modulation

If the bandwidth is defined as the extremes of frequency beyond which none of the side-frequency amplitudes are greater than 1 per cent of the carrier amplitude that would be obtained if the modulation were removed, the variation of bandwidth with modulation index can be computed from the equations for the side-frequency amplitudes. Curve A of Fig. 17 shows how the bandwidth increases as the repetition rate is increased. For a more precise definition of bandwidth, either curve B or curve C can be used.

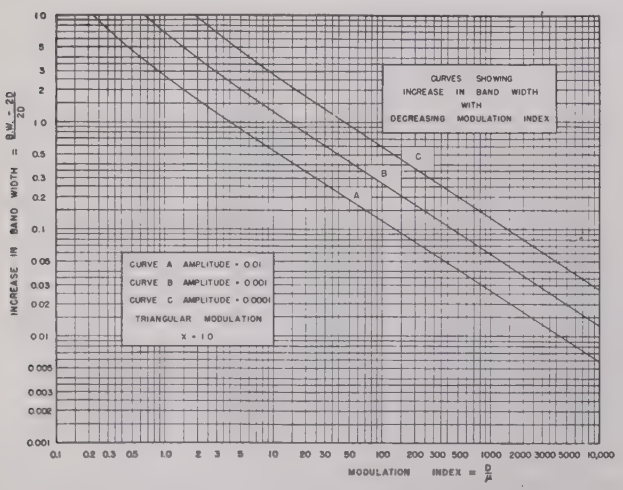

Fig. 17—Variation of bandwidth with modulation index.

If x is reduced to 0.1, the signal becomes a series of triangular pulses with blank spaces between. Most of the sideband energy will occur near the frequency which the carrier wave has between pulses, but the pulses will cause energy to be distributed on both sides of this frequency. Fig. 18 shows the spectrum for a modulation index of 10. The amplitudes decrease much more slowly than in the case of triangular or sinusoidal modulation.

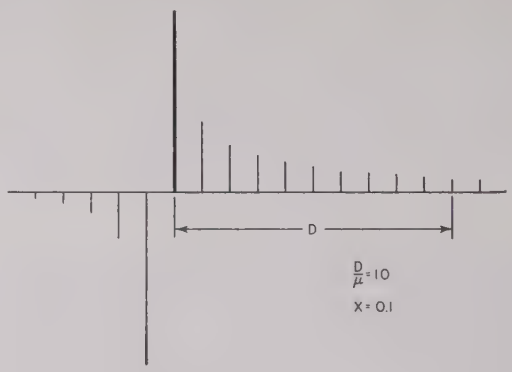

Fig. 18—Spectrum for triangular pulse modulation.

Conclusions

When a carrier wave is modulated in frequency, an infinite number of side frequencies is produced. As the modulation index is changed, the amplitudes of the side frequencies change and the carrier is likewise reduced and may even become zero. Although the bandwidth is theoretically infinite, in practice the side frequencies gradually decrease in amplitude for frequencies beyond the extremes of the total frequency excursions. The bandwidth can be defined as the extremes of frequency beyond which none of the side-frequency amplitudes are greater than 1 per cent of the carrier voltage obtained when the modulation is removed.

The bandwidth so defined always exceeds the total frequency excursion, but is nevertheless limited. For large modulation indexes, i.e., the deviation much greater than the repetition rate, the bandwidth approaches the actual variation in frequency and is only slightly greater. For small modulation indexes, the bandwidth may be several times the actual frequency excursion. Curves are given to show the bandwidth for modulation indexes from 0.1 to 10,000 for sinusoidal, square, rectangular, and triangular modulation. For a more precise definition of bandwidth, curves are also given for amplitude limits of $0.001E$ and $0.0001E$.

When several modulating tones are on simultaneously, the side frequencies are produced at frequencies separated from the carrier by all combination frequencies that can be obtained by taking sums and differences of all the harmonics of the tone frequencies. The same curves can be used to determine the bandwidth when several audio tones are used simultaneously, since the bandwidth will be equal approximately to the sum of the bandwidths for each tone separately.

The Influence of Amplitude Limiting and Frequency Selectivity Upon the Performance of Radio Receivers in Noise*

W. J. CUNNINGHAM†, MEMBER, I.R.E., S. J. GOFFARD‡, AND J. C. R. LICKLIDER§

Summary—This paper describes an experimental study of the relations which exist between the effectiveness of voice communication, measured in terms of the intelligibility of received speech, and the amplitude- and frequency-selective characteristics of amplitude-modulation receivers. The results lead to the following conclusions:

(1) Amplitude limiters are ineffective against fluctuation noise. Against impulse noise, however, they provide marked improvement in performance if they are incorporated in receivers with appropriate selectivity characteristics.

(2) When no limiter is used, best performance in the presence either of fluctuation noise or of impulse noise is provided by narrow-band circuits, but the advantage of narrow-band circuits over wide-band circuits is small.

(3) When a limiter is used, best performance against fluctuation noise is again provided by narrow-band circuits, and again the advantage of narrow-band circuits over broad-band circuits is small. For optimal reception in the presence of impulse noise, however, the selectivity curve of the circuits preceding the limiter must have gradually sloping skirts. When a limiter is used, therefore, advantage rests with broad-band rather than with narrow-band circuits.

I. Interference

THE FLUCTUATION noise used in the experiments was generated with the aid of a 6D4 gas tube and wide-band amplifiers. The spectrum, approximately uniform from 100 to 5000 kilocycles, covered the frequency range important for these tests, which were conducted at carrier frequencies of 465 and 520 kilocycles.

The impulse noise consisted of pulses of constant amplitude, spaced irregularly in time. The average number of pulses per second was approximately 1000, and the irregularity of spacing was such that there were few 1-second intervals with less than half, or more than twice, that number of pulses. The spectrum of the impulse noise was approximately uniform from 100 to at least 20,000 kilocycles. Noise with these characteristics was generated by an irregularly triggered thyratron circuit which provided output pulses of approximately 0.02-microsecond duration.[1]

* Decimal classification: R261.51×R361.211. Original manuscript received by the Institute, July 12, 1946; revised manuscript received, December 1, 1946. This work was begun under Contracts OEMsr-1441 and OEMsr-658 between the Office of Scientific Research and Development and Harvard University, where it is continuing under Contract N5ori-76 with the United States Navy, Office of Naval Research, as a joint project between the Electronics Research Laboratory (Project Order I) and the Psycho-Acoustic Laboratory (Project Order II, Report No. PNR-15).

† Formerly, Harvard University, Cambridge, Mass.; now, Yale University, New Haven, Conn.

‡ Formerly, Harvard University, Cambridge, Mass.; now, University of Minnesota, Minneapolis, Minn.

§ Harvard University, Cambridge, Mass.

[1] C. J. Mullin and H. W. Rudmose, Psycho-Acoustic Laboratory Report PNR-8, pp. 1–29; October 28, 1945. This report describes in detail the generator, Electro-Acoustic Laboratory Static Generator Model X-1, and may be obtained through the Office of Technical Services, United States Department of Commerce, Washington, D. C.

II. Amplitude Limiting

The amplitude limiter used in the experiments was a simple series-diode circuit, incorporated into the receiver at a point immediately following the detector. A schematic diagram of the limiter and its connection to the detector and to the cathode-follower output circuit is shown in Fig. 1. The limiter itself operates only upon the negative side of the audio wave, clipping off extreme negative peaks in the received signal.

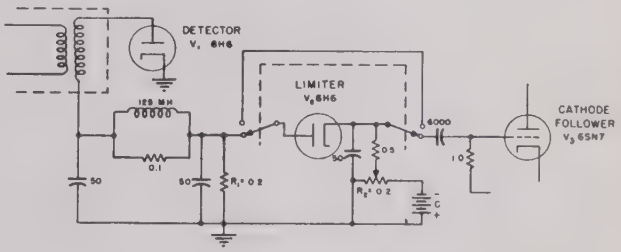

Fig. 1—Schematic diagram showing the amplitude limiter and its connection to the detector. Identical limiting circuits were used in the two test receivers. Values of resistance are in megohms, values of capacitance in micromicrofarads.

The action of the diode detector limits the positive swing at an amplitude level corresponding to 100 per cent modulation when the noise limiter is not connected. When the noise limiter is switched into the circuit, this positive-swing limitation is made more severe because part of the negative bias from R_2 is thrown across R_1. This bias shifts the amplitude at which detector limitation takes place with the result that the detector clips the positive swings approximately as much as the noise limiter clips the negative swings. Thus, although the noise limiter uses only a single diode, the circuit provides full-wave limitation. In the main series of experiments reported herein, the circuit was so adjusted that the limiting took place at an amplitude corresponding approximately to 50 per cent modulation.

III. Frequency Selectivity

The frequency-selective circuits used in the experiments provided control over two characteristics of the selectivity curve: (1) the bandwidth, important in determining the over-all level of the interference passed by the receiver; and (2) the slope of the skirts of the curve, important in determining the wave form of the output when the interference is impulsive. In order to obtain a wide range of control over each of these characteristics, two test receivers were prepared. Receiver I was a laboratory set which consisted of a variable-band

radio-frequency amplifier and the detector and audio circuits shown in Fig. 1. Receiver II consisted of the (modified) intermediate-frequency amplifier of a Hallicrafters SX-28-A receiver, followed by detector and audio circuits which were duplicates of those in receiver I.

Control over bandwidth was achieved by varying the coupling of the interstage transformers, and control over the slope of the skirts of the selectivity characteristics by varying the dissipation factor ($D=1/Q$) of the coupling circuits. Actually, changes in coupling produce some effect upon slope and changes in Q produce some effect upon bandwidth, but these effects are secondary.

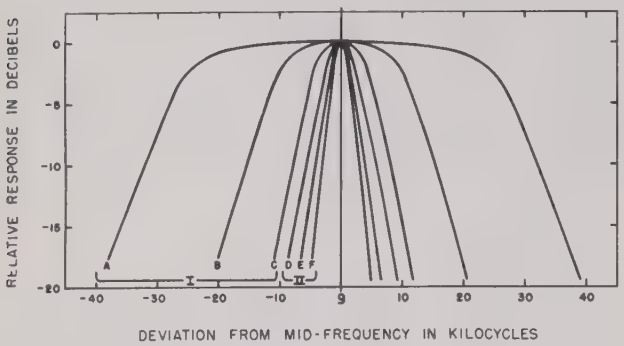

Fig. 2—Frequency-selective characteristics of the test receivers. The curves labeled *A*, *B*, and *C* are three of the selectivity characteristics which could be obtained with receiver I. Those labeled *D*, *E*, and *F* are three additional characteristics provided by receiver II.

Selectivity characteristics representative of those provided by the two test receivers are shown in Fig. 2. Three of the curves (*A*, *B*, and *C*) were obtained with receiver I; the other three (*D*, *E*, and *F*) were obtained with receiver II. It was possible, with other adjustments of the test receivers, to provide other characteristics besides those shown—in particular, to set up characteristics with the same bandwidths at half-power but with different slopes, and characteristics with the same slopes but different bandwidths.

IV. Listening-Test Procedure

In studying the influence of amplitude limiting and frequency selectivity upon intelligibility, two types of listening tests were used: threshold tests and articulation tests. Threshold tests were employed in preliminary experiments in order to determine, under a variety of experimental conditions, the signal-to-interference ratios required for satisfactory reception of speech. Articulation tests were then employed in the principal series of tests to provide, under a more restricted set of conditions, quantitative measures of intelligibility.

Threshold Tests

In the threshold tests, meaningful paragraphs were read over the communication system to the listeners, who in some instances worked individually and in other instances as a group. The radio-frequency signal-to-interference ratio was adjusted until the listeners could follow with little difficulty the sense of the paragraphs. The signal-to-interference ratio thus determined is referred to as the "threshold of intelligibility."

Articulation Tests

In the articulation tests, the announcers read discrete words instead of meaningful material, and the observers, listening in a group, wrote down the words as they heard them. The test vocabulary consisted of 1000 monosyllabic words, organized into twenty 50-word sets approximately equal in difficulty. The words of each set were "scrambled" to provide a large number of equivalent test lists.[2] Each test word was read as part of the *carrier sentence:* "You will write _____." The results of the articulation tests were expressed in terms of the percentage of the test words recorded correctly. Percentages for two talkers, each reading 50 words to the group of listeners, were averaged to determine the value of "per cent word articulation" for each experimental condition.

The test setup shown in Fig. 3 was used for both the threshold and the articulation tests.

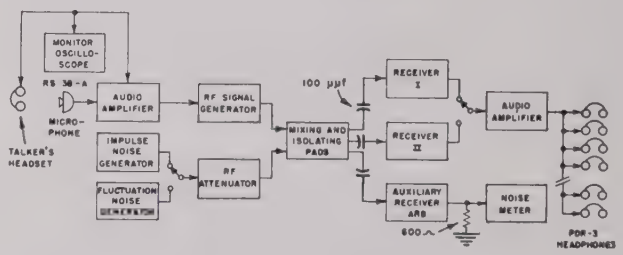

Fig. 3—Schematic diagram of test setup. The arrangement provided a speech-modulated carrier and either of two types of noise. The carrier and the noise were added in a resistive mixing circuit and applied together to the input terminals of the test receivers. An auxiliary receiver and noise meter, calibrated with the aid of the signal generator, were used in measuring the carrier-to-noise ratios.

Speech-modulated carrier: The amplitude-modulated carriers (520 and 465 kilocycles, 50 microvolts) were obtained by modulating a General Radio Type-805-A signal generator with a speech signal produced externally. The speech modulation was provided by two experienced talkers who read the test words into a carbon microphone (Navy Type RS 38-A) and monitored their speech at a level suitable for communication under adverse conditions. The speech amplifier was adjusted to provide 100 per cent modulation of the carrier on the average instantaneous peaks of the speech wave. Both sidebands were used.

Interference: Fluctuation noise and impulse noise were generated as described above. The intensity of the interference was controlled by a radio-frequency attenuator connected at the output of the interference generator. This attenuator permitted either continuous variation or variation in 5-decibel steps.

[2] The lists, known as the Psycho-Acoustic Laboratory PB Lists, were developed in connection with an extensive wartime program in which articulation tests were used to evaluate communication systems.

Method of mixing: The speech-modulated carrier and the interference were mixed in a resistive network and fed separately (from isolating pads of 10 ohms output impedance through 100-micromicrofarad capacitors) to the test receivers and to the receiver used in measuring the signal-to-interference ratio.

Signal-to-interference ratio: In the tests, the carrier intensity was held constant at 50 microvolts, and various signal-to-interference ratios were obtained by varying the interference level. The intensity of the interference (equivalent noise sideband input) was measured with an auxiliary receiver (Navy Type ARB, pass band approximately 10 kilocycles wide) and an output meter (RCA Type 302-B). The level was determined by substituting a carrier which was modulated 100 per cent at 400 cycles and varying its intensity until it produced the same indication on the noise meter as did the interference.[3]

Headsets and listeners: The audio amplifier of the test receiver was adjusted to deliver 5 milliwatts to each headset. The headsets, which consisted of Permoflux PDR-3 headphones mounted in small sponge-rubber cushions (MX-41/AR), provided approximately uniform response to 4500 cycles. With 5 milliwatts input, the output level was 115 decibels above 0.0002 dyne/cm^2.

Except in some of the preliminary work in which the experimenters served as listeners, the listeners were a group of nine to twelve women who had, in previous experiments, made articulation scores which agreed very closely with those of a comparable group of men. The listeners were seated in a relatively quiet room adjoining that in which the test equipment was set up. They could neither watch the talker nor hear his voice directly as he read the test words.

V. Results

Threshold-of-Intelligibility Tests

The carrier-to-noise ratios required to reach the threshold of intelligibility in the presence of impulse noise (1000 pulses per second) with six different bandwidths and five different amounts of amplitude limiting are shown in Fig. 4. The selectivity characteristics were those shown in Fig. 2. Four of the clipping levels corresponded, as indicated in the figure, to 18, 32, 56, and 100 per cent modulation, and the fifth was "no clipping." Fig. 4 shows (1) that the minimum carrier-to-noise ratio required for satisfactory reception was, in general, markedly lower when amplitude limiting was introduced than when it was not; (2) that the advantage provided by amplitude limiting depended markedly upon the width of the pass band; and (3) that the amplitude level at which limiting took place was not, within the range tested, a critical factor. Inasmuch as a level corresponding to about 50 per cent modulation gave consistently good results, that adjustment of the amplitude limiter was adopted as one of the two amplitude-limiting characteristics to be used in the principal series of tests. The other characteristic, no amplitude limiting, was obtained by disconnecting the limiter.

At the top of Fig. 4, the duration of the output pulses (measured at a level approximately 20 decibels below the peaks) has been indicated along a scale which parallels the (lower) scale of half bandwidth. It is not clear from these data whether the significant relation is between performance (with limiter) and bandwidth, or between performance and pulse duration. In order to distinguish between bandwidth and pulse duration as factors influencing the effectiveness of amplitude limiting, threshold tests were conducted with several additional combinations of the adjustments of coupling and Q.

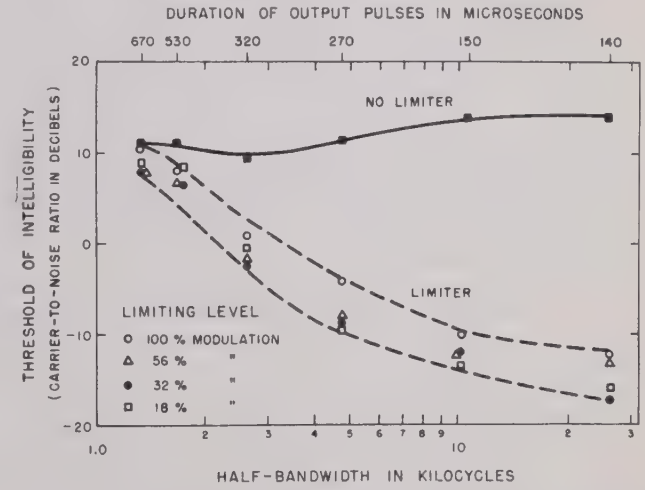

Fig. 4—Threshold-of-intelligibility curves showing the superior performance of broad-band circuits when used in conjunction with amplitude limiting against impulse interference. Performance is measured in terms of the carrier-to-noise ratio required for usable reception. The upper solid curve indicates that, when no limiter is used, slightly higher ratios were required with broad-band circuits than with narrow-band circuits. But, as shown by the lower dashed curves, broad-band circuits were much the more effective when an amplitude limiter was employed.

Some of these combinations provided equal bandwidths, as measured at the half-power points, but different pulse durations. Others provided equal pulse durations but different bandwidths. The results indicated clearly that, with a given type and amount of interference, the duration of the output pulses, as measured near the base of the pulse, is the primary factor in determining the effectiveness of amplitude limiting.

Using the variety of selectivity characteristics just described, threshold tests were conducted also with fluctuation noise. The differences between the thresholds for the various selectivity curves were very small, and it was apparent that neither frequency selectivity nor amplitude limiting was markedly effective against fluctuation noise.

[3] Actually, the carrier set up to provide equivalent output was modulated only 56 per cent, and a correction was made by multiplying the carrier intensity by 0.56.

Articulation Tests

The relationships obtained between per cent word articulation and carrier-to-interference ratio are presented in Figs. 5 and 6. These curves bear out the conclusions based on the threshold tests and afford more significance only when the carrier-to-interference ratio is low.

In the presence of impulse noise (Fig. 6), amplitude limiting is highly effective in improving performance if the frequency-selective circuits which precede the

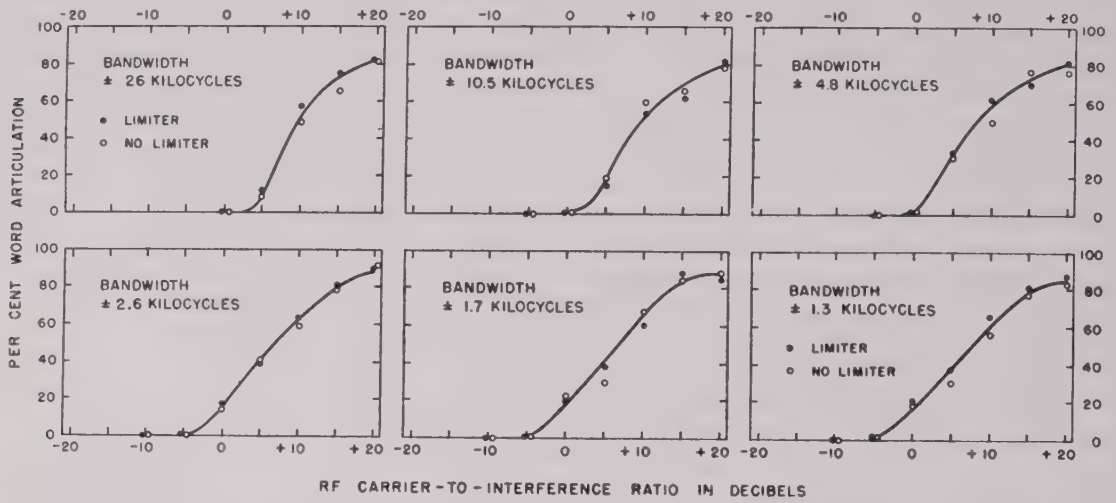

Fig. 5—Results of articulation tests with fluctuation noise. Word articulation is plotted as a function of radio-frequency carrier-to-interference ratio for the six frequency-selective characteristics shown. In the tests with the limiter (filled circles) the audio wave was limited sharply at the level corresponding to 50-per-cent modulation. In the tests in which the limiter was not used, the only amplitude limitation was that introduced by the normal action of the detector.

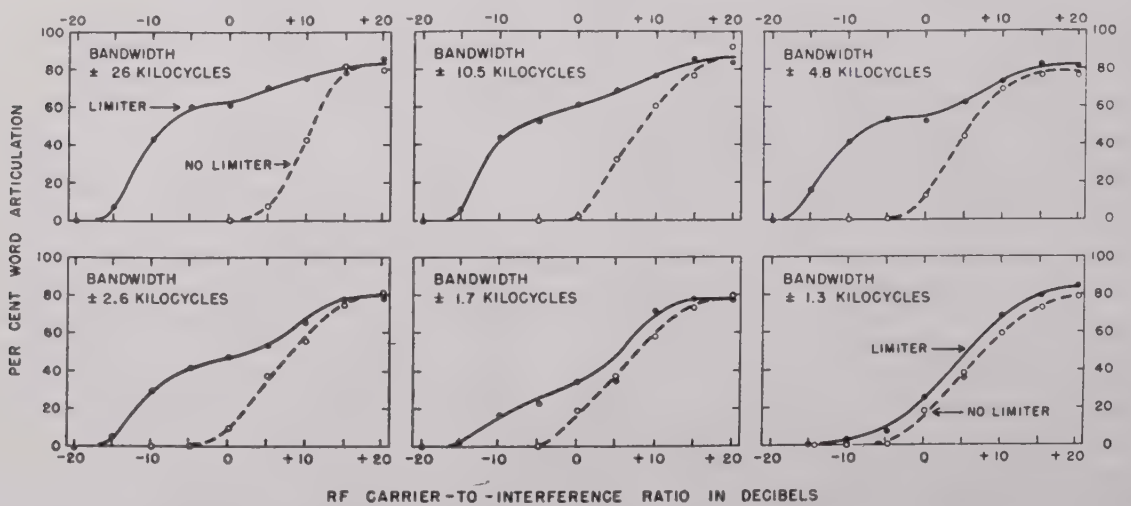

Fig. 6—Results of articulation tests with impulse noise. These results were obtained with the same frequency-selective and amplitude-limiting circuits as those shown in Fig. 5, but in the presence of irregularly spaced pulses (average pulse-repetition frequency 1000 pulses per second) instead of fluctuation noise.

quantitative indexes of the performance provided by the several combinations of frequency-selective and amplitude-limiting characteristics.

In the presence of fluctuation noise (Fig. 5) the effect of amplitude limiting upon intelligibility is essentially nil, no matter what the bandwidth. Performance is better with narrow-band coupling circuits than it is with broad-band coupling circuits, whether amplitude limiting is used or not; the advantage of narrow-band circuits is never great, however, and it appears to be of practical limiter have the (broad-band, low-Q) characteristics which are required to preserve the spike-like wave form of the pulses.

In conjunction with narrow-band coupling circuits which broaden the pulses, amplitude limiting is relatively ineffective. If no amplitude limiter is used, however, some advantage results from the employment of narrow-band coupling circuits. This advantage is roughly equivalent to that found in the tests with fluctuation noise.

VI. Discussion of Results

Frequency Selectivity Without Amplitude Limiting

In the presence of uniform spectrum noise, noise output power is directly proportional to bandwidth.[4] It is therefore not at all surprising to observe that, in the presence of fluctuation noise or in the presence of impulse noise when no limiter is used, narrow-band circuits provide better performance than broad-band circuits. But it is surprising to find that, even when bandwidths in the ratio of 1 to 20 are considered, the margin in favor of narrow-band circuits is so small.

It must be noted that, in the experiments reported herein, not all of the broad-band noise output reached the listeners' ears because the earphones were relatively insensitive at frequencies above 5000 cycles. But supplementary listening tests indicated that intelligibility was not noticeably changed when earphones with uniform response to 7500 cycles were substituted, and it is probable that it would not have been altered markedly if the headphones had passed the highest audio frequencies in the detector output. The significant factor appears to be not the frequency response of the audio equipment but the "masking" in the listener's auditory system. It is well known that low-frequency sounds mask high-frequency sounds, but high-frequency sounds do not mask low-frequency sounds.[5] Noise components above 2000 cycles are, therefore relatively ineffective in masking speech, and noise components above 4000 cycles may be disregarded in so far as influence upon intelligibility is concerned. The disadvantage of broad-band receiving circuits is, in this respect, much less pronounced than uncritical consideration of noise power as noise power—without regard to frequency—would suggest.

Frequency Selectivity and Amplitude Limiting

In considering the action of the amplitude limiter against interference, it is helpful to think in terms of amplitude selectivity, i.e., of discrimination in favor of signal and against noise on the basis of some characteristic difference between the amplitude patterns of the signal and the noise. When the problem is considered in these terms, it is apparent that amplitude selectivity can be effective in improving performance only if a characteristic difference between the wave forms of signal and noise exists. It is apparent, also, that for maximal effectiveness the particular type of amplitude selectivity chosen must be one appropriate for the difference in wave form.

Since both speech and fluctuation noise have continuous, irregular wave forms, and since their ratios of peak[6] to root-mean-square amplitude are, on the average, about equal, it is not surprising that amplitude limiting provides no marked improvement in performance against fluctuation noise. Against highly peaked impulse noise, on the other hand, limiters are effective because, simply by clipping off the peaks, a considerable reduction in noise intensity can be achieved with very little disruption of the speech wave—and low-Q coupling circuits maintain the abrupt, transient wave form of impulse noise.

The relation between the effectiveness of amplitude limiting and the bandwidth of the circuits which precede the limiter is thus a reflection of the relation between bandwidth and pulse duration.[7] The way in which pulse duration controls intelligibility when amplitude limiting restricts all of the output pulses to the same amplitude may, for practical purposes, be thought of as follows: Each pulse blanks out the speech signal during a short time interval. As the duration of the pulse is increased, the disruptive effect upon intelligibility is increased. As the duration is increased still further, each pulse fills up a considerable time interval and successive pulses start to overlap. When this occurs the interference loses the characteristics of impulse noise and takes on the characteristics of fluctuation noise. There is then no distinguishing characteristic on the basis of which the amplitude limiter may discriminate against the noise and in favor of the speech, and amplitude limiting becomes ineffective.

It is unfortunate that the type of selectivity characteristic which is required in order to permit effective amplitude limiting in the presence of impulse noise is just the type of selectivity characteristic which is least effective in rejecting adjacent-channel signals. However, a certain amount of impulse interference is encountered even in the range of very-high frequencies in which it has not proved feasible to use narrow pass bands. The present results would suggest, therefore, that very-high-frequency amplifiers be designed with low-Q circuits rather than with staggered or overcoupled high-Q circuits. Furthermore, even in medium- and low-frequency applications it is sometimes more important to minimize impulse interference than to avoid adjacent-channel interference. In such an event, a broad selectivity characteristic would be preferable to a narrow one.

The advantages of effective amplitude limiting can perhaps be reconciled to some degree with the advantages of a narrow over-all pass band by incorporating the amplitude limiter into the intermediate-frequency section of the receiver.[8] Or, the selective circuits of the receiver might be so arranged that their characteristics could be altered, perhaps automatically, in accordance with the requirements for optimal handling of the received wave.

[4] John R. Carson, "Selective circuits and static interference," *Trans. A.I.E.E.* (*Elec. Eng.*, June, 1924), vol. 43, pp. 789–797; June, 1924.

[5] S. S. Stevens and Hallowell Davis, "Hearing: Its Psychology and Its Physiology," John Wiley and Sons, New York, N. Y., 1938.

[6] The term "peak amplitude" as used here should be qualified. It is convenient to consider not the highest amplitude ever to be reached by the wave, but the highest amplitude to be exceeded some fixed small percentage (e.g., 1 per cent) of the time.

[7] Martin Wald, "Noise suppression by means of amplitude limiters," *Wireless Eng.*, vol. 17, pp. 432–438; October, 1940.

[8] J. J. Lamb, "Silencing circuits for radio receivers," United States Patent No. 2,101,549.

Performance of Short Antennas*

CARL E. SMITH†, SENIOR MEMBER, I.R.E., AND EARL M. JOHNSON‡, SENIOR MEMBER, I.R.E.

Summary—The purpose of this paper is to present experimental data on the performance of vertical antennas having a physical height of less than one-eighth wavelength. These data cover many conditions of top loading performed on a 300-foot, self-supporting, tapered vertical tower with measurements of antenna resistance and reactance from 120 to 400 kilocycles. For these conditions, field-intensity measurements were made to determine the unattenuated field intensity at one mile over a frequency range from 139 to 260 kilocycles. Field-intensity measurements along eight radials were made to determine the horizontal pattern and root-mean-square field intensity.

The best results are obtained when adequate top loading is used in conjunction with a good ground system. Such top loading increases the value of the radiation-resistance component and lowers the capacitive-reactance component of the driving point impedance. Since the loss resistance remains essentially constant with various types of loading, the radiation efficiency of the antenna is materially improved by raising the value of the radiation resistance. Increasing the radiation resistance and lowering the capacitive reactance both tend to lower the effective Q of the antenna circuit. In wide-frequency-band applications a low value of Q is very important.

With short antennas having a small resistance and a large capacitive reactance, extra precautions should be taken to minimize base insulator losses. With high humidity, mist, fog, or rain the input loss resistance of a short unloaded tower may increase several times over its normal dry value. Extensive ground systems and high-Q loading coils are also of prime importance.

I. Introduction

A REVIEW of the literature regarding vertical antennas reveals that most investigations in the past few years have been made on antennas having a height of from one-eighth wavelength to the order of one-half wavelength.[1–3] Most of these studies have been directed toward improving broadcasting coverage by increasing the ground-wave signal and reducing the fading caused by the sky wave.

In the past, it has been rather common practice at the low frequencies to use antennas about one-quarter wavelength in height, where possible, or to use loading of the T or inverted-L types for very short antennas. It has been the opinion of the authors for some time that other types of top loading would be practical. It is the purpose of this paper to discuss this problem and to report on a series of experiments that were made to prove or disprove the validity of top loading to improve the performance of short antennas.

* Decimal classification: R320. Original manuscript received by the Institute, July 25, 1946; revised manuscript received, December 2, 1946.

† Formerly, Office of Chief Signal Officer, United States Army; now, United Broadcasting Company, Cleveland, Ohio.

‡ Formerly, Office of Chief Signal Officer, United States Army; now, Mutual Broadcasting System, New York, N. Y.

[1] W. L. McPherson, "Electrical properties of aerials for medium and long wave broadcasting," *Elec. Commun.*, vol. 16, pp. 306–320; April, 1938; and vol. 17, pp. 44–65; July, 1938.

[2] G. H. Brown, R. F. Lewis, and J. Epstein, "Ground systems as a factor in antenna efficiency," PROC. I.R.E., vol. 25, pp. 753–787; June, 1937.

[3] C. E. Smith, "A critical study of two broadcast antennas," PROC. I.R.E., vol. 24, pp. 1329–1341; October, 1936.

II. Theoretical Considerations

1. Vertical Patterns

An antenna of infinitesimal height, assuming no loss, will radiate a field having an intensity of 186 millivolts per meter at one mile in the horizontal plane for 1.0 kilowatt input. An antenna one-eighth wavelength in height under similar conditions provides 189 millivolts per meter at one mile, an improvement of only 1.6 per cent. A one-fourth wavelength antenna has a field intensity of only 195 millivolts per meter at one mile, which is an improvement of 4.8 per cent over an antenna of infinitesimal height. The vertical patterns have essentially the same semicircular shape, which accounts for the horizontal fields having nearly the same strength.

2. Power Radiated and Dissipated

In actual practice the above theoretical values of the field intensity can not be realized because of loss resistance in the conductors of the antenna and coupling network, finite conductivity of the ground system, and dielectric losses in the insulators. Due to the fact that the radiation resistance approaches zero as the height is reduced and the loss resistance increases due to the dielectric losses in the base insulators, the efficiency of the antenna system must approach zero.

The ratio of power radiated to power input to the antenna system can be taken as the criterion of over-all performance of the antenna system. In equation form:

$$\text{antenna system efficiency} = \frac{P_R}{P_I} 100 \text{ per cent} \qquad (1)$$

where P_R = antenna power radiated in watts and P_I = antenna-system input power in watts.

The power radiated from the antenna can be determined by measuring the unattenuated root-mean-square field intensity at one mile and comparing it with the theoretical unattenuated field intensity which can be computed for a given antenna configuration. Thus,

$$P_R = 1000\left[\frac{E_m}{E_t}\right]^2 \qquad (2)$$

where E_m = measured unattenuated field intensity at one mile in millivolts per meter for 1.0 kilowatt input and E_t = theoretical unattenuated field intensity at one mile in millivolts per meter for 1.0 kilowatt input.

The antenna-system input power can also be considered as the transmitter output power since the input power supplies the losses in the antenna-system coupling

network between the transmitter terminals and the antenna as shown in Fig. 1. The total power lost in the

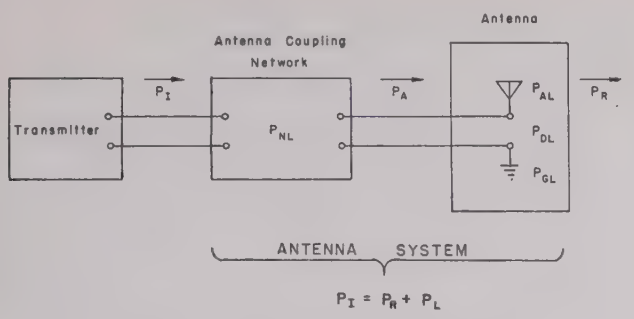

Fig. 1—Power in various parts of the antenna system.

antenna system can be expressed as follows:

$$P_L = P_{NL} + P_{AL} + P_{DL} + P_{GL} \tag{3}$$

where P_L = total power lost in the antenna system measured in watts, P_{NL} = antenna-system coupling-network power lost measured in watts, P_{AL} = antenna-resistance power lost measured in watts, P_{DL} = insulator-dielectric power lost measured in watts, and P_{GL} = ground-system power lost measured in watts.

The power lost in the antenna-system coupling network can be determined by measuring the input and output power and using the equation:

$$P_{NL} = P_I - P_A \tag{4}$$

where P_A = antenna input in watts measured at the antenna terminals as shown in Fig. 1.

The power lost in the antenna itself, P_{AL}, in the insulator dielectric, P_{DL}, and the ground system, P_{GL}, can be lumped together and determined from the following equation:

$$P_A - P_R = P_{AL} + P_{DL} + P_{GL}. \tag{5}$$

3. *Antenna Impedance*

For an antenna without top loading that is shorter than one-eighth wavelength (45 degrees), the radiation resistance is small and approximately proportional to the square of the height. A useful approximation is

$$R_R \doteq \frac{h^2}{312} \tag{6}$$

where R_R = base radiation resistance in ohms, and h = height of antenna in degrees.

This equation has been plotted (see Fig. 13) to show its accuracy as compared with the theoretical radiation-resistance curve for a thin vertical wire with sinusoidal current distribution. Equation (6) gives fair accuracy up to one-eighth wavelength. Above this wavelength the values are too low. As the top loading is increased the slope of the radiation-resistance curve increases and this approximation loses its accuracy.

The reactance of a short antenna is capacitive and becomes larger with decreasing height. An approximate formula is

$$X_c \doteq Z_0 \cot h \tag{7}$$

where X_c = base capacitive reactance in ohms, $Z_0 = 60(\log_e(h/r) - 1)$ ohms, h = height of antenna in degrees, and r = radius of antenna in degrees.

This equation assumes a uniform cross-section tower with sinusoidal current distribution and no shunting insulator capacitance at the base.

4. *Antenna-System Performance*

The performance of a nondirectional antenna system depends upon the vertical directivity gain of the antenna and the losses in the system. For short antennas the directivity gain will not change appreciably from one condition to another so long as there is not a reversal of current on the antenna. The vertical pattern for most cases will be somewhere between that of an infinitesimal antenna and a quarter-wave antenna.

The term "antenna system" is used in this discussion to include the coupling network between the transmitter and the antenna proper as shown in Fig. 1. It is important to include this network since its losses P_{NL} may be an appreciable factor in determining the over-all efficiency of the antenna system. In both the theoretical and practical case, as the antenna is made shorter the radiation resistance decreases and the capacitive reactance increases. To transform this antenna impedance to a value that will properly load the transmitter, it is common practice to insert a coil in series with the antenna that will neutralize the capacitive reactance and leave enough inductive reactance so that a capacitor in parallel will antiresonate the circuit to give the desired value of impedance for the transmission line or transmitter as the case may be. The losses in this network can be determined by capacitor (3). Since the loss in this network may be large for very short antennas, it is desirable to take measures to increase the antenna terminal resistance and lower the capacitive-reactance component. Both of these conditions are improved by proper top loading of the antenna.

The power P_{AL} lost in heating the antenna itself will usually be quite small providing the conductor surface is large, the antenna-tower members are thoroughly bonded and the material of the tower is itself a good conductor. In any event, it would be difficult to separate this loss from that of the ground-system loss P_{GL} and the insulator loss P_{DL}.

During the course of these experiments, measurements indicated that the reactance of the base insulator was small in comparison to its loss-resistance component. Under these conditions the power lost in the insulator P_{DL} may be considered separately if it is first considered that the equivalent circuit of a short antenna consists of a resistance R and a capacitive re-

actance X in series, as shown in Fig. 2(a). The resistance R is assumed to be made up of all resistances as measured at the antenna terminals except the insulator loss resistance. The impedance of this circuit is given by,

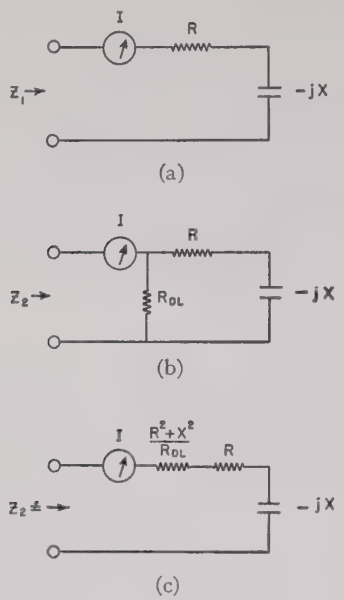

Fig. 2—Equivalent circuits for determining power loss in base insulators: (a) assuming no insulator loss, (b) insulator shunting antenna terminals with resistance R_{DL}, and (c) insulator effective series loss resistance R^2+X^2/R_{DL}.

$$Z_1 = R - jX. \tag{8}$$

If the antenna circuit is shunted with a lossy insulator represented by a resistance R_{DL}, the circuit becomes that shown in Fig. 2(b), with impedance Z_2 given by

$$Z_2 = \frac{R^2R_{DL} + X^2R_{DL} + RR_{DL}^2 - jXR_{DL}^2}{(R + R_{DL})^2 + X^2}. \tag{9}$$

In practice the insulator loss resistance R_{DL} is usually very much greater than the resistance R and the reactance X, so that the equivalent circuit may, to a very close approximation, be represented by Fig. 2(c) and the equation for Z_2 simplifies to,

$$Z_2 \doteq \frac{R^2 + X^2}{R_{DL}} + R - jX. \tag{10}$$

Comparing (8) and (10), it may be seen that they differ only in the term $(R^2+X^2)/R_{DL}$, the insulator effective series loss resistance. Since the antenna current I must flow through both resistances, $(R^2+X^2)/R_{DL}$ and R, the power is divided between them and the power lost in the insulator P_{DL} is given by

$$P_{DL} = I^2\frac{R^2 + X^2}{R_{DL}}. \tag{11}$$

The percentage of the antenna input power P_A lost in the insulator is equal to

$$P_{DL} = \frac{100}{1 + \dfrac{RR_{DL}}{R^2 + X^2}}. \tag{12}$$

An adequate ground system is of extreme importance where short antennas are employed. The per cent power loss for various types of buried-copper-wire radial ground systems, expressed as a function of antenna height for an unloaded tower, is shown in Fig. 3. These curves are derived from field-intensity measurements made in the standard broadcast band and on file with the Federal Communications Commission and from those shown in the paper of Brown, Lewis, and Epstein.[2]

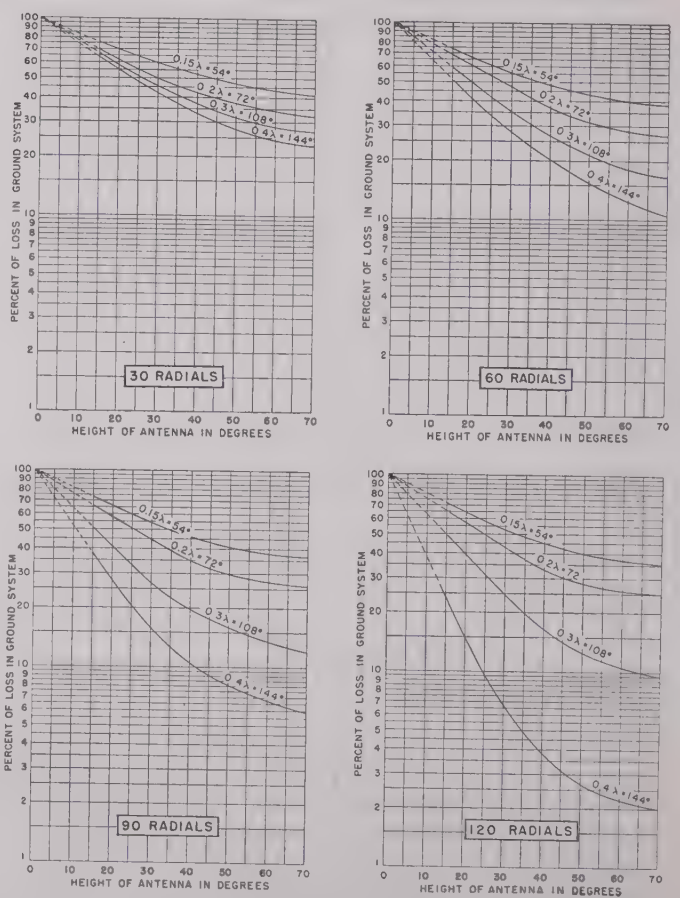

Fig. 3—Per cent power loss in the ground system for various lengths of buried-copper-wire radials, as identified on the curves, plotted as a function of antenna height for the indicated number of radials.

The effect of conductivity in the immediate vicinity of the transmitter becomes very important when poor ground systems are used. Under such conditions the losses will be different from those shown in Fig. 3, which are for average soil conductivities. On low frequencies, where physical limitations may prevent the installation of an ideal ground system, careful selection of trans-

mitter sites is essential. Whenever possible, a site having a high conductivity for the first few miles should be selected.

It should be noted that these curves have been prepared for an unloaded vertical tower. Where top loading is used, it is necessary to determine the radiation resistance for that structure and select an unloaded tower having a height that will give the same radiation resistance. The equivalent unloaded height is then used to estimate the power lost in the ground system. This procedure assumes that the ground-loss resistance R_{GL} remains constant for loaded and unloaded towers. Although there is some change in R_{GL} with loading, it is generally not of sufficient magnitude to alter the results appreciably.

Preparation of the curves to indicate the per cent power loss in the ground system allows direct addition of this loss in (3) for determination of over-all antenna-system loss P_L.

For a given quantity of copper wire, less loss will occur if the ground radials are made in the order of 0.4-wavelength long rather than placing this same quantity of wire in a greater number of shorter radials. Due to the physical dimensions of a 0.4-wavelength ground system, it may not always be practical to install such a system. Where the number of ground radials is limited, the use of a ground screen will improve stability as well as reduce losses.

In many applications of radio, the effective Q or bandwidth of the antenna circuit is of greater significance than the efficiency of the system. The bandwidth of the antenna may be determined from the resistance and reactance measurements made at the base of the tower. If the bandwidth is considered to be the frequency band within which the power is equal to or greater than one-half the power at resonance, then in equation form

$$\Delta f = \frac{2R_A}{\frac{dX}{df}} \tag{13}$$

where Δf = bandwidth in kilocycles between half-power points, R_A = measured antenna resistance in ohms, and dX/df = slope of reactance curve at resonant frequency.

This equation assumes a generator impedance of zero ohms. When the generator is matched to the antenna circuit, the effective bandwidth will be doubled.

III. Experimental Data

1. Impedance-Measuring Equipment

A General Radio type 516-C radio-frequency bridge was modified with a type 578-C low-frequency transformer and a ratio arm with 1000 ohms in each arm to give better sensitivity in this frequency range. A specially constructed composite oscillator having an output up to 25 volts was used as the generator voltage for the bridge. A Hammarlund receiver with two low-frequency bands was used as the bridge detector. The operating frequency was measured with a type SCR-211 frequency meter.

In making the measurements over a range of frequencies from 120 to 400 kilocycles, care was taken to get accurate values of the resistance component. Corrections were made to take into account the loss in the capacitor placed in series with the unknown. The loss of this capacitor varied considerably over the frequency range. The generator signal was unmodulated and the null point was determined by the dip of the "R" meter in the Hammarlund receiver.

2. Determination of the Unattenuated Root-Mean-Square Field Intensity at 1 Mile

The initial tests were made on a 300-foot self-supporting tower without top loading. A photograph of this tower with the eight umbrella wires connected is shown in Fig. 4. The ground system installed consisted of 500 buried-copper-wire radials out to a distance of 75 feet, and 250 buried-copper-wire radials out to a distance of 400 feet. To measure the performance of this antenna, a rather complete survey was made to determine the unattenuated root-mean-square field intensity at one mile when operating on a frequency of 170 kilocycles. Top-loading conditions were then referred to this unloaded condition of operation.

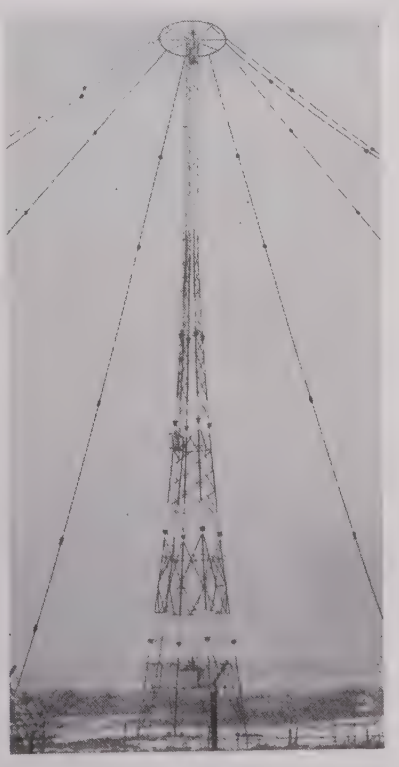

Fig. 4—View of WHK's 300-foot tower with the eight umbrella wires in place.

The antenna was driven with a type BC-191 transmitter. The field-intensity measurements were made

with a Radio Corporation of America type 308-A field-intensity meter mounted in a four-wheel-drive carry-all truck. This truck was also equipped with two-way radio-communication equipment.

In order to determine the power radiated, field-intensity measurements were made along 8 radials. A plot of the measurements along the respective radials was used to determine the unattenuated field intensity at one mile. From these data the horizontal pattern was constructed as shown in Fig. 5.

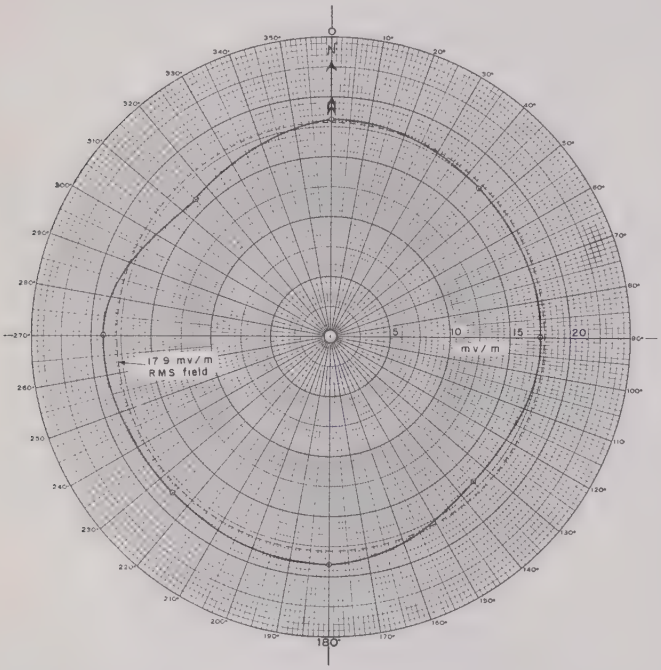

FIG. 5—Plot of unattenuated field intensity at 1 mile: frequency, 170 kilocycles; antenna, 300-foot self-supporting tower with top loading; ground system, 500 radials under asphalt pavement out 75 feet, plus 250 radials out 400 feet; impedance, $2.5-j\,465$ ohms; antenna current, 3.8 amperes; and root-mean-square field, 17.9 millivolts per meter.

3. *Ratio Method of Determining the Root-Mean-Square Field Intensity for the Tower with the 30-Foot-Diameter Capacitive Hat*

The capacitive hat was connected to the top of the tower through the contacts of a relay which could be readily controlled from the tuning house at the base of the tower. Resistance and reactance measurements for both conditions were made over the frequency range 120 to 400 kilocycles. Field-intensity measurements were then made at a few established points along each radial, first with the capacitive hat on and then with it off. The work was speeded up with the aid of two-way radio communication between the tuning house and the field car. Enough measurements were made to establish the fact that the horizontal patterns were essentially the same for both conditions of operation. At 170 kilocycles and with the same input current the field intensity with the capacitive hat was 11 per cent greater than for the tower without top loading.

4. *Ratio Method of Determining the Root-Mean-Square Field Intensity for the Various Conditions of Operation over a Frequency Range*

To determine the performance for numerous conditions of loading, a reference point was selected 1.5 miles from the antenna. Field-intensity measurements were made at this point on the following frequencies: 139, 150, 159, 170, 183, 193, 230, and 260 kilocycles, for each condition of loading. During these measurements, the antenna current was maintained at 3.0 amperes or the field measurements were corrected to correspond to this value of antenna current. This method gives a check on measurements at a given frequency in addition to adding the frequency-range parameter.

Field-intensity measurements indicated that the horizontal pattern remains substantially unchanged from the condition of zero top loading; hence, the unattenuated root-mean-square field intensity at one mile and the radiation resistance can be computed over a frequency range for each condition of top loading.

5. *Top Loading with Eight Umbrella Wires*

The loading afforded by the use of the 30-foot-diameter capacitive hat, although increasing the power radiated, did not appear to offer the optimum degree of loading. The mechanical difficulties involved in enlarging the size of the hat made such a procedure impractical. As a means of increasing the amount of loading, eight umbrella wires were fastened between the top of the tower and ground. These wires were uniformly spaced in the horizontal plane and were made taut by means of blocks and tackles fastened to stakes driven in the ground 350 feet from the center of the tower. Each wire was broken with insulators at regular intervals. By opening and shorting pertinent insulators, it was possible to vary the length of these wires so as to present different amounts of top loading. Two types of umbrella loading were tried. The first involved varying the length of the eight umbrella wires, so that their lengths were 100, 200, 300, 375, and 450 feet. The second involved connecting the outer or free ends of the umbrella wires with a wire skirt and varying the radial length to 100, 200, and 300 feet.

Resistance, reactance, and field-intensity measurements were made over a frequency range for each of the nine conditions of umbrella loading. The radiation resistances were determined and are plotted along with the measured base resistance and reactance in Figs. 6 and 7. A sketch of the installation is shown on each curve. For comparison purposes, the values of reactance have been replotted as families of curves in Figs. 8 and 9.

If the measured base resistance is plotted against length of umbrella wires for the lower frequencies, considerable variation will be observed. This arises from the fact that resistance measurements for the

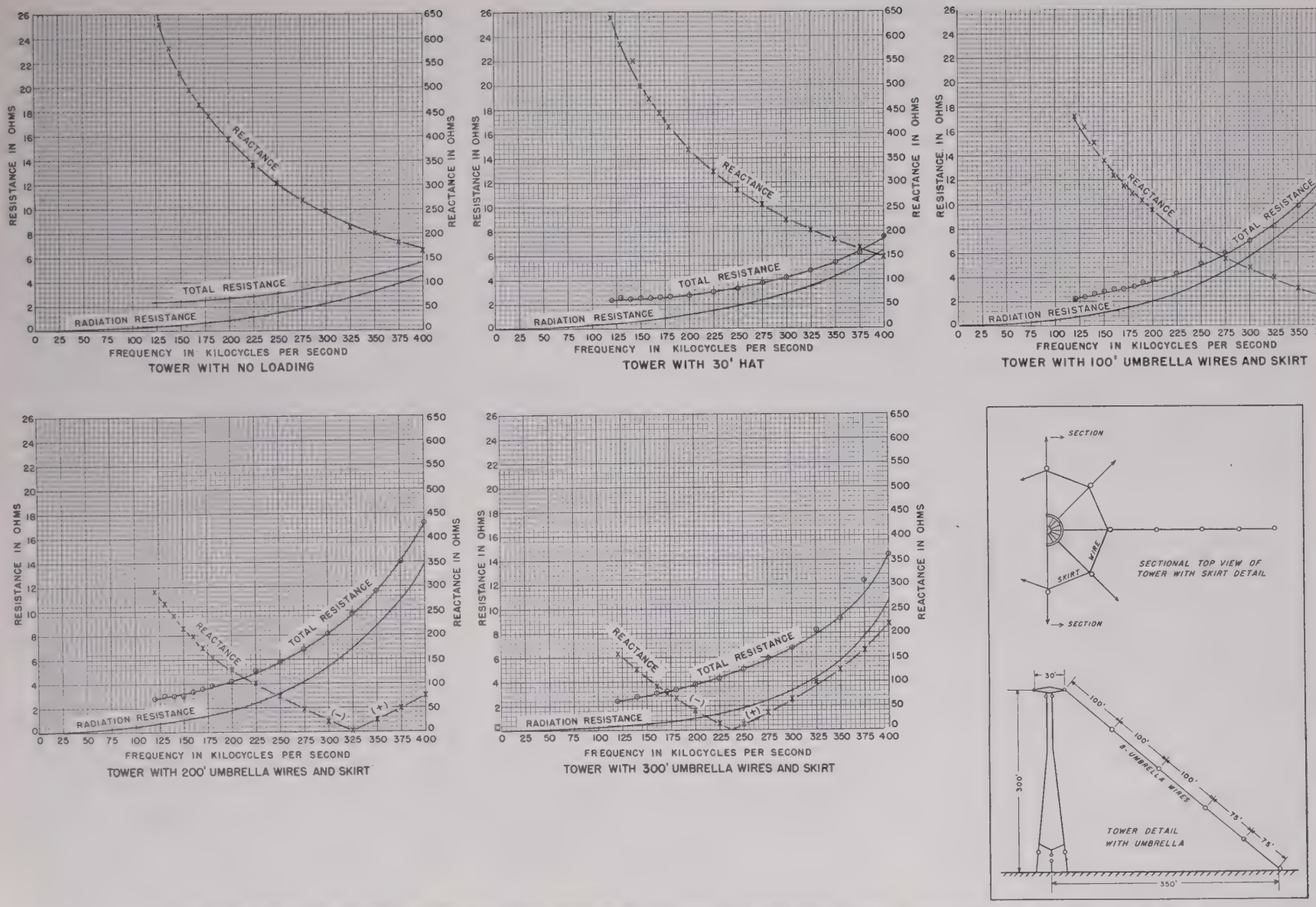

Fig. 6—Plot of resistance and reactance measurements on a 300-foot self-supporting tower, top-loaded with eight uniformly spaced umbrella wires connected at the ends with a wire skirt as shown in the sketch.

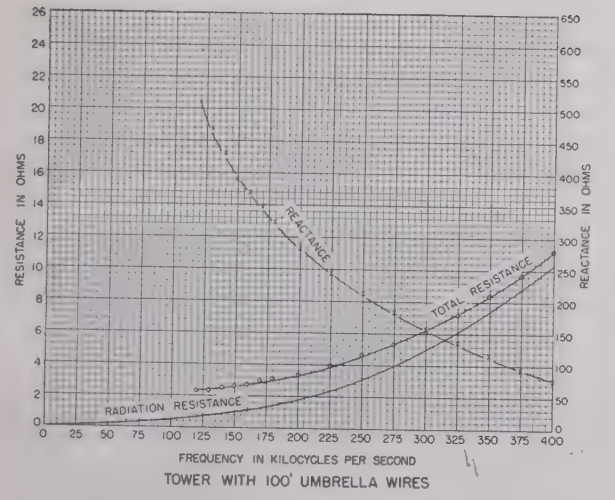

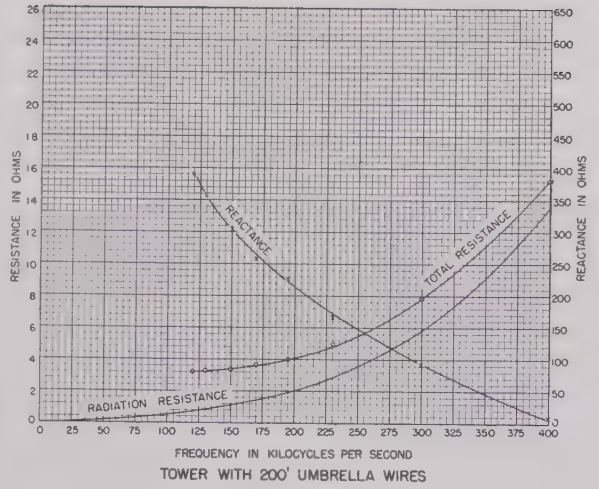

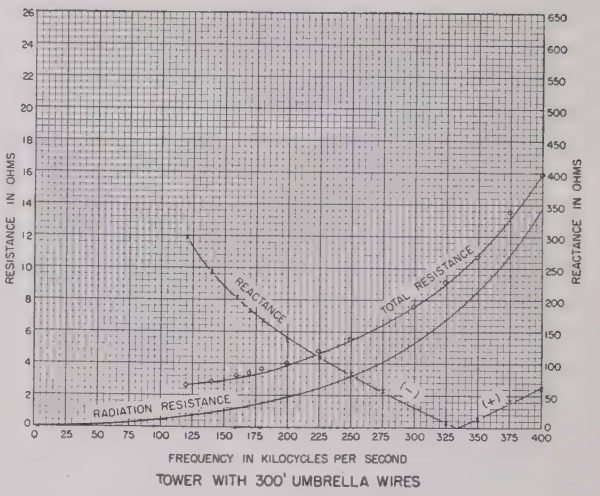

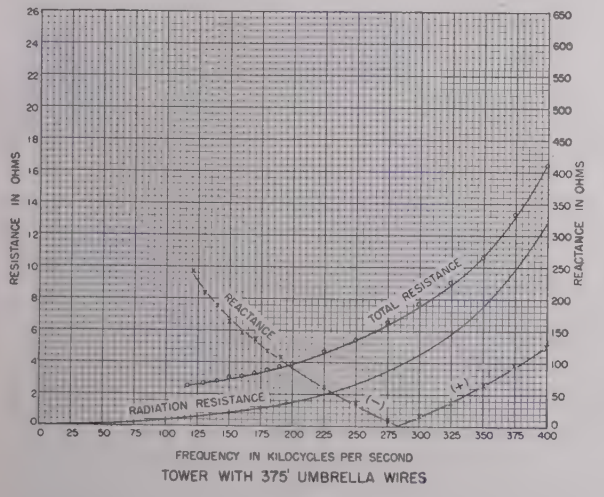

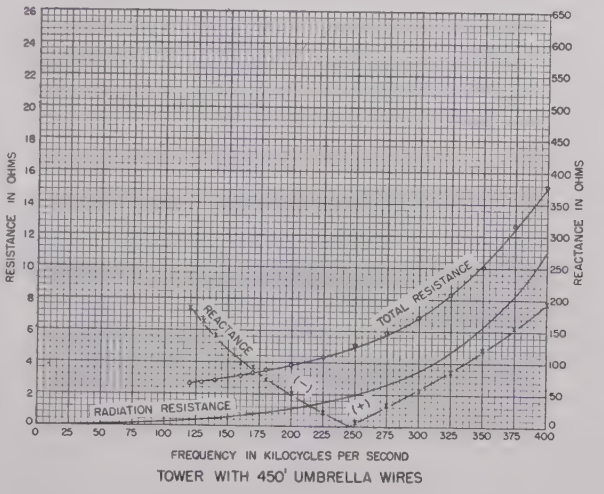

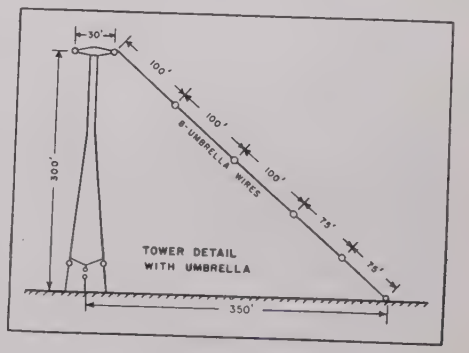

Fig. 7—Plot of resistance and reactance measurements on a 300-foot self-supporting tower, top-loaded with eight uniformly spaced umbrella wires.

various amounts of loading were made on different nights under different weather conditions, and thus at variable values of insulator dielectric loss P_{DL}.

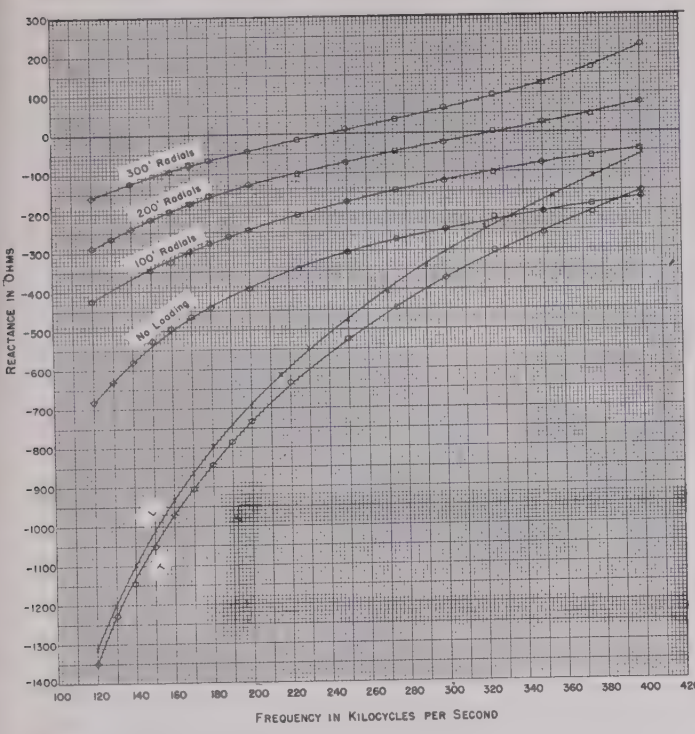

Fig. 8—Reactance curves of inverted-L- and T-type antennas compared with various lengths of eight umbrella wires, with skirt wire connecting the outer extremity, used as top loading on a self-supporting tower.

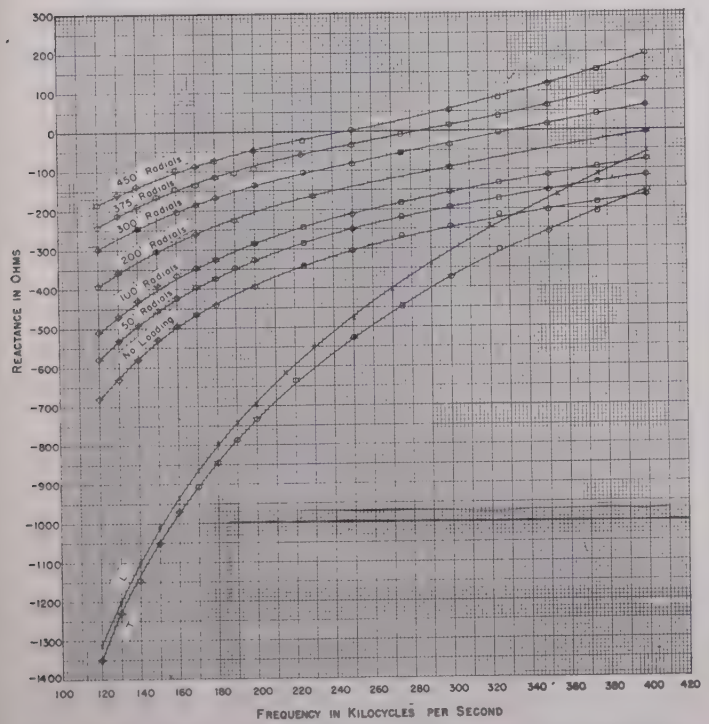

Fig. 9—Reactance curves of inverted-L- and T-type antennas compared with umbrella-type loading with eight radial wires of various lengths, as indicated.

Fig. 10 gives the calculated percentage of antenna input power P_A lost in the insulator-dielectric loss resistance R_{DL} as a function of the amount of loading at a number of frequencies and for a number of assumed values of leakage resistance for the measured tower. The diagrams in this figure demonstrate the importance of having insulators with low leakage resistance when using antennas with high base reactance and low radiation resistance.

The tower insulators consisted of six porcelain compression members and two bakelite strain members at

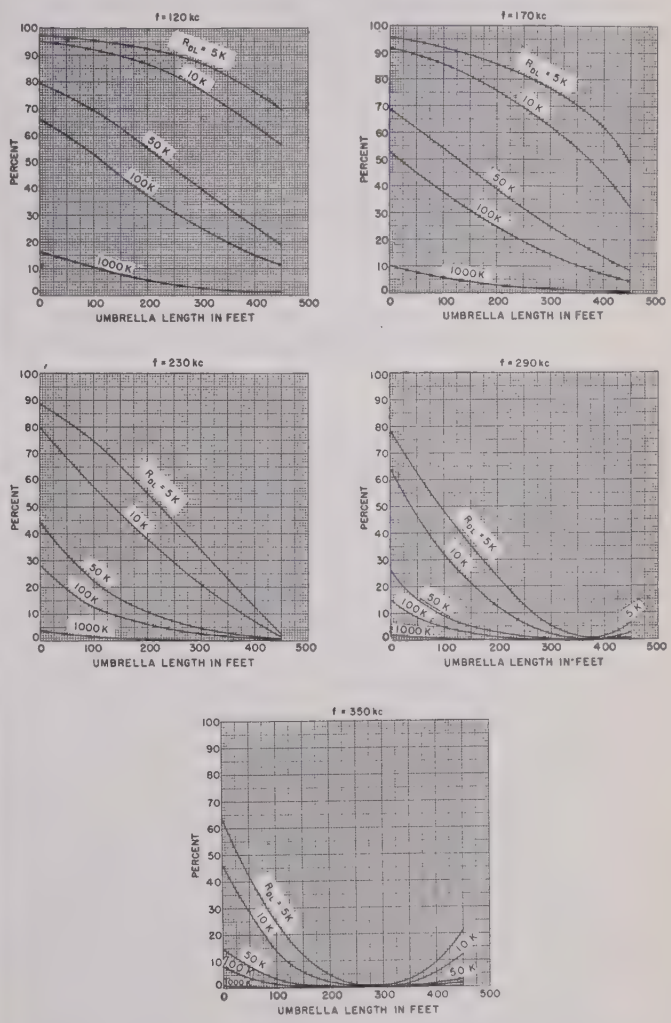

Fig. 10—Per cent antenna input power lost in base insulator versus length of eight umbrella wires for various values of insulator leakage resistance shunted across measured base impedance of antenna at low operating frequencies.

each of the four tower legs. The insulators were in need of maintenance since the surface of the bakelite strain members had become rough and dirty from exposure to the weather. Measurements were made of actual leakage resistance to determine the order of magnitude of insulator leakage resistance which may be encountered in practice with dirty insulators when adverse weather conditions exist.

Under particularly bad foggy or sleety weather conditions, the series base resistance at 170 kilocycles was measured to be 12.8 ohms; whereas the measured value under dry conditions was only 2.8 ohms. The measured

reactance was 391 ohms and was not appreciably different than under dry conditions. This increase in base resistance represents an equivalent insulator leakage resistance R_{DL} of approximately 15,000 ohms, as determined by solving for R_{DL} in (10). The fact that the insulator leakage was responsible for this effect was definitely ascertained by throwing a pitcher of water on one of the base insulators and observing the measured base resistance increase from 2.6 to 7.6 ohms at 130 kilocycles. This represents an insulator loss resistance of approximately 200,000 ohms. Insulator leakage losses can be kept at a minimum by the selection of proper insulators and regular maintenance. In this connection, the use of heated insulators having water shields and surfaces which tend to prevent the formation of water films may prove beneficial.

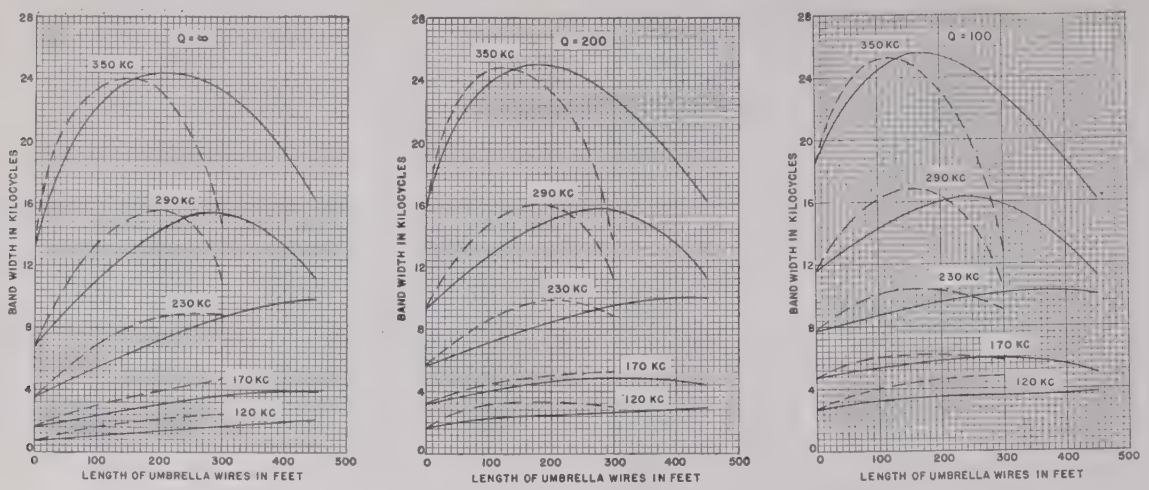

Fig. 11—Bandwidth in kilocycles for a 300-foot self-supporting tower, top-loaded with eight umbrella wires, as a function of length of umbrella wires for five frequencies, with loading coils having Q's of ∞, 200, and 100. (— — — with skirt, ——— without skirt.)

At standard broadcast frequencies, where the base resistance of this tower is comparatively high and the reactance low, the dielectric losses in the insulator are so small that they are of no practical importance.

The effective bandwidth has been calculated for each condition of umbrella loading. Since the Q of the antenna-loading coil will alter the results, the calculations have been made for coils having a Q of ∞, 200, and 100. A plot of bandwidth versus length of umbrella wires for frequencies of 120, 170, 230, 290, and 350 kilocycles is shown in Fig. 11. From these curves it can be seen that, for maximum bandwidth, the optimum length of umbrella wires is dependent upon both the frequency involved and the Q of the loading coil.

The field-intensity measurements have been analyzed and the radiation resistance calculated for the above five frequencies. A plot of the resistance versus length of umbrella wires for each of these frequencies is shown in Fig. 12. It is interesting to note that the degree of top loading which produces maximum radiation resistance is essentially independent of frequency.

The radiation resistance of a thin, vertical wire top-loaded with a nonradiating capacitive hat has been calculated for a number of conditions as shown in Fig. 13. The formula for these calculations is given in the figure. These curves have been prepared to show the correlation with the experimental results plotted in Figs. 6 and 7. It will be noted that for the unloaded tower the radiation resistance curve is approximately a squared

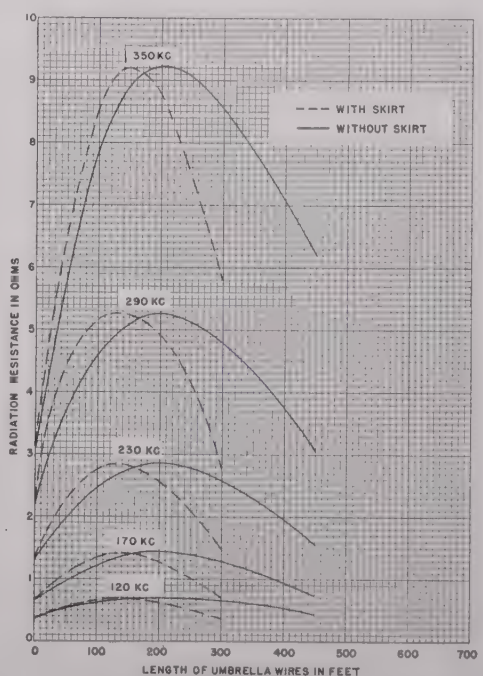

Fig. 12—Radiation resistance for various conditions of umbrella top loading.

function up to 45 degrees. As the degree of top loading is increased, the radiation resistance increases at an exponential rate greater than the squared power.

The unattenuated field intensity at one mile has been determined for each condition of top loading for the frequencies 120, 170, 230, 290, and 350 kilocycles. A

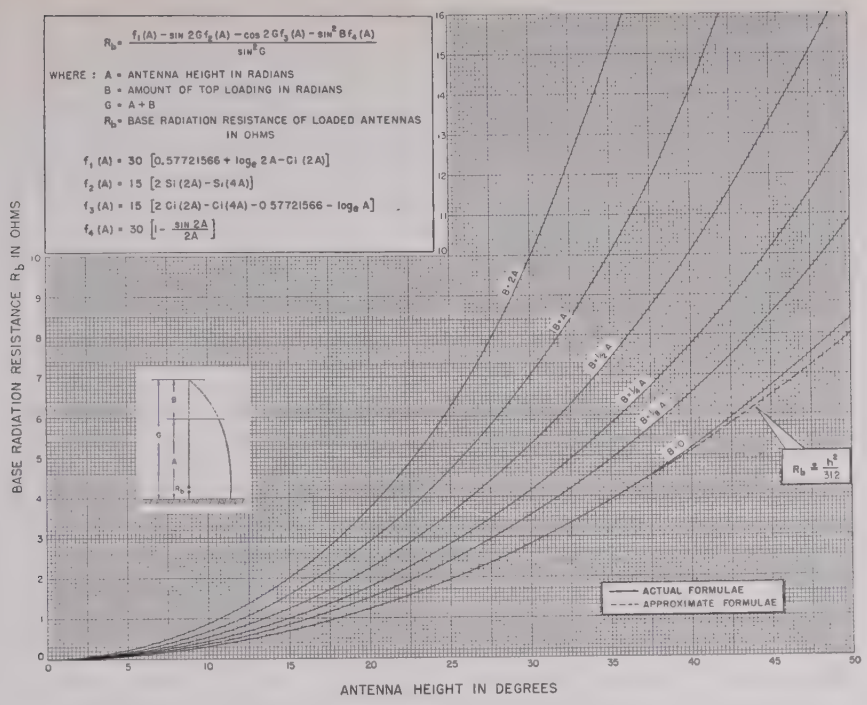

Fig. 13—Theoretical radiation resistance for various degrees of top loading.

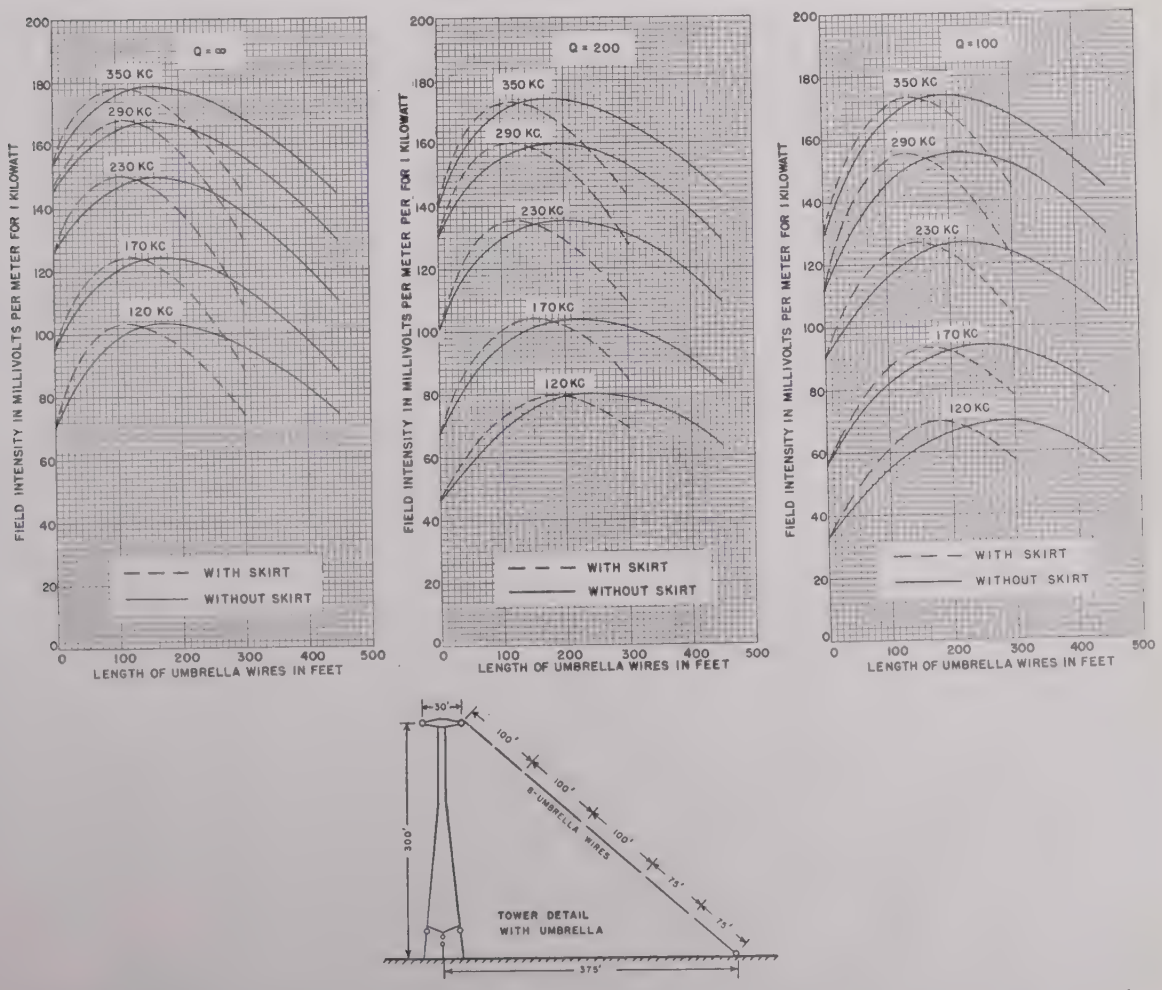

Fig. 14—Unattenuated field intensity at 1 mile radiated in millivolts per meter for 1.0 kilowatt from a 300-foot self-supporting tower, employing umbrella-type loading, as a function of length of eight umbrella wires for five frequencies with loading coils having a Q of ∞, 200, and 100.

plot of the unattenuated field as a function of length of umbrella wires for loading coils having Q's of ∞, 200, and 100 is shown in Fig. 14. In viewing these curves, it is necessary to keep in mind that the ground system as well as the antenna increases in electrical length with increasing frequency.

The amount of gain to be realized from top loading of a short antenna is dependent upon the losses in the system. If there are no losses in the system, the gain in field intensity is negligible. However, with optimum top loading at 120 kilocycles, the experimental results indicate that, when using a loading coil having a Q of 100, a gain of 6.5 decibels, which is equivalent to a power increase of 4.5, is realized. On 350 kilocycles, using a coil having the same Q, the gain is 2.6 decibels, or a power increase of 1.8.

The results indicate that substantial gains in power radiated and bandwidth acceptance can be realized with umbrella-type loading on short towers. It is an easy and inexpensive way to buy power and improve performance. The placing of a wire skirt around the outer end of the umbrella wires shortens the radial length of the umbrella wires required to produce a particular result, as shown in Figs. 11, 12, and 14. Where high powers are involved, a wire skirt is a useful method of reducing corona losses. Another method of accomplishing substantially the same results would be to increase the number of umbrella wires. Also, if the size of the umbrella wires is increased, the corona loss will be further decreased. The formation of wire cages is a common method of increasing the effective size of conductors. The construction and maintenance of an umbrella with a wire skirt is more difficult than increasing the number or size of umbrella wires.

6. *Top Loading by Means of Inverted-L- and T-Type Antennas*

Inverted-L- and T-type antennas were erected between two 300-foot towers spaced 410 feet apart. The height of the vertical lead of the inverted-L-type antenna was 290 feet and the T-type was 280 feet. The length of the flat-top in each case was 350 feet. Resistance, reactance, and field-intensity measurements were made for both types of antennas. A plot of the resistance and reactance measurements is shown in Fig. 15. At the lower frequencies, where loading afforded by

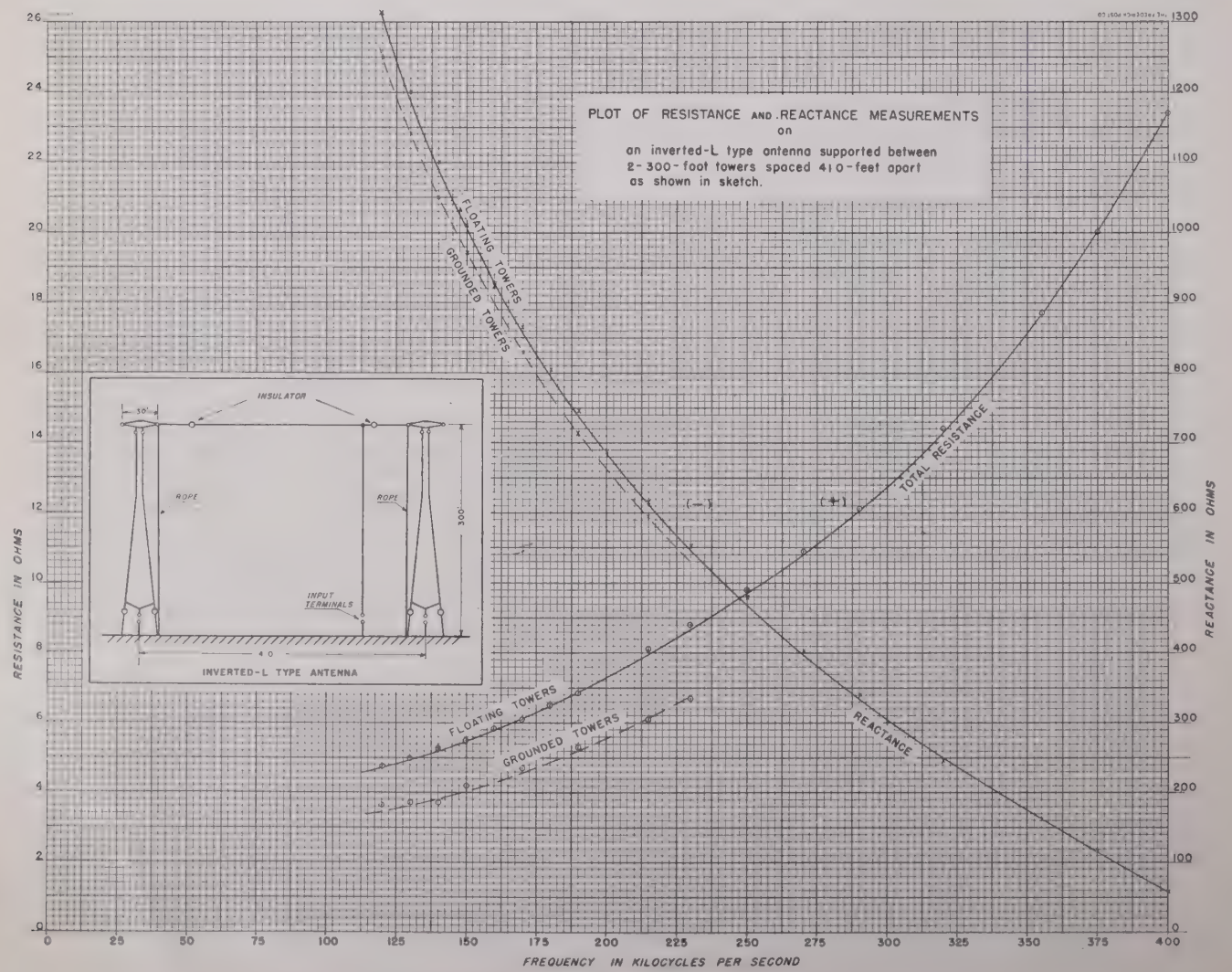

Fig. 15(a)—Plot of resistance and reactance measurements for an inverted-L- type antenna.

the 350-foot flat-top is inadequate, the reactance component of both the inverted-L- and the T-type antennas is appreciably higher than that offered by umbrella-type loading. This is as expected, since the characteristic impedance of a thin wire is much higher than of a tower having considerable cross section. Where wide-band transmission is of importance, the cross section of the antenna should be as large as practical. The bandwidth of both the inverted-L- and T-type antennas have been plotted as a function of frequency in Fig. 16.

The field-intensity measurements indicate that, over the frequency range considered, the unattenuated field for both the inverted-L- and T-type antennas were inferior to the optimum afforded by umbrella-type loading as shown in Table I. Had a larger flat-top been used, the efficiencies of the various types of loading would probably be about the same. However, the bandwidth afforded by umbrella-type loading will be superior unless cages having dimensions comparable to a tower are used. Both the inverted-L- and T-type antennas require the installation of two towers. In addition to the extra cost involved, there are certain other disadvantages of requiring two towers. As pointed out early in this paper, it is important to have an area of good conductivity immediately surrounding the antenna. In certain instances, it might be possible to erect a single tower where an effective salt-water ground would prevail but, due to physical limitations, it might not be feasible to install a second tower with the required separation. In the case of the inverted-L-type antenna, there is also the problem of radiation from the flat-top. When the length of the flat-top is less than the height of vertical lead and the combined electrical length is less than 90 degrees, the radiation from the flat-top will be a small percentage of the total power radiated.

TABLE I

FIELD INTENSITY AT ONE MILE FOR 1.0 KILOWATT ON 170 KILOCYCLES FOR LOADING COILS HAVING Q'S AS INDICATED

Type of Antenna	$Q=\infty$	$Q=200$	$Q=100$
Inverted L	103	78.5	66
T	115	76.6	61.4
Tower with no loading	94	67	56
Tower with optimum umbrella loading	125	104	92

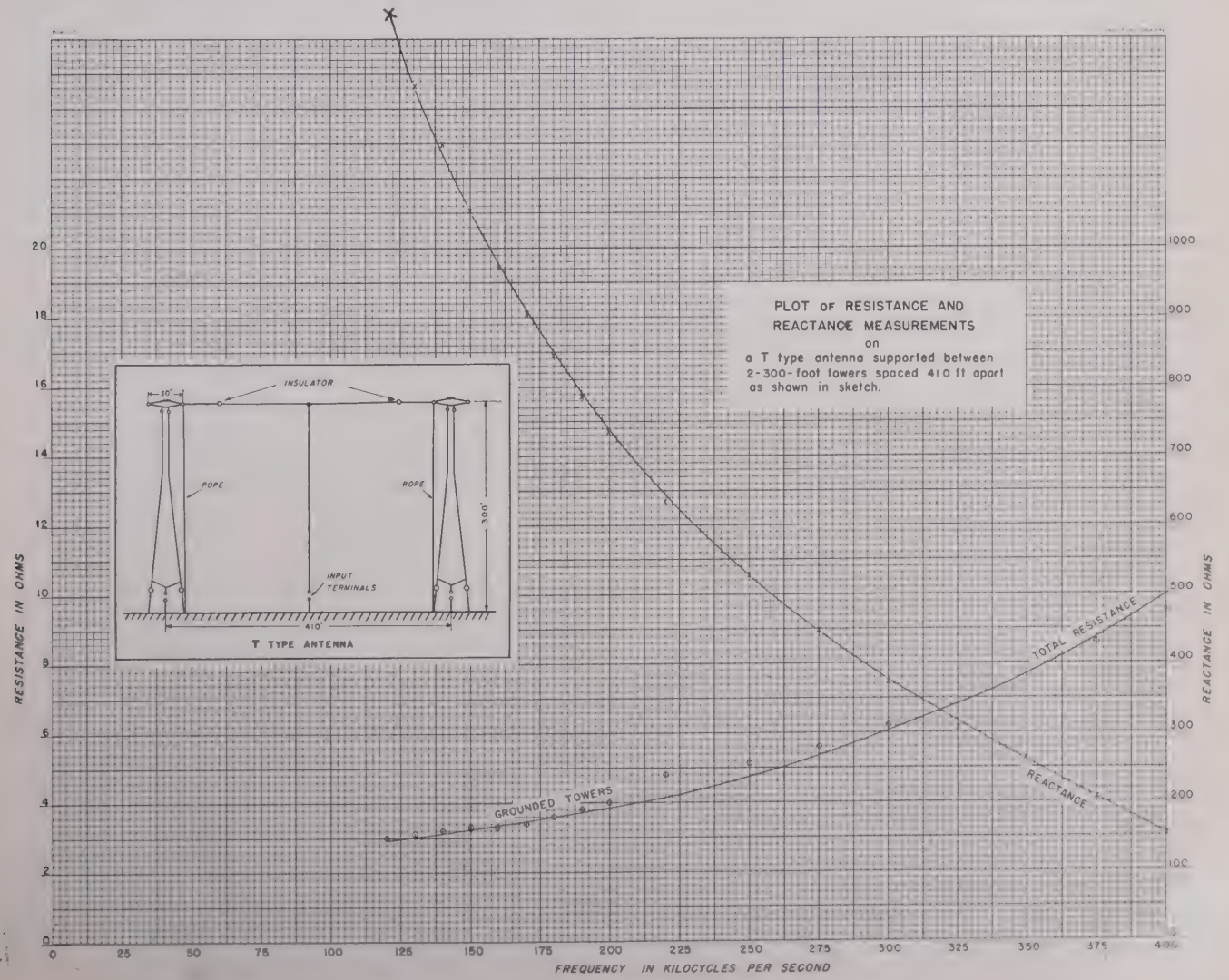

Fig. 15(b)—Plot of resistance and reactance measurements for a T-type antenna.

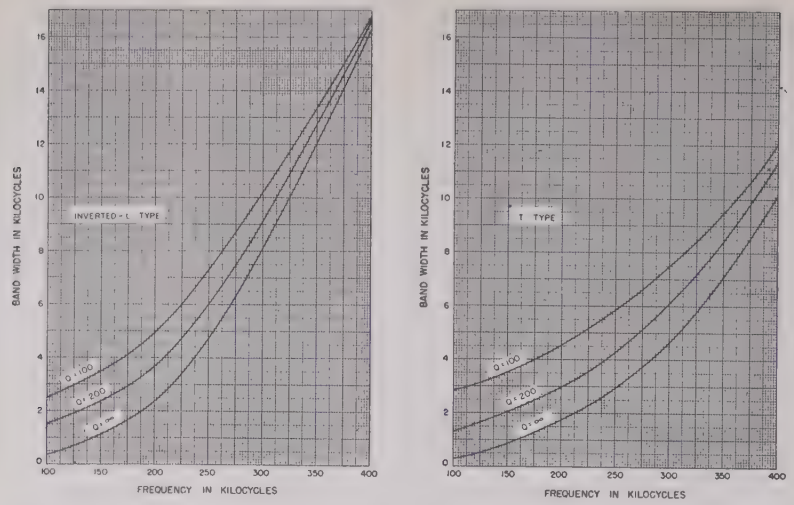

Fig. 16—Bandwidth for various conditions of inverted-L- and T-type antennas.

7. *Top Leading With Capacitive Hat and Coil*

To increase the degree of loading afforded by the 30-foot diameter hat, a coil was connected between the capacitive hat and top of the tower. This coil had a Q of approximately 100 and an inductance range up to 1.9 millihenries. The amount of coil inserted was varied by means of a slider connection. Resistance, reactance, and field-intensity measurements were made at 170 kilocycles for each condition of loading. A plot of the measured base resistance and reactance and the radiation resistance at 170 kilocycles as a function of the amount of reactance in the coil is shown in Fig. 17; the unattenuated field at one mile has been plotted against the reactance of the top-loading coil in Fig. 17. It is seen that an increase in power radiated is obtained by inserting a small portion of the coil. However, on increasing the amount of coil, the antenna efficiency is reduced. Above a certain quantity of coil the reflected loss resistance more than offsets the gain made by increasing radiation resistance. Unless a coil having a Q considerably greater than 100 is used, the results obtained do not appear to justify such an installation. Similar measurements were made for the coil between the tower and the 100-foot umbrella wires connected with a wire skirt. A plot of these measurements is also shown in Fig. 17.

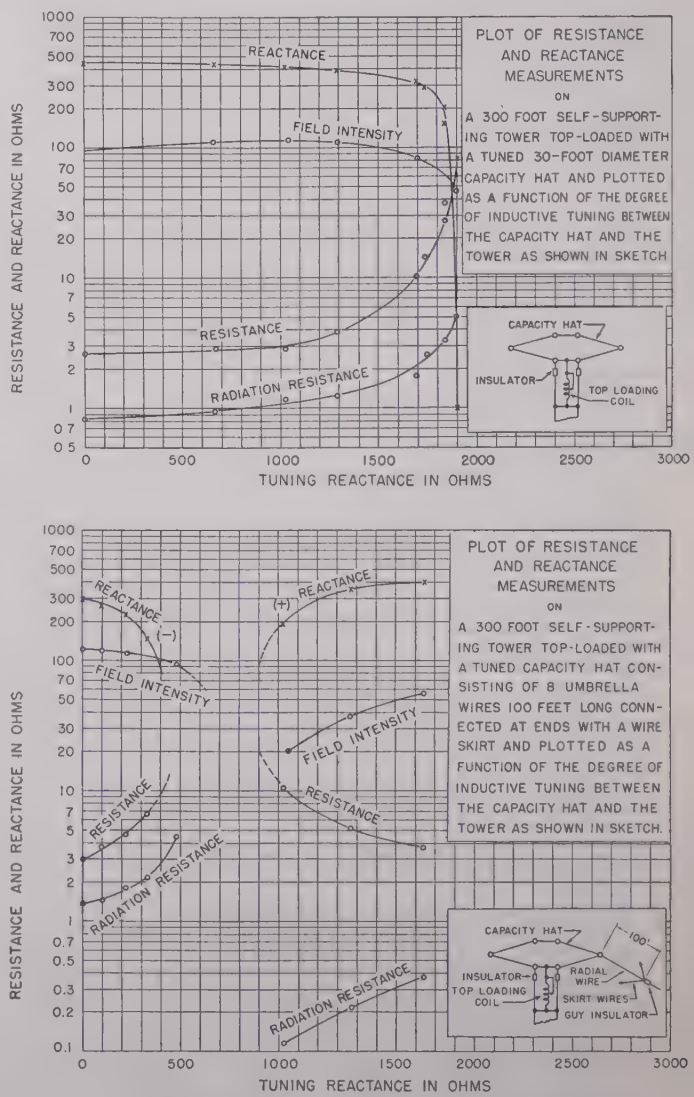

Fig. 17—Plot of resistance, reactance, and field intensity for various degrees of tuning a top-loaded tower.

IV. Acknowledgments

The authors wish to acknowledge the assistance given by Anthony Carnavale and Eugene Smith, both of the Camp Coles Signal Laboratory, Red Bank, N. J., for their part in collecting the field data; and to Ross Bateman and Jack W. Herbstreit, both of the Radio Propagation Section, Communication Liaison Branch, Plans and Operation Division, Office of the Chief Signal Officer, for their part in the calculation of theoretical curves presented in Figs. 10 and 13. This work was carried out under W. L. Everitt, director Operational Staff, Office of the Chief Signal Officer, United States Army. Finally, the authors wish to thank H. K. Carpenter, executive vice president of the United Broadcasting Company, for making the facilities of station WHK available for this experimental project.

Time Modulation*

BRITTON CHANCE†, SENIOR MEMBER, I.R.E.

Summary—**The techniques of time modulation and demodulation have been extensively developed in the past five years for radar range-finding, pulse communication, and data transmission. This paper presents a brief review of the basic processes employed in time modulation and gives representative examples of practical circuits. In military applications considerable emphasis has been placed upon high precision, and many methods for achieving a linearity and stability of 1 part in 10^4 are available.**

THE PROBLEMS of radar range-finding have led to many extensions and improvements in the well-known physical techniques employed in the measurement of the velocity of light and the height of the ionosphere. Especially significant improvements have been made in methods for the variation of the time interval between two randomly recurring wave forms. Accurate control of this interval in response to signal information is the process of time modulation and is the subject of this paper. The generation of pairs of time-modulated pulses requires, in all cases, nonlinear circuit elements for achieving abrupt discontinuities in timing wave forms. Since such circuit elements often are used to select portions of a timing wave form, the operation is called amplitude selection. A related problem is that of marking the instant of equality of two voltages (one of which may be a timing wave) by a pulse. This process is termed amplitude comparison. Since these two processes are basic in time modulation and both depend upon the properties of nonlinear circuit elements, some of the idealized types will be presented.

Fig. 1 shows the well-known nonlinear characteristic of the ideal diode. This nonlinear characteristic, which is

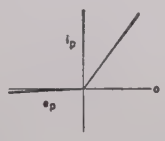

Fig. 1—The ideal broken-line characteristic of a diode.

exhibited at the cutoff point of many thermionic tubes and contact rectifiers, is termed a "broken-line" characteristic. Its use in the selection of the amplitudes of a wave which are less than or which exceed a given amplitude is well known as the process of separation or limiting, and a typical example is illustrated in Fig. 2. Diode V_1 is used to select the positive portions of sinusoidal wave (a) which exceed its cathode potential. A more general term for this process is, therefore, amplitude selection.

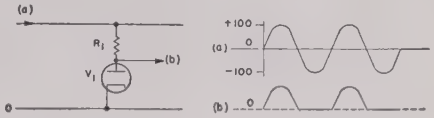

Fig. 2—A diode amplitude selector. Positive excursions of sinusoidal wave (a) exceeding the cathode potential of diode V_1 are selected as indicated in (b). Approximately ideal operation is obtained for input amplitudes of a few hundred volts.

A nonlinear characteristic which permits the selection of amplitudes lying between two bounds is illustrated in Fig. 3, and the characteristic obtained at the grid of

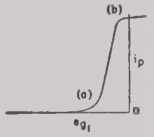

Fig. 3—The broken-line characteristic obtained at the grid of a triode or pentode. The characteristic is broken at two points: (a) near cutoff, and (b) near the grid-current point or, in the case of a pentode, near the "bottom" of the pentode characteristic.

a triode or pentode is often employed. The application of this circuit to selecting the portions of a sinusoidal wave lying between two limits is well known as clipping or squaring, and is represented in Fig. 4. The pentode is, of course, more useful for this purpose, since the upper

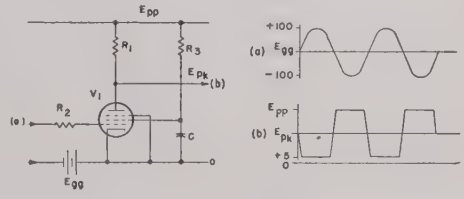

Fig. 4—A pentode circuit for amplitude selection between two limits: cutoff, and bottoming. The sinusoidal wave form (a) is selected between these limits as indicated in (b); the excursions of the plate extend from the supply voltage to a few volts positive with respect to the cathode. Screen resistor R_3 is necessary to avoid excessive current when the plate "bottoms."

limit is not necessarily set by grid current but may be set by "bottoming" of the plate. The selection of portions of sinusoidal wave (a) between two limits is indicated in (b).

This characteristic may be obtained with a pair of diodes as in Fig. 5 and has the advantage that the break in the characteristic is more abrupt than that of Fig. 3, and furthermore the characteristic may be symmetrical about the point *O-O*, as shown in Fig. 6. The selection of portions of irregular wave (a) lying between the limits E_1 and E_2 is shown in (b) of Fig. 5.

* Decimal classification: R148.6. Original manuscript received by the Institute, July 17, 1946; revised manuscript received, November 12, 1946. This paper is based on work done for the Office of Scientific Research and Development under Contract No. OEMsr-262 with the Massachusetts Institute of Technology.

† Formerly, Massachusetts Institute of Technology, Cambridge, Mass.; now, Medicinska Nobelinstitutet, Biokemiska Avdelningen, Hantverkaregatan 3, Stockholm, Sweden.

The cutoff point of triodes and pentodes is poorly defined, and variations of $\pm\frac{1}{4}$ volt with time may be expected. Variations in excess of $\frac{1}{4}$ volt may be expected on changing tubes. In addition, the cutoff point depends upon the cathode temperature. For these reasons the broken-line characteristic exhibited at the grid

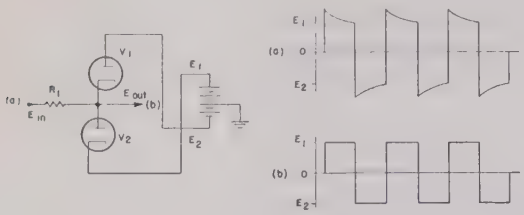

Fig. 5—A double-diode amplitude selector. Portions of wave (a) are selected between the limits $+E_1$ and $-E_2$, giving rectangular wave (b).

of a vacuum tube is rarely used where high stability is required. The reproducibility and stability observed at the plate of a diode is considerably better, and drifts of contact potential may be held to considerably less than a few tenths of a volt, providing the heater voltage is stabilized. The symmetrical characteristics have a major advantage in this respect, since variations in con-

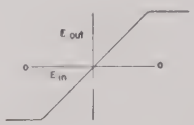

Fig. 6—The symmetrical broken-line characteristic, passing through the point *O-O*.

tact potential are partially compensated. The germanium crystal appears to be extremely promising for precision applications, and preliminary experiments indicate that it may be at least an order of magnitude more stable than the thermionic diode.

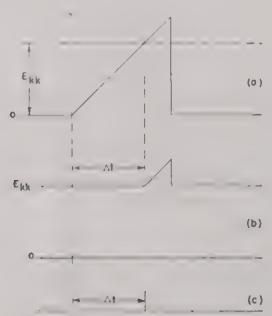

Fig. 7—Amplitude selection of a portion of a triangular wave form. The portion of triangular wave (a) is delayed by an interval Δt as indicated in (b). Further amplification and differentiation convert (b) to a sharp pulse (c).

The amplitude selection of a portion of a triangular wave form is one of the basic processes in electrical time measurement. If, for example, the triangular wave of Fig. 7(a) is applied to the diode amplitude selector V_1 of Fig. 8, in which the cathode potential E_{kk} is biased positively with respect to ground, a time delay Δt between the initiation of the triangular wave and the selection of portion (b) of Fig. 7 will be defined. Furthermore, for an accurately linear rise of triangular wave (a) and an abrupt discontinuity of the broken-line characteristic,

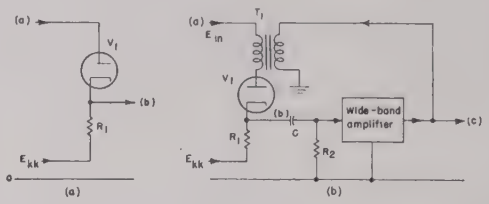

Fig. 8—Diode amplitude selector and comparator. Fig. 8(a) shows a diode amplitude selector with a variable reference potential E_{kk}, for obtaining a time-modulated pulse. Fig. 8(b) shows an amplitude comparator depending upon a wide-band regenerative amplifier. The output of diode amplitude selector V_1 is amplified and fed back regeneratively by means of pulse-differentiating transformer T_1, which gives a hysteresis or backlash characteristic.

the time delay Δt will be linearly related to the control voltage E_{kk}. The slope discontinuity of the selected portion of the triangular wave is seldom abrupt enough for accurate time measurements, and the wave is therefore converted into a pulse or step by wide-band regenerative or nonregenerative amplification, as shown in Fig. 7(c). A generalized circuit for obtaining such a pulse is indicated in Fig. 8(b), where the output of a wide-band amplifier is coupled back to the plate of V_1 in a regenerative fashion. Since transformer T_1 is usually a "differentiating transformer," it may determine the duration of the pulse of Fig. 7(c).

The over-all characteristic of the circuit of Fig. 8(b) for a time short compared to the time constant of T_1 is indicated in Fig. 9. The output voltage is zero until amplitude selection occurs in V_1 and the loop gain of the feed-back amplifier exceeds unity. At this time regeneration occurs, and rapid transition to a new state is indicated. The break in the characteristic is much more abrupt than that obtainable without amplification. On the other hand, the positive feedback leads to a backlash or hysteresis effect, and the characteristic often takes these names.

Fig. 9—The hysteresis or backlash characteristic. An abrupt change of the output level occurs when the input voltage exceeds the cathode potential of the diode amplitude selector.

A large number of circuits have this characteristic, and they may be called "flop-over," "flip-flop," "pick-off," or "trigger" circuits. But it is proposed here to define the process as that of indicating the moment of equality of two wave forms, and to name the circuit components accomplishing this function "amplitude comparators" regardless of the means by which the

abrupt discontinuity of characteristic is obtained. The methods for obtaining these discontinuities range from blocking-oscillator circuits to wide-band nonregenerative amplifiers. But the latter type of circuit is relatively

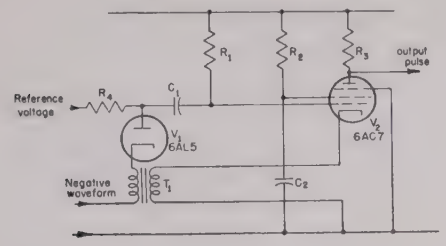

Fig. 10—An amplitude comparator for a negative-going wave. T_1 is a pulse-differentiating transformer.

inefficient compared to some regenerative amplifiers.

A practical circuit for indicating the instant of equality of a negative-going triangular wave and a reference voltage is indicated in Fig. 10. Cathode voltages rate at which V_2 cuts off. For wave forms of several hundred volts amplitude, the instant of equality of the wave form and the reference voltage is indicated with a short-time stability exceeding 0.1 per cent. The practice of using the diode characteristic of V_1 for amplitude selection in place of the grid characteristic of V_2 is well-

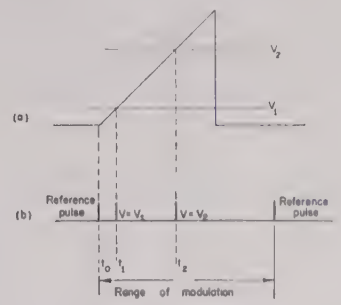

Fig. 11—Electrical time modulation of the spacing between the reference pulse and the pulses occurring at t_1 and t_2 in accordance with the variation of the reference voltage of an amplitude comparator from V_1 to V_2.

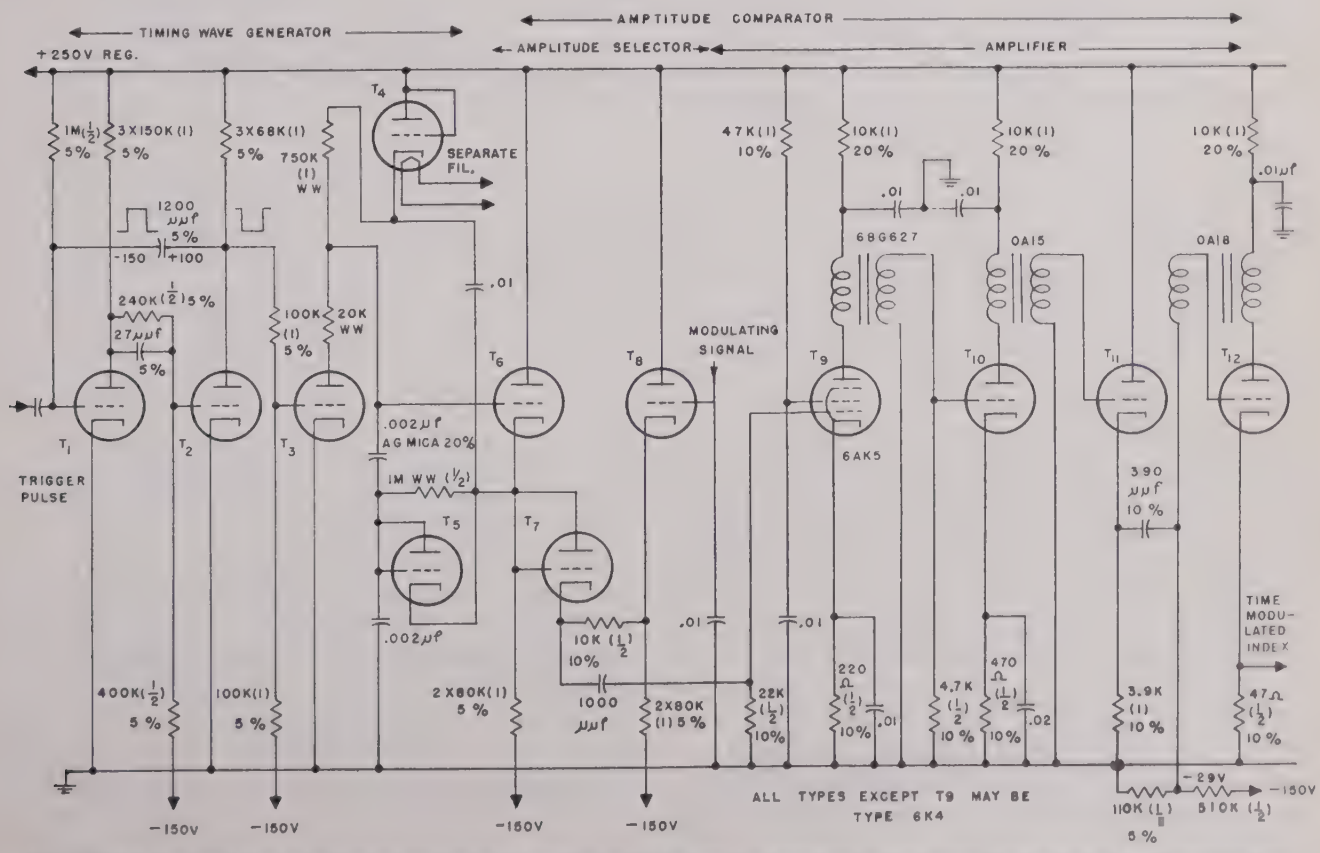

Fig. 12—An accurate time modulator employing a positive-going triangular wave and a diode amplitude selector and regenerative amplifier for amplitude comparison. For the particular constants indicated, this circuit covers a range of 250 microseconds with a linearity of better than 0.1 per cent.

of V_1 less than the reference voltage will cause conduction of the diode and cutoff of the normally conducting amplifier V_2. The transformer windings of T_1 are arranged so that a fall of the cathode potential of V_2 causes a fall of the cathode potential of V_1 and increases the established in these circuit techniques. This circuit[1] is called the "Multiar."

[1] F. C. Williams and F. J. U. Ritson, "Automatic strobes and recurrence frequency selectors," presented, Institute Electrical Engineers Convention, London, England, March, 1946.

A variation of the reference voltage of the amplitude comparators of Fig. 8(b) and Fig. 10 gives a linear variation of the time delay between the initiation of the triangular wave form of Fig. 11(a) and the output pulse of Fig. 11(b). This variation of the interval between two pulses or between two portions of a rectangular wave form is termed *time modulation*, and the earlier pulse is called the "reference pulse." Since triangular wave forms of extremely high linearity (1 part in several thousand) may be generated with relatively simple circuits, an over-all linearity of modulation of this order of magnitude is readily obtained from an accurate amplitude comparator.

Repetition of the timing wave form at a rapid rate compared to signal variations gives a time-modulated carrier useful for precise data transmission or high-fidelity communication. The range or percentage modulation is usually limited between 75 and 90 per cent of the repetition interval, owing to the recovery time of the wave-form generator and associated circuits.

Fig. 12 represents a circuit for an accurate time modulator which has been used for range measurements in conjunction with methods presented in a companion paper.[2] T_1, T_2, and T_3 form a negative rectangular switching impulse which initiates the operation of a linear sawtooth generator consisting of T_4, T_5, and T_6. The amplitude comparator consists of diode amplitude selector T_7 and a wide-band amplifier, T_9, T_{10}, T_{11}, and T_{12}. The linearity of this sawtooth is 1/10 per cent or better and it has an amplitude of roughly 150 volts. Its slope is, of course, determined by the 1-megohm wire-wound resistor and the 0.002-microfarad mica capacitors. Complete details of this type of sawtooth generator will be found elsewhere.[3]

The sawtooth is connected to the plate of a diode amplitude selector T_7 whose cathode potential is set by means of the grid voltage of the cathode follower T_8. The selected portion of the sawtooth instantly initiates the operation amplifier T_9, T_{10}, T_{11}, and T_{12}, giving an index which marks the time of equality of the modulating signal and the triangular wave form. The duration of the output pulse is 0.2 microsecond and its rise time is between 0.02 and 0.05 microsecond. The over-all linearity of a system of this type is as good as the linearity of the timing wave form, which is 0.1 per cent, and the stability, in spite of moderate variations of temperature, time, and voltage, is 0.2 per cent. This particular circuit has a full range of modulation of 250 microseconds.

This circuit is designed for the solder-in vacuum tube, type 6K4. The whole unit is calibrated for the particular vacuum tubes with which it has been built, and upon failure of a vacuum tube, the complete unit which is replaced will, of course, have already been calibrated for its particular vacuum tubes. Unless this procedure is employed, variations on changing vacuum tubes may run as high as 0.4 per cent full scale.

A much simpler but considerably less accurate method of electrical time modulation depends upon a cathode-coupled multivibrator,[4] shown in Fig. 13. In this multivibrator, V_{1b} is normally conducting, and operation is initiated by a positive pulse applied to the grid of V_{1a}, which cuts off V_{1b} and generates a triangular wave form at its grid. The operation of the circuit is now identical with Fig. 11, since the time at which V_{1b} recovers depends upon its cathode potential, which is set by E_1. Thus a variation of E_1 produces waves of variable duration at the plate of V_{1b}. Differentiation of this rectangular wave form will give an output corresponding to that obtained in Fig. 11. Since only a small sawtooth is generated

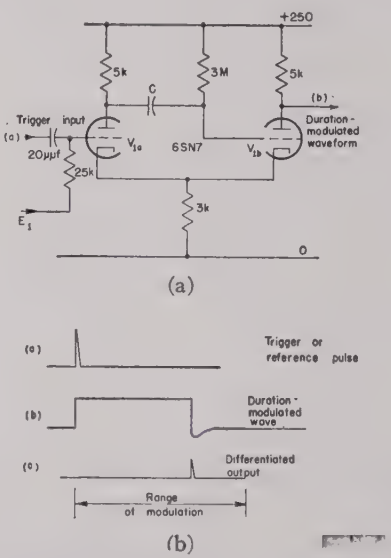

Fig. 13—A multivibrator for producing a time-modulated rectangular wave. A time-modulated pulse is readily obtained by differentiation and amplitude selection.

(20 to 30 volts) and amplitude selection occurs at the grid of a triode, the stability of this circuit is but 1 or 2 per cent. Its linearity is, however, considerably better than this.

The use of time modulation for obtaining phase modulation was recently pointed out.[5] The reverse process is a well-known radar technique, as the next section indicates.

Time Modulation Through Phase Modulation

Time modulation in response to mechanical signals can be obtained in the previous case by controlling the

[2] Britton Chance, "Time demodulation," Proc. I.R.E., vol. 35, pp. 1045–1049: this issue.

[3] Radiation Laboratory Series, "Waveforms," McGraw-Hill Book Co., New York, N. Y., 1947; vol. 19, chap. 7.

[4] See chapter 13 of footnote reference 3.

[5] J. F. Gordon, "A new angular-velocity-modulation system employing pulse techniques," Proc. I.R.E., vol. 34, pp. 328–335; June, 1946.

reference potential of the amplitude computer by means of a linear potentiometer. There are a number of very useful devices for time modulation which can only be controlled mechanically.

The first of these devices depends upon phase modulation of sinusoidal or other wave forms. A number of phase shifters have been used; for example, the two-phase to one-phase synchro supplied with sinusoidal currents in quadrature gives a voltage which shifts phase continuously in accordance with the mechanical signal, as indicated in Fig. 14. Similarly, a capacitance phase shifter supplied with three-phase voltages will give continuous phase shift, as indicated in Fig. 15. An extremely useful and versatile phase shifter is the circu-

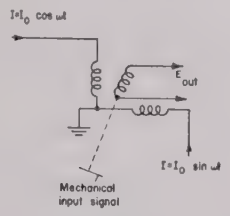

Fig. 14—A synchro used for continuous phase modulation. An accuracy of somewhat better than ½ degree is obtained with Bendix autosyns.

lar sweep or type-J cathode-ray-tube display. It is useful for manual measurements when the signal is applied as a radial deflection by means of a center electrode (type 3DP1). In all these devices linearities of

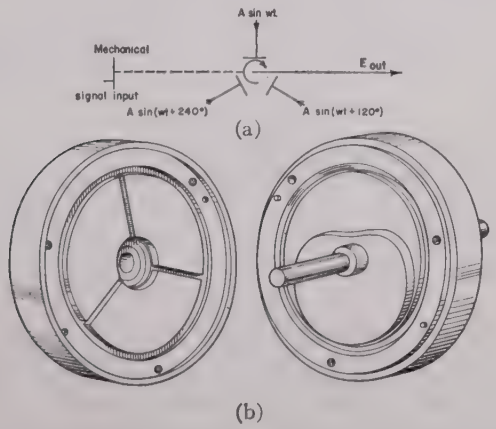

Fig. 15—A three-phase variable capacitor used in phase modulation. An accuracy of approximately 1 degree is obtainable.

approximately 1 degree (0.3 per cent) are obtainable[4] as compared to 0.1 per cent for the electrical time modulators. Since phase-shift methods are less linear, more complicated, and unsuitable for direct electrical control, they are rarely used as a single-scale time-measuring device. Their use is restricted to an important class of time modulators employing multiple scales for extremely high precision, and these are discussed later.

The generation of a time-modulated pulse from the output of the phase shifters of Figs. 14 and 15 is carried out by an amplitude comparator using a fixed reference voltage, as shown in Fig. 16. A time-modulated pulse is

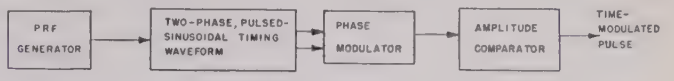

Fig. 16—Block diagram of the use of a phase shifter in time modulation.

readily obtained from a circular trace on a cathode-ray tube by a photocell pick-off (type 931).

Devices Depending Upon Wave-Propagation Velocity

A second class of electromechanical time modulators depends upon the velocity of propagation of electric or

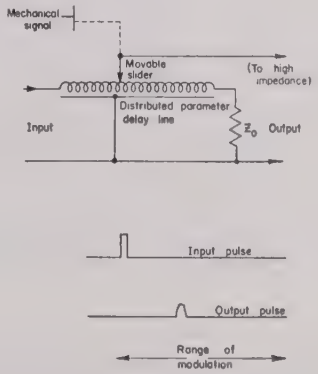

Fig. 17—Electromechanical time modulation obtained from an electrical delay line.

acoustic waves through various media. The simplest type is shown in Fig. 17. A pulse is applied to the input terminals of a distributed-parameter delay line. A high-impedance probe moved in accordance with a mechanical signal determines the delay of the output pulse with respect to the input pulse.

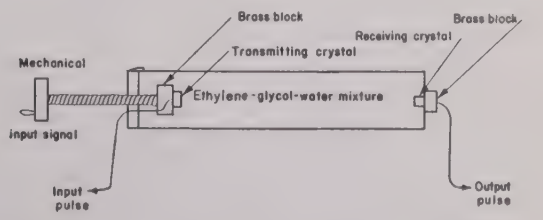

Fig. 18—Electromechanical time modulation obtained from a supersonic delay tank.

Similar devices depend upon the propagation velocity of supersonic waves through liquids. In Fig. 18 a supersonic transmitter mounted on a lead screw is movable

with respect to a receiver to vary the time delay of the output pulse with respect to the input. Extremely high accuracy may be obtained with this system. For example, in a tank 30 inches long an accuracy of one part in 8000 is achieved.[6] Much longer delays and higher precision are obtained in more recent supersonic delay lines.[7]

The most common and the most accurate method of time modulation employs the propagation velocity of a radio wave as in a radar system, as shown in Fig. 19. In this case, the mechanical movement of a reflector with respect to the transmitter varies the duration of the interval between the transmitted and received pulse. The accurate demodulation of this information is presented in a companion paper.[2]

Fig. 19—Time or range modulation obtained in a radar system.

Multiple-Scale Systems

Accurate subdivision of the range of modulation is accomplished by a train of fixed pulses synchronized with the pulse-repetition frequency of the time-modulation system. These pulses, derived from a continuous crystal or pulsed inductance-capacitance oscillator, are of more than adequate accuracy for most requirements.

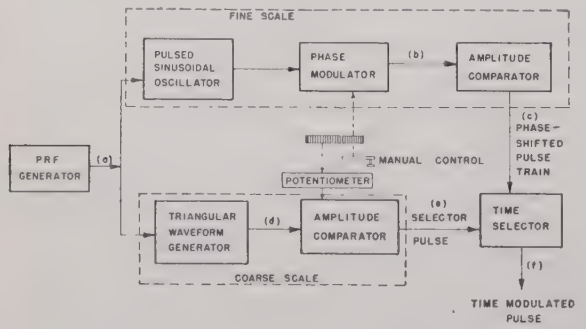

Fig. 20—Block diagram of a double-scale time-modulation system. The over-all accuracy is roughly the product of that of the coarse and fine scales. The two scales are geared together at an appropriate ratio so that a single control of the time-modulated pulse is obtained over the full range of modulation.

The over-all accuracy is therefore increased by the number of subdivisions employed, as any one of the circuits described above may be used to interpolate between any desired pair of fixed pulses. But a more advantageous method depends upon continuous phase modulation of the sinusoidal timing wave, as is shown in Fig. 20. A train of pulses generated as already indicated in Fig. 16 may be phase-shifted over the full range of modulation, as shown in Fig. 21. A particular member of the pulse train is selected by a coarse time-modulation system covering the entire range. This is preferably of the type shown in Fig. 12, and the scale factors are adjusted so that the rate of the selector pulse from the coarse scale is approximately equal to that of the fine scale. The selected pulse is then continuously variable over the whole range in response to a single control. The circuit has a theoretical accuracy equal to the product of that of the coarse and fine scales (one part in 360,000), but accuracies of one part in 50,000 are achieved in practice.[8]

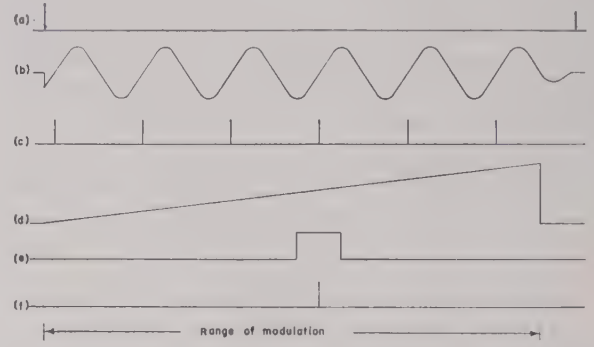

Fig. 21—Wave-form diagram of the double-scale time-modulation system. The pulses at the recurrence frequency are shown in (a), the phase-shifted sinusoid in (b), and the phase-shifted pulse train in (c), (d) shows the triangular timing wave form, (e) the selector pulse, and (f) the selected member of the phase-shifted pulse train. The rate of travel of (c) and (e) are equalized by the gear ratio and the scale factors of the coarse scale.

No multiple-scale systems are suitable for a control by a single electrical modulating signal, but this rarely causes difficulties as the information usually demodulated is slowly varying as, for example, in the case of a radar echo.

Acknowledgment

Since range-measuring circuits are a component of all radar systems, the methods of accurate time modulation were developed at many different laboratories in this country and in the British Commonwealth. It is therefore impossible to give special credit to single individuals or institutions, and grateful thanks are given to all those who have contributed to this material. A most beneficial and fruitful aspect of this collaborative effort was the freedom of exchange of information that scientists and engineers enjoyed during the war.

[6] A Bell Telephone Laboratories development for the Model SJ radar.

[7] Radiation Laboratory Series, "Electrical Time Measurements," McGraw-Hill Book Co., New York, N. Y., 1947; vol. 20, chap. 12.

[8] See chapters 3 and 6 of footnote referenec 7.

Time Demodulation*

BRITTON CHANCE†, SENIOR MEMBER, I.R.E.

Summary—**The demodulation of the signals imparted to carriers by the process of time modulation is an essential process of radar range finding, pulse data transmission, and communication. This paper describes methods for precision demodulation which depend upon a time modulator operating in synchronism with the input information, a time-discrimination element, and negative feed-back connections to control the local time modulator to reproduce the modulating signal in an electrical or mechanical form. Accuracies are usually set by the bandwidth of the radio link and may be 5 parts in 10^4 or better.**

Introduction

IN A COMPANION paper,[1] the principles and methods of time modulation have been discussed. The companion process, time demodulation, defined as the process by which information is obtained from a time-modulated wave about the signal imparted in modulation, is described here.

The greater accuracy requirements of radar range-finding have led to relatively restricted use of the demodulation methods commonly used in amplitude- or frequency-modulation systems. Direct demodulation of signals is rarely employed and negative-feedback methods have been developed to a high degree of accuracy. Usually time-modulated information is transmitted by variations in the interval between two pulses; the first termed the reference pulse, and the second, the time-modulated pulse. Radar information is, of course, of this form, where the interval between the transmitted and received pulses bears information on the target distance. These circuits are used for automatic time

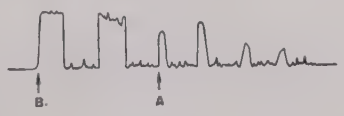

Fig. 1—Radar video signals, containing time-modulated pulse *A* due to target motion. Pulse *B* is the transmitted or reference pulse.

demodulation or range tracking to obtain accurate and continuous information for navigation, bombing, and fire control. In such cases the range of modulation corresponding to the maximum target distance is many times the pulse duration (~1000 times), and special methods responsive to only one echo and accurate over the whole range must be employed. In addition, interference and noise are serious, and the repetition interval of the carrier is usually variable. A typical input signal is indicated in Fig. 1 and is representative of signals received in radar range-finding or pulse data-transmission systems, operating either at the limit of their range or in the presence of interference.

General Description of a Negative-Feedback Time Demodulator

Illustrated in Fig. 2 is a block diagram of a typical negative-feedback time demodulator. The time-modulated input signals are generated, for example, by the motion of a reflector in a radar system, or in response to signal inputs to a data-transmission system. Synchronism between this time modulator and the demodulator system is achieved by the time-reference pulse (*B*) which is readily available in radar systems and is transmitted along with the time-modulated signal in data-transmission and communication systems. This refer-

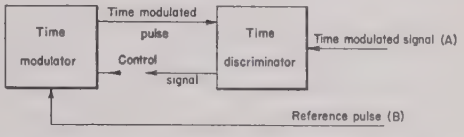

Fig. 2—A negative-feedback time demodulator. The error signal from the time discriminator may be used to control the time modulator automatically.

ence pulse initiates the operation of a local time modulator to which the input signals are to be compared. The output of the local time modulator and the time-modulated input signal are connected to a time-discriminating circuit, the output of which is a voltage indicating the sign and approximate magnitude of the time difference between the input pulses. This "error" signal may control the local time modulator directly or may operate a servomechanism if mechanical output is desired.

In communication or data-transmission systems the reference pulse *B* is obtained by pulse-recurrence-frequency selection, often involving control of a frequency-modulated oscillator by a time discriminator.

The precision of this process can be made extremely high, since it depends only upon the modulation characteristics of the local time modulator, and, as indicated in the previous paper,[1] this may be made 1 part in 1000 for single-scale systems or 1 part in 50,000 or better for multiple-scale systems.

One of the great advantages of the time-modulation–demodulation systems is the fact that amplitude distortions do not give rise to errors. However, adequate bandwidth is essential lest amplitude variations be converted into time variations in the receiver. It has been found desirable to employ rapidly acting automatic-gain-control circuits to minimize amplitude fluctuations.

* Decimal classification: R148.6. Original manuscript received by the Institute, July 17, 1946; revised manuscript received, November 12, 1946. This paper is based on work done for the Office of Scientific Research and Development under Contract OEMsr-262 with the Massachusetts Institute of Technology.

† Formerly, Massachusetts Institute of Technology, Cambridge, Mass.; now, Medicinska Nobelinstitutet, Biokemiska Avdelningen, Hantverkaregatan 3, Stockholm, Sweden.

[1] Britton Chance, "Time modulation," PROC. I.R.E., vol. 35, pp. 1039–1044; this issue.

Nonlinear Circuit Elements Used in Time Discrimination and Detection

The time modulators useful for this purpose have been described.[1] Time discriminators, while operated as null indicators in these systems, depend upon two important operations: time selection and detection. The

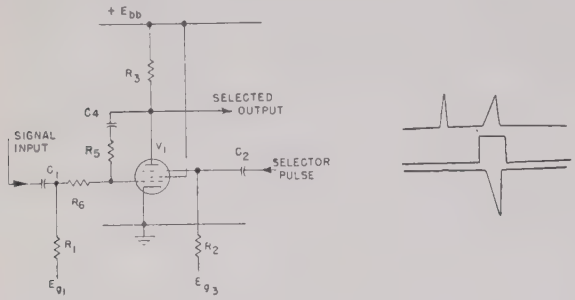

Fig. 3—Multigrid-tube time selector with negative feedback. The wave forms indicate, on the top line, the signal input; on the second line, the selector pulse; and on the third line, the selected output. The anticoincident signal produces a nearly negligible effect in the output, and the desired pulse is reproduced with reasonably good linearity. Typical values for the components are: $R_3 = 15{,}000$ ohms, $R_5 = 30{,}000$ ohms, $R_6 = 62{,}000$ ohms, $E_{g_1} = -6$, $E_{g_3} = -42$, V_1 = type 6AS6.

first is essential not only to protect the discriminator from interfering signals but also to give sensitive indications of the overlap of the input pulses. The second converts the pulse to a steady voltage suitable for control of the time modulator.

Time selectors depend upon the characteristics of an important class of nonlinear circuit elements. An example is indicated in Fig. 3, where the process of time selection is carried out. A time-modulated input signal is connected to control grid g_1 and the output of the local time modulator to the suppressor grid g_3. Both of

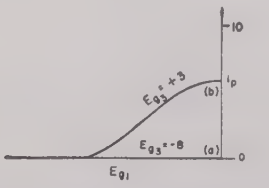

Fig. 4—A nonconstant double-valued characteristic. The particular values indicate the characteristic obtainable from the type 6AS6.

these electrodes normally have fixed negative bias. If both pulses are simultaneous, the signal is reproduced in the plate circuit as indicated by the wave form of Fig. 3, which indicates the excellent linearity of this circuit. Fig. 4 gives in case (a) the transfer characteristic of the time selector with respect to the signal applied to g_1 in the absence of the potential applied to g_3, and it is observed that the transconductance of g_1 is substantially zero. If, however, a potential is applied to g_3, a finite transconductance is obtained as indicated in curve (b). Thus the circuit of Fig. 3 has a multivalued characteristic. The characteristic should not, however, be nonlinear, since faithful reproduction of the selected signal is required.

This circuit has been called a "coincidence," "separator," "switch," or "pip-selector" circuit, but the name *time selector* is proposed since its purpose is entirely analogous to that of the amplitude selector previously described.[1] The actuating pulse, often called a "gate" or "pedestal," is termed the *selector pulse*.

The quality of nonlinearity differs markedly from the broken-line characteristic used for amplitude selection. As before, linear operation is obtained for two slopes of the transfer characteristic, but the discontinuity does not exist in the characteristic of the input electrode; it is dependent upon a second signal operating upon another electrode. The term "multivariable" more accurately describes this circuit element than does the term "nonlinear."

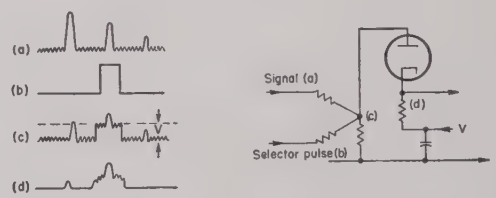

Fig. 5—Time selection by addition and amplitude selection. The signal and selector pulses (a) and (b), added as shown in (c), are amplitude-selected at (d). As is characteristic of these circuits, an unwanted pulse preceding the desired pulse appears in the output.

Imperfect simulations of this characteristic are obtained by addition of signal and selector pulses and separating the signal by amplitude selection, as indicated in Fig. 5. This circuit has the obvious disadvantage that large values of the signal can appear in the output regardless of the presence of the selector pulse, as shown by the signal preceding the desired one.

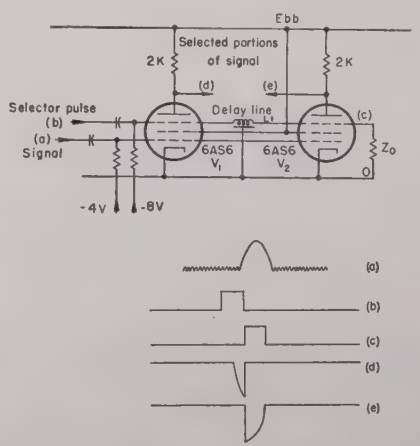

Fig. 6—Adjacent time selectors. The selector pulse is split into two adjacent pulses (b) and (c) of equal duration by delay line L_1. Portions of the input signal (a) are selected at the plates as indicated at (d) and (e).

Many other combinations of circuit elements have useful multivariable characteristics and are described in detail elsewhere.[2]

Time discrimination requires an indication of the *sense* and the approximate magnitude of the time difference between the input signal and the local time-modulated signal. This is accomplished in a pair of time

[2] Radiation Laboratory Series, "Waveforms," McGraw-Hill Book Co., New York, N. Y., 1947; vol. 19, chap. 10.

selectors, employing, for example, the circuit of Fig. 6. The time-modulated input signal is applied to control grids of both tubes. A double selector pulse is obtained by means of an electric delay line giving rise to a second selector pulse adjacent to the first one, and the outputs at the plates of V_1 and V_2 represent the portions of the input wave overlapping the two selector pulses, as indicated in the diagrams of Fig. 6. Alternatively, the signal may be split into two parts by a delay line.

Subtraction of the amplitude of the output of the differential time selector is accomplished in what may be called a *difference detector*, indicated in Fig. 7. Negative pulses from V_1 or V_2 will respectively cause an increase and decrease of the potential of C'. The net potential of C' will depend upon the difference of the amplitude or

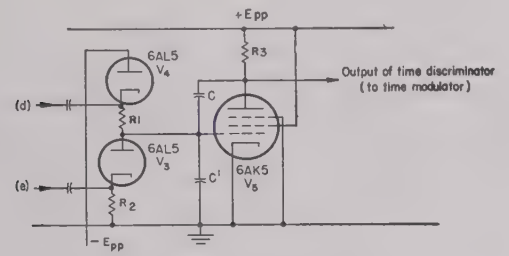

Fig. 7—A difference detector and memory circuit. The difference of the areas of the selected pulses (d) and (e) of Fig. 6 is measured on capacitor C' and smoothed by a storage circuit.

area of these pulses, depending upon the relative values of the circuit components. The value of the difference of these two pulses is sustained during the repetition interval by the memory circuit, composed of V_5 and C. Furthermore, bias applied to the plate of V_4 and the operating potential of the grid of V_5 is such that the input voltage is disconnected from C' in the absence of output from V_1 and V_2. Sensitivities of about 100 volts per microsecond misalignment are obtainable in such circuits with pulses rising in 0.1 microsecond.

The output of this circuit is suitable for direct control of an electrically controlled time modulator which adjusts the position of the selector apertures to follow the modulation of the input signal exactly. In this case, rapid response and smooth operation are obtained. The accuracy is, however, limited by the time modulator to a few parts in 10^3. For higher accuracy, mechanical control of a multiple-scale system is obtained through a servomechanism.

The stabilization problems involved in this type of negative-feedback loop are similar to those found in other systems. The intermittency of the input data gives rise to interesting problems. Nevertheless, the principles of band shaping apply equally well to these systems, as to those operating with signals of more continuous nature. A detailed analysis of the stabilization of these systems is given elsewhere.[3,4]

[3] F. C. Williams, and F. J. U. Ritson, "Automatic strobes and recurrence frequency selectors," presented, Institute of Electrical Engineers Convention, London, England; March, 1946.

[4] Radiation Laboratory Series, vol. 20, "Electrical Time Measurements," McGraw-Hill Book Co., New York, N. Y.; 1947, chaps. 7–9.

Simplified Negative-Feedback Time Demodulator

The discussion of highly precise time demodulators is beyond the scope of this paper, but an example of a simplified circuit is included here to illustrate the general principles of operation. Fig. 8 indicates the use of the double-triode delay multivibrator for a time modulator and a combined time selector and difference detector for a time discriminator. The range of modulation is between 2 to several hundred microseconds, and the accuracy is roughly 1 per cent. The circuit is designed to operate with $\frac{1}{2}$-microsecond pulses at a pulse-recurrence frequency of roughly 1000 per second. It will, however, maintain proper operation in spite of the possible loss of a number of these pulses as a result of interference or fading.

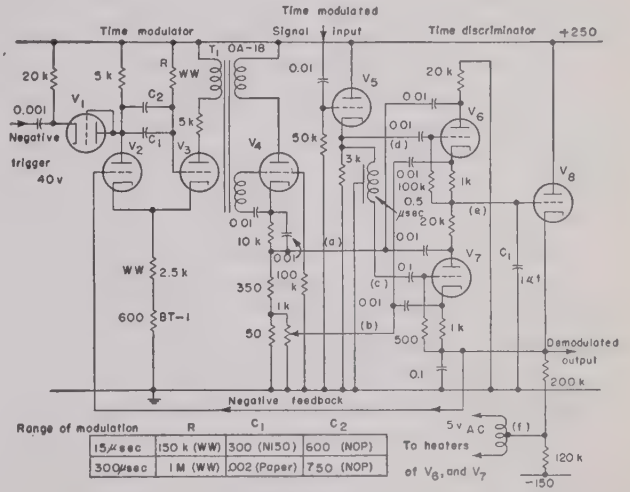

Fig. 8—A negative-feedback time demodulator. This circuit, operating at a pulse-recurrence frequency in the neighborhood of 1000 cycles per second, is suitable for demodulating $\frac{1}{2}$-microsecond time-modulated input signals over the ranges which depend upon the choice of R and C. Typical values are included in the figure.

A negative trigger applied to diode V_1 initiates the operation of time modulator, V_2, V_3, which gives a rectangular pulse at the plate of V_3. The duration of this pulse is linearly related to the control potential applied to the grid of V_2. Differentiation of this rectangular pulse occurs in pulse transformer T_1 (Utah OA-18). The plate-to-grid-coupled blocking oscillator[5] V_4 gives a current pulse in its cathode of approximately 0.2 ampere, and selector pulse (a) has an amplitude of roughly 80 volts and a duration of $\frac{1}{2}$ microsecond. This selector pulse is, of course, time modulated in accordance with the potential of the control grid of V_2.

The $\frac{1}{2}$-microsecond time-modulated input signal which is to be demodulated by this circuit is connected to cathode follower V_5, which in turn drives a terminated $\frac{1}{2}$-microsecond delay line L_1. In this way the time-modulated signal is split into two adjacent portions each $\frac{1}{2}$ microsecond in duration. Coincidence of these two signal pulses and the selector pulse obtained from V_4 energizes the differential detector composed of V_6 and

[5] See chapter 6 of footnote reference 2.

V_7 to give a potential at (e) which depends upon the difference of the areas of the overlap of selector pulse (a) and the split pulses (d) and (c).

For normal values of the potential of point (e) and in the absence of signal and selector pulses, V_6 and V_7 are nonconducting since the cathode of V_7 is maintained positive with respect to its plate by the grid bias of V_8, and the plate of V_6 is held negative with respect to its cathode by the difference of potential between point (e) and ground. In the absence of a time-modulated signal coincident with the selector pulse (a), negligible conduction of V_6 and V_7 occurs, since a positive pulse (b) is applied to the cathodes of V_6 and V_7 at the same time as the selector pulse (a) is applied to their plates, and sufficient bias is developed to maintain V_6 and V_7 very nearly nonconducting. Therefore, the potential of point (e) is undisturbed in the absence of a coincident input signal. On the other hand, a coincident signal causes a decrease of grid bias in V_6 and V_7 and conduction of either one of these tubes for a time determined by the overlap of the split signal and selector pulse. A charge then accumulates on C_1 which represents the integral of the time error. If the selector pulse exactly bisects the split input signal, i.e., there is no time error, then the potential of C_1 is unchanged, as equal conduction will occur in V_6 and V_7 for balanced components. The potential of C_1 is, therefore, fed back to the control grid of the time modulator by cathode follower V_8 and adjusts the position of the selector pulse to follow exactly the modulation of the input signal.

For demodulating pulses of a relatively high intermittency, heater-cathode leakage in V_6 and V_7 would cause discharge of the storage capacitor C_1. Therefore, the heaters of these tubes are operated at 5 volts and are maintained at a constant negative potential with respect to the cathodes by connection to the cathode follower at point (f). In this way leakages of 3×10^{-3} microamperes are obtained in this particular circuit.

The gain of the time demodulator circuit is not very high, and hence no difficulty arises due to instability. The bandwidth of the demodulator is not high; it is suitable for following signals which cover the full range of modulation in 10 or 20 seconds. The speed of following could, however, be considerably increased by reduction of C_1.

Cathode-Ray-Tube Methods

The processes described above can be duplicated by means of cathode-ray-tube displays, and a large number of manual-range-tracking methods have been employed.[4] But automatic time discrimination may be carried out by means of a pair of photocells and an intensity-modulated display. The output signals may operate an electromechanical time modulator. A photograph of an experimental model is shown in Fig. 9, and is suitable for operating with a circular-sweep display.

The problem of obtaining initial coincidence of the selector pulses and the time-modulated signal requires the use of a manual or automatic searching device which will permit this coincidence to exist long enough for the automatic operation of the circuits to be initiated. In radar systems this is usually done with cathode-ray-tube displays. However, several automatic searching circuits have been made which scan the entire range of the time modulation in one second or less. A momentary coincidence of the selector pulses and the signal is adequate to initiate the operation of the time demodulator and to disconnect the automatic searching voltage; usually several pulses are sufficient. The cathode-ray-tube displays are, therefore, unnecessary in this type of operation.

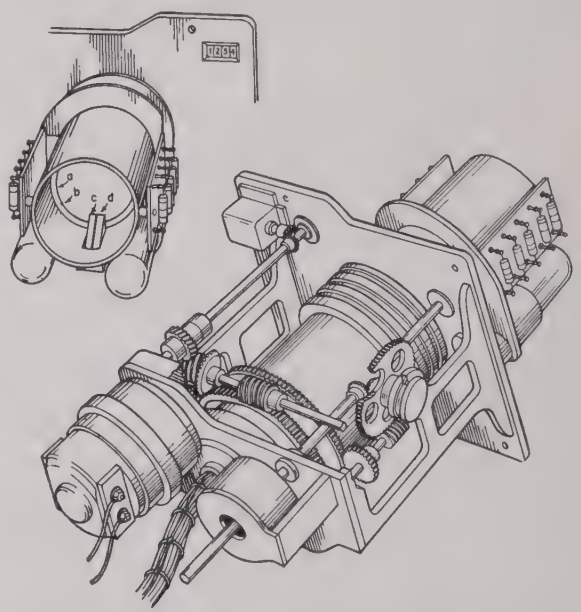

Fig. 9—Perspective view of an automatic range-tracking mechanism employing an intensity-modulated signal displayed on a circular sweep and a photocell tracking system. Intensity-modulated signal (b) is displayed upon the circular trace (a) of a 2-inch cathode-ray tube. Split prisms (c) and (d) reflect light onto type 931 photomultipliers. The photomultiplier assembly is rotatable about the fixed cathode-ray tube by means of a motor-driven worm gear, and the output voltage is obtained through slip rings and is then connected to a power amplifier to drive the motor. Using a circular trace of a 12-microsecond period, an accuracy of roughly 8 yards may be obtained in a full range of several hundred thousand yards. A greater accuracy over a shorter interval may be obtained by employing a circular sweep of a 1.2-microsecond interval. The distance is displayed upon a Veeder-Root counter.

Conclusion

The accuracy obtainable with negative-feedback methods for automatic range measurement depends upon the character of the input signals, the accuracy of the local time modulator, and the sensitivity of the time discriminator. The last two can be made accurate to a few yards in 10 or 20 miles. The limitation has usually been found to be in the bandwidth of the receiver and the characteristics of the reflector. With receiver bandwidth of 16 megacycles, corresponding to a pulse rise time of 0.05 microsecond, the measurements of the distance of a fixed object are repeated to an accuracy of less than one yard. But the fluctuations of aircraft echoes due to variations in the point from which the

reflection originates give errors five or ten times this amount. In the absence of satisfactory radar reflectors, beacons have been used to give distance measurements accurate to 50 feet in 200 miles.

ACKNOWLEDGMENT

The methods and principles described in this paper represent the contributions of many individuals at many government and industrial laboratories in this country and in the British Commonwealth.

The work was, however, carried on intensively and continuously in the Precision Group of the Radiation Laboratory by E. F. MacNichol, Jr., and R. I. Hulsizer, and in Group 19 of the Telecommunications Research Establishment by F. C. Williams and his co-workers.

Analysis of Lengthening of Modulated Repetitive Pulses*

S. C. KLEENE†

Summary—**Pulse lengtheners are circuits which lengthen a series of pulses without changing the relative pulse amplitudes. An ideal "box-car" pulse lengthener produces flat-topped pulses prolonged throughout the interval between pulses. It has been shown by Ming-Chen Wang and G. E. Uhlenbeck that if a pulse with repetition frequency f_0, periodically modulated by a signal with fundamental frequency f_m, is put through the ideal pulse lengthener, the expression for the output pulse contains terms with frequencies $|sf_0+qf_m|$ where $s=0, 1, 2, \cdots$ and $q=\cdots, -2, -1, 0, 1, 2, \cdots$. The amplitudes of terms with frequencies $sf_0 (s=1, 2, \cdots)$, however, are zero. The present paper contains a derivation of the result in more detail, and without the restriction to the ideal case. In the present derivation, the pulse form is taken initially to be quite general. Both a formula and graphs are then presented for the amplitudes associated with the output frequencies of the pulse lengthener, when the output pulse height decays exponentially with the time constant α, and lasts throughout the fraction β of the interval between pulses. This reduces further to the ideal case when $\alpha=0$ and $\beta=1$. The frequencies sf_0 $(s=1, 2, \cdots)$ are ordinarily present, except in the ideal case. An example of a pulse-lengthening circuit is given.**

I. INTRODUCTION

CIRCUITS which are used to lengthen a series of pulses without changing the relative pulse amplitudes are finding many applications in video work. Such pulse lengtheners are amplifiers, in that they increase the power of the pulse wave form. Since the amplification can be obtained without any increase in peak voltage, this is a decided advantage. Another advantage is the elimination in the so-called ideal "box-car" lengthener[1] of any power components at the repetition frequency.

This was brought out by Ming-Chen Wang and G. E. Uhlenbeck,[2] who analyzed the action of the ideal pulse lengthener on a sinusoidally modulated pulse wave form, obtaining the amplitudes and frequencies of the components in the resulting output wave form. Interest has been expressed in having a derivation of their result set down in greater detail than they gave, and without their restriction to the ideal pulse lengthener. It is proposed here to begin by analyzing the output wave form for an arbitrary pulse form.

II. MODULATING SIGNAL, PULSE, AND OUTPUT SIGNAL

The action of the pulse lengthener can be analyzed mathematically as consisting in the conversion of a modulating signal $f(t)$, i.e., the function which gives the amplitude of the unlengthened input pulses, into an output signal $F(t)$.[3]

If the modulating signal were a constant signal of amplitude 1, the output of the pulse lengthener would

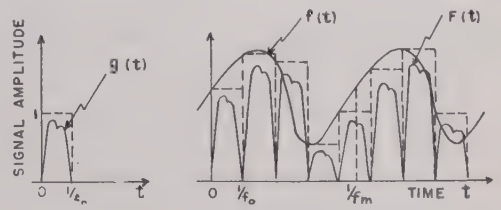

(a) (b)

Fig. 1—General case. (a) Unmodulated pulse $g(t)$. (b) Modulating signal $f(t)$, and output $F(t)$.

be a succession of lengthened pulses, each one identical with its predecessor. Let f_0 be the pulse-repetition frequency, and $1/f_0$ the length of the pulse interval. Let the signal amplitude of one of these standard pulses be represented by the function $g(t)$, as shown in Fig. 1(a) where t is time measured from the beginning of the pulse interval.

Now let the modulating signal be a signal of varying amplitude, shown as $f(t)$ in Fig. 1(b), where t is time measured from the initial instant of some pulse interval.

* Decimal classification: R148.6. Original manuscript received by the Institute, June 6, 1946; revised manuscript received, February 10, 1947.

This paper comprises material contained in Naval Research Laboratory report R-2555 (July 2, 1945, changed from secret to unclassified February 7, 1946), with the addition of a section on pulse-lengthening circuits contributed by A. E. Hastings of the Naval Research Laboratory.

† Formerly, Naval Research Laboratory, Washington, D. C.; now, University of Wisconsin, Madison, Wis.

[1] An ideal "box-car" pulse lengthener produces flat-topped pulses which last until the next succeeding pulse.

[2] Radiation Laboratory Classified Report S-10, J. L. Lawson, editor, appendix by Wang and Uhlenbeck, p. 103; May 16, 1944.

[3] The quantities $f(t)$, $g(t)$, $F(t)$ as functions of t will be referred to as "signal amplitude" to avoid confusion with "amplitude" as applied to the frequency components into which the functions are analyzed.

The output signal $F(t)$ now consists of a succession of pulses which differ from the standard pulses just described in that the signal amplitude $g(t)$ throughout each pulse interval is multiplied by the modulating signal amplitude $f(t)$ for the initial instant of that pulse interval. Let the initial instant of the pulse interval in which t occurs be written $\{t\}$; i.e., $\{t\}=k/f_0$ where k is the greatest integer such that $k/f_0 \leqq t$. Then[4]

$$F(t) = f(\{t\})g(t-\{t\}). \tag{1}$$

III. The General Case: Fourier Analysis

We now further assume that $f(t)$ is periodic,[5] with the fundamental frequency f_m or the period $1/f_m$. Let it be developed in the Fourier series

$$f(t) = \sum_{q=-\infty}^{\infty} c_q e^{2\pi i q f_m t}$$

$$= c_0 + \sum_{p=1}^{\infty} 2|c_p| \cos(2\pi p f_m t + \arg c_p). \tag{2}$$

It is shown in Appendix I that then

$$F(t) = \frac{1}{2}A(0,0) + \sum_{s=1}^{\infty} A(s,0) + \sum_{p=1}^{\infty}\left\{A(0,p) + \sum_{s=1}^{\infty}[A(s,p)+A(s,-p)]\right\} \tag{3}$$

where

$$A(s,q) = 2|c_q|\,|w_{sf_0+qf_m}| \cos(2\pi(sf_0+qf_m)t + \arg c_q + \arg w_{sf_0+qf_m}), \tag{4}$$

and $w_{sf_0+qf_m}$ is the value for $f=sf_0+qf_m$ of

$$w_f = f_0 \int_0^{1/f_0} g(t)e^{-2\pi i f t}dt. \tag{5}$$

IV. Relative Amplitude and Relative Phase

By (4), $A(s,q)$ is of the frequency $|f|=|sf_0+qf_m|$. By (3), the frequencies (ordinarily) present in $F(t)$ are thus $|sf_0+qf_m|$ for $s=0, 1, 2, \cdots, q=\cdots, -2, -1, 0, 1, 2, \cdots$; or in other notation, $|sf_0 \pm pf_m|$ for $s=0, 1, 2, \cdots, p=0, 1, 2, \cdots$.

By (4), the amplitude of $A(s,q)$ is $2|c_q|\,|w_{sf_0+qf_m}|$. Here by (2), $2|c_q|=2|c_p|$ is the amplitude of the term of frequency $pf_m=|q|f_m$ in $f(t)$ (except for $q=0$ when it is twice that amplitude; however, for $q=0$ and $s=0$, only half of $A(s,q)$ is used in (3)). The other factor $|w_{sf_0+qf_m}|$ we call the *relative amplitude* of the output frequency $|f|=|sf_0+qf_m|$. Since $|w_{-f}|=|w_f|$, it depends only on the frequency $|f|$.

This product gives the amplitude of the particular $A(s,q)$ of frequency $|f|=|sf_0+qf_m|$ in the expansion (3) of $F(t)$. In special cases another $A(s',q')$ of (3) might have the same frequency, i.e., when $|sf_0+qf_m| = |s'f_0+q'f_m|$, with s and s' not both 0, and $s'\neq s$ or $q'\neq q$.[6] In such cases the total amplitude of the frequency $|f|$ in $F(t)$ is obtained by combining all the terms of (3) of that frequency, considering both amplitudes and phases.

By (4), the phase of $A(s,q)$ considered as a cosine is $\arg c_q + \arg w_{sf_0+qf_m}$ if $f=sf_0+qf_m \geqq 0$, and $-\arg c_q - \arg w_{sf_0+qf_m}$ if $f \leqq 0$. Using $\arg c_{-q} = -\arg c_q$ and $\arg w_{-f} = -\arg w_f$, the expression for the phase becomes $\pm\arg c_p + \arg w_{|sf_0+qf_m|}$, where $\pm\arg c_p$ is the cosine phase $\arg c_p$ of the term of frequency $pf_m=|q|f_m$ in $f(t)$, taken with either $+$ or $-$ sign according as q and $f=sf_0+qf_m$ have the same or opposite signs (or with either sign when $q=0$ or $f=0$). The other angle $\arg w_{|sf_0+qf_m|}$ we call the *relative phase* of the output frequency $|f|=|sf_0+qf_m|$.[7]

V. A Special Case

We now specialize the pulse function $g(t)$ to the following,[8] where $0<\beta\leqq 1$:

$$g(t) = \begin{cases} e^{-\alpha t} & \text{when } 0 < t < \beta/f_0, \\ 0 & \text{when } \beta/f_0 < t < 1/f_0. \end{cases} \tag{6}$$

For illustration, the modulating function $f(t)$ may be taken as follows, where $S_0,\ \epsilon \geqq 0$:

$$f(t) = S_0[1+\epsilon \sin 2\pi f_m(t+\delta)]. \tag{7}$$

In this case the frequencies pf_m are present in $f(t)$ only for $p=0$ and $p=1$; (3) simplifies accordingly (terms for $p>1$ disappearing); and $c_0=S_0$, $2|c_1|=\epsilon S_0$, $\arg c_1 = 2\pi f_m\delta - \pi/2$. However, the discussion will be carried out so that its application when there are more frequencies present in the modulating function will be evident. Fig. 2 illustrates the special case.

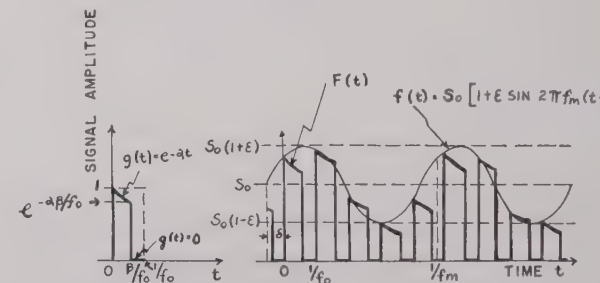

(a) (b)

Fig. 2—Special case. (a) Unmodulated pulse $g(t)$. (b) Modulating signal $f(t)$, and output $F(t)$.

The integration of (5) leads to the following when α and f are not both 0:[9]

[4] Except for $t=k/f_0$, when $F(t)=\frac{1}{2}F(t-0)+F(t+0)$ to accord with footnote 13.

[5] Although only the case of a periodic modulating function $f(t)$ is being treated in this paper, it is surmised that the analysis would carry over in its essentials to the case of an aperiodic modulating function $f(t)$ having a convergent Fourier integral which would then take the place of the Fourier series of $f(t)$ in the developments below.

[6] This possibility may be neglected in the important case that the fundamental and its lower harmonics predominate in both $f(t)$ and $g(t)$ and $f_0 \gg f_m$.

[7] If $g(t)$ is known empirically, w_f can be computed using an harmonic analyzer.

[8] We might have $\gamma e^{-\alpha t}$ instead of $e^{-\alpha t}$ (where $\gamma>0$), but the present formulas will fit that case if $F(t)$ is measured in units γ times those used for $f(t)$ and $g(t)$.

[9] The graphical representation of w_f in the complex plane can be used to advantage in resolving w_f into $|w_f|$ and $\arg w_f$ and in computation.

$$|w_f| = \beta \left\{ \frac{1+e^{-2\alpha\beta/f_0} - 2e^{-\alpha\beta/f_0}\cos 2\pi\beta f/f_0}{(\alpha\beta/f_0)^2+(2\pi\beta f/f_0)^2} \right\}^{1/2}, \quad (8)$$

$$\arg w_f = \sin^{-1} \frac{e^{-\alpha\beta/f_0}\sin 2\pi\beta f/f_0}{(1+e^{-2\alpha\beta/f_0} - 2e^{-\alpha\beta/f_0}\cos 2\pi\beta f/f_0)^{1/2}} - \tan^{-1}\frac{2\pi\beta f/f_0}{\alpha\beta/f_0} \quad (9)$$

where for $\alpha>0$ the inverse functions take their principal values. Integrating separately for $\alpha=f=0$ ((8) and (9) being indeterminate then),

$$w_f = |w_f| = \beta \quad \text{and} \quad \arg w_f = 0. \quad (10)$$

present results in the study of a practical pulse lengthener.[11]

VI. The Relative-Amplitude Curve

The family of the curves of $|w_f|$ as a function of $|f|$ is shown in Fig. 3 for the family of special pulse functions $g(t)$ depending on parameters α, β, f_0. The curves, computed from (8) and (11), are drawn for a number of fixed values of $\alpha\beta/f_0$, and show $|w_f|$ in multiples of β for $|f|$ in multiples of f_0/β.

For example: Let $\alpha=200$, $\beta=0.75$, $f_0=300$, $f_m=700$, $\epsilon=0.5$, $S_0=1$. One of the frequencies in the output is $|f| = |3f_0-f_m| = 200$. What is the amplitude of the term

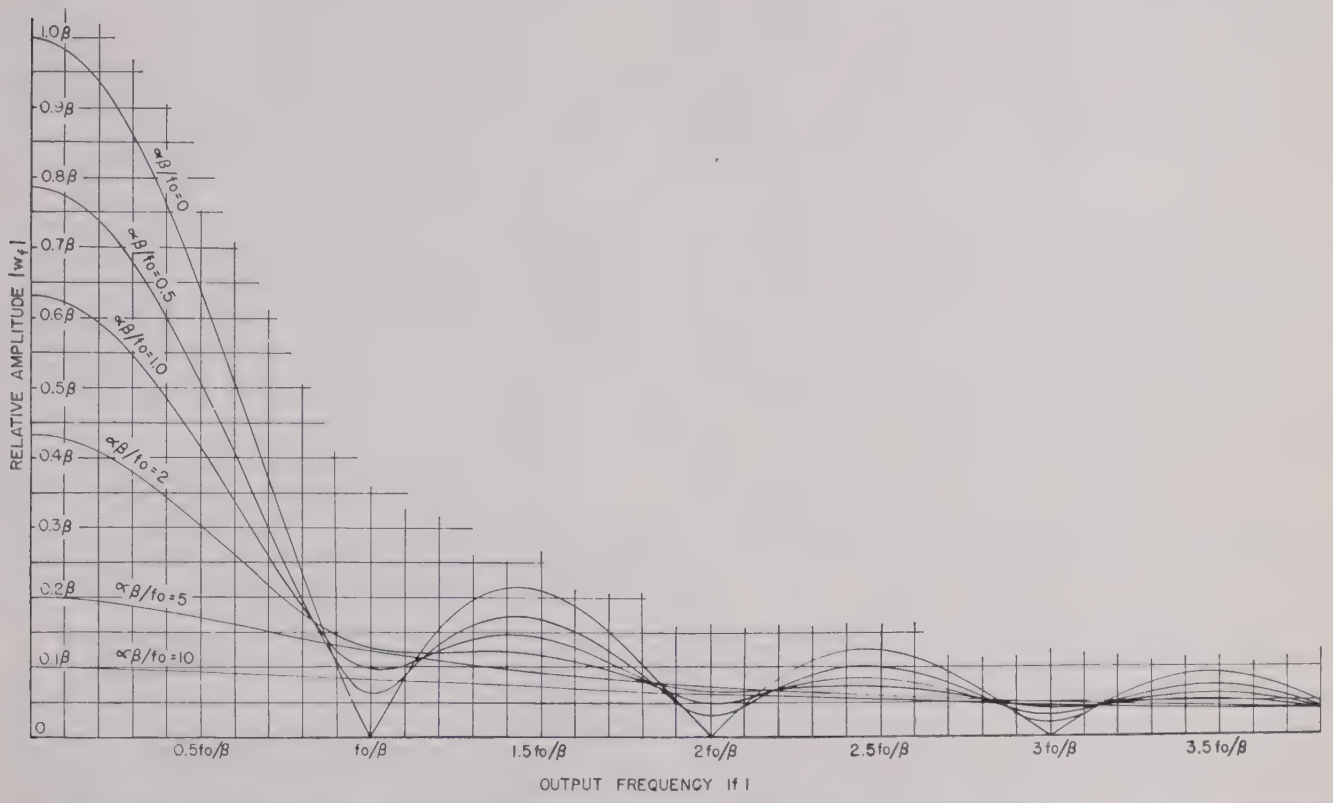

Fig. 3—Relative amplitude versus output frequency. f_0=generator frequency, α=attenuation constant, β=fractional pulse width.

When $\alpha=0$ but $f\neq 0$, (8) and (9) simplify to

$$w_f | = \beta \left| \frac{\sin \pi\beta f/f_0}{\pi\beta f/f_0} \right|, \quad (11)$$

$$\arg w_f = -\pi\beta f/f_0 + \arg \frac{\sin \pi\beta f/f_0}{\pi\beta f/f_0}. \quad (12)$$

It is easily verified that these formulas lead to Wang and Uhlenbeck's formula for the case $\alpha=0$ and $\beta=1$ which gives the ideal box-car pulse.[10] Use has been made of the

[10] Wang and Uhlenbeck's formula is as follows, where their $F_s(t)$ is our $F(t)/S_0$:

$$F_s(t) = 1 + \epsilon \frac{f_0}{\pi f_m} \sin \frac{\pi f_m}{f_0} \left[\sin \left\{ 2\pi f_m t - \frac{\pi f_m}{f_0} + 2\pi f_m \delta \right\} + \sum_{s=1}^{\infty} \frac{f_m}{sf_0+f_m} \sin \left\{ 2\pi(sf_0+f_m)t - \frac{\pi f_m}{f_0} + 2\pi f_m\delta \right\} \right] + \sum_{s=1}^{\infty} \frac{f_m}{sf_0-f_m} \sin \left\{ 2\pi(sf_0-f_m)t + \frac{\pi f_m}{f_0} - 2\pi f_m\delta \right\} \Big].$$

$A(3, -1)$ which has this frequency? The amplitude of the correlated term of frequency $1\cdot f_m$ in $f(t)$ is $\epsilon S_0=0.5$. Now $\alpha\beta/f_0=0.5$, and $\beta|f|/f_0=0.5$ or $|f|=0.5f_0/\beta$. Entering the curve of Fig. 3 for $\alpha\beta/f_0=0.5$ from the abscissa $0.5\ f_0/\beta$, we read $|w_f|=0.5^+\beta$. Hence $|w_f|=0.38$. The amplitude of $A(3, -1)$ is $\epsilon S_0\cdot|w_f| = 0.19$.

In the example, $A(3, -1)$ is the only term with the frequency $|f|=200$. Should a practical need arise to study phases (e.g., to find the total amplitude of a frequency $|f|$ when several terms of (3) give the same $|f| = |sf_0+qf_m|$), a second set of curves could be prepared giving arg $w_{|f|}$ as a function of $|f|$.

A simple geometrical model, briefly described in Appendix II, is useful in thinking about the situation,

[11] Section VIII, and Naval Research Laboratory Classified Report R-2561; May 1, 1945.

particularly as it sets in order certain exceptions to the general rule.

VII. Amplitude Nulls

For $\alpha=0$ and $\beta=1$, the frequencies $sf_0(s=1, 2, \cdots)$ are absent. This appears in Fig. 3 since the curve for $\alpha\beta/f_0=0$ has nulls at the frequencies sf_0/β (compare (11)), and with $\beta=1$ the sf_0 frequency points from which the curve is entered coincide with these nulls. The amount by which these frequencies reappear if β decreases from 1, so that the points sf_0 no longer coincide with the nulls, is indicated by the steepness of the curve at those points.[12] If $\alpha\neq 0$, so that $\alpha\beta/f_0\neq 0$, the curves no longer have nulls, but for small values of $\alpha\beta|f_0|$ they have pronounced minima occurring approximately at the points sf_0/β with approximately the values $\beta|1-e^{-\alpha\beta/f_0}|/((\alpha\beta/f_0)^2+(2\pi s)^2)^{1/2}$ (compare (8)). These considerations are of interest for designing pulse lengtheners in the effort to eliminate pulse-repetition frequencies.

VIII. A Pulse-Lengthening Circuit

Fig. 4 gives the circuit of a practical pulse lengthener. The modulated pulsed signal is applied to the grid of

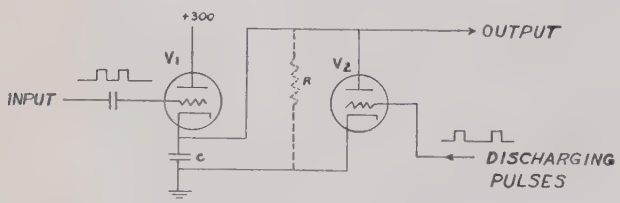

Fig. 4—A pulse-lengthening circuit.

the cathode-coupled amplifier V_1. Each pulse charges the capacitor C to a value proportional to the pulse amplitude. The capacitor C remains charged until just before the next pulse, when it is discharged by the plate current of V_2. The grid of V_2, normally biased to cutoff, is supplied with a series of short positive pulses, each just preceding the pulses in the signal wave form, which may be obtained in various ways, depending on the circuit application. One simple method is to feed the signal pulses directly to the grid of V_2, but to apply them to the grid of V_1 through a delay line. Then V_2 is nonconducting except for a brief period just before each signal pulse. The resulting wave form across C is then a series of pulses with amplitudes proportional to those in the signal.

The output pulses will not be flat-topped because of the leakage across the capacitor given by the exponential function $e^{-\alpha t}$, where $\alpha=1/RC$, though α can be made to approach 0. Since a finite time is required to discharge the capacitor, the length of the output pulse can only approach the repetition period, the ratio β of the pulse length to the repetition period approaching 1.

[12] For special values of s and the other quantities, a frequency sf_0 might be absent because of coincidence with some $s'f_0/\beta$; or conceivably due to complete phase cancellation among terms of that frequency for several values of p.

IX. Acknowledgment

Acknowledgment is due A. E. Hastings for assistance in the re-editing of the Naval Research Laboratory report as the present paper, Jeanne Schwartz for preparing the figures and editing the original report, and Bertram Yood for valuable criticism in connection with the preparation of that report.

Appendix I—Derivation of the Fundamental Formula[13]

Using (2) to express $f(\{t\})$ in (1) as a series, and multiplying $g(t-\{t\})$ into the series term by term,

$$F(t) = \sum_{q=-\infty}^{\infty} c_q e^{2\pi i q f_m \{t\}} g(t-\{t\}). \tag{13}$$

Writing $\{t\}$ in the exponent as $t-(t-\{t\})$, and factoring,

$$F(t) = \sum_{q=-\infty}^{\infty} c_q e^{2\pi i q f_m t} e^{-2\pi i q f_m (t-\{t\})} g(t-\{t\}). \tag{14}$$

The expression $e^{-2\pi i q f_m (t-\{t\})} g(t-\{t\})$ represents $e^{-2\pi i q f_m t} g(t)$ in the first pulse interval, and the periodic repetition of this function in other pulse intervals. Developing it in a Fourier series, and inserting this series into (14),

$$F(t) = \sum_{q=-\infty}^{\infty} c_q e^{2\pi i q f_m t} \cdot \sum_{s=-\infty}^{\infty} \left[f_0 \int_0^{1/f_0} e^{-2\pi i q f_m t} g(t) e^{-2\pi i s f_0 t} dt \right] e^{2\pi i s f_0 t}. \tag{15}$$

Multiplying $c_q e^{2\pi i q f_m t}$ into the series summed on s, and combining the exponential factors,

$$F(t) = \sum_{q=-\infty}^{\infty} \sum_{s=-\infty}^{\infty} c_q \left[f_0 \int_0^{1/f_0} g(t) e^{-2\pi i (s f_0 + q f_m) t} dt \right] \cdot e^{2\pi i (s f_0 + q f_m) t}. \tag{16}$$

Calling the expression under the summation signs $C(s, q)$, and setting $A(s, q)=C(s, q)+C(-s, -q)$, one easily obtains thence the real form of the expansion given as (3)–(5) in the text.

Appendix II—A Geometrical Model of the Output

A frequency nomograph is shown as the horizontal quarter-plane in Fig. 5 with axis of abscissas labeled "output frequency $|f|$" and axis of ordinates labeled "modulating frequency pf_m." Lines are ruled on the nomograph at angles of ± 45 degrees with the axes, which therefore have the equations $|f|=|sf_0 \pm pf_m|$, if $|f|$ is considered as a continuously varying abscissa and pf_m as a continuously varying ordinate. Hence, when to each of the modulating frequencies pf_m for $p=0, 1, 2, \cdots$, a line parallel to the axis of abscissas is drawn at the ordinate pf_m (shown in Fig. 5 only for

[13] A practical set of assumptions under which the Fourier expansions will all exist and converge to the functions represented for every t is that $f(t)$ and $g(t)$ and their first derivatives each be continuous except at isolated values of t. Then $f(t)$ shall be defined at a point of discontinuity as $\frac{1}{2}(f(t-0)+f(t+0))$, and the same convention shall apply to $g(t)$ and $F(t)$.

$p=0$ and $p=1$), the abscissas of the intersections of this line with the lines of the frequency nomograph will be the output frequencies associated with the modulating frequency pf_m. Vertical lines erected at these intersections and terminated above by the appropriate curve of Fig. 3 (for $\alpha\beta/f_0=0.5$ with $\beta=0.75$ in our illustration) represent the corresponding relative amplitudes.

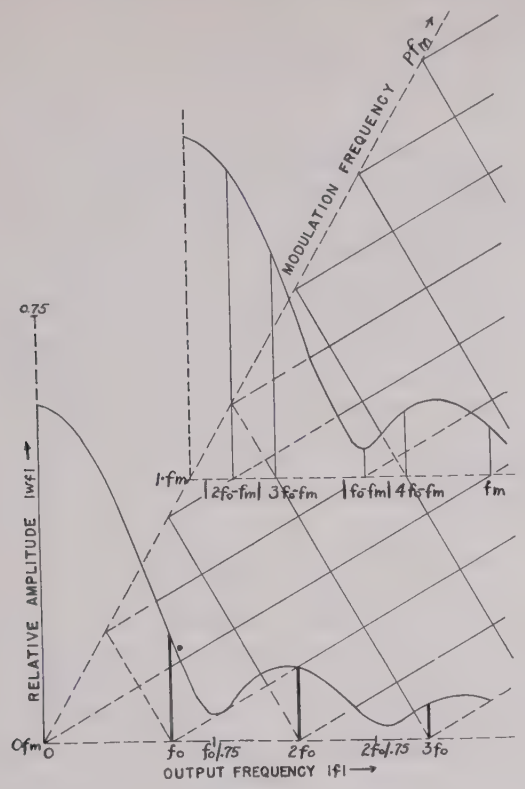

Fig. 5—Relative amplitudes of output terms. Attenuation constant $\alpha=2f_0/3$, pulse width $\beta/f_0=3/4f_0$.

On the $p=0$ panel, the relative-amplitude lines are shown double (except for $|f|=0$), corresponding to the fact that for $p=|q|=0$ (except for $s=0$) the absolute amplitude is twice the relative amplitude times the amplitude of the corresponding component of $f(t)$ (compare with Section IV). This appears natural on observing that, had the panel been positioned for a very small ordinate pf_m, there would be for each $sf_0(s\neq 0)$ two lines erected at near-by frequencies, which would come together at sf_0 when $pf_m\rightarrow 0$.

If a panel for $p>0$ passes through double points of the frequency nomograph (as it might in another example), two lines are likewise erected at each of those double points, but those two lines belong to distinct terms $A(s, q)$ and $A(s', q')$ with a phase difference of 2 arg c_p.

If a panel for $p>0$ passes through a point where the nomograph lines meet the axis of ordinates, a single line is erected there which represents the relative amplitude $|w_0|$ of a term of 0 frequency. But $2|c_p||w_0|$ is not (ordinarily) the absolute value of that term, as the phase factor cos (arg c_p+arg w_0) (ordinarily) differs in absolute value from 1. The term may be thought of as originating from a sinusoidal fluctuation with relative amplitude $|w_f|$ which as $|f|\rightarrow 0$ is frozen in the phase arg c_p+arg w_0.[14]

[14] The idea of the model can be carried further, by varying the vertical scales of the several panels in proportion to the amplitudes of the modulating frequencies so that the lines erected will represent absolute amplitudes; and by showing the phases.

Abstract of "Recording of Sky-Wave Signals From Broadcast Stations"*

WILBERT B. SMITH†, MEMBER, I.R.E.

IN ORDER TO obtain data on sky-wave propagation conditions, equipment was developed for making graphical records of the signal intensities of certain broadcasting stations, and for the rapid analysis by electronic means of the charts so taken.

The recording sets consist of communications-type receivers arranged for the automatic-volume-control voltage to drive a 0–5 recording milliammeter, and operating in conjunction with special signal generators and coupling gear, so that calibration marks may be placed directly on the graphical record to supply the scale for subsequent analysis.

An electronic device is provided in series with the recording milliammeter to return the pen to zero periodically, so that the area between the curve drawn and the base line or zero is completely blanked in. This device consists of a 6J5 triode whose plate circuit is in series with the recorder, and whose grid potential varies from cutoff to about 4 volts positive under the action of a thyratron sawtooth-wave generator of period about 1 to 10 seconds. Under these conditions, the triode plate resistance varies from about 200 ohms to infinity.

Analysis of the charts to obtain the field intensities which were exceeded for certain specified percentages of time is done on a special scanning device. This scanner consists of a drum around which the chart is wound, a scale and chart onto which the calibration marks are transferred and from which the signal intensities are read, a light spot, photocell, amplifier, and integrating circuit and meter from which is read the percentage of time.

As the drum revolves rapidly, the spot of light travels the length of the portion of the chart under observation. Light reflected from the unmarked paper of the chart actuates the photocell and amplifier, and blocks the flow of current through the integrating milliammeter. When the photocell is not illuminated, current is permitted to flow through the meter which therefore reads directly the percentage of time during which the spot of light has been on the blanked-in portion of the chart. The corresponding field intensity which has been exceeded for that percentage of time can be read directly from the calibration scale.

The field-intensity recording sets are extremely simple and reliable, and are under the care of regular station personnel. Analysis of the charts is rapid, averaging less than 10 minutes for a two-hour recording period, as compared with several hours by manual methods. There is also a much greater over-all accuracy, because personal and judgment errors are practically eliminated and other sources of error are reduced to a minimum or arranged to be largely self-compensating.

* Decimal classification: R271.32×R112.63. Original manuscript received by the Institute, March 25, 1947; abstract received, July 16, 1947.

† Department of Transport, Government of Canada, Ontario, Canada.

Investigation of Frequency-Modulation Signal Interference*

IGOR PLUSC†, MEMBER, I.R.E.

Summary—The cause and mechanism of interference between two frequency-modulation signals are analyzed. It is shown that, while the interference of two frequency-modulation signals on the same channel is practically independent of receiver design, off-channel interference depends on the shape of discriminator curve beyond 120 kilocycles off resonance.

Methods are developed to calculate the amount of interference for a given receiver, in terms of the relative strength of the interfering signal. Receiver design modifications, which will reduce the amount of interference from different channels, are indicated.

Introduction

INTERFERENCE between several frequency-modulation signals operating on, or near, the same frequency is becoming an important receiver design problem with the steadily increasing number of transmitters being put into operation.

The object of this work is to present a quantitative analysis of the interference under conditions likely to be encountered in a frequency-modulation receiver, particularly in regard to the action of the discriminator. This phase of a frequency-modulation receiver has been neglected by most writers on the general subject, probably because of the widespread belief that the shape of the discriminator curve beyond the limits of modulation is of no consequence provided the limiter is operating perfectly. Methods are developed for analyzing and evaluating the effect of the shape of the discriminator curve upon the susceptibility to interference. Also, some of the possible remedies are outlined.

Interference from other frequency-modulation stations may be divided into two classifications: interference arising from stations on the same channel, and that from stations on different channels. These cases are treated separately, as follows: (1) co-channel interference, and (2) adjacent-and alternate-(second-) channel interference.

Definitions of the Symbols

F_c = the carrier frequency to which the receiver is tuned (desired signal)
F_n = the carrier frequency of the interfering signal
$F_{cn} = (F_c - F_n)$ = the beat frequency between the desired and interfering signals
F_m = modulating frequency
$\rho = c/n$ = the ratio of the amplitudes of the desired to interfering signals at the output of intermediate frequency
F_d = maximum frequency deviation due to frequency modulation ($F_d = 75$ kilocycles)
$\beta = F_d/F_m$
F_i = the frequency deviation (modulation due to the interfering signal)
S = output of desired signal corresponding to 75-kilocycle deviation (100 per cent modulation)
S/N = the signal-to-interference ratio in the audio
N = the output of the interfering signal
$W_c = 2\pi F_c$
$W_n = 2\pi F_n$
$W_{cn} = 2\pi F_{cn} = W_c - W_n$
$p = 2\pi F_m$
A = the amplitude.

General Theory

The two signals, desired and interfering, reach the limiter to form a composite signal, both frequency- and amplitude-modulated. This modulation has a fundamental frequency corresponding to the frequency difference between the two signals and in certain cases is high in harmonic content.

An amplitude limiter with ideal characteristics is used throughout this analysis. The expression for the composite signal at the output of such a limiter has been derived many times,[1] and so the derivation will not be given here. The expression is:

$$e = A \sin \left\{ \omega_c t + \beta \cos pt + \tan^{-1} \frac{\sin \left[\omega_{cn} t - \phi(t) + \beta \cos pt \right]}{\rho + \cos \left[\omega_{cn} t - \phi(t) + \beta \cos pt \right]} \right\}. \quad (1)$$

This is the most general form, when both signals are frequency modulated. The expression $\beta \cos pt$ is due to the desired signal modulation. The term $\phi(t)$ is due to the interfering signal modulation.

Let

$$\tan^{-1} \frac{\sin \left[\omega_{cn} t - \phi(t) + \beta \cos pt \right]}{\rho + \cos \left[\omega_{cn} t - \phi(t) + \beta \cos pt \right]} = \alpha. \quad (1a)$$

Frequency deviation due to the interfering signal can be found from

$$F_i = \frac{1}{2\pi} \frac{d\alpha}{dt} = \frac{F_{cn} - \dfrac{d\phi}{dt} - F_d \sin pt}{\dfrac{\rho + \cos \left[\omega_{cn} t - \phi(t) + \beta \cos pt \right]}{\dfrac{1}{\rho} + \cos \left[\omega_{cn} t - \phi(t) + \beta \cos pt \right]} + 1}. \quad (2)$$

* Decimal classification: R171×R430.11. Original manuscript received by the Institute, July 1, 1946; revised manuscript received, September 30, 1946.

† Formerly, Colonial Radio Corporation, Buffalo, N. Y.; now, Syracuse University, Syracuse, N. Y.

[1] M. G. Crosby, "Frequency modulation noise characteristics," PROC. I.R.E., vol. 25, pp. 472–514; April, 1937.

When both signals are unmodulated carriers, $\phi(t)$, $\beta \cos pt$, and their derivatives vanish, and (2) becomes

$$F_i = \frac{F_{cn}}{\dfrac{\rho + \cos \omega_{cn} t}{\dfrac{1}{\rho} + \cos \omega_{cn} t} + 1}. \qquad (2a)$$

This equation shows that F_i is not symmetrical; its two peaks can be obtained by substituting $\cos \omega_{cn} t \pm 1$.

First peak $$F_{i_1} = \frac{F_{cn}}{\rho + 1}; \qquad (\cos \omega_{cn} t = 1) \qquad (3)$$

Second peak $$F_{i_2} = \frac{F_{cn}}{\rho - 1}; \qquad (\cos \omega_{cn} t = -1). \qquad (4)$$

The asymmetry increases as ρ decreases. Expanded, (2a) becomes

$$F_i = F_{cn} \sum_{r=1}^{r=\infty} (-1)^{r+1} \frac{\cos r\omega_{cn} t}{\rho^r}. \qquad (5)$$

There is no constant term in this expression: although nonsymmetrical, F_i has an average value equal to zero. Consequently, there is no frequency shift.

Co-Channel Interference

When the desired and interfering signals are on the same channel and the difference in frequency is within the audio range, it has been found experimentally that interference is strongest when both signals are unmodulated carriers. This case will be examined first.

(a) The root-mean-square value of the interference N can be found from (5).

$$N_{rms} = \frac{F_{cn}}{\sqrt{2}} \sqrt{\sum_{r=1}^{r=r_0} \frac{1}{\rho^{2r}}}$$

where

$$r_0 \leqq \frac{15}{F_{cn}} \quad (F_{cn} \text{ in kilocycles}). \qquad (6)$$

The results were plotted as S/N(in decibels) against ρ, for different values of F_{cn} (Fig. 1). These curves were plotted for two cases: with no de-emphasis and with 75-microsecond de-emphasis. Without de-emphasis the total interference is proportional to F_{cn}, while with 75-microsecond de-emphasis it increases much more slowly with F_{cn} and for higher F_{cn} approaches asymptotically a constant value.

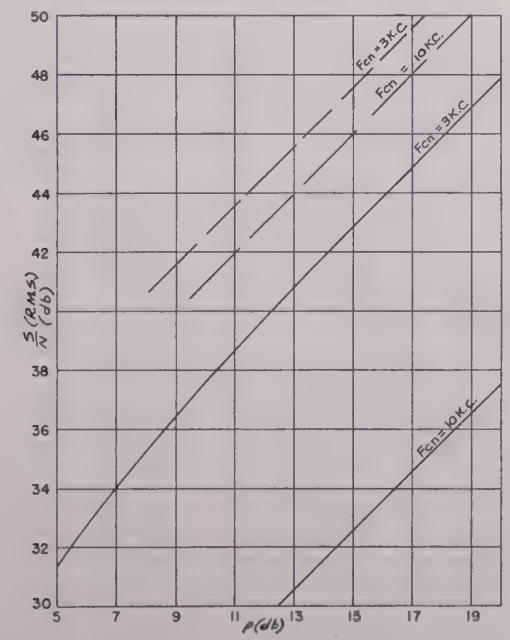

Fig. 1—Signal-to-interference ratio in output due to interfering signal on the same channel (both signals unmodulated) for two beat frequencies (F_{cn}).
———— Without de-emphasis
— — — — With de-emphasis.

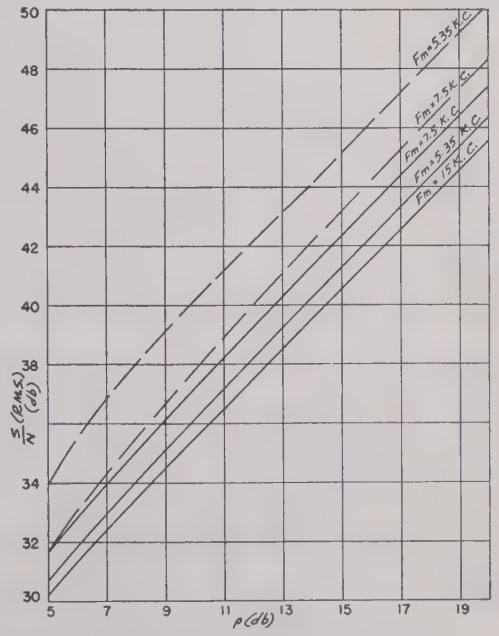

Fig. 2—Signal-to-interference ratio when both signals are on the same channel (one signal modulated)
———— $F_{cn} = 3$ kilocycles
— — — — $F_{cn} = 10$ kilocycles.

(b) When only one of the signals is frequency modulated, $\phi(t)$ in (2) vanishes and it becomes

$$F_i = \frac{F_{cn} - F_d \sin pt}{\dfrac{\rho + \cos [\omega_{cn} t + \beta \cos pt]}{\dfrac{1}{\rho} + \cos [\omega_{cn} t + \beta \cos pt]} + 1}. \qquad (7)$$

This equation is expanded by binomial formula, then using sine and cosine addition formulas, the Bessel Functions expansion and recurrence formula, whereupon it is brought to a more convenient form:

$$F_i = \sum_{n=1}^{n=\infty} \sum_{r=0}^{r=\infty} \left\{ J_r(n\beta) \left[(F_{cn}+rF_m) \cos\left(n\omega_{cn}t + rpt + \frac{\pi r}{2}\right) + (F_{cn}-rF_m) \cos\left(n\omega_{cn}t - rpt + \frac{\pi r}{2}\right) \right] \right\}. \quad (8)$$

The root-mean-square values of N were calculated from this formula for different values of F_{cn} and F_m and were plotted against ρ (Fig. 2). In calculating the root-mean-square values only the components of audio frequencies (less than 15 kilocycles) were taken into consideration.

Equation (8) shows that the components of higher frequencies have greater amplitudes. Consequently, in this case, interference is much more affected by the de-emphasis than in case of two unmodulated carriers, because the higher frequencies are attenuated much more. Without de-emphasis, interference would be almost the same in both cases with and without modulation. With de-emphasis, however, interference will be considerably weaker when modulation is present.

Adjacent-Channel Interference

According to present Federal Communications Commission standards, 200-kilocycle adjacent-channel spacing is the closest that needs to be considered above that of 4-kilocycle common channel maximum spacing. After that, 400-kilocycle spacing will be considered. While the analysis is identical for both of these cases, the evaluation of the magnitudes to be expected in a practical receiver is different.

Suppose a frequency-modulation receiver is tuned to a certain signal of a frequency F_c (desired signal). There is another signal on the adjacent ($F_{cn}=200$ kilocycles) channel which interferes with the first. Let us assume that, at first, both signals are unmodulated carriers. Then F_{cn} and the harmonics will be far above the audio range, so there will be no audio interference.

If, then, the interfering signal is modulated 100 per cent, its frequency will swing 75 kilocycles in each direction. F_{cn} will vary with the modulation, from 125 to 275 kilocycles. The selectivity curve of an ordinary receiver is very steep between 125 and 275 kilocycles from resonance, and the gain of the receiver changes greatly between those frequencies. Thus, the amplitude of the interfering signal at the last intermediate-frequency circuit will change together with the frequency variation, and the signal will become amplitude, in addition to frequency, modulated at the output of the intermediate-frequency amplifier. The amount of this amplitude modulation depends upon the shape of the selectivity curve. With a typical selectivity curve of a present commercial receiver, amplitude modulation reaches 100 per cent at a frequency deviation between 35 and 45 kilocycles.

When the interfering signal is both frequency and amplitude modulated, ρ is no longer a constant, but becomes a function of time. When modulation is sinusoidal

$$\rho = \frac{c}{m(1+\cos pt)}.$$

If we substitute this expression into (1a) and get

$$F_i = \frac{1}{2\pi}\frac{d\alpha}{dt},$$

we find that all the terms that contain functions of F_m (modulating frequency) cancel out, only the terms that contain functions of beat frequency and its harmonics remaining in the final expression. As long as the discriminator curve is linear, frequency variation F_i will be transformed into corresponding amplitude modulation without distortion. Therefore, the amplitude variations at the output of the discriminator will not contain any modulating frequencies, and there will be no audible effect of the interference.

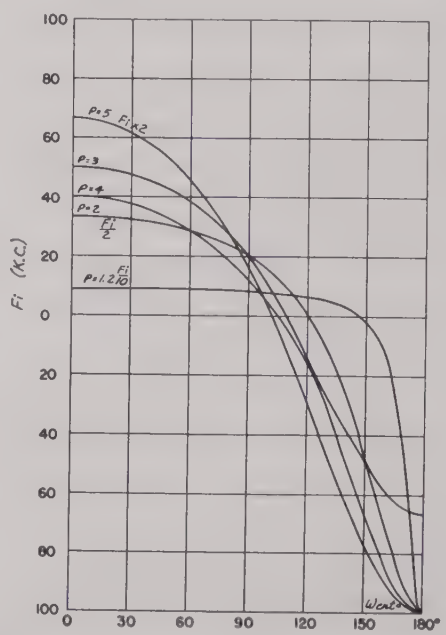

Fig. 3—Frequency deviation of the desired signal produced by interfering signals of different strengths ($F_{cn}=200$ kilocycles).

In order to determine the effect of the nonlinear part of the discriminator curve on the interference, we shall once more examine (3) and (4). For low ρ, F_i is not symmetrical; one of its peaks is much greater than the other. As was shown earlier (5), the average value of F_i is zero. As long as F_i is changed into amplitude variation A without distortion, the average value of A will also be zero, and so there will be no direct-current component in the output of the discriminator. However, as soon as one of the peaks extends into the nonlinear part of the discriminator curve, distortion is introduced, the average value of the discriminator output is no longer zero, and a direct-current component appears. For a fixed discriminator curve, the magnitude of this component depends on both F_{cn} and ρ. As was shown before, when the interfering signal is frequency modulated, it also becomes

amplitude modulated. Then ρ and F_{cn} both vary with F_m, but ρ varies much faster (due to steepness of the selectivity curve). Since the magnitude of the direct-current component depends upon ρ, it will vary with ρ and consequently with F_m, thus introducing an audible interference.

The easiest method to find the magnitude of the direct-current component is graphical. First F_i (2a) is plotted for a half cycle against $W_{cn}t$ (Fig. 3). Then the values of F_i for different $W_{cn}t$ are applied to the discriminator curve[2] and the corresponding values of the amplitude are found. These amplitudes are plotted against $W_{cn}t$ and represent a half cycle of the discriminator output (Fig. 3). The direct-current component is then found from Fig. 4:

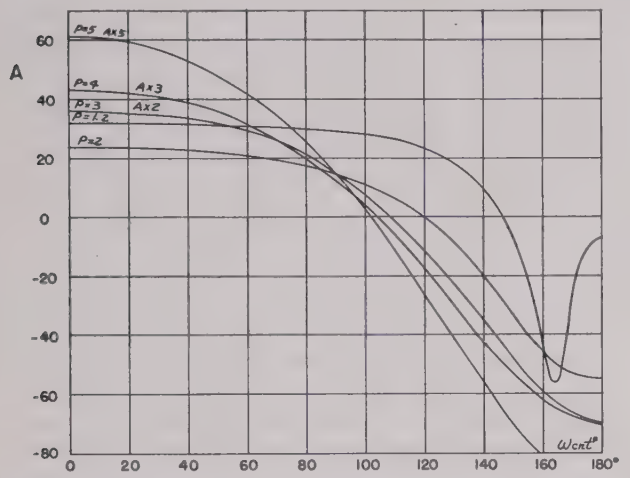

Fig. 4—Amplitude variations resulting from frequency deviation due to the interfering signals of different strength (Fig. 3).

$$\text{direct current} = \frac{\sum \text{area}}{\text{abscissa}}.$$

The actual amount of interference would depend on variation of ρ, and therefore on the particular selectivity curve used. It was found, however, that with the selectivity curves of the commercial receiver available, the actual interference with F_{cn} both 200 and 400 kilocycles was very close to that caused by the direct-current component 100 per cent modulated. The results calculated on this assumption were plotted as S/N for adjacent channel (Fig. 5).

In the case where the actual selectivity curve is available, the procedure to find the variation of direct-current component would be as follows: Three direct-current curves are plotted against ρ, for F_n and $F_{cn} \pm 75$ kilocycles. The variation of ρ corresponding to ± 75-kilocycle deviation of the interfering signal is found from the selectivity curve. Knowing how much ρ changes between $F_{cn}+75$ and $F_{cn}-75$ kilocycles, the exact variation of the direct-current component is then found from the three curves.

Although the above-described method is comparatively simple and easy to visualize, it is accurate only when the interfering-signal frequency falls between the peaks of the discriminator curve. In other cases a general method of sideband components must be used.

The general method is to expand expression (1) (simplified for the case of two unmodulated carriers). After expansion it takes a form:

$$e = \alpha_0 + \sin \omega_c t + \sum_{r=1}^{r=\infty} (-1)^r [b_r \sin (\omega_c - r\omega_{cn})t - a_r \sin (\omega_c + r\omega_{cn})t]. \quad (9)$$

(The derivation of this expression and the coefficients a_r and b_r is shown in the appendix.) The absolute values of the coefficients a_r, b_r were plotted against ρ (Fig. 6).

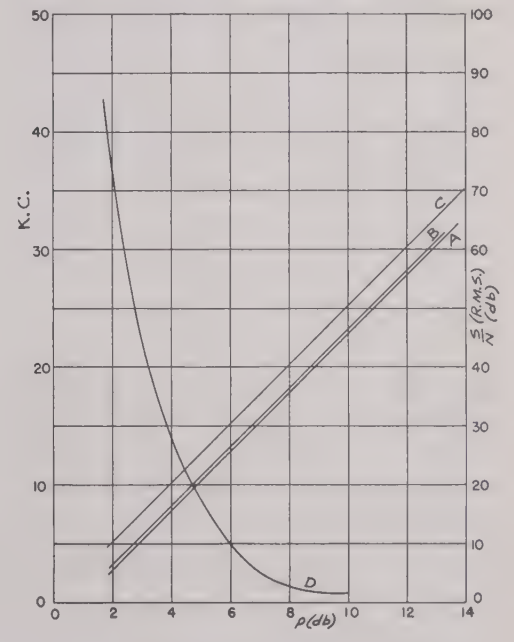

Fig. 5—Curves A, B, and C show signal-to-interference ratio in output due to interfering signals from adjacent and alternate channels.
A—$F_n = 200$ kilocycles (calculated by equivalent-frequency-deviation method).
B—$F_{cn} = 200$ kilocycles (sideband-components method).
C—$F_{cn} = 400$ kilocycles (sideband-components method).
D—Detuning (in kilocycles) required to reduce interference from signal in adjacent channel.

When signal e is applied to each diode circuit of a balanced discriminator, there is a direct-current component in the output of each diode. The difference of these components from two diodes is the resultant direct-current component D in the output of the balanced discriminator. $D = D_1 - D_2$ where D_1 and D_2 are the direct-current components in the output of each diode. The method to calculate D_1 and D_2 is shown in the appendix. As was shown before, when the interfering signal becomes frequency modulated, D changes with F_m and thus introduces an audible interference. From

[2] Discriminator curve taken from *RCA Report* LB-326, "Automatic-frequency control," Fig. 4, page 9 ($Q = 25$).

(9) it can be seen that the sideband components have frequencies $F_c \pm rF_{cn}$, $r=1, 2, 3$. Fig. 6 shows that symmetrical components (those having the same value of r) have unequal amplitudes. When the discriminator curve is a straight line, the coefficients a_r, b_r (9) are such that $D_1=D_2$, that is, $D=0$, and there is no interference. If the discriminator curve deviates from a straight line, D

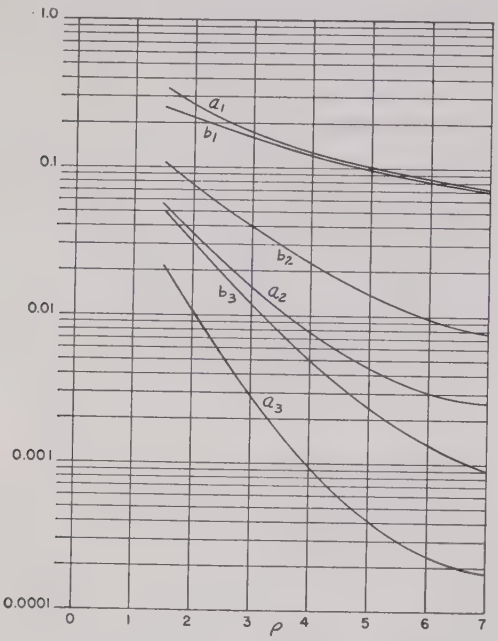

Fig. 6—Coefficients of equation (14) versus desired-to-interfering signals ratio in intermediate-frequency output.

is not equal to zero. In a symmetrical discriminator, with two diode circuits having their selectivity curves of the same shape (though tuned to different frequencies), D will increase when all the sideband frequencies are attenuated except the first two ($F_c \pm F_{cn}$). The maximum possible interference with a symmetrical discriminator would occur when the first pair of sideband components fall on the peaks of the discriminator curve, while the rest of the components are completely eliminated. If the circuits of the discriminator are not symmetrical, the interference may become still higher if one sideband is more attenuated than the other. When all the sideband components are attenuated, D_1 and D_2 both approach the same value, so D approaches zero.

It was found that, for a good degree of approximation, when $\rho \geqq 2$ at least two of the sideband components on each side of the carrier have to be taken into consideration. The direct-current component is represented by an infinite series (17) whose terms become so long and complicated that it would be impractical to go any further than the first two terms. Fortunately, for $\rho \geqq 2$ the first term only gives an accuracy within 20 per cent and the second term would bring it within less than 5 per cent. Numerical calculations require an accuracy to at least six figures, which makes the whole procedure long and tedious. So, when valid, the equivalent-frequency-deviation method is easier to use.

Conclusion

As was shown earlier, the interference of two transmitters working on the same channel is caused by the beat frequency between the signals. The carrier of the desired signal becomes frequency modulated by the beat frequency during the process of limiting. This kind of interference cannot be eliminated, or even materially reduced by modifications in the receiver design. The co-channel frequency-modulation interference decreases with decrease of F_{cn}. This effect is partially offset by the increase of the residual amplitude-modulation interference for small F_{cn}. So the only way to reduce the frequency-modulation co-channel interference is to keep the difference between the frequencies of the transmitters as low as practical, while the residual amplitude-modulation interference can be reduced by more effective limiters and accurate tuning.

When the interference is caused by transmitters working on adjacent or alternate channels, the beat frequency is far beyond the audio range. In such a case, interference is due to two factors: First, a direct-current component in the output of the discriminator. This component appears when one or both peaks of the frequency deviation (due to the interfering signal) extend into the nonlinear part of the discriminator curve. As long as the interfering signal is an unmodulated carrier, the direct-current component will remain constant. So, by itself, this component will not produce any audible effect, unless the second factor is present. The second factor is the amplitude variation of the frequency-modulated interfering signal, caused by the steep sides of the receiver selectivity curve. The variation of the amplitude of the interfering signal (with the modulation frequency) causes the direct-current component to vary at the same rate, thus producing an audible interference. So a reduction or elimination of either factor will result in a reduction, or almost complete elimination, of the interference. It must be understood, however, that this is true only as long as the peaks of the interfering signal always remains weaker than the carrier of the desired signal; that is, $\rho > 1$.

The amplitude variation of the interfering signal can be eliminated (or at least considerably reduced) by making the selectivity curve almost flat from 120 to 280 kilocycles and from 320 to 480 kilocycles off resonance (for adjacent and alternate channels, respectively).

The direct-current component at the output of the discriminator can be reduced considerably by the following methods:

(a) By retuning the receiver after a transmitter from an adjacent or alternate channel begins to interfere with the received signal. However, it would not be practical to retune a receiver everytime an interfering signal comes on, or changes in strength, unless it is done automatically. An efficient automatic frequency control would reduce this kind of interference appreciably.

Thus, a receiver with crystal-tuned push buttons is at a disadvantage. The amount of detuning necessary to reduce the direct-current component to zero was plotted against ρ for adjacent-channel interference (Fig. 5, curve D).

(b) Theoretically, the direct-current component can be completely eliminated by making the linear part of the discriminator curve infinitely long. The direct-current component would be reduced appreciably if the linear part was extended, at least as far as $2F_{cn}$ on each side of the carrier. This would mean a reduction of interference at the expense of sensitivity. Many compromises and combinations of the methods described are possible.

Appendix

The composite signal at the output of the limiter can be represented by the expression

$$e = A \sin \left\{ \omega_c t + \beta \cos pt + \tan^{-1} \frac{\sin \left[\omega_{cn} t - \phi(t) + \beta \cos pt\right]}{\rho + \cos \left[\omega_{cn} t - \phi(t) + \beta \cos pt\right]} \right\}. \quad (10)$$

When neither signal is modulated, (1) becomes

$$e = A \sin \left[\omega_c t + \tan^{-1} \frac{\sin \omega_{cn} t}{\rho + \cos \omega_{cn} t} \right].$$

Let

$$\tan^{-1} \frac{\sin \omega_{cn} t}{\rho + \cos \omega_{cn} t} = \alpha. \quad (11)$$

$$e = A \sin (\omega_c t + \alpha) = A(\sin \omega_c t \cos \alpha + \cos \omega_c t \sin \alpha) \quad (12)$$

where $\sin \alpha = \sin \omega_{cn} t(1+\rho^2+2\rho \cos \omega_{cn} t)^{-1/2}$ and $\cos \alpha = (\rho + \cos \omega_{cn} t)(1+\rho^2+2\rho \cos \omega_{cn} t)^{-1/2}$. Substituting $(1+\rho^2) = g$, $2\rho/g = g$, and expanding $(1+\rho^2+2\rho \cos \omega_{cn} t)^{-1/2}$ in terms of the harmonics $\cos n\, \omega_{cn} t$,

$$\sin \alpha = \frac{\sin \omega_{cn} t}{q^{1/2}} \sum_{r=0}^{r=\infty} (-1)^r h_r \cos r\omega_{cn} t \quad (13)$$

where

$$\cos \alpha = \frac{\rho + \cos \omega_{cn} t}{q^{1/2}} \sum_{r=0}^{r=\infty} (-1)^r h_r \cos r\omega_{cn} t$$

$$h_0 = 1 + \sum_{k=1}^{k=\infty} \frac{(4k-1)!\, g^{2k}}{2^{2(3k-1)} k!(2k)!(k-1)!} \quad (13a)$$

and

$$h_r = \sum_{k=0}^{k=\infty} \frac{(4k+2r-1)!\, g^{2k+r}}{(2k+r-1)!\, 2^{(6k+3r-2)} k!(k+r)!}.$$

Substituting (13) and (13a) into (12), we obtain

$$e = \alpha_0 \sin \omega_c t + \sum_{r=1}^{r=\infty} (-1)^r [b_r \sin (\omega_c - r\omega_{cn})t - a_r \sin (\omega_c + r\omega_{cn})t] \quad (14)$$

where

$$a_0 = \left(\rho h_0 - \frac{h_1}{2}\right) A \qquad a_3 = (\rho h_3 - h_4) \frac{A}{2}$$

$$a_1 = \left(h_0 - \frac{\rho h_1}{2}\right) A \qquad a_4 = (h_3 - \rho h_4) \frac{A}{2}$$

$$a_2 = (h_1 - \rho h_2) \frac{A}{2} \qquad b_r = (\rho h_r - h_{r+1}) \frac{A}{2}$$

$$r = 1, 2, 3, \cdots.$$

For reasonable accuracy a fundamental and four sideband components (two pair) would be sufficient. When applied to a diode circuit, this expression will have different coefficients due to the selectivity of the circuit. Equation (14) will become

$$e = \alpha_0 \sin \omega_c t + \sum_{r=1}^{r=\infty} (-1)^r [\beta_r \sin (\omega_c - r\omega_{cn})t - \alpha_r \sin (\omega_c + r\omega_{cn})t]. \quad (15)$$

The output of the diode (linear detector) is[3]

$$E = [\alpha_0^2 + \alpha_1^2 + \alpha_2^2 + \beta_1^2 + \beta^2 + 2(\alpha_0\alpha_1 + \alpha_0\beta_1 + \alpha_1\alpha_2 + \beta_1\beta_2) \cos \omega_{cn} t + 2(\alpha_0\alpha_2 + \alpha_0\beta_2 + \alpha_1\beta_1) \cos 2\omega_{cn} t + 2(\alpha_1\beta_2 + \beta_1\alpha_2) \cos 3\omega_{cn} t + 2\alpha_2\beta_2 \cos 4\omega_{cn} t]^{1/2}. \quad (16)$$

Let

$$\alpha_0^2 + \alpha_1^2 + \alpha_2^2 + \beta_1^2 + \beta_2^2 = \psi$$

and the rest of the expression under the radical $= \epsilon$.

Then

$$E = (\psi + \epsilon)^{1/2} = \psi^{1/2} \left(1 + \frac{\epsilon}{\psi}\right)^{1/2}$$

$$= E = \psi^{1/2} \left[1 + \frac{\epsilon}{2\psi} - \frac{1}{2 \cdot 4}\left(\frac{\epsilon}{\psi}\right)^2 + \frac{1 \cdot 1 \cdot 3}{2 \cdot 4 \cdot 6}\left(\frac{\epsilon}{\psi}\right)^3 - \cdots\right]. \quad (17)$$

$\psi^{1/2}$ is the first approximation of direct-current component $= D$. The odd powers of (ϵ/ψ) do not contain constant term and, as we are interested only in the direct-current component, can be neglected. The constant part of the second term is:

$$\gamma = \frac{2}{8\psi^2} [(\alpha_0\alpha_1 + \alpha_0\beta_1 + \alpha_1\alpha_2 + \beta_1\beta_2)^2 + (\alpha_0\alpha_2 + \alpha_0\beta_2 + \alpha_1\beta_1)^2 + (\alpha_1\beta_2 + \beta_1\alpha_2)^2 + (\alpha_2\beta_2)^2]. \quad (18)$$

For $\rho > 2$ the series for D converges rapidly and the first two terms give an accuracy sufficient for all practical purposes.

The direct-current component of a diode is $D_1 \cong \psi_1^{1/2} + \gamma$.

[3] W. L. Everitt, "Communication Engineering," chap. 13, pp. 407; McGraw-Hill Book Co., New York, N. Y.

High-Frequency Excitation of Iron Cores*

J. D. COBINE†, SENIOR MEMBER, I.R.E., J. R. CURRY‡, ASSOCIATE, I.R.E., CHARLES J. GALLAGHER†, AND STANLEY RUTHBERG§

Summary—**Several iron alloys intended for use in wide-band transformers were studied from the point of view of core loss and exciting impedance. Techniques for studying these properties are described, using both high-frequency sine-wave and wide-band random-noise excitation. The frequency range of 0.1 to 5 megacycles was covered. Materials investigated include hipersil, monimax, molybdenum permalloy, and B9W4A.**

Introduction

THE OBJECT of this research was to make a thorough study of the electrical properties of iron-core coils, such as are used in transformers, at frequencies up to 5 megacycles for both sine-wave and random noise excitation.

Simple Theory of Core Losses and Exciting Impedance

The core losses of transformer iron are usually determined as a function of the magnetic-flux density B. For low-frequency sine-wave excitation, the eddy-current power loss P_e is given by

$$P_e = \alpha f^2 t^2 B_m^2 V \tag{1}$$

where f is the frequency, t is the thickness, B_m is the maximum value of flux density, V is the volume of iron, and α is a constant for the material. The hysteresis loss P_h for sine wave is proportional to the number of loops traced per second, and to the maximum flux density raised to some power. Usually the Steinmetz law holds, namely,

$$P_h = \gamma f B_m^{1.6} V \tag{2}$$

where γ is another constant for the material. The value of B_m is proportional to E/fNA where E is the root-mean-square voltage across the core winding, N is the number of turns, and A is the cross-sectional area of the core.

With noise excitation, no simple relations exist between E and B_m, since the applied voltage varies in a completely random manner, and contains not one frequency but a whole band of frequency components. The eddy-current loss with noise excitation has been studied theoretically by Middleton.[1] The theory of hysteresis loss with noise excitation has not been developed. The solution of this problem is very difficult because the loss depends both on B_m and on the relation between B and H, the magnetic field. The relation between B and H depends on the wave form, and, for noise, the exact B-H curve cannot be determined. Fig. 1 shows a possible B-H path with noise, together with a normal induction curve and a sine-wave loop.

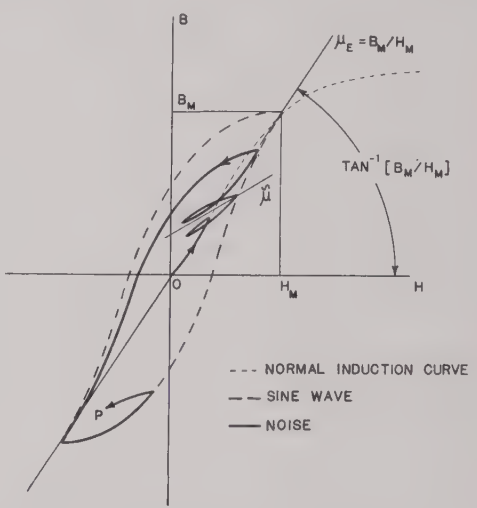

Fig. 1—B-H characteristics.

To study sine wave and noise, it seems reasonable to determine the total iron loss as a function of E/NA, the quantity which determines B_m for a fixed frequency or frequency band. For convenience, we shall refer to E/NA, the "excitation." In obtaining losses with noise, we are concerned in general only with flat voltage spectra; i.e., the root-mean-square noise voltage measured by a narrow-band spectrum analyzer is independent of frequency. In general, losses with noise will depend on the frequency limits of the noise. Thus we shall obtain a series of curves of loss versus excitation, with different frequencies for sine wave, and different frequency limits for noise. Since the losses will depend on the size of the iron core, it is convenient to obtain the loss per gram, or specific loss.

The factors which contribute to the exciting impedance may be considered in an elementary way. An ordinary iron-core inductance is represented elec-

* Decimal classification: R282.3. Original manuscript received by the Institute, July 20, 1946; revised manuscript received, January 9, 1947. This work was done in whole or in part under Contract No. OEMsr-411 between the President and Fellows of Harvard College and the Office of Scientific Research and Development.

† Formerly, Radio Research Laboratory, Harvard University; now, Research Laboratory of General Electric Co., Schenectady, N. Y.

‡ Formerly, Radio Research Laboratory, Harvard University; now, Thompson Chemical Laboratory, Williams College, Williamstown, Mass.

§ Formerly, Radio Research Laboratory, Harvard University; now, University of Michigan, Ann Arbor, Mich.

[1] D. Middleton, "An approximate theory for eddy-current loss in transformers excited by sine-wave or by random noise," Radio Research Laboratory Report No. 411-264. Available at Harvard War Archives, Littauer Building, Harvard University; also, PROC. I.R.E., vol. 35, pp. 270–282; March, 1947.

trically by Fig. 2(a), where E_p is the voltage applied across the winding, E is the voltage actually effective in exciting the core after the voltage drop in the leakage inductance L_p is subtracted, L is the inductance of the core, and R is the effective resistance which is produced by the core losses. If the winding contains only a few turns and is close to the core, E may be assumed equal to E_p, and we then have the simplified circuit of Fig. 2(b).

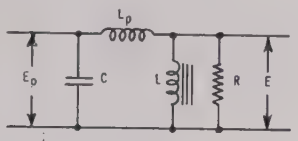

(a)

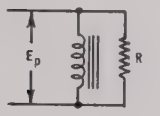

(b)

Fig. 2—Equivalent circuits of an iron-core coil.

The loss component of the exciting impedance R can be estimated from the simple theory. As a reasonable approximation for low excitations,[2] assume that the exponent in the Steinmetz equation may be set equal to 2, rather than 1.6. The volume of the core may be taken as the product of the area A and the mean length of the magnetic circuit l.

$$P_e = \alpha f^2 t^2 B_m^2 A l \tag{3}$$

and

$$P_h \doteq \gamma f B_m^2 A l. \tag{4}$$

For sine-wave excitations

$$E = \delta N A f B_m \tag{5}$$

where δ is a constant. The value of R is defined by the relation

$$R = \frac{E^2}{P_e + P_h}. \tag{6}$$

From (3), (4), (5), and (6), we obtain

$$R = \frac{N^2 A/l}{\left(\frac{\alpha t^2}{\delta^2} + \frac{\gamma}{\delta^2 f}\right)} = \frac{N^2 A/l}{F}. \tag{7}$$

It will be noted that F depends on the frequency, the material, and the lamination thickness, but does not depend on the core geometry. Thus, from this simple theory, the power loss for different cores should be roughly proportional to l/N^2A, if E is assumed constant.

The inductance L of the core is

$$L = \beta \tilde{\mu} N^2 A/l \tag{8}$$

where β is a constant and $\tilde{\mu}$ is the variational permeability. Then the reactive component of the exciting impedance is

$$X = 2\pi f L = 2\pi \beta \tilde{\mu} f N^2 A/l. \tag{9}$$

The exciting impedance is

$$Z = \frac{RX}{\sqrt{R^2 + X^2}} = \frac{2\pi\beta f\tilde{\mu}}{\sqrt{1 + (2\pi F \beta f \mu)^2}} \frac{N^2 A}{l}. \tag{10}$$

Thus, both the resistance and the impedance can be expressed as the product of two factors. One contains the frequency, the thickness, and the constants of the material, and the other depends on the number of turns and the geometry.

Types of Transformer Materials

The materials studied were as follows:

hipersil —0.001 and 0.002 inch ("C" Butt)
molybdenum permalloy —0.001 inch (continuous ribbons)
B9W4A —0.004 inch ($C-I$ Punchings)
monimax —0.003 inch ($C-I$ Punchings).

The investigation covered core sizes ranging from $\frac{1}{4} \times \frac{3}{8}$-inch area with a mean length of $3\frac{1}{2}$ inches to $1\frac{1}{2} \times 1\frac{1}{2}$ inches with a mean length of 14 inches.

Experimental Methods of Investigation

The exciting impedance of a core may be studied directly by current-voltage measurements. For sine-wave excitation the technique is well understood and presents no special problems. With noise, it is necessary to specify how the currents and voltages are to be measured. In general, the quantities of interest are the root-mean-square values of current and voltage, which may be measured with wide-band thermocouple instruments. The ratio of root-mean-square noise voltage to root-mean-square noise current defines a noise-exciting impedance which depends on the shape and frequency limits of the noise spectrum. This we may call the "wide-band impedance," Z_w.

A pseudo-sine-wave impedance for noise may be defined by taking the ratio of the noise voltage in a small frequency range to the noise current in that same range. This ratio we shall call the "narrow-band noise impedance," to be denoted by the symbol Z_n. In general, it will be a function of frequency. This impedance must be measured with a wave analyzer[3] which measures the noise voltage in a small frequency range centered at the desired frequency. The noise voltage is obtained by

[2] Electrical Engineering Staff, M.I.T., "Magnetic Circuits and Transformers," p. 129, John Wiley and Sons, Inc., New York, N. Y., 1943.

[3] G. P. McCouch and P. S. Jastram, "Video spectrum analyzer," Radio Research Laboratory Report No. 411-96, July 10, 1944.

measuring the spectrum of the voltage across the core. The noise current is obtained by measuring the spectrum across a known series resistor.

The total core loss may be measured directly for both sine wave and noise excitation. For sine wave the hysteresis and eddy-current components can be separated.[4] For noise no such separation is possible. Two methods were used in measuring total losses:

1. Calorimeter Measurements

This method involves a direct measurement of power dissipated by immersing the core in a calibrated calorimeter filled with transformer oil, and noting the temperature rise for a definite interval of time. To calibrate the calorimeter, a known amount of power is introduced into the calorimeter for the same time interval. This method gives results with errors of the order of 10 per cent. Care must be taken to make calibrations and heat runs under approximately the same conditions of room temperature. This method is applicable to both sine-wave and noise excitation. The chief disadvantage is the time required to make a single measurement.

2. Current-Voltage Method

This method can best be explained by considering the circuit of Fig. 3. The effective resistance and reactance

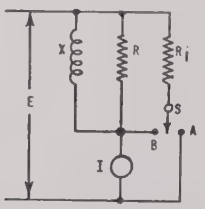

Fig. 3—Circuit for power measurement.

of the core are represented by R and X, respectively. Both R and X will depend on frequency and, to some extent, on excitation. The current through the shunting resistance R_1 can be passed through the meter or shunted around it by the switch S. Let E be the root-mean-square voltage across the core. Then, with the switch at A, the root-mean-square current through the meter is

$$I = \frac{E}{Z} = E\sqrt{\frac{1}{R^2} + \frac{1}{X^2}}. \tag{11}$$

With E held constant (both amplitude and frequency characteristics), the switch is shifted to B. The root-mean-square current through both R_1 and core then passes through the meter. This current is

$$I_1 = E\sqrt{\left(\frac{1}{R} + \frac{1}{R_1}\right)^2 + \frac{1}{X^2}}. \tag{12}$$

Squaring both equations, and subtracting (11) from (12), we obtain

$$I_1^2 - I^2 = E^2\left[\left(\frac{2}{R} + \frac{1}{R_1}\right)\left(\frac{1}{R_1}\right)\right]. \tag{13}$$

Since the power dissipated in the core is

$$P = \frac{E^2}{R}, \tag{14}$$

we obtain for the power finally

$$P = \frac{1}{2}\left[(I_1^2 - I^2)R_1 - \frac{E^2}{R_1}\right]. \tag{15}$$

Thus, if the currents and voltages are measured on root-mean-square-reading meters and the value of R_1 is known, the power is obtained from a simple calculation. It must be emphasized that the value of E must be identically the same in both current measurements.

The current-voltage method in general is more satisfactory than the calorimeter method. The errors are about the same in magnitude, i.e., 10 per cent, and the time required for measurements is much less. Careful checks were made to compare the two methods and the power losses obtained were in good agreement, even though the current-voltage method is not rigorously applicable to noise. Some of the data presented in this paper were obtained by calorimeter and some by current-voltage technique. No attempt will be made to distinguish between the two in the discussion to follow.

Experimental Results

Impedance Measurements

The expression for $Z(10)$ indicates that Z is independent of excitation except for the variation in $\tilde{\mu}$, which is small in the range covered. It was found that Z increased only slightly with excitation, and the error in assuming it independent of excitation is less than 10 per cent.

The dependence of Z on N^2A/l is shown graphically in Fig. 4(b) for sine wave. The ratio of the impedance to N^2A/l is plotted as a function of frequency for a number of cores of 2-mil hipersil. Although the cores were quite different in size, the curves should lie fairly close together, if (10) is a good approximation. As the curves show, the agreement with the equation is not very satisfactory. A better result is obtained by plotting Z/N^2A against frequency (Fig. 4(a)). Apparently the length of the magnetic circuit does not play an important part in determining the impedance, possibly

[4] See page 151 of footnote reference 2.

because of the presence of small air gaps. The spread in the curves of Fig. 4(a) is probably caused by core-to-core variations in $\tilde{\mu}$.

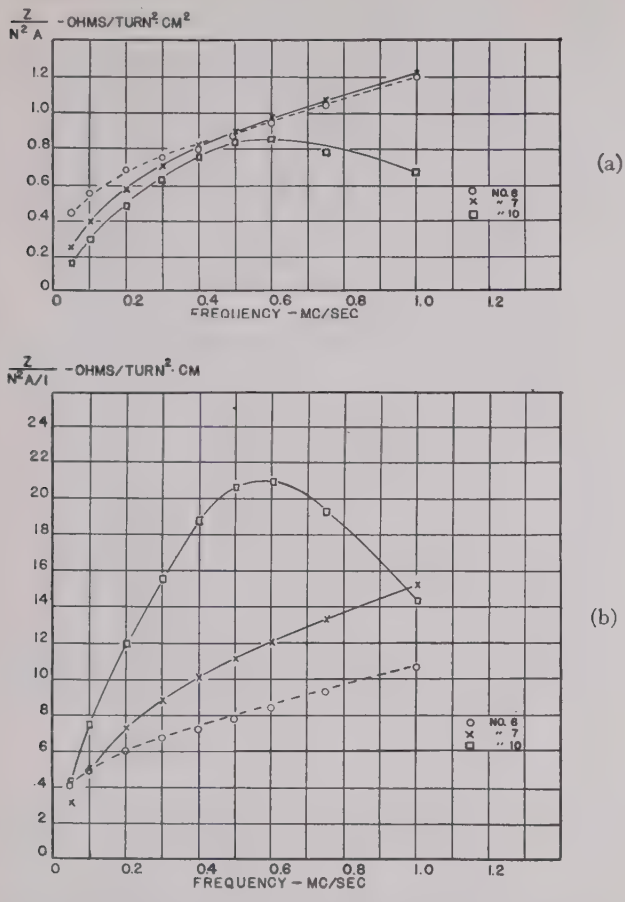

Fig. 4—Impedance characteristics of 0.002-inch hipersil with sine-wave excitation.

No.	Area (cm.²)	Mean length (cm.)
6	0.605	8.9
7	1.61	12.5
10	10.1	24.3

$N = 30$

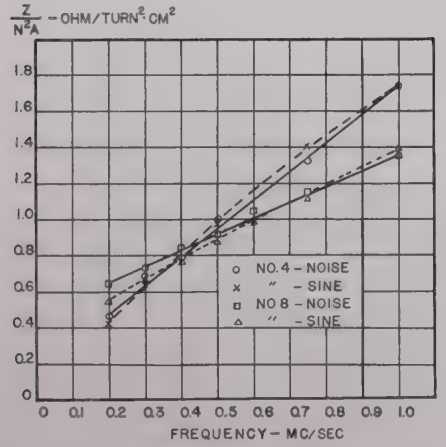

Fig. 5—Sine-wave and narrow-band noise impedances (Z and Z_n) as functions of frequency for 0.002-inch hipersil.
Core No. 4, mean length = 6.75 centimeters
cross section = 0.95 × 0.635 centimeter
Core No. 8, mean length = 14.9 centimeters
cross section = 0.48 × 1.27 centimeters.

Fig. 5 shows Z/N^2A and Z_n/N^2A for two hipersil cores of different length and substantially the same cross-sectional area as functions of frequency. The agreement between Z and Z_n is remarkably close over the frequency range studied. In fact, we may consider them to be identical.

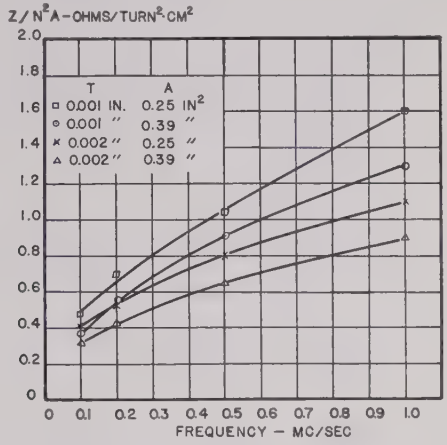

Fig. 6—Z/N^2A versus frequency for hipersil cores of different cross-section A and thickness T.

Fig. 6 shows Z/N^2A for two sizes of hipersil core, each size available in 1-mil and 2-mil thickness. As (10) indicates, the impedance increases as the thickness is decreased. Each curve represents the average value for five cores. Deviations from the average value may be as high as 50 per cent, due to variations in $\tilde{\mu}$. Fig. 7

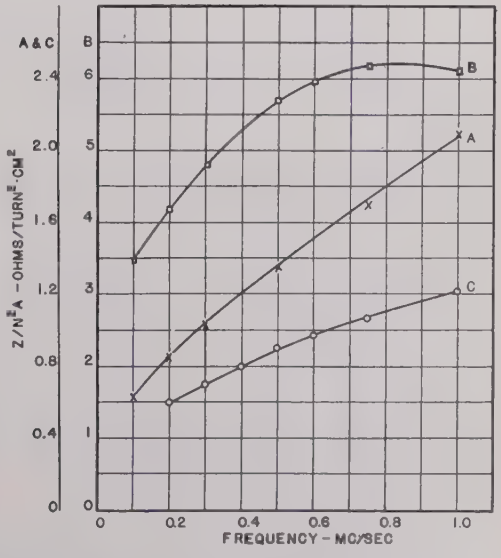

Fig. 7—Z/N^2A versus frequency for three materials.
(a) 0.003-inch monimax
(b) 0.001-inch molybdenum permalloy
(c) 0.002-inch hipersil.

permits a comparison between the impedance values of hipersil, monimax, and molybdenum permalloy. The impedance is lowest for hipersil, highest for permalloy.

The dependence of wide-band impedance (Z_w) on bandwidth is shown in Fig. 8 for one hipersil core. The

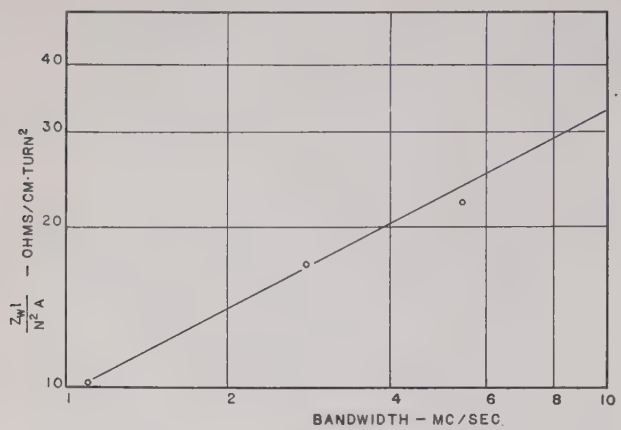

Fig. 8—Wide-band impedance versus bandwidth for 0.002-inch hipersil. Slope of line = 0.5.

lower frequency limit was kept at 100 kilocycles per second. The line is drawn to have a slope of 0.5. The near coincidence of the points with the line shows that the impedance is nearly proportional to the square root of the bandwidth, as long as the frequency is not high enough to permit shunting capacitances to be important.

the ratio of ordinate to abscissa is $Z_n/N^2A/l$. This curve is useful in predicting the exciting current of a core.

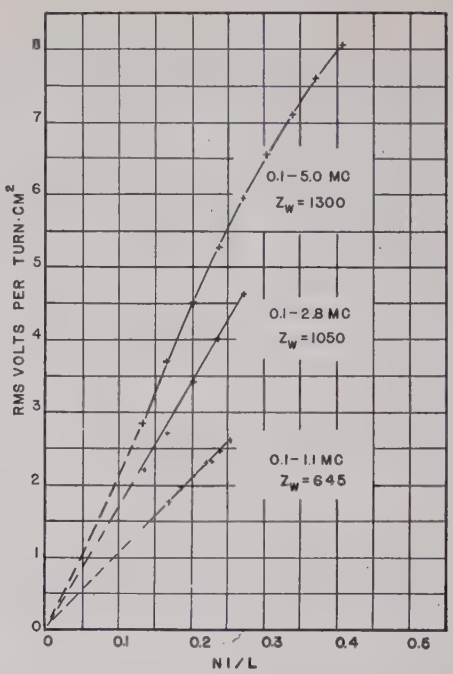

Fig. 9—Wide-band excitation characteristics for 0.002-inch hipersil. N = turns; I = root-mean-square exciting current; l = mean core length.

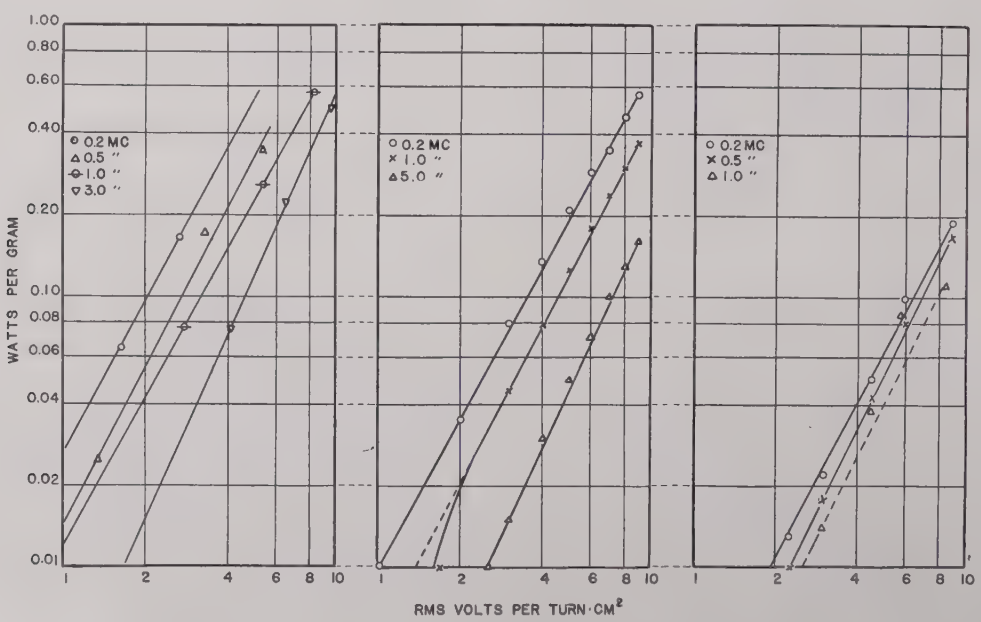

Fig. 10—Core loss characteristics for sine-wave excitation.
(a) 0.002-inch hipersil
(b) 0.001-inch hipersil
(c) 0.001-inch molybdenum permalloy.

Fig. 9 presents essentially the same data from a different aspect. Here are plotted values of E/NA (excitation) against NI/l where I is the exciting current. Note that

Core Losses

Curves of specific core loss (watts per gram) versus excitation are shown in Fig. 10 for sine wave, and in

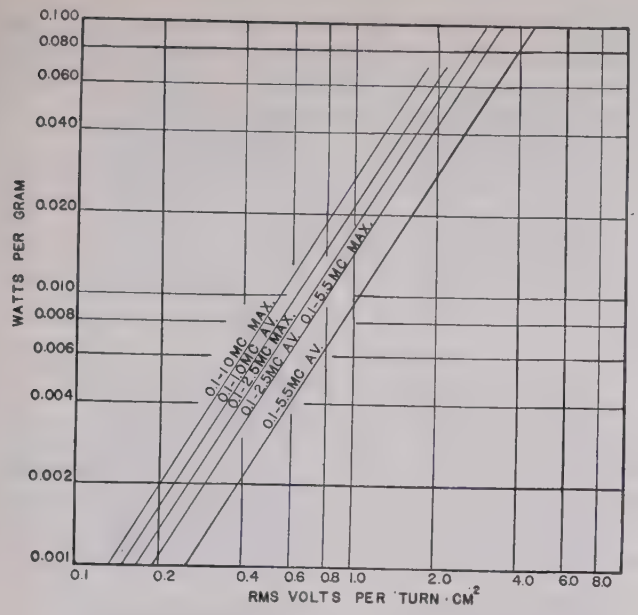

(a)

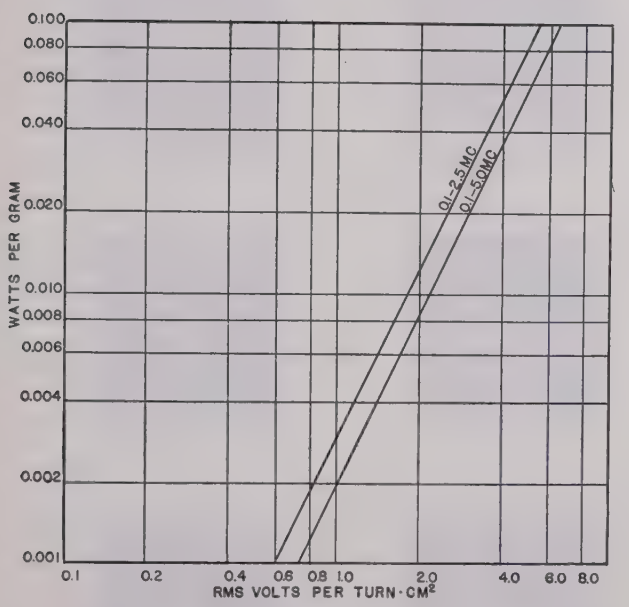

(b)

Fig. 11—Core-loss characteristics for noise excitation of different bandwidths.

(a) 0.002-inch hipersil
(b) 0.004-inch B9W4
c) 0.003-inch monimax.

(These curves are for a number of different cores, "Max." indicating the maximum loss observed and "Av." the average of all the cores.)

Fig. 11 for noise. Note that all curves can be represented by equations of the form $P=K(E/NA)^x$, where x varies between 1.8 and 2.1. Fig. 10(a) and (b) show the loss for 2- and 1-mil hipersil cores at different frequencies. It will be noted that the losses for the 1-mil are less than for the 2-mil core. Fig. 10(c) presents loss data for 1-mil permalloy.

Fig. 11 shows the variations of specific loss with excitation for different noise bandwidths. The materials here are 2-mil hipersil, 4-mil B9W4A, and 3-mil

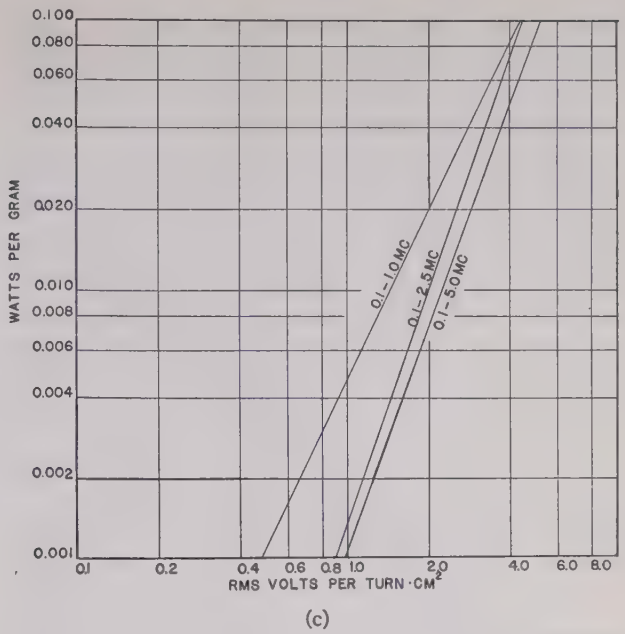

(c)

monimax. The losses in general decrease as the bandwidth is increased at constant excitation. In fact, the loss appears to be inversely proportional to the square root of the bandwidth (see Fig. 12).

Fig. 13 shows a plot of specific loss versus noise-volt-amperes per gram for a number of hipersil cores with different turns and sizes, and for different bandwidths. The ratio of the ordinate to the abscissa is readily shown to be the power factor of the core. Curve A is drawn to have unity power factor. The minimum power

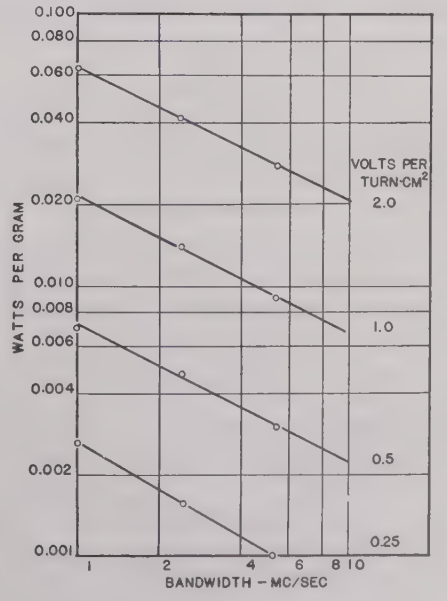

Fig. 12—Core loss versus bandwidth of noise for 0.002-inch hipersil.

factor for the various points is about 0.46. The average value is 0.69, as shown in curve B. This curve represents most of the points quite well, especially in the high-excitation range. Despite the arbitrary differences

in size of core, number of turns, and noise bandwidth, the points fall quite close to the average line, so that this line may be used to predict approximately the losses from 2-mil hipersil.

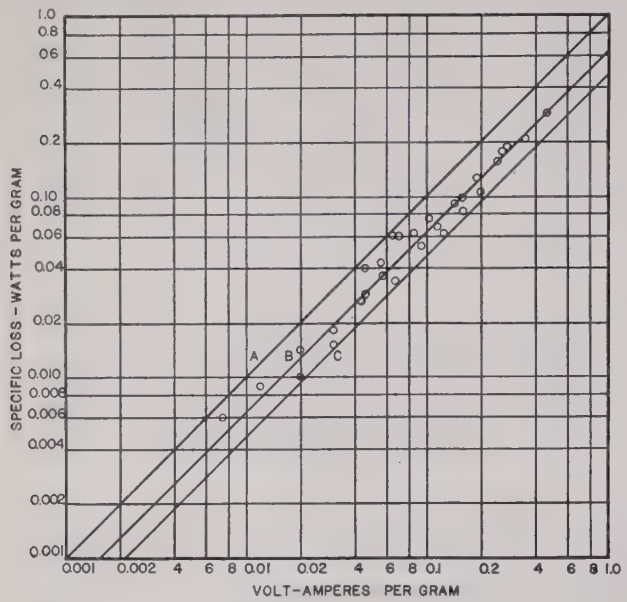

Fig. 13—Specific losses as function of specific volt-amperes for 0.002-inch hipersil.
(A) Power factor = 1.000
(B) Power factor = 0.690
(C) Power factor = 0.465.

The hysteresis and eddy-current losses may be separated in the usual manner for sine wave.[4] The calculated eddy-current loss is plotted as a function of frequency in Fig. 14. The curve agrees qualitatively with the theoretical curve obtained by Middleton.[1]

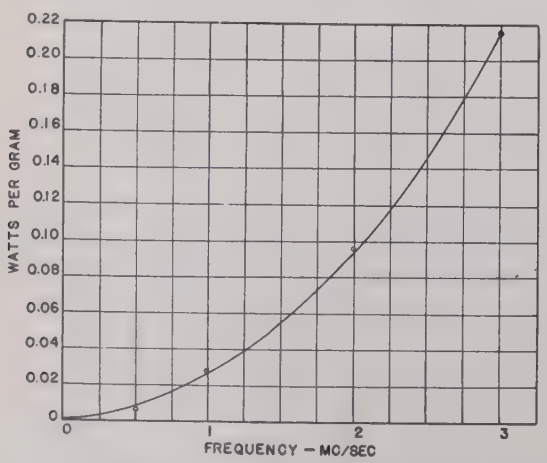

Fig. 14—Eddy-current loss for 0.002-inch hipersil with sine-wave excitation; $B = 400$ gauss.

B-H Curves

A picture of the hysteresis effect may be obtained by studying the *B-H* loops for a core. These loops may be obtained on an oscilloscope screen by using the circuit shown in Fig. 15. According to Faraday's law, $B = -(1/NA)\int e dt$. Thus, if we shunt the core with a simple resistance-capacitance integrating circuit, the integrated voltage developed across the capacitor C will be proportional to B. The voltage developed across a small series resistor is proportional to the existing current, and hence to H. These two voltages are applied simultaneously to the vertical and horizontal deflecting plates of an oscilloscope, and the pattern obtained has the shape of the *B-H* curve. Distributed capacitance was kept to a minimum to reduce the uncertainty in H.

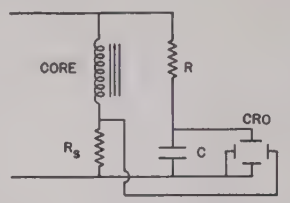

Fig. 15—Circuit for *B-H* cyclograms.

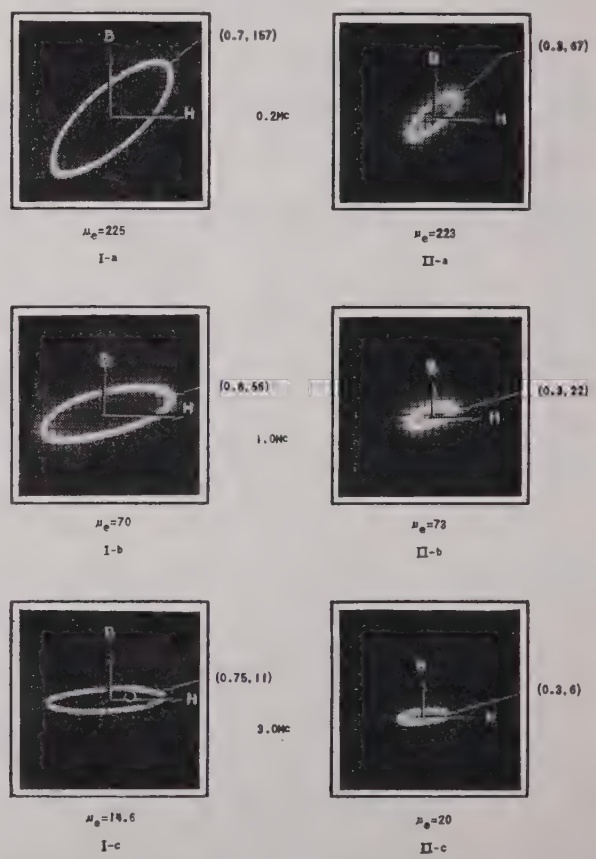

Fig. 16—Sine wave *B-H* curves for 0.002-inch hipersil for two values of excitation. $N = 30$, $A = 0.605$ centimeter squared, $l = 8.85$ centimeters. Parentheses indicate peak values of H in oersteds and B in gauss.
(a) $f = 0.2$ megacycle
(b) $f = 1.0$ megacycle
(c) $f = 3.0$ megacycles.

Photographs of the resulting patterns are shown in Figs. 16 and 17 for a 2-mil hipersil core. The photographs in Fig. 16 were obtained with sine wave for two values of excitation (I and II) and at three frequencies (0.2, 1.0, and 3.0 megacycles). Similar photographs are shown in Fig. 17, I-b and II-b for noise, for

approximately the same values of excitation, for a bandwidth of 2.7 megacycles. In Fig. 17, I-a and II-a show the "wave form" of the noise voltage applied to the core, I-c and II-c show the wave form of the integrated voltage across the capacitor, and I-d and II-d show the current wave form.

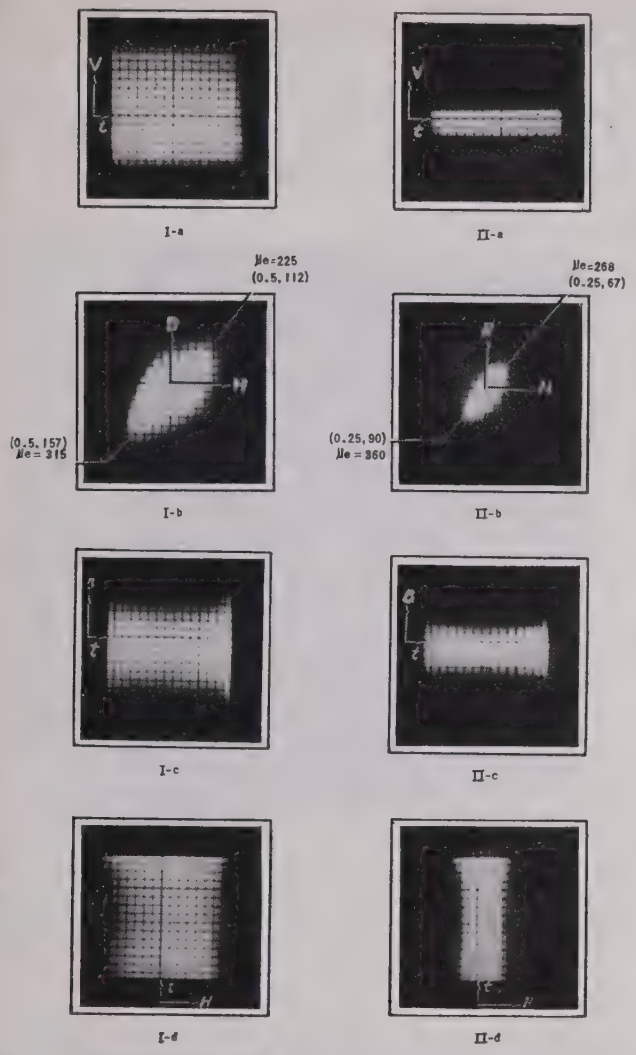

Fig. 17—Noise characteristics of 0.002-inch hipersil. $N=30$, $A=0.605$ centimeter squared, $l=8.85$ centimeters. Parentheses indicate peak values of H in oersteds, and B in gauss.

	Exciting Current	Peak-to-Peak Voltage
I	66 milliamperes root-mean-square	307
II	20 milliamperes root-mean-square	72
	(a) Voltage versus time	
	(b) B versus H	
	(c) B versus time	
	(d) H versus time.	

From the hysteresis loops shown, the effective permeability μ_e can be calculated from the relation

$$\mu_e = \frac{B_{\max}}{H_{\max}}.$$

Values of μ_e obtained for the sine-wave case are plotted in Fig. 18 as a function of frequency. The permeability is seen to decrease with increasing frequency, just as might be expected from theory.[1] The evaluation of the effective noise permeability is not quite so simple because the loops are not symmetrical. This dissymmetry is probably the result of clipping in the noise source, i.e., the applied voltage itself is not symmetrical. One can calculate an average permeability, however, by using the maximum values at both extremes of the loop. The average values of μ_e thus obtained is about 270, which corresponds to the value for a sine wave of about 100 kilocycles. Thus the lower-frequency limits of the noise determine the envelope of the B-H noise loop.

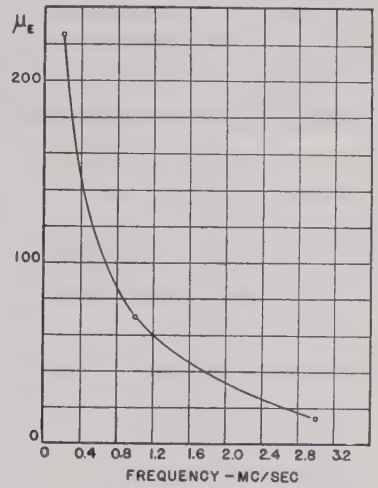

Fig. 18—Dependence of μ_e of 0.002-inch hipersil on frequency for constant excitation.

The hysteresis loss per cycle can also be calculated from the area of the sine-wave loop.[5] For noise, the value of the loss as obtained from the hysteresis loop is meaningless because of the frequency factor. Also, the noise loop is itself made up of many re-entrant loops (see Fig. 1), so that the area enclosed is indeterminate.

It was found that a large superimposed direct-current magnetizing force is required to produce any appreciable change in core loss. In fact, for 1-mil hipersil, with a variational component of the magnetizing force of the order of 0.1 oersted, a direct-current magnetizing force of 2 oersteds caused no change at all, and further increasing the direct-current force to 4.8 oersteds reduced the losses by about 10 per cent. The variational ~ is low and most of the loss is associated with small random loops and is not affected by their location on the magnetization curve.

The data obtained in these studies were used to design an iron-core transformer delivering 350 watts of random noise into a 50-ohm load. The frequency range was from 0.1 to 2.5 megacycles.

Acknowledgment

The authors wish to express their appreciation of the service of Hiram Gratrix and Guy Sanders, whose mechanical ingenuity greatly facilitated the research.

[5] See page 489 of footnote reference 2.

Wide-Range Double-Heterodyne Spectrum Analyzers*

L. APKER†, J. KAHNKE‡, ASSOCIATE, I.R.E., E. TAFT†, AND R. WATTERS†, ASSOCIATE, I.R.E.

Summary—Spectrum analyzers using double-heterodyne converter units can cover very wide frequency bands. A typical instrument described in this paper covers the range from 10 to 3000 megacycles. The signal frequency is changed to 24,600 megacycles by a crystal mixer and a special beating oscillator. A band-pass filter network rejects undesired frequencies and passes the output of the first mixer to a second crystal, where the frequency is reduced to 115 megacycles. A narrow-band amplifier increases the level at this frequency and drives a cathode-ray presentation unit.

Also mentioned are two other analyzers using production oscillators and covering smaller ranges. The succeeding sections of the paper discuss qualitatively the following points: frequency stability, losses and noise figure, and suppression of spurious responses.

I. Introduction

IT HAS been known since 1925 that a receiver using two heterodyne stages separated by a relatively high-frequency band-pass filter is capable of reception over a very wide range.[1,2] In previous applications of this principle, the filter was incorporated in an amplifier. The noise figure was accordingly determined only by the quality of the first mixer and by that of the first tube in the amplifier. The frequency range over which such a receiver will operate is equal to that covered by the beating oscillator which drives the first mixer. A very wide frequency band may be covered, therefore, by using ultra-high-frequency oscillators.

This scheme is useful in spectrum analyzers. Since amplifiers are not available at the high frequencies most useful in this work, however, the noise figure and the suppression of spurious responses are affected by the quality of both the first and second mixers as well as that of the band-pass filter. This paper discusses qualitatively some general considerations useful in the design of this type of analyzer.

II. Typical Experimental Analyzers

Fig. 1 is a photograph of an analyzer[3] designed to cover, with a single tuning control, the frequency range from 10 to 3000 megacycles. Fig. 2 is a schematic diagram showing its principal components.

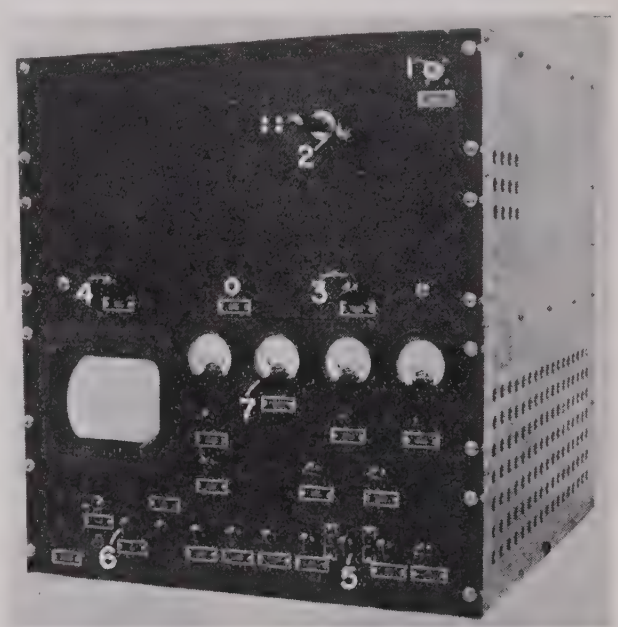

Fig. 1—Front view of analyzer for the frequency range 10 to 3000 megacycles. 1. Signal input. 2. Frequency meter. 3. Main tuning control. 4. Second-beating-oscillator tuning control. 5. "Presentation switch." 6. Gain control. 7. Automatic-frequency-control crystal-current meter.

The signal is applied to the first crystal mixer in a two-crystal converter unit shown schematically in Fig. 3. The pertinent components are enclosed in a dashed line in Fig. 2. In the first crystal, the signal is mixed with the output of the first reflex beating oscillator, which is thermally tunable from 24,590 to 21,600 megacycles.[4] The frequency of this oscillator is also swept electronically in synchronism with an oscilloscope trace in the usual way.[5] A band-pass filter rejects undesired components in the output of the first mixer and delivers the 24,600-megacycle power to a second crystal mixer, which reduces the frequency to 115 megacycles. The level is increased at the latter frequency by a narrow-band amplifier until it is sufficient to permit detection, video amplification, and presentation in the usual fashion.[6]

* Decimal classification: R371.2. Original manuscript received by the Institute, July 10, 1946; revised manuscript received, September 19, 1946. Presented, New York Section, I.R.E., May 1, 1946; presented, Williamsport Section, I.R.E., Williamsport, Pa., September 4, 1946. This paper is based on work done for the Office of Scientific Research and Development under Contract, No. OEMsr-931 with the General Electric Company.

† Research Laboratory, General Electric Company, Schenectady, N. Y.

‡ Engineering Research Associates, Inc., St. Paul, Minn.

[1] H. F. Elliot, U. S. Patent No. 1,867,214; December, 1925.

[2] Harvey Kees, "Receiver with 2 megacycle i.f.," *Electronics*, vol. 18, pp. 129–131; April, 1945.

[3] The predecessor of this analyzer is one developed by J. H. Rubel to cover the range from 100 to 1400 megacycles. The following frequencies are used in this earlier instrument to drive a single crystal mixer connected to the input of a 50-megacycle narrow-band amplifier: (1) the signal; (2) the output of a beating oscillator variable in frequency from 8300 to 9600 megacycles; and (3) the output of a beating oscillator fixed in frequency at 9750 megacycles. This work was done for the Office of Scientific Research and Development under Contract No. OEMsr-931 with the General Electric Company. At this date it has been discussed only in reports having limited distribution.

[4] The authors are indebted to J. O. McNally and P. Kusch of the Bell Telephone Laboratories for the special beating oscillators used in this work. To J. M. Lafferty of this laboratory the authors are indebted for special mechanically tunable oscillators.

[5] F. J. Gaffney, "A spectrum analyzer for microwave pulsed oscillators," presented, I.R.E. Winter Technical Meeting, January 25, 1946, New York, N. Y.

[6] Everard M. Williams, "Radio-frequency spectrum analyzers," PROC. I.R.E., vol. 23, pp. 18–22; January, 1946.

Two resonant-cavity transmission filters separated by a quarter-wavelength of wave guide and tuned to 24,600 megacycles make up the band-pass filter. The pass band is about 40 megacycles wide. There is a resonant-cavity rejection filter with roughly the same bandwidth coupled to the wave guide approximately one-half wavelength from each of the crystal mixers.

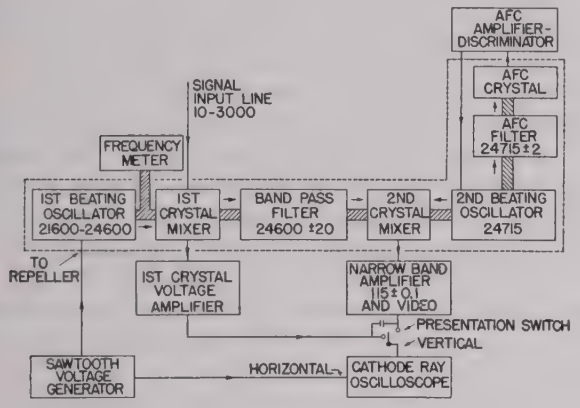

Fig. 2—Schematic diagram showing principal components of the analyzer in Fig. 1. Low-frequency lines are shown single; waveguides, crosshatched. The dashed line encloses the converter unit. Frequencies are given in megacycles.

These cavities are also tuned to 24,600 megacycles and act at this frequency as high impedances in series with the guide. They serve to decouple the mixers from the beating-oscillator lines and reduce the loss of 24,600-megacycle power. Their effect at other frequencies is negligible, of course. They are placed at the proper positions to effect optimum transfer of 24,600-megacycle power from the first mixer to the second. They should be considered part of the filter network.

The input line is standard 50-ohm coaxial cable terminated at the converter unit with a 55-ohm disk resistor. The signal is applied by way of the usual type of "crossbar" perpendicular to the plane of Fig. 3 at the middle of the wave guide. The first crystal is connected in parallel with the disk. Since the impedance of the crystal at signal frequencies is of the order of magnitude of 500 ohms, the input line remains reasonably well terminated as the analyzer is tuned over its range.

The frequency meter is a standard type of absorption cavity coupled through a small hole in the broad side of the first-oscillator wave guide. At the frequency for which it is tuned it reduces the power incident on the first crystal, producing about a 5 per cent decrease in the voltage across the unit. The first-crystal-voltage amplifier, shown in Fig. 2, is connected to the crystal through a 2000-ohm decoupling resistor to prevent any appreciable influence on the impedance of the signal input line. The "presentation switch" permits the display of the crystal voltage on the oscilloscope as a function of the horizontal sweep voltage and therefore, of course, as a function of frequency. The effect of the frequency meter is to produce a small reversed "pip" on the crystal-voltage display. Because of the small coupling capacitor shown in Fig. 2, any signals present on the output of the 115-megacycle amplifier will also appear as small differentiated "pips" on the first-crystal-voltage oscilloscope display.

The horizontal sweep frequency is normally 60 cycles. A phasing control is provided to facilitate inspection of signals which happen to be pulsed or modulated at this frequency. In addition, the sweep frequency may be varied from 40 to 90 cycles if desired.

The second beating oscillator is held close to an average frequency of 24,715 megacycles by a standard type of automatic frequency control. A small 60-cycle sine-wave voltage is applied to the repeller of the oscillator in order to produce about 1 megacycle of frequency modulation on its output. A portion of the output power is delivered to a resonant-cavity transmission filter with a bandwidth of about 5 megacycles centered at 24,715 megacycles. The amplitude-modulated output of the filter is rectified by the automatic-frequency-control crystal shown in Fig. 2 and is applied to the input of a 60-cycle amplifier and phase discriminator. The phase of the amplitude modulation changes by 180 degrees as the frequency of the second beating oscillator passes from one side of the filter resonance point to the other.

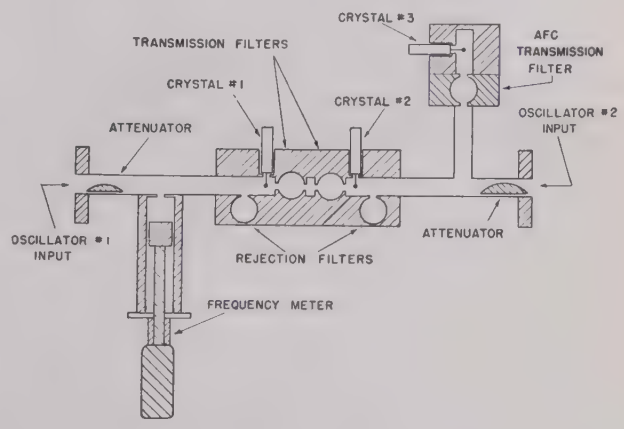

Fig. 3—Schematic diagram of the converter unit. The input and output lines are perpendicular to the plane of the diagram and are shown by dots at the ends of the center conductors to the crystal cartridges.

The direct-current output of the discriminator accordingly changes sign and passes through zero at resonance. It is returned to the thermal tuner of the beating oscillator in such a direction that the 60-cycle component in the output of the crystal is reduced to zero. The frequency of the oscillator is thus held at the center of the pass band of the automatic-frequency-control transmission filter.

The 115-megacycle amplifier is made up of seven sharply tuned stages operated at a maximum gain of about 17 decibels per stage. The over-all bandwidth is 200 kilocycles, and this is roughly the resolving power

of the analyzer.[7] The tuning elements are high-Q, capacitance-loaded sections of coaxial line connected in the grid circuits of the amplifier tubes. The amplifier proper is followed by a diode detector, a logarithmic video-amplifier stage, and a cathode-follower stage, all mounted on the same chassis. A photograph of the top chassis of the analyzer is shown in Fig. 4. The resonant-line tuning elements may be seen projecting from the top of the amplifier chassis.

Other converters have been constructed for the ranges from 10 to 1200 megacycles and from 1100 to 2400 megacycles by using production beating oscillators operating over various parts of the frequency range from 7000 to 9600 megacycles.

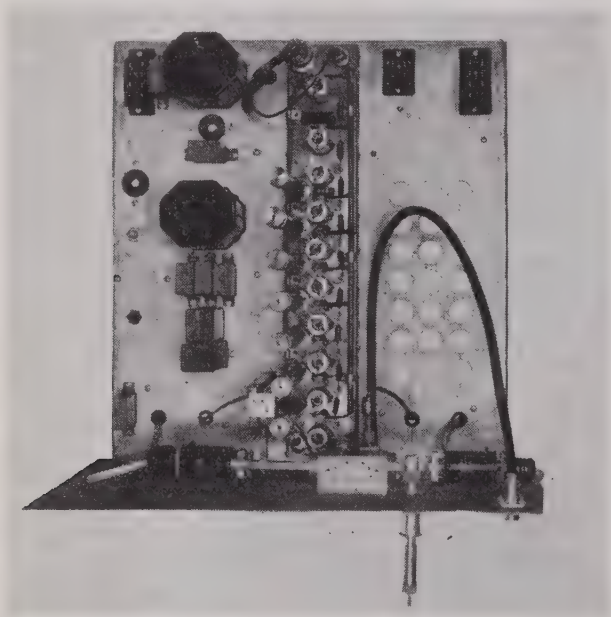

Fig. 4—Top view of the upper chassis showing the mounting of the converter unit and the 115-megacycle amplifier.

The power supplies in all cases are of the usual electronically regulated type. The ripple on the 300-volt beating-oscillator plate supply is held to less than 5 millivolts.

The analyzer described first in this section will be mentioned to illustrate points in the following parts of this paper. Except as noted, the arguments apply equally well to the other analyzers mentioned.

III. Frequency Stability

A relatively high degree of frequency stability is required of the beating oscillators in double-heterodyne analyzers. This stability is attainable, however, with modern reflex oscillators and with properly regulated power supplies. Types of instability are the following:

(1) Slow drifts in frequency, principally due to thermal effects (if automatic frequency control is used, this source of trouble is limited to the first beating oscillator).

(2) Irregular rapid changes in frequency due mainly to vibration.

(3) Rapid changes occurring at a 60-cycle rate and due to magnetic effects from the alternating currents in the heaters or to ripple on the plate power-supply voltages.

(4) The 60-cycle frequency modulation deliberately produced on the output of the second beating oscillator by the automatic-frequency-control circuits.[8]

If both the first and second beating oscillators drift simultaneously by the same amount, the signal "pips" will, of course, remain stationary on the oscilloscope. Rapid changes of type (3) are frequently of this nature. Slow drifts of this sort occur only when automatic frequency control is not used, and then only fortuitously. In order that the sensitivity remain constant, the attenuation of the band-pass filter must be constant over a frequency range equal to the amount of the frequency drift.

It is evident that cyclic variations in beating oscillator frequency occurring in synchronism with the oscilloscope sweep will produce no instability of the signal "pip." In the analyzers of Section II, both the frequency modulation (4) and the sweep frequency are normally fixed at 60 cycles. A phasing control on the sweep-generator trigger permits examination of signals pulsed or modulated at this frequency. The only effect, then, of frequency variations of types (3) and (4) is to produce a slight shift of the signal "pip" when the phasing control is used. This shift corresponds to a frequency change of less than 1 megacycle.

If sweep frequencies other than 60 cycles are used, variations (3) and (4) cause a periodic shift of the signal "pip" equal to that produced when the phasing control is used. Since most of this shift is due to variation (4), it may be minimized by driving the automatic-frequency-control circuits and the sweep circuits at the same frequency, if variable sweep frequencies are often used.

When the sweep bandwidth is set at its minimum value of 10 megacycles, instability due to the irregular frequency variations (2) is not observable unless the analyzer is given an appreciable shock. Slow drifts of type (1) are such that no readjustment of the main tuning control is required over a period of ten minutes.

IV. Losses and Noise Figure

Since a spectrum analyzer is almost invariably in the vicinity of the signal source being investigated, large signal intensities are available. The noise figure is obviously not as important as it is in the case of receivers for distant and weak signals. The production of spurious re-

[7] A detailed discussion of the factors determining the resolving power of an analyzer is given by Williams in footnote reference 6.

[8] This difficulty may be eliminated in a refined instrument through the use of the automatic-frequency-control system recently proposed by R. V. Pound, "Electronic frequency stabilization of microwave oscillators," presented, I.R.E. Winter Technical Meeting; January 24, 1946, New York, N. Y.

sponses in the type of instrument discussed here becomes more noticeable, however, as the signal power is increased. There is, in addition, the obvious restriction that the signal power must not be so great that the first crystal mixer is damaged. This point is not trivial when frequency spectra extending over wide ranges are to be examined. For these reasons, the large losses inherent in double-heterodyne reception at high frequencies must be held within reason and noise production must be minimized.

The important losses of signal power occur as follows: (1) in the resistance disk that terminates the signal input line; (2) in the resonant cavities of the band-pass filter network; and (3) in the first and second mixers. The noise arises mainly in the second mixer crystal and in the first tube of the 115-megacycle amplifier.

When operated efficiently, the normal crystal mixer presents an impedance of about 500 ohms to signals applied at its low-frequency terminals. The coaxial signal-input line has an impedance of 50 ohms, however, and for quantitative work it is important that this line be terminated over the entire frequency range in something close to its characteristic impedance. To avoid the prohibitive difficulties of broad-band transformers for transferring the signal power to the crystal efficiently, the 55-ohm disk is used to terminate the line and efficiency is sacrificed. When the 500-ohm mixer terminals are shunted across this disk, the termination is quite satisfactory. The slight variation in mixer impedance as the analyzer is tuned causes no difficulty. There is, of course, roughly a 10-decibel loss of signal power involved in this procedure.

The losses in the resonant cavities are small compared to the other losses in the converter unit. The measured "unloaded Q" of the 24,600-megacycle cavities is about 5000. The "loaded Q" is about 1000. Assuming that the effects of impedance mismatches in the converter unit are small, we arrive at a total attenuation of roughly 5 decibels due to the two transmission filters. Approximately 0.5-decibel attenuation is due to each of the two rejection filters,[9,10] since they produce merely high shunt impedances across the crystal terminals instead of the infinite impedances produced by cavities with no dissipation.

The first and second crystal mixers are responsible for the most serious losses in the converter unit. The second mixer, converting 24,600 megacycles to 115, operates under almost the same conditions as the crystal in the normal superheterodyne receiver for the former frequency. Roughly the usual 8.5-decibel loss is to be expected, then, at this point,[11] and the level of the power from the second beating oscillator is important in determining the noise generated by the crystal.

The first mixer, however, converts the relatively low-frequency signal to 24,600 megacycles. It is well known that mixer networks do not in general have the same transmission in both directions.[12] The same crystal may, accordingly, show different losses as a first and as a second mixer.[13,14] Standard silicon crystals, however, usually show very nearly the same loss in the two positions.

In the preceding discussion of losses we have treated the individual components of the converter unit as isolated circuit elements. We have naively assumed that impedances were matched for maximum power transfer at the terminals of each component. Combining these individual losses, therefore, to obtain the total loss of the converter unit leads only to an estimate of the true value, since the assumption of an impedance match at all terminals is not justified.

More accurate calculations treating the converter unit as a single complex network are tedious and will not be presented here. It may be interesting to mention, however, that such calculations verify the following points: (1) The input impedance of the first crystal mixer is about 500 ohms. As stated previously, this is to be expected from the behavior of the usual type of superheterodyne crystal mixer. This impedance is quite insensitive to the load impedance connected to the output of the converter unit. This is not surprising, since the losses in the converter network are relatively high. (2) The total loss in the converter network and input termination agrees within 1 decibel with the value of 33 decibels obtained by combining the losses of the individual components. The effect of internal impedance mismatches is, therefore, small.

The measured noise output of the converter unit is essentially that of the second crystal[15] and corresponds to a "noise temperature" of about 2.5 (a level 4 decibels above thermal noise in the output resistance). This figure added to the 33-decibel total loss of the converter unit and input termination gives a noise figure of 37 decibels for the converter unit. The noise figure of the amplifier is 3 decibels. Using the well-known relations

---

[9] If Q_0 is the "unloaded Q" and if Q_1 is the "loaded Q" of a single transmission filter, the transmission is given very closely by the quantity $1-2Q_1/Q_0$. The dissipation due to a single rejection filter is given by $Q_1/2Q_0$. See footnote reference 10.

[10] A. L. Samuel, "An equivalent circuit for a microwave TR tube," Paper X9, Cambridge meeting, American Physical Society, April 27, 1946. This information is also available in reports having limited distribution.

[11] Since this was written the performance of these crystals has been improved. It should also be noted that the resonant cavities in the converter unit make the second crystal mixer a "high-Q" system. The loss is, therefore, not exactly the same as in the usual broad-band superheterodyne mixer.

[12] L. C. Peterson and F. B. Llewellyn, "The performance and measurement of mixers in terms of linear-network theory," PROC. I.R.E., vol. 33, pp. 458–478, July, 1945.

[13] This phenomenon, termed "reciprocity failure," is especially pronounced when some types of germanium rectifiers are used. Such crystals were furnished for experimental purposes by H. Q. North.

[14] This subject is treated in detail in a book, "Crystal Rectifiers," by H. C. Torrey and C. A. Witmer, to be published in the near future. We are indebted to Dr. Torrey for information given us in advance of publication.

[15] Measurements show (principally because of the subsequent losses in the converter network) that the noise generated in the first crystal is not important. The power level of the first beating oscillator, in contrast to that of the second, is thus not limited by noise generation in the crystal. The loss in the first mixer may therefore be decreased somewhat by raising this power level until it is limited by the oscillator itself or by crystal damage.

for the noise figure of two networks in cascade,[16] we arrive at an over-all noise figure for the analyzer of 38.5 decibels. The sweep frequency of the analyzer is sufficiently low to allow the 115-megacycle amplifier response to build up to its equilibrium value in the time required for the analyzer to sweep across a single-frequency signal. Although the situation is complicated by the logarithmic response of the amplifier, the noise figure quoted should determine the order of magnitude of the smallest signal observable on the oscilloscope screen.

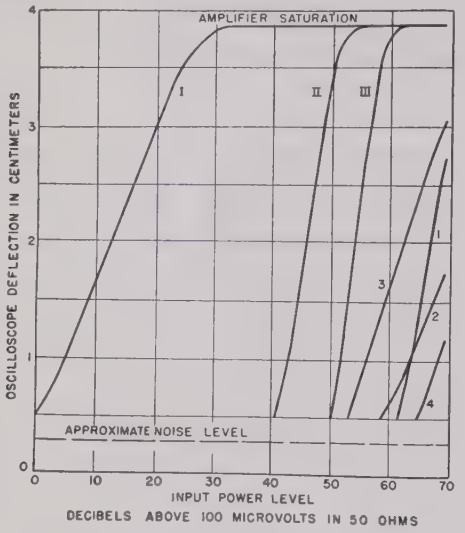

Fig. 5—Response characteristic of the analyzer with gain control at normal setting.
I. Signal, S
II. Second harmonic, $2S$
III. Third harmonic, $3S$
1. Spurious response, $S-(115/2)$
2. Spurious response, $S-(2\times115)$; this is the "115-megacycle-image response"
3. Spurious response, $(S/2)-(115/2)$
4. Spurious response, $(S/3)-2(115/3)$.

A signal of 20 microvolts in the 50-ohm input line (a level 40 decibels above the available thermal noise power from the line) gives a response that is just detectable in the noise on the oscilloscope presentation. The deflections for signal input powers higher than this are shown in curve I of Fig. 5. It is evident that the deflections are proportional to the signal level in decibels over a range of about 30 decibels. An arbitrary reference level of 100 microvolts in 50 ohms is used in this diagram. Because of disturbances due to the noise, signal levels below this value do not give oscilloscope deflections that can be measured reliably. Deviations from the straight line of curve I also occur in this region.

[16] H. T. Friis, "Noise figures of radio receivers," PROC. I.R.E., vol. 32, pp. 419–422; July, 1944. The noise figure of two networks is given by

$$F_{\text{over-all}} = F_1 + \frac{F_2 - 1}{G_1}.$$

In the case above this gives

$$5000 \text{ (or 37 db)} + \frac{2-1}{1/2000 \text{ (33 db)}} = 7000 \text{ (or 38.5 db} = F_{\text{analyzer}}.$$

V. Spurious Responses

Because of the untuned input circuit, all signals within the frequency range of the analyzer are impressed on the first crystal simultaneously. This leads immediately to the possibility of two types of spurious responses. The first of these is due to the production of beat frequencies when two large signals enter the receiver at the same time. This is not as serious in a spectrum analyzer, of course, as it would be in a receiver, since in the analyzer the signal of interest is usually larger than the others. Fig. 6 shows the magnitude of a typical response of this type. Signal number 1 has a frequency of 700 megacycles, and number 2 is 300 megacycles. The powers required at these frequencies to produce reference-level and saturation responses at 400 megacycles are shown by the two straight lines in the figure. Thus, two such signals each 40 decibels above the 100-microvolt reference level will produce a response equal to that produced by a 100-microvolt, 400-megacycle signal. To produce amplifier saturation, two signals each 58 decibels above the reference level are required. It is evident from the straight lines in Fig. 6 that the magnitude of the spurious response is proportional to the product of the two signal powers that produce it. It is also evident that this sort of spurious response is not observable if the signal of interest is not more than 35 decibels below the level of the strongest signal entering the receiver.

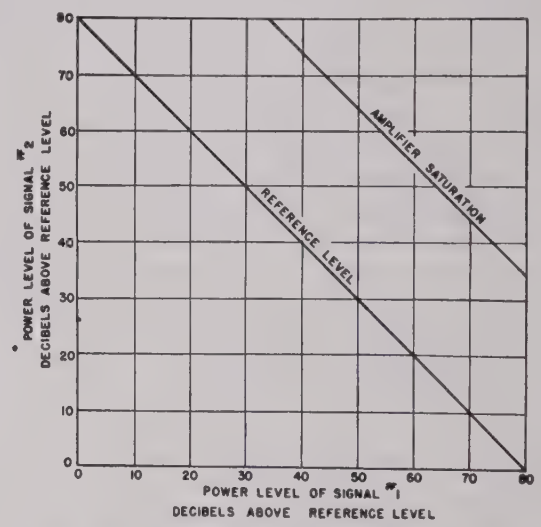

Fig. 6—Response characteristics of the analyzer for typical "cross modulation" of two strong signals in the first mixer crystal. Signal No. 1, 700 megacycles, Signal No. 2, 300 megacycles. Response appears when the analyzer is tuned to 400 megacycles.

The second type of spurious response is due to harmonic generation in the first crystal mixer. The second and third harmonics are the only ones that are normally observable. They are shown as curves II and III, respectively, in Fig. 5. The second-harmonic voltage increases roughly as the square of the fundamental voltage, and the third harmonic increases as the cube. These responses become more noticeable as the absolute magni-

tude of the signal input power increases, therefore, and the slopes of curves I, II, and III are roughly in the ratio of 1:2:3 in Fig. 7. Again, none of these responses is troublesome if the signal of interest is not more than 35 decibels below the level of the strongest signal entering the receiver.

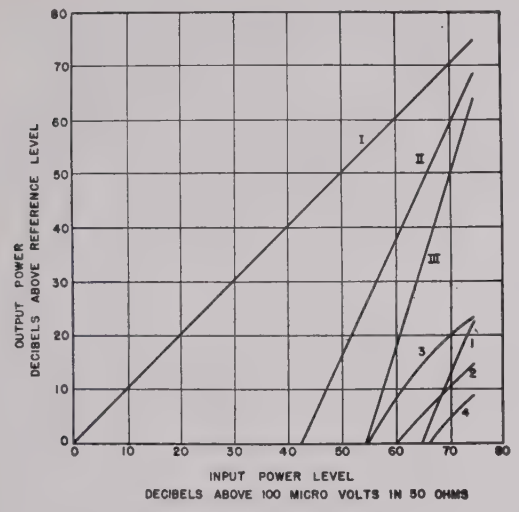

Fig. 7—Response characteristic of converter unit at large signal levels. The labeling of the curves is the same as in Fig. 5.

The 115-megacycle-image response is greatly suppressed in this type of analyzer since it must leak through the band-pass filter at a frequency 230 megacycles away from the center of the pass band. The attenuation characteristic of the filter network is shown in Fig. 8. The values are referred to the attenuation of a signal at the center of the pass band. Actually, this characteristic was measured by tuning the first and second beating oscillators simultaneously by the same amount, and by applying signals in the range from 400 to 1000 megacycles to the first mixer. Since the characteristics of the mixers do not change appreciably in this range, the resulting attenuation curve represents essentially the characteristic of the filter network. It is evident from Fig. 8 that the attenuation of the image in passing through the filter is about 55 to 60 decibels more than that of the signal. The actual image response is shown in curve 2 of Fig. 5. It agrees roughly with the expected value.

Response 1 in Fig. 5 appears when the analyzer is tuned for a frequency 57.5 megacycles below the frequency of the signal producing the response. It is produced because power leaks through the band-pass filter at a frequency 57.5 megacycles below that at the center of the pass band. This leakage power suffers an attenuation (see Fig. 8) of about 30 decibels and produces a 57.5-megacycle beat note in the second crystal mixer. The second harmonic of this beat note, also generated in this crystal, produces a response in the 115-megacycle amplifier. This spurious response determines the maximum bandwidth allowable for the filter network, since the response would become objectionable if the attenuation were much less than 20 decibels.

Responses 3 and 4 in Fig. 5 both arise because power from the second beating oscillator leaks through the bond-pass filter to the first crystal mixer. If the signal power producing the response is of frequency S, response 3 appears when the analyzer is tuned to a frequency of $(S/2)-(115/2)$ megacycles. The second harmonic of the first beating oscillator, the leakage from the second beating oscillator, and the signal all mix in the first crystal to produce 24,600 megacycles. This power proceeds through the filter to the second crystal and produces a response in the ordinary manner. Response 4 is more complex; it involves the second harmonic of the second beating oscillator. It is observable when the analyzer is tuned to a frequency of $(S/3)-2(115/3)$ megacycles.

Fig. 5 gives the oscilloscope deflections observed for the various responses discussed above. When any signal is large enough to saturate the amplifier at the normal gain setting, the operator is warned that there is a possibility of spurious responses. Fig. 7 gives the behavior both of the signal response and of the spurious responses at signal input levels up to 80 decibels above the 100-microvolt reference level. The responses are measured

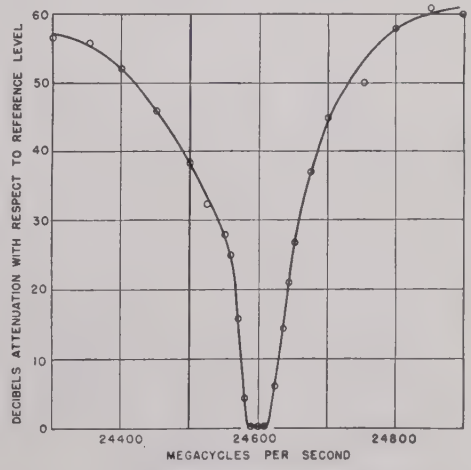

Fig. 8—Attenuation characteristic of filter network.

at the output of the converter unit with respect to the response produced by the 100-microvolt reference signal. The characteristics of the amplifier are not involved, of course. For observation of responses at these levels, however, the gain of the amplifier must be decreased in order that they lie in the region below saturation.

Acknowledgments

We are indebted to A. W. Hull, J. P. Blewett, and J. H. Rubel for helpful discussions. To Miss J. E. Dickey we are indebted for aid in the design of the mixers.

The Behavior of "Magnetic" Electron Multipliers as a Function of Frequency*

L. MALTER†, SENIOR MEMBER, I.R.E.

Summary—**This paper consists of a theoretical and experimental study of the frequency variation of gain of magnetic electron multipliers. It is shown that, for multipliers of the type studied, the behavior as a function of over-all electron transit angle is very similar to that observed for electrostatic electron multipliers previously described.[1] Up to frequencies of about 500 megacycles, loss in gain can be ascribed to a spread in transit angle resulting from the emission velocities of secondary electrons and the varying paths of electrons through the stages of the multiplier. From the results given, it is possible to predict the useful upper frequency limit of a magnetic electron multiplier of the type studied.**

Introduction

IN AN EARLIER paper[1] (hereinafter referred to as Paper I), wherein the behavior of electrostatic electron multipliers was analyzed, it was shown that for multipliers of any type the amplification of a radio-frequency signal will fall off with increasing frequency. The decrease of amplification at higher frequencies is due to the spread in the transit times of electrons after passing through several stages of the multiplier. The spread has two principal causes: (1) the nonuniformity in the emission velocities of secondary electrons, and (2) the differing paths traversed by various electrons between stages.

Decrease in amplification with increasing frequency can have still another cause. If the transit time between the output electrode and the one preceding it is appreciable, then the radio-frequency current flowing in the output circuit is less than that present as modulation in the beam. This arises from the fact that the current flow in the output circuit may be considered as arising from the change in the image charges in the output electrode, and in the one preceding it, as produced by the motion of electron charge between them. Thus, e.g., it is obvious that if the transit time between these electrodes is a full period, no radio-frequency current will flow in the output circuit.

By use of a screen electrode adjacent to the output electrode, the critical transit time becomes that between these two electrodes. In this work as well as in that of Paper I, the electrode spacings and potentials were such that the effect of the transit time between the screen and output electrode, in contributing to a decrease in amplification over the frequency range studied, could be neglected.[2]

On the basis of the results obtained it was found possible to make predictions regarding the frequency response of electrostatic multipliers of the forms now in most common use,[3] regardless of the scale to which they are built or the number of stages employed. These multipliers are characterized by the feature that there is an intense accelerating field at the secondary emitting surface. Reduced over-all transit times result in reduced spreads with consequent superior high-frequency performance.

Another type of multiplier having intense accelerating fields for secondary electrons is the so-called magnetic[4] type. (See Fig. 1.) Electrons emitted from any of the lower electrodes are accelerated upward by the action of the more positive potential applied to the electrode above it. However, a magnetic field parallel to the plane of the electrodes causes the electrons to bend over and strike the next succeeding lower electrode. Since this type of multiplier has an intense accelerating field at the secondary emitting surfaces, it was considered desirable to investigate its behavior as a function of frequency, in order to see whether it possessed any advantages over the purely electrostatic type studied in Paper I.

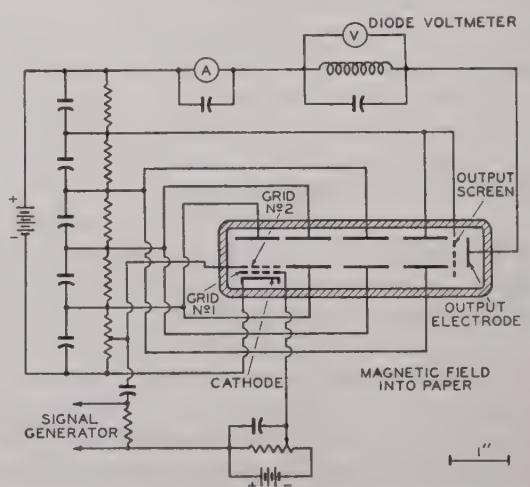

Fig. 1—Magnetic-multiplier setup employed in determination of frequency response.

Theory

It has been shown[3] that the positional co-ordinates of an electron in the crossed fields (see Fig. 1) are given by

$$x = \alpha\beta t + \frac{\mu_0}{\alpha} - \beta' \sin(\alpha t + \theta) \tag{1}$$

$$y = \beta - \frac{\lambda_0}{\alpha} - \beta' \cos(\alpha t + \theta) \tag{2}$$

* Decimal classification: R138.6. Original manuscript received by the Institute, March 13, 1946; revised manuscript received, December 31, 1946.

† Formerly, RCA Laboratories, Inc., Princeton, N. J.; now, Naval Research Laboratory, Washington D. C.

[1] L. Malter, "The behavior of electrostatic electron multipliers as a function of frequency," PROC. I.R.E., vol. 29, pp. 587–589; November, 1941.

[2] R. D. Sard, "Calculated frequency spectrum of the shot noise from a photo-multiplier tube," *Jour. Appl. Phys.*, vol. 17, pp. 768–777; October, 1946.

[3] V. K. Zworykin and J. A. Rajchman, "The electrostatic electron multiplier," PROC. I.R.E., vol. 27, pp. 558–566; September, 1939.

[4] V. K. Zworykin, G. A. Morton, and L. Malter, "The secondary emission multiplier, a new electronic device," PROC. I.R.E., vol. 24, pp. 351–375; March, 1936.

where

$\alpha = e/m\,H$
e = charge of electron
m = mass of electron
H = magnetic field strength
$\beta = (1/\alpha)(E/H)$
E = electric field between electrodes
λ_0, μ_0 = initial velocities in x and y directions, respectively.

$$\theta = \tan^{-1}\left(\frac{\mu_0/\alpha}{\beta - \lambda_0/\alpha}\right) \tag{3}$$

$$\beta' = \sqrt{\left(\beta - \frac{\lambda_0}{\alpha}\right)^2 + \left(\frac{\mu_0}{\alpha}\right)^2}. \tag{4}$$

It should be noted that (1) and (2) apply for the motion of an electron in crossed electric and magnetic fields of a multiplier only for the case wherein there is no increase of potential from stage to stage. While such is actually not the case, it is felt that serious error will not result in making use of the simplified theoretical picture in arriving at a measure of the performance of the actual multiplier. That such is actually the case is borne out by the results described below.

Let τ_m be the time it takes the electron to reach its maximum y displacement. Then the time taken for the electron to return to the axis (the transit time) is given by

$$\tau = 2\tau_m. \tag{5}$$

From (1) and (2) it may be shown that

$$\tau = 2\left(\frac{\pi - \theta}{\alpha}\right).$$

Then, if $\mu_0/\alpha \ll \beta$,

$$\theta = \frac{\mu_0/\alpha}{\beta - \lambda_0/\alpha} \tag{6}$$

and

$$\tau = \frac{2\pi}{\alpha}\left[1 - \frac{1}{\pi}\,\frac{\mu_0/\alpha}{\beta - \lambda_0/\alpha}\right] = \frac{2\pi}{\alpha}\,\Phi. \tag{7}$$

If

$$\mu_0 = \lambda_0 = 0,$$

then

$$\tau = \tau_0 = \frac{2\pi}{\alpha}$$

where τ_0 is the transit time for electrons emitted with zero velocity. Then

$$\tau = \tau_0\Phi. \tag{7a}$$

In order to permit of a determination of the spread of τ,

$$\Phi = \frac{\tau}{\tau_0}$$

was computed for a typical multiplier wherein

E = 175 volts per centimeter

H = 48 gauss.

Let l_0 and m_0 be the potential differences thru which electrons must fall in order to attain velocities respectively of λ_0 and μ_0. If V_p is the potential difference through which an electron falls between emission and impact at a secondary emitting surface, and if $V_p = 200$ volts, then m_0/V_p corresponds to V_e/V_p of Fig. 1 in Paper I.[1] Φ as a function of m_0, for various values of l_0, is plotted in Fig. 2. It is seen that the effects of initial velocity are about the same in both electrostatic and magnetic multipliers, as regards their effect on the relative transit angle.

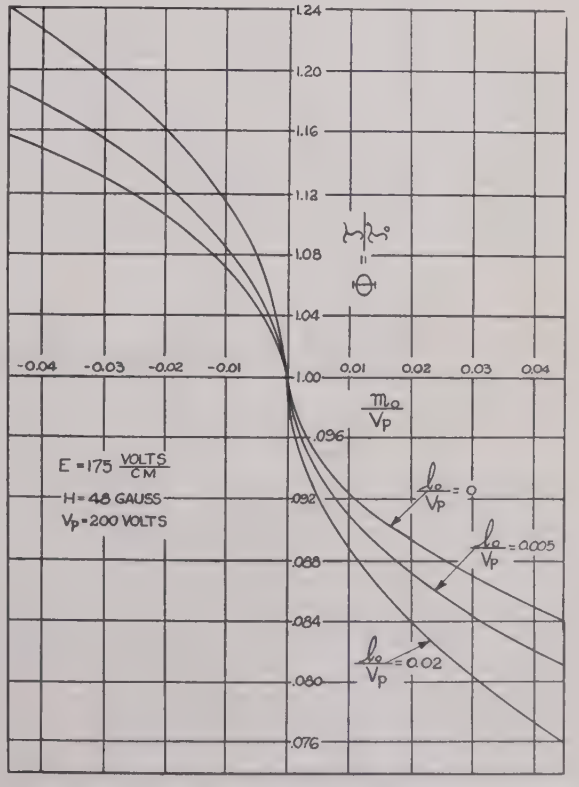

Fig. 2—Spread in transit angle in a single stage of a magnetic multiplier as a function of initial velocities of secondary electrons.

An effort to carry through a more complete analysis of the frequency response of a magnetic multiplier appears a fruitless task for the following reasons:

1. The theory outlined above applies to the case of uniform fields between lower and upper plates of the multiplier. Since in the actual multiplier the potential increases from stage to stage, with consequent nonuni-

form fields, the multiplier behavior cannot conform to the actual occurrences in other than a qualitative fashion.

2. There are insufficient data available regarding the angular distribution of secondaries to make an accurate determination of transit-time spreads possible.

Experimental Method

It is shown in Paper I that the frequency response of any multiplier of a given form can be represented as a function of the over-all transit angle regardless of the scale to which the multiplier is built. Thus it is unnecessary to build more than a single multiplier of any form in order to be able to predict the performance of any multiplier of the same form but of different size.

A magnetic multiplier of conventional form and to the scale shown in Fig. 1 of this paper was constructed. A known signal was fed into the input from a calibrated signal generator. The output voltage was then measured with a close-spaced-diode voltmeter. Corrections for the effects of input and output lead inductance and stray capacitances were made in accordance with the methods outlined in Paper I.

Results and Conclusions

The relative output for constant-signal grid voltage is plotted as a function of over-all transit angle in Fig. 3. (This is the "Frequency Response," as defined in Paper I.) For purposes of comparison, the results for an electrostatic multiplier are reproduced from Fig. 13 of Paper I. The similarity between the results for these two so widely different forms is quite surprising.

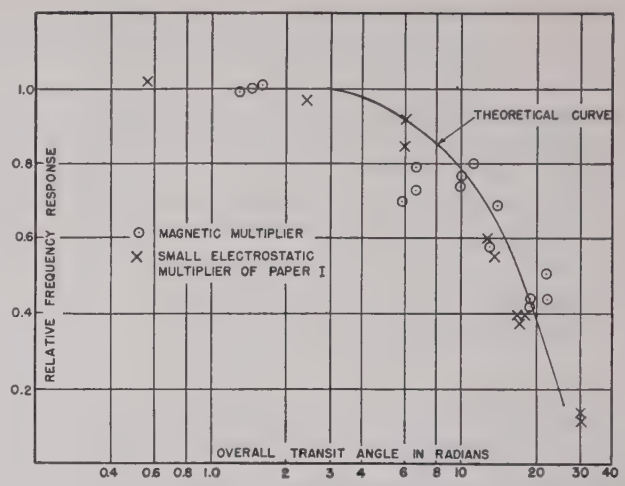

Fig. 3—Frequency response of "magnetic" and "electrostatic" multipliers as a function of over-all transit angle.

From these results it appears that the magnetic multiplier approximately equals in performance the best (as far as is known) of electrostatic multipliers. However, in view of the additional complexities introduced by the need for a magnetic field, the use of electrostatic multipliers is suggested in cases where frequency response is a major consideration.

Transit-Time Effect in Klystron Gaps*

H. B. PHILLIPS†, associate, I.R.E., and L. A. WARE†, senior member, I.R.E.

Summary—**The theory of the klystron is usually based upon a simplified configuration in which it is assumed that the grid spacing in the buncher is so small that, during the flight of the electron through it, the electric field changes very little. This assumption leads to a certain ideal value for the drift distance *S*. It is of interest to calculate the effect on the ideal value of *S* caused by a finite spacing of the buncher grids. This calculation is carried through by means of a graphical method suggested by R. Kompfner. It is found that, in general, as the grid spacing is increased, the value of S is also increased. In the case of the depth of modulation *M* equal to 0.5, *S* is found to increase by 47 per cent as the grid spacing is varied from 0 to 2 millimeters for an accelerating voltage of 1200 volts and a frequency of 3×10^9 cycles per second.**

Introduction

THE THEORY of the klystron, as usually developed,[1] depends upon the assumptions that the depth of modulation is small and that the time of flight of an electron through the grids of the resonators can be neglected. The first assumption means that the ratio of the maximum voltage V_1 between the buncher grids to the accelerating voltage V_0, i.e., V_1/V_0, is small. The second assumption considers the entire change in the velocity of the electron to occur at a point midway between the buncher grids. Obviously, this is not the case, for with a reasonable spacing between the grids, and with the very high frequencies involved, the field between the grids may change appreciably during the electron's flight between them. The object of this paper is to determine the effect of this second assumption upon the so-called ideal drift distance, as compared with the solution that takes into account the magnitude of V_1/V_0 only.

The ideal drift space, designated as S', is defined as the distance from the buncher at which electrons will form a sheath of infinite space-charge density during each cycle. Although optimum bunching, from a standpoint of efficiency, is somewhat different from ideal

* Decimal classification: R138.5. Original manuscript received by the Institute, June 10, 1946; revised manuscript received, August 26, 1946.

† State University of Iowa, Iowa City, Iowa.

[1] D. L. Webster, "Cathode ray bunching," *Jour. Appl. Phys.*, vol. 10, pp. 501–508; July, 1939.

bunching, any effects caused by resonator transit time should be expected to appear in both cases. The elementary solution for an arbitrary V_1/V_0 has been worked out elsewhere.[2] The value of S' will now be worked out, taking into consideration the value of grid spacing d. From the results of previous work and this development an estimate of the importance of considering grid spacing can then be made.

A Solution Considering Grid Spacing

A solution taking into consideration the finite time of flight between the buncher grids follows the method suggested by Kompfner.[3] In treating this condition use

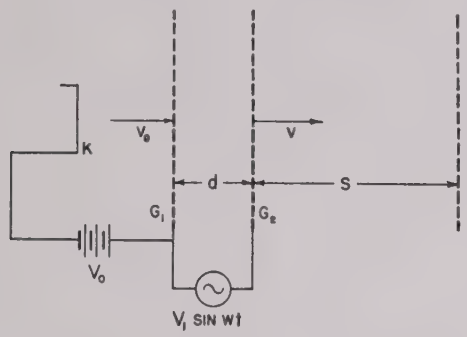

Fig. 1—Klystron configuration for theory involving finite grid spacing.

will be made of Fig. 1, in which d is the separation of the buncher grids, and S is measured from the second grid G_2. In the space d the electric field intensity is

$$E = \frac{V_1 \sin \omega t}{d}.$$

The acceleration of an electron at any time t is

$$\alpha = \frac{dv}{dt} = \frac{eV_1 \sin \omega t}{md} \tag{1}$$

from which the velocity may be obtained by integration.

$$v = \frac{eV_1}{\omega md}(\cos \omega t_1 - \cos \omega t) + v_0 \tag{2}$$

where t_1 is the time of crossing the grid G_1, and t is the time at which the electron is found at some point such as z between the grids. The distance z, traveled in time $(t-t_1)$, is given by another integration.

$$z = \left(v_0 + \frac{eV_1}{m\omega d}\cos \omega t_1\right)(t - t_1) - \frac{eV_1}{m\omega^2 d}(\sin \omega t - \sin \omega t_1) = d. \tag{3}$$

[2] R. Kompfner, "Velocity modulation," *Wireless Eng.*, vol. 17, pp. 478–488; November, 1940.
[3] R. Kompfner, "Transit-time phenomena in electron tubes," *Wireless Eng.*, vol. 19, pp. 2–6; January, 1942.

z is set equal to d because we are interested in conditions at G_2.

In order to simplify (3), make the following identifications:

$$x = \omega t_1 \qquad \theta = \frac{\omega d}{\sqrt{V_1}}\sqrt{\frac{m}{2e}} = \frac{\omega d}{v_1}$$

$$y = \omega t \qquad \phi = \frac{\omega d}{\sqrt{V_0}}\sqrt{\frac{m}{2e}} = \frac{\omega d}{v_0}.$$

Equation (3) is then written

$$\frac{2\phi^2}{M} = \left(\frac{2\phi}{M} + \cos x\right)(y - x) - \sin y + \sin x \tag{4}$$

where M is the depth of modulation.

The expression for the velocity of the electron as it leaves G_2 becomes

$$v = v_0\left[\frac{eV_1}{m\omega d}(\cos x - \cos y) + 1\right] = v_0\left[\frac{M}{2\phi}(\cos x - \cos y) + 1\right]. \tag{5}$$

Thus the velocity at G_2 can be determined if the value of y corresponding to a chosen value of x is first found from (4).

The evaluation of y in terms of x from (4) may be accomplished graphically, as in Fig. 2. In any particular case the parameters M and ϕ are known, and x is selected arbitrarily. Draw two sine waves of unit

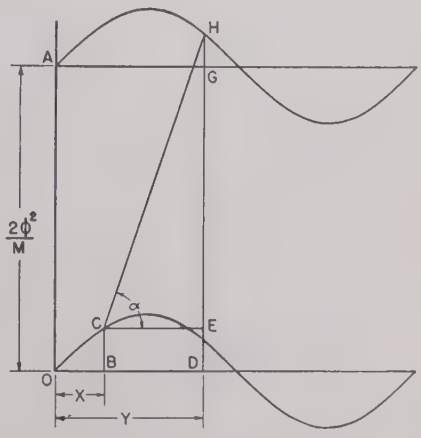

Fig. 2—Graphical solution of equation (4).

amplitude and separated vertically by a distance $2\phi^2/M$. At a point x draw an ordinate BC. At C draw the horizontal CE and the line CH making an angle α with CE, where $\tan \alpha = (2\phi/M) + \cos x$. Drop a perpendicular from H to D; the distance OD is the value of y corresponding to x. This may be proved by writing

$$\tan \alpha = \frac{DG + GH - DE}{y - x} = \frac{2\phi}{M} + \cos x,$$

by construction, or

$$(y - x)\left(\frac{2\phi}{M} + \cos x\right) = \frac{2\phi^2}{M} + \sin y - \sin x,$$

which is the same as (4). The results of these calculations provide a means of determining v in terms of t_1, the time of crossing the grid G_1.

The following equation may now be written

$$a = t + \frac{S}{v} \tag{6}$$

where a is the time of arrival at a plane a distance S from the grid G_2, v is given by (5), and t is the time of leaving G_2.

An expression for the current at S may be developed from the following considerations. Electrons entering the buncher during short time intervals Δt_1 arrive at S during short intervals Δa. In the case of overbunching, faster electrons may overtake and pass slower ones, so that a single interval Δa may correspond to several intervals Δt_1.[3,4] In order to conserve charge, then,

$$i\Delta a = \sum i_0 \Delta t_1 = i_0 \sum \Delta t_1.$$

The instantaneous current at S is then, taking the limit,

$$i = i_0 \sum \frac{dt_1}{da}. \tag{7}$$

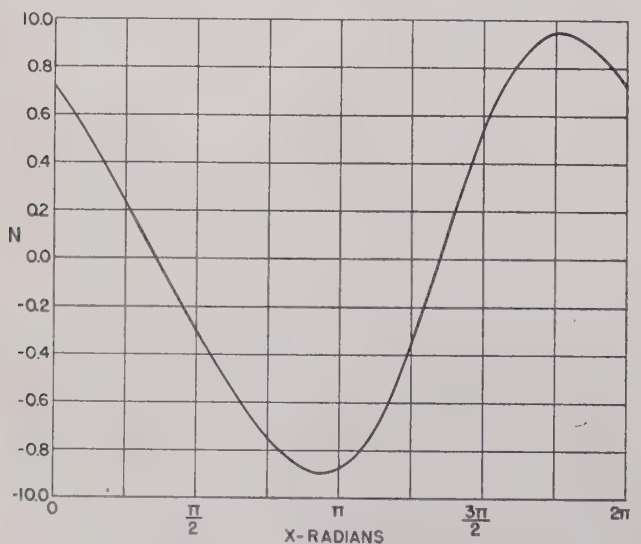

Fig. 3—The auxiliary quantity N as a function of x.

Since the sign of dt_1/da merely denotes the sequence in which electrons arrive at S, and does not affect the value of i, we write

$$i = i_0 \sum \left|\frac{dt_1}{da}\right|. \tag{8}$$

[4] L. J. Black and P. L. Morton, "Current and power in velocity-modulation tubes," PROC. I.R.E., vol. 32, pp. 477–482; August, 1944.

From (6),

$$\frac{da}{dt_1} = \frac{dt}{dt_1} - \frac{S}{v^2}\frac{dv}{dt_1}. \tag{9}$$

Thus

$$i = i_0 \sum \left|\frac{\dfrac{dt_1}{dt}}{1 - \dfrac{S}{v^2}\dfrac{dv}{dt}}\right|. \tag{10}$$

From (5),

$$\frac{dv}{dt} = v_0\left[\frac{M}{2\phi}\left(\omega \sin \omega t - \omega \frac{dt_1}{dt}\sin \omega t\right)\right]$$

$$= \frac{\omega v_0 M}{2\phi}\left(\sin \omega t - \frac{dt_1}{dt}\sin \omega t_1\right) \tag{11}$$

and (10) becomes

$$i = i_0 \sum \frac{dt_1}{dt}\left|\frac{1}{1 - \dfrac{SMN}{2d}}\right| \tag{12}$$

where

$$N = \frac{\sin \omega t - \dfrac{dt_1}{dt}\sin \omega t_1}{\left[\dfrac{M}{2\phi}(\cos \omega t_1 - \cos \omega t) + 1\right]^2}. \tag{13}$$

A typical graph of N versus ωt_1 is shown in Fig. 3. If N is set equal to its maximum value, N_{max}, and if S is chosen so that

$$\frac{SMN_{max}}{2d} = 1,$$

i will be infinite once during each cycle, giving the ideally bunched condition. For this case, then,

$$S' = \frac{2d}{MN_{max}} \tag{14}$$

where S' is the ideal drift distance.

Solution for d Equal to Zero

When d is allowed to approach zero, giving the case usually considered, N_{max} also becomes zero, making (14) indeterminate. In order to evaluate this expression when $d=0$, consider d to be very small so that the transit angle of an electron passing through the buncher is very small. Thus

$$y - x = z \ll 1. \tag{15}$$

The time of flight through the buncher z/ω is then equal to the grid separation divided by the average velocity of the electron, or

$$\frac{z}{\omega} = \frac{d}{\bar{v}} = \frac{d}{\frac{1}{2}(v_0 + v)}$$

and

$$z = \frac{2\omega d}{v_0 + v}. \tag{16}$$

Since

$$\cos y = \cos x \cos z - \sin x \sin z$$
$$\doteq \cos x - z \sin x,$$

the velocity, v, as given by (5) may be written

$$v = v_0\left[\frac{Mv_0}{2\omega d}(z \sin x) + 1\right].$$

Substituting from (16) for z,

$$v = \frac{Mv_0^2}{v_0 + v}\sin x + v_0. \tag{17}$$

Solving (17) for v yields

$$v = v_0\sqrt{1 + M \sin x}. \tag{18}$$

Equation (6) now becomes

$$a = t + \frac{S}{v} = t_1 + \frac{z}{\omega} + \frac{S}{v_0\sqrt{1 + M \sin x}} \tag{19}$$

and

$$\frac{da}{dt_1} = 1 - \frac{S}{2v_0}(M\omega \cos x)(1 + M \sin x)^{3/2}. \tag{20}$$

Upon substituting (20) into (8), there is obtained

$$i = i_0 \sum \left| \frac{1}{1 - \frac{SM\omega \cos x}{2v_0(1 + M \sin x)^{3/2}}} \right|. \tag{21}$$

Here, again, i will be infinite once during each cycle if

$$S = \frac{2v_0}{\omega M}\left[\frac{(1 + M \sin x)^{-3/2}}{\cos x}\right]_{\max}. \tag{22}$$

Upon maximizing the bracketed term of (22), it is found that

$$\sin x = \frac{1 - \sqrt{1 + 3M^2}}{M} \tag{23}$$

and it follows that

$$\cos x = \frac{\sqrt{2}}{M}\sqrt{\sqrt{1 + 3M^2} - M^2 - 1}. \tag{24}$$

Substituting (23) and (24) into (22) gives

$$S' = \frac{v_0}{\pi f M} \cdot C$$

where

$$C = \frac{(2 - \sqrt{1 + 3M^2})^{3/2}}{\sqrt{2}\left(\frac{1}{M}\sqrt{\frac{1}{M^2} + 3} - \frac{1}{M^2} - 1\right)^{1/2}}.$$

These two equations agree with the results of Kompfner and tie the two developments together for $d = 0$.[2]

Conclusion

The value of S', the ideal drift distance as defined above and given by (14), has been calculated for values of $M = 0.2$, 0.3, 0.4, and 0.5, using the following parameters:

$V_0 = 1200$ volts

$v_0 = 2.06 \times 10^9$ centimeter per second

$f = 3 \times 10^9$ cycles per second

$\omega = 6\pi \times 10^9$ radians per second.

The results are presented in Fig. 4, where S' is plotted as a function of the grid spacing d. In this figure, S' is measured from the midpoint between the two buncher grids, i.e., S' here is (24) plus $d/2$. It is evident from Fig. 4 that there is an increase in the ideal drift distance

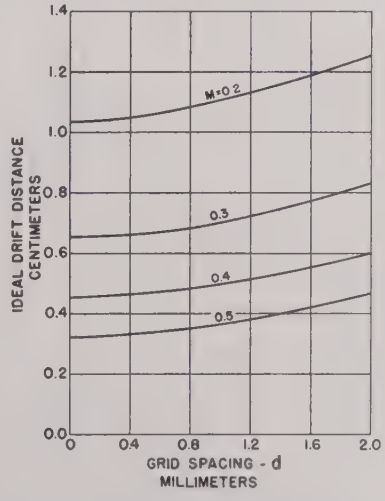

Fig. 4—Effect of grid spacing on S'.

as the spacing between the buncher grids is increased. This increase is very little for smaller grid spacings but becomes appreciable for larger values of grid spacing. A table presenting the per cent increase of S' for $d = 2$ millimeters as M is varied is given below.

M	*Per cent increase in* S'
0.2	21 per cent
0.3	27 per cent
0.4	30 per cent
0.5	47 per cent.

Broad-Band Wave-Guide Admittance Matching by Use of Irises*

R. G. FELLERS† AND R. T. WEIDNER‡, ASSOCIATE, I.R.E.

Summary—A procedure is described for broad-band admittance matching of wave-guide devices by the use of simple irises. Slotted-line measurements yield the standing-wave ratio and position of voltage minimum for several wavelengths and allow the determination of the transverse plane along the axis of the wave guide at which the dispersion with wavelength of the reflection-coefficient phase is a minimum. For regions in which the standing-wave ratio is approximately independent of wavelength, this information determines the optimum position and dimensions of a purely susceptive iris which matches the admittance of the load to that of the wave guide.

TRANSMISSION-LINE admittance matching has been treated in great detail for a single wavelength by use of stubs, transformers, resonant circuits, and lumped capacitances and inductances.[1] These methods are directly applicable to wave guides by using the wave-guide equivalents for the transmission-line matching devices.[2] Many of the wave-guide matching devices are not desirable because of their mechanical and analytical complexity In this paper a method is presented for admittance matching in wave guides by use of irises, the wave-guide equivalents of lumped capacitances and inductances, as shown in Fig. 1.

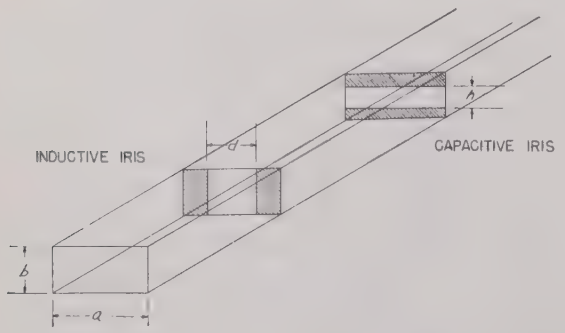

Fig. 1—Inductive and capacitive irises in rectangular wave guide.

A close analogy exists between a wave guide transmitting only the dominant mode and an ordinary two-wire transmission line; for, if a wave guide is not terminated in its characteristic admittance Y_0, a standing-wave pattern exists in the wave guide, and a knowledge of this pattern permits the determination of the equivalent admittance of the wave guide at any transverse plane, just as a knowledge of the standing-wave pattern for the two-wire transmission line permits the determination of the admittance terminating the line or the admittance at any other point along the line.

The standing-wave pattern is determined by the slotted-line technique in which a probe is moved along an axial slot in the broad face of a rectangular wave guide to give the voltage as a function of position along the line.[3] In order to apply the slotted-line technique it is assumed (a) that the wave guide supports only the dominant mode, (b) that the probe produces negligible distortion of the standing-wave pattern, and (c) that the wave-guide attenuation is negligible for the lengths of wave guide used in the measurements. The voltage standing-wave ratio (v.s.w.r.), is the ratio of the maximum to the minimum voltage, i.e., v.s.w.r. $= V_{max}/V_{min}$. The distance between adjacent maxima or minima is $\frac{1}{2}\lambda$ where the wave-guide wavelength λ is related, for the dominant TE_{10} mode, to the wave-guide width a and the free-space wavelength λ_0 by

$$\lambda = \lambda_0\left[1 - \left(\frac{\lambda_0}{2a}\right)^2\right]^{-1/2}. \qquad (1)$$

A probe measurement at a given wavelength determines, therefore, v.s.w.r., the position of $V_{min.}$ and λ.[4]

These data are best represented on a Smith admittance chart[5] (see Fig. 4), where the reflection coefficient R is represented by a vector with its origin at the center of the chart. The v.s.w.r. determines the amplitude of R, and the scale of the values of v.s.w.r. is given along the lower half of the vertical line. Concentric circles of constant v.s.w.r. surround the center point. The angular position of R (measured counterclockwise on the inner circular scale) is determined by the distance along the line (measured in fractional parts of λ) between the point V_{min} and the point with which R is associated.

On the chart Y_0 is represented by the center point, for which v.s.w.r. = 1. All values of admittance are given as fractions of Y_0; that is, normalized to 1. A precise definition of Y_0 in terms of parameters (dimensions, properties of medium, wavelength) of the wave guide[6] has not been agreed upon and is unnecessary for this analysis. The conductance G is represented by the family of circles which pass normally through the lower

* Decimal classification: R118. Original manuscript received by the Institute, July 2, 1946; revised manuscript received, December 2, 1946.

† United States Naval Research Laboratory, Washington 20, D. C.

‡ Formerly, United States Naval Research Laboratory; now, Sloane Physics Laboratory, Yale University, New Haven, Conn.

[1] R. W. P. King, et al., "Transmission lines, antennas, and wave guides," McGraw-Hill Book Co., New York, N. Y.; pp. 44–64, 1945.

[2] See pp. 286–288, of footnote reference 1.

[3] R. I. Sarbacher and W. A. Edson, "Hyper and Ultra-High Frequency Engineering," John Wiley and Sons, New York, N. Y., 1943; pp. 292–300.

[4] See p. 191 of footnote reference 1.

[5] P. H. Smith, "Transmission line calculator," *Electronics*, vol. 12, pp. 29–31; January, 1939.

[6] S. A. Schelkunoff, "Electromagnetic Waves," D. Van Nostrand Company, Inc., New York, N. Y.; p. 319, 1943.

end of the vertical line on the chart; the susceptance B is represented by the family of circles which are orthogonal to the G circles. Positive susceptance is represented on the right half of the chart; negative susceptance on the left. The terminus of R gives the values of G and B, and, therefore, Y, at any point along the line.[7] When R is different from zero, Y varies periodically along the line at intervals of $\frac{1}{2}\lambda$. If the admittance Y is measured looking toward the load, motion along the line toward the load is represented by counterclockwise rotation of R, and motion toward the generator corresponds to clockwise rotation of R. It is important to understand that Y as represented on the chart is the value looking toward the load for a specific position along the line (or points distant by an integral multiple of $\frac{1}{2}\lambda$).

The admittance of a guide in which there is reflection from a physical discontinuity is determined over a band of wavelengths and represented in the following manner. First, a position along the line, point P of Fig. 2, is

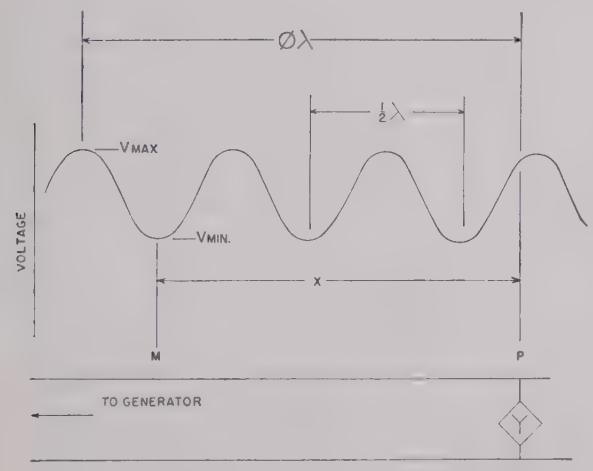

Fig. 2—Standing-wave pattern along the wave guide.

selected, relative to which the admittance is to be measured. This point should be chosen close to the physical discontinuity in the wave guide. The v.s.w.r. and the distance x between P and M (the position of V_{min}) are determined for several wavelengths of the band by means of the standing-wave indicator. X is measured positively toward the load. The admittance Y at point P for a given wavelength is represented on the admittance chart by the terminus of R of a length determined by the v.s.w.r. and at an angular position determined by the phase fraction (angular length) ϕ. For a given guide wavelength λ, ϕ, the phase fraction for point P is

$$\phi = x/\lambda + 1/4. \tag{2}$$

[7] Since the Smith charts of Figs. 2 and 4 are used for registering admittance here rather than impedance, the words reactance and resistance appearing there should be replaced by susceptance and conductance, respectively.

x/λ is the corresponding phase fraction for impedance representation. For a different wavelength $\eta\lambda$,

$$\phi_\eta = \frac{x_\eta}{\eta\lambda} + \frac{1}{4}. \tag{3}$$

It should be noted that if ϕ exceeds one-half, $\phi - (n/2)$ is plotted, where n is an integer, and any ambiguity as to the curve between the points representing λ and $\eta\lambda$ is removed by plotting the admittance for one or more intermediate wavelengths.

A very important fact which can be observed at this juncture is that, since a given distance along the axis of the wave guide is a larger fraction of a shorter wavelength than it is of a longer wavelength, a particular distance moved along the guide will represent a larger phase fraction ϕ for the shorter wavelength than it does for the longer wavelength. Therefore, reference of the admittances to a point different from P will change the value of $\phi_\eta - \phi$. That is, by reference to the proper point along the guide, different wavelengths may be made to possess the same phase fraction and to lie on the same radial line on the chart ($\phi_\eta - \phi = 0$).

In order to locate this point, the reference point, first chosen at P, is now displaced Δx along the guide toward the load or generator, which represents an increment of phase fraction $\Delta\phi$ for the wavelength λ. For the wavelength $\eta\lambda$ this corresponds to an increment $\Delta\phi/\eta$. In order that the resultant phase fractions for λ and $\eta\lambda$ be equal,

$$\phi + \Delta\phi = \phi_\eta + \frac{\Delta\phi}{\eta}. \tag{4}$$

Therefore,

$$\Delta\phi = \frac{\phi_\eta - \phi}{\eta - 1}\eta. \tag{5}$$

The positive direction of measurement of phase fraction is taken as counterclockwise on the chart, which represents motion toward the load. The distance (measured positively toward the load) which must be traveled along the guide from P to produce this zero difference in phase fraction is

$$\Delta x = \lambda\Delta\phi = \frac{\lambda(\phi_\eta - \phi)}{\eta - 1}\eta. \tag{6}$$

This phenomenon is employed in the broad-band matching of wave-guide devices by means of a simple susceptance. The curve C of Fig. 3 is a bandwidth curve of a device in which the v.s.w.r. varies only slightly over the desired band of wavelengths. Such behavior is typical of many common wave-guide devices, such as transitions from rectangular to circular wave guide and simple horns.

This may be illustrated on the admittance chart with the aid of curve C of Fig. 3, which uses an enlarged center section of the full admittance chart. Curve C represents a plot of admittance of a typical wave-guide

device relative to some point P for a band of wavelengths from λ to $\eta\lambda$ where η has the value 1.146 for the chosen band of wavelengths. Calculations for intermediate wavelengths are not usually necessary because of the smooth variation of ϕ with λ. From the chart it may be seen that $\phi_\eta - \phi = 0.111$. From (6) it follows that the distance moved along the guide for the two phase fractions to coincide is 0.871λ.

This means that at the point 0.871λ distant from P toward the load, the phase fraction for λ is equal to that for $\eta\lambda$. This can readily be seen from Fig. 3. A rotation of $\Delta\phi = 0.871$ for the wavelength λ will carry the point through one complete revolution and return it to a point at a phase fraction of 0.371 past its original spot on the admittance chart. It is now at the phase fraction 0.014 at point D. However, 0.871λ represents an increment of phase fraction $0.871\lambda/\eta\lambda$ for the wavelength $\eta\lambda$, and the point representing $\eta\lambda$ will move only $0.871/1.146 = 0.760$ in phase fraction. This carries the point representing $\eta\lambda$ through one complete revolution on the chart, which carries it to the phase fraction 0.014, where it has the phase fraction of the point representing λ. It is seen that, by referring the admittance to a point 0.871λ along the guide toward the load, the bandwidth curve representing the band of wavelengths from λ to $\eta\lambda$ is contracted to the short radial line extending

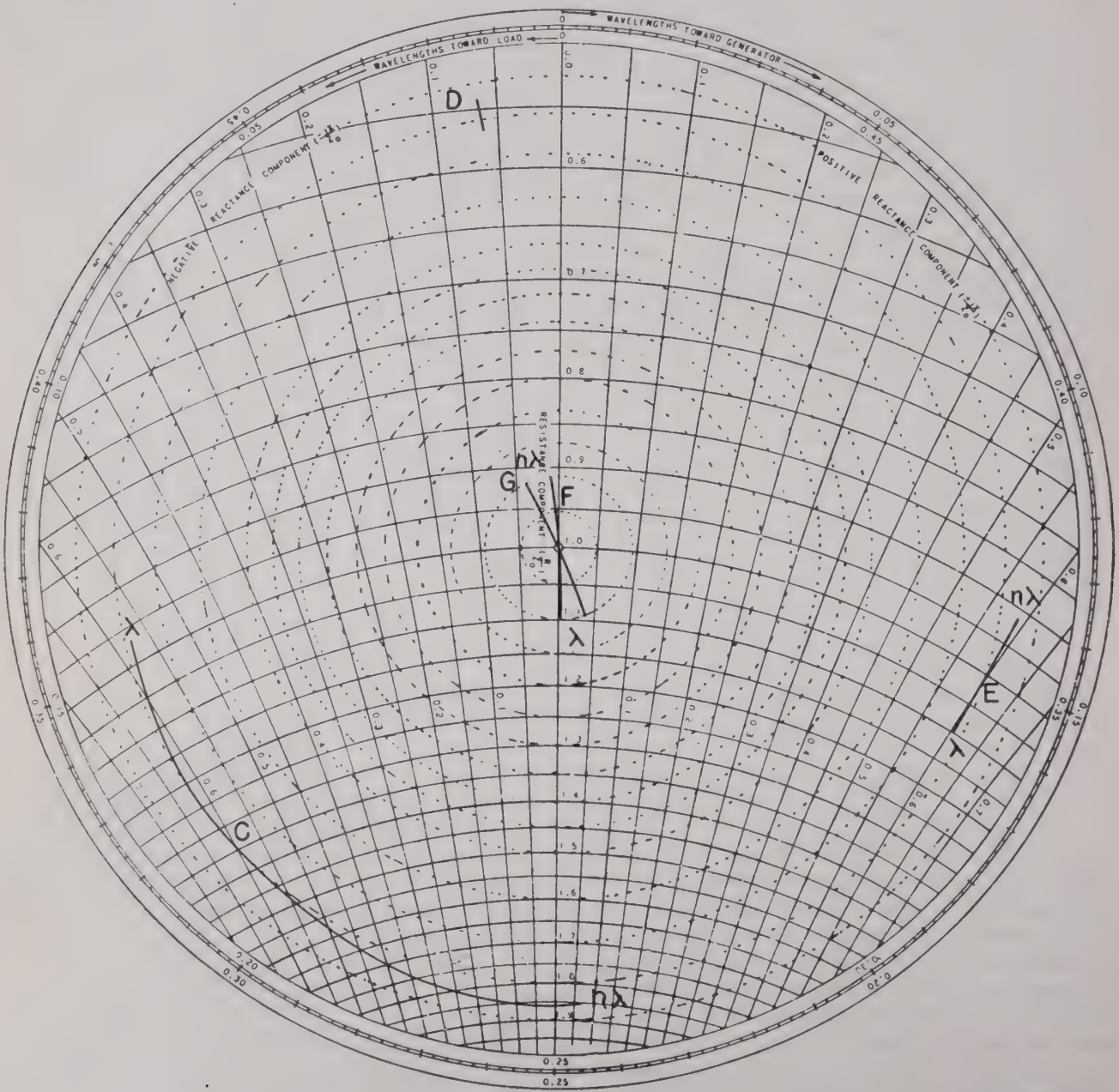

Fig. 3—Enlarged center section of admittance chart.

from v.s.w.r. = 1.78 to v.s.w.r. = 1.85 at the phase fraction 0.014.[8] This is shown as curve *D* on the admittance chart of Fig. 3. In order to match the admittance represented by this curve to the characteristic admittance Y_0, addition of both conductance and susceptance would necessary to move some distance along the line until the position of the curve is such that a purely susceptive device will match the point of median wavelength to the characteristic admittance 1.0 of the wave guide. When the point of minimum dispersion falls on the

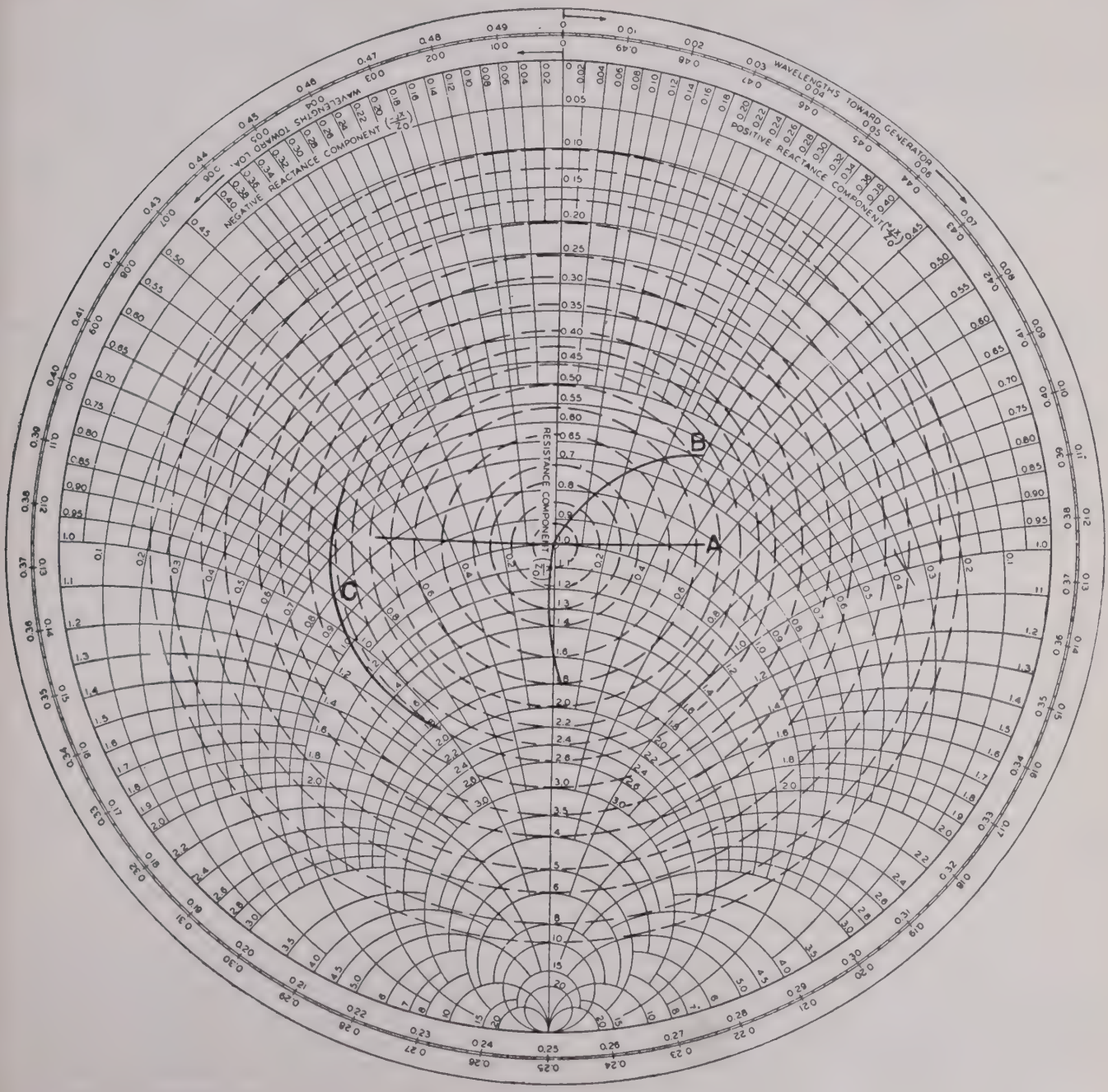

Fig. 4—Smith admittance chart.

be necessary. This type of matching device is not impossible, but purely susceptive irises are more convenient mechanically and simpler to design. In order to make use of suceptive matching devices, then, it is upper section of the zero susceptance line (along the vertical), the angular difference between it and the position of 1.0 conductance is a maximum. Therefore, our example represents almost the worst angular position of the point of minimum dispersion for matching with pure susceptance. The curve *D* is rotated back toward the generator by such an amount that it will

[8] In many cases the contracted curve is not a straight radial line; divergence from such a radial line can be attributed largely to errors in the experimental data.

be bisected by the 1.0 conductance line in the positive susceptance region. Since the clockwise rotation required to center curve E on the 1.0 conductance line is 0.162, the rotation $\Delta\phi$ required for the λ extremity of the line can be found from the equation

$$\frac{1}{2}\left(\Delta\phi + \frac{\Delta\phi}{1.146}\right) = 0.162. \tag{7}$$

This represents clockwise rotation of 0.174 in phase fraction toward the generator for wavelength λ. Upon subtracting this figure from the angle obtained above to be traversed toward the load from point P, a net rotation of $0.871-0.174=0.697$ is obtained. (This represents incremental movement of $0.174/1.146=0.151$ in phase fraction back toward the generator for the wavelength $\eta\lambda$.)

The resultant bandwidth curve is shown as curve E on the chart of Fig. 3. When the point of minimum dispersion falls on the pure conductance line (close to D), rotation to the 1.0 conductance line represents the maximum lengthening of the bandwidth curve which can occur for a given η; that is, usually a curve of considerably less spread with wavelength is found at the pure conductance line. Addition of 0.60 normalized negative susceptance at a distance 0.697λ from P is necessary to center the curve about the characteristic admittance $Y_0=1$. Addition of 0.60 susceptance for all wavelengths shifts the curve E to the final position F. The curve at F now represents a v.s.w.r. of 1.1 at the ends of band with a v.s.w.r. of 1.0 at the center wavelength, over a 14 per cent band of wavelengths. It should be mentioned that this situation for which the point of minimum dispersion falls far from the 1.0 conductance line represents maximum deviation from optimum position, and that usually less spread in v.s.w.r. is obtained.

If it had been desired, as is often the case, the final point chosen could have placed the curve C on the 1.0 conductance line in the negative susceptance region, where matching is accomplished by addition of a positive susceptance.

The values of susceptance, both positive and negative, can be calculated from relationships indicated in (8) and (9).[9] The negative susceptance is produced by an inductive iris similar to that in Fig. 1. The value for the normalized susceptance of an inductive iris of small thickness in rectangular wave guide is given by the following relation:

$$B = -\frac{\lambda}{a}\cot^2\frac{\pi d}{2a}. \tag{8}$$

The symbols refer to Fig. 1. Positive normalized susceptance corresponding to the capacitive iris is given by the relation:

$$B = \frac{4b}{\lambda}\log_e \operatorname{cosec}\frac{\pi h}{2b}. \tag{9}$$

Extensive experimental tests indicate these theoretical relations to be valid to a high degree of accuracy for thin irises. For both irises the aperture is symmetrical with respect to the axis of the wave guide. It is seen that guide wavelength λ enters into the expression for susceptance. In practical applications the value of B calculated for the center of the band of wavelengths may be used, or, if more precise results are desired, B may be calculated for as many wavelengths as may be desired on the bandwidth curve. This latter procedure produces curve G of Fig. 3, instead of curve F, which differs from G only slightly in phase and v.s.w.r.

If the bandwidth curve does not represent approximately constant v.s.w.r. for the varying wavelengths, other steps may be necessary in the matching procedure. A bandwidth curve similar to curve A in Fig. 4 is typical of many practical wave-guide devices such as transitions from wave guide to coaxial line and crystal-detector terminations. The admittance of this type of curve may be matched by use of an additional step. If the admittance of the device is referred to a point approximately one-eighth wavelength along the line toward the generator ($\Delta\phi\cong 0.125$), the curve will assume position B by a rotation process similar to that discussed above. Some increase in curvature will occur. Susceptance of the appropriate amount and sign may be added at this point to move the curve to position C,[10] which represents approximately constant v.s.w.r. over the band of wavelengths. Then the method discussed previously may be applied to contract the curve and produce an admittance match.

If the curve actually encircles the center it may be "unwrapped" by reference of the admittance to the proper point along the line, and one of the above matching methods may be applied. The more important limitation of this method lies in the possibility that the point of minimum phase dispersion, Δx distant from P, is outside the physical dimensions of the device in question or behind the physical discontinuity which causes the reflection, since data employed here give meaning to admittance only up to the first physical discontinuity. In this case, complete admittance matching cannot be achieved by this method. However, considerable contraction of the original bandwidth curve can be produced by retreating along the guide until it becomes physically possible to insert the matching device; then the insertion of the matching susceptance will improve the v.s.w.r. over the entire band but will produce an admittance match which is more frequency sensitive.

Admittance matching by means of this system is extremely useful in work with wave-guide devices. Experience has shown that many of the devices regularly encountered in practical wave-guide work have curves

[9] J. W. Miles, "The equivalent circuit for a plane discontinuity in a cylindrical wave guide," PROC. I.R.E., vol. 34, pp. 728–742; October, 1946.

[10] Not to be confused with curve C of Fig. 3.

of admittance over the wavelength band of the simpler types discussed here, and are readily amenable to matching by this method. Complete contraction of the curve and admittance matching is not always physically possible, but considerable improvement in v.s.w.r. can often be obtained. The method outlined here is simple and straight-forward in analysis and procedure, and the construction of the matching device presents no mechanical difficulty.

The capacitive and inductive irises are equivalent to frequency-insensitive shunt inductances and capacitances. (The susceptance of capacitive and inductive irises varies inversely and directly as λ, respectively, whereas the susceptance of lumped capacitances and inductances varies inversely and directly as λ_0, respectively.) Therefore, in many ways irises are preferable to stubs, transformer sections, and similar devices whose frequency sensitivity limits their use as matching devices (described here for wave-guide work). Stubs and similar devices are essentially resonant elements operated near resonant frequency, and hence are extremely frequency sensitive. This method is also applicable to coaxial lines.

List of Symbols

a = greater inside dimension of rectangular wave guide
B = susceptance
b = lesser inside dimension of rectangular wave guide
d = separation in a symmetrical inductive iris (see Fig. 1)
G = conductance
h = separation in a symmetrical capacitive iris (see Fig. 1)
M = position of V_{min} along the wave guide
P = point relative to which admittance is to be measured
R = reflection coefficient = v.s.w.r. -1/v.s.w.r. $+1$
V_{max} = voltage maximum of standing-wave pattern
V_{min} = voltage minimum of standing-wave pattern
v.s.w.r. = voltage-standing-wave ratio
x = distance along the wave guide between point P and point M
Y = admittance
Y_0 = characteristic admittance of wave guide
η = bandwidth as ratio of extreme values of guide wavelength
λ_0 = free-space wavelength
λ = wave-guide wavelength ($\lambda/2$ is the distance between adjacent maxima of the standing-wave pattern)
ϕ = phase fraction (angular length). Its magnitude is given by the distance from P to M measured in fractions of λ plus 0.25.

Broad-Band Noncontacting Short Circuits for Coaxial Lines

Part II—Parasitic Resonances in the Unslotted S-Type Plunger*

W. H. HUGGINS†, Associate, I.R.E.

Summary—**The problems involved in the design of wide-tuning-range resonators suitable for use with reflex-klystron oscillators have been discussed elsewhere.[1] When these resonators are tuned with noncontacting short circuits,[2] parasitic resonances, caused by waves propagating circumferentially around the small gaps between the plunger and the inner and outer conductors, may occur. In this paper it is shown that for a typical coaxial-line resonator incorporating noncontacting S-type plungers:**

(1) These resonances may occur in the outer gap when the wavelength is somewhat less than a submultiple of the mean circumference of this gap.

(2) Parasitic resonances occurring in the inner gap will be affected by the resonator tuning since these fields can propagate in the resonator. For the usual 3/4-wave resonator, two resonances may be expected; one at a wavelength somewhat greater than and the other at a wavelength somewhat less than the mean circumference of the inner gap.

(3) Plunger eccentricity produces a strong coupling between the principal resonator mode and the "one-cycle" circumferential resonances, but only a slight coupling to the "multiple-cycle" circumferential resonances. Hence, all one-cycle resonances must be made to occur at a wavelength outside of the tuning range either by suitable choice of resonator dimensions or by a slotting technique to be described in another paper.[3]

(4) Plunger eccentricity splits the circumferential resonances into "direct-axis" and "quadrature-axis" types which have differing resonant wavelengths.

* Decimal classification: R117.112. Original manuscript received by the Institute, August 13, 1946; revised manuscript received, January 13, 1947.

† Communications Laboratory, Cambridge Field Station, Air Material Command, Army Air Forces, Cambridge 39, Mass. This paper is based in part upon work done for the Office of Scientific Research and Development under Contract No. OEMsr-411 with the President and Fellows of Harvard College.

I. Introduction

ALL NONCONTACTING plungers of the type described elsewhere[1,2] possess parasitic resonances which at certain wavelengths will be excited by the principal mode of the coaxial line. These parasitic reasonances are very harmful because they produce frequency discontinuities and greatly reduce the Q of the principal resonance. Hence, it is necessary to design the plunger so that the most severe of these resonances will occur at wavelengths outside of the tuning range. This may sometimes be accomplished by selecting the proper dimensions for the coaxial resonator. It is the purpose of the following sections to establish a basis for coaxial-resonator design by showing how the wavelengths at which the parasitic resonances may occur are related to the resonator dimensions. When the desired dimensions cannot be used because of other limitations, it is necessary to control the parasitic resonances by slotting the plunger. The theory of plunger slotting is described in a subsequent paper.[3]

Since these resonances are caused by waves propagating circumferentially around the small gaps between the plunger and the inner and outer conductors, as a first approximation these resonances might be expected to occur when the circumference of the gap under consideration is an integral number of wavelengths in length. For example, in a typical oscillator incorporating a simple S-type plunger having outer-gap and inner-gap circumferences of 13.9 and 7.6 centimeters, respectively, one might expect to find parasitic resonances at wavelengths of 13.9, 7.6, 6.95, 4.63, etc., centimeters.

Actual measurements made on this oscillator showed, not *one* resonance at 13.9 centimeters, but two distinct resonances; one at 13.58 and the other at 12.80 centimeters. Also, instead of a single inner-gap resonance at 7.6 centimeters, resonances occurred at 7.90, 7.83, and 7.00 centimeters. This discrepancy is sufficiently great to warrant the more refined theory and method of calculating the resonant wavelengths now to be presented.

Although we are interested in the resonance effect of a wave which may be considered to propagate circumferentially around the plunger, because of the cylindrical geometry the wave may be treated more readily as a $TE_{n,1}$ coaxial-line wave where n is the number of circumferential cycles.[4] This change in viewpoint enables one to apply uniform transmission-line theory to a problem that would be very difficult to treat otherwise. It should be emphasized, however, that both viewpoints are simply different ways of looking at the same phenomenon.

[1] Radio Research Laboratory Staff, "Very High-Frequency Techniques," McGraw-Hill Book Co., New York, N. Y., 1947, chap. 32.

[2] W. H. Huggins, "Broad-band noncontacting short-circuits for coaxial lines—Part I," Proc. I.R.E., vol. 35, pp. 906–913; September, 1947.

[3] W. H. Huggins, Part III—"Control of parasitic resonances in S-type plungers," Proc. I.R.E., to be published.

[4] Robert A. Kirkman and Morris Kline, "The transverse electric modes in coaxial cavities," Proc. I.R.E., vol. 34, pp. 14–17; January, 1946. See also Discussion by W. H. Huggins, vol. 35, pp. 931–935; September, 1947.

The behavior of plungers and cavities to the $TE_{n,1}$ modes may be calculated from the usual transmission equations in much the same way that the TEM behavior was calculated in a previous paper.[2] The only complication is that the "wave-guide" property of these modes must be included so that both the characteristic impedance and propagation parameter become functions of the wavelength.

In a uniform coaxial line of inner and outer radii a and b, respectively, the cutoff wavelength for the $TE_{n,1}$ wave[1] may be calculated to a good approximation from

$$\lambda_c \simeq \frac{\pi(a+b)}{n}, \qquad n = 1, 2, 3, \cdots . \tag{1}$$

The propagation and characteristic-impedance parameters of the $TE_{n,1}$ wave are then (ignoring losses)

$$\gamma = j\frac{2\pi}{\lambda}\sqrt{1-(\lambda/\lambda_c)^2} \tag{2}$$

$$Z_0 = \frac{Z_0'}{\sqrt{1-(\lambda/\lambda_c)^2}} \tag{3}$$

where $Z_0' = 60\ 1n(b/a)$ is the characteristic impedance at infinite frequency.

If $\lambda < \lambda_c$, the propagation parameter is imaginary and the characteristic impedance is real, but for wavelengths greater than cutoff the propagation parameter is real and the characteristic impedance is imaginary, indicating attenuation of the wave. With this in mind we may return to the analysis of the plunger resonances. Since the inner and outer plunger gaps are effectively in series, they may be analyzed separately.

II. Resonance in Outer Plunger Gap

Fig. 1 shows the cross section of a coaxial cavity with an S plunger in position. For purposes of analysis, the

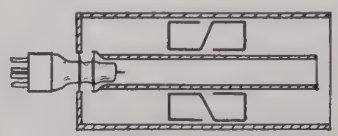

Fig. 1—Coaxial resonator with S plunger.

actual cavity may be replaced with the conventional cavity shown in Fig. 2. It is an interesting fact that, although the tube acts as an open circuit (with capacity loading) to the principal TEM mode, the tube end of the cavity is essentially *short-circuited* for modes having circumferential variations. Thus, in the equivalent cavity of Fig. 2, it is assumed that some *a priori* information is available as to the equivalent length d of the front cavity at the circumferential resonant wavelengths.

The length of the plunger resonant sections will be l; the mean *radii* of the cavity, inner, and outer gaps will be c, a, and b, respectively; and the mean *circumferences* of the cavity, inner, and outer gaps will be λ_c, λ_a, and λ_b.

Anticipating later results, the $TE_{1,1}$ resonances in the plunger may be expected to occur at wavelengths slightly less than the mean circumference λ_b of the gap.

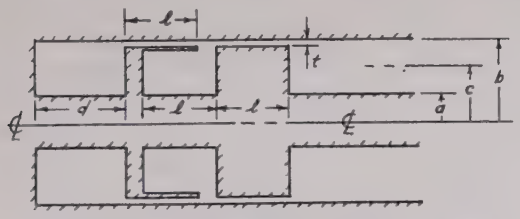

Fig. 2—Conventionalized cavity and plunger for outer-gap resonance.

If λ_b is used as the first approximation, we can obtain a better approximation to the resonant wavelength by setting

$$\lambda = \lambda_b(1 - \delta) \tag{4}$$

where δ is a small quantity now to be determined by establishing the equivalent circuit for the $TE_{1,1}$ resonance.

Consider first the rear low-impedance gap. If the impedance presented to the rear of the plunger by the rear cavity is Z_L, the input impedance of this rear gap will be given by the familiar formula:

$$Z_{\text{input}} = Z_0 \frac{Z_L \cosh \gamma l + Z_0 \sinh \gamma l}{Z_0 \cosh \gamma l + Z_L \sinh \gamma l} \tag{5}$$

where Z_0 and γ are given by (2) and (3).

But when $\lambda = \lambda_b(1-\delta)$, since λ_b is also the cutoff wavelength,

$$\gamma = j\frac{2\pi}{\lambda}\sqrt{1 - (\lambda/\lambda_b)^2} \simeq j\frac{2\pi}{\lambda_b}\sqrt{2\delta} \tag{6}$$

$$Z_0 = \frac{Z_0'}{\sqrt{1 - (\lambda/\lambda_b)^2}} \simeq \frac{Z_0'}{\sqrt{2\delta}}. \tag{7}$$

It should be noted that at wavelengths approximating the circumference of the gap, the guide wavelength becomes very great. Hence, at wavelengths near resonance the low-impedance gap is electrically short, and $\tanh \gamma l \cong \gamma l$. Using this approximation together with (6) and (7), the input impedance (5) becomes

$$Z_{\text{input}} = \frac{Z_0'\left(Z_L + j\frac{2\pi l}{\lambda}Z_0'\right)}{Z_0' + jZ_L\frac{2\pi l}{\lambda}2\delta}. \tag{8}$$

If $Z_L \gg 2\pi l Z_0'/\lambda$, (8) may be approximated by

$$Z_{\text{input}} = \frac{1}{\frac{1}{Z_L} + j\frac{4\pi l}{\lambda Z_0'}\delta}. \tag{9}$$

This is recognized as the load impedance Z_L in parallel with a capacitive susceptance $j(4\pi l/\lambda Z_0')\delta$, and the approximate equivalent circuit of the low-impedance gap and terminal impedance is shown in Fig. 3. Since, for usual plunger design, $Z_0' \ll Z_L$, this approximate circuit may be expected to hold quite generally.

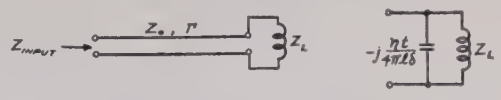

Fig. 3—Exact and simplified circuits for low-impedance gaps when $Z_L \gg 2\pi l Z_0'/\lambda$.

Because of the approximations just developed, it may be concluded, for the $TE_{1,1}$ resonance, *the low-impedance gaps act as shunt capacitive susceptances of value* $4\pi l\delta/\lambda Z_0'$. We may, therefore, replace the conventionalized cavity and plunger of Fig. 2 with the approximate equivalent circuit of Fig. 4. The inductive susceptances B_f and B_r are the $TE_{1,1}$ susceptances of the front- and

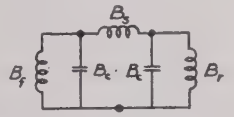

Fig. 4—Approximate equivalent circuit for $TE_{1,1}$ plunger resonance.

rear-cavity sections, respectively, and B_s is the $TE_{1,1}$ susceptance of the internal plunger "stub." Both B_f and B_s are the input susceptances of short lengths of transmission line short-circuited on the far ends for the $TE_{1,1}$ mode, and their values may be calculated from

$$jB = \frac{1}{Z_0}\cdot \operatorname{ctnh} \gamma l, \tag{10}$$

Z_0 and γ being defined by (2) and (3) with the radical sign so chosen that the inductive susceptance is negative.

Since the mean circumference λ_c of the cavity is less than that of the outer gap, the $TE_{1,1}$ wave in the main cavity will be "cut off" and will have appreciable amplitude only in the immediate vicinity of the plunger gap. For this same reason, the inductive susceptances of Fig. 4 will be slow-changing in comparison to the rapid variation of B_c with wavelength near resonance. Hence, in this equivalent circuit, values of B_f, B_s, and B_r may be calculated at the first approximation λ_b to the true resonant wavelength without introducing serious error.

To obtain the second approximation of the resonant wavelength, we note that resonance of the equivalent circuit will be obtained when the capacitive susceptance B_c is such that

$$B_c^2 + (B_f + B_r + 2B_s)B_c + [(B_f + B_s)(B_r + B_s) - B_s^2] = 0. \tag{11}$$

Equation (11) may be solved for the two values of B_c which will result in resonance. Designating these two

values by B_1 and B_2, we find, in consideration of $B_c = 4\pi l\delta/\lambda Z_0'$ and $Z_0' \cong \eta t/\lambda_b$ (where $\eta = 377$ ohms), that

$$\delta_{1,2} \cong \frac{\eta t}{4\pi l} B_{1,2} \tag{12}$$

from which the second-order approximation to the resonant wavelengths may be calculated by (4).

Experimental Agreement with Theory

Whereas the first-order approximation yielded only one resonance at wavelength λ_b, the second-order approximation gives two resonant wavelengths corresponding to B_1 and B_2. Physically, this "splitting may be attributed to interaction between the front and rear low-impedance sections. When the parasitic fields in the front and rear sections are in phase, the resonant frequency will be lower than when the fields are of opposite phase. These two possibilities result in two distinct resonant wavelengths.

Space does not permit presentation of the detailed calculations, but application of the above equations to the typical oscillator previously mentioned[5] yielded the comparison of wavelengths shown in Table I at which the outer-gap resonance occurred.

TABLE I

Calculated (centimeters)	Experimental (centimeters)
13.52	13.58
12.95	12.80

III. Inner-Gap Resonance

In the calculation of the outer-gap resonances, the $TE_{1,1}$ reactances presented by the front and rear cavity sections were relatively independent of tuning since the $TE_{1,1}$ mode in the main cavity was beyond cut-off. But

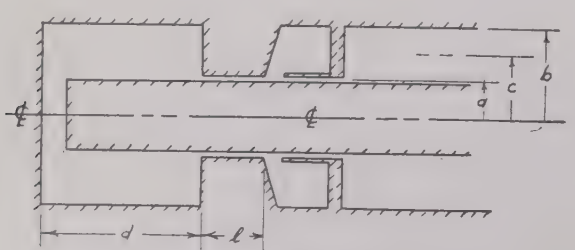

Fig. 5—Idealized coaxial cavity with inner plunger gap.

for the inner-gap resonances, now to be considered, the $TE_{1,1}$ mode can propagate in the main cavity (λ_a being always less than λ_c) and the impedances presented by the main cavity sections may vary rapidly over wide ranges depending upon the cavity length and frequency.

For this reason, the inner-gap resonance is similar to resonance in a *variable* circuit in which there exists some functional relation between the value of the circuit parameters and frequency of the driving force. Of course, this same situation was true for the outer-gap resonance, but in that case the circuit parameters B_f, B_s, and B_r varied so slowly with frequency that they could be considered as constants.

Let us consider for the moment an idealized coaxial resonator such as that shown in Fig. 5. This cavity will resonate for the principal or TEM mode when the cavity is an odd multiple of a quarter-wave long. (This, of course, ignores the capacity loading of the tube.) Also, the cavity will resonate to a $TE_{n,1}$ mode when the equivalent cavity length is any multiple of one-half the guide wavelength. Assuming that the plunger presents a perfect short circuit to all TE modes, the resonant wavelengths as a function of cavity lengths would plot as the solid curves of Fig. 6.

The $TE_{1,1}$ resonance curve shown in Fig. 6 is based upon an idealized cavity with a perfect plunger. It does

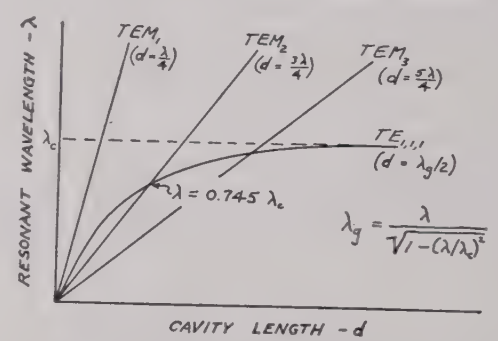

Fig. 6—Simultaneous resonance of the $TE_{1,1,1}$ and TEM_2 modes in a coaxial cavity.

show, however, that a parasitic resonance may be expected in a coaxial oscillator operating on the 3/4-wave cavity mode when the wavelength is about 3/4 of the mean circumference.

Actually, however, the plunger may not present a short circuit to the $TE_{n,1}$ waves. In the vicinity of inner-gap resonance the conditions of short electrical length and high-impedance termination of the gap are essentially the same as those assumed in the calculation of the outer-gap impedance. Consequently, the same analysis applies for the input $TE_{1,1}$ impedance of the inner gap, and hence to a reasonable approximation the plunger impedance to the $TE_{1,1}$ wave is the reciprocal of the admittance of the front low-impedance line section, or

$$Z_p = -j\frac{\eta t}{4\pi l\delta} \tag{13}$$

where in this case

$$\delta = 1 - \frac{\lambda}{\lambda_a}.$$

[5] Major dimensions of this plunger (footnote reference 2) were as follows:

$\lambda_a = 7.6$ centimeters	$t = 0.025$ centimeter
$\lambda_b = 13.9$ centimeters	$l = 1.7$ centimeter
$\lambda_c = 10.7$ centimeters	$d = 0.6$ centimeter.

Now, the $TE_{1,1}$ resonance will occur when the cavity impedance is the negative of the plunger impedance. That is, when

$$j\frac{Z_c'}{\sqrt{1-\left(\frac{\lambda}{\lambda_c}\right)^2}}\tan\left[\frac{2\pi d}{\lambda}\sqrt{1-\left(\frac{\lambda}{\lambda_c}\right)^2}\right] = j\frac{\eta t}{4\pi l\delta}. \quad (14)$$

For all except the smallest values of δ, the right side of (14) is practically zero and the curve shown in Fig. 6,

$$d=\frac{\lambda}{2\sqrt{1-\left(\frac{\lambda}{\lambda_c}\right)^2}},$$

results as a solution.

However, at wavelengths nearly equal to the inner-gap circumference λ_a, the $TE_{1,1}$ resonance characteristic is distorted by a discontinuity at $\lambda=\lambda_a$. The tuning characteristic may be calculated by solving (14) for d, thus:

$$d=\frac{\lambda}{2\pi\sqrt{1-\left(\frac{\lambda}{\lambda_c}\right)^2}}\tan^{-1}\left\{\frac{\eta t}{4\pi l\delta}\frac{\sqrt{1-(\lambda/\lambda_c)^2}}{Z_c'}\right\}. \quad (15)$$

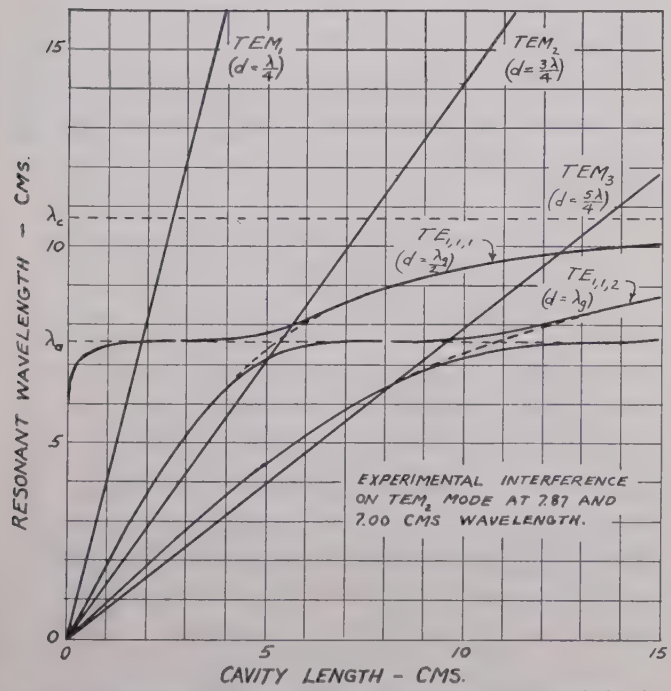

Fig. 7—Calculated *TEM* and $TE_{1,1}$ resonance characteristics including effect of inner-gap circumferential resonance.

The distortion resulting from this resonance is illustrated in Fig. 7. The multiple-valued $TE_{1,1}$ tuning curves, as calculated from (15) for the same cavity dimensions as used in the outer-gap resonance calculations, are shown together with *TEM* or dominant tuning curves.

The undistorted $TE_{1,1}$ resonance curve is also shown in Fig. 7 as a broken line. It should be pointed out that the wavelength of theoretical crossover of the 3/4-wave *TEM* mode by the $TE_{1,1}$ mode should occur at $0.745\lambda_c$. That this crossover point coincides with λ_a is mere happenchance.

Experimental Agreement with Theory

The curves of Fig. 7 indicate that parasitic resonances may be expected to occur in an oscillator operating on any of the *TEM* cavity modes; the following comparisons apply specifically to resonances observed with the oscillator operating on the 3/4-wave *TEM* mode.

Values read from the curve are 7.98 and 7.2 centimeters. Experimental measurements made on an oscillator having the cavity and plunger dimensions used in these calculations showed parasitic resonances at 7.90, 7.83, and 7.00 centimeters. The first two resonances are probably a single resonance which has been split either because of plunger eccentricity or a double-resonance effect similar to that occurring in the outer gap. It is interesting that if the *TEM* 3/4-wave curve is shifted slightly (as it well may be in an actual oscillator due to tube capacitance and corner effects), the agreement between calculated and measured resonances is as shown in Table II. Again, this is considered to be a satisfactory agreement of theory and experiment.

Table II

Calculated (centimeters)	Experimental (centimeters)
7.9	7.87 (average)
7.0	7.00

The one-cycle resonances that have been observed to occur around the inner and outer plunger gaps have thus been explained and found to be in close agreement with theoretical considerations. It is believed that the same theory may be extended to explain multiple-cycle resonances as well.

IV. Excitation of Plunger Circumferential Resonances

It will now be shown that an eccentric plunger acts as a transformer which couples the dominant *TEM* mode to the various *TE* modes in the cavity and in the plunger. A perfectly round plunger in a perfectly round cavity, while coupling into the $TE_{1,1}$ mode by an amount proportional to the eccentricity, will produce little direct coupling to the $TE_{2,1}$ and higher-order $TE_{n,1}$ waves.

It is significant that there are actually always *two* $TE_{1,1}$ modes that may exist in the plunger and cavity. These modes usually exist at approximately right angles to each other, and their behavior is reminiscent of the "two-reaction theory" in rotating machinery. If cavity

and plunger asymmetries are sufficient and of the proper spatial relationship, it will be observed that what would otherwise be a single $TE_{1,1}$ resonance will split into two resonances at slightly different wavelengths. A plausible explanation of this behavior will now be presented.

Consider the eccentric plunger gap shown in Fig. 8. As a first approximation it may be assumed that the voltage $V(\phi)$ across the gap at any angle ϕ will be proportional to the gap thickness and the radial current density $i(\phi)$. Thus, the voltage across the gap will be, approximately,

$$V(\phi) = CZ_p(1 - \alpha \cos \phi) \cdot i(\phi) \tag{16}$$

where C is the circumference of the gap and α is the eccentricity factor. If the plunger gap is driven exclusively by a current corresponding to the TEM mode,[6] the current density $i_0(\phi)$ will be constant, I_0/C, and the induced voltage drop across the front of the gap will be

$$V(\phi) = Z_pI_0 - \alpha Z_pI_0 \cos \phi. \tag{17}$$

The first term on the right of (17) is the TEM voltage drop that might be expected in the absence of any plunger eccentricity.

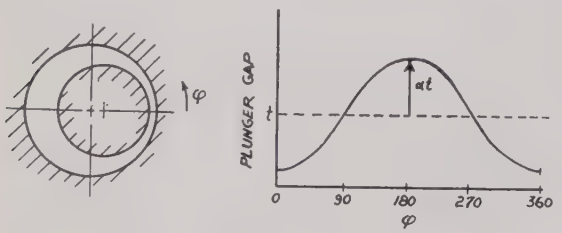

Fig. 8—Eccentric plunger gap.

The second term on the right of (17), however, represents a new voltage arising from the eccentricity. *This voltage is a $TE_{1,1}$ voltage*, since it makes one complete cycle in the gap circumference. Thus, the TEM mode can excite the $TE_{1,1}$ mode through an eccentric plunger gap.

Consider next the plunger voltage drop induced by a $TE_{1,1}$ radial current. Since the current I_1 flows in a given direction only over half of the circumference of the gap, the radial current density may be expressed as

$$i_1(\phi) = \frac{I_1}{C/2} \cos (\phi - \psi)$$

$$= \frac{2}{C} [I_{1d} \cos \phi + I_{1q} \sin \phi]$$

where ψ is the angle at which the $TE_{1,1}$ radial current is a maximum. Because the "cos ϕ" field is in the direction of the axis of the eccentricity, it is referred to as the "direct-axis" field, while the "sin ϕ" field is the "quadrature-axis" field. The direct-axis and quadrature-axis components are designated by subscripts d and q, respectively.

We shall separately consider the voltage drops arising from each of the two components, the fields of which are

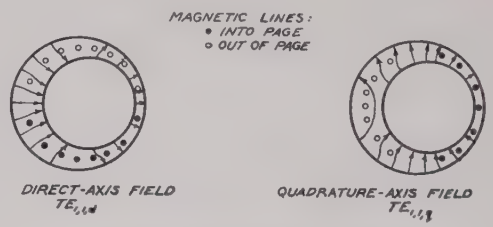

Fig. 9—Two possible $TE_{1,1}$ fields.

sketched in Fig. 9. The voltage drops resulting from the impressed $TE_{1,1,d}$ current will be, by (16),

$$V(\phi) = CZ_p(1 - \alpha \cos \phi) \frac{I_{1d}}{C/2} \cos \phi$$

$$= -\alpha Z_p \cdot I_{1d} + 2Z_p \cdot I_{1d} \cos \phi - \alpha Z_p \cdot I_{1d} \cdot \cos 2\phi$$

$$= V_{0d} + V_{1d} + V_{2d}. \tag{18}$$

The first term on the right of (18) is a *constant* in ϕ and, as such, represents a TEM component of voltage drop. The second represents the $TE_{1,1}$ or self-voltage drop, while the third represents a $TE_{2,1}$ voltage drop. *Thus, in general, we may show that a current wave having n circumferential variations will produce a voltage drop component of n variations, but in addition there will be two "side-band" voltage-drop components of $n-1$ and $n+1$ circumferential variations.*

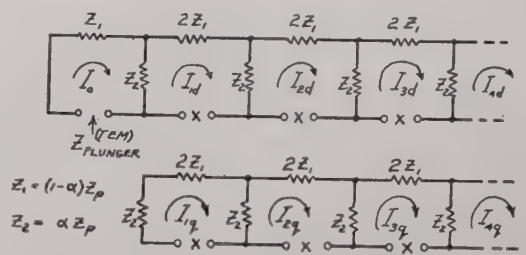

Fig. 10—Equivalent circuit of eccentric plunger.

On the other hand, the voltage drop resulting from the quadrature-axis $TE_{1,1,q}$ impressed current will be

$$V(\phi) = CZ_p(1 - \alpha \cos \phi) \frac{I_{1q}}{C/2} \sin \phi$$

$$= 2Z_pI_{1q} \sin \phi - \alpha Z_pI_{1q} \sin 2\phi$$

$$= V_{1q} + V_{2q}$$

and it is observed that the $TE_{1,1,q}$ field does not couple to the principal mode.

If we identify each of the TEM, $TE_{n,1,d}$, and $TE_{n,1,q}$ currents impressed upon the plunger face with the individual mesh currents of a linear lumped circuit, the

[6] In establishing these relations the voltage drops resulting from each mode current (with all other mode currents reduced to zero) are required. This is exactly the same procedure as followed in setting up the mesh equations of a linear lumped network.

equivalent circuit of an eccentric plunger may be constructed as shown in Fig. 10. At each terminal pair marked "x," the impedance of the cavity, as seen from the face of the plunger for the mode represented by that particular mesh, is to be inserted. Conversely, if the impedance of the plunger to any particular mode is desired, the equivalent circuit may be "viewed" from the corresponding "x" pair.

In the idealized, lossless plunger assumed in setting up Fig. 10, there is no coupling between the dominant- and quadrature-axis meshes. That is, quadrature-axis resonances would not effect the direct-axis and principal modes, and vice versa. Actually, because of power losses, there does exist a coupling between the direct- and quadrature-axis fields, with the result that a quadrature-axis resonance introduces a *resistive* component into the dominant plunger impedance. The reason why this is so may be seen by analogy to the standing-wave components in a resonant line which is terminated in a very small resistance used to simulate the circuit losses. If $R=0$ for the lossless case, the instantaneous voltage along the line shown in Fig. 11 will be

$$e = [E \cos \omega t] \cos \theta. \tag{20}$$

On the other hand, if $R \neq 0$,

$$e = [E \cos \omega t] \cos \theta + \frac{R}{Z_0} [E \sin \omega t] \sin \theta. \tag{21}$$

Thus it is seen that the effect of the loss is to add to the original voltage (20) an additional term which differs both in *time* and *space* phase by 90 degrees. In other words, associated with each *quadrature-axis reactive*

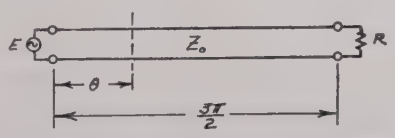

Fig. 11—Resonant line possessing a small dissipation resistance R.

voltage drop there will be induced because of losses a direct-axis resistive voltage drop, and vice versa. For this reason, the plunger reactance presented to the TEM mode will be distorted appreciably only by the $TE_{1,1,d}$ resonance. The principal effect of the $TE_{1,1,q}$ resonance is greatly to increase the plunger dissipation. This may "load" an oscillator sufficiently to produce a "hole."

Experimental Verification of Two-Reaction Theory

It is admitted that the foregoing analysis is grossly oversimplified. If the structure of the equivalent circuit shown in Fig. 10 is at all justified, it is certainly true that the values of the individual impedances in the circuit should all be different and include the various refractive indexes, etc. Nevertheless, the circuit is helpful in explaining qualitatively various experimental observations. Fig. 12 shows the actual mode plot made on a coaxial cavity having a short circuit at one end and an insulated choke plunger at the other. The data pre-

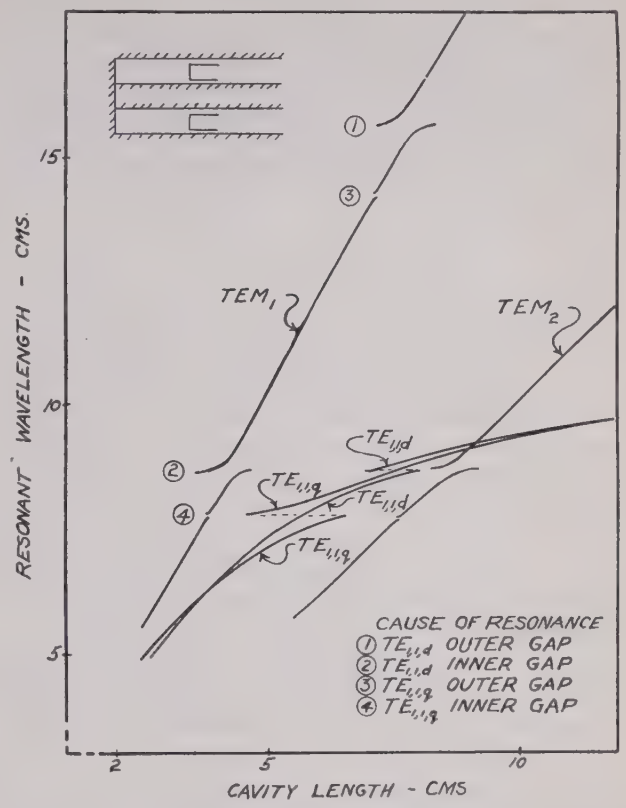

Fig. 12—Experimental mode plot of coaxial cavity with eccentric choke plunger.

sented in this figure are of special significance in that they illustrate the marked difference that may be obtained between direct- and quadrature-axis resonant wavelengths. Furthermore, they show that the direct-axis $TE_{1,1}$ resonances at points 1 and 2 introduce large *reactances* into the principal-mode plunger impedance and hence distort the TEM tuning curves, whereas the quadrature-axis resonances at points 3 and 4 result primarily in *resistive loading* of the principal mode. Notice also that two $TE_{1,1}$ resonant plots appear; one for the direct- and the other for the quadrature-axis cavity fields.

With reference to Fig. 9, observe that in the case of the direct-axis field the eccentricity tends to increase the capacitance more on one side than it is decreased on the other, with the result that the effective capacitance of the plunger is increased. On the other hand, the permeance of the magnetic path (the axial magnetic lines being of maximum density at nearly 90 degrees from the maximum electric field) is practically unchanged. The effect of a marked eccentricity is, therefore, to increase the resonant wavelength of the direct-axis field and to change only slightly the resonant wavelength of the quadrature-axis field. This is in accord with the experimental data of Fig. 12.

Microwave Antenna Analysis*

SAMUEL SEELY†, SENIOR MEMBER, I.R.E.

Summary—The diffraction theory of Stratton and Chu is applied to a calculation of the vertical polar diagram and the gain of a parabolic cylindrical antenna. This antenna is fed by a line source having a known energy distribution and polarization. A numerical calculation for a particular profile is carried out, and the results are compared with those obtained experimentally. Satisfactory agreement between these results is found.

I. Introduction

A. General

A DIRECTIONAL antenna in the wavelength range from approximately 1 to 10 meters usually consists of a broadside array of dipole radiators backed by an appropriate plane reflector. At the microwave frequencies the antenna ordinarily consists of a shaped reflector which is illuminated by a relatively simple feed.

If the reflector is a paraboloid of revolution with the diameter of the face plane d much greater than the wavelength λ, and if the antenna feed is placed at the focus, the assemblage is somewhat analogous to a searchlight with an arc at the focus. The analogy would be almost complete if the feed were a true point source with regards to its own equiphase surfaces, since the resulting illumination at all points in the face plane or aperture plane of the reflector would have the same phase. Because of this similarity with the optical problem, the Kirchoff-Huygens method in physical optics is sometimes used to study the details of antenna systems.

Owing to the fact that many of the problems of interest in microwave systems are those for which the assumptions inherent to the Kirchoff theory are not valid, this method cannot always be expected to yield significant results. In microwave antennas the length of the wave may be of the same order as the dimensions of the opening, and, moreover, the polarization of the diffracted radiation is easily observed. As a result, the Kirchoff theory, which replaces the vector wave equation by a scalar wave equation, neither relates the vectors E and H nor satisfies the proper boundary conditions.

The general problem of diffraction has been examined by Stratton and Chu[1] who have developed a method for the direct integration of the field equations. They examined the limitations of the method, and considered the approximations that are necessary in order to apply the results to the problem of diffraction at a slit. It is found possible to make the appropriate assumptions in order to satisfy the boundary conditions. The present paper is an application of the method to an evaluation of the polar diagram from a reflector having a known profile which is illuminated by a feed of known energy distribution and polarization. The method is substantially that of T. J. Keary, now of the Naval Radio and Sound Laboratory.

B. Fundamental Considerations

A particular type of problem is to be examined, although the general principles remained in evidence. This problem, which is one that possesses practical importance, can be solved by a relatively direct application of the general theory.

A formal statement of the problem is the following: An antenna system having the general features illustrated in Fig. 1 consists of a parabolic cylinder of length l which is illuminated by a linear feed having a known energy distribution and polarization. The feed is placed on the focal axis of the cylinder. It is desired to calculate the polar diagram in the median plane, and the gain of this antenna.

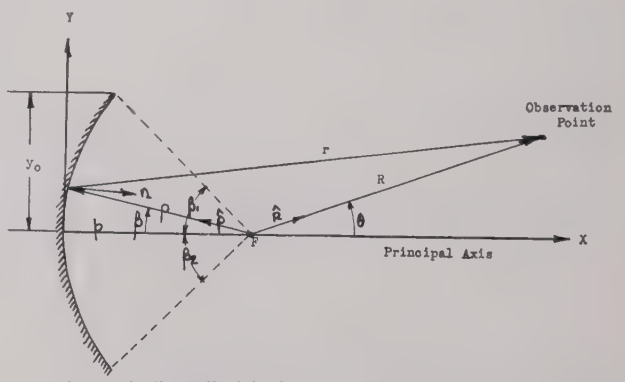

Fig. 1—A parabolic cylindrical antenna illuminated by a line feed.

The problem actually resolves itself into two problems; first, that of finding the charge and current distribution induced on the reflector due to the field of the feed, and second, that of finding a solution of Maxwell's equations for $\boldsymbol{E}$ and $\boldsymbol{H}$ at all points in space, and which satisfy the appropriate boundary conditions.

The general solution is expressible in terms of the retarded vector potential $\boldsymbol{A}$, and the retarded scalar potential ϕ, which are given by

$$\left.\begin{aligned} A &= \frac{\mu_0}{4\pi}\int \frac{[i]}{r}\,d\tau = \frac{\mu_0}{4\pi}\int_S \frac{[i]}{r}\,dS \\ \phi &= \frac{1}{4\pi\epsilon_0}\int \frac{[\rho]}{r}\,d\tau = \frac{1}{4\pi\epsilon_0}\int_S \frac{[\sigma]}{r}\,dS \end{aligned}\right\} \tag{1}$$

with

$$\left.\begin{aligned} H &= \nabla \times A \\ \text{and} \quad E &= -\nabla\phi - \frac{\partial A}{\partial t} \end{aligned}\right\}. \tag{2}$$

* Decimal classification: R326.8. Original manuscript received by the Institute, June 26, 1946; revised manuscript received, November, 5, 1946.

† Formerly, Naval Postgraduate School, United States Naval Academy, Annapolis, Md.; now, Syracuse University, Syracuse, N.Y.

[1] J. A. Stratton, "Electromagnetic Theory," pp. 464 et seq., McGraw-Hill Book Co., New York, N. Y., 1941.

The current density i and the charge density σ are those that are induced in the reflector surface by the fields of the feed. They are, of course, related by the continuity equation $\Delta \cdot i + (\partial\sigma/\partial t) = 0$. However, in order to reconcile the discontinuities in the tangential components of E and H at the edges of the reflector, it is necessary to assume the existence of a line distribution of charge or currents about the contour of the reflector.

C. Field Considerations

Separate considerations are required for the E vector parallel to the principal plane (horizontal polarization) and the E vector in the normal plane (vertical polarization. For the case of horizontal polarization, $\sigma = 0$, and the total distant field is given in terms of the vector potential

$$A = \frac{\mu_0}{4\pi}\int_S \frac{[i]}{r}\,dS. \tag{3}$$

For the case of vertical polarization, the conditions are somewhat more involved. It is not necessary to find an expression for ϕ, as it can be shown that it, and the line distribution at the edges of the reflector, contribute radial components, whereas the surface current contributes both radial and transverse components to the distant field. But as these radial components must cancel to order $1/R$ at large distances, it is only necessary to compute the transverse component of the field. This is given by the expression

$$A_\theta = \frac{\mu_0}{4\pi}\int_S \frac{[i]\cos(n, \widehat{R})}{r}\,dS. \tag{4}$$

For the particular problem under survey, the feed is vertically polarized, and this latter expression must be evaluated.

II. Detailed Calculation

By taking into account the incident and reflected fields at the surface of the reflector arising from the presence of the antenna feed, the following expression for the current induced in the surface of the reflector results

$$i = 2\sqrt[4]{\frac{\epsilon_0}{\mu_0}}\sqrt{\frac{P}{\pi l}}\sqrt{\frac{G(\beta)}{p}}\,e^{-jkp}. \tag{5}$$

In this expression, P denotes the power emitted from a length l of the line source; and $G(\beta)$ is the power gain of the line source, and is the ratio of the power per radian in the direction β to the average power per radian. The expression for A then assumes the form

$$A = \sqrt{\frac{\epsilon_0\mu_0}{2\pi}}\sqrt[4]{\frac{\mu_0}{\epsilon_0}}\sqrt{\frac{P}{\pi}}\sqrt{lp}\,\frac{e^{-jk(R+2p)}}{R} \int_{\beta_1}^{\beta_2}\sqrt{G(\beta)}\,\frac{\cos(n, \widehat{R})}{\cos(n, -\hat{\rho})}\sqrt{\frac{\rho}{p}}\,e^{2jkp[1-\rho/2p[1+\cos(\beta+\theta)]]}d\beta. \tag{6}$$

It is this expression that must be combined with (2) to give E and H at all points in space.

The polar diagram, denoted by $g(\theta)$, is a measure of the absolute value of the electric field intensity at a fixed distance R from the source. It is given by

$$g(\theta) = |RE| = NI(\theta) \tag{7}$$

where N is a normalizing factor, and $I(\theta)$ is the integral

$$I(\theta) = \int_{\beta_1}^{\beta_2}\sqrt{G(\beta)}\sqrt{\frac{\rho}{p}} \cdot \frac{\cos(n, \widehat{R})}{\cos(n, -\hat{\rho})}\,e^{2jkp[1-\rho/2p[(1+\cos(\beta+\theta)]]}d\beta. \tag{8}$$

The gain of the antenna is defined as

$$G(\theta) \equiv \frac{\text{power per solid angle in direction } \theta}{\text{average power per solid angle}}.$$

An evaluation of the optimum value of this expression leads to the form

$$G(\theta)_m = \left(4\pi\frac{A'}{\lambda^2}\right)\left[\frac{p}{4\pi y_0}\,|I(\theta)_m|^2\right] \tag{9}$$

where A' is the face area of the reflector, and where $I(\theta)_m$ is the optimum value of (8), and is

$$I(\theta)_m = \int_{\beta_1}^{\beta_2}\sqrt{G(\beta)}\sqrt{\frac{\rho}{p}}\,\frac{\cos(n, \widehat{R})}{\cos(n, -\hat{\rho})}\,d\beta. \tag{10}$$

The first term in (9) is that for a uniformly illuminated reflector, and the second term is the factor which takes account of the fact that the array is not uniformly illuminated.

For the parabolic cylinder, and for the case of small angles θ, the integral in (8) may be simplified. The expression becomes

$$I(m) = 2\int_{\mu_1}^{\mu_2}\sqrt{G(\mu)}\,\frac{1}{\sqrt{1+\mu^2}}\left[1 - \frac{m\mu}{2kp}\right]e^{jm\mu}d\mu \tag{11}$$

where

$$\left.\begin{aligned} m &= 2kp\theta \\ \mu &= \tan\beta/2 \end{aligned}\right\}. \tag{12}$$

III. Comparison of Calculated and Experimental Results

As a verification of this expression, the polar diagram in the horizontal plane of the AN/MPN-1 10.7-centimeter search radar system, as obtained experimentally by C. F. Porterfield and L. J. Chu of the Radiation Laboratory, M.I.T., will be compared with the results obtained from theory. This antenna consists of a $4' \times 8' \times f = 27.5$-inch reflector which is illuminated by a feed consisting of a dipole and reflector. For this system $\beta_1 = \beta_2 = 47$ degrees.

A plot of the primary or feed pattern is given in Fig. 2. Also plotted on the same curve sheet is the function

$\cos^4 \beta$. It will be observed that the agreement between the two curves is reasonably satisfactory over the range

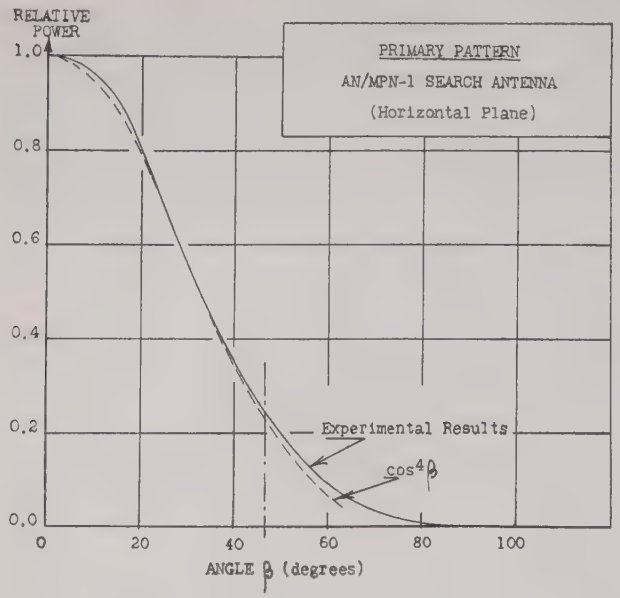

Fig. 2—Primary pattern of the AN/MPN-1 search antenna in the horizontal plane.

of interest, namely, 0 to 47 degrees. Over this range, the gain of the feed is given by the expression

$$G(\beta) = 5.16 \cos^4 \beta \tag{13}$$

where 5.16 is the peak gain of the feed. The resulting expression for $I(m)$ becomes

$$I(m) = 2 \times 5.16 \int_{-0.435}^{0.435} \frac{(1-\mu^2)^2}{(1+\mu^2)^{5/2}} \left[1 - \frac{m\mu}{2kp}\right] e^{jm\mu} d\mu. \tag{14}$$

This is a difficult expression to integrate in its present form, and it is found convenient to replace the integrand by an equivalent, though less complicated, analytical form. First, however, it is noted that the second term in the integrand can be neglected, since for small θ it is only a few per cent of the first term. To find a simpler analytical form to replace the first term, one plots the integrand and then seeks an expression that approximates it. For this problem it is found that over the range of interest we may write with good approximation

$$\frac{(1-\mu^2)^2}{(1+\mu^2)^{5/2}} \simeq [1 - (1.16\mu)^2]^3. \tag{15}$$

By noting that the resulting function is an even function, the integral for solution becomes, finally,

$$I(n) = \frac{2 \times 5.16}{1.16} \int_{-.504}^{.504} (1 - z^2)^3 \cos nz dz \tag{16}$$

where

$$\left.\begin{aligned} n &= \frac{m}{1.16} = \frac{2kp\theta}{1.16} = 70.8\theta \\ z &= 1.16\mu \end{aligned}\right\}. \tag{17}$$

This expression may be integrated by parts to yield the expression

$$g(n) = N' \left\{ \frac{2}{n} \sin .504n \left[0.415 - \frac{1.206}{n^2} - \frac{19.44}{n^4} + \frac{720}{n^6} \right] - \frac{1.008}{n^2} \cos .504n \left[3.342 + \frac{41.5}{n^2} + \frac{720}{n^4} \right] \right\}. \tag{18}$$

A plot of this expression, normalized to unity, is given in Fig. 3. Also included in this figure is the experimentally determined curve of Porterfield and Chu.

To calculate the peak gain of the array, we must evaluate (10). The integral becomes

$$I(n)_m = \frac{2 \times 5.16}{1.16} \int_{-.504}^{.504} (1 - z^2)^3 dz = 3.10.$$

By combining this result with (9) there results

$$G(\theta)_m = 0.875 \left(4\pi \frac{A'}{\lambda^2}\right) = 2870.$$

A comparison of the curves given in Fig. 3 shows that the result obtained analytically agrees quite well with the result that was obtained experimentally. A number of factors contribute to the difference between them, among which are: (a) neglecting the

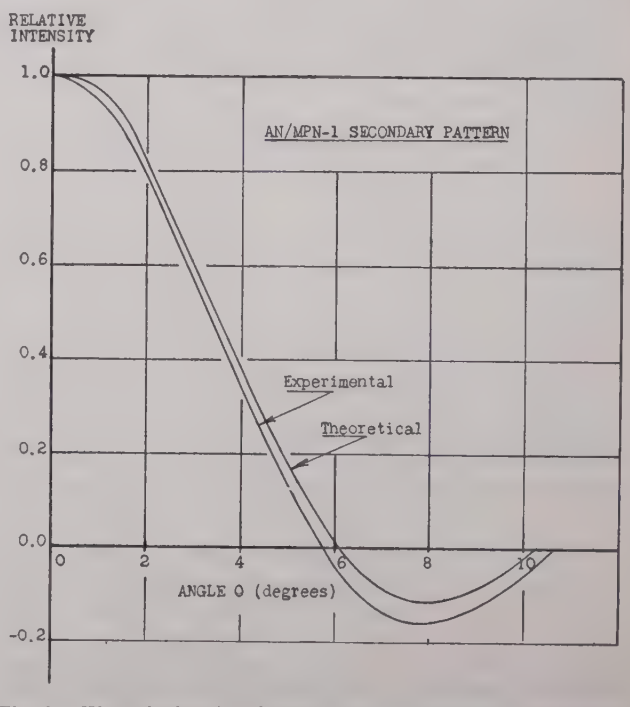

Fig. 3.—The calculated and experimental secondary polar pattern of the AN/MPN-1 radar.

effect of the presence of the feed in the field of the reflector; (b) the error in the approximation by replacing the experimental feed pattern by the analytic form given in (13); (c) neglecting the second term in (14); (d) the error in the approximation in replacing one analytic function by an equivalent form (15); (e) the implicit as-

sumption that the current at a given point on the reflector is produced only by the field from the feed, and is not affected by radiation from currents on other parts of the reflector; and (f) experimental inaccuracies.

As to the gain of the array, a direct comparison with the experimentally determined value is not possible. This is so because the AN/MPN-1 antenna is actually quite different from that considered herein. It consists of a four-foot section cut out of an eight-foot paraboloid of revolution. Moreover, the feed consists of two spaced dipoles placed near the focus of the paraboloid. Consequently the geometry relative to one of the principal planes is identical with that of the parabolic cylinder, although the geometry relative to the other principal plane in no way resembles that of the assumed cylindrical shape. However, it is possible to show that the gain of the AN/MPN-1 antenna should be very nearly equal to one-half that of the antenna herein discussed. One should therefore compare the estimated value of $0.5 \times 2870 = 1435$ with the measured 1450 ± 10 per cent to see that the results as calculated are entirely reasonable.

IV. Acknowledgment

The author wishes to acknowledge the several discussions with Samuel Silver, now of the Naval Research Laboratories.

Approximate Equivalent Circuit for a Resonator Transducer*

WILLIAM R. MacLEAN†, ASSOCIATE, I.R.E.

Summary—**The equivalent circuit of a high-Q resonator transducer is given as a set of unit transducers connected in series on both ends. Each unit is a tank circuit with $\sqrt{L/C} = 120\ \pi$, and two ideal transformers whose turns ratios are given for loops or probes in terms of electrode geometry and a quantity called relative volume.**

CONDON[1] HAS derived formulas for the impedance of loops and probes in hollow reasonators. By slight changes, similar results may be had with variable ϵ, u. The necessary changes to accomplish this are indicated in the appendix. Here the result in meter-kilogram-second units of such a modified derivation is merely stated:

$$Z_c = Z_s + \sum_a \frac{j\omega M_a^2}{U\left(\omega_a^2 - \omega^2 + j\frac{\omega\omega_a}{Q_a}\right)} = Z_s + \sum_a Z_a \quad (1)$$

with

$$U = \int \epsilon A_a^2 dv \qquad \text{instead of Condon's (1),}$$

and

$$M_a = \frac{1}{I}\int \mathbf{G}\cdot\mathbf{A}_a dv \qquad \text{instead of Condon's (9),}$$

where $\mathbf{G}$ is current density, I is driving-point current, and Z_s is the ohmic resistance R_s for a loop, or the reactance of the direct-current capacitance C_s for a probe. This Z_s is taken care of immediately by extracting it as a series element.

* Decimal classification: R119.35. Original manuscript received by the Institute, July 8, 1946; revised manuscript received, February 3, 1947.

† Polytechnic Institute of Brooklyn, Brooklyn, N. Y.

[1] E. U. Condon, "Forced oscillations in cavity resonators," *Jour. Appl. Phy.*, vol. 12, pp. 129–32; February, 1941.

Suppose there are two electrodes, 1 and 2, in the resonator. Then for the open circuit Z_{11} and Z_{22} of such a transducer, immediately two such equations as (1) with the corresponding M's subscripted 1 and 2 appear. For the open-circuit transfer impedance Z_{12} it can be shown that the same (1) holds, except that $(M_{a1}\ M_{a2})$ replaces M_a^2.

Using $\eta_0 = \sqrt{\mu_0/\epsilon_0} = 120\pi$, it was decided to write a general formula for $Z_{nm}(n, m = 1, 2)$ in the form:

$$Z_{nm} = \sum_a \frac{M_{an}}{\sqrt{U\omega_a\eta_0}} \frac{M_{am}}{\sqrt{U\omega_a\eta_0}} \left(\frac{j\omega\omega_a\eta_0}{\omega_a^2 - \omega^2 + j\frac{\omega\omega_a}{Q_a}} \right). \quad (2)$$

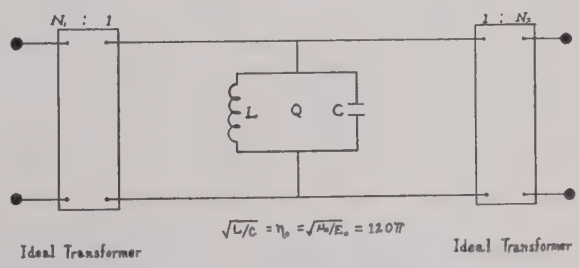

Fig. 1—A unit transducer for one mode.

The last factor is the impedance Z_{a0} of a high-Q parallel-resonant circuit, resonant at ω_a with quality Q_a and surge impedance η_0. The first factors are called N_{an} and N_{am}, respectively, and are written:

$$Z_{nm} = \sum_a N_{an}N_{am}Z_{a0} = \sum_a Z_{anm}. \quad (3)$$

Consider a transducer representing only one term of

this series. Its equivalent circuit would be as shown in Fig. 1: its open-circuit impedances check with (3).

If several such units were connected in series on both ends, all the open-circuit impedances would add. But this is exactly what happens if more terms of (3) are used.

Consequently, the equivalent circuit of a resonator transducer consists of such a double series arrangement of the unit transducers shown in Fig. 1, with a Z_{s1} and Z_{s2} finally added in series on each end.

What is needed now is a better formula for the N's.

Loops

For a loop, M_{an} is easily shown equal to $(s_{an}B_{an})$ where B_{an} is the magnitude of $\boldsymbol{B}_a$ (by phase choice it is made real) associated with the standard $\boldsymbol{A}_a$ at the locale of electrode n, and s_{an} is the projected area of the loop in the direction of $\boldsymbol{B}_{an}$.

Put

$$V_{an} = \frac{\mu_0}{B_{an}^2}\int \frac{1}{\mu}\boldsymbol{B}_a^2 dv \qquad (4)$$

and note that by invoking the undamped wave equation which the $\boldsymbol{A}_a$ obey, the equation for U can be changed into

$$U = \frac{1}{\omega_a^2}\int \frac{1}{\mu}\boldsymbol{B}_a^2 dv$$

as a result of which the formula for N_{an} can be written:

$$\boxed{N_{an}^2 = \frac{\beta_a s_{an}^2}{V_{an}}} \quad \text{for a loop.} \qquad (5)$$

Here β_a is $2\pi/\lambda_{0a}$, i.e., the vacuum phase factor of ω_a. This equation is usable practically if the simple nature of V_{an} is pointed out; it is a relative volume of the resonator, i.e., the vacuum volume it would have to have to contain the stored magnetic energy of mode a if B_a had everywhere the magnitude obtaining at electrode n. Fortunately, this is often easy to estimate.

Probes

For probes V_{an} is defined on the basis of stored electric, rather than magnetic, energy, and since in the undamped modes $\boldsymbol{A}_a$ the stored electric and magnetic energies are equal, U can be given in terms of electric energy as well. A short, straight probe will have a current distribution that is linear from zero at the tip to the driving-point value at the base. Letting $2h_{an}$ be the projected height in the direction of the electric field $\boldsymbol{E}_a$, associated with $\boldsymbol{A}_a$, M_{an} can be calculated as:

$$M_{an} = \frac{E_{an}h_{an}}{j\omega_a}$$

which is real, since $\boldsymbol{E}_a$ is imaginary by the choice of phase. h_{an} is the effective height. Using these facts, one can obtain for N_{an}:

$$\boxed{N_{an}^2 = \frac{h_{an}^2}{\beta_a V_{an}}} \quad \text{for a probe.} \qquad (6)$$

The relatively simple equivalent circuit obtained in this way is limited to high Q's, and moreover the Q actually depends on ω. Hence, the circuit is not equivalent in the full sense of the word. It is, however, a good approximation since Q_a is of little influence except near ω_a, so the resonance value can be used.

In practice, we know that the modes far off resonance contribute negligibly to Z_{12}. Near any resonance these modes merely add a nearly constant impedance to Z_{sn}, so they can be accounted for satisfactorily in most cases by adding them to Z_{sn}. This leaves essentially only one unit transducer together with two modified Z_{sn} which often can be calculated by other means. If there is a frequency degeneracy at the desired resonance, several units would be required and irregularities would probably split their frequencies and cause a multiple-peak effect. However, usually only one would be strongly coupled.

Electron-beam coupling can be handled like a probe by dropping the factor $\frac{1}{2}$ in the effective height.

By "resonator transducer" is implied a distinction with "wave-guide transducer"; in the former, frequency and dimensions are such that no appreciable power transfer can occur except near the resonances. The final simplification rests on this distinction.

Appendix

To modify Condon's results for arbitrary μ, ϵ, start with Maxwell's equations in the field quantities $\boldsymbol{E}$ and $\boldsymbol{B}$ Introduce the Lorentz potentials in the usual way, but work with the gauge:

$$\text{div}\,(\epsilon \boldsymbol{A}) = 0.$$

In this case ϕ becomes the instantanecus static potential. The ordinary wave and Laplacian equations are not obtained since μ, ϵ are variable. In the force-free case, eigen $\boldsymbol{A}_a$'s exist orthogonal against ϵ.

The modified wave equation for $\boldsymbol{A}$, in the driven case, has the driving term $\boldsymbol{G} - \epsilon$ grad $\partial\phi/\partial t$. This has no divergence and is expandable in a series of $\epsilon\boldsymbol{A}_a$ due to the choice of gauge, and only G contributes to the coefficients.

With these changes one obtains the results given.

In the case of loops, one is forced to the approximation that the current is constant and hence no charges. This is the inexactitude in (1) and restricts it to loops small compared to λ.

In the case of probes, one assumes the current distribution to be the same as at low frequencies. This is approximately so for probes short compared to λ and so restricts (1). Condon's "internal electrode" is not necessary with the form of M_a used here.

Discussion on

"High-Impedance Cable"*

HEINZ E. KALLMANN

M. R. Winkler:[1] The paper by Kallmann is interesting, but additional comment is in order.

Unfortunately, Kallmann's formula for inductance is in error because it assumes that the magnetic field is not confined within the outer shield. Since it is confined within the shield, the reluctance of the magnetic path between the shield and the coil must be taken into account. A good simple handbook formula for inductance is

$$L = \frac{10^{-9}4\pi N^2}{R} \text{ henries,} \qquad (1)$$

which is taken from Pender and McIlwain.[2] Here R is the total magnetic reluctance of the flux path. It is the sum of the reluctances of the flux paths both inside the coil and between the coil and the shield. For a long solenoid, each of these reluctances is inversely proportional to its respective cross-sectional area. Using the same nomenclature as Kallmann, except letting N = turns per centimeter, the inductance formula becomes:

$$L = 10^{-9}\pi^2 N^2 d^2\left[1 - \left(\frac{d}{a}\right)^2\right] \text{ henries per centimeter.} \qquad (2)$$

This formula becomes equivalent to Kallmann's equation (4) as a becomes large. The inductance reaches an optimum value when $d = 0.707a$, as it obviously should.

If the capacitance is written in terms of natural logarithms to facilitate differentiating, etc., and if the thickness of the wire is neglected, the characteristic impedance becomes:

$$Z = \frac{133Nd}{\sqrt{k}}\sqrt{\left[1 - \left(\frac{d}{a}\right)^2\right]\left[\log_e\left(\frac{a}{d}\right)\right]}, \qquad (3)$$

which becomes a maximum when

$$2\log_e\left(\frac{a}{d}\right) = \left[\frac{\left(\frac{a}{d}\right)^2 - 1}{\left(\frac{a}{d}\right)^2 - 2}\right]$$

or approximately when $a = 2.06d$. Then

$$Z = [\text{constant}] \times \frac{Na}{\sqrt{k}}. \qquad (4)$$

The above constant has a numerical value of 48 if wire size and other factors are neglected. Using data Kallmann gives regarding cable type RG-65/U, manufactured by the Federal Telegraph and Radio Corporation, we have $w = 0.0089$ inch (No. 32F wire), $N = 112$ turns per inch, $a = 0.285$ inch, $k = 2.25$, and $Z = 950$ ohms, whence the experimentally determined constant should be 45.

The fact that $d = 0.119$ inch is smaller than for optimum Z reduces the constant less than 2 per cent; the effect of the wire size is to increase the capacitance and reduce the inductance (due to skin effect), thereby decreasing the required constant approximately 5 or 6 per cent. These considerations also indicate that the constant should be about 45.

The agreement between theory and experiment is therefore excellent. In spite of the limited experimental data it seems fitting to state that a general formula useful to engineers might be

$$Z = 45\frac{Na}{\sqrt{k}}$$

where N = turns per unit length and a = inside diameter of the outer shield measured in the same units. Certain obvious limitations apply.

This correspondent has been interested in high-impedance lines of this type for several years. Early in 1943 a piece of flexible coaxial high-impedance cable was submitted to the Radio Research Laboratory of Harvard University, along with a mathematical analysis similar in form to that in this discussion.

Prior art exists, however; such devices are disclosed in a French patent No. 853,398. United States patents of related interest are Nos. 789,738; 1,026,150; and 2,139,055.

Heinz E. Kallmann:[3] I learn from the letter of M. R. Winkler that here was another of those inevitable cases of duplicated effort, this one notable for proximity in both time and space. I am obliged to him for the patent references showing that the method of distributed inductive loading of cables by coiling the inner conductor was proposed as early as 1901 and 1905, though then for different purposes. I had, myself, looked for just such references, but not far enough back.

I feel that I cannot accept Mr. Winkler's correction for the calculated cable impedance. Possible effects of eddy currents induced in the outer conductor were investigated on the sample cable described. More serious

* Heinz E. Kallman, "High-impedance cable," PROC. I.R.E., vol. 34, pp. 348–351; June, 1946.

[1] 3318 South Main Street, South Bend 14, Ind.

[2] H. Pender and K. McIlwain, "Electrical Engineers' Handbook," John Wiley and Sons, New York, N. Y.; third edition, section 4, p. 28, 1936.

[3] 417 Riverside Drive, New York 25, N. Y.

than some adjustment in the computation would have been an increase in transmission loss and, particularly, the danger of noise whenever the contact resistances between braid wires is changed by flexing of the cable. No such effects were found, and a cable sheath braided of individually Formex-insulated wires—held ready for the purpose—was therefore not used.

The inductance of the coiled conductor of the sample cable as computed from its dimensions was compared with $L=T^2/C$ where the capacitance C was measured at audio frequencies and the delay T, with considerable accuracy, as described elsewhere for delay lines.[4] While I have now no access to the notes, I can say from memory that the values agreed well within the expected accuracy of about ± 2 per cent of the impedance so found. Direct measurements of the impedance, somewhat less precise, also showed no disagreement.

The basis of Mr. Winkler's computation is his equation (2). I wonder how he arrived at the conclusion that it represents the inductance of a solenoid loaded by a short-circuited secondary winding. Actually, his equation merely represents the primary stray inductance. While his reference does not refer to this matter at the cited place, the problem of a shielded coil is discussed at length two pages earlier (pp. 4–26), but only the case of a spherical shield is discussed, hardly a suitable approximation to the cable. However, more or less accurate solutions of the problem of the cylindrical coil shield have been published,[5–7] all leading to rather formidable equations.

It may be remembered that the calculations of the effective cable inductance are exact only at such low frequencies where out-of-phase turns are still very far apart, and the calculations are true in any case only for the straight parts of the cable. It therefore seems adequate to compute the very small effect of the metal braid on the inductance of the coiled conductor quite simply, as follows. The effective inductance L_c of the coiled conductor is considered as the effective inductance of a long solenoid forming the primary of a coaxial transformer with short-circuited secondary winding. This inductance[8] is $L_c=L_p(1-k^2)$ where L_p is the inductance of the primary alone and k the coupling coefficient of the transformer. The coupling coefficient of two coaxial solenoids of equal length[9] is $k=r^2$ where r is the ratio of the inner coil diameter to the outer coil diameter. Thus it follows that $L_c/L_p=(1-r^4)$. The correction so computed for the impedances of the sample and of the manufactured cable thus amount to 1 per cent and 1.6 per cent, respectively.

[4] Heinz E. Kallmann, "Equalized delay lines," PROC. I.R.E., vol. 34, pp. 646–657; September, 1946.
[5] J. Hak, *Zeit. für Hoch.*, vol. 43, pp. 76–81; 1934.
[6] J. Hak, *Zeit. für Hoch.*, vol. 45, pp. 14–19; 1935.
[7] M. J. O. Strutt, *Zeit. für Hoch.*, vol. 43, pp. 121–123; 1934.
[8] F. E. Terman, "Radio Engineer's Handbook," McGraw-Hill Book Co., New York, N. Y., 1943, p. 152, Fig. 14.
[9] See p. 71, equation (87) of footnote reference 8.

M. R. Winkler:[1] Kallmann feels that he cannot accept my equation for inductance and that any correction which might exist is trivial.

Fortunately, the validity of my equation is substantiated by some excellent references which he has not mentioned. Kallmann's equation (4) gives the correct inductance of a long solenoid in free space. My equation (2) gives the inductance of a long solenoid whose magnetic field is confined within an impenetrable coaxial cylindrical shield. The ratio between these two equations is

$$\left[1-\left(\frac{d}{a}\right)^2\right].$$

This relationship is corroborated fully and exactly by information in Terman[10] and Howe.[11] Both the above references specifically concern the inductance of solenoids surrounded by a cylindrical coaxial metal shield. These references not only show Kallmann's equations to be incorrect but the equation and the data agree perfectly with my equation (2).

The writer will agree that in many cases the correction for inductance is small. However, it is not as small as Kallmann suggests. His experimental study of "effects of eddy currents" was done in a region of low ratios of coil diameter to shield diameter where discrepancies in inductance are difficult to discern. Should the coil diameter be 90 per cent of the shield diameter, the inductance as calculated by Kallmann's formula would have been more than five times as large as indicated by the curves in the above reference. The calculated inductance per unit length of the coiled inner conductor of the commercial cable is about 83 per cent of its inductance in free space. If the diameter of the coiled inner conductor is increased until it approaches the diameter of the outer shield, the calculated inductance approaches zero. This correction materially changes the character of many of the curves and equations of Kallmann's original paper and is not to be considered trivial.

Heinz E. Kallmann:[2] The disagreement between Mr. Winkler and myself has now reduced to the question by how much the inductance of a long solenoid is reduced when it is shielded by a coaxial metal cylinder. With r denoting the ratio of coil to shield diameter, Mr. Winkler states that the correction coefficient should be $(1-r^2)$ while I think that it should be $(1-r^4)$. Both expressions lead, of course, to the same result when r is very small and when the coil diameter equals that of the shield, $r=1$. In the case at hand, the value of r for

[10] See p. 129, Fig. 87 of footnote reference 8, taken from "Graphic determination of the decrease in inductance produced by a coil shield," RCA Application Note 48; June 12, 1935.
[11] See equation (149) of footnote reference 8 which is taken from results given by G. W. O. Howe, "The effect of screening cans on the effective inductance and resistance of coils," *Wireless Eng.*, vol. 11, p. 155; March, 1934.

the high-impedance cable is 0.42; thus Mr. Winkler's correction coefficient for its inductance is about 0.83, while my analysis leads to the value 0.97. The error in computed cable impedance, if these corrections are omitted, would be about 9 per cent according to Mr. Winkler, a negligible $1\frac{1}{2}$ per cent in my opinion.

I notice that, in his second letter, Mr. Winkler does not care to discuss either my simple analysis nor his own as given in his first letter and questioned in my reply; nor does he discuss the references I quoted as pertinent. He adduces, instead, two other references which appear to confirm his result. Let us examine these references.

The one is the RCA Application Note No. 48. The brief analysis given there leads explicitly to $L_c/L_p = (1-k^2)$, identical with my first equation. The values of k^2 are given as a family of curves, as functions of r and of l/d, similar to Fig. 87 in Terman's handbook. Since the curves are plotted against l/d of the coil, I am inclined to suspect that they were derived for short coils of the usual type, and not necessarily applicable to the case at hand. Since neither author nor sources nor any clues as to the derivation are given in the Note and since my efforts to find out about them failed, I cannot definitely decide on the relevance of this reference.

The other reference is to the editorial of Howe for March, 1934. This is based wholly on a study by H. Kaden who had approximated the usual cylindrical coil can by a hollow metal sphere. This approximation is certainly not suitable for the long slim shield of the case at hand. Being familiar with the content of both papers, I had refrained from citing them as references. Moreover, the footnote (2) on the very page of Terman's handbook that Mr. Winkler cites, explains at length that a sphere had been substituted for the cylindrical coil can. Yet Mr. Winkler writes, "Both the above references specifically concern the inductance of solenoids surrounded by a cylindrical coaxial metal shield."

M. R. Winkler:[1] Kallmann's reply attempts to lead this discussion to an erroneous conclusion. Had Kallmann confined his remarks to what could be substantiated in experiment, this discussion would have had fewer controversial equations.

It is imperative that this matter be settled because my equation (2) is not the only issue at stake; more important and to the point is the fact that the theory of design of high-impedance lines as defined by Kallmann's paper is in error and must be materially modified as related in my first discussion.

Further discussion of my equation (2) was not given in my second letter because it was felt the two substantiating references would suffice. My equation (1) is a formula useful where the reluctance of the magnetic circuit can be determined by the geometry of the problem. The manner of determining the reluctance has been defined. The remaining steps are elementary. Kallmann does not question any particular step of my derivation; instead, he infers that the result does not apply, either for reasons of intuitiveness or choice. He has made an error by incorrectly inferring that I ever "arrived at the conclusion that it (equation (2)) represents the inductance of a solenoid loaded by a short-circuited secondary winding."

Kallmann's derivation was not criticized because its inadequacy was considered obvious in the face of other references cited. It is based on an equation listed by Terman as "approximate" and limited to configurations which Terman has shown in an accompanying Fig. 44 of the reference cited. Since Kallmann has gone beyond the limitations, his derivation is erroneous.

Kallmann's comments regarding Howe are misleading. He cleverly skips the fact that my reference was to Terman's equation (149), which emphatically concerns cylindrical shields.

The data given in Fig. 87 of Terman's handbook concern coils having lengths up to 40 diameters which are not short in any sense. These data are definitely correct, especially for long coils. Kallmann questions the data without proof. He admits his implied irrelevance is based on what he suspects.

Let us determine with a simple experiment which laws apply and which laws are worthless. A 6-inch length (approximately 50 coil diameters) of type RG-65/U cable is observed at approximately 2 megacycles to have 13 per cent less inductance with the braid than without it. The measured dimensions of interest were $d = 0.118$ inch and $a = 0.292$ inch. The agreement is good, but two corrections should be made regarding how to measure d and a. First, the braid allows some penetration and its effective diameter should be used instead of its inside diameter. By substituting solid cylinders which reduce the inductance an equivalent amount, and allowing for "skin depth," its effective diameter is found to be 0.314 inch. Second, due to skin effect wherein the current flows close to the inside of the coil, the effective coil diameter is less than the mean diameter. Using an effective coil diameter of 0.113 (plus or minus 0.004) inch the agreement is essentially perfect.

Summarizing, the reduction of inductance of the sample tested, according to Kallmann's formula, should be 2.6 per cent; according to my formula, 16 per cent for uncorrected dimensions and 13 per cent for corrected dimensions; and from experiment the reduction of inductance was found to be 13 per cent. Kallmann's correction factor in this instance is in error by a factor of 5 to 1.

Obviously this discussion reverts back to the principles laid down in my first letter. It is regrettable that much time and space has been used because of Kallmann's contentions which can find no justification in experiment.

Heinz E. Kallmann:[3] It appears that Mr. Winkler is jumping to conclusions about me; one need not be clever to notice that he had cited that reference against its plain language. Anybody who cares may check that for himself.

Mr. Winkler's straightforward measurement, however, appealed to me very much and there I am glad to join him. Since the core of the cable tends to curl I simulated it by a single-layer coil, 8 inches long, close-wound with No. 32 HF Formex wire on an insulating rod of 0.093-inch diameter. The inductance of this coil was then measured at 2 megacycles in the open, and when surrounded by one of six different heavy-walled seamless copper tubes, each 8 inches long. Fig. 1 shows the relative decrease of the coil inductance L/L_0 due to these shields, as a function of d/a. The single separate point shows the effect of the braid on the core of an 8-inch piece of RG-65/U.

Since all these observed correction factors are much closer to those expected by Mr. Winkler than to my estimates, appears that the resulting decrease in cable impedance is not "very small" as previously thought but, for the RG-65/U, amounts to about 6 per cent.

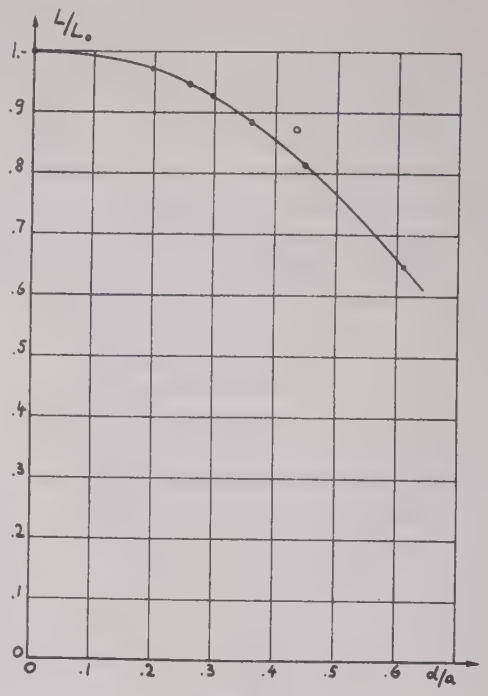

Fig. 1.

Contributors to the Proceedings of the I.R.E.

L. Apker

L. Apker was born in Rochester, N. Y., on June 11, 1915. He received the A.B. degree in 1937 and the Ph.D. degree in physics in 1941 from the University of Rochester. He was a Charles A. Coffin Fellow in 1940. After spending the summer of 1939 at the General Electric Research Laboratory, he returned to that laboratory in 1941. He has been engaged in research on nonlinear microwave networks, and on the properties of semiconductors.

Dr. Apker is a member of the American Physical Society and of Sigma Xi.

❖

Britton Chance (M'46–SM'46) was born in Pennsylvania on July 24, 1913. He received the Ph.D. degree in physical chemistry from the University of Pennsylvania in 1940, and the Ph.D. degree in biology from Cambridge University in 1942. From 1939 to 1941 he carried on biochemical research at the Johnson Foundation for Medical Physics of the University of Pennsylvania.

Since 1941 Dr. Chance has been assistant professor of biophysics at the University of Pennsylvania, from which he is presently on leave. From 1941 to 1946 he was associated with the Massachusetts Institute of Technology Radiation Laboratory. Since 1946 Dr. Chance has been a John Simon Guggenheim Fellow at the Nobel Medical Institute, Stockholm, engaged in research on timing rapid spectrophotometric changes in enzyme-substrate reactions.

Dr. Chance's interests are also in the fields of automatic ship steering, low-frequency amplification techniques, and sensitive spectrophotometry. He is a Fellow of the American Physical Society, and a member of Sigma Xi and Tau Beta Pi.

Britton Chance

❖

Thomas Studios

Murlan S. Corrington

❖

Murlan S. Corrington was born at Bristol, S.D., on May 26, 1913. He received the B.S. degree in electrical engineering in 1934 from the South Dakota School of Mines and Technology, and the M.Sc. degree in 1936 from Ohio State University.

From 1935 to 1937 Mr. Corrington was a graduate assistant in the physics department of Ohio State University. In 1937 he joined the Rochester Institute of Technology, and taught mathematics, mechanics, and related subjects. Since 1942 he has been

W. J. Cunningham

❖

engaged in mathematical engineering in the advanced-development section of the RCA Victor Division of the Radio Corporation of America. He is the author of "Applied Mathematics for Technical Students," and co-author of "Machine Shop Practice and Instrument Making."

❖

W. J. Cunningham was born August 21, 1917, at Comanche, Texas. He received the A.B. and A.M. degrees from the University of Texas in 1937 and 1938, respectively, and the Ph.D. degree from Harvard University in 1947. During the war he was at Harvard where, for a time, he did research on problems in acoustics and radio communications. For several years during this period he taught radar theory to Army and Navy officers, and general communications courses to civilian students at Harvard. He has been with the department of electrical engineering, Yale University, for the past year.

❖

Rufus G. Fellers was born at Columbia, South Carolina, in 1920. He received the B.S. degree in electrical engineering from the University of South Carolina in 1941, and the Ph.D. degree from Yale University in 1943. During 1943 and 1944 he was an instructor in electrical engineering at Yale. From 1944 to date he has been engaged as a radio engineer and physicist in the radio-frequency research section of the Naval Research Laboratory, including the period from March to September, 1945, when he was on active duty as a member of the United States Naval Reserve.

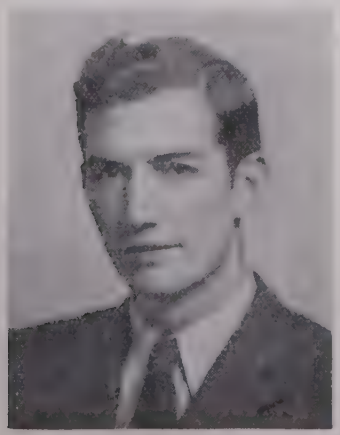

Rufus G. Fellers

Dr. Fellers is a member of Phi Beta Kappa, and the American Institute of Electrical Engineers.

❖

Charles J. Gallagher was born in Philadelphia, Pa., on October 16, 1917. He received the B.S. degree in education in 1938 from Temple University, and the M.A. and Ph.D. degrees in physics in 1940 and 1942 from the University of Notre Dame.

For three years following his graduation Dr. Gallagher was engaged as a research associate at the Radio Research Laboratory, Harvard University, studying applications of gaseous discharges to radar countermeasures. He joined the staff of the Research Laboratory of General Electric Company at Schenectady, New York, in November, 1945, where he is currently engaged in the study of arc phenomena.

Charles J. Gallagher

❖

S. James Goffard was born at Minneapolis, Minn., on September 24, 1916. He received the B.A. degree in 1938 and the M.A. degree in 1940 from the University of Michigan, and is now finishing his work for the Ph.D. degree at the University of Minnesota. From 1942 to 1946 he was a special research associate at the Psycho-Acoustic Laboratory, Harvard University.

Mr. Goffard's interest in radio communication is principally in the people who talk and the people who listen, since he is a psychologist and a statistician rather than an engineer. He likes to think of power as a variance, and of root-mean-square voltages as standard deviations.

❖

Earl M. Johnson (S'40–A'41–M'44–SM'47) was born in Frankfort, S.D., on October 3, 1915. He received the degree of electrical engineer from the University of Cincinnati in 1940. In 1937 he joined the engineering staff of the Crosley Corporation, first as a transmitter engineer for station WSAI, and later doing analysis work on propagation effects encountered with the 500-kilowatt operation of station WLW. In 1940 Mr. Johnson joined the engineering department of the Federal Communications Commission as a monitoring officer, later becoming assistant chief of the Standard Broadcast Section of the Washington office. In 1944 he transferred to the War Department, acting as an expert consultant on matters of wave propagation for the operational research staff in the Office of the chief signal officer. Since 1945 he has been associated with the Mutual Broadcasting System, where he is Director of Engineering. He is a licensed professional engineer in the State of Ohio.

S. James Goffard

❖

J. Kahnke (S'41–A'44) was born in Rochester, Minn., on September 25, 1919. He received the B.E.E. degree in 1941 from the University of Minnesota. During 1941 he worked for KSTP, Inc., in St. Paul, Minn. In 1943 he joined the General Electric Research Laboratory.

Mr. Kahnke is now engaged in circuit research at Engineering Research Associates, Inc., St. Paul, Minn.

❖

Stephen C. Kleene was born at Hartford, Conn., on January 5, 1909. He received the A.B. degree from Amherst College in 1930, and the Ph.D. degree in mathematics from Princeton University in 1934.

❖

Earl M. Johnson

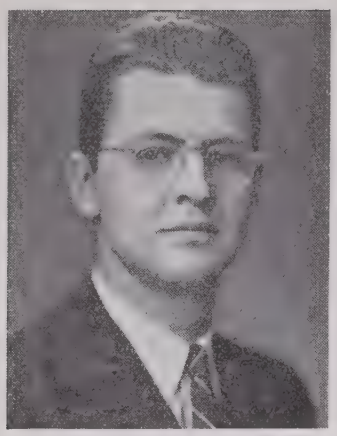

J. KAHNKE

❖

He was an instructor in mathematics at the University of Wisconsin from 1935 to 1937, and assistant professor from 1937 to 1941. During 1939 and 1940 he was a member of the Institute for Advanced Study at Princeton, N. J. In 1941 he went to the mathematics department of Amherst College as associate professor. Commissioned Lieutenant (j.g.) in the United States Naval Reserve in May, 1942, he taught navigation at the United States Naval Reserve, Midshipmen's School, New York, N. Y., until May, 1944, when he was transferred to the Naval Research Laboratory, becoming project engineer in charge of the applied mathematics group of the fire-control division.

Lieutenant Commander Kleene returned to inactive duty in January, 1946. He is now associate professor of mathematics at the University of Wisconsin. He is a member of Phi Beta Kappa, Sigma Xi, the American Mathematical Society, the Mathematical Association of America, and the Association for Symbolic Logic.

❖

J. C. R. Licklider was born at St. Louis, Mo., on March 11, 1915. He received the B.A. degree in 1937 and the M.A. degree in 1938 from Washington University, and the Ph.D. degree in 1942 from the University of Rochester. He traces his interest in radio interference to his Ph.D. thesis problem, which was to find out in what part of its brain a cat hears high-pitched tones and in what part, low-pitched tones. Some of the intervening steps, most of which were taken at the Psycho-Acoustic Laboratory, Harvard University, include: hearing, communication, amplitude distortion, nonlinear circuits, and noise-reducing devices. At present, Dr. Licklider is teaching in the department of psychology and doing further research on communication in the Psycho-Acoustic Laboratory at Harvard University.

❖

STEPHEN C. KLEENE

❖

Louis Malter (A'37–SM'45) was born in New York, N. Y., on April 27, 1907. He received the B.S. degree from the College of the City of New York in 1926, and the M.A. and Ph.D. degrees in physics from Cornell University in 1931 and 1936, respectively.

❖

J. C. R. LICKLIDER

❖

From 1926 to 1928 Dr. Malter was an instructor of physics at the College of the City of New York. In 1928 he joined the Radio Corporation of America, where he was associated with the acoustic research and photophone divisions until 1930, and during the summer of 1931. From 1933 to 1942 he was with RCA Manufacturing Company at Camden, N. J.; from 1942 to 1943 with RCA Laboratories Division at Princeton, N. J.; and from 1943 to 1946 was in charge of the special development division of RCA Manufacturing Company at Lancaster, Pa. Since May, 1946, he has been in charge of the vacuum-tube research section of the Naval Research Laboratory, Washington, D. C.

Dr. Malter is a Fellow of the American Physical Society, and a member of Sigma Xi.

❖

W. R. MACLEAN

William R. MacLean (A'42) was born on July 14, 1908 at Marinette, Wis. He became interested in radio in grade school and operated a spark-coil, crystal-detector station in 1921. Later he operated two licensed amateur stations while in high school, and a third at Massachusetts Institute of Technology, where he received the B.Sc. degree in electrical engineering in 1929. For the following year he worked in the Bell Telephone Laboratories. Thereafter, during the Weimar Republic, he studied physics a semester each at the Universities of Munich and Berlin. This was followed by most of a third semester at the Sorbonne. He did actuarial work from 1932 to 1937.

Dr. MacLean returned to electrical engineering in civil service from 1937 to 1941, and then went to the Polytechnic Institute of Brooklyn where he received the M.E.E. degree in 1942 and the D.E.E. degree in 1945, and is now a member of the electrical engineering department. He is a member of Sigma Xi and of the Acoustical Society of America.

❖

Warren P. Mason (A'35–F'45) was born in Colorado Springs, Col., in 1900. He

❖

LOUIS MALTER

WARREN P. MASON

graduated from the University of Kansas in 1921, and obtained the A.M. degree in 1924 and Ph.D. degree in 1928 from Columbia University. From 1921 to date he has been a research engineer and physicist with Bell Telephone Laboratories. His principal contributions have been in the fields of piezoelectric crystals and ultrasonics.

Dr. Mason is a member of Sigma Xi and Tau Beta Pi, and is a Fellow of the American Physical Society, and the Acoustical Society of America. He is the author of numerous technical papers and of the book "Electromechanical Transducers and Wave Filters."

❖

H. Bruce Phillips (A'45) was born in Iowa, on November 19, 1921. He was graduated from the State University of Iowa in December, 1943, with the B.S. degree in electrical engineering. Upon graduation he was employed by the Radio Corporation of America in the Power Tube Development Laboratory at Lancaster, Pennsylvania. In August, 1945, he returned to the State University of Iowa as a research associate with a proximity-fuze development project, and entered the Graduate College in September. He obtained the M.S. degree in electrical engineering in June, 1946, and at present is doing graduate work toward a Ph.D. degree in the department of physics at the State University of Iowa. He is a member of Tau Beta Phi, Eta Kappa Nu, and Sigma Xi.

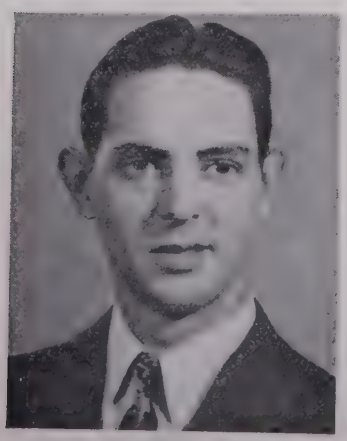

H. BRUCE PHILLIPS

❖

Igor Plusc (M'45) was born in Kiev, Russia, in 1904. He received the B.S. degree in electrical engineering from Robert College Engineering School in 1927. From 1928 to 1937 he was associated with the Turkish Radio Company, in charge of studio and control of Turkish Broadcasting Stations. He was an official tutor part time in Robert College engineering school from 1932 to 1937, and from 1937 to 1939 he was head of the technical department of Turkish Phillips Ltd.

Mr. Plusc received the M.S. degree in electrical engineering from Michigan University in 1940, and remained at Michigan

IGOR PLUSC

as research assistant of Professor W. G. Dow, doing graduate work from 1941 to 1942. He served as associate professor of engineering at Pennsylvania Military College from 1942 to 1944. From 1944 to February, 1947, he was a research physicist and mathematician at the Colonial Radio Corporation, Buffalo, N. Y. He is now an assistant professor, in the electrical engineering department, Syracuse University, N. Y.

Mr. Plusc is an Associate of Sigma Xi.

❖

Stanley Ruthberg was born on July 29, 1920, in Middletown, N. Y. He received the A.B. degree in 1942, and the M.A. degree in physics in 1944, from Syracuse University. He was associated with the Radio Research Laboratory, Harvard University, until the latter part of 1945, when he joined the physics department of Purdue University, where he remained for the first part of 1946.

Mr. Ruthberg is now at the University of Michigan, as a graduate student of physics.

❖

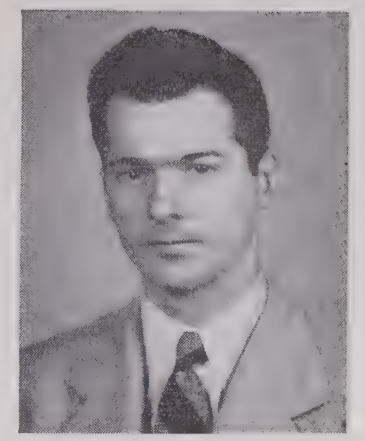

STANLEY RUTHBERG

❖

Samuel Seely (A'39–SM'45) was born in New York, N. Y., on May 7, 1909. He received the E.E. degree from the Polytechnic Institute of Brooklyn in 1931; the M.S. degree from Stevens Institute of Technology in 1932; and the Ph.D. degree in physics from Columbia University in 1936. He was a member of the staff of the department of electrical engineering of the School of Technology of the College of the City of New York from 1936 until 1946, but was on extended leave of absence at the Radiation Laboratory at the Massachusetts Institute of Technology from January, 1941, until January, 1946. He was associate professor of electronics at the Naval Postgraduate School at Annapolis, Md., from July, 1946, until February, 1947. He joined the staff of Syracuse University in February, 1947, as professor of electrical engineering.

Dr. Seely is a member of the American Institute of Electrical Engineers, the American Physical Society, the American Society of Engineering Education, Tau Beta Pi, Sigma Xi, and of the Papers Review Committee of the I.R.E. He is coauthor of the textbook, "Electronics."

SAMUEL SEELY

CARL E. SMITH

Carl E. Smith (A'30–M'39–SM'43) was born near Eldon, Iowa, on November 18, 1906. He received the B.S. degree in electrical engineering from Iowa State College in 1930. From then until the summer of 1931 he was a student engineer for the Radio Corporation of America, Victor Division, Camden, N. J., and took evening postgraduate work at the University of Pennsylvania. A year of postgraduate study at the Ohio State University resulted in the M.S. degree in electrical engineering in 1932. In the summer of 1932 he joined the technical staff of the United Broadcasting Company, became assistant chief engineer in 1936, chief engineer in 1941, and vice-president in charge of engineering in 1946. In 1936 he received the professional degree of electrical engineer from the Ohio State University for research work on broadcast transmitter-antenna design.

In 1934 the Smith Practical Radio Institute was founded by Mr. Smith. Early in 1946 the Cleveland Institute of Radio Electronics Inc., was organized as successor to the Smith Practical Radio Institute of Cleveland, Ohio, and Nilson Radio School of New York City. Mr. Smith was elected president of this Institute, which now offers a variety of home-study training courses. During World War II, from 1942 to 1946, Mr. Smith took leave of absence to become assistant director of the operational research staff of the Chief Signal Officer of the United States Army.

He is a member of the American Institute of Electrical Engineers and the American Society for Engineering Education, and a registered professional engineer in the State of Ohio.

Mr. Smith is the author of "An Advanced Radio and Communication Engineering Course"; a reference volume on "Directional Antennas" published by the Cleveland Institute of Radio Electronics, and "Applied Mathematics."

❖

E. TAFT

E. Taft was born in Globe, Ariz., on June 24, 1919. He received the B.S. degree in electrical engineering from the University of Arizona in 1940. Since then he has been with the General Electric Company, joining the Research Laboratory in 1942. At the laboratory he has been engaged in research on microwave networks and on the properties of semiconductors. Mr. Taft is a member of the American Physical Society.

❖

LAWRENCE A. WARE

Lawrence A. Ware (A'41–M'45–SM'46) was born at Bonaparte, Iowa, on May 21, 1901. He received the B.E. degree in electrical engineering in 1926, the M.S. degree in physics in 1927, the Ph.D. degree in physics in 1930, and the E.E. degree in 1935, all from the University of Iowa. From 1929 to 1933 Dr. Ware was a transmission engineer with the Bell Telephone Laboratories; from 1935 to 1937 he was assistant professor of physics at Montana State College; and since 1937 he has been assistant and associate professor of electrical engineering at the State University of Iowa. He is a member of the American Institute of Electrical Engineers, American Physical Society, American Society for Engineering Education, American Association of University Professors, American-Soviet Science Society, Eta Kappa Nu, Sigma Xi, and Tau Beta Pi.

R. WATTERS

R. Watters (S'40–A'42) was born at Monroe, Mich., on October 29, 1919. He received the B.S. degree in electrical engineering from the University of Notre Dame in 1941. Since that time he has been associated with the General Electric Research Laboratory, engaged in circuit research.

❖

For photographs and biographies of J. D. COBINE, J. R. CURRY, and W. E. HUGGINS, see the September, 1947, issue of the PROCEEDINGS OF THE I.R.E.

❖

Richard T. Weidner (A'44) was born in Allentown, Pa., in 1921. He received the B.S. degree from Muhlenberg College in 1943, and the M.S. degree from Yale University in 1943. He was an instructor in physics at Yale University during 1943 and 1944, and served as a physicist in the radio-frequency research section of the Naval Research Laboratory from 1944 to 1946. At present he is engaged as a research assistant in physics at Yale University.

Mr. Weidner is a member of the American Physical Society, Sigma Xi, and the American Association for the Advancement of Science.

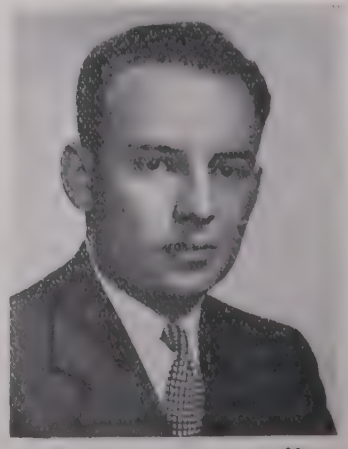

Metzger

RICHARD T. WEIDNER

Correspondence

Radar Reflections from the Lower Atmosphere

June 19, 1947*

The correspondence on "Radar reflections from the lower atmosphere," by H. T. Friis[1] is of particular interest, since the reported echoes may parallel phenomena observed at Evans Signal Laboratory, Belmar, N. J., during the past two years. Radar equipment operating on a wavelength of approximately 1.25 cm. and directed vertically has given fairly consistent unexplainable echoes at altitudes between approximately 300 and 3000 yards (Figs. 1–6). For want of a better term, these echoes have been dubbed "Angels" by Signal Corps personnel. The possibility exists that these "Angels" may be echoes from the same phenomena as has been occasionally observed on wavelengths in the vicinity of 10 and 3 cm.; but no convincing correlation has as yet been established.

As noted by Dr. Friis, the number of echoes varies greatly during the day and from day to day. They are most numerous in the first 1000 yards above the ground, and none have been observed much in excess of 3000 yards. The duration of the echoes is short, varying from a fraction of a second to perhaps a maximum of 10 seconds. The short duration may, in part, be explained by the possible motion of the reflecting medium through the relatively narrow radar beam produced by the equipments. "Angels" have been observed on four different 1.25-cm. radar systems, which lessens the possibility of equipment peculiarities. The obvious explanation that the echoes might be birds has been discarded by optical checks. Insects have been ruled out, since the echoes have been recorded in midwinter.

The early observations of this phenomena were carried on largely by Herbert Brett of Evans Signal Laboratory.

WILLIAM B. GOULD
Evans Signal Laboratory
Signal Corps Engineering Laboratories
Belmar, N. J.


Fig. 1

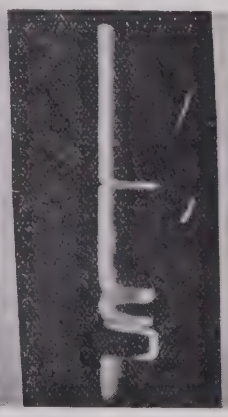
Fig. 2

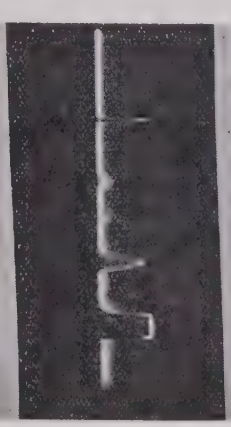
Fig. 3

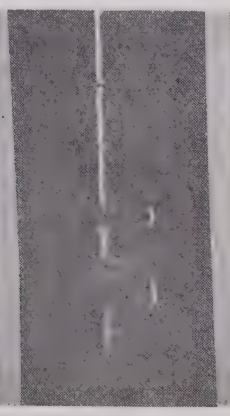
Fig. 4

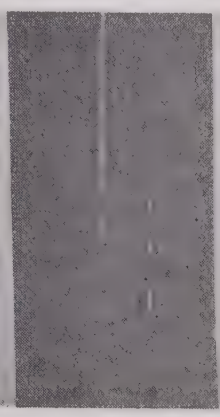
Fig. 5

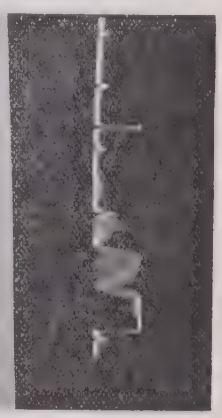
Fig. 6

Fig. 1—A 3-second exposure showing numerous "angels" up to 2000 yards. The range marker at the top of the picture is set at 3000 yards.
Fig. 2—Two "angels" within 1000 yards. Range marker set at 2000 yards.
Fig. 3—"Angels" at 900 and 2000 yards. Marker set at 3000 yards. One-half second exposure.
Fig. 4—"Angels" at 600 and 1200 yards. Marker at 3000 yards. One-tenth second exposure.
Fig. 5—"Angels" at 1000 and 1600 yards. Marker at 3000 yards. One-fifth second exposure.
Fig. 6—Numerous "angels." Small range markers at 1000-yard intervals.

* Received by the Institute, June 25, 1947.
[1] H. T. Friis, "Radar reflections from the lower atmosphere," PROC. I.R.E., vol. 35, pp. 494–495; May, 1947.

Network Transmission of a Frequency-Modulated Wave

July 3, 1947*

In a recent paper[1] Frantz described a method for obtaining the output signal from a network when the input signal is frequency modulated. (For an excellent generalized treatment of this problem, when the network characteristics are expressed by means of a power series, or by means of a trigonometric series, the reader is referred to a paper by Block.[2]) In the application of Frantz's method it is necessary that the network response be expressed as a Fourier series or, as was also indicated, by other series approximations. However, it is possible to obtain the amplitude and phase of the output signal by using point-by-point data from the network response curve; contrary to Frantz's statement, this can be accomplished without plotting the output r.f. signal point by point as a function of time. The additional work of obtaining a series expression, as well as questions as to the proper convergence of this expression, are thus avoided. It is believed that the method of calculation to be described is, therefore, simpler and more straightforward, and in any event may be of interest as an alternate method of solution.

To rephrase the problem: a network having a gain-versus-frequency characteristic given by $R(\omega)$ and a phase-versus-frequency characteristic given by $\theta(\omega)$ is driven by a single-tone f.m. voltage (assumed to be of unit amplitude for convenience, as network is assumed to be linear with amplitude) given by

$$e_{in} = \sin(\omega_0 t + m_f \sin vt)$$

$$= \sum_{n=-\infty}^{\infty} J_n(m_f) \sin(\omega_0 + nv)t. \quad (1)$$

It is desired to determine the output voltage from the network.

The input signal indicated in (1) consists of a multiplicity of individual sinusoidal signals comprising the carrier and the upper- and lower-side frequencies. These individual sinusoidal signals can be pictured as vectors of proper length given by $J_n(m_f)$ rotating counterclockwise about the center at an angular frequency given by $(\omega_0 + nv)$. The upper- and lower-side frequencies can be paired off by rewriting (1)

* Received by the Institute, July 7, 1947.
[1] W. J. Frantz, "The transmission of a frequency-modulated wave through a network," PROC. I.R.E., vol. 34, pp. 114P–125P; March, 1946.
[2] A. Block, "Modulation theory," *Jour. I.E.E.* (London), pt. III, vol. 91, pp. 31–42; March, 1944.

$$e_{in}=J_0(m_f)\sin\omega_0 t + J_1(m_f)[\sin(\omega_0+v)t-\sin(\omega_0-v)t] + J_2(m_f)[\sin(\omega_0+2v)t+\sin(\omega_0-2v)t] + J_3(m_f)[\sin(\omega_0+3v)t-\sin(\omega_0-3v)t] + \cdots . \quad (2)$$

To better visualize the action that is taking place, it is convenient to assume that the frame of reference rotates counterclockwise with an angular frequency ω_0 so that the carrier vector $J_0(m_f)$ remains stationary. If this is done, then the vectors with the higher angular frequencies will rotate counterclockwise with angular frequencies of nv, and the vectors with the lower angular frequencies will rotate clockwise with the same angular frequencies nv. This is pictured in Fig. 1(a) for the case where $m_f=1.0$ and $vt=30°$. It is readily seen from this figure (as well as from (2) by subtracting ω_0 from each angular frequency) that the even-order sidebands pair off to give a vector sum in phase with the carrier vector and the odd-order sidebands pair off to give a vector sum in phase-quadrature with the carrier vector. Thus it is seen either from Fig. 1(a) or from (2) that

$$|e_{in}| = \sqrt{[J_0(m_f)+2J_2(m_f)\cos 2vt+2J_4(m_f)\cos 4vt+\cdots]^2+[2J_1(m_f)\sin vt+2J_3(m_f)\sin 3vt+\cdots]^2} \quad (3)$$

and

$$\beta = \text{phase of } e_{in} \text{ with respect to signal of phase } \omega_0 t = m_f \sin vt = \arctan\left\{\frac{[2J_1(m_f)\sin vt+2J_3(m_f)\sin 3vt+\cdots]}{[J_0(m_f)+2J_2(m_f)\cos 2vt+2J_4(m_f)\cos 4vt+\cdots]}\right\}. \quad (4)$$

The network output voltage is obtained, as indicated by Frantz, by treating each of the sideband terms as an individual signal and altering its amplitude by $R_n(\omega)$ and its phase by $\theta_n(\omega)$. Thus, the output voltage derived from (2) is

$$e_{out} = R_0J_0(m_f)\sin(\omega_0 t+\theta_0) + J_1(m_f)[R_1\sin\{(\omega_0+v)t+\theta_1\} - R_{-1}\sin\{(\omega_0-v)t+\theta_{-1}\}] + J_2(m_f)[R_2\sin\{(\omega_0+2v)t+\theta_2\} + R_{-2}\sin\{(\omega_0-2v)t+\theta_{-2}\}] + \cdots . \quad (5)$$

If (5) is pictured on the counterclockwise rotating reference frame, it is seen (as indicated in Fig. 1(b) for same conditions as 1(a) with hypothetical network characteristics) that

$$|e_{out}| = \sqrt{\{R_0J_0(m_f)\cos\theta_0+J_1(m_f)[R_1\cos(vt+\theta_1)-R_{-1}\cos(vt-\theta_{-1})]+J_2(m_f)[R_2\cos(2vt+\theta_2)+R_{-2}\cos(2v-\theta_{-2})]+\cdots\}^2 + \{R_0J_0(m_f)\sin\theta_0+J_1(m_f)[R_1\sin(vt+\theta_1)+R_{-1}\sin(vt-\theta_1)]+J_2(m_f)[R_2\sin(2vt+\theta_2)-R_{-2}\sin(2vt-\theta_{-2})]+\cdots\}^2} \quad (6)$$

and

$$\beta \text{ phase of } e_{out} \text{ with respect to signal of phase } \omega_0 t = \arctan\left\{\frac{R_0J_0(m_f)\sin\theta_0+J_1(m_f)[R_1\sin(vt+\theta_1)+R_{-1}\sin(vt-\theta_{-1})]+\cdots}{R_0J_0(m_f)\cos\theta_0+J_1(m_f)[R_1\cos(vt+\theta_1)-R_{-1}\cos(vt-\theta_{-1})]+\cdots}\right\}. \quad (7)$$

Using (6) and (7) the point-by-point amplitude and phase of the output voltage as a function of vt can be obtained either by algebraic or graphical calculation. Sufficient terms are retained to give the desired accuracy with more terms being necessary when m_f is large. If the series indicated in (6) can be summed up analytically, then a closed analytic expression for the output is possible.

If the network-gain characteristic is symmetrical so that $R_{-n}=R_n$, and the network phase characteristic is skew symmetrical so that $\theta_{-n}=-\theta_n$ (which is the case treated in detail by Frantz) then (6) and (7) simplify to

$$|e_{out}| = \sqrt{\{R_0J_0(m_f)+2R_2J_2(m_f)\cos(2vt+\theta_2)+2R_4J_4(m_f)\cos(4vt+\theta_4)+\cdots\}^2+\{2R_1J_1(m_f)\sin(vt+\theta_1)+2R_3J_3(m_f)\sin(3vt+\theta_3)+\cdots\}^2} \quad (8)$$

and

$$\beta = \arctan\left\{\frac{[2R_1J_1(m_f)\sin(vt+\theta_1)+2R_3J_3(m_f)\sin(3vt+\theta_3)+\cdots]}{[R_0J_0(m_f)+2R_2J_2(m_f)\cos(2vt+\theta_2)+2R_4J_4(m_f)\cos(4vt+\theta_4)+\cdots]}\right\}. \quad (9)$$

If $vt=180°+\gamma$ it is seen that $|e_{out}|$ is the same as for $vt=\gamma$, and that β is negative the value for $vt=\gamma$, so that for (8) and (9) only the region of $vt=\theta$ to $vt=180°$ need be investigated. In order to compare (8) and (9) with similar results by Frantz, one should keep in mind that the phase angle of e_{out} used by Frantz is the phase of e_{out} with respect to the phase of the f.m. wave. Thus

θ = phase of e_{out} with respect to the phase of the input

$$\text{f.m. wave} = \beta - m_f \sin vt. \quad (10)$$

A sample calculation of e_{out} is shown in Table I for $vt=60°$ for the same e_{in} used by Frantz, and using values of $R(\omega)$ and $\theta(\omega)$, interpolated from curves given by him.

It is perhaps worth noting that the complete value of e_{out} is known, since its amplitude is given by $|e_{out}|$ and its phase is $\omega_0 t+\beta$ or $\omega_0 t+m_f \sin vt+\theta$, i.e., $e_{out}=|e_{out}|\sin(\omega_0 t+\beta)$. In the event one is interested only in the frequency distortion caused by transmission through a network (as, for instance, when limiters remove all amplitude variation), the angular frequency distortion term is given by the time derivative of θ with respect to time.

TABLE I

COMPUTATION OF POINTS ON CURVES

Shown in Fig. 5 in Article by Frantz[1] for $vt=60°$ Instantaneous Frequency = 1.0125 Mc.

n	C_n	$nvt-\theta_n$	$C_n\cos(nvt-\theta_n)$
0	+10	0°	+10
2	−20	95	+ 2
4	+21	−163	−20
6	−21	− 51	−13
8	+16	63	+ 7
10	− 7	177	+ 7
12	− 6	− 67	− 2
14	+12	49	+ 8
16	− 4	166	+ 4
18	− 9	− 76	− 2
20	+ 2	42	+ 2
22	+ 9	161	− 9
24	+ 8	− 80	+ 1
26	+ 4	39	+ 3
28	+ 1	158	− 1
			− 3

n	C_n	$nvt-\theta_n$	$C_n\sin(nvt-\theta_n)$
1	−25	48°	−18
3	+19	143	+11
5	− 9	−108	+ 9
7	− 1	6	0
9	+10	120	+ 9
11	−14	−125	+12
13	+ 7	− 9	− 1
15	+ 6	107	+ 6
17	−10	−135	+ 7
19	− 4	− 17	+ 1
21	+ 7	102	+ 7
23	+ 9	140	− 6
25	+ 5	− 20	− 2
27	+ 2	99	+ 2
29	+ 1	−143	0
			+37

$C_n=Kf(\omega)/g_m x_s J_n(25)$; $K=1$ when $n=0$ and $K=2$ when $n\neq 0$; $f(\omega)/g_m x_s=R(\omega)$ is interpolated from Fig. 4(c) of the article;[1] θ_n is interpolated from Fig. 4(d) of the article. Then $|e_{out}|=\sqrt{(-3)^2+(37)^2}=37$: $\beta=\tan^{-1}(+37/-3)=95°$, and since $25\sin 60°=160$ $\phi=\beta-160°=-65°$. For $vt=180°+60°$, instantaneous frequency = 0.9875 Mc. $|e_{out}|=37$, $\beta=-95°$, and, $\phi=\beta+160°=65°$.

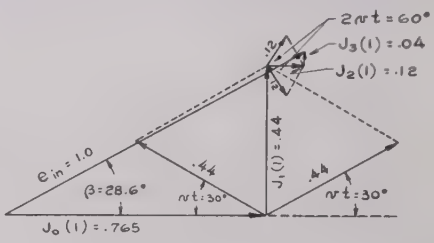

(a)

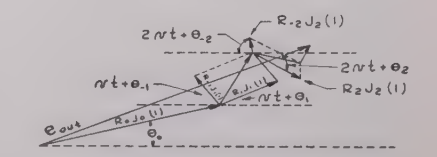

(b)

Fig. 1—Vector summation of (a) input signal, and (b) output signal for an arbitrary network (assuming modulation index = 1.0, $vt=30°$).

L. J. GIACOLETTO
Radio Corporation of America
RCA Laboratories Division
Princeton, N. J.

Institute News and Radio Notes

I.R.E. Telephone Number

The telephone number of I.R.E. Headquarters at 1 East 79 Street, New York City, is REgent 7-9600.

Louisville Section

On behalf of the Board of Directors, the Executive Committee, at its meeting of August 5, 1947, approved the petition for the formation of the Louisville Section of the I.R.E.

New RTPB Officers

The Radio Technical Planning Board Administrative Committee has elected the following officers for the year beginning October 1, 1947: Chairman, Haraden Pratt; Vice-Chairman, Alfred N. Goldsmith; Treasurer, Will Baltin; Secretary, George W. Bailey.

Note from the Executive Secretary

Fellow Members:

A great engineering society such as the I.R.E. assists its membership in many ways which may not be immediately clear. Consider, for example, how greatly the Institute helps each of us through its Proceedings, its standards reports, and its Technical Committee operations. In these ways the Institute gathers the most advanced and valuable engineering information. It distributes this information to tens of thousands of capable and active engineers, technicians, and executives. This helps each engineer to carry out his own job by placing the latest dependable information before him; by enabling him to avoid "technical blind alleys"; and by assisting him in getting the job done quickly and correctly.

This in turn results in the creation of better products, and the manufacture, sale, and use of larger quantities of communications and electronic equipment. Thus our industry develops—and new jobs are created. And existing jobs become more important, with, it is hoped, corresponding returns.

Not only does the I.R.E. advance the communications and electronic sciences and technologies—it contributes directly to the opportunities and success of each of its members and of the organizations with which they work.

George W. Bailey

Nineteenth Annual Rochester Fall Meeting

November 17, 18, 19, 1947
Sheraton Hotel, Rochester, N. Y.

The 1947 Rochester Fall Meeting of members of The Institute of Radio Engineers and members of the Radio Manufacturers Association engineering department will be held at the Sheraton Hotel, Rochester, New York, November 17, 18, and 19, 1947. The meeting will be sponsored by the Rochester Fall Meeting Committee.

PROGRAM

Monday, November 17, 1937

Technical Sessions—9:30 A.M. and 2:00 P.M.

1. "V.H.F. Direction Finder for Airport Use," A. G. Richardson, Federal Telecommunication Laboratories.
2. "R.F. Inductance Meter with Direct-Reading Linear Scale," Harold A. Wheeler, Wheeler Laboratories Inc.
3. "Design and Layout of Radio Receivers and The Maintenance Man," A. C. W. Saunders, Saunders Radio and Electronics School.
4. "Use of Miniature Tubes in A.C.-D.C. Receivers for A.M. and F.M.," R. F. Dunn, Radio Corporation of America.
5. "Two-Signal Performance of Some F.M. Receiver Systems," B. D. Loughlin and D. E. Foster, Hazeltine Electronics Corporation.

General Session—8:15 P.M.

1. "Engineering Responsibilities in Today's Economy," E. F. Carter, Sylvania Electric Products, Inc.

Tuesday, November 18, 1947

Technical Sessions—9:30 A.M. and 2:00 P.M.

1. "Avenues of Improvement in Present-Day Television," Donald G. Fink, McGraw-Hill Publishing Company, Inc.
2. "Standardization of Transient Response of Television Transmitters and Receivers," R. D. Kell and G. L. Fredendall, RCA Laboratories.
3. "Psychoacoustic Factors in Radio-Receiver Loudspeaker Selection," Hugh S. Knowles, Jensen Manufacturing Company.
4. "Spectral Energy Distribution of Cathode-Ray Phosphors," R. M. Bowie and A. E. Martin, Sylvania Electric Products, Inc.
5. "Quality Control in Receiving-Tube Manufacture," J. A. Davies, General Electric Company.

Fall Meeting Dinner—6:30 P.M.

Toastmaster—R. A. Hackbusch, Stromberg-Carlson Company.
Speaker—F. S. Barton, Ministry of Supply, England. "The British Radio Industry Today."

Wednesday, November 19, 1947

Technical Sessions—9:00 A.M. and 2:00 P.M.

1. "Metallized-Film Coaxial Attenuators," John W. E. Griemsmann, Polytechnic Institute of Brooklyn.
2. "I.F. Selectivity Considerations in F.M. receivers," R. B. Dome, General Electric Company.
3. "A New Television Projection System," William E. Bradley, Philco Corporation.
4. "The Organization of the Work of the I.R.E. Technical Committees," L. G. Cumming, Institute of Radio Engineers.
5. "V.H.F. Bridge for Impedance Measurements Between 20 and 140 Megacycles," Robert A. Soderman, General Radio Company.

Photographic Session—8:15 P.M.

1. "The Problem of Amateur Color Photography," Ralph M. Evans, Eastman Kodak Company.

The officers of the Rochester Fall Meeting Committee are as follows: *Chairman*, V. M. Graham, Sylvania Electric Products, Inc.; *Vice-Chairman*, H. A. Brown, Rochester Gas and Electric Corp.; *Treasurer*, H. J. Klumb, Rochester Gas and Electric Corp.; *Secretary*, O. L. Angevine, Rochester Engineering Society.

Second Joint I.R.E.—U.R.S.I. Meeting

The American Section of the International Scientific Radio Union and the Washington Section of the Institute of Radio Engineers will hold a second joint meeting this year on Monday, Tuesday, and Wednesday, October 20, 21, and 22, 1947, in the auditorium of the new Interior Department Building, C Street between 18 and 19 Streets N.W., Washington, D. C. The program will, as usual, be devoted to the more fundamental and scientific aspects of radio and electronics. The program of titles and abstracts will be available in booklet form for distribution before the meeting. Correspondence should be addressed to The Institute of Radio Engineers, 1 East 79 Street, New York 21, N. Y., or to Dr. Newbern Smith, Secretary, American Section, U.R.S.I., National Bureau of Standards, Washington 25, D. C.

Louis N. Persio

Louis N. Persio (A'30–M'46), Chairman of the Williamsport Section of the Institute of Radio Engineers, died on August 6, 1947. A graduate of Valparaiso University and the University of Chicago, Mr. Persio joined Radio Station WRAK as an engineer when it first began broadcasting in 1932. He was made chief engineer in 1934, and held that position until his death. He was also maintenance supervisor for the radio equipment of the Williamsport Police Department.

Industrial Engineering Notes[1]

Cosmic-Noise Research Project

A comprehensive and continuing study of cosmic noise and its relation to radio reception, particularly in the high frequencies, and with emphasis on the design and construction of f.m. receivers and their ability to suppress this phenomena, is being undertaken by the National Bureau of Standards scientists at the Sterling, Va., receiving station.

Facsimile Service

The F.C.C. has indicated that facsimile may soon become a regular broadcast service. The Radio Technical Planning Board recently submitted proposed transmission standards for facsimile operation by f.m. broadcast stations. Upon completion of further tests it is believed that these will be adopted, providing the necessary basis for regular operation.

F.C.C. Engineering Department Reorganized

A reorganization of its engineering department, including new divisions; the promotion of G. S. Turner to assistant chief engineer, filling the vacancy caused by the recent naming of G. E. Sterling as chief engineer; and the promotion of G. K. Rollins to chief of a new Radio Operator and Amateur Division, have been announced by the F.C.C.

Licenses Needed for Radar and Electronic Devices

Purchasers in the United States of surplus radar and other electronic devices capable of radio emissions have been cautioned by the F.C.C. that appropriate licenses must be obtained for both the transmitter and the operator of this type of equipment.

"Wired-Wireless" Investigated by F.C.C.

The F.C.C. has received reports that "wired-wireless" broadcast service over local power lines has been begun or planned by some individuals or groups under the mistaken assumption that this type of operation does not come under Commission jurisdiction. The F.C.C. points out that "unlicensed radio operation, which normally results when low-power devices exceed the limitations provided, creates a definite menace to important communications and may subject the operator to serious penalties provided for in the Communications Act."

[1] The data on which these NOTES are based were drawn, by permission, from "Industry Report," issues of July 11, 18, and 25, and August 1, 1947, published by the Radio Manufacturers Association, whose courteous co-operation in this matter is gratefully acknowledged.

Handie-Talkie Improvements

The Signal Corps has announced that its handie-talkie radio set has been improved by several modifications. Chief among these are a homing device and a single carrying case for the whole apparatus.

Navy Electronic Funds

The United States Navy Department has requested appropriations for electronics amounting to $100,000,000 for the 1947–1948 fiscal year. Of this, $85,750,000 would be used by the Bureau of Ships for equipment and maintenance; and $12,550,000 by the Bureau of Aeronautics for radio and radar equipment, including guided-missile control and antisubmarine purposes.

Army Signal Corps Funds

The United States Army Signal Corps has listed more than $30,000,000 of its requested appropriation to be expended on procurement of equipment, construction, and research and development. Included were radiosonde equipment, radio and radar for army boats, and construction of administrative and army-airways radio systems.

New Television Stations

The first commercial television license issued since the war went to WNBT of the National Broadcasting Company, in New York. This license covers changed facilities of the station, which was one of the six commercial stations functioning during the war. As of July 18, 1947, there were six licensed television stations, 59 under construction, and 10 pending applications.

F.M. Stations Frequency Separation

The F.C.C. has announced that, under its recent reallocation plan for f.m. stations, a frequency separation of 800 kc. is provided between Class B stations in the same area. However, because of the demand for channels, Class A stations have been assigned which are only 400 or 600 kc. removed from Class B stations in the same area.

F.M. Educational Networks

Active interest in the establishment of state-wide f.m. educational networks has been expressed by 23 states, according to a recent F.C.C. poll. In five states planning has reached the legislative stage; in six more, planning committees are active; some planning has been done in another four; and eight show interest but no present planning.

As of July 15, 1947, six noncommercial educational broadcast stations held regular licences, 32 construction permits were outstanding, and eight applications were pending. On the same date, nine such stations were on the air. The Iowa State College of Agriculture and Mechanical Arts, at Ames, Iowa, which, on September 19, 1946, received the first construction permit for a noncommercial television broadcast station, is the only educational institution to hold a television authorization.

New F.M. Stations

Conditional grants for 12 new f.m. stations and construction permits for 34 other f.m. outlets have been authorized by the F.C.C. The first four licenses to be issued since the war were sent the week ending July 17, 1947, to stations which have met the necessary requirements. This makes a total of 52 f.m. broadcast stations now licensed. However, a total of 253 such stations were in operation as of July 24, 1947.

Air Navigation Aids

The House Interstate and Foreign Commerce Committee has recommended the continued development of an instrument-landing system and the inauguration of the most modern ground-control-approach installations to replace the present systems. The standardization of airborne radar equipment employed by military and civil air transport was urged. The committee also proposed the substitution of v.h.f. fixed-course ranges for the l.f. range system now in use.

Installation of Electronic Proximity Indicators Urged

A Special Board of Inquiry on Air Safety has submitted to President Truman recommendations that scheduled airliners install special electronic devices which would measure the true distance of the airplane above the ground. It also urged that the minimum clearance of aircraft flying in mountainous country be raised to 2,000 feet from the present 1,000 feet. It was felt that the terrain-proximity indicators would act as a secondary aid to the aneroid altimeters already installed, and, with the additional clearance requirements, would aid in averting "collisions with terrain."

Receiver and Phonograph Production

Production of radio receiving sets by RMA member-companies, including electric, battery, auto, and television, private and factory brands, totaled 1,213,142 for the month of June, and 8,610,644 for the first six months of 1947. Their phonograph production, including record players as radio attachments, amounted to 28,086 for June, and 273,090 for the first half of 1947.

Income and Product Statistics

A report issued by the Department of Commerce shows expenditures of $905 million for radios, phonographs, parts, and records by consumers in 1929, and reflects a decline to $171 million in 1933. The figure for 1946 was $1,056 billion, and included also expenditures for other musical instruments.

The report, "National Income Supplement to Survey of Current Business, July, 1947," may be obtained at 25 cents per copy from the Superintendent of Documents, United States Government Printing Office, Washington 25, D. C.

Radio Manufacturers Sales

A recent survey by the Securities and Exchange Commission shows an increase in sales by radio and television receiver manufacturers and parts manufacturers for the first quarter of 1947 over the last quarter of 1946.

A total of 1,286 corporations in 139 industry groups, out of 1,402 reporting, showed an increase of $676,000,000 in sales or operating revenues. Thirteen radio and television companies reported a similar increase of $6,146,000. Seven companies, included under radio, television, and electronic parts and equipment manufacturers, showed an increase of $305,000.

Radio and Phonograph Tax Collection

The Bureau of Internal Revenue reports that excise-tax collections on radio sets, components, phonographs, etc., for the fiscal year 1946–1947 totalled $63,856,292.16; $27,402,335.23 being collected in the first six-month period (July, 1946, through December, 1946), and $36,453,956.93 in the second (January, 1947, through June, 1947). Figures for the fiscal year 1945–1946 were, in the same order: $13,387,132.31; $2,702,-070.63; and $10,685,061.68.

Phonograph-record excise-tax collections amounted to $8,491,543.44 for the 1946–1947 fiscal year: $3,485,293.93 in the first six months, and $5,006,249.51 in the second. Figures for corresponding periods in the 1945–1946 fiscal year were $3,902,192.80; $1,258,030.55; and $2,644,162.25.

Radio Exports

The United States Department of Commerce reports that exports of radio receiving equipment during the first four months of 1947 were valued at $31,175,055. In 1946, exports of radio receivers, radio receiving tubes, components, and accessories, had a total value of $39,637,427.

May, 1947, exports of radio transmitting and receiving equipment amounted to 10,044,591 items, with a value of $11,209,734. The total quantity for 1947 was thus 42,013,234, valued at $49,099,764.

RMA Parts Division New Section Heads

Chairman J. J. Kahn, of Chicago, has completed a reorganization of the RMA Parts Division and announced the appointment of Section Chairmen for the 1947–1948 fiscal year as follows:

Coil, E. I. Guthman; Fixed Capacitor, W. M. Owen; Fixed Resistor, J. H. Stackpole; Instrument and Test Equipment, R. L. Triplett; Insulations, J. W. Apgar; Metal Stampings and Metal Specialties, S. L. Gabel; Phonograph Cartridges and Pickups, G. B. Fraser; Plastics and Molded Parts, J. J. Bachner; Record Changer and Phono-Motor, A. W. Fritzsche; Socket, Frank Holmstrom; Speaker, L. A. King; Speaker Parts, A. D. Plamondon, Jr.; Special Products Section, W. R. MacLeod; Switch, W. S. Parsons; Transformer, R. A. Hoagland; Variable Condenser, G. F. Behringer; Variable Resistor, D. S. W. Kelly; Vibrator, R. F. Sparrow; Wire, R. G. Zender; Wire Wound Resistor, D. T. Siegel.

RMA Transmitter Division New Section Chairmen

Broader activities for the members of the RMA Transmitter Division have been arranged by Chairman S. P. Taylor and the Division's Executive Committee. The following chairmen for 1947–1948 service have been appointed:

Aviation, H. M. Hucke; Broadcast Transmitter, C. W. Miller; General Communications, Natale Gada; Marine, C. E. Maass; Transmitter Tube, A. Frankel.

RMA Activities

The following RMA engineering meetings were held:

August 15—Executive Committee

August 27—Committee on Television Receivers

August 28—Subcommittee on Depth Sounding.

◇

National Electronics Conference

The program of the National Electronics Conference, which will be held at the Edgewater Beach Hotel, Chicago, Ill., on November 3, 4, and 5, 1947, will include 20 technical sessions with a total of about 50 papers, two luncheons, and the main banquet, in addition to the general session on Monday morning, November 3. Dr. George D. Stoddard, president of the University of Illinois, will deliver the keynote address at the general session.

A comprehensive technical program has been arranged, covering many fields of interest. Major emphasis will be on Industrial Electronics, to which three sessions will be devoted.

Various new types of antennas, including aircraft antennas, will be discussed. One session will be devoted to commercial, f.m., and television broadcasting, and another to color television and oscillography. Several papers will be presented on instrumentation, and a panel discussion on electronics research operations will be led by experts in the field.

Of general interest will be such subjects as guided missiles, electronic computors, supersonics and infrared, microwaves, and detection of particles. Technical details of the new dynamic noise suppressor, invented by Hermon Hosmer Scott, will be released, and other papers on audio frequencies have been scheduled. Educational exhibits will be displayed by various manufacturers.

Dr. Jolliffe Urges "Scientific Method" as Solution For Social Problems

Dr. C. B. Jolliffe (M'25–F'30), executive vice-president in charge of Radio Corporation of America's RCA Laboratories, declared in an address before the graduating class of the University of West Virginia that social problems threatening civilization with chaos can be solved by the same "scientific method" that has given the world so many of its material benefits.

"Many of the causes and effects of social disruption are known," Dr. Jolliffe said. "What we need to do is to amplify this knowledge, develop it as a body of scientific fact, and formulate general laws by which human conduct can be guided and regulated. . . .

"Man has made amazing progress, especially in the last three hundred years, in his unceasing fight to control and to utilize the physical elements of his environment. But in the all-important field of human relations, where one would expect the greatest advances, progress has been slow. This imbalance between material and social development has brought on a dangerous state in human affairs. . . .

"Scientific method is nothing more than the art of thinking developed to the highest degree. It is the key to insight. By it, in my opinion, we will continue the rapid unfolding of material accomplishment and, in addition, achieve that high level of human understanding so necessary to lasting peace and prosperity. . . .

"The first thing to be done is to make people aware of the power of logic and reason to solve the economic and political problems of our times. This is a task that must be assumed by our more progressive leaders of thought—men and women of education, government, the professions, industry, labor, and the arts. . . .

"A thinking people will insist upon a logical approach to any kind of problem, whether its character is physical or social. It will resort less frequently to falsely conceived panaceas, quack nostrums, and to expedience."

Reprints and Preprints

In most cases, The Institute of Radio Engineers does *not* have available reprints or preprints of papers published in the Proceedings, papers presented at Conventions, or papers presented at Section meetings. Reprints *can* be obtained *only* if ordered in advance of publication and in quantities of fifty or more copies. However, the following three papers *are* available in reprint form and may be obtained by writing to the Institute.

"Radar," by Edwin G. Schneider. Published in the August, 1945, issue of the Proceedings of the I.R.E. and Waves and Electrons. Price, $.50.

"The Presentation of Technical Developments Before Professional Societies," by William L. Everitt. Published in the July, 1945, issue of the Proceedings of the I.R.E. Obtainable on request without charge.

"Preparation and Publication of I.R.E. Papers," by Helen M. Stote. Published in the January, 1946, issue of the Proceedings of the I.R.E. Obtainable on request without charge.

Please address your inquiries to:

The Institute of Radio Engineers, Inc.
1 East 79 Street
New York 21, N. Y.

It would be appreciated if a large stamped, self-addressed envelope accompanied each request.

Emporium Section Summer Seminar

FRIDAY AND SATURDAY, AUGUST 1 AND 2, 1947

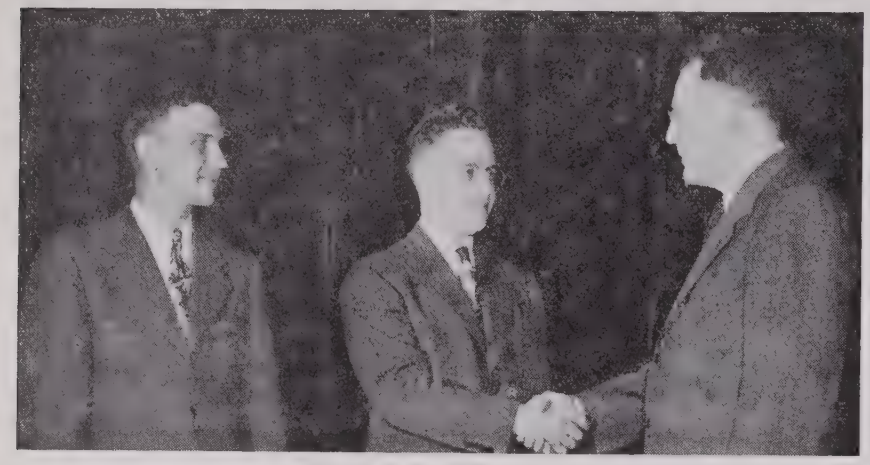

Virgil M. Graham, I.R.E. Director, congratulates H. D. Johnson, Seminar Chairman, and N. J. Reitz, Section Chairman.

Speakers at the Seminar

Left to right: B. F. Wheeler, Radio Corporation of America; R. Beardsley Graham, Bendix Aviation Corporation; George R. Towne, Stromberg Carlson Company.

The Emporium Section of the Institute of Radio Engineers held its Eighth Summer Seminar Friday and Saturday, August 1 and 2, 1947.

Five technical papers, including demonstrations of new types of radio receivers and a sound moving picture, were presented in the two days by leading engineers.

Inspection trips were arranged for those wishing to tour the Emporium plant of Sylvania Electric Products, Inc., on Friday, August 1.

The social part of the program consisted of a picnic with various outdoor sports and supper, on Saturday, August 2.

Details of the program were as follows:

TECHNICAL SESSIONS

Friday, August 1—7:30 p.m.

1. "Microwave Relaying," by B. F. Wheeler, Radio Corporation of America.
2. "Signal-Seeking Receiver" (with demonstration), by V. W. Wiley, Colonial Radio Corporation.
3. "Micromicrowave Radar" (with demonstration), by M. G. Nicholson, Colonial Radio Corporation.

Sound Moving Picture, "Proximity Fuses"

Saturday August 2—10:00 a.m.

1. "Guided Missiles," by R. Beardsley Graham, Bendix Aviation Corporation.
2. "Television Today," by Dr. George R. Town, Stromberg Carlson Company.

INSPECTION TOURS

Friday, August 1—1:00 p.m. to 4:00 p.m.

Emporium plant of Sylvania Electric Products, Inc.

OUTING

Saturday, August 2—2:30 p.m. to 8:30 p.m.

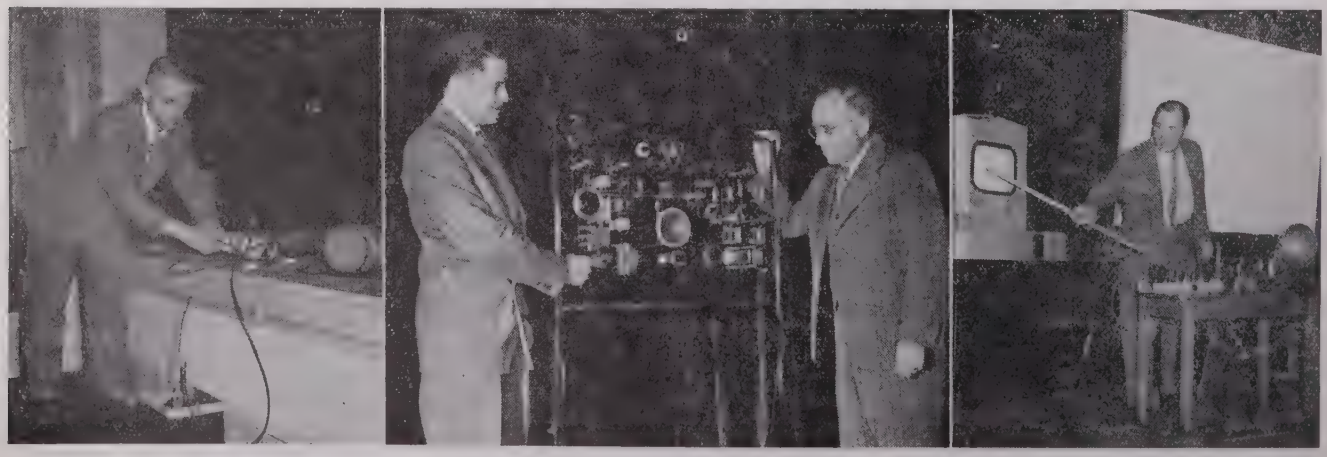

Left: V. W. Wiley, Colonial Radio Corporation, demonstrates a new type of automobile receiver.
Center: L. A. Milton, Colonial Radio Corporation, and W. R. Jones, Chief Engineer, Radio Tube Division, Sylvania Electric Products, Inc., show a demonstration receiver used in training radio service men.
Right: M. G. Nicholson, Colonial Radio Corporation, demonstrates radar effects at extremely short wavelengths.

Minutes of Technical Committee Meetings

The following brief abstracts of I.R.E. technical committee minutes are intended to keep the membership informed as to the activities of such groups Members having views or proposals of interest to the committees, or desiring possibly available information from them, should write directly to the chairman of the particular committee, sending a copy of the letter to Mr. Laurence G. Cumming, Technical Secretary, The Institute of Radio Engineers, 1 East 79 Street, New York 21, N. Y.

Standards

Date.....May 22, 1947
Place.....I.R.E. Headquarters, New York, N. Y.
Chairman.....A. B. Chamberlain

Present

A. B. Chamberlain, *Chairman*

W. G. Cady	G. D. O'Neill
P. S. Carter	(for R. S. Burnap)
L. G. Cumming	R. E. Shelby
E. Dietze	(for Paul Larsen)
V. A. Harrington	W. O. Swinyard
F. R. Lack	H. M. Turner
E. A. Laport	H. A. Wheeler

Mr. Lack gave a useful description of the intended missions of the American Standards Association and the proposed relationship between the I.R.E. Standards Committe activities and the ASA. Mr. Swinyard agreed to have his proposed Standards on Methods of Testing F.M. Receivers ready for circulation to the Standards Committee within two weeks time. Professor Turner made a motion, which was approved by the entire committee, that the Piezoelectric Crystals Committee be changed from a special committee to a regular standing Technical Committee of the Institute.

Electron Tubes

Date.....May 23, 1947
Place.....I.R.E. Headquarters, New York, N.Y.
Chairman.....R. S. Burnap

Present

R. S. Burnap, *Chairman*

J. E. Gorham	L. S. Nergaard
J. W. Greer	G. D. O'Neill
H. L. Krauss	H. J. Reich
J. A. Morton	A. C. Rockwood
I. E. Mouromtseff	C. M. Wheeler

Next year's Electron Tube Conference was discussed and Mr. O'Neill reported that a reply had been received from Cornell University suggesting possible dates for this Conference. The report of the Gas Tube Subcommittee was to be sent to members with a letter requesting comments to Messrs. Burnap and Marshall. A letter from W. W. Watrous, Chairman of Joint Electron Tube Executive Committee's Gas Tube Committee was referred to the Power-Output High-Vacuum Tube and Gas Tube Subcommittees for action.

Mr. O'Neill reported on a meeting of representatives of I.R.E. and RMA to discuss the relative scopes of the organizations. The Small-Signal High-Vacuum Tube Committee's proposed definitions of December 6, 1946, were presented to the committee.

Electron Tubes

Date.....July 18, 1947
Place.....I.R.E. Headquarters, New York, N. Y.
Chairman.....R. S. Burnap

Present

R. S. Burnap, *Chairman*

L. B. Headrick	I. S. Nergaard
S. B. Ingram	G. D. O'Neill
H. L. Krauss	H. J. Reich
D. E. Marshall	A. C. Rockwood
I. E. Mouromtseff	J. R. Steen

C. M. Wheeler

The Chairman of the Electron-Tube Conference Subcommittee reported that the Electron-Tube Conference was a great success both technically and financially. He advised that next year's conference would be held June 28 and 29, 1948, at Cornell University. A review of the Small Signal Vacuum Tube Subcommittee definitions and methods of testing was made.

Radio Transmitters

Date.....July 14, 15, 1947
Place.....I.R.E. Headquarters, New York, N. Y.
Chairman.....E. A. Laport

Present

E. A. Laport, *Chairman*

L. T. Bird	C. H. Meyers
Cledo Brunetti	R. L. Robbins

Robert Serrell

Messrs. Crosby and Laport had met to discuss the differences of opinion between this committee and the Modulation Systems Committee on definitions for clipper, limiter, and clipper-limiter. It was decided that the definitions would be prepared for publication in alphabetical order. The committee deliberated on the definitions previously prepared by the subcommittees on Circuits and Advanced Developments, Television, A.M. Transmitters, F.M. Transmitters, and a list prepared by the Chairman; the definitions were processed and adopted.

Piezoelectric Crystals

Date.....June 9, 1947
Place.....I.R.E. Headquarters, New York, N. Y.
Chairman.....W. G. Cady

Present

W. G. Cady, *Chairman*

W. L. Bond	Paul Smith
Hans Jaffee	R. A. Sykes
W. P. Mason	K. S. Van Dyke

It was voted that Mr. Bond was to ask the committee of The Crystallographic Societies to participate in a joint meeting with the I.R.E. committee in mid-August for the discussion of standard nomenclature. The committee reviewed a paper on "Crystal Rotation Systems," and decided to submit the paper to the Executive Committee of the I.R.E. and urge its early publication as part of the standard report on Piezoelecric Crystals.

Dr. Van Dyke reported that he finds considerable simplification in the elastic piezoelectric matrices follows if he uses the symmetrized system suggested by Dr. Baewald at the last meeting. It was unanimously carried that Dr. Baewald should be urged to publish a paper on this system and that he supply the Chairman of the Piezoelectric Committee with 100 copies of a draft of this paper as soon as possible in order that it may be studied by interested people.

Modulation Systems

Date.....August 1, 1947
Place.....I.R.E. Headquarters, New York, N. Y.
Chairman.....Murray G. Crosby

Present

Murray G. Crosby, *Chairman*

H. S. Black	V. D. Landon
F. L. Burroughs	C. T. McCoy
C. C. Chambers.	Dale Pollack
L. G. Cumming	O. L. Prestholdt
W. F. Goetter	(for J. W. Wright)
D. D. Grieg	Bertram Trevor

W. G. Tuller

The committee status reports were passed out to the committee members and it was decided that the differences in definitions of this committee and those of the F.C.C. would be taken up by the Chairman of the Standards Committee when this set of definitions was approved by the Standards Committee and submitted to the F.C.C. A list of simplified definitions was proposed by Mr. Trevor, and definitions proposed by Messrs. Grieg and Black were reviewed. The Transmitter Committee proposed definitions to be defined by the Modulation Systems Committee. Mr. Landon pointed out the urgent necessity for a definition of the term "Noise Factor."

Subcommittees

Power-Output High-Vacuum Tubes

Date.....June 10, 1947
Place.....Hotel Syracuse, Syracuse, N. Y.
Chairman..I. E. Mouromtseff

Present

I. E. Mouromtseff, *Chairman*

C. E. Fay	E. C. Okress
J. W. Greer	H. J. Reich
G. R. Kilgore	C. M. Wheeler
H. E. Mendenhall	A. K. Wing

Consideration of the material for the revised Section 4 was the main business of the meeting. This material had been prepared by a group of the members of the committee in a meeting on May 20, 1947, and was now submitted to the full committee. Some changes were agreed to and the revised draft was left with Professor Reich for further editing.

Institute Committees—1947

(*Revised as of September 17, 1947*)

Executive

W. R. G. Baker, *Chairman*

R. F. Guy, *Treasurer and Vice-Chairman*

Haraden Pratt, *Secretary*

A. N. Goldsmith, *Editor*

S. L. Bailey
Keith Henney
F. R. Lack

Board of Editors

A. N. Goldsmith, *Chairman*

F. W. Albertson
J. S. Allen
G. M. K. Baker
W. L. Barrow
R. R. Batcher
A. E. Bowen
R. M. Bowie
Ralph Bown
R. S. Burnap
O. H. Caldwell
C. W. Carnahan
L. W. Chubb
L. M. Clement
J. D. Cobine
M. G. Crosby
R. B. Dome
W. G. Dow
E. W. Engstrom
W. L. Everitt
W. G. H. Finch
D. G. Fink
H. C. Forbes
I. A. Getting
G. W. Gilman
P. C. Goldmark
A. W. Graf
F. W. Grover
L. B. Headrick
E. W. Herold
J. A. Hutcheson
C. M. Jansky, Jr.
J. K. Johnson
L. F. Jones
H. S. Knowles
J. D. Kraus
J. B. H. Kuper
J. T. Lawson
D. G. Little
F. B. Llewellyn
S. S. Mackeown
Nathan Marchand
E. D. McArthur
Knox McIlwain
J. W. McRae
L. A. Meacham
G. F. Metcalf
E. L. Nelson
D. O. North
H. F. Olson
R. M. Page
H. O. Peterson
G. W. Pickard
Haraden Pratt
C. A. Priest
J. R. Ragazzini
Simon Ramo
H. J. Reich
J. D. Reid
F. X. Rettenmeyer
P. C. Sandretto
S. W. Seeley
V. W. Sherman
L. C. Smeby
C. E. Smith
J. A. Stratton
W. C. Tinus
K. S. Van Dyke
E. K. Van Tassel
E. C. Wente
H. A. Wheeler
J. R. Whinnery
W. C. White
L. E. Whittemore
G. W. Willard
William Wilson
I. G. Wolff
V. K. Zworykin

Awards

F. B. Llewellyn, *Chairman*

E. W. Engstrom
D. G. Fink
V. M. Graham
R. A. Hackbusch
D. D. Israel
I. J. Kaar

Education

William H. Radford, *Chairman*

W. E. Arcand
R. E. Beam
A. B. Bronwell
Melville Eastham
G. H. Fett
A. W. Graf
E. A. Guillemin
Alan Hazeltine
G. B. Hoadley
L. N. Holland
A. H. Howell
H. H. Newell
R. G. Porter
H. J. Reich
E. H. Schulz
W. J. Seeley
F. R. Stansel
W. O. Swinyard
G. R. Town
Ernst Weber
A. H. Wing, Jr.

Papers Procurement

Dorman D. Israel, *Chairman*

Andrew Alford
B. B. Bauer
R. M. Bowie
A. B. Bronwell
J. W. Butterworth
I. F. Byrnes
T. J. Carroll
Madison Cawein
K. A. Chittick
B. J. Chromy
J. T. Cimorelli
Harry Diamond
Eginhard Dietze
G. V. Eltgroth
M. K. Goldstein
H. Grossman
R. C. Guthrie
D. E. Harnett
J. R. Harrison
J. V. L. Hogan
F. V. Hunt
T. A. Hunter
Hans Jaffe
J. J. Jakosky
Martin Katzin
C. E. Kilgour
A. V. Loughren
I. G. Maloff
H. B. Marvin
W. P. Mason
Pierre Mertz
B. J. Miller
I. E. Mouromtseff
A. F. Murray
J. R. Nelson
L. L. Nettleton
G. M. Nixon
D. E. Noble
T. M. Odarenko
H. F. Olson
W. E. Reichle
J. D. Reid
F. X. Rettenmeyer
H. W. G. Salinger
Robert E. Shelby
W. P. Short
Daniel Silverman
P. L. Smith
J. Q. Stansfield
G. R. Town
L. G. Trolese
H. J. Tyzzer
K. S. Van Dyke
W. L. Webb
J. R. Whinnery
W. C. White
G. S. Wickizer
R. H. Williamson
R. J. Wise
C. J. Young

Papers Review

Murray G. Crosby, *Chairman*

H. A. Affel
E. W. Allen
C. F. Baldwin
B. de F. Bayly
F. J. Bingley
H. S. Black
F. T. Bowditch
H. A. Chinn
J. K. Clapp
I. S. Coggeshall
S. B. Cohn
J. M. Constable
F. W. Cunningham
H. D. Doolittle
O. S. Duffendack
R. D. Duncan, Jr.
I. E. Fair
E. H. Felix
V. H. Fraenckel
R. L. Freeman
Stanford Goldman
W. M. Goodall
W. C. Hahn
G. L. Haller
O. B. Hanson
A. E. Harrison
J. R. Harrison
T. J. Henry
C. N. Hoyler
F. V. Hunt
Harley Iams
D. L. Jaffe
Hans Jaffe
W. R. Jones
D. C. Kalbfell
A. G. Kandoian
J. G. Kreer, Jr.
Emil Labin
V. D. Landon
H. C. Leuteritz
C. V. Litton
H. R. Lubcke
Louis Malter
W. P. Mason
R. E. Mathes
H. F. Mayer
H. R. Mimno
R. E. Moe
R. M. Morris
F. L. Mosely
I. E. Mouromtseff
G. G. Muller
A. F. Murray
J. R. Nelson
K. A. Norton
H. W. Parker
L. J. Peters
A. P. G. Peterson
W. H. Pickering
A. F. Pomeroy
S. O. Rice
T. H. Rogers
H. E. Roys
M. W. Scheldorf
Samuel Seely
Harner Selvidge
C. M. Slack
J. E. Smith
P. L. Smith
E. E. Spitzer
E. K. Stodola
H. P. Thomas
Bertram Trevor
Dayton Ulrey
A. P. Upton
G. L. Usselman
L. Vieth
S. N. Van Voorhies
R. M. Wilmotte
J. W. Wright
H. R. Zeamans

Constitution and Laws

B. E. Shackelford, *Chairman*

G. W. Bailey
A. B. Chamberlain
I. S. Coggeshall
R. F. Guy
R. A. Heising
F. R. Llewellyn
F. E. Terman
H. R. Zeamans

Admissions

G. T. Royden, *Chairman*
F. A. Polkinghorn, *Vice-Chairman*

R. D. Avery
H. H. Beverage
R. M. Bowie
J. T. Brothers
J. L. Callahan
H. A. Chinn
J. D. Cobine
E. D. Cook (W. A. Ford, alternate)
E. T. Dickey
W. A. Dickinson
O. M. Dunning
Lloyd Espenschied
T. T. Goldsmith, Jr.
A. R. Hodges
A. R. Morton
R. S. O'Brien
D. S. Rau
C. E. Scholz
S. W. Seeley
R. F. Shea
E. R. Shenk
M. E. Strieby
J. C. Stroebel
W. L. Webb
F. D. Webster
G. R. White
G. S. Wickizer
R. C. G. Williams

Membership

Beverly Dudley, *Chairman*

A. L. Albert
R. E. Beam
E. D. Cook
A. V. Eastman
D. G. Fink
R. P. Glover
George Grammer
R. F. Guy
J. W. Horton
P. B. Laeser
I. E. Mouromtseff
W. H. Radford
Donald Sinclair
J. A. Stratton
Ernst Weber
W. C. White
P. D. Zottu
(Section Secretaries *Ex Officio*)

Public Relations

Virgil M. Graham, *Chairman*

G. W. Bailey
E. L. Bragdon
W. C. Copp
C. B. DeSoto
O. E. Dunlap
W. C. Evans
H. C. Forbes
Charles Fry
R. A. Hackbusch
Keith Henney
George Lewis
R. H. Manson
E. A. Nicholas
R. C. Poulter
H. B. Richmond
E. L. Robinson
Crump Smith
D. B. Smith
Will Whitmore

Sections

W. O. Swinyard, *Chairman*

S. L. Bailey
E. D. Cook
A. W. Graf
J. A. Green
R. A. Heising
G. B. Hoadley
Earl Kent
P. B. Laeser
L. E. Packard
J. E. Shepherd
(Section Chairmen *Ex Officio*)

Nominations

Haraden Pratt, *Chairman*

S. L. Bailey
J. E. Brown
E. W. Engstrom
J. J. Farrell
L. C. F. Horle
F. B. Llewellyn

Tellers

H. A. Chinn, *Chairman*

W. A. Cobb
J. E. Shepherd

Technical Committees—May 1, 1947-May 1, 1948

(Revised as of September 1, 1947)

Annual Review

L. E. Whittemore, *Chairman*

G. P. Bosomworth, George Brown, R. S. Burnap, W. G. Cady, P. S. Carter, A. B. Chamberlain, I. S. Coggeshall, M. G. Crosby, Eginhard Dietze, B. S. Ellefson, D. G. Fink, Keith Henney, J. V. L. Hogan, E. A. Laport, P. J. Larsen, W. B. Lodge, E. W. Schafer, S. A. Schelkunoff, W. O. Swinyard, F. E. Terman

H. A. Wheeler

Antennas

P. S. Carter, *Chairman*

Andrew Alford, T. M. Bloomer, G. H. Brown, Harry Diamond, W. S. Duttera, J. E. Eaton, Sidney Frankel, George Grammer, R. F. Guy, R. F. Holtz, R. B. Jacques, E. C. Jordan, W. E. Kock, K. A. MacKinnon, W. W. Mieher, D. C. Ports, M. W. Scheldorf, S. A. Schelkunoff, J. C. Schelleng, George Sinclair, P. H. Smith, L. C. Van Atta

J. W. Wright

Circuits

J. G. Brainerd, Cledo Brunetti, C. R. Burrows, F. C. Everett, W. L. Everitt, R. M. Foster, S. G. Goldman, E. A. Guillemin, H. L. Krauss, E. E. Overmier, E. H. Perkins, J. B. Russell, Jr., S. W. Seeley, W. M. Smith

W. N. Tuttle

Electroacoustics

Eginhard Dietze, *Chairman*

P. N. Arnold, B. B. Bauer, S. J. Begun, R. H. Bolt, R. K. Cook, M. J. Di Toro, W. D. Goodale, Jr., E. C. Gregg, F. L. Hopper, F. V. Hunt, H. S. Knowles, G. M. Nixon, Benjamin Olney, H. F. Olson, R. A. Schlegel, E. S. Seeley

Lincoln Thompson

Electron Tubes

R. S. Burnap, *Chairman*

A. Y. Bentley, K. C. De Walt, W. G. Dow, A. M. Glover, J. E. Gorham, George Grammer, J. W. Greer, L. B. Headrick, E. C. Homer, D. R. Hull, S. B. Ingram, H. L. Krauss, Louis Malter, D. E. Marshall, J. A. Morton, I. E. Mouromtseff, L. S. Nergaard, G. D. O'Neill, L. M. Price, H. J. Reich, A. C. Rockwood, A. L. Samuel, J. R. Steen, C. M. Wheeler

Facsimile

J. V. L. Hogan, *Chairman*

J. C. Barnes, Henry Burkhard, J. J. Callahan, A. G. Cooley, R. E. Mathes, Pierre Mertz, H. C. Ressler, Arthur Rustad, W. E. Stewart, E. F. Watson

R. J. Wise

Handbook

H. A. Wheeler, *Chairman*

C. T. Burke, R. S. Burnap, J. D. Crawford, C. B. DeSoto, R. L. Dietzold, D. G. Fink, Sidney Frankel, Knox McIlwain, Frank Massa, F. E. Terman, B. F. Wheeler, J. R. Whinnery

R. M. Wilmotte

Industrial Electronics

G. P. Bosomworth, *Chairman*

W. B. R. Agnew, J. E. Brown, R. D. Campbell, C. A. Ellert, C. W. Frick, Merle Gander, H. C. Gillespie, Otto Glasser, Guy Harris, A. C. Holt, Eugene Mittelmann, H. W. Parker, H. O. Peterson, Walther Richter, W. C. Rudd, P. C. Sandretto, V. W. Sherman, D. E. Watts, Julius Weinberger, R. M. Wilmotte, T. L. Wilson, P. D. Zottu

Modulation Systems

M. G. Crosby, *Chairman*

H. S. Black, J. E. Brown, F. L. Burroughs, C. C. Chambers, F. M. Doolittle, C. W. Finnigan, W. F. Goetter, A. C. Goodnow, George Grammer, D. D. Grieg, R. F. Guy, D. M. Hill, V. D. Landon, B. D. Loughlin, C. T. McCoy, C. R. Miner, G. W. Olive, E. M. Ostlund, Dale Pollack, S. W. Seeley, Bertram Trevor, W. G. Tuller

J. W. Wright

Navigation Aids

D. G. Fink, *Chairman*

H. G. Busignies, P. A. D'Orio, F. C. Dyer (C. R. Banks, alternate), R. C. Ferrar, N. L. Harvey, C. J. Hirsch, A. B. Hunt, W. E. Jackson, H. R. Mimno, H. K. Morgan, Marcus O'Day, J. A. Pierce, J. A. Rankin, P. C. Sandretto, Ben Thompson

R. R. Welsh

Piezoelectric Crystals

W. G. Cady, *Chairman*

C. F. Baldwin, W. L. Bond, J. K. Clapp, Clifford Frondel, Hans Jaffe, W. P. Mason, P. L. Smith, R. A. Sykes, K. S. Van Dyke, J. M. Wolfskill

Railroad and Vehicular Communication

M. G. Brown, *Chairman*

F. T. Budelman, W. T. Cooke, W. A. Harris, C. N. Kimball, Jr., D. E. Noble, W. W. Salisbury, David Talley, F. W. Walker

W. R. Young

Research

F. E. Terman, *Chairman*

W. L. Barrow, F. T. Bowditch, R. M. Bowie, E. W. Engstrom, W. L. Everitt, D. G. Fink, H. T. Friis, L. C. Van Atta, A. F. Van Dyck, Julius Weinberger

Radio Receivers

W. O. Swinyard, *Chairman*

G. L. Beers, J. E. Brown, W. F. Cotter, W. L. Dunn, H. C. Forbes, D. E. Foster, C. J. Franks, A. R. Hodges, K. W. Jarvis, J. K. Johnson, C. R. Miner, Garrard Mountjoy, H. O. Peterson, J. M. Pettit, Dale Pollack, F. H. R. Pounsett, J. D. Reid, R. F. Shea, H. L. Shortt, R. M. Wilmotte

C. F. Wolcott

Radio Transmitters

E. A. Laport, *Chairman*

L. T. Bird, M. R. Briggs, Cledo Brunetti, H. R. Butler, George Grammer, A. E. Kerwien, J. B. Knox, L. A. Looney, C. H. Meyer, J. C. R. Punchard, R. L. Robbins, J. C. Schelleng, Robert Serrell, I. R. Weir

Radio Wave Propagation and Utilization

S. A. Schelkunoff, *Chairman*

S. L. Bailey, C. R. Burrows, T. J. Carroll, A. E. Cullum, W. S. Duttera, A. G. Fox, M. C. Gray, D. E. Kerr, K. A. Norton, H. O. Peterson, J. A. Pierce, George Sinclair, R. L. Smith-Rose, J. A. Stratton, H. W. Wells, J. W. Wright

Standards

A. B. Chamberlain, *Chairman*
L. G. Cumming, *Vice Chairman*

G. M. K. Baker, G. P. Bosomworth, G. M. Brown, R. S. Burnap, W. G. Cady, P. S. Carter, M. G. Crosby, Eginhard Dietze, D. G. Fink, V. M. Graham, Keith Henney, J. V. L. Hogan, L. C. F. Horle, E. A. Laport, P. J. Larsen, A. V. Loughren, E. W. Schafer, S. A. Schelkunoff, W. O. Swinyard, H. M. Turner, H. A. Wheeler, L. E. Whittemore

Symbols

E. W. Schafer, *Chairman*

A. E. Anderson, R. R. Batcher, M. R. Briggs, R. S. Burnap, C. R. Burrows, H. F. Dart, J. H. Dellinger, E. T. Dickey, H. S. Knowles, O. T. Laube, C. A. Nietzert, A. F. Pomeroy, Duane Roller, A. L. Samuel, J. R. Steen, H. M. Turner

Television

P. J. Larsen, *Chairman*

W. F. Bailey, J. E. Brown, K. A. Chittick, D. G. Fink, C. J. Franks, P. C. Goldmark, R. N. Harmon, A. G. Jensen, I. J. Kaar, R. D. Kell, H. T. Lyman, J. B. Minter, Garrard Mountjoy, J. A. Ouimet, D. W. Pugsley, R. E. Shelby, D. B. Smith, M. E. Strieby

N. H. Young, Jr.

Special Committees

(Revised as of September 1, 1947)

Office Practices

R. F. Guy, *Chairman*
S. L. Bailey, F. R. Lack, W. C. White

Building Fund Administrators

Melville Eastham, E. A. Nicholas, Haraden Pratt

Convention Policy

J. E. Shepherd, *Chairman*
Austin Bailey, E. J. Content, G. W. Bailey, B. E. Shackelford

Editorial Administrative

A. N. Goldsmith, Editor—*Chairman*
R. S. Burnap, F. B. Llewellyn, M. G. Crosby, Donald McNicol, E. W. Herold, Haraden Pratt, L. E. Whittemore

Founders

R. F. Guy, *Chairman*

Fiscal

Haraden Pratt, *Chairman*
A. N. Goldsmith, F. R. Lack, R. F. Guy, F. B. Llewellyn

International Liaison

Ralph Bown, *Chairman*
F. S. Barton, E. M. Deloraine, F. B. Llewellyn

Office Quarters

R. A. Heising, *Chairman*
G. W. Bailey, F. B. Llewellyn, A. N. Goldsmith, Haraden Pratt

Planning

R. A. Heising, *Chairman*
S. L. Bailey, Keith Henney, A. N. Goldsmith, D. B. Sinclair, B. E. Shackelford

Professional Recognition

W. C. White, *Chairman*
E. F. Carter, J. V. L. Hogan, C. C. Chambers, H. A. Wheeler, H. R. Zeamans

Special Publication Fund

F. R. Lack, *Chairman*
S. L. Bailey, J. R. Miller, J. E. Brown, B. E. Shackelford, R. V. Howard, D. B. Sinclair, D. B. Smith

RMA-I.R.E. Co-ordinating

V. M. Graham, *Chairman*
L. G. Cumming, D. D. Israel, J. J. Farrell, Keith Henney, L. C. F. Horle

Institute Representatives in Colleges—1947

(Revised as of September 17, 1947)

Alabama Polytechnic Institute: Appointment Later
*Alberta, University of: J. W. Porteous
Arkansas, University of: G. H. Scott

British Columbia, University of: H. J. MacLeod
Brooklyn, Polytechnical Institute of: G. B. Hoadley

California Institute of Technology: S. S. Mackeown
*California, University of: L. J. Black
Carleton College: Appointment Later
Carnegie Institute of Technology: E. M. Williams
Case School of Applied Science: P. L. Hoover
Cincinnati, University of: A. B. Bereskin
Colorado, University of: Appointment Later
Columbia University: J. R. Ragazzini
Connecticut, University of: F. P. Fischer
Cooper Union: J. B. Sherman
Cornell University: True McLean

Detroit, University of: Appointment Later
Drexel Institute of Technology: Appointment Later
Duke University: W. J. Seeley

Florida, University of: F. H. Pumphrey

Georgia School of Technology: M. A. Honnell

Harvard University: E. L. Chaffee

Idaho, University of: Appointment Later
Illinois Institute of Technology: Appointment Later
*Illinois, University of: E. C. Jordan
Iowa, State University of: L. A. Ware
Iowa State College: W. L. Cassell

Johns Hopkins University: Ferdinand Hamburger, Jr.

*Kansas State College: K. Martin
Kansas, University of: C. L. Coates, Jr.

Lawrence Institute of Technology: H. L. Byerlay
Lehigh University: D. E. Mode
Louisiana State University: W. E. Owen

Maine, University of: W. J. Creamer, Jr.
Manhattan College: E. N. Lurch
Maryland, University of: G. L. Davis
Massachusetts Institute of Technology: E. A. Guillemin and W. H. Radford
McGill University: F. S. Howes
Michigan State: J. A. Strelzoff
*Michigan, University of: L. N. Holland
Minnesota, University of: O. A. Becklund
Missouri, University of: D. L. Weidelich

Nebraska, University of: F. W. Norris
Newark College of Engineering: Solomon Fishman
New Hampshire, University of: W. B. Nulsen
New Mexico, University of: Appointment Later
*New York, College of the City of: Harold Wolf
*New York University: Philip Greenstein
*North Carolina State College: W. S. Carley
North Dakota, University of: Clifford Thomforde
Northeastern University: G. E. Pihl
*Northwestern University: R. E. Beam
Notre Dame, University of: H. E. Ellithorn

Ohio State University: E. M. Boone
Oklahoma Agriculture and Mechanical College: H. T. Fristoe
Oregon State College: A. L. Albert

Pennsylvania State College: G. L. Crossley
Pennsylvania, University of: C. C. Chambers
Pittsburgh, University of: Appointment Later
Princeton University: H. M. Chandler
*Purdue University: R. P. Siskind

Queen's University: H. H. Stewart

Rensselaer Polytechnic Institute: H. D. Harris
Rice Institute: M. V. McEnany
Rose Polytechnic Institute: H. A. Moench
*Rutgers University: J. L. Potter

Southern Methodist University: H. J. Smith
*Stanford University: Karl Spangenberg
Stevens Institute of Technology: Carl Neitzert
Syracuse University: C. S. Roys

Tennessee, University of: E. D. Shipley
*Texas, University of: A. W. Straiton
Toronto, University of: Appointment Later
Tufts College: A. H. Howell

Union College: F. W. Grover
United States Military Academy: L. E. Johnson
United States Naval Academy: G. R. Giet
*Utah, University of: O. C. Haycock

Virginia, University of: L. R. Quarles
Virginia Polytechnic Institute: R. R. Wright

*Washington, University of: A. V. Eastman
Washington University: S. H. Van Wambeck
Wayne University: H. M. Hess
Western Ontario, University of: G. W. Woonton
West Virginia University: R. C. Colwell
Wisconsin, University of: Glenn Koehler
*Worcester Polytechnic Institute: H. H. Newell

Yale University: H. M. Turner

* Colleges with approved Student Branches.

Sections

Chairman		Secretary
P. H. Herndon c/o Dept. in charge of Federal Communication 411 Federal Annex Atlanta, Ga.	ATLANTA October 17	M. S. Alexander 2289 Memorial Dr., S.E. Atlanta, Ga.
F. W. Fischer 714 Beechfield Ave. Baltimore 29, Md.	BALTIMORE	E. W. Chapin 2805 Shirley Ave. Baltimore 14, Md.
W. H. Radford Massachusetts Institute of Technology Cambridge, Mass.	BOSTON	A. G. Bousquet General Radio Co. 275 Massachusetts Ave. Cambridge 39, Mass.
A. T. Consentino San Martin 379 Buenos Aires, Argentina	BUENOS AIRES	N. C. Cutler San Martin 379 Buenos Aires, Argentina
R. G. Rowe 8237 Witkop Avenue Niagara Falls, N. Y.	BUFFALO-NIAGARA October 15	R. F. Blinzler 558 Crescent Ave. Buffalo 14, N. Y.
J. A. Green Collins Radio Co. Cedar Rapids, Iowa	CEDAR RAPIDS	Arthur Wulfsburg Collins Radio Co. Cedar Rapids, Iowa
Karl Kramer Jensen Radio Mfg. Co. 6601 S. Laramie St. Chicago 38, Ill.	CHICAGO October 17	D. G. Haines Hytron Radio and Electronics Corp. 4000 W. North Ave. Chicago 39, Ill.
J. F. Jordan Baldwin Piano Co. 1801 Gilbert Ave. Cincinnati, Ohio	CINCINNATI October 14	F. Wissel Crosley Corporation 1329 Arlington St. Cincinnati, Ohio
W. G Hutton R.R. 3 Brecksville, Ohio	CLEVELAND October 23	H. D. Seielstad 1678 Chesterland Ave. Lakewood 7, Ohio
C. J. Emmons 158 E. Como Ave. Columbus 2, Ohio	COLUMBUS November 14	L. B. Lamp 846 Berkeley Rd. Columbus 5, Ohio
L. A. Reilly 989 Roosevelt Ave. Springneld, Mass.	CONNECTICUT VALLEY October 16	H. L. Krauss Dunham Laboratory Yale University New Haven, Conn.
Robert Broding 2921 Kingston Dallas, Texas	DALLAS-FT. WORTH	A. S. LeVelle 308 S. Akard St. Dallas 2, Texas
E. L. Adams Miami Valley Broadcasting Corp. Dayton 1, Ohio	DAYTON October 16	George Rappaport 132 E. Court Harshman Homes Dayton 3, Ohio
P. O. Frincke 219 S. Kenwood St. Royal Oak, Mich.	DETROIT October 17	Charles Kocher 17186 Sioux Rd. Detroit 24, Mich.
N. J. Reitz Sylvania Electric Products, Inc. Emporium, Pa.	EMPORIUM	A. W. Peterson Sylvania Electric Products, Inc. Emporium, Pa.
F. M. Austin 3103 Amherst St. Houston, Texas	HOUSTON	C. V. Clarke, Jr. Box 907 Pasadena, Texas
H. I. Metz Civil Aeronautics Administration 84 Marietta St., NW Atlanta, Ga.	INDIANAPOLIS	M. G. Beier 3930 Guilford Ave. Indianapolis 5, Ind.
C. L. Omer Midwest Eng. Devel. Co. Inc. 3543 Broadway Kansas City 2, Mo.	KANSAS CITY	Mrs. G. L. Curtis 6003 El Monte Mission, Kansas
R. C. Dearle Dept. of Physics University of Western Ontario London, Ont., Canada	LONDON, ONTARIO	E. H. Tull 14 Erie Ave. London, Ont., Canada
C W. Mason 141 N. Vermont Ave. Los Angeles 4, Calif.	LOS ANGELES October 21	Bernard Walley RCA Victor Division 420 S. San Pedro St. Los Angeles 13, Calif.
O. W. Towner Radio Station WHS Louisville, Ky.	LOUISVILLE	D. C. Summerford Radio Station WHS Louisville, Ky.

Chairman		Secretary
E. T. Sherwood Globe-Union Inc. Milwaukee 1, Wis.	MILWAUKEE	J. J. Kircher 2450 S. 35th St. Milwaukee 7, Wis.
R. R. Desaulniers Canadian Marconi Co. 211 St. Sacrement St. Montreal, P.Q., Canada	MONTREAL, QUEBEC November 12	R. P. Matthews Federal Electric Mfg. Co. 9600 St. Lawrence Blvd. Montreal 14, P.Q., Canada
J. E. Shepherd 111 Courtenay Rd. Hempstead, L. I., N. Y.	NEW YORK November 5	I. G. Easton General Radio Co. 90 West Street New York 6, N. Y.
L. R. Quarles University of Virginia Charlottesville, Va.	NORTH CAROLINA-VIRGINIA	J. T. Orth 4101 Fort Ave. Lynchburg, Va.
K. A. Mackinnon Box 542 Ottawa, Ont. Canada	OTTAWA, ONTARIO October 16	D. A. G. Waldock National Defense Headquarters New Army Building Ottawa, Ont., Canada
P. M. Craig 342 Hewitt Rd. Wyncote, Pa.	PHILADELPHIA November 6	J. T. Brothers Philco Radio and Television Tioga and C Sts. Philadelphia 34, Pa.
E. M. Williams Electrical Engineering Dept. Carnegie Institute of Tech. Pittsburgh 13, Pa.	PITTSBURGH November 10	E. W. Marlowe 560 S. Trenton Ave. Wilkinburgh PO Pittsburgh 21, Pa.
Francis McCann 4415 N.E. 81 St. Portland 13, Ore.	PORTLAND	A. E. Richmond Box 441 Portland 7, Ore.
N. W. Mather Dept. of Elec. Engineering Princeton University Princeton, N. J.	PRINCETON	A. E. Harrison Dept. of Elec. Engineering Princeton University Princeton, N. J.
A. E. Newlon Stromberg-Carlson Co. Rochester 3, N. Y.	ROCHESTER October 16	J. A. Rodgers Huntington Hills Rochester, N. Y.
E. S. Naschke 1073-57 St. Sacramento 16, Calif.	SACRAMENTO	G. W. Barnes 1333 Weller Way Sacramento, Calif.
R. L. Coe Radio Station KSD Post Dispatch Bldg. St. Louis 1, Mo.	ST. LOUIS	N. J. Zehr Radio Station KWK Hotel Chase St. Louis 8, Mo.
Rawson Bennett U. S. Navy Electronics Laboratory San Diego 52, Calif.	SAN DIEGO November 4	C. N. Tirrell U. S. Navy Electronics Laboratory San Diego 52, Calif.
W. J. Barclay 955 N. California Ave. Palo Alto, Calif.	SAN FRANCISCO	F. R. Brace 955 Jones San Francisco 9, Calif.
J. F. Johnson 2626 Second Ave. Seattle 1, Wash.	SEATTLE November 13	J. M. Patterson 7200—28 N. W. Seattle 7, Wash.
C. A. Priest 314 Hurlburt Rd. Syracuse, N. Y.	SYRACUSE	R. E. Moe General Electric Co. Syracuse, N. Y.
C. A. Norris J. R. Longstaffe Ltd. 11 King St., W. Toronto, Ont., Canada	TORONTO, ONTARIO	C. G. Lloyd 212 King St., W. Toronto, Ont., Canada
O. H. Schuck 4711 Dupont Ave. S. Minneapolis 9, Minn.	TWIN CITIES	B. E. Montgomery Engineering Department Northwest Airlines Saint Paul, Minn.
L. C. Smeby 820—13 St. N. W. Washington 5, D. C.	WASHINGTON October 13	T. J. Carroll National Bureau of Standards Washington, D. C.
	WILLIAMSPORT November 5	R. G. Petts Sylvania Electric Products, Inc. 1004 Cherry St. Montoursville, Pa.

Sections

SUBSECTIONS

Chairman		Secretary
J. D. Schantz Farnsworth Television and Radio Company 3700 E. Pontiac St. Fort Wayne, Ind.	Fort Wayne (Chicago Subsection)	S. J. Harris Farnsworth Television and Radio Co. 3702 E. Pontiac Fort Wayne 1, Ind.
F. A. O. Banks 81 Troy St. Kitchener, Ont., Canada	Hamilton (Toronto Subsection)	E. Ruse 195 Ferguson Ave., S. Hamilton, Ont., Canada
A. D. Emurian HDQRS. Signal Corps Engineering Lab. Bradley Beach, N. J.	Monmouth (New York Subsection)	Ralph Cole Watson Laboratories Red Bank, N. J.
A. R. Kahn Electro-Voice, Inc. Buchanan, Mich.	South Bend (Chicago Subsection) October 16	A. M. Wiggins Electro-Voice, Inc. Buchanan, Mich.
W. M. Stringfellow Radio Station WSPD 136 Huron Street Toledo 4, Ohio	Toledo (Detroit Subsection)	M. W. Keck 2231 Oak Grove Place Toledo 12, Ohio
W. A. Cole 323 Broadway Ave. Winnipeg, Manit., Canada	Winnipeg (Toronto Subsection)	C. E. Trembley Canadian Marconi Co. Main Street Winnipeg, Manit., Canada

Books

Television, Volume III (1938–1941) and Television, Volume IV (1942–1946), edited by Alfred N. Goldsmith, Arthur F. Van Dyke, Robert S. Burnap, Edward T. Dickey, and George M. K. Baker

Published (1947) by RCA Review, Radio Corporation of America, RCA Laboratories Division, Princeton, N. J.

Television III: 460 pages+26-page appendix+xii pages. 307 figures. 6×9 inches. Price, $2.50 cloth, $1.50 paper.

Television IV: 498 pages+12-page appendix+xiv pages. 338 figures. 6×9 inches. Price, $2.50 cloth, $1.50 paper.

Before the war, "Television, Volumes I and II," consisting of a collection of papers by Radio Corporation of America authors on various phases of television, were published by the RCA Institute's Technical Press. During the war, the publication of the series of books, including "Television, Volumes I and II," was discontinued. Since the war, the RCA Review has compiled and edited material to bridge the gap and bring the television books up to date.

Volume III contains papers by RCA authors published during the years 1938–1941, and, in addition, summaries of other important television papers. The papers in this volume are grouped in four sections under the headings: Pickup, Transmission, Reception, and General.

An Appendix gives summaries of the papers published in the books, "Television, Volumes I and II." Unfortunately, these summaries include neither reference to the publication in which they originally appeared nor the date of publication.

Volume IV presents the papers and summaries for the period 1942–1946. The papers are divided under the same headings as in Volume III, with the addition of groups on color television and military television, the latter group covering the war-time developments on which wartime restrictions have been removed. In addition, the Appendix holds a rather complete bibliography of television papers by RCA authors for the period 1929–1946.

The judicious choice of papers in full form and summaries has minimized repetition and increased the usefulness of these books. The wide scope of the subject matter, the wide difference in treatment, and the well-balanced presentation of papers on the various phases of television, make these volumes of great value to engineers, scientists, and all others interested in television.

With the exception of a few papers which are of a general type and some introductions, no new information or new treatment of old information is presented, since most of the information is available in other publications.

Although the books, by their very nature, cannot present an integrated, complete, technical treatise, the advantage of having a large number of papers on television, covering a wide range of subjects in readily available form, should not be underestimated. It would appear that the editors can confidently "hope" the material here assembled may lead to speedy developments and advance the position of television among the companion arts and sciences.

Lewis M. Clement
Crosley Radio Corporation
Cincinnati 25, Ohio

Writing the Technical Report (New Second Edition), by J. Raleigh Nelson

Published (1947) by McGraw-Hill Book Company, Inc., 330 W. 42 St., New York 18, N. Y. 382 pages+6-page index+xiv pages. 22 figures. 5½+9 inches. Price, $3.00.

This book is the second edition of a book initially published in 1940. While the basic scheme of this new edition is unchanged from that of the earlier edition, the author has revised the details of presentation in numerous instances, has supplied additional cross references to help the reader, and has added a useful index.

Prepared for the dual objectives of assisting both students and practitioners in writing better technical reports, the book is well organized for the intended use. It is divided into four parts.

Part I, representing about one-third of the material, discusses in seventeen chapters the design of the report. Such matters as the purpose of a report, its organization, use of headings, constructing the paragraph, and testing of progress, all liberally illustrated by practical examples, are covered in logical and adequate detail.

Part II gives some suggestions as to the form of the report. It covers stenographic details, style, format, and use of figures and tables, and includes about 100 pages of illustrative annotated reports in both long and short forms.

Part III, entitled "The Criticism of the Report," treats in five so-called clinics the problems of preparing the introduction, organizing the material, providing coherence, achieving good sentence structure, and of avoiding common editorial errors.

Part IV, comprising some 45 pages, gives suggestions specifically for the use of the book in the classroom and is, therefore, of minor interest to the practitioner.

The reviewer finds much in the book to commend and little to criticize. On such basic matters as the function of a report, its viewpoint, and its organization, the author has emphasized sound principles which have stood the test of practical use. On the other hand, he has avoided the pitfalls of a dogmatic approach, leaving latitude for the exercise of judgment in individual cases. By providing liberal examples of various forms of reports, he, of course, greatly increased the difficulties of preparing the text, but the examples as a group stand up successfully under critical analysis, and are, therefore, a valuable contribution.

This book is well worth reading by the engineer. For the man inexperienced in report writing, it provides professional assistance in competently organized form; for the man of greater experience, it is an excellent refresher course.

R. S. Burnap
Radio Corporation of America
Harrison, N. J.

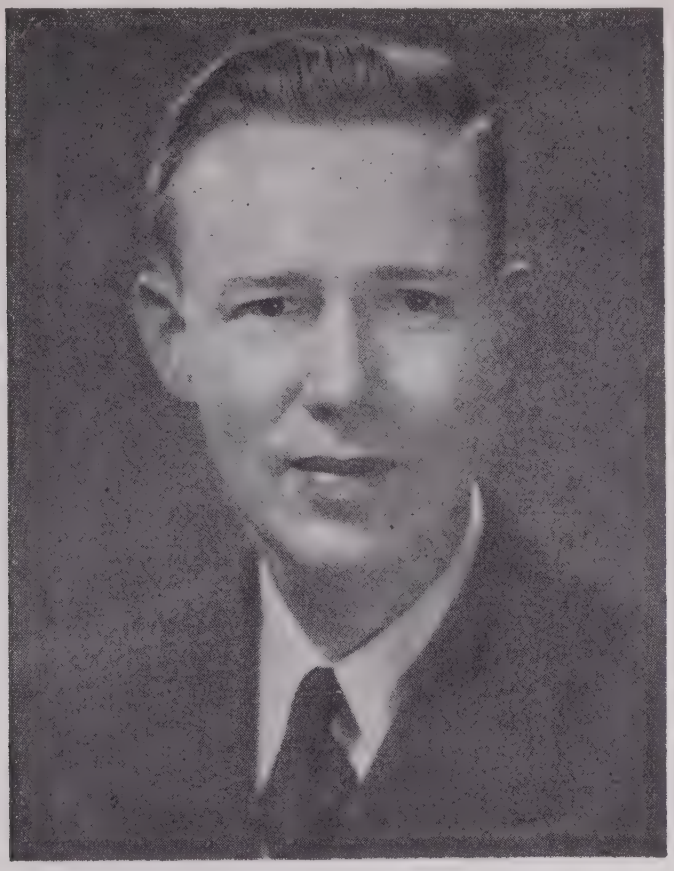

Henry I. Metz

Chairman, Indianapolis Section, 1944–1947

Henry I. Metz was born August 17, 1904, in Pittsburgh, Pennsylvania. He received the B.S. degree in electrical engineering from the University of Pittsburgh in 1927.

Mr. Metz joined Westinghouse Electric Manufacturing Corporation in 1925 through a co-operative training program, and in 1927 was transferred to the company's radio division in Chicopee Falls, Mass. There, he supervised the development, intercompany co-ordination, and manufacturing engineering of speech-input equipment. He was also placed in charge of the division's publicity and technical information.

In March, 1935, Mr. Metz went to the Bureau of Air Commerce (now Civil Aeronautics Administration) in Washington, D. C., where he handled the development of radio markers and instrument landing systems. He was transferred to Indianapolis in 1939 for the installation and testing of the first C.A.A. consolidated instrument landing system. The C.A.A. Experimental Station at Indianapolis was opened, and from 1942 to 1946 Mr. Metz was in charge of these laboratories as chief of the station. In 1946 he became chief of the radar section of the C.A.A.'s consolidated Technical Development Services. During October of that year he was coordinator for the ten-day demonstration of air navigation developments for the Provisional International Civil Aviation Organization assembly at Indianapolis. In March, 1947, Mr. Metz was appointed superintendent of communications for the C.A.A. second region, covering the southeastern states and with headquarters in Atlanta. He directs the region's program for conversion of C.A.A. airways facilities to v.h.f. and the adaption of omniranges, instrument-landing, and radar to civil aviation. Overseas airways radio teletype stations at Miami, Bermuda, and San Juan are maintained by his staff.

Mr. Metz joined The Institute of Radio Engineers in 1938 as an Associate and became a Senior Member in 1946. During his chairmanship, the Indianapolis Section became a charter member of the Indianapolis Technical Societies Council which was formed in 1945. Mr. Metz became president of the Council in 1946.

Officials of a government which is truly democratic in its guiding principles must be fully determined to represent not one special group or interest but rather the best interests of *all* the people. Their task accordingly requires broadness of outlook, honesty of purpose, a judicial temperament, absence of striving for power for its own sake, and a wide fund of knowledge of current events and underlying trends. Some of these basic requirements are effectively discussed in the following illuminating guest editorial by a prominent radio-engineering consultant, who was as well Chief Engineer of the Federal Communications Commission, and is Vice-Chairman of the Washington Section of the Institute.—*The Editor.*

Government and Industry

GEORGE P. ADAIR

Too often and too long we have used and heard used the expression, "Government versus Industry." In court controversies that is correct phraseology, but except for specific and limited points where there is a difference of opinion the government is not against industry nor is industry against government. Industry and government are both essential parts of our nation and neither can function properly without the other. It must be "Industry and Government," each performing its own responsibilities.

As it was possible to win the war only by full co-operation between government and industry, it will be possible to win the peace and continued prosperity only by full and continued co-operation. Only by a full understanding of each other's problems, limitations, and facilities can the best results flow. Since in the communications and electronics fields most of these mututal problems arise from technical considerations, particularly spectrum space and its proper utilization, the burden and privilege of responsibility fall largely upon the engineers of both government and industry. They are the liaison between government and industry; they hold the key to proper regulation, both technical and non-technical. With adequate and proper technical facilities, competition and the public's good taste would appear to render the need of other regulation negligible.

Engineers of both must mix freely, both formally and informally, to establish and maintain this liaison which is the only way the desired result, industry growth in all phases in the public interest, can be obtained. The government engineer cannot sit in his ivory tower and devise regulations or propound engineering decisions that make any sense. The technical developments and the problems of the industry are changing too rapidly. He must have day-to-day first-hand knowledge. Valuable information can, of course, be obtained through the trade journals, but far more than this is required. It is only natural that much of such information is either too general or too specific to be applied without interpolations or extrapolations which often result in very erroneous conclusions. It is the duty of the industry engineer to be the liaison, making sure of the flow of up-to-the-minute, accurate information on one hand; and on the other hand assisting in making sure that the regulations and decisions that result are the best obtainable.

The radio industry in all its branches is highly competitive, which is a healthy situation indeed, but which makes the problems of regulation most difficult at best. A ruling for one company is a ruling against another; spectrum space assigned to one is lost by another. This makes it doubly important that full and proper liaison be maintained. Fortunately, but as would be expected, with few exceptions industry engineers have given accurate information to the best of their ability, and government engineers have done their best to apply this information with judgment and integrity. Biased and half-truth information and testimony is worse than none, and is usually easily spotted and is given its due weight and consideration. On the other side of the fence, the government engineer with a "bureaucratic" attitude, making regulations simply to make regulations, is as much a traitor to his trust as if he were actually dishonest. Regulations should serve a definite purpose in the public interest or should be abolished.

Competition, ability, imagination, ingenuity, integrity, and co-operation are the fundamentals of a great industry under proper regulation. A good measure of all these has been demonstrated in Communications. I urge only that each realize his privilege and responsibility as a liaison member. In this way alone can the use of technological developments be regulated and guided to harvest the fullest benefits and prevent their use for destructive purposes.

The Electronic Research Sponsored by the Office of Naval Research*

E. R. PIORE†, SENIOR MEMBER, I.R.E.

Summary—**A survey is given of the research being sponsored by the electronics branch of the Physical Sciences Division of the Office of Naval Research. The philosophy from which the electronics program evolves is presented.**

Introduction

THE OFFICE of Naval Research has been supporting basic research in educational institutions and some commercial companies. The Research Group is the agency within the Office of Naval Research (ONR) which has been performing this function.

This paper is a report on the electronic aspects of the program. It is my purpose here to give you the background of the thinking that evolved the electronic program, so that we may have a common coordinate system or point of reference for an evaluation of the program.

The motivation for the support of basic research is national welfare, with the realization that national scientific health or well-being, will reflect itself directly in naval technical growth. The emphasis of this program is naturally placed at universities, the traditional source of basic knowledge and the source of technical manpower. Part of the mission of the program is to alleviate the critical shortage of technical manpower.

The actual program, in the ultimate analysis, is evolved in the laboratories. The research worker is the man most competent to determine or formulate the program. ONR does mold it, of necessity, because the available funds are limited. However, the program is constructed on the basis of the composite thinking in the country's laboratories. The scientist is invited to submit his proposed research problems to ONR. It is not the policy to present a list of projects and state that these are the ones that will be supported.

Definition of Electronics

To evolve a basic research program in any field, it is necessary to define the field. Very broadly, it can be stated that electronics covers the production and control of radio waves, or electromagnetic radiation (specifying some limits as to frequency or wavelength) and the study and control of the motion of charged particles. Although the motion of charged particles is the very heart of electronics, it is necessary to restrict the latter field and exclude chemistry and quantum mechanics. The boundary cannot be defined in detail.

Although the emphasis in electronic research of necessity must be placed on radio and vacuum tubes, it is well to point out that other fields of science directly determined the direction that electronic research could take in the past. If electronics is to grow and prosper there must be basic research in properties of matter.

The role of other fields can be best indicated by a few examples. The thermionic cathode, which is the core of the vacuum tube and limits the realization of theoretical efficiency of the magnetron, requires the attention of the physicist, the chemist, and even the metallurgist. The luminescent material that coats the cathode-ray tube and makes it a useful instrument is developed by the combined effort of the physicist and the chemist. The electronic specialists must rely on the physicist, chemist, and metallurgist for research that will extend the electronic art in the use of capacitors, high-frequency cables, and new types of core materials for inductors. Even the mathematician is making a direct contribution through the current activities in analogue and digital computers. When the growth of electronics is examined historically, immediately evident is the large role played by other basic scientific fields in this growth. Langmuir and Dushman are chemists. Hull, Tuve, Breit, and DuBridge are physicists.

Thus, in planning any program, it is necessary to maintain a balance between direct support in electronics and these bordering fields of scientific research which will have direct impact on electronics. The study of the properties of matter as it affects the future growth of electronics requires encouragement.

The Division of Electronics

For planning purposes the field of electronics has been divided into five major categories. These divisions are propagation, the interaction of radio radiation and matter, components and the physics of components, systems research, and instrumentation.

Let me review some selected problems in these various fields. The selection is arbitrary, with little emphasis on conventional lines of research such as circuit theory and analysis. I should like to stress that these problems had their origin in the laboratories reviewed. I shall occasionally indicate the institutions that are conducting the research. I shall not be able to cover all the tasks nor all the institutions receiving ONR support in electronics.

Where appropriate, I shall emphasize the deficiencies in the over-all program. The cause of these deficiencies is hard to analyze. Some problems are too difficult. Some lack the necessary appeal to research workers, and others require a new fundamental approach.

Through the war years emphasis naturally was placed on the development of equipment to meet specific military requirements. As a result, two apparently opposite tendencies occurred simultaneously: (a) the dormant character of basic research in that period and (b) the creation of new tools for research. Thus, in reviewing the current research activities, one finds a renewed effort in problems that were dormant and the utilization of the newly created tools to push back the borders of science.

In preparing a review of this type, one is struck with the tremendous impact of electronics on other fields of science.

Propagation

The emphasis in propagation since the end of the war demonstrates the following tendencies: (a) the use of newly-created tools; (b) a renewed attack on old problems; and (c) the contribution of electronics to other fields, specifically astronomy and meteorology.

The field that has received recently a great deal of emphasis, especially in the British Empire, is the study of radiation from stellar space and celestial bodies. One can get the magnitude of the activity by thumbing through last year's issue of *Nature*. In this country work has just been started in this field, with emphasis on radiation from the sun rather than noise from stellar space. Southworth[1,2] has measured radiation from the sun in the microwave region, and found that the radiation in terms of a black body corresponds to temperatures of 20,000° K. Reber[3] using 480 Mc. found that the temperature at that frequency, in terms of a black body, corresponds to 10°K. The optical measurements assign a temperature of 6000°K. Both Saha[4] and Martyn[5] deal with the origin and the source of the radio radiation in the sun's atmosphere, and the sun proper, as a function of frequency. In general, the experimental behavior fits the theoretical consideration. However, experimentation must be pushed with narrower and narrower beams, so that, at least in the microwave region, the antenna can resolve the larger sun spots. This will give valuable data to astronomers and at the same time may permit better prediction of propagation on conventional wavelengths. To encourage research in this field, the

* Decimal Classification: R563×R010. Original manuscript received by the Institute, June 23, 1947. This work was carried on by the Planning Division, Office of Naval Research, Washington, D. C. Presented, 1947 I.R.E. National Convention, March 6, 1947, New York, N. Y.

† Research Group, Office of Naval Research, Washington 25, D. C.

[1] G. C. Southworth, "Microwave radiation from the sun," *Jour. Frank. Inst.*, vol. 239, pp. 285–298; April, 1945.

[2] G. C. Southworth, "Microwave radiation from the sun," *Jour. Frank. Inst.*, vol. 241, p. 231; March, 1946.

[3] G. Reber, "Solar radiation at 480 Mc/s.," *Nature* (London), vol. 158, p. 945; December 28, 1946.

[4] M. N. Saha, "Conditions of escape of radio-frequency energy from suns and the stars," *Nature* (London), vol. 158, p. 549; October 9, 1946.

[5] D. F. Martyn, "Temperature radiation from the quiet sun in radio spectra," *Nature* (London), vol. 158, pp. 632–633; November 2, 1946.

Office of Naval Research is supporting research at Cornell University.

As we drop millions of miles toward the earth, we come to the well-known F and E layers. The studies of the interaction of these layers with radio radiation is being continued in many places. The principal governmental agency in this field is the Central Radio Propagation Laboratory of the National Bureau of Standards. Work in this field is being sponsored by this office at the Cruft Laboratories at Harvard University and at Cosmic Terrestrial Laboratory at the Massachusetts Institute of Technology. Resuming a program that was discontinued during the war, meteors have proven to be a powerful tool in supplying data on ionized layers. Recent papers on this subject can be found in the *Physical Review*—one by J. A. Pierce[6] of Cruft Laboratory and another by a group from Stanford University.[7] Here again electronics can supply useful instrumentation to astronomers interested in meteors.

As we further descend through our atmosphere we come to clouds, motions of air masses, and all the associated thermodynamic and statistical mechanical problems. High-frequency radar has been able to detect clouds, typhoons, and various types of discontinuities in the atmosphere. These studies currently are qualitative in nature. The available meteorological data are either not sufficient in detail or not proper in character to give this general field a quantitative approach not get it out of the descriptive stage. The development on the quantitative approach level will be useful not only in propagation studies but also in meteorology.

Another problem in propagation that relies on meteorological data for the interpretation of results is the existence of transmission paths beyond the radio horizon when there is a temperature inversion in the atmosphere. The measurement of the angle-of-arrival is a method that studies the deviation of the path from normal conditions. The most recent publication in this field, in this country, comes from the Bell Telephone Laboratories.[8,9]

This effect is of prime importance to all users of narrow-beam microwave radiation. The Office of Naval Research has continued to sponsor this work at the University of Texas. One will find here, again, that the meteorological data may not be sufficiently fine-grain to permit detailed interpretation of results.

These few examples indicate the obvious conclusion that progress in propagation research will rely more and more on cross-fertilization of this field with astronomy and meteorology.

The attenuation of radiation by the atmospheric gases is included under the subdivision of interaction of radiation and matter. Propagation actually is the study of interaction of radiation and matter. The division is made on the basis of techniques and where the experiments are performed. In one case you are stuck in the laboratory; in the other case you must be an outdoor man.

Interaction of Radiation and Matter

The tremendous increase of activity in this field is due to the development of microwave techniques. The war trained many people in the manipulation of microwave techniques and circuits. Let us examine the type of information that can be obtained with radio radiation in the study of the properties of matter. There are three approaches: energy, frequency, and wavelength; and they are fundamentally the same.

Using the energy relative $E=h\nu$, one finds that microwaves correspond to approximately 0.001 electron volt, which is of same order of magnitude as room temperature. Energies of this order of magnitude appear in atoms in the coupling of the nuclear and electron spins. A method of tremendous resolution compared to optical spectroscopy is available for the study of hyperfine structure in atomic spectra and the determination of nuclear spin.

In the molecules, energies of vibration, rotation, and space inversion correspond to energies that can be reached by microwave radiation. A new tool is available to study moments of inertia, the contribution of various electric and magnetic moments of the molecules in the radiation processes, and because of the resolution inherent in the technique, isotope effects can be readily detected. A general review of this field before the war is contained in the *Review of Modern Physics*[10] Since the war the journals have had many papers in this field. Some of this type of research is being supported by ONR at Harvard, Massachusetts Institute of Technology, Yale, Stanford, and Princeton. It is too early to speculate and state in definite terms the impact that this research will have on electronics. One obvious result that can be made available in the immediate future is a frequency standard.

An instrument that would be of tremendous value in this work is a wideband spectroscope, so that large regions of the spectrum would appear simultaneously on some indicator—something analogous to the optical grating or prism spectroscope.

Another approach to radio radiation can be made in terms of frequency or accurate time pieces. Here again this technique was used to study nuclear spin and hyperfine structure separation. Rabi[11] and his student exploited this method. The oscillator is required to be at the same frequency as the Larmor frequency of procession of angular moment.

As a third approach, let us consider microwaves through the concept of length and, more specifically, length in terms of skin effect. Measurement of superconducting lead at 3 centimeters has been reported by a group from M.I.T.[12] The skin effect determines the penetration of the field. In this experiment, the Q of the cavity that contained the refrigerant was 2000 at room temperature and increase to 10^6 at 4°K. The skin effect can also be a powerful tool in studying domain size in ferromagnetism.[13] All of us appreciate the value of large Q in the microwave region. The ferromagnetic studies may permit the utilization of ferromagnetic materials at higher and higher frequences.

Properly the behavior of dielectrics as a function of frequency should be included here. However, since their use is so intimately tied in with components. they are grouped in that general category.

Components and the Physics of Components

Basic research in components covers all fields in science, and of necessity our activities have to be restricted. However, general goals can be set. These goals are high power, frequency extension, narrower- and wider-frequency components, higher reliability, greater flexibility, and components to perform new functions. A few selected topics will be discussed and the direction of the program indicated.

The basic components are resistors, inductors and capacitors. Nonlinear components have been very important in the extension of the electronic art. There has been a great deal of work on nonlinear resistance elements. The transformer, a nonlinear inductor, is known but has not been exploited to the fullest extent in this country. In this field, basic work is in progress at the Carnegie Institute of Technology, and more limited work at the Polytechnic Institute of Brooklyn, both under ONR sponsorship.

Nonlinear capacitors have received very little attention. Now it is possible to start work in this field. Shepard Roberts,[14] working at the Laboratory of Insulation Research, has submitted to M.I.T. a doctor's dissertation on barium titanate and barium-strontium titanate. Under certain conditions it displays nonlinear characteristics. Apart from the basic information that is obtained in understanding matter, the circuit designer acquires an additional degree of freedom.

The vacuum tube has equal importance in electronics to coils, capacitors, and resistors. ONR activities in this field have been restricted to projects that are basic in nature, are too long-range for the Bureaus or industry, or that are vital to a new field of science.

The history of the vacuum tube can be viewed through Maxwell's field equations. Langmuir and Childs, through the manipulation Div $D=\rho$, gave us the 3/2-power law. The study of transit-time phenomena placed

[6] J. A. Peirce, "Ionization by meteoric bombardment," *Phys. Rev.*, vol. 71, pp. 88–93; January 15, 1947.

[7] L. A. Manning, R. A. Helliwell, O. G. Villard, and W. E. Evans, Jr., "On the detection of meteors by radio," *Phys. Rev.*, vol. 70, p. 767; November 1 and 15, 1946.

[8] W. M. Sharpless, "Measurements of the angle of arrival of microwaves," Proc. I.R.E., vol. 34, pp. 845–848; November, 1946.

[9] A. B. Crawford and W. M. Sharpless, "Further observations of the angle of arrival of microwaves," Proc. I.R.E., vol. 34 pp. 845–848; November, 1946.

[10] J. B. M. Kellogg and S. Millman, "Molecular beam magnetic resonance method—the radio-frequency spectra of atoms and molecules," *Rev. Mod. Phys.*, vol. 18, pp. 323–352; July, 1946.

[11] I. I. Rabi, "Space quartization in a gyrating magnetic field," vol. 51, pp. 652–654; April 15, 1937.

[12] F. Bitter, J. B. Garrison, J. Halpern, E. Maxwell, J. C. Slater, and C. F. Squire, *Phys. Rev.*, vol. 70, p. 97; July 1 and 15, 1946.

[13] C. Kittel, "Theory of the structure of ferromagnetic domain in films and small particles," *Phys. Rev.*, vol. 70, pp. 965–971; December 1 and 15, 1946.

[14] S. Roberts, (Doctoral dissertation), Massachusetts Institute of Technology, 1946.

emphasis on the last term of Curl $H=i+\dot{D}^{\circ}$. The betatron operates on the base of $\dot{B}^{\circ}$ in Curl $E=\dot{B}^{\circ}$. It is a transformer with the electrons acting as the secondary. To date, the electronic industry has not developed any tube which has this last equation as its basis of operation. It would be interesting to exploit this thought.

The tube that may have the same effect on the future of the electronic art as the magnetron and klystron have had in the past is the travelling-wave tube, which was reported for the first time in this country by Pierce and Fields.[15,16] Although there are many patents on this device, it seems that the first careful experiments were performed by Kompfner.[17] Now and then there are indications that every industrial company is constructing a traveling-wave tube. In a tube of the klystron and the interaction between the electron beam and the electromagnetic fields occurs in a small region in a short time. In the traveling-wave tube, by having the beam and the field traveling at the same velocity, the region of interaction is extended. Basic studies on this tube are taking place at Stanford, M.I.T., and Harvard, and under ONR sponsorship.

The capabilities and limitations of the klystron and the magnetron are being studied at Yale, Stanford, and Harvard.

Another form of traveling-wave tube can be found in some linear accelerator.[18] A number are under construction to be used in nuclear research. The beam and field travel at the same velocity through a long tube. The beam extracts energy from the field and is thus accelerated. The activity in the linear accelerator is providing very-high-power sources at ultra-high frequency. Historically, there is a close connection between linear accelerators and high-power tubes. Before the war, the resnatron was initially conceived, as a power source for a linear accelerator by Sloane and Marshall at the University of California. The present activity through the country on linear accelerators will produce high-power sources of one form or another from 200 to 3000 Mc. Industry has limited use for this, and the educational institutions are in a position to bring radical ideas to bear on the problem.

In closing the gap between infrared and the microwave region, there is a need for power generators below 1 centimeter. The limit has been reached with present types of tubes. Inspiration is required to get practical generators as most of the present work is along conventional lines.

The core of vacuum tubes is the cathode. It may be a thermionic cathode or a cold second-electron-emission cathode. In many tubes the cathode limits the power output. The study of the solid state in its surface aspects is receiving very limited attention by the academic institutions. This field is important not only in the cathode development but also in the design of such devices as storage tubes which are becoming so important in electronic computers both of the analogue and digital type. A great deal of experimental work and theoretical speculation are required in this field before improvement in electronic gadgetry can be achieved.

Before concluding this section of the paper, let me mention two more topics which would give valuable information and extend the electronic art but which have been receiving limited attention: (a) discharge in gases, especially in the microwave region; and (b) general microwave plumbing problems, such as wideband plumbing and plumbing that will take greater and greater power as the frequency is increased. If wideband plumbing can be evolved, a partial solution to the spectroscope may be a by-product.

The discussion has not touched on circuit analysis, nor signal and electron dynamics. There is a great deal of work in these fields, but I think most of you are familiar with the work, and one must make arbitrary omissions.

Systems

With the knowledge of propagation, the interaction of radiation and matter, and the components readily available, one is prepared to design the electronic system.

The whole purpose, or goal, of basic research in a field such as electronics, which is essentially an engineering field, is to have available all the parameters to permit the selection of the best frequency; to perform certain operations with the knowledge of the limitations imposed by nature on our physical universe, the limitations imposed by the state of the art; and finally, the limitations imposed by man, the rate of human reactions, the physiological processes and the like.

Let us speculate. The air navigation and traffic control problem is of major importance. The results of basic research should enable us to lock a group of engineers in a large room, give them the operation requirements, all the data from basic research, and have the engineers come out with the design of a complete system that solves the problem. The system would be aware of every aircraft in the air, would through data made available by computers, give automatic instructions to the aircraft to maintain schedule and avoid collision. The men on the ground and the pilot would only monitor instruments.

This type of speculation clearly indicates the tremendous fields that require the attention of basic research activity. In any system, even of limited complexity, we are always forced to determine the design parameters *a posteriori*.

Within the Navy, the bureau's construct systems, CNO evaluates them, the Fleet uses them, and ONR merely analyzes, studies, and sponsors basic research to extend them. Some of the work that is being encouraged through ONR support is: (a) research in direction finders at the University of Illinois, (b) wideband oscillators at Stanford, and (c) stabilizing microwave systems at M.I.T. and Harvard. The results will be useful not only for communications but also in the laboratories using microwave technique. Other institutions are concerned with signal, large and small: frequency modulation, pulse, and amplitude modulation as they travel through various types of networks.

A problem of some interest is the actual bandwidth required to transmit a specific quantity of information per second.

Instruments

The field of instrumentation is part of the design of systems. Personnel working in electronics design a variety of instruments not only for their own use but also for use in other scientific fields. A typical example is the electron microscope. Once the design is completed and the theoretical resolution attained, the electronist has no use for his instrument.

In supporting work in this field, it is necessary to confine one's enthusiasm. All the instruments in nuclear physics, from the big machines to the small counters, are electronic instruments. Certain nuclear machinery has been supported, such as linear accelerator. The motivation for this support was principally electronic. The interesting problems in the linear accelerator are a group of high-power sources operating in parallel, the study of power in a waveguide, the geometric retention of an electron beam through a long path, and possible interaction of high-speed electron beam and the field. Other instruments that have been supported are the high-speed oscilloscopes, spectrophotometers, and computers.

In conclusion, I would like to state that there is no implied criticism in the omission of any project or institution. Omissions were made in the accepted fields in electronics, but it was my desire to give some indication of the breadth of the electronic field.

The Research Laboratory of Electronics at M.I.T. is partially supported through a Signal Corps Contract by the Signal Corps, ONR, and the Air Matériel Command. The Cruft Laboratory at Harvard, and the Laboratory for Insulation Research at M.I.T. are partially supported through an ONR contract by the Signal Corps and ONR.

[15] J. R. Pierce and L. Field, "Traveling-wave tubes," Proc. I.R.E., vol. 35, pp. 108–111; February, 1947.

[16] J. R. Pierce, "Theory of the beam-type traveling-wave tube," Proc. I.R.E., vol. 35, pp. 111–123; February, 1947.

[17] R. Kompfner, "The traveling-wave tube as amplifier at microwaves," Proc. I.R.E., vol. 35, pp. 124–128; February, 1947.

[18] J. C. Slater, "The design of linear accelerators," New York Meeting, American Physical Society, September, 1946.

Radio Propagation at Frequencies Above 30 Megacycles*

KENNETH BULLINGTON†, ASSOCIATE, I.R.E.

Summary—Radio propagation is affected by many factors, including the frequency, distance, antenna heights, curvature of the earth, atmospheric conditions, and the presence of hills and buildings. The influence of each of these factors at frequencies above about 30 megacycles is discussed, with most of the quantitative data being presented in a series of nomograms. By means of three or four of these charts, an estimate of the received power and the received field intensity for a given point-to-point radio transmission path ordinarily can be obtained in a minute or less.

The theory of propagation over a smooth spherical earth is presented in a simplified form that is made possible by restricting the frequency range to above about 30 megacycles, where variations in the electrical constants of the earth have only a secondary effect. The empirical methods used in estimating the effects of hills and buildings and of atmospheric refraction are compared with experimental data on shadow losses and on fading ranges.

I. Introduction

METHODS of calculating ground-wave propagation over a smooth spherical earth have been given by Burrows and Gray and by Norton for all values of distance, frequency, antenna height, and ground constants.[1,2] These two methods are different in form but they give essentially the same results. Both methods are relatively simple to use at the lower frequencies where grounded antennas are in common use, but their complexity increases as the frequency increases. At frequencies above 30 or 40 megacycles, elevated antennas are in common use, and the radio path loss between two horizontal antennas tends to be equal to the loss between two vertical antennas. In addition, both types of transmission tend to be independent of the electrical constants of the ground, so that considerable simplification is possible. This paper presents a series of nomograms which have been found useful in solving radio propagation problems in the very-high-frequency range and above. These charts are arranged so that radio transmission can be expressed in terms of either the received field intensity or the received power delivered to a matched receiver. The field-intensity concept may be more familiar, but the power-transfer concept becomes more convenient as the frequency is increased.

In addition to the smooth-earth theory, an approximate method is included for estimating the effects of hills and other obstructions in the radio path. The phenomena of atmospheric refraction (bending away from straight-line propagation), atmospheric ducts (tropospheric propagation), and atmospheric absorption are discussed briefly, but the principal purpose is to provide simplified charts for predicting radio propagation under average weather conditions. It is expected that, normally, the nomograms will provide the desired answer directly without any additional computation, except the addition of the decibel values obtained from three or four individual charts. The basic formulas are presented as an aid to understanding the principles involved and as a more accurate method, should one be required. This paper does not consider sky-wave propagation, although ionospheric reflections may occur at frequencies above 30 megacycles and may cause occasional long-distance interference between systems operating on the same frequency.[3]

A convenient starting point for the theory of radio propagation is the condition of two antennas in free space, which is discussed in terms of both received field intensity and received power. Since most radio paths cannot be considered to be free-space paths, the next step is to determine the effect of a perfectly flat earth, and this is followed by the effect of the curvature of the earth. After the basic smooth-earth theory is completed, there is a discussion of the variations in received power caused by atmospheric conditions and by irregularities on the earth surface, but the methods used in predicting these factors are necessarily less exact than the data for a smooth spherical earth in a uniform atmosphere.

II. Free-Space Field

A free-space transmission path is a straight-line path in a vacuum or in an ideal atmosphere, and sufficiently removed from all objects that might absorb or reflect radio energy. The free-space field intensity E_0 at a distance d meters from the transmitting antenna is given by

$$E_0 = \frac{\sqrt{30 g_1 P_1}}{d} \text{ volts per meter} \qquad (1)$$

where P_1 is the radiated power in watts and g_1 is the power-gain ratio of the transmitting antenna. The subscript $_1$ refers to the transmitter and the subscript $_2$ will refer to the receiver. For an ideal (isotropic) antenna that radiates power uniformly in all directions, $g=1$. For any balanced antenna in free space (or located more than a quarter-wavelength above the ground), g is the power-gain ratio of the antenna relative to the isotropic antenna. A small doublet or dipole whose over-all physical length is short compared with a half-wavelength has a directivity gain of $g=1.5$ (1.76 decibels) and a half-

* Decimal classification: R112×R113. Original manuscript received by the Institute, October 23, 1946; revised manuscript received, December 23, 1946.

† Bell Telephone Laboratories, Inc., New York, N. Y.

[1] C. R. Burrows and M. C. Gray, "The effect of earth's curvature on ground-wave propagation," PROC. I.R.E., vol. 29, pp. 16–24; January, 1941.

[2] K. A. Norton, "The calculation of ground-wave field intensities over a finitely conducting spherical earth," PROC. I.R.E., vol. 29, pp. 623–639; December, 1941.

[3] E. W. Allen, "Very-high-frequency and ultra-high-frequency signal ranges as limited by noise and co-channel interference," PROC. I.R.E., vol. 35, pp. 128–136; February, 1947.

wave dipole has a gain of $g=1.64$ (2.15 decibels) in the direction of maximum radiation. In other directions of transmission the field is reduced in accordance with the free-space antenna pattern obtained from theory or measurement. Consequently, the free-space field intensity in a direction perpendicular to a half-wave dipole is

$$E_0 = \sqrt{\frac{30 \times 1.64 P_1}{d}} \sim 7\sqrt{\frac{P_1}{d}}. \qquad (2)$$

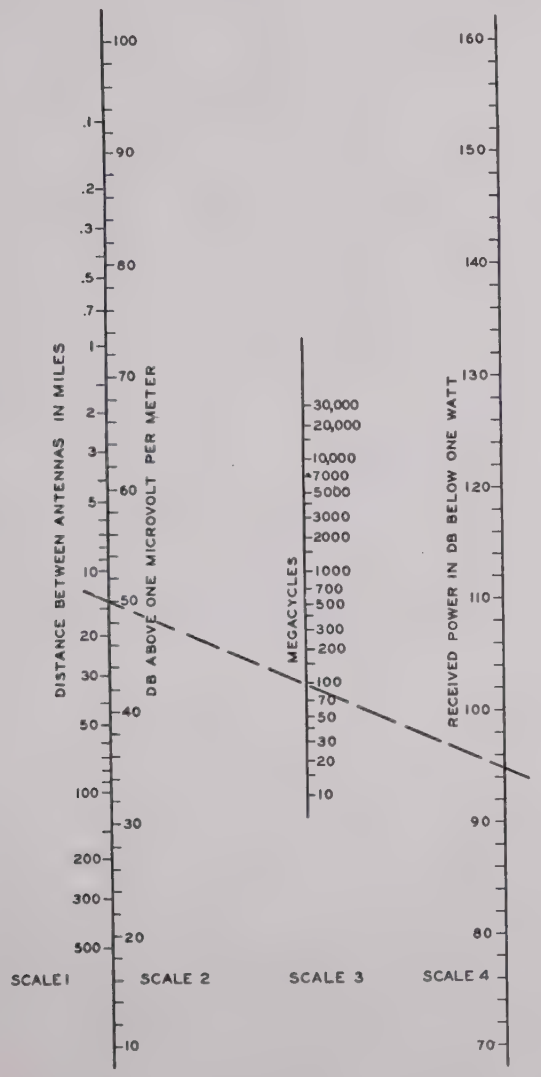

Fig. 1—Free-space field intensity and received power between half-wave dipoles, 1 watt radiated.

This field intensity in microvolts per meter for 1 watt of radiated power is shown on scale 2 of Fig. 1 as a function of the distance in miles shown on scale 1. For radiated power of P watts, the correction factor to apply to the field intensity or power is 10 log P decibels. For example, the free-space field intensity at 100 miles from a half-wave dipole radiating 1 watt is 33 decibels above 1 microvolt per meter (about 45 microvolts per meter). When the radiated power is 50 watts (17 decibels above 1 watt), the received field intensity is 33+17 = 50 decibels above 1 microvolt per meter (about 315 microvolts per meter). It will be noted that the field intensity is related to the energy density of the radio wave at the receiving antenna, but is independent of the type of the receiving antenna.

The directivity gain of an array of n dipoles (sum of driven and parasitic elements) of optimum design is approximately equal to n times the gain of one dipole, although some allowance should be made for antenna power losses. The theoretical power-gain ratio of a horn, paraboloid, or lens antenna whose aperture has an area of B square meters is $g=4\pi B/\lambda^2$; however, the effective area is frequently taken as one-half to two-thirds of the actual area of the aperture to account for antenna inefficiencies.

III. Relation Between the Received Power and the Radiated Power

Before discussing the modifications in the free-space field that result from the presence of the earth, it is convenient to show the relation between the received field intensity (which is not necessarily equal to the free-space field intensity) and the power that is available to the receiver. The maximum useful power P_2 that can be delivered to a matched receiver is given by

$$P_2 = \left(\frac{E\lambda}{2\pi}\right)^2 \frac{g_2}{120} \text{ watts} \qquad (3)$$

where

E = received field intensity in volts per meter
λ = wavelength in meters = $300/F$
F = frequency in megacycles
g_2 = power-gain ratio of the receiving antenna.

This relation between received power and the received field intensity is shown by scales 2, 3, and 4 in Fig. 1 for a half-wave dipole. For example, the maximum useful power at 100 megacycles that can be picked up by a half-wave dipole in a field of 50 decibels above 1 microvolt per meter is 95 decibels below 1 watt.

A general relation for the ratio of the received power to the radiated power obtained from (1) and (3) is

$$\frac{P_2}{P_1} = \left(\frac{\lambda}{4\pi d}\right)^2 g_1 g_2 \left(\frac{E}{E_0}\right)^2. \qquad (4)$$

When both antennas are half-wave dipoles, the power-transfer ratio is

$$\frac{P_2}{P_1} = \left(\frac{1.64\lambda}{4\pi d}\right)^2 \left(\frac{E}{E_0}\right)^2 = \left(\frac{0.13\lambda}{d}\right)^2 \left(\frac{E}{E_0}\right)^2 \qquad (4a)$$

and is shown on Fig. 1 for free-space transmission ($E/E_0=1$).

When the antennas are horns, paraboloids, or multi-element arrays, a more convenient expression for the ratio of the received power to the radiated power is given by

$$\frac{P_2}{P_1} = \frac{A_1 A_2}{(\lambda d)^2} \left(\frac{E}{E_0}\right)^2 \qquad (4b)$$

where B_1 and B_2 are the effective areas of the transmitting and receiving antennas, respectively. This relation is obtained from (4) by substituting $g=4\pi B/\lambda^2$, and is shown on Fig. 2 for free-space transmission when $B_1=B_2$. For example, the free-space loss at 4000 megacycles between two antennas of 10 square feet effective area is about 72 decibels for a distance of 30 miles.

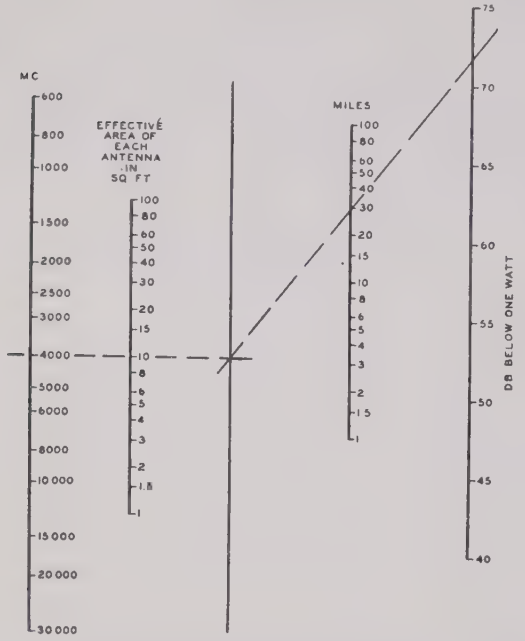

Fig. 2—Received power in free space between two antennas of equal effective areas, 1 watt radiated.

IV. Transmission Over Plane Earth

The presence of the ground modifies the generation and the propagation of the radio waves so that the received field intensity is ordinarily less than would be expected in free space. The ground acts as a partial reflector and as a partial absorber, and both of these properties affect the distribution of energy in the region above the earth. The principal effect of plane earth on the propagation of radio waves is indicated by the following equation:[4,5]

$$E = E_0[1 + Re^{j\Delta} + (1-R)Ae^{j\Delta} + \cdots]. \qquad (5)$$

(Direct Wave; Reflected Wave; Surface Wave; Induction Field and Secondary Effects of the Ground)

R is the reflection coefficient of the ground and is approximately equal to -1 when the angle θ between the reflected ray and the ground is small. The commonly used concept of a *perfectly conducting* earth, for which the reflection coefficient for vertical polarization is $+1$ for any angle of incidence, may cause some misunderstanding at this point. In practice, the principal interest is in low angles, and as the angle θ approaches zero the reflection coefficient approaches -1 for any finite value for the conductivity of the earth, even if it were made of solid copper. The magnitude and phase of the reflection coefficient can be computed from the following equation:[6]

$$R = \frac{\sin\theta - z}{\sin\theta + z} \qquad (6)$$

where

$z=\sqrt{\epsilon_0-\cos^2\theta}/\epsilon_0$ for vertical polarization
$z=\sqrt{\epsilon_0-\cos^2\theta}$ for horizontal polarization
$\epsilon_0=\epsilon-j60\sigma\lambda$
ϵ = dielectric constant of the ground relative to unity in free space
σ = conductivity of the ground in mhos per meter
λ = wavelength in meters
$j=\sqrt{-1}$
$e^{j\Delta}=\cos\Delta+j\sin\Delta$.

The quantity A is the surface-wave attenuation factor which depends upon the frequency, ground constants, and type of polarization. It is never greater than unity and decreases with increasing distance and frequency, as indicated by the following approximate equation:[7]

$$A \simeq \frac{-1}{1+j\dfrac{2\pi d}{\lambda}(\sin\theta+z)^2}. \qquad (7)$$

[4] Charles R. Burrows, "Radio propagation over plane earth-field strength curves," *Bell Sys. Tech. Jour.*, vol. 16, pp. 45–75; January, 1947.

[5] Kenneth A. Norton, "The propagation of radio waves over the surface of the earth and in the upper atmosphere, part II," Proc. I.R.E., vol. 25, pp. 1203–1236; September, 1937.

[6] It will be noted that for vertical polarization this expression agrees with the data given by Burrows and subsequently included in Terman's "Radio Engineer's Handbook," p. 699, first edition, but for horizontal polarization it is the negative of that given in these references. This change was necessary in order to make equations (5) and (6) independent of polarization. The pseudo-Brewster angle frequently mentioned in the literature occurs when the reflection coefficient is a minimum and is approximately equal to the value of θ for which $\sin\theta=|z|$; this occurs with vertical polarization only, since $z>1$ for horizontal polarization. The reflection coefficient is sometimes modified by a divergence factor to give a first approximation of the effect of the curvature of the earth, but this additional complication does not seem essential here. The effect of the curvature of the earth is discussed in the next section, and for conditions of frequency and antenna height where some interpolation is required, the possible variations due to atmospheric conditions are usually greater than the error introduced by the omission of the divergence factor. The measured data on the plane-earth reflection coefficient agrees reasonably well with the theoretical values at frequencies below about 1000 megacycles. At higher frequencies the magnitude of the reflection coefficient is sometimes less than 1, presumably due to multiple reflections from the irregularities on the earth's surface. Measured values as low as -0.2 at 10,000 megacycles over rolling country have been reported by W. M. Sharpless. The low value of reflection coefficient is not expected to be important for ground-to-ground transmission, but it tends to smooth the lobes that occur in high-angle radiation and, hence, may be important in air-to-ground transmission.

[7] This approximate expression is sufficiently accurate as long as $A<0.1$, and it gives the magnitude of A within about 2 decibels for all values of A. However, as A approaches unity, the error in phase approaches 180 degrees. More accurate values are given by Norton, where in his nomenclature $A=f(P,B)e^{i\Phi}$.

The angle Δ used in (5) is the phase difference in radians resulting from the difference in the length of the direct and reflected rays. It is equal to $4\pi h_1 h_2/\lambda d$ radians, when the distance d between antennas is greater than about five times the sum of the two antenna heights h_1 and h_2.

The effect of the ground shown in (5) indicates that ground-wave propagation may be considered to be the sum of three principal terms; namely, the direct wave, reflected wave, and surface wave. The first two types correspond to our common experience with visible light, but the surface wave is less familiar. Since the earth is not a perfect reflector, some energy is transmitted into the ground and is absorbed. As this energy enters the ground, it sets up ground currents, which is another way of saying that the distribution of the electromagnetic field in the region near the surface of the earth is distorted relative to what it would have been over an ideal perfectly reflecting surface. The surface wave is defined as the vertical electric field for vertical polarization, or the horizontal electric field for horizontal polarization, that is associated with these ground currents.[8] The practical importance of the surface wave is limited to a region above the ground of about 1 wavelength over land or 5 to 10 wavelengths over sea water, since for greater heights the sum of the direct and reflected waves is larger in magnitude. Thus the surface wave is the principal component of the total ground wave at frequencies less than a few megacycles, but it is of secondary importance in the very-high-frequency range (30 to 300 megacycles) and it usually can be neglected at frequencies above 300 megacycles.

A physical picture of the various components of the ground wave can be obtained from (5), but an equivalent expression which is more convenient for this discussion is

$$\frac{E}{E_0} = 2 \sin \frac{\Delta}{2} + j[(1 + R) + (1 - R)A]e^{j(\Delta/2)}. \qquad (8)$$

When the angle $\Delta = 4\pi h_1 h_2/\lambda d$ is greater than about 0.5 radian, the terms inside the brackets (which include the surface wave) are usually negligible, and a sufficiently accurate approximation is given by

$$\frac{E}{E_0} = 2 \sin \frac{2\pi h_1 h_2}{\lambda d}. \qquad (8a)$$

In this case the principal effect of the ground is to produce interference fringes or lobes so that the field intensity, at a given distance and for a given frequency, oscillates around the free-space field as either antenna height is increased.

When the angle Δ is less than about 0.5 radian, the receiving antenna is below the maximum of the first lobe and the surface wave may be important. A sufficiently accurate approximation for this condition is[9]

$$\left|\frac{E}{E_0}\right| = \left|\frac{4\pi h_1' h_2'}{\lambda d}\right|. \qquad (8b)$$

In this equation $h' = h + jh_0$ where h is the actual antenna height and $h_0 = \lambda/2\pi z$ has been designated as the minimum effective antenna height. The magnitude of the minimum effective height $|h_0|$ is shown in Fig. 3 for sea water and for "good" and "poor" soil. "Good" soil corresponds roughly to clay, loam, marsh, or swamp, while "poor" soil means rocky or sandy ground.

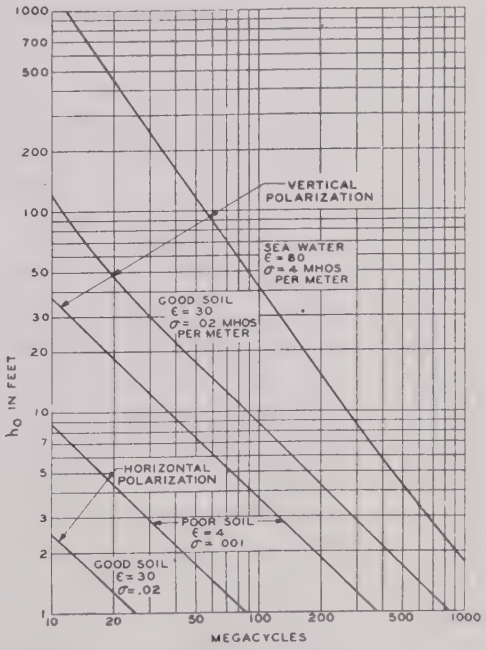

Fig. 3—Minimum effective height.

The surface wave is controlling for antenna heights less than the minimum effective height, and in this region the received field or power is not affected appreciably by changes in the antenna height. For antenna heights that are greater than the minimum effective height, the received field or power is increased approximately 6 decibels every time the antenna height is doubled until free-space transmission is reached. It is ordinarily sufficiently accurate to assume that h' is equal to the actual antenna height or the minimum effective antenna height, whichever is the larger.

The ratio of the received power to the radiated power

[8] Another component of the electric field associated with the ground currents is in the direction of propagation. It accounts for the success of the wave antenna at lower frequencies, but it is always smaller in magnitude than the surface wave as defined above. The components of the electric vector in three mutually perpendicular co-ordinates are given by Norton.

[9] This approximate expression is obtained from (8) by assuming:

$$\sin\theta = \frac{h_1 + h_2}{d} \ll z, \qquad (1)$$

$$\sin\frac{2\pi h_1 h_2}{\lambda d} = \frac{2\pi h_1 h_2}{\lambda d} \qquad (2)$$

$$A = -\frac{\lambda}{j2\pi d z^2}. \qquad (3)$$

for transmission over plane earth is obtained by substituting (8b) into (4), resulting in

$$\frac{P_2}{P_1} = \left(\frac{\lambda}{4\pi d}\right)^2 g_1 g_2 \left(\frac{4\pi h_1' h_2'}{\lambda d}\right)^2 = \left(\frac{h_1' h_2'}{d^2}\right)^2 g_1 g_2. \qquad (9)$$

This relation is independent of frequency, and is shown on Fig. 4 for half-wave dipoles ($g = 1.64$). A line through the two scales of antenna height determines a point on the unlabeled scale between them, and a second line through this point and the distance scale determines the

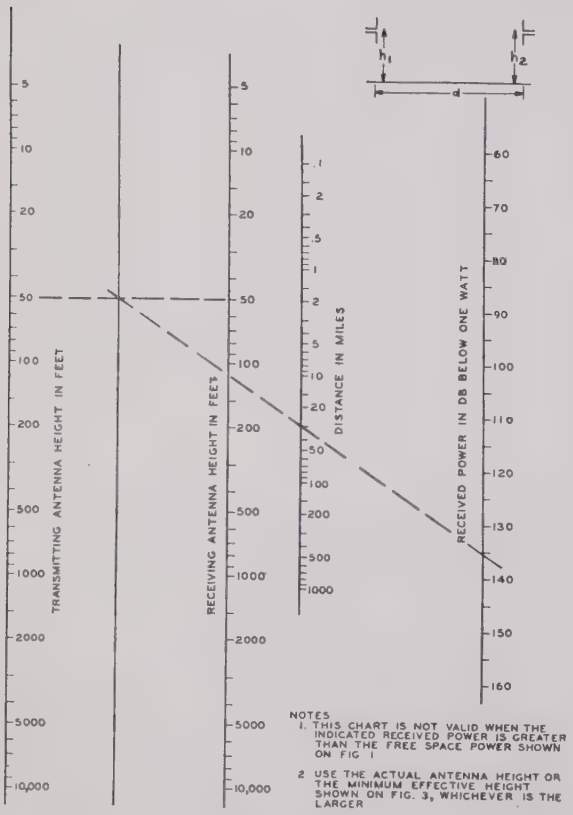

Fig. 4—Received power over plane earth between half-wave dipoles, 1 watt radiated.

received power for 1 watt radiated. When the received field intensity is desired, the power indicated on Fig. 4 can be transferred to scale 4 of Fig. 1, and a line through the frequency on scale 3 indicates the received field intensity on scale 2. The results shown on Fig. 4 are valid as long as the value of received power indicated is lower than shown on Fig. 1 for free-space transmission. When this condition is not met, it means that the angle Δ is too large for (8b) to be accurate and that the received field intensity or power oscillates around the free-space value as indicated by (8a).

As an example, consider a 250-watt, 30-megacycle transmitter with both transmitting and receiving dipoles mounted 50 feet above the ground and separated by a distance of 30 miles over *plane* earth. The transmission loss is shown on Fig. 4 to be 135.5 decibels. Since 250 watts is 24 decibels above 1 watt, the received power is $135.5 - 24 = 111.5$ decibels below 1 watt. (The free-space power transfer shown on Fig. 1 indicates a received power of $91 - 24 = 67$ decibels below 1 watt, so Fig. 4 is controlling.) The received field intensity can be obtained from Fig. 1, which shows that a received power of 111.5 decibels below 1 watt corresponds to a received field intensity of about 23 decibels above 1 microvolt per meter at a frequency of 30 megacycles. Should one antenna be only 10 feet above "good" soil, rather than 50 feet, the minimum effective height of 30 feet shown on Fig. 3 should be used on one of the height scales on Fig. 4 in determining the transmission loss. It will be noted that this example assumes a perfectly flat earth. The curvature of the earth introduces an additional loss of about 4 decibels, as discussed in the next section.

In addition to the effect of plane earth on the propagation of radio waves, the presence of the ground may affect the impedance of an antenna and thereby may have an effect on the generation and reception of radio waves. This effect usually can be neglected at frequencies above 30 megacycles, except where whip antennas are used. The impedance in the presence of the ground oscillates around the free-space value, but the variations are unimportant as long as the center of the antenna is more than a quarter-wavelength above the ground. A convenient method of showing the effect of the change in impedance of a balanced antenna near the ground is to replace the directivity gain g in the preceding formulas by the arbitrary factor of $g' = g/r$ where r is the ratio of the input resistance in the presence of the ground to the input resistance of the *same* antenna in free space. This assumes an impedance match between the antenna and the transmitting equipment with proper tuning to balance out any reactance.

For horizontal dipoles less than a quarter-wavelength above the ground, the ratio r is less than unity. It approaches zero as the antenna approaches a perfectly conducting earth, but in practice it does not reach zero at zero height because of the finite conductivity of the earth. The wave antenna and the top-loaded antenna frequently used at lower frequencies are sometimes called horizontal antennas, but since they are used to radiate or receive vertically polarized waves they are not horizontal antennas in the sense used here.

For vertical half-wave dipoles the factor r is approximately equal to unity, since the height of the center of the antenna can never be less than a quarter-wavelength above the ground. For very short vertical dipoles, however, the ratio r is greater than unity and it approaches a value of $r = 2$ for antennas very near to the ground. This means that, whereas a short vertical dipole whose total length $2l$ is small compared with the wavelength has an input radiation resistance of $80(\pi l/\lambda)^2$ ohms in free space, it has a resistance of $160\ (\pi l/\lambda)^2$ ohms near the ground.

Correct results for a vertical whip antenna working against a perfect counterpoise are obtained by using

$r=2$. This means that a vertical whip antenna of length l is 3 decibels less efficient than a dipole of length $2l$ (located more than a quarter-wavelength above the ground) for either transmitting or receiving. The poorer efficiency at the receiver is not important when external noise is controlling.

V. Diffraction Around the Curvature of the Earth

Radio waves are bent around the earth by the phenomenon of diffraction, with the ease of bending decreasing as the frequency increases. Diffraction is a fundamental property of wave motion, and in optics it is the correction to apply to geometrical optics (ray theory) to obtain the more accurate wave optics. In other words, all shadows are somewhat "fuzzy" on the edges and the transition from "light" to "dark" areas is gradual, rather than infinitely sharp. Our common experience is that light travels in straight lines and that shadows are sharp, but this is only because the diffraction effects for these very short wavelengths are too small to be noticed without the aid of special laboratory equipment. The

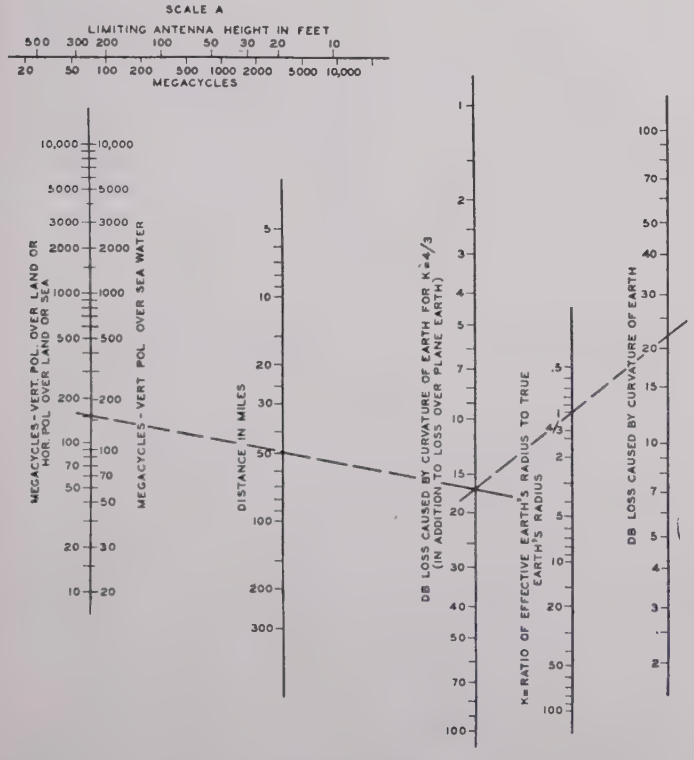

Fig. 5—Diffraction loss caused by curvature of the earth, assuming neither antenna height is higher than shown on scale A.

order of magnitude of the diffraction at radio frequencies may be obtained by recalling that a 1000-megacycle radio wave has about the same wavelength as a 1000-cycle sound wave in air, so that these two types of waves may be expected to bend around obstacles with approximately equal facility.

The effect of diffraction around the earth's curvature is to make possible transmission beyond the line-of-sight, but it introduces an additional loss. The magnitude of this loss increases as either the distance or the frequency is increased and it depends to some extent on the antenna height. The loss resulting from the curvature of the earth is indicated by Fig. 5 as long as neither antenna is higher than the limiting value shown at the top of the chart. This loss is in addition to the transmission loss over plane earth obtained from Fig. 4.

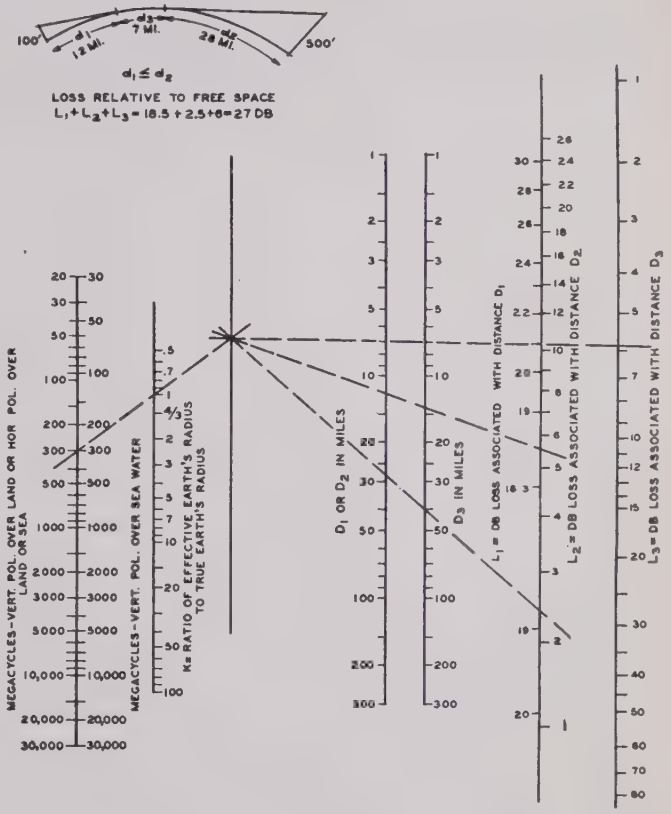

Fig. 6—Decibel loss relative to free-space transmission at points beyond line-of-sight over a smooth earth.

For example, at 150 megacycles, with antenna heights of less than 175 feet, the curvature of the earth in a 50-mile land path introduces a loss of 22 decibels (for $k=1$) in addition to the loss over plane earth. (The losses for $k=1$ are pure diffraction phenomena which would occur even in a vacuum. In the next section it will be shown that atmospheric refraction may cause a similar effect, although the cause is different. The parameter k is introduced to account for refraction in the earth's atmosphere, so that Fig. 5 shows the combined effects of diffraction and refraction.)

When either antenna is as much as twice as high as the limiting value shown on Fig. 5, this method of correcting for the curvature of the earth indicates a loss that is too great by about 2 decibels, with the error increasing as the antenna height increases. An alternate method of determining the effect of the earth's curvature is given by Fig. 6. This method is derived in the Appendix and is approximately correct for any antenna

height, but it is theoretically limited in distance to points at or beyond the line-of-sight, assuming that the curved earth is the only obstruction. Fig. 6 gives the loss relative to free-space transmission (and hence is used with Figs. 1 or 2) as a function of three distances: d_1 is the distance to the horizon from the *lower* antenna, d_2 is the distance to the horizon from the higher antenna, and d_3 is the distance beyond the line-of-sight. In other words, the total distance between antennas $d=d_1+d_2+d_3$. The distance to the horizon is shown in Fig. 7 for various values of k and antenna height. As an example,

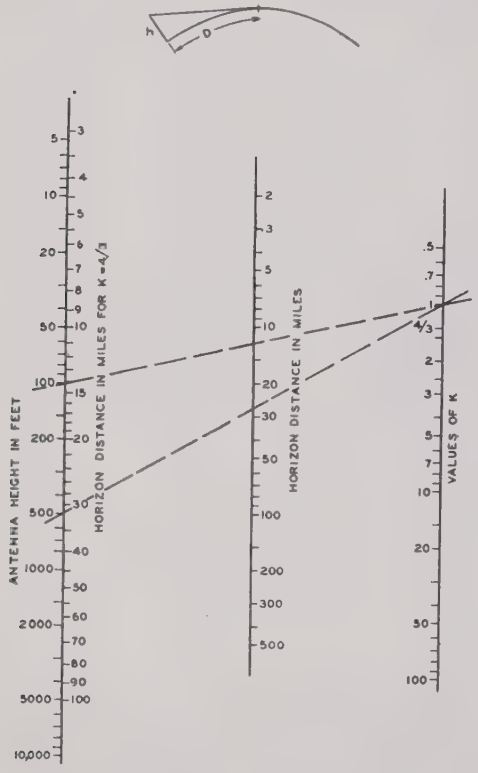

Fig. 7—Distance to the horizon.

consider a radio system operating at 300 megacycles over smooth earth with antenna heights of 500 and 100 feet. Fig. 7 indicates that $d_1=12$ miles and $d_2=28$ miles for a value of $k=1$. Table I shows the loss relative to free-space transmission, as obtained from Fig. 6, for various distances at and beyond the line-of-sight.

In Table I, the estimated received power at line-of-sight is 21 decibels less than would be expected in free space, and it decreases about 0.8 decibels for each mile beyond line-of-sight. At distances well within line-of-sight, the earth can be considered flat. There is no accurate method of joining the curve for points well within line-of-sight to the curve for points beyond line-of-sight, but one or both of the following empirical methods may be helpful. The data for flat earth, given in Fig. 4, can be used at distances near grazing, provided that each antenna height is interpreted as the height above an imaginary plane drawn tangent to the earth at the point of reflection. An alternate method is to use Fig. 6 at points near grazing by considering the loss L_3 to be negative whenever d_3 is negative. In either case, the estimated received power should not be greater than would be obtained over flat earth.

For more accurate results at and beyond the line-of-sight, the field intensity or received power computed by means of Fig. 6 should be increased by

$$10 \log \left[\frac{1}{\sqrt{2}} \left(1 + \frac{d_1}{d_2} + \frac{d_3}{d_2} \right) \right]$$

decibels as long as one antenna height is higher than the value shown on the top of Fig. 5. In the region of antenna heights where Fig. 5 is applicable, it is easier to use and more accurate than the data on Fig. 6.

TABLE I
SAMPLE COMPUTATIONS BEYOND LINE-OF-SIGHT
300 Megacycles—Antenna Heights, 500 and 100 Feet

Miles				Decibel Losses			Decibel Loss in Addition to the Free-Space Loss
d	d_1	d_2	d_3	L_1	L_2	L_3	
40	12	28	0	18.5	2.5	0	21
45	12	28	5	18.5	2.5	4	25
50	12	28	10	18.5	2.5	8.5	29.5
55	12	28	15	18.5	2.5	13.5	34.5
60	12	28	20	18.5	2.5	19	40
65	12	28	25	18.5	2.5	24	45

VI. Atmospheric Refraction and Absorption

Thus far it has been assumed that the radio waves are traveling through a vacuum, or through an ideal atmosphere which has a dielectric constant of unity at all points and has zero absorption. Actually, the dielectric constant of the air is slightly greater than 1 and is variable. It depends on the pressure and temperature of the air and on the amount of water vapor present, so that it varies with weather conditions and with the height above the ground. The change in dielectric constant in several thousand feet is never more than a few parts in ten thousand, but this variation is sufficient to have an appreciable effect on radio propagation.

Whenever the dielectric constant varies with the height above the ground, the path of a radio wave deviates from a straight line. This change in direction is called refraction. A general solution of the problem which would allow any possible distribution of dielectric constant with the height above the ground at any point along the radio path is virtually impossible because of a large number of variables involved, so some simplifying assumptions are needed in order to obtain an engineering solution. The first assumption usually made is that of horizontal stratification, which means that for any given height the dielectric constant has the

same value at all distances along the radio path. Typical solutions based on this assumption have been worked out, but the problem is still too complex for most applications. A simple engineering solution can be obtained by making the additional assumption that the dielectric constant is a linear function of the height. On this basis, the effect of atmospheric refraction can be included in the expression of diffraction around the smooth earth (without discarding the useful concept of straight-line propagation) by multiplying the actual earth's radius by

$$k = \frac{1}{1 + \frac{a}{2}\frac{\Delta\epsilon}{\Delta h}}$$

where a is the radius of the earth and $\Delta\epsilon$ is the change in dielectric constant in going from height h to $h+\Delta h$. Physically, the phenomenon of refraction is entirely separate from the concept of diffraction discussed in the preceding section, although for computational purposes the two effects are combined by introducing the parameter k in Figs. 5 and 6.

The dielectric constant normally decreases with increasing height ($k>1$) and the radio waves are bent toward the earth. However, under certain atmospheric conditions the dielectric constant may increase ($0<k<1$) over a reasonable height, thereby causing the radio waves in this region to bend away from the earth. Since the earth's radius is about 2.1×10^7 feet, a decrease in dielectric constant of only 2.4×10^{-8} per foot of height results in a value of $k=4/3$, which is commonly assumed to be a good average value. When the dielectric constant decreases about four times as rapidly (or by about 10^{-7} per foot of height), the value of $k=\infty$. This means that, as far as radio propagation is concerned, the earth can be considered flat, since any ray that starts parallel to the earth will remain parallel.

When the dielectric constant decreases more rapidly than 10^{-7} per foot of height, radio waves that are radiated parallel to or at an angle above the earth's surface may be bent downward sufficiently to be reflected from the earth. After reflection the ray is again bent toward the earth, and the path of a typical ray is similar to the path of a bouncing tennis ball. The radio energy appears to be trapped in a duct or wave guide between the earth and the maximum height of the radio path. This phenomenon is variously known as trapping, duct transmission, anomalous propagation, or guided propagation. It will be noted that in this case the path of a typical guided wave is similar in form to the path of sky waves, which are lower-frequency waves trapped between the earth and the ionosphere. However, there is little or no similarity between the virtual heights, the frequencies, or the causes of refraction in the two cases.

In addition to the simple form of a duct where the earth is the lower boundary, trapping may also occur in an elevated duct. For example, assume an ideal case where the curve of the dielectric constant versus the height above the ground can be represented by three straight lines. The lower segment corresponds to the height interval of 0 to 100 feet above the ground and in this region the dielectric constant decreases very slowly, or it may even increase. The middle segment corresponds to a height interval of 100 to 150 feet and in this region the dielectric constant decreases more rapidly than 10^{-7} per foot. The third section corresponds to heights greater than 150 feet and the dielectric constant decreases at a rate less than 10^{-7} per foot. In this ideal case it can be shown that most of the radio energy (at frequencies above about 300 megacycles) is trapped within a height interval of about 50 to 150 feet above the ground, and that the actual path for any given ray is approximately a sine wave whose axis is 100 feet above the ground.

The phenomenon of trapping is of considerable interest, but quantitative data on radio propagation in a duct are beyond the scope of this paper. The concept of an effective earth's radius used in Figs. 5 and 6 fails in this case because the parameter k is negative, and negative values are contrary to the original assumptions in diffraction theory. However, experience indicates that the received field intensity or received power is seldom greater than would be expected for plane earth ($k=\infty$), so this limitation is not expected to be serious.

Meteorological measurements indicate that the actual curve of dielectric constant versus the height above the ground is frequently a curved line which may have one or more sharp bends, rather than a straight line as required in using the concept of an effective earth's radius.[10] Theoretical considerations indicate that this curve can be approximated with reasonable accuracy by a series of straight lines as long as each individual line corresponds to a change in height of not more than 20 to 50 wavelengths. At 30 megacycles, for example, the actual curve of dielectric constant versus height can be approximated by a number of straight lines, each of which has a slope corresponding to the average change in dielectric constant over a height interval of 600 to 1500 feet. Since most of the radio energy transmitted between two ground stations travels in the first of these height intervals, the concept of effective earth radius is a useful one and is sufficiently accurate at 30 megacycles. As the frequency increases, however, more than

[10] The investigators in this field usually use M units rather than the dielectric constant. The M unit is defined as

$$M = \left(\sqrt{\epsilon} - 1 + \frac{h}{a}\right) 10^6$$

where ϵ is the dielectric constant at height h, and a is the radius of the earth. The M unit provides a number of convenient size (usually 200 to 500) and is modified by the term h/a for use on a flat earth diagram. The relation between the parameter k and M units is given by

$$k = \frac{10^6}{M'a} \simeq \frac{.048}{M'},$$

where M' is the change in M units per foot of height.

one segment must be considered, since the straight-line approximation is valid over smaller and smaller height intervals. At 3000 megacycles, for example, this interval is only 6 to 15 feet, and the concept of effective earth radius becomes inadequate for analytical use. Considerable progress has been made toward formulating a method of correcting for atmospheric refraction that avoids these limitations, but the complexity of the problem and the amount of basic data required indicate that ordinarily a statistical study of fading ranges may be preferred to an analytical solution.

The experimental data on fading in the 30- to 150-megacycle range can be correlated reasonably well with the concept of effective earth's radius, if it be assumed that the value of k is rarely less than 0.8 and is seldom greater than 2 or 3. At higher frequencies the received signal at distances beyond the line-of-sight is seldom less than would be expected for $k=0.8$ and may be equal to or above the free-space value.[11] This means that the fading range at 3000 megacycles over a path 10 miles beyond the optical line-of-sight may be as much as 60 or 70 decibels. The per cent of time that the signal is either extremely high or extremely low depends on meteorological conditions, which, in turn, are functions of the geography and season of the year as well as the daily weather variations. Within the line-of-sight, the received power at frequencies above 2000 or 3000 megacycles may vary from several decibels above to 15 decibels or more below the free-space value, even over a good optical path. A good optical path is defined as one with full first-Fresnel-zone clearance, as discussed in the next section. The fading appears to be more severe over sea water than over land, but whether this difference results primarily from a difference in atmospheric conditions or from a difference in the reflecting properties of sea water and land has not been clearly established.

The atmosphere not only affects the direction of a radio wave but also it may introduce some absorption in the transmission path. The presence of rain, snow, or fog introduces an additional attenuation which depends on the amount of moisture and on the frequency. During a rain of cloudburst proportions the attenuation at 10,000 megacycles (3 centimeters) may reach 5 decibels per mile, and at 30,000 megacycles (1 centimeter) it may be in excess of 25 decibels per mile.[12,13] In addition to the effect of moisture, some selective absorption may result from the oxygen, nitrogen, and other components of the atmosphere. The first absorption peak due to water vapor occurs at a wavelength of about 1.25 centimeters and the first peak for oxygen occurs at about 0.5 centimeters. These absorption bands are well known at frequencies of infrared and visible light, and are to be expected as the radio spectrum is extended to higher frequencies.

VII. Transmission Over Sharp Ridges

The preceding discussion assumes that the earth is a perfectly smooth sphere. The modification in these results caused by the presence of hills, trees, and buildings is difficult or impossible to compute, but the order of magnitude of these effects may be obtained from a consideration of the other extreme case, which is propagation over a perfectly absorbing knife edge.

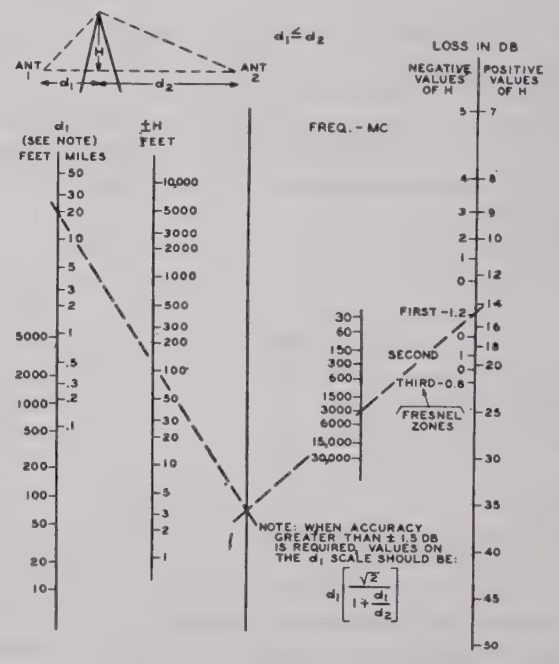

Fig. 8—Shadow loss relative to free space.

The diffraction of plane waves over a knife edge or screen causes a shadow loss whose magnitude is shown on Fig. 8.[14] The height of the obstruction H is measured from the line joining the two antennas to the top of the ridge. It will be noted that the shadow loss approaches 6 decibels as H approaches 0 (grazing incidence), and that it increases with increasing positive values of H. When the direct ray clears the obstruction, H is negative, and the shadow loss approaches 0 decibels in an oscillatory manner as the clearance is increased. In other words, a substantial clearance is required over line-of-sight paths in order to obtain "free-space" transmission.

There is an optimum clearance, called the first-Fresnel-zone clearance, for which the transmission is theoretically 1.2 decibels better than in free space. Phys-

[11] The theory of trapping would indicate that the received signal may be considerably higher than indicated by free-space transmission. Instantaneous peaks of 18 to 20 decibels above free space have been reported, but the average signal is greater than 3 or 4 decibels above the free-space value for only a small percentage of the total time.

[12] S. D. Robertson and A. P. King, "The effect of rain upon the propagation of waves in the 1- and 3-centimeter regions," Proc. I.R.E., vol. 34, pp. 178–180; April, 1946.

[13] G. E. Mueller, "Propagation of 6-millimeter waves," Proc. I.R.E., vol. 34, pp. 181–183; April, 1946.

[14] The theory of diffraction over a knife edge is discussed in several textbooks including J. C. Slater and N. H. Frank, "Introduction to Theoretical Physics," McGraw-Hill Book Co., New York, N. Y. 1933, pp. 315–323.

ically, this clearance is of such magnitude that the phase shift along a line from the antenna to the top of the obstruction and from there to the second antenna is about ½ wavelength greater than the phase shift of the direct path between antennas. When this phase difference is 1 wavelength, the path clears the first two Fresnel zones, and there is theoretically a loss of about 1 decibel relative to free space. Similarly, when the phase difference is 3/2 wavelengths the path clears the first three Fresnel zones, and this is a gain of about 0.8 decibel relative to free space. The locations of the first three Fresnel zones are indicated on the right-hand scale on Fig. 8, and by means of this chart the required clearances can be obtained. At 3000 megacycles, for example, the direct ray should clear all obstructions in the center of a 40-mile path by about 120 feet to obtain full first-zone clearance. The corresponding clearance for a ridge 100 feet in front of either antenna is 4 feet. Should the ridge project above the direct path by 4 feet, the shadow loss is about 15 decibels. It will be noted that the effective clearance obtained on a particular path will vary with the weather conditions, since the effect of atmospheric refraction is neglected in Fig. 8.

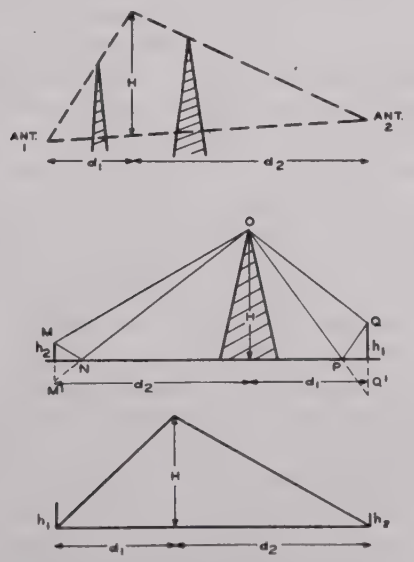

Fig. 9—Ideal profiles used in developing theory of diffraction over hills.

The problem of two or more knife-edge obstructions between the transmitting and receiving antennas, such as is shown in Fig. 9(a), has not been solved rigorously. However, graphical integration indicates that the shadow loss for this case is equivalent within 2 or 3 decibels to the shadow loss for the knife edge represented by the height of the triangle composed of a line joining the two antennas and a line from each antenna through the top of the peak that blocks the line-of-sight from that antenna.

Thus far it has been assumed that the transmission between the two antennas would be approximately the same as in free space, if the obstacles could be removed. This assumption is usually valid only at centimeter wavelengths, and at lower frequencies it is necessary to include the effects of waves reflected from the ground. This results in four paths, namely, MOQ, MOQ', $M'OQ$, and $M'OQ'$, shown on Fig. 9(b) for a single obstruction. Each of these paths is similar in form to the single path illustrated by Fig. 9(a). The sum of the field intensities over these four paths, considering both magnitude and phase, is given by the following equation:

$$\left|\frac{E}{E_0}\right| = S_1\left[1-\frac{S_2}{S_1}e^{-j(\Delta+b)}-\frac{S_3}{S_1}e^{-j(\Delta+c)}+\frac{S_4}{S_1}e^{-j(b+c)}\right] \quad (12)$$

where

E = received field intensity
E_0 = free-space field intensity
S_1 = magnitude of the shadow loss over path MOQ
S_2 = magnitude of the shadow loss over path MOQ'
S_3 = magnitude of the shadow loss over path $M'OQ$
S_4 = magnitude of the shadow loss over path $M'OQ'$
$\Delta = 4\pi h_1 h_2/\lambda(d_1+d_2)$ radians
b is approximately equal to $4\pi h_2 H/\lambda d_2$ radians
c is approximately equal to $4\pi h_1 H/\lambda d_1$ radians.

This equation assumes that the reflection coefficient is -1 and that the actual antenna heights are greater than the minimum effective antenna height h_0. This means that the surface wave is neglected, and the equation fails when either antenna height approaches zero. The angles b and c are phase angles associated with the diffraction phenomena, and the approximate values given above assume that H is greater than h_1 or h_2. This assumption permits the shadow losses to be averaged so that $S_1=S_2=S_3=S_4=S$. After several algebraic manipulations, (12) can be reduced to

$$\left|\frac{E}{E_0}\right| = 2(2S)\left|\sin\frac{\Delta}{2}\cos\frac{b-c}{2} + j\left(\sin^2\frac{b+c}{4}-\sin^2\frac{b-c}{4}\right)e^{j(\Delta/2)}\right| \quad (13)$$

where S is the average shadow loss for the four paths. This means that the shadow triangle should be drawn from a point midway between the location of the actual antenna and the image antenna, as shown in Fig. 9(c). For small values of H this equation is approximately equal to

$$\left|\frac{E}{E_0}\right| = 2\,(2S)\sin\frac{\Delta}{2}. \quad (14)$$

Since the field intensity over plane earth (assuming that the antenna heights are greater than the minimum effective height h_0) is $2E_0\sin\Delta/2$, the first-order effect of

the hill is to add a loss of 20 log $2S$ decibels, which is shown by the nomogram on Fig. 10.

The complete expression given in (12) indicates that, under favorable conditions, the field intensity behind sharp ridges may be greater than over plane earth. This result has been found experimentally in a few cases, but the correlation between theory and experiment is not

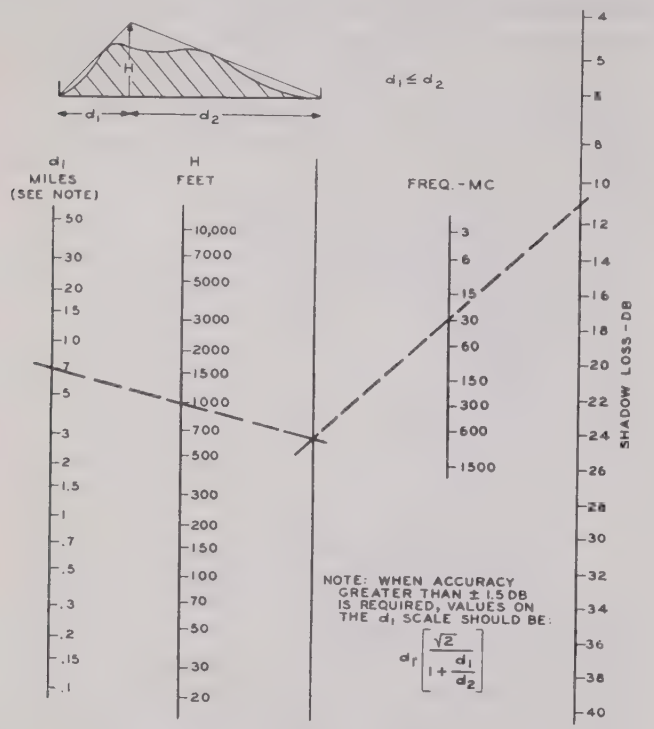

Fig. 10—Shadow loss relative to smooth earth.

complete. In general, the field intensity predicted by either (12) or (13) tends to be too high; that is, shadow losses rather than gains occur on most of the paths on which measured data are available. The less-approximate expression given in (14) agrees more closely with experimental data, is more conservative, and is easier to use. Consequently, it is usually assumed that the effect of obstructions to line-of-sight transmission (at least in the 30- to 150-megacycle range), is to introduce the loss shown on Fig. 10 in addition to the normal loss over smooth earth for the antenna heights and distances involved. Measured results on a large number of paths in the 30- to 150-megacycle range indicate that about 50 per cent of the paths are within 5 or 6 decibels of the values predicted on this basis. The correlation on 10 per cent of the paths is no better than 10 to 12 decibels, and an occasional path may differ by 20 decibels.

VIII. Miscellaneous Factors Affecting Propagation

The height of an antenna located over plane earth is the height of the center of the antenna above ground level. Locating an antenna on a hill which slopes downward toward the distant terminal usually increases the received power. The magnitude of this improvement can be estimated by assuming that the effective antenna height (for use on Fig. 4) is the difference in elevation between the antenna and the bottom of the hill, *providing* that first-Fresnel-zone clearance is obtained over the immediate foreground. At 30 megacycles this means a clearance of about 20 feet at a distance of 20 feet, 40 feet at a distance of 100 feet, 90 feet at a distance of 500 feet, etc. The required clearance decreases as the square root of the wavelength, and may be obtained from Fig. 8. When these clearances are not met, it is convenient to assume that the effective antenna height is the difference in elevation between the antenna and the point where the actual profile intercepts the curve of required clearance (first Fresnel zone).

Built-up areas have little effect on radio transmission at frequencies below a few megacycles, since the size of any obstruction is usually small compared with the wavelength, and the shadows caused by steel buildings and bridges are not noticeable except immediately behind these obstructions. However, at 30 megacycles and above, the absorption of a radio wave in going through an obstruction and the shadow loss in going over it are not negligble, and both types of losses tend to increase as the frequency increases. The attenuation through a brick wall, for example, may vary from 2 to 5 decibels at 30 megacycles and from 10 to 40 decibels at 3000 megacycles, depending on whether the wall is dry or wet. Consequently most buildings are rather opaque at frequencies of the order of thousands of megacycles. Shadow losses at street level in the downtown area of large cities may be of the order of 30 decibels or more at frequencies in the 30- to 150-megacycle range, and the received power may vary 15 to 20 decibels within a few feet because of wave interference caused by multiple-path transmission. As the frequency increases the number of possible multiple paths also increase, so that there is some tendency to fill in the deep shadow regions. This means that the average shadow loss at street level may not increase as rapidly with frequency as the shadow loss behind an isolated ridge, and this is one reason for limiting the distance scale on Fig. 10 to values greater than 0.1 mile.

When an antenna is surrounded by moderately thick trees and below tree-top level, the average loss at 30 megacycles resulting from the trees is usually 2 or 3 decibels for vertical polarization and is negligible with horizontal polarization.[15] However, large and rapid variations in the received field intensity may exist within a small area, resulting from the standing-wave pattern set up by reflections from trees located at a distance of as much as 100 feet or more from the antenna. Consequently, several near-by locations should be inves-

[15] National Defense Research Council Report, Division 13, "Effect of hills and trees as obstructions to radio propagation," C. M. Jansky and S. L. Bailey; November, 1943.

tigated for best results. At 100 megacycles the average loss from surrounding trees may be 5 to 10 decibels for vertical polarization and 2 or 3 decibels for horizontal polarization. The tree losses continue to increase as the frequency increases, and above 300 to 500 megacycles they tend to be independent of the type of polarization. Above 1000 megacycles trees that are thick enough to block vision present an almost solid obstruction, and the diffraction loss over or around these obstructions can be obtained from Fig. 8.

IX. Minimum Allowable Input Power

The effective use of the preceding data for estimating the received power requires a knowledge of the power levels needed for satisfactory operation, since the principal interest is in the signal-to-noise ratio. The signal level required at the input to the receiver depends on several factors, including the noise introduced by the receiver (called first-circuit or set noise), the type and magnitude of any external noise, the type of modulation, and the desired signal-to-noise ratio. A complete discussion of these factors is beyond the scope of this paper, but the fundamental limitations are listed below in order to show the order of magnitude. The theoretical minimum noise level is that set by the thermal agitation of the electrons, and its root-mean-square power in decibels below 1 watt is 204 decibels minus 10 log (bandwidth) where (bandwidth) is approximately equal to twice the audio (or video) bandwidth.[16] The set noise of a typical receiver may be 5 to 15 decibels higher than the theoretical minimum noise. The lower values in this range of "excess" noise are more likely to be met in the very-high-frequency range, while the higher values are more probable in the super-high-frequency range. This means that the set noise in a 3000-cycle audio band may be 151 to 161 decibels below 1 watt. Measured data indicate that the carrier power needs to be 12 to 20 decibels higher than the noise power to provide an average signal-to-noise ratio that is sufficient for moderate intelligibility. This assumes that the modulation level has been adjusted so that most of peaks of speech power can be transmitted without causing overmodulation in the transmitter. It follows that the required input power for a single-channel voice circuit is of the order of 140 decibels below 1 watt, which is roughly equivalent to 1 microvolt across a 70-ohm input resistance. This limiting input power is approximately correct (within 3 or 4 decibels) for both amplitude and frequency modulation, since the radio-frequency signal-to-noise ratio must be above that required for marginal operation before the use of frequency modulation can provide appreciable improvement in the audio signal-to-noise ratio.

The input power must be greater than 140 decibels below 1 watt when circuits of above marginal quality or greater bandwidth are desired, and when external noise rather than set noise is controlling. Man-made noise is frequently controlling at 30 megacycles, but is less serious at 150 megacycles. Above 500 megacycles, set noise is almost always controlling. For circuits requiring a high degree of reliability, a margin should also be included for the fading range to be expected during adverse weather conditions.

Table II
Figures to Use

Type of Terrain	Both Antennas Lower in Height than Shown on Fig. 5	One or Both Antenna Heights Higher than Shown on Fig. 5	
		Within Line-of-Sight	Beyond Line-of-Sight
Plane earth	Fig. 4 or 1	Figs. 4 or 1 or 2	
Smooth earth	Figs. 4 and 5	Figs. 4 or 1 or 2	Figs. 1 or 2 and 6
Irregular terrain	Figs. 4, 5, and 10	Figs. 4 and 10 or 1 or 2 and 8	Figs. 1 or 2 6 and 10

X. Summary and Examples

In any given radio propagation problem some of the factors described above are important, while others can be neglected. Table II indicates the figures that apply to any given situation.

Whenever Fig. 4 is used, reference should be made to Figs. 1 and 3 as a check on its proper use. When Fig. 10 is used in determining the effects of hills, the profile is usually drawn on rectangular co-ordinates (neglecting the earth's curvature), and the shadow triangle is drawn to the base of the antenna (half way between the antenna and its image). Curved co-ordinates are sometimes used, but they are not necessary since the loss caused by the curvature of the earth is either negligible or has already been considered in Figs. 5 or 6. Fig. 8 is used for determining the first-zone clearance and for estimating the shadow losses, when the transmission without the obstruction is expected to be the same as in free space. In the latter case, the shadow triangle is

[16] Harald T. Friis, "Noise figures of radio receivers," Proc. I.R.E., vol. 32, pp. 419–422; July, 1944.

drawn from the actual antennas, and curved co-ordinates are useful since the curvature of the earth should be included in the profile.

Various examples of the use of these figures have been given during the discussion of each individual chart, but further examples may help to illustrate the relations between the various figures. Assume a transmitting dipole located 250 feet above the ground and a receiving dipole on a 30-foot mast. The estimated transmission losses at 30, 300, and 3000 megacycles over smooth earth are shown on Fig. 11 for $k=4/3$ for various distances between these two dipoles. The solid lines indicate values obtained from the figures and the dashed lines show the region where some interpolation is required.

The received power depends on the radiated power and the antenna-gain characteristics, as well as on the transmission loss between dipoles. A typical 30-megacycle transmitter may radiate 250 watts, so that at a

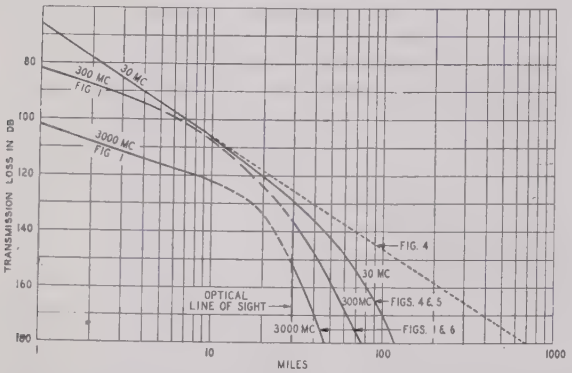

Fig. 11—Transmission over smooth earth at 30, 300, and 300 megacycles; half-wave dipoles at 250 and 30 feet.

distance of 30 miles the received power is 10 log 250 $-129=105$ decibels below 1 watt. (The value of 129 decibels is obtained from Fig. 11.) Similarly, a 300-megacycle transmitter may radiate 50 watts from a 5-decibel antenna, and when a 5-decibel receiving antenna is used the estimated received power at 30 miles is 10 log $50+5+5-137=110$ decibels below 1 watt. At 3000 megacycles the radiated power may be 0.1 watt and antenna gains of 28 decibels each are not uncommon, so the received power at 30 miles is 10 log $0.1+28+28-152=106$ decibels below 1 watt. (The values of radiated power used in this example are not the maximum continuous-wave powers that can be obtained, but the downward trend with increasing frequency is a characteristic of the available tubes.)

Over irregular terrain it is assumed that the shadow loss based on knife-edge diffraction theory is to be added to the transmission loss obtained from smooth-earth theory. The computation of shadow losses for the profile shown on Fig. 12(a) is given in Table III.

The estimated transmission loss for 30 and 300 megacycles, including the shadow loss from Table III, is shown by the solid lines on Fig. 12(b), while the dashed lines are the corresponding values over smooth earth taken from Fig. 11. Superimposed on these average val-

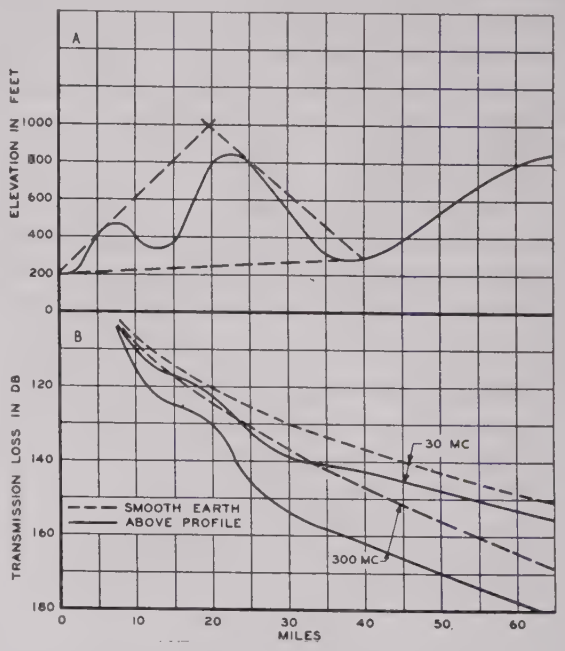

Fig. 12—Transmission loss over irregular terrain at 30 and 300 megacycles; half-wave dipoles at 250 and 30 feet.

ues will be unpredictable variations of ± 6 to 10 decibels resulting from the effects of trees and buildings and from profile irregularities that were smoothed out in drawing the profile shown in Fig. 12(a).

TABLE III
SHADOW-LOSS COMPUTATIONS

Miles from Transmitter	H (feet)	d_1 (miles)	Shadow Loss in Decibels Obtained from Fig. 10	
			30 megacycles	300 megacycles
12.5	200	4.5	3.5	9
20	70	6.5	2	4
25	310	4.5	5.5	13
35	750	14.5	7	16
40	760	20	6	14
50	610	18	5	12
60	490	16.5	4.5	11

APPENDIX

DERIVATION OF DIFFRACTION LOSS BETWEEN ELEVATED ANTENNAS

The derivation of the method shown in Fig. 6 for determining the effect of the curvature of the earth is based on the data in the appendix to the paper by Burrows and Gray,[1] and their nomenclature is used in the following discussion.

The best available equation for radio propagation over spherical earth below the line of sight is

$$\frac{E}{E_0} = (8\pi\zeta_a)^{1/2} \left| \sum_{s=0}^{\infty} f_s(h_1) f_s(h_2) \frac{\exp(-i\tau_s\zeta_a)}{\delta + 2\tau_s} \right| \qquad (15)$$

where the parameters τ_s are functions of the ground constants and the height functions $f_s(h)$ are independent of the distance between antennas. The other symbols are defined below:

$$\zeta_a = \frac{\frac{2\pi d}{\lambda}}{\left(\frac{2\pi ka}{\lambda}\right)^{2/3}} = \zeta_1 + \zeta_2 + \zeta_3$$

$$\delta = z^2\left(\frac{2\pi ka}{\lambda}\right)^{2/3}$$

d = distance between antennas

a = radius of the earth

λ = wavelength

k = ratio of $\dfrac{\text{effective earth's radius}}{\text{true earth's radius}}$

$z = \dfrac{\sqrt{\epsilon_0 - 1}}{\epsilon_0}$ for vertical polarization

$= \sqrt{\epsilon_0 - 1}$ for horizontal polarization.

The height function $f_s(h_1)$ can be represented by

$$f_s(h_1) = \frac{3}{\sqrt{2\pi\zeta_1}} \frac{\exp(i\tau_s\zeta_1)N_1}{\sqrt{-2\tau_s}[J_{1/3}(z_s) + J_{-1/3}(z_s)]} \qquad (16)$$

where

$$\zeta_1 = \frac{\frac{2\pi d_1}{\lambda}}{\left(\frac{2\pi ka}{\lambda}\right)^{2/3}}$$

$d_1 = \sqrt{2kah_1}$ = distance to horizon from antenna height h_1

Z_s = is a function of τ_s.

The factor N_1 is approximately equal to 1 for values of $\xi_1 > 6$, but its value for $\xi_1 < 6$ is still to be determined.

Substituting the value of $f_s(h_1)$ given in (16) and a similar one for $f_s(h_2)$ into (15) results in

$$\left|\frac{E}{E_0}\right| = \sqrt{\frac{\zeta_a}{8\pi\zeta_1\zeta_2}} N_1N_2 \sum_{s=0}^{\infty} 4[\delta + 2\tau s] \left[\frac{\exp\left(-\frac{i\tau_s}{2}(\zeta_a - \zeta_1 - \zeta_2)\right)}{1/3\sqrt{-2\tau_s}[J_{1/3}(z_s) + J_{-1/3}(z_s)][\delta + 2\tau_s]}\right]^2. \qquad (17)$$

The quantity inside the second pair of brackets after the summation sign is in the same form as in (4a) in the paper by Burrows and Gray,[1] so that their solution $[L(\delta)F_L]$ can be substituted in the above equation, resulting in

$$\frac{E}{E_0} = \sqrt{\frac{\zeta_1 + \zeta_2 + \zeta_3}{8\pi\zeta_1\zeta_2}} N_1N_2[2F_{L/2}]^2[L(\delta)]^2\delta \qquad (18)$$

when $\delta \gg \tau_s$.

This step involves the assumption that

$$\sum_{s=0}^{\infty} A_s^2 = \left[\sum_{s=0}^{\infty} A_s\right]^2$$

where A_s is any function of s. This assumption is not justifiable in the general case, but in this instance it affects the loss L_3 (shown on Fig. 6) only in the region near

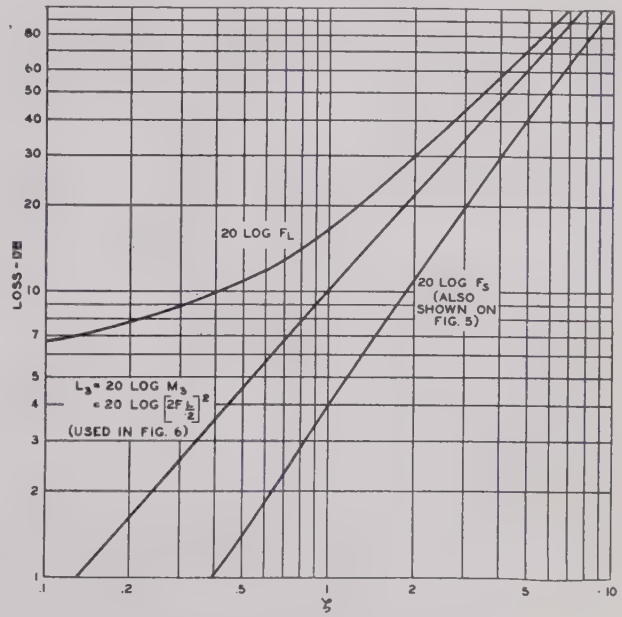

Fig. 13—Attenuation factors used in theory of diffraction over smooth earth.

the line-of-sight. When the loss L_3 is greater than about 30 decibels, the first term ($s=0$) is accurate within one or two decibels; when the loss L_3 is less than 30 decibels (which occurs near the line-of-sight), the above assumption may introduce an error of about ± 3 decibels. Since these possible errors are no greater than the effect of a small change in the assumed value of the parameter k, the over-all accuracy is not greatly impaired, and this procedure simplifies the problem considerably.

The parameter 20 log F_L (taken from Fig. 10 of the Burrows and Gray paper) is shown on Fig. 13 as a function of ξ_3, since $L = \xi_3$ for large values of δ. Also, for large values of δ, $L(\delta) = 1/\sqrt{\delta}$. Consequently, (18) reduces to

$$\frac{E}{E_0} = \sqrt{\frac{1 + \frac{d_1}{d_2} + \frac{d_3}{d_2}}{8\pi\zeta_1}} N_1N_2M_3$$

$$= \left[\frac{N_1}{\sqrt{5.656\pi\zeta_1}}\right][N_2][M_3]\left[\frac{1}{\sqrt{2}}\left(1 + \frac{d_1}{d_2} + \frac{d_3}{d_2}\right)\right]^{1/2} \qquad (19)$$

where $M_3=[2F_{L/2}]^2$ and 20 log M_3 is plotted in Fig. 13. The term in the first set of brackets is a function of d_1 (since N_1 depends on d_1 but is independent of d_2 and d_3); the factor in the second set of brackets is a function of d_2; and the factor in the third set of brackets is a function of d_3. The fourth term is small, *providing* that d_1 is defined as the distance to the horizon from the *lower* antenna, and it ordinarily can be neglected.

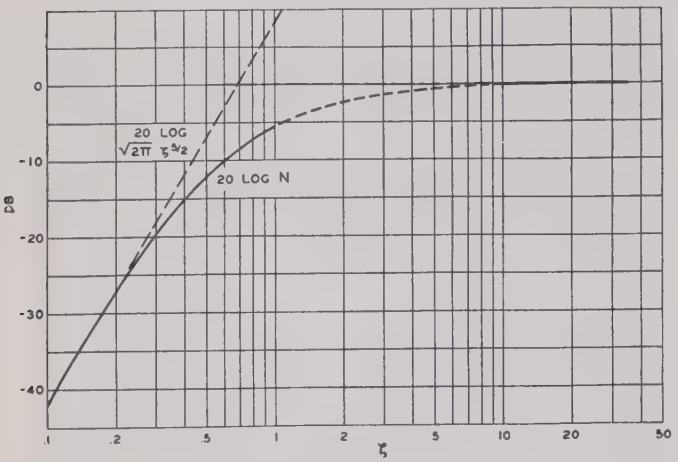

Fig. 14—Values of N.

The factor N is equal to unity when ζ is greater than about 6, but more information about the factor N is required in order that (19) can be used at lower antenna heights. When one antenna is high so that $\zeta_2>6$, and the other antenna low ($\zeta_1<1$), (19) at line-of-sight reduces to

$$\frac{E}{E_0}=\frac{N_1}{\sqrt{8\pi\zeta_1}}.$$

A solution to this same problem is given by Burrows and Gray (19) which can be shown to be equivalent to

$$\frac{E}{E_0}=\frac{\zeta_1^2}{2}.$$

By setting these two expressions equal it is found that

$$N_1=\sqrt{2\pi}\,\zeta_1^{5/2} \tag{20}$$

for low values of ζ_1.

The asymptotic value of 20 log $\sqrt{2\pi}\,\xi_1^{5/2}$ is shown by the dashed line on the left side of Fig. 14, while the other asymptotic value of 20 log $N=0$ for high antenna heights is also shown by a dashed line. The true value of N must be a smooth curve or a family of curves joining these two asymptotic values.

A second method for determining the magnitude of N is to assume a grazing path with two antennas of equal height. This means that $\zeta_1=\zeta_2$; $N_1=N_2$; $\zeta_a=2\zeta_1$. For this case (19) reduces to

$$\frac{E}{E_0}=\frac{N_1^2}{\sqrt{4\pi\zeta_1}}.$$

Another solution to this problem is well known for the case of $\xi_1<1$. It is

$$\frac{E}{E_0}=\frac{4\pi h_1h_2}{\lambda d}F_s=\frac{\zeta_1^2\zeta_2^2}{2\zeta_a}F_s$$

where F_s is the diffraction loss caused by the curvature of the earth when both antennas are near the ground. The value of 20 log F_s is shown on Fig. 13 as a function of ζ_a and is also given by the nomogram in Fig. 5. By setting these two expressions equal, it is found that

$$\frac{N_1^2}{\sqrt{4\pi\zeta_1}}=\frac{\zeta_1^4}{4\zeta_1}F_s$$

$$N_1^2=\sqrt{\frac{\pi}{4}}\,\zeta_1^{7/2}F_s$$

or $$20\log N_1=-0.5+35\log\zeta_1+10\log F_s \tag{21}$$

where F_s is a function of $2\zeta_1$.

The value of 20 log N_1 is shown on Fig. 14, as a function of ζ_1 (or N_2 as a function of ζ_2). The values of N for the range of $0.3<\zeta<1$ have been computed from (21). (The quantity ζ_1 is greater than 0.3 whenever the antenna height is greater than 50 feet at 30 megacycles, or greater than 10 feet at 300 megacycles.) The values of N in the range of $1<\zeta<6$ have been interpolated, but there seems little chance of serious error in this procedure.

In the nomogram on Fig. 6, the decibel loss

$$L_1=20\log\frac{N_1}{\sqrt{5.656\pi\zeta_1}},$$

the decibel loss $L_2=20$ log N_2, and the decibel loss $L_3=20$ log M_3.

Wide-Range Ultra-High-Frequency Signal Generators*

A. V. HAEFF†, SENIOR MEMBER, I.R.E., T. E. HANLEY†, ASSOCIATE MEMBER, I.R.E., AND C. B. SMITH†, ASSOCIATE MEMBER, I.R.E.

Summary—**A series of wide-range signal generators, covering a frequency range from 90 to 9700 megacycles, was developed during the war at the Naval Research Laboratory. The radio-frequency-oscillator circuits are of low capacitance, resulting in good pulse as well as continuous-wave operation. The mutual-inductance-type attenuators give a range in output level of over 100 decibels below 0.1 volt across 50-ohm output impedance with an absolute accuracy of the order of 1 decibel. Versatile pulsing, synchronizing, and modulating circuits make the instruments particularly useful in pulse system studies. The usefulness of these signal generators led to their large-scale production and use in the laboratory and in the field. Experience gained in their design and use forms the basis for future progress in this field.**

Introduction

ONE OF the most versatile instruments in electronic research is the calibrated signal generator. Its use makes it relatively easy to solve many problems experimentally whose solutions otherwise may be extremely difficult.

Great intensification of research in the field of ultra-high-frequency electronics took place shortly before the war, and a need for ultra-high-frequency signal generators became particularly apparent at that time. Since no satisfactory instruments were available, a program of research on signal generators was initiated at the Naval Research Laboratory early in 1941. This work was prosecuted by a small group under the direction of the senior author of this paper and was carried as an extra activity outside the official laboratory program until satisfactory results in the form of successful laboratory instruments were obtained. At that time the Bureau of Ships initiated the procurement of signal generators, based on the laboratory design, for use by other government laboratories, the United States Fleet, and the commercial organizations, particularly in connection with the development and production of countermeasure equipment. In order to expedite the introduction and use of signal generators by all organizations in need of these instruments, complete design and performance information on Naval Research Laboratory models was supplied to several organizations, such as the Radio Corporation of America, Federal Telephone and Radio Corporation, and others, even before the plans for the production of these units outside of the laboratory were completely formulated.

The successful prosecution of the program resulted in the development of a series of signal generators covering the frequency range from 90 to 10,000 megacycles. Because much of the war work at this and other laboratories involved development of pulse radar equipment, these signal generators were designed to provide either continuous-wave or pulsed output with radio-frequency pulses of known amplitude and of adjustable duration.

It is the purpose of this paper to give a general picture of this development by brief descriptions of the design, performance, and limitations of the different models of this series and to point out features which should be considered for future designs.

Frequency Ranges of Models

The work on the signal generators began with the design of oscillators which would cover the desired frequency range. The ranges of the resulting units were not arrived at arbitrarily but rather evolved as a function of tube and circuit limitations. Table I shows the frequency ranges and the types of high-frequency tubes used in the signal generators.

TABLE I

Frequency Range (megacycles)	Radio-Frequency-Oscillator Tube Type	Laboratory and Production Model Designation	Remarks
90 to 600	446(2C40)	E (LAF)	Continous wave; pulse; external amplitude modulation
500 to 1350	446(2C40)	A (LAE)	Continuous wave; pulse; external amplitude modulation
1200 to 4000	707B(2K28)	D (LAG)	Continuous wave; pulse; internal frequency modulation; wavemeter
3700 to 9700	1289CT(BTL)	F (—)	Continuous wave; pulse; wavemeter
2000 to 3800	446(2C40)	B (—)	Continuous wave; pulse; external amplitude modulation; wavemeter
9200 to 9700	723A/B	G (—)	Continuous wave; pulse; internal frequency modulation; wavemeter

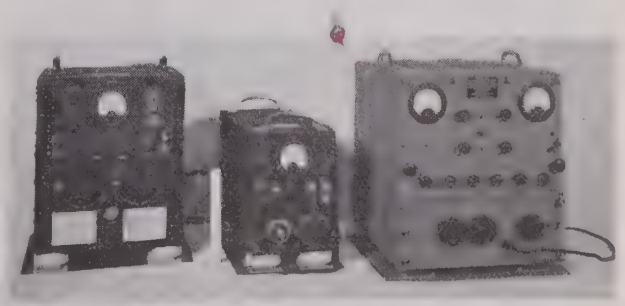

Fig. 1—The Navy-type signal generators. Left to right: LAF (90 to 600 megacycles), LAE (500 to 1350 megacycles), and LAG (1200 to 4000 megacycles).

Oscillator Circuit Design

Figs. 1 and 2 show the external appearance of some of the units. In addition to a tunable radio-frequency oscillator provided with an output monitor and attenua-

* Decimal classification: R355.913.2. Original manuscript received by the Institute, June 25, 1946; revised manuscript received, September 9, 1946.

† Naval Research Laboratory, Washington, D. C.

tor, the signal-generator circuits comprise the following: the power supply, level-control, pulse-forming, and synchronizing circuits, frequency-modulation and phasing circuits, and a frequency meter. The requirement of pulse modulation made it desirable to use radio-frequency circuits having a minimum of capacitance.

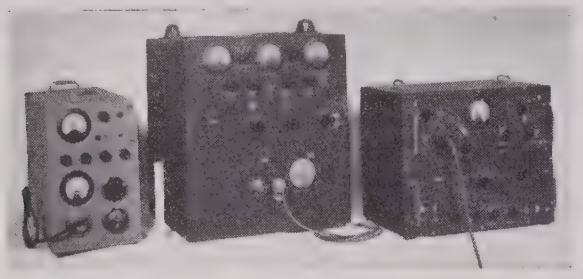

Fig. 2—The laboratory models of signal generators. Left to right: NRL Type B (2000 to 3800 megacycles), NRL Type F (3700 to 9700 megacycles), and the NRL Type G (9200 to 9700 megacycles).

Therefore, a general type of transmission-line circuit tuned by sliding shorting pistons was chosen. The electrical limitations of the tubes and their mechanical design governed the choice of circuit arrangement most suitable for a particular frequency range.

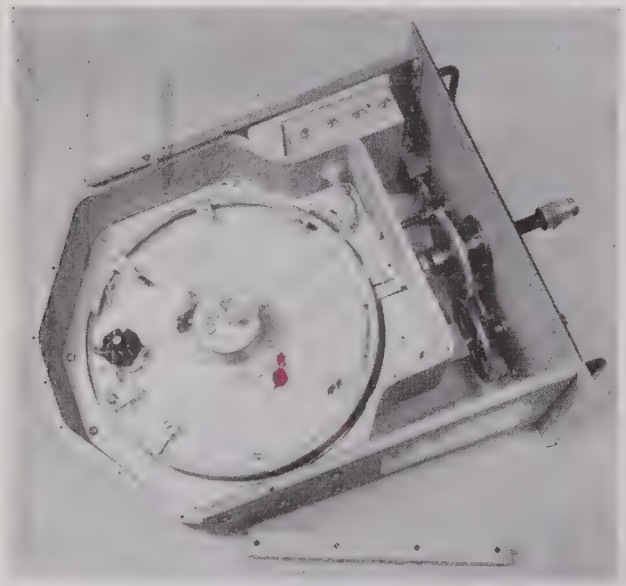

Fig. 3—The oscillator compartment of the type E (model LAF) showing the rotor, the frequency drive, the attenuator drive, and the position of the stationary shorting bar.

For the lowest-frequency generator where the lighthouse tube is used, a parallel-line oscillator was designed with lines formed into portions of a circle, since straight concentric lines would have been too cumbersome. As shown in Fig. 3, the plate and cathode lines are mounted on opposite sides which can be rotated by the frequency dial.

To cover the range from 500 to 4000 megacycles, concentric-line oscillators are used, and these are of several kinds. The lower-frequency unit, illustrated schematically in Fig. 4, covers a range of from 500 to 1300 megacycles and uses the lighthouse tube mounted in a

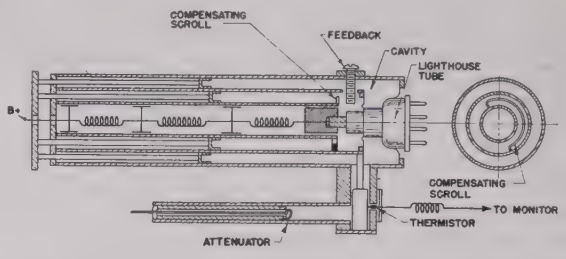

Fig. 4—A schematic drawing of the oscillator and attenuator assembly for the LAE model.

circuit in which the cathode cavity is "folded" back over the plate cavity, thus permitting both of the shorting pistons to move in the same direction and to be easily ganged. Both pistons operate in the one-quarter-wave mode and the capacitative feedback between plate and cathode cavities is accomplished by means of a

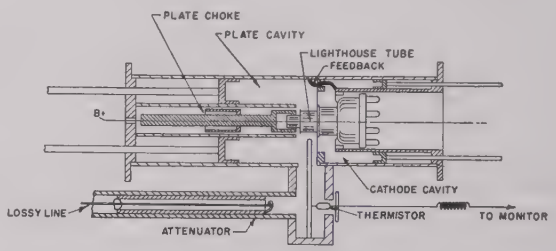

Fig. 5—A schematic drawing of the oscillator and attenuator assembly for the NRL type-B signal generator.

screw. This circuit is used in the Naval Research Laboratory type-A and the Navy type-LAE signal generators.

Another concentric-line lighthouse-tube oscillator used in the Naval Research Laboratory type-B signal

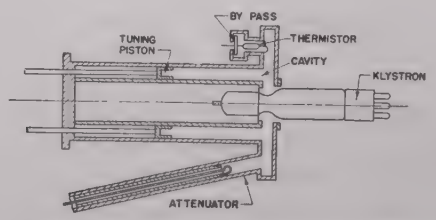

Fig. 6—The oscillator and attenuator assembly of the LAG signal generator.

generator covers the range of 2000 to 3800 megacycles. This circuit is illustrated in Fig. 5. The plate-grid line operating in the $7/4\lambda$ mode and the cathode line in the $5/4\lambda$ mode are arranged on opposite sides of the grid plane separating the two circuits. A feedback loop is provided which is tied directly to the tube end of the

cathode line and forms a small loop on the plate side of the grid-separation plane. The use of this feedback arrangement makes possible the operation over a very wide frequency range without readjustment of the feedback.

A third type of concentric-line oscillator is illustrated in Fig. 6. The Naval Research Laboratory type-D and the Navy type-LAG signal generators use this type of circuit involving a single coaxial cavity tunable with a shorting piston. This circuit makes it possible for the 707B reflex klystron to cover from 1200 to 4000 megacycles. This oscillator also has a specially designed ring cavity which extends the main cavity outward, making it possible to couple conveniently the attenuator, the output monitor unit, and the wavemeter to the main oscillator circuit.

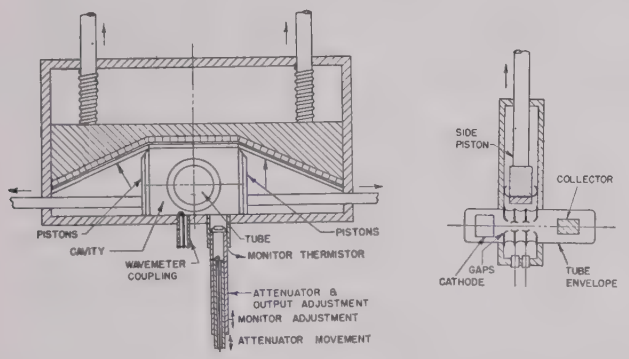

Fig. 7—(a) The oscillator cavity and the attenuator arrangement in the NRL type-F signal generator, showing the cavity-tuning mechanism and the attenuator monitor adjustment. (b) End view of the type-F oscillator cavity showing the position of the 1289 tube.

For the frequencies beyond the 10-centimeter range, a wave-guide-type cavity is used. The Naval Research Laboratory type-F signal generator uses such a cavity containing a 1289CT(BTL) tube, which is a magnetically focused three-gap klystron designed for use with an external cavity. Fig. 7(a) and (b) give a cross-sectional view of this tube and the cavity. The cavity design is unusual in that it changes width as well as length as the single frequency dial is turned. By means of this "two-way stretch" feature, it is possible to eliminate frequency "holes" due to conflicting modes, so that the oscillator covers a frequency range from 3800 to 9700 megacycles without hiatus.

The type-G signal generator uses the wave-guide type of cavity and is designed to cover the narrow frequency band around 9500 megacycles. This generator uses a 723A/B tube, which is coupled to an external wave-guide cavity tuned to resonance, thus making available high magnetic fields for coupling to the usual type of attenuator. This generator covers only the range of the 723A/B tube (approximately 500 megacycles centered about 9700 megacycles). Figs. 8 and 9 illustrate the wave-guide cavity and the control mechanisms for this generator.

The oscillator circuit consists of a section of wave guide terminated by a thermistor-type monitor at one end and by a tuning piston at the other. The 723A/B oscillator is coupled to this cavity through a probe, and

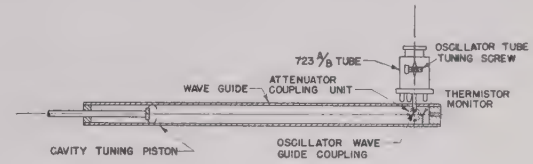

Fig. 8—The type-G oscillator assembly showing the relative positions of the 723A/B tube, the monitor, the attenuator coupling orifice, and of the cavity-tuning piston.

the coupling can be adjusted externally by moving the tube with respect to the wave guide. The attenuator is of the usual wave-guide type, the movable output loop coupling directly to the field within the oscillating cavity. Fig. 9 shows the general arrangement of the components within the radio-frequency shielding compartment and the controls brought out to the front panel: the wave-guide tuning control, the coupling adjustment, the attenuator, and the tuning mechanism for the 723A/B tube.[1]

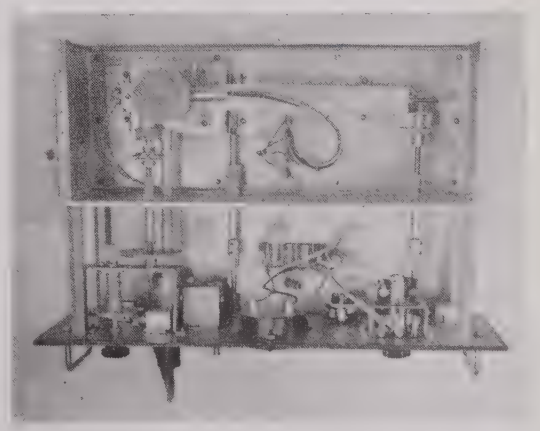

Fig. 9—The top view of the type-G oscillator chassis (with cover removed from the shielded compartment), showing the tuning mechanisms for the 723A/B tube and for the cavity, the coupling and attenuator controls, and the monitor meter and repeller potentiometer mounted on the front panel.

Attenuators

The attenuators used on all of these signal generators are the mutual-inductance, cylindrical-wave-guide type.[2] The diameter d selected is such that the cylinder is well

[1] In addition to the generator using the 723A/B tube, two units were built following the general design of the type-G generator but using oscillator tubes covering other frequency bands.

[2] E. G. Linder, "Attenuation of electromagnetic fields in pipes smaller than the critical size," Proc. I.R.E., vol. 30, p. 556; December, 1942.

below cutoff at the frequency range used in order to minimize the frequency correction in the attenuator calibration. In each case the attenuator consists of a cylindrical chamber in which a pickup loop connected to a coaxial line can be moved. This loop is made to couple directly to the magnetic field of the resonant cavity of the oscillator in order to obtain the highest output within the linear portion of the attenuator. The movement of the attenuator is accomplished by means of a threaded section which moves the loop in the cylindrical wave guide. The position of the loop in the wave guide determines the amount of attenuation present. Theoretically, for the H mode, the attenuation in decibels is given by the formula:

$$a = 32\frac{z}{d}\sqrt{1-\left(\frac{f}{f_c}\right)^2}$$

where f is the operating frequency, $f_c=(1.84/d)3\times10^{10}$ is the cutoff frequency, d is the diameter of the attenuating wave guide, and z is the displacement of the loop. The position of the loop is recorded on a counter. The threads on the attenuator and the gears on the counter were selected so as to make the counter numbers indicate decibels below a given level. These attenuators can be set to one-tenth of a decibel.

In the case of the parallel-line oscillator, the attenuator loop is coupled through the unit which shorts the lines, thus always coupling at a point of maximum current. In the concentric-line lighthouse-tube oscillators, the attenuator loop couples inductively to a "probe" which in turn is coupled to the oscillator cavity. In the 500- to 1300-megacycle unit this probe is conductively coupled to the main oscillator circuit and thus forms an integral part of it. In order to make the plate and cathode circuits track, a compensating circuit in the form of a "scroll" is connected between the plate and grid conductors, as shown in Fig. 4. Because this circuit is similar electrically to the probe circuit, its effect on the plate-line tuning is the same as the effect of the probe on the cathode line. This makes it possible to have the two circuits track over the entire frequency range. In the 2000- to 4000-megacycle unit the probe is coupled capacitively in the plate line, and since the plate and cathode circuits are tuned independently, no compensating circuit is used in the cathode line.

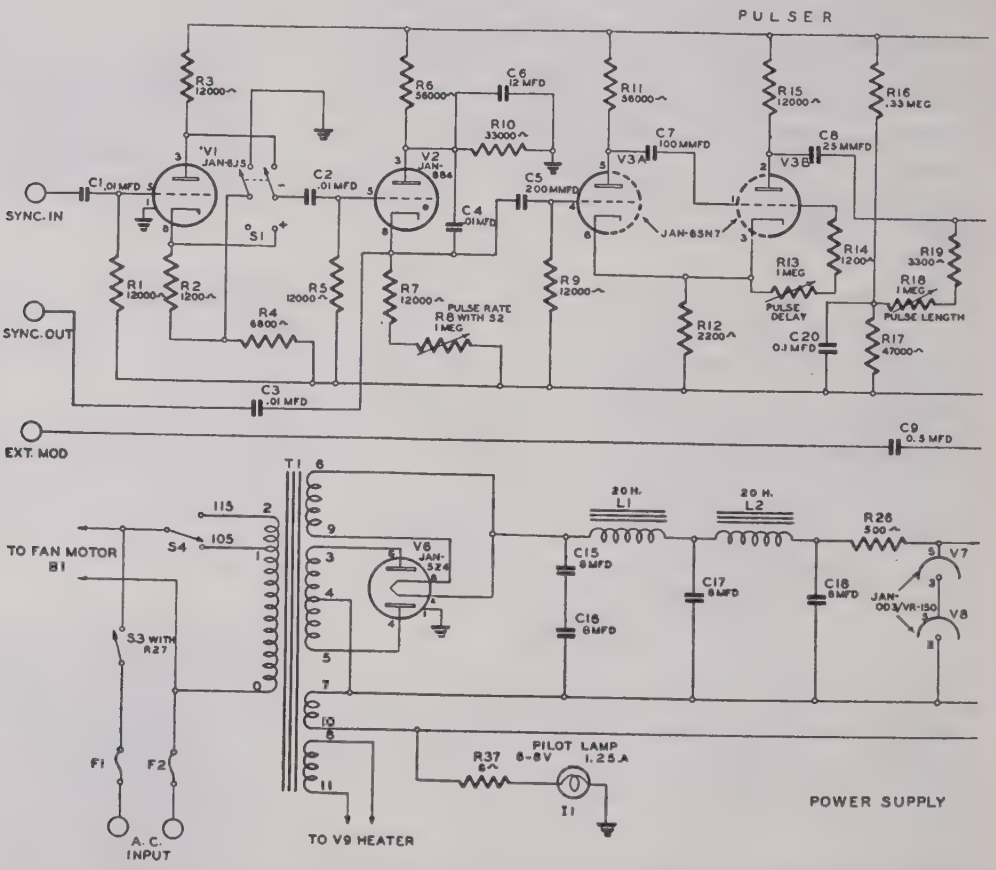

Fig. 10—A circuit schematic for the type-LAE signal generator showing the radio-

In the case of the oscillators using the 707B reflex klystron, the attenuator couples to the ring-shaped cavity which is an integral part of the main circuit, as was shown in Fig. 6. This serves to provide a region of high current density in the region of attenuator coupling. The cavity ring also makes it possible to separate the attenuator dial from other dials on the front panel.

Internal Impedance of the Signal Generator

In order that the signal generator shall present a constant impedance over the frequency range, the attenuator loop is made to have a minimum of inductance, and a 50-ohm resistor at the loop is used to terminate the 50-ohm coaxial output cable. These resistors are ½-watt carbon resistors made by the Erie Resistor Corporation in the radio-frequency field of the oscillator and connected in a resistance bridge with the output meter across the bridge so as to indicate the unbalance when the resistance of the thermistor changes. The unbalance current is very nearly proportional to the radio-frequency power. A typical monitor circuit is shown in Fig. 10.

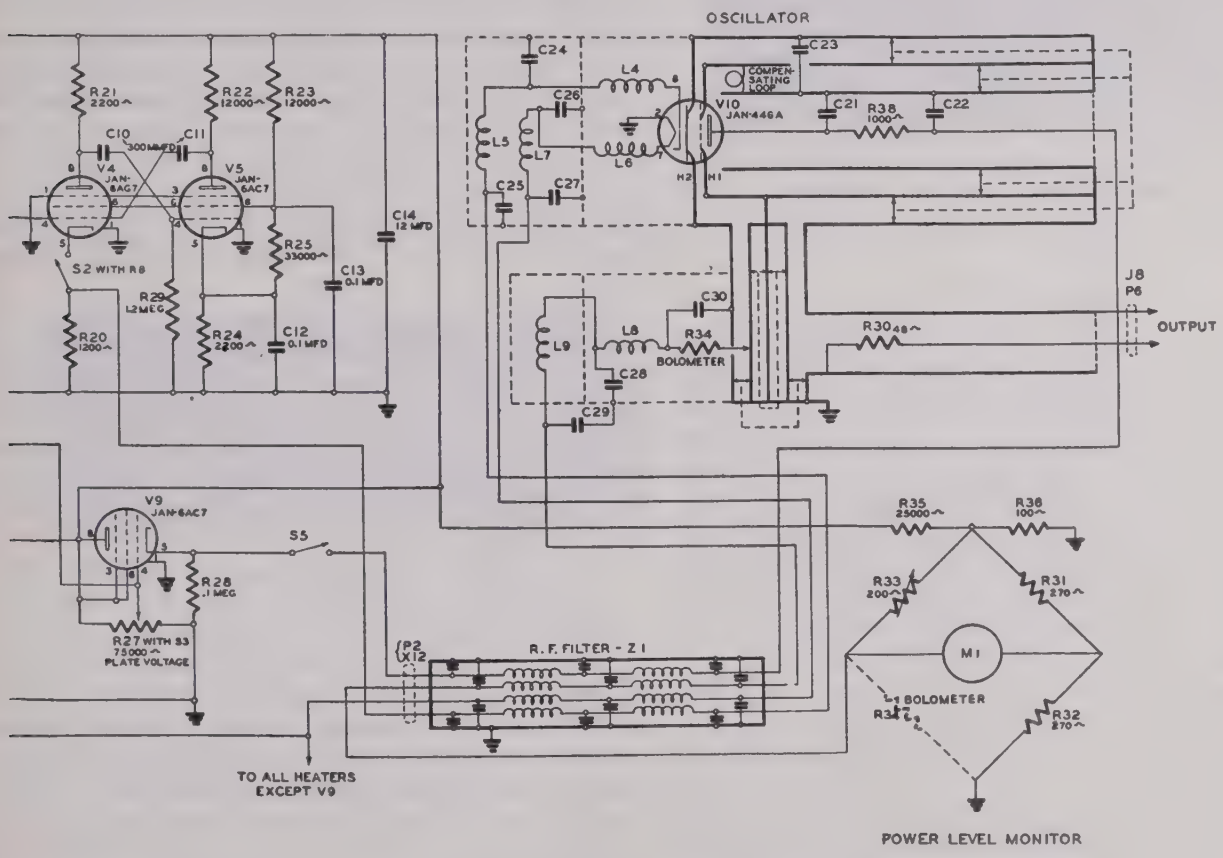

frequency oscillator, the filter, the pulser, the monitor, and the power-supply circuits.

and have inductive reactance low compared to 50 ohms up to frequencies of 1200 megacycles. The signal generators above 1200 megacycles, in addition to a terminating resistor, use a special lossy output cable having between 6 and 8 decibels of loss at the higher frequency. At the lower frequencies the loss is considerably less, but then the resistor provides good termination. In all cases the voltage-standing-wave ratio proves to be better than 1.2 to 1, as measured by feeding a signal into the signal generator from an external source.

Output Monitor

In order that the signal generator give a known output, it is necessary to provide a monitor and means for adjusting the output level. In all of these generators the monitor is located near the point of coupling of the attenuator-output loop, so that the variation in the monitor-meter reading accurately corresponds to output-level variation. The monitor consists of a thermistor placed

Output-Level Control

To set the output level to its normal value as indicated by the monitor, it is necessary to have some control over the radio-frequency energy delivered by the oscillator. In generators using the lighthouse-tube triodes, the plate voltage is made manually adjustable in order to obtain the desired output. A 6AG7 in a cathode-follower arrangement is used as shown in Fig. 10. This arrangement combines ease in adjusting output level and permits good voltage regulation.[8] In order to control the output of the 707B klystron, the voltage which is applied to the grid is varied. This voltage is controlled by the same type of cathode-follower arrangement as is used in the lighthouse-tube circuits.

In the type-F signal generator, which uses the 1289 tube, the output is varied by a double-attenuator ar-

[8] The use of the cathode-follower arrangement for this application was first suggested by F. H Harris of the Naval Research Laboratory.

rangement. The monitor element and the output attenuator can be moved together in a section of cylindrical guide which is below cutoff so as to change the coupling between the oscillator and the monitor and thus set the level. Then the output attenuator is moved with respect to the monitor element. This system has the advantage that the output can be varied without the necessity of changing the voltages on the oscillator. This arrangement is illustrated in Fig. 7(a).

In the type-G signal generator, which uses the 723A/B tube, the output is varied by varying the coupling of the oscillator tube to the auxiliary resonant circuit, as shown in Fig. 8. The last two methods make it possible to vary the output reference level without varying any of the voltages on the oscillator tube, which has a considerable advantage since optimum operating voltages can be used at all times.

Frequency Calibration

The low-frequency generators (up to 1350 megacycles) have stable oscillator circuits and have the frequency indicated directly by the position of the calibrated tuning dial. In the signal generators above 1350 megacycles, special wavemeters are provided which form an integral part of the generator. These wavemeters make possible a more accurate setting of the generator frequency, and also make it possible to change tubes without recalibration of the frequency dial. The wavemeters also provide a continuous monitoring of the frequency. In the case of the LAG, type-D, and type-B signal generators, the wavemeter is an accurately tunable quarter-wave coaxial-line section loosely coupled to the oscillator cavity. In the type-G signal generator, the 723A/B tube is coupled into an auxiliary circuit tuned to resonance by means of a piston, and this auxiliary circuit serves as a wavemeter. Resonance for all of the wavemeters is indicated by a meter on the front panel which reads current rectified by a 1N21 crystal. For the LAG, type-D, and type-B signal generators, the wavemeter calibration is accurate to about 2 megacycles, and frequencies as close as one-tenth megacycle can be distinguished.

Shielding

The shielding of the signal generator is a requirement which becomes increasingly more stringent when measurements on sensitive receivers are contemplated. The method used on all of the Naval Research Laboratory signal generators is to include the oscillator in a tight metal compartment which, together with the pulser and power supply, fits into the outer metal cabinet. In all cases, the oscillator proper is also shielded, since at these frequencies the oscillator itself is self-contained so that the radio-frequency fields are confined within the metal enclosures. Also, in the case of the generators using cavities, the leads entering the oscillator have choke-capacitance-type filters in them. The shielding box into which the oscillator is placed is closed on all sides except the front, with all seams welded and soldered. The radio-frequency section is usually suspended on a subpanel which slips into the front of the shield can and is held in place by screws.

Pulser Design

Since these signal generators were primarily designed to check the performance of radar receivers, it was necessary to develop a versatile pulsing unit in order to simulate radar signals. The Naval Research Laboratory generators all provide pulsers which permit independent control of repetition rate, pulse delay, pulse length and synchronization of or by external devices. A typical pulser circuit is illustrated in Fig. 10. In these units an 884 gas tube is used in a relaxation circuit to provide original pulses at a repetition rate which is adjustable between 30 and 3000 pulses per second with a single control.

A 6SN7 tube in a multivibrator circuit provides the delay which makes it possible to delay the radio-frequency pulse with reference to the triggering pulse and thus to position the pulse on the viewing scope at any point between 2 microseconds and 3000 microseconds after the trace has been keyed. This delay tube in turn keys the pulse-length-determining circuit, which in most cases is a multivibrator.

After a suitable video pulse has been obtained, there still is the problem of applying the pulse to the radio-frequency oscillator in such a manner that its pulse output can be calibrated. Since the average radio-frequency energy obtained from the pulsed oscillator is usually too small to calibrate accurately by direct measurement of power, a system of pulsing was chosen whereby the signal generator can be calibrated on continous waves, and when the switch is thrown to pulse, the pulse power rises to this continuous-wave level. Such an arrangement is shown in Fig. 10. In the generators using the lighthouse tube, when the switch is in the pulse position the oscillator is biased off except when the pulse is applied. The bias is obtained by drawing heavy current from the tube V_4, the cathode of which is connected to the cathode of the oscillator tube. When a negative pulse is applied to the grid of the bias tube V_4 the cathode of the oscillator tube assumes the potential which would be attained under the unmodulated continuous-wave condition.

This method of pulsing has the advantage of requiring only a negative pulse of relatively low amplitude, the shape of the pulse on top being unimportant as long as the amplitude is sufficient to cut off the bias tube (V_4). Thus, regardless of the length of the pulse, the oscillator output reaches the value equal to the continuous-wave value, which can be calibrated directly by power measurement.

Since the impedance of the cathode-bias resistor is of the order of 200 ohms, it is relatively easy to generate video pulses with short rise and decay time, even when the lead from bias tube to the cathode of the oscillator

tube has to pass through a high-capacitance radio-frequency filter. Thus the limit to the "squareness" of the pulse is usually imposed by the starting time of the oscillator itself, rather than by the applied video pulse.

In order to pulse the generators using the 707 and the 1289 klystron tubes, the bias tube is placed in series with their cathodes, and this bias tube, which is normally biased off, is pulsed on. In the case of the 723A/B, the repeller of the klystron is pulsed from a nonoscillating bias to a voltage corresponding to an oscillating mode. A diode is used as a clipper to maintain the proper amplitude for the pulse.

Modulation

In addition to pulse modulation, the LAG and the type-D and type-G signal generators have built into

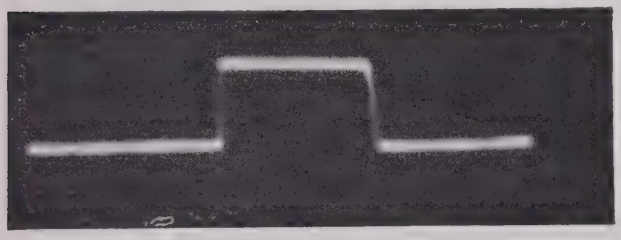

Fig. 11—The "unmodulated" radio-frequency pulse (rectified).

them provisions for frequency modulation by applying a 60-cycle voltage to the repeller of the klystron. This gives about 8 megacycles of frequency modulation. A phasing circuit is also included which makes it possible to phase the frequency-modulation pattern as viewed on the oscilloscope.

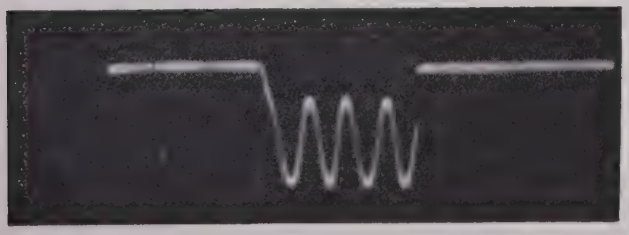

Fig. 12—The radio-frequency pulse modulated with a high-frequency sine wave.

All of the signal generators using the lighthouse tube have provisions for external modulation on the plate. This makes it possible to superimpose other types of modulation in addition to the pulse modulation. Fig. 11 shows an example of just the pulse modulation. Fig. 12 gives the pulse with a high-frequency sine wave superimposed. This frequency is high with respect to the repetition rate. Fig. 13 gives a series of pulses with low-frequency sine wave superimposed, thus giving amplitude-modulated square pulses. External modulation at frequencies up to 0.1 to 0.5 megacycle is quite effective in most of the units described.

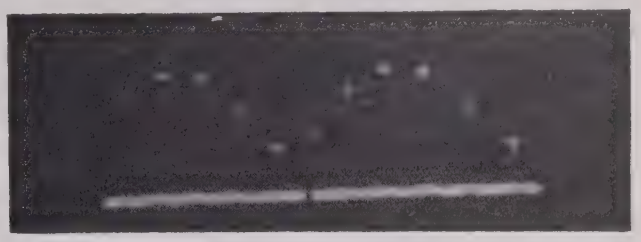

Fig. 13—The radio-frequency pulse modulated in amplitude at a frequency low compared to the pulse-repetition rate.

Conclusion

The signal generators described in this paper have proved quite useful for laboratory and field measurements. In addition, experience gained in their design and use served to point the way to better equipments. One improvement would be a single and direct-reading frequency control. Another desirable feature would be a smaller and lighter unit through the use of miniature components. The pulsing circuits could be improved to make synchronization more stable by eliminating the gas tube and providing shorter and sharper pulses by the use of multivibrator circuits. Improvements such as these will be incorporated in the signal generators of the near future. A more fundamental improvement would be the development of a method for direct calibration of pulsed output.

Acknowledgment

The original development work on the above equipments, including building of complete models, was done entirely at the Naval Research Laboratory. The manufacturers who undertook production of the equipment for laboratory or field use were supplied with complete design information. Several improvements which were incorporated during the minor redesign of the equipment for production should be credited to E. W. Weimer and J. P. Leiphart who conducted the Navy type-approval tests on the developmental, preproduction, and production models, and to the engineers of the manufacturers who participated in the production of the equipment. The authors take this opportunity to express their appreciation of the engineering effort supplied by the Hewlett-Packard Company in the production of the Naval Research Laboratory type-A, -B, and -G models, the Line Material Company in the production of the Naval Research Laboratory type-D and -E models, the Airadio Company in the production of the LAE, the F. Rieber Company in the production of the LAF, and the General Communications Company in the production of the LAG.

Center-Frequency-Stabilized Frequency-Modulation System*

E. M. OSTLUND†, SENIOR MEMBER, I.R.E., A. R. VALLARINO†, ASSOCIATE, I.R.E., AND MARTIN SILVER†, ASSOCIATE, I.R.E.

Summary—A system comparing the phase between two frequencies in a balanced phase detector utilizes the output to maintain synchronization between two oscillators. The phase detector operates between ±90 degrees.

By dividing the frequency of a frequency-modulated oscillator, the frequency swing is reduced to less than ±24 degrees. The mean divided modulated oscillation is compared in the phase detector to the same frequency obtained by dividing the frequency of a crystal oscillator. The correction voltage resulting from a change in phase between the two oscillators changes the capacitance injected into the tank of the modulated oscillator, and thus maintains synchronization.

A modulator utilizing the linear relationship between the input capacitance and the transconductance of a vacuum-tube amplifier is used to control the total capacitance of the frequency-determining circuit of a master oscillator. Part of the output of the master oscillator is multiplied in frequency and power to produce the transmitter output, and part goes to a frequency divider having a ratio of 1 to 256. This practically eliminates the frequency swing resulting from modulation and permits the output frequency to be synchronized with that of a similarly frequency-divided crystal oscillator. Any shift in phase between these two synchronized frequencies produces a correcting voltage which is applied to the modulator of the master oscillator. This correcting voltage acts to maintain the synchronization of the two divided frequencies.

1. Modulator

VARIATION of the effective capacitance of the modulator-tube grid circuit is reflected across the master-oscillator tank circuit, as shown in Fig. 1. This capacitive change is proportional to the total bias voltage on the 6AB7 modulator-tube grid which is the sum of the program audio-frequency input and the center-frequency-stabilizing phase-detector output voltages. Thus the modulator not only converts the audio-frequency voltage into the desired frequency variations, but also acts in conjunction with the center-frequency-stabilizing system to maintain the mean carrier frequency in exact coincidence with that of a temperature-controlled crystal.

The linear relationship between the input capacitance and the transconductance of a vacuum-tube amplifier is used to swing the frequency of a Hartley oscillator. Operating the modulator in the region of linear transconductance and applying a modulating signal to its control grid results in an input capacitance applied to the oscillator which is directly proportional to the amplitude of the modulating signal.

To a first approximation, and for a qualitative discussion of the mechanism of action of the modulator, it can be shown that the input capacitance of the vacuum tube is given by

$$C_{in} = C_{gp}(1 + g_m R_L), \tag{1}$$

where

C_{in} = input capacitance
C_{gp} = grid-plate capacitance
g_m = transconductance
R_L = load impedance at resonance.

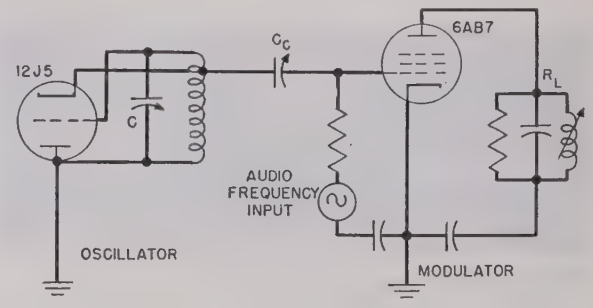

Fig. 1—The grid-cathode capacitance of the modulator tube is a function of the input audio-frequency voltage. The variations in this capacitance cause the frequency of the grounded-plate Hartley oscillator to change, thus producing frequency modulation.

As the frequency of oscillation is approximately $\omega_0 = 1/(LC)^{1/2}$, the differential of frequency for an increment of capacitance is

$$\left.\begin{aligned} d\omega &= \left(\frac{d\omega}{dC}\right)\Delta C \\ &= \frac{-1}{2L^{1/2}C^{3/2}}\Delta C \\ &= \frac{-\omega_0}{2C}\Delta C \end{aligned}\right\} \tag{2}$$

where

$\omega = 2\pi$ times frequency of oscillation
$d\omega$ = differential of frequency
ΔC = increment of capacitance
L = inductance
C = capacitance
$\omega_0 = 1/(LC)^{1/2}$.

This shows that the frequency swing is directly proportional to the change in injected capacitance, and inversely proportional to the fixed tank capacitance C. To obtain a fixed frequency swing for a given change in input capacitance, over the range of oscillator capacitance required to cover the transmitting frequency band an adjustable capacitance C_c couples the modulator to

* Decimal classification: R630. Original manuscript received by the Institute, August 2, 1946; revised manuscript received, November 15, 1946.

† Federal Telecommunication Laboratories, Inc., New York, N. Y.

the oscillator. To reduce the radio-frequency signal on the modulator grid, the capacitance is injected across only a portion of the tank inductance.

2. Center-Frequency Stabilization

The center-frequency-stabilization system is based on the automatic synchronization of two oscillators, a crystal oscillator and a frequency-modulated master oscillator. The outputs of the crystal oscillator and of the frequency-modulated master oscillator are passed through separate frequency dividers and combined in a balanced phase detector. The rectified integrated difference output actuates the modulator so as to pull-in and lock the master oscillator mean frequency to that of the crystal oscillator. This arrangement is shown in Fig. 2.

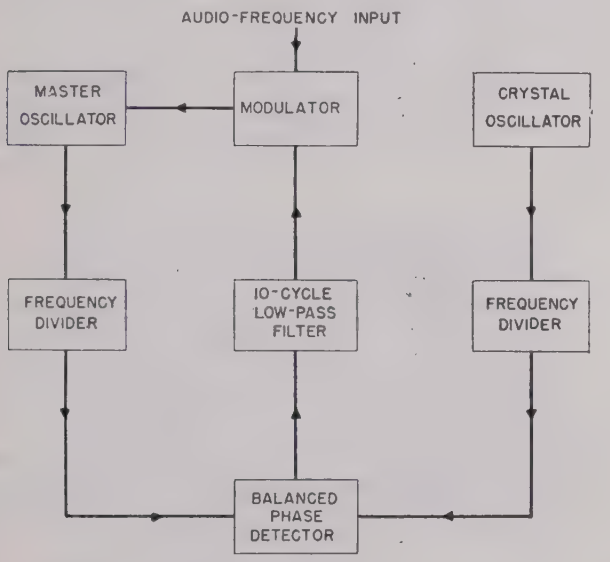

Fig. 2—Schematic diagram of the center-frequency-stabilized modulation system.

If synchronization of the two frequencies is assumed, the output of the balanced phase detector depends on their relative phase. Any attempt of the mean frequency of the master oscillator to drift from the crystal frequency results in an instantaneous change of the phase difference of the two oscillations and a corresponding variation in the rectified output of the phase detector, which will act on the modulator to increase or decrease the total master-oscillator tank capacitance and maintain synchronization.

If synchronization of the two frequencies is not assumed, the output of the detector is the beat difference between the frequency-divided crystal oscillation and the frequency-divided modulated master oscillation. This beat frequency, acting on the modulator, swings the carrier frequency of the master oscillator at a rate equal to the beat frequency and with a deviation proportional to the amplitude of the beat. If the deviation is sufficiently large and the beat rate sufficiently low, the instantaneous frequency of the modulated oscillator will be in near-synchronization with the crystal oscillation for a sufficient number of oscillation cycles for synchronization to occur and be maintained. Thereafter, the condition described in the preceding paragraph is effective.

It would not be possible to synchronize a frequency-modulated oscillator with a crystal oscillator at the carrier frequency because under modulation the carrier-frequency-component amplitude passes through innumerable conditions of zero amplitude. But if frequency division is performed, the effect is to reduce the frequency swing (modulation index) to an extent where the reduction of carrier-frequency-component amplitude is very small. If, for example, a maximum swing of 3 kilocycles occurs at an oscillator center frequency of 4 megacycles, a frequency division of 256 will reduce the maximum swing to $3000/256 \approx 12$ cycles. Considering an audio frequency of 30 cycles, the maximum modulation index is $12/30 = 0.4$ radians ≈ 24 degrees. This index reduces the carrier to 0.96 of its unmodulated value, giving an essentially constant carrier for synchronization. The crystal-oscillator frequency is also divided to correspond to the divided frequency of the master oscillator.

Frequency division is accomplished through untuned multivibrator circuits which depend mainly on resistive and capacitive components for both critical and noncritical functions. This results in stable operation over long periods of time as well as extreme ease in initial alignment and a minimum of operational maintenance.

The use of a balanced phase detector imposes the condition that the instantaneous phase variation at the detector must not exceed ± 90 degrees as this is the maximum range over which the detector operates as a phase-control device. Frequency division reduces the phase variation due to modulation to less than 24 degrees and operation is always within the control of the phase detector when the system is under synchronization. As a matter of fact, continuous modulation exceeding 200 per cent may be used without losing control.

The output circuit of the phase detector is essentially an integrator and low-pass 10-cycle filter; it responds only to slow mean frequency drifts and removes the residual modulation. A meter is provided to give continuous check of the phase relations between the crystal and master-oscillator frequencies.

3. Balanced Phase Detector

Under conditions of synchronization the output voltage of the balanced phase detector, shown in Fig. 3, is given by

$$V_{out} = |V_{ca}| - |V_{cb}| = 1.414\hat{V}_{0c}[(1 + \cos\delta)^{1/2} - (1 - \cos\delta)^{1/2}] \qquad (3)$$

where δ is the phase angle between the frequency-divided master-oscillator input and the frequency-divided crystal input. This is shown in Fig. 4. The output voltage is plotted against δ in Fig. 5.

The physical picture of the action of the balanced

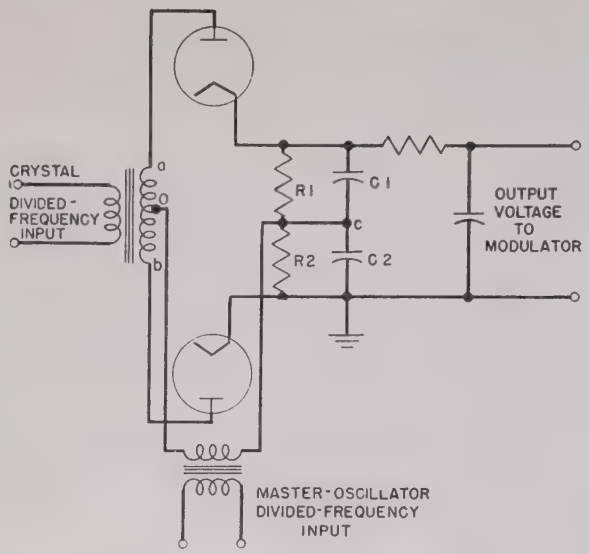

Fig. 3—Balanced phase detector. If the synchronized crystal and master-oscillator frequencies, after division, are 90 degrees out of phase, the output voltage to the modulator will be zero.

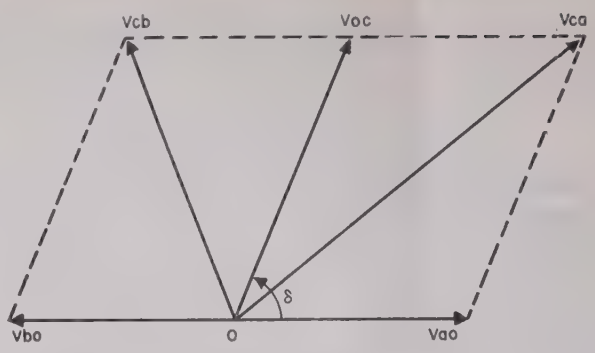

Fig. 4—Vector diagram of balanced phase detector.

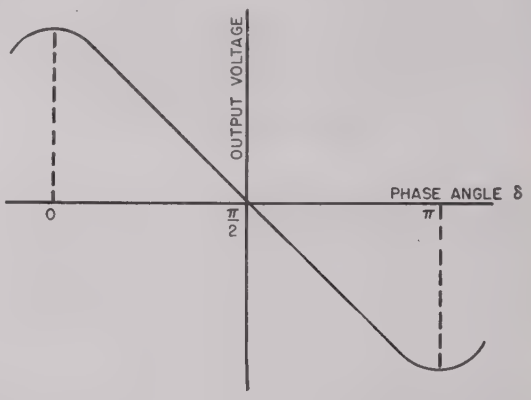

Fig. 5—Response characteristic of the balanced phase detector.

phase detector may be considered as the action of two peak-reading diode detector circuits whose outputs are combined in opposition. V_{ca} is the peak voltage acting on the upper diode and V_{cb} is the peak voltage acting on the lower diode. The time constants of the output network R_1C_1 and R_2C_2 are high enough to prevent any appreciable decay in the peak voltage during the time when the diode is not conducting. If a 90-degree phase relation between the two identical frequencies is assumed, $|V_{ca}|$ is equal to $|V_{cb}|$ and their difference gives zero output voltage. This is the normal operating condition.

Any attempt at slow drift of the master-oscillator frequency will shift the phase in a direction to give a correcting output voltage to the modulator. This voltage will change the injected capacitance to the master oscillator so that the total capacitance and the frequency will remain constant. Therefore, operation may occur

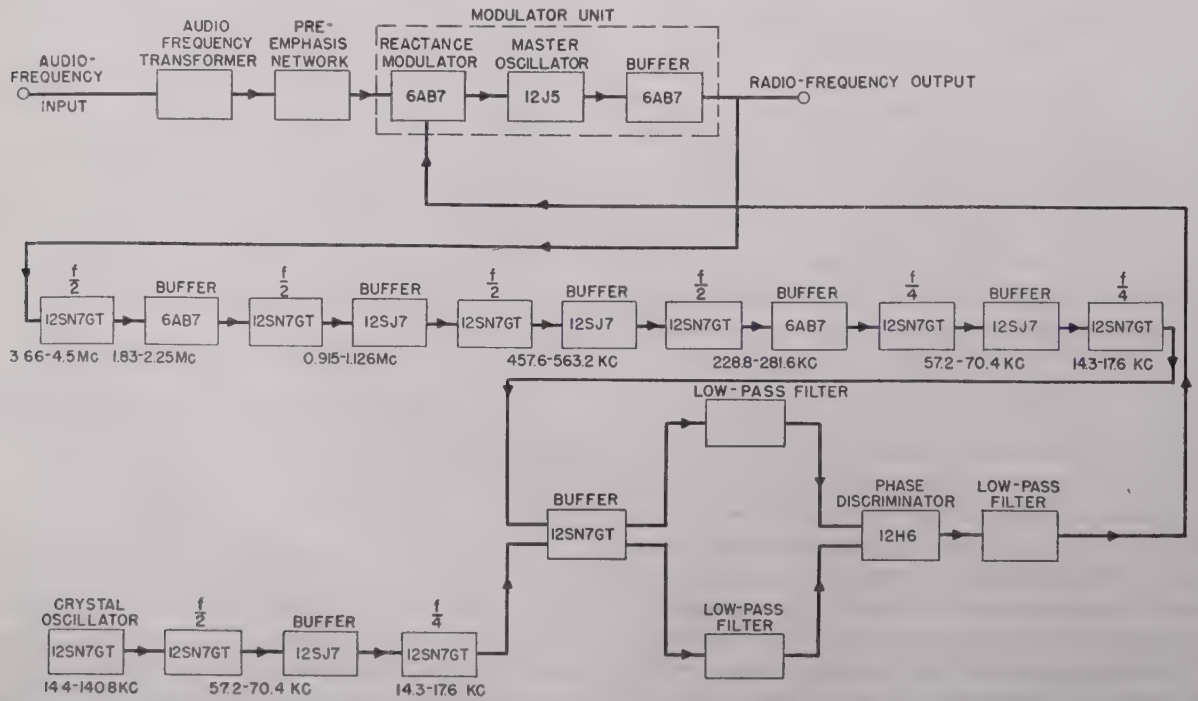

Fig. 6—Schematic diagram of the modulator and center-frequency stabilization system. The frequency notations for the various stages are the limits for operation in the 88- to 108-megacycle band assigned to frequency-modulation broadcasting in the United States. The radio-frequency output from the modulator is multiplied 24 times to produce power in that band.

at any point within the region of control of the S curve and the system will be in synchronization. Similarly, should there be a modification in any parameter of the oscillator circuit which would normally cause a change in frequency, the phase will shift to compensate for the parameter variation and the frequency will remain constant.

It has been previously noted that the phase swing resulting from normal modulation is well within the limits of control of the balanced phase detector. As the lowest modulating frequency is 30 cycles, the 10-cycle low-pass filter following the detector removes residual modulation.

4. Over-All Performance

Fig. 6 is a schematic arrangement for the modulator and center-frequency-stabilization system. Figs. 7 and 8 are front and rear views of the modulator unit. A complete 1-kilowatt transmitter is shown in Fig. 9. The radio-frequency output from the modulator unit is frequency multiplied 24 times to produce power in the frequency-modulation band from 88 to 108 megacycles.

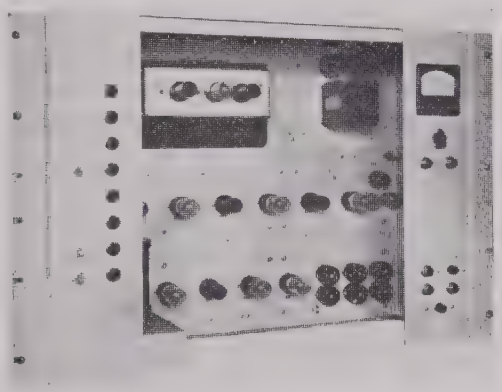

Fig. 7—Federal 1-kilowatt frequency-modulated transmitter. In the upper left is the frequency multiplier and driver stage; next below is the modulator and center-frequency stabilizer. The two lower panels are for the regulated power supply, controls, and contactors. In the lower right is the high-voltage power supply. Above it is the power output stage and the bazooka coupler to the antenna transmission line.

In operation the unmodulated frequency is firmly synchronized with the crystal frequency. The divided master-oscillator frequency will pull into synchronization with the divided crystal frequency over a range of ± 50 kilocycles about the carrier frequency. A carrier-to-crystal-frequency phase-comparison meter is included.

Audio-frequency distortion at full frequency deviation of 75 kilocycles is only 0.5 per cent. The frequency-modulation noise is 75 decibels below 100 per cent modulation and the amplitude-modulated noise is 60 decibels below the carrier level. Normal operation of the transmitter is unaffected by disabling of the center-frequency control system. This permits uninterrupted emergency operation under such conditions.

5. Appendix

One of the functions of the modulator is precisely and continuously to keep all oscillator influences balanced so that the mean frequency does not change or, in more general terms, so that the total frequency drift is zero.

If synchronization is assumed, the center-frequency-stabilization system can be considered as a linear, continuously operating, zeroing type of control mechanism that corrects for any change in the frequency-determining capacitance of the oscillator resulting from any inside influence.

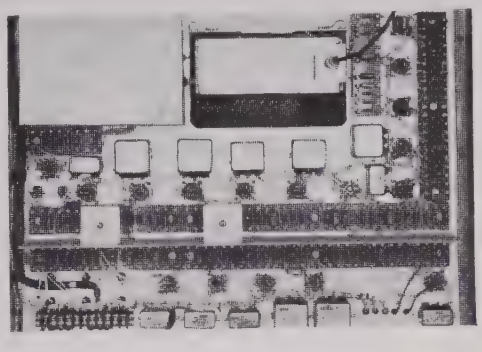

Fig. 8—Center-frequency-stabilized frequency-modulation unit, front view. The master oscillator, modulator, and buffer are mounted in the cabinet in the upper center of the equipment. The phase-comparison meter is in the right corner. The two rows of tubes are frequency dividers.

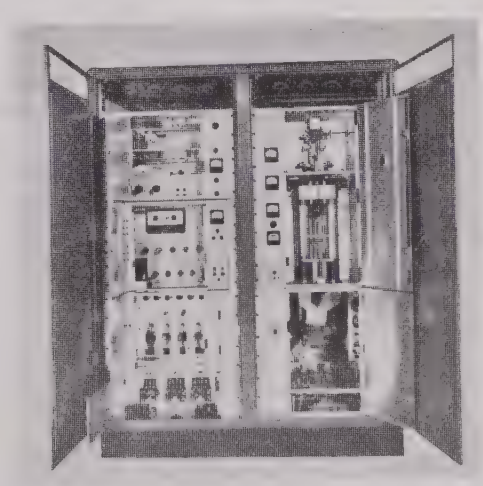

Fig. 9—Center-frequency-stabilized frequency-modulation unit, rear view.

In examining the mathematical basis for the control action,

let x = change in tank capacitance due to any inside influence

y = voltage output of phase detector

$\theta_3 y$ = injected capacitance due to action of phase detector-modulator

θ_1 = conversion coefficient of capacitance to phase at the oscillator

θ_2 = conversion coefficient of phase to voltage at phase detector

θ_3 = conversion coefficient of voltage to capacitance at oscillator

ϕ_0 = reference phase of crystal oscillator
ϕ_1 = phase of oscillator output
$\theta = \theta_1 \theta_2 \theta_3$.

In Fig. 10 the time rate of change of the output voltage y of the phase detector is proportional to the phase deviation at the detector. The output voltage of the phase detector is given by an expression having a transient term $v = Ve^{-\alpha t}$. The time derivative is given by $dv/dt = -V\alpha e^{-\alpha t}$, i.e., it is proportional to the maximum impressed voltage V. As the maximum voltage V is directly proportional to the maximum phase deviation, the above statement follows directly and gives

$$\dot{y} = \theta_2(\phi_1 - \phi_0)$$
$$\phi_1 = \theta_1(x - \theta_3 y)$$
$$\dot{y} = \theta_1\theta_2(x - \theta_3 y) - \theta_2\phi_0$$
$$\dot{y} + \theta_1\theta_2\theta_3 y = \theta_1\theta_2 x - \theta_2\phi_0$$
$$\dot{y} + \theta y = \theta_1\theta_2 x - \theta_2\phi_0.$$

Under the assumption that the coefficients θ_1, θ_2, and θ_3 are constants, and considering the changes in the parameter x of the oscillatory circuit to take place at a slow drift rate, the solution for the quasi-stationary state can be considered the same as that for x = constant. Under these general assumptions the solution evidently is

$$y = \theta_3^{-1}x + Ae^{-\theta t} - \theta^{-1}\phi_0 \tag{4}$$

where A is an arbitrary constant of integration. Observe that under the special conditions of operation, where at times $t=0$, $x=0$, $y=-0^{-1}\phi_0$, then $A=0$ and y would remain at a value corresponding to x thereafter. Actually, this condition is not met, and so the effect of the transient term $Ae^{-\theta t}$ must be examined. There are two cases to consider when $A \neq 0$.

$$\theta_1 = \frac{d\phi_1}{dC} = \frac{d\left(\int_0^t \frac{d\phi_1}{\partial t}\,dt\right)}{dC} \quad \text{[Fig. 11(a)]} \tag{5}$$

$$\theta_2 = \frac{dV}{d\phi} = \frac{d\left(\int_0^\phi \frac{\partial V}{\partial \phi}\,d\phi\right)}{d\phi} \quad \text{[Fig. 11(b)]} \tag{6}$$

$$\phi = \phi_0 - \phi_1$$

$$\theta_3 = \frac{dC}{dV} = \frac{d\left(\int_0^V \frac{\partial C}{\partial V}\,dV\right)}{dV} \quad \text{[Fig. 11(c)]} \tag{7}$$

where C, V, and ϕ can all be functions of time.

If θ is negative, the magnitude of y increases without limit and is the condition for an unstable system. If θ is positive, the magnitude of $Ae^{-\theta t}$ decreases and y approaches the steady value corresponding to x. It has been assumed that x is constant, but it is evident that if θ is positive and if the time constant of x is large compared with the time constant of θ, in a general sense y will be equal to the value corresponding to the instantaneous value of x. This shows roughly that, if the system is stable, y tends to be proportional to x. Incidentally, it is worth noting that our control mechanism acts as an integrator, for if it makes y proportional to x it makes the output voltgage of the phase detector proportional to the integral of the output phase.

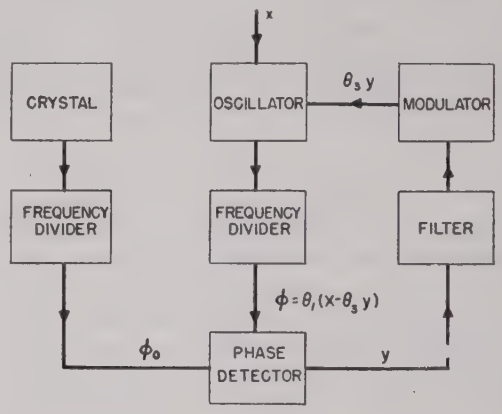

Fig. 10—Center-frequency-stabilizer control loop.

It may not be amiss to mention that a more rigorous solution could be obtained using the fundamental steady-state equation of linear control mechanisms where the coefficients are not assumed constant.

$$y = \frac{Y_0(P)\theta^{-1}x}{1 + Y_0(P)} \tag{8}$$

where $\theta^{-1}Y_0(P)$ is the steady-state-transmission ratio around the feedback loop of the control mechanism. For our particular case this is not warranted.

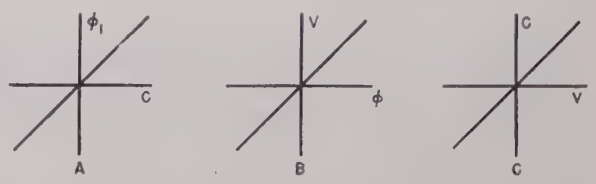

Fig. 11—Center-frequency-stabilizer parameter conversion.

If synchronization is not assumed, then the action of the phase detector is that of a diode mixer whose output has, among other frequencies, the beat difference between the divided crystal frequency and the divided modulated frequency. These beats are applied to the modulator to modulate the frequency of the carrier. The value of the frequency swing (ΔF) fed back depends on the amplitude of the beat, and this determines the pull-in region. When the amplitude of the beat corresponds to the difference between the mean carrier and the crystal frequency, the two frequencies will pull into step.

An investigation of a mathematical analysis of the process whereby pull-in action is obtained leads to the conclusion that this is essentially a nonlinear mechanism

and has no simple solution. But it is fortunate that in this region we are interested only in the transient effect whereby the pull-in action takes place.

A 10-cycle low-pass filter, inserted following the phase detector, determines the maximum beat which can be utilized in obtaining pull-in. The output frequency of the transmitter is divided by 6000 to obtain the beat, and the control frequency is therefore $\pm 6000 + 10 = \pm 60$ kilocycles. In other words, beat action is able to control ± 60 kilocycles. But the determining factor is how far pull-in can be used is the change in capacitance the modulator can insert across the tank of the oscillator. Thus, knowing the static change in capacitance which the modulator is able to produce, the range over which pull-in take place may be determined. Of the transmission coefficients θ_1, θ_2, and θ_3 which have been discussed, the only one that has an appreciable time delay is θ_2. This comes about because of the time constant R_1C_1 of the phase detector. The beat frequency modulating the carrier is itself frequency-modulated at the beat rate, and reaches a condition where zero beat occurs and the two signals have identical frequencies. Furthermore, if we examine the period of any of the beats, they will always have a period $T > 1/\text{beat frequency}$. It is evident that, if the time constant of the transmission coefficient $\theta_2 \ll T$, synchronization can be obtained. For the constants as used, $\theta_2 = E_1C_1 = 1000$ microseconds and $T = 100{,}000$ microseconds. This gives a ratio of 100 to 1 which allows the coefficient $Ae^{-\theta_1\theta_2\theta_3 t}$ to decay much faster than the rate at which the frequency of the modulated oscillator is moving away from synchronization, and so lock-in holds.

Intermodulation Distortion Analysis as Applied to Disk Recording and Reproducing Equipment*

H. E. ROYS†, ASSOCIATE, I.R.E.

Summary—**Measuring the sidebands generated due to nonlinearity when using a test signal consisting of two different frequencies has been found to be a useful way of analyzing distortion in disk recording systems.**

The method is more sensitive than the single-frequency harmonic method and gives results which seem to agree very well with listeners' observations.

Tests made at various groove velocities with playback tips of different sizes show the expected increase in distortion at the lower velocities with the larger tips. The importance of a good fit between stylus and groove is illustrated.

Introduction

FOR SOME time a method of measuring distortion has been needed that is readily applicable to disk recording, with good correlation to what is heard by the ear. Methods which measure the individual harmonic components of a single frequency are difficult to apply. Usually special equipment is required because of the shifting of the phase and frequency due to speed variations of the turntable. Much time is usually involved in making such measurements, and the correlation with what is heard is not very good unless the results are carefully analyzed. Equipment that filters out the fundamental and measures the residue (which consists of the harmonic components and the noise) is simple to operate. Noise is a problem, however, and the scope is limited unless the equipment is designed to pass all of the essential harmonics, and again the correlation with the ear is not very good.

Intermodulation Method

The two-frequency method of analyzing distortion has been widely used in variable-density photographic sound recording, and we have found it a valuable tool for similar studies in disk recording. The term *intermodulation* is preferred to *cross modulation* for this method of distortion analysis in order to distinguish it from a test used by the film industry which is called cross modulation, and which uses an amplitude-modulated carrier as the test signal.

In the intermodulation method of distortion testing,[1] two frequencies, preferably one low and the other high, are combined in a linear network to make up the test signal. The usual practice is to have the higher frequency 12 decibels lower in level than the low frequency and to maintain this relation for all tests. According to Frayne and Scoville,[2] when a 12-decibel difference in level between the upper and lower frequencies exists, the sensitivity of the intermodulation method is somewhere between 3.2 and 4 times greater than the harmonic-measurement, single-recorded-frequency method. This ratio is not fixed but depends upon the order of the harmonics and their amplitudes.

The advantage of the intermodulation method of distortion testing lies in its ease of application: adjustments are simple; a single reading is obtained for each measurement; and the method is insensitive to phase and frequency changes caused by turntable speed varia-

* Decimal classification: R391.1×534. Original manuscript received by the Institute, June 7, 1946; revised manuscript received, December 5, 1946.

† Radio Corporation of America, RCA Victor Division, Camden, N. J.

[1] J. K. Hilliard, "Distortion tests by the intermodulation method," PROC. I.R.E., vol. 29, pp. 614–620: December, 1941.

[2] J. G. Frayne, and R. R. Scoville, "Analysis and measurements of distortion in variable-density recording," *Jour. Soc. Mot. Pict. Eng.*, vol. 32, p. 648; June, 1939.

tions. The combination of a low and a high frequency permits measurements at frequencies higher than the harmonic method. This is because the only requirement is that the sideband frequencies created by intermodulation distortion fall within the range of the equipment.

Equipment

In operation, the combination of frequencies is fed to the equipment under test. The output from the device is fed to an analyzer, shown in Fig. 1, which consists of a filter that eliminates the original low-frequency component, and passes only the higher frequency and the sidebands (generated because of curvature or nonlinearity in the device). The amplitude of modulation of the high frequency is then measured by rectifying, filtering out the high frequencies, and measuring the fluctuation in the rectified current. We find good correlation between distortion as measured by the intermodulation test and impairment of sound quality as judged by the ear.

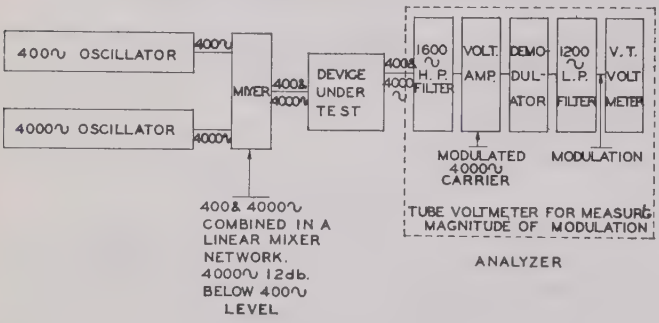

Fig. 1—Intermodulation distortion equipment.

For our tests, frequencies of 400 and 4000 cycles were used, as the equipment available operated at these frequencies. A lower frequency, such as 100 cycles, might constitute a better choice, but for lateral disk recording 400 cycles is in the constant-amplitude portion of the recording characteristic and therefore is subjected to the maximum displacement.

Distortion with Change in Groove Velocity

In order to obtain some data on the variation of distortion with groove velocity, lacquers were recorded with intermodulation bands at different diameters and turntable speeds. The records were processed and pressings were made for test purposes. A recording tip radius much smaller than normal was used so that reproducing styli having tips of various radii could be used while the principle was maintained that the spherical reproducing tip should contact the two side walls but not reach the bottom. The results of these tests are shown in Fig. 2. Curve A was obtained with a pickup having a 2.8-mil tip radius. Curve B was obtained with a pickup which was thought to have a 2.5-mil tip radius, but the results indicated a larger radius by showing greater distortion at the lower groove velocities than those shown for the 2.8-mil tip. The pickup had been in use for some time, and upon rechecking after these measurements, the tip was found to have a flat of about 1.2 mils. We are not aware of any other reproduction test which shows up a flat on the playback tip so readily and clearly. Curves C and D give the expected results, and show that the distortion is less at the lower groove velocities for smaller playback tips.

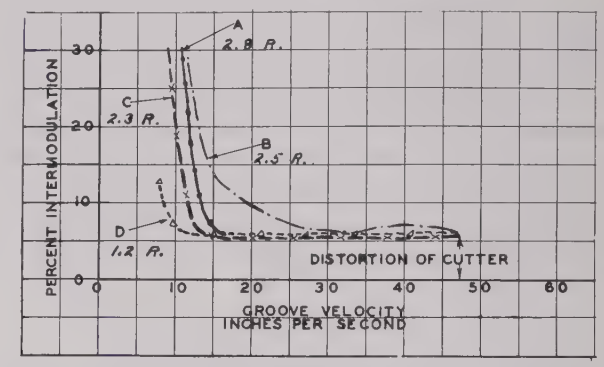

Fig. 2—Intermodulation distortion with pickups of different tip radii.
A ———— 2.8-mil tip radius
B —·—·— 2.5-mil tip radius (with approximately 1.2 mil flat)
C —×—× 2.3-mil tip radius
D ---△---△ 1.2-mil tip radius.

Calculated Results

It is always interesting to compare measured results with calculated values (providing they are fairly in agreement). Using the equations from a paper by Lewis and Hunt[3] on the theory of tracing distortion and calculating the intermodulation distortion, we obtained the solid curves shown in Fig. 3. The measured curves, after correction for distortion of the recording head and system, are shown with these, and it is believed that the agreement between calculated and measured results is remarkably good. Only the intermodulation at low linear velocities is significant in this check,

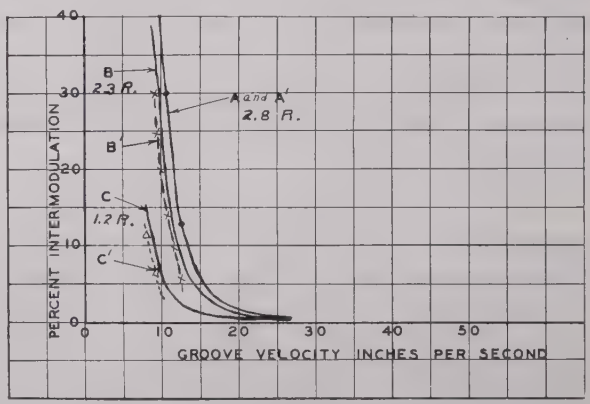

Fig. 3—Comparison of measured and calculated results of intermodulation distortion tests with pickups of different tip radii.
A ———— calculated A′ ———— measured 2.8-mil tip
B ———— calculated B′ —×—×— measured 2.3-mil tip
C ———— calculated C′ --△--△- measured 1.2-mil tip.

[3] W. D. Lewis and F. V. Hunt, "A theory of tracing distortion in sound reproduction from phonograph records," *Jour. Acous. Soc. Amer.*, vol. 12, pp. 348–365; January, 1941.

since at higher velocities the predicted tracing distortion is so low that it would be masked by distortion known to be inherent in the cutter. It will be of interest to repeat the tests using a cutter of lower distortion than was available to us at the time these tests were made. It is gratifying to have the results check so well as it strengthens one's confidence in both the calculations and in the experimental work.

Results with Excessively Polished Master

In order to obtain results due to excessive polishing, a second lacquer (cut identically with the first) was processed, and the metal master polished excessively during the processing. The results are shown in Fig. 4. The pickup with the largest tip radius now shows the least distortion, since it contacts the side walls farthest above the bottom of the groove. The change in groove contour should be greatest at the bottom for it is formed

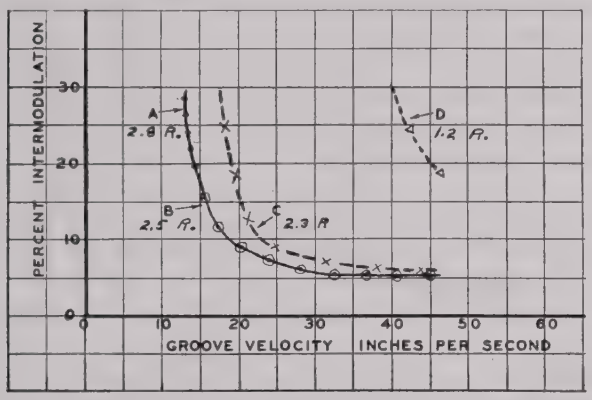

Fig. 4—Intermodulation distortion tests with pickups of different tip radii; pressing from excessively polished master.
A ———— 2.8 mil tip radius
B ———— 2.5 mil tip radius (with approximately 1.2 mil flat)
C --X--X 2.3 mil tip radius
D ---△---△ 1.2 mil tip radius.

by the top of the ridge of the stamper, where the wear is greatest because of polishing. It is interesting to note that the least change in distortion (compared with the unpolished master) was obtained with the 2.5-mil tip which had a flat of about 1.2 mil; also, the 2.8-mil tip gave the same results. The smaller tips showed greater distortion. With the 1.25-mil tip, only one measurement is indicated. This was at the outside of the 12-inch, 78 revolution-per-minute disk; at lower velocities the distortion exceeded the range of the measuring equipment.

Single-Frequency Measurements

Since 400-cycle bands had been recorded on these test records, in addition to the intermodulation bands, 400-cycle distortion measurements were possible. These were made using a distortion meter which filters out the 400-cycle fundamental and measures the residue. The results of the test with the 2.8-mil pickup are shown in Fig. 5 and are compared with the results obtained by the intermodulation method. Curves A and B show only a slight difference in 400-cycle distortion between the two pressings, and in no way indicate the difference which the intermodulation method shows. It is interesting to note that the break in the curve indicating a

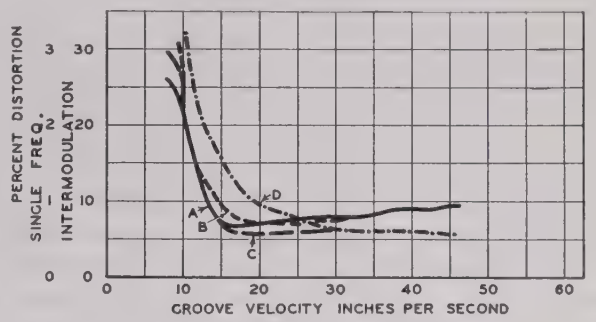

Fig. 5—Comparison of single-frequency and two-frequency (intermodulation) distortion tests. 2.3-mil playback tip radius.
A—Single-frequency (400 cycles) distortion, unpolished master
B—Single-frequency (400 cycles) distortion, polished master
C—Two-frequency (400 and 4000 cycles) distortion, unpolished master
D—Two-frequency (400 and 4000 cycles) distortion, polished master.

rapid increase in distortion occurs at the same groove velocity (about 12 inches per second) for both methods when the pressing from the unpolished master was used.

These measurements were repeated using the pickup with the 1.2-mil tip radius. The results, shown in Fig. 6, show a much greater difference in distortion between the single- and double-frequency methods with this pickup. Curve A shows the 400-cycle distortion obtained with the pressing from the unpolished master. Curve B is that obtained with the pressing from the polished mas-

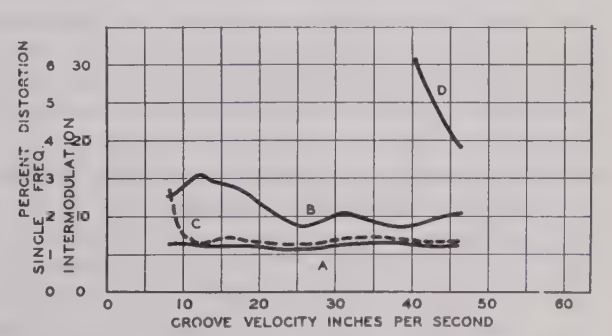

Fig. 6—Comparison of single-frequency and two-frequency (intermodulation) distortion tests. 1.2-mil playback tip radius.
A—Single-frequency (400 cycles) distortion, unpolished master
B—Single-frequency (400 cycles) distortion, polished master
C—Two-frequency-(400 and 4000 cycles) distortion, unpolished master
D—Two-frequency (400 and 4000 cycles) distortion, polished master.

ter. There is some difference between these curves; approximately one per cent at a groove velocity of thirty inches per second. But the difference is not great, and not at all comparable to that measured by the intermodulation method. This is illustrated by Curves C and D. The intermodulation distortion at thirty inches per second for the pressing from the polished master was so

great as to exceed the upper range of equipment (30 per cent). The sidebands due to intermodulation were plainly evident during listening tests, and, judging by ear, the intermodulation measurements were far more significant than the 400-cycle measurements.

Listening Tests

Good correlation was found between distortion as measured by the intermodulation tests and impairment of sound quality as judged by ear. For these tests, music obtained directly from a studio was recorded between bands of intermodulation frequencies. The processing included various degrees of polishing, and it is believed that the distortion measurements obtained from the intermodulation bands were indicative of the condition that existed in the corresponding music portions. In all cases of recordings which were judged to be inferior in quality during listening tests on a wide-range system, measurement of the corresponding intermodulation test showed high intermodulation distortion, and the magnitude of the sound impairment also accorded well with the intermodulation measurements. Fig. 4 indicates that use of a fairly large-radius reproducing tip reduces distortion of the type caused by excessive polishing, and this improvement was plainly evident in the listening tests.

Flats on the reproducer tips, which cause a noticeable impairment in quality when playing a low-distortion record, were found to cause an appreciable increase in intermodulation.

Conclusions

1. The intermodulation method of distortion testing offers many advantages in the study of distortion of disk recording and reproducing equipment. Judging by listening tests, it provides means of measuring distortion that is obnoxious to the ear, but difficult to evaluate by the single-frequency harmonic method.

2. As predicted by the theory developed by Lewis and Hunt,[3] distortion goes up almost abruptly when the linear speed falls below a certain value. The smaller the radius of the reproducing stylus, the lower the permissible minimum speed. The advantages of small tip styli, particularly for use with long-playing records, provided the record grooves are suitably shaped, have been recognized for a number of years,[4,5] but the increased refinements in record manufacture, required in order to realize this benefit, have militated against radical steps in this direction.

3. Improper relation between stylus tip and groove walls due to a stylus which is worn and no longer spherical, or to a groove which is worn or improperly shaped, can be readily detected by the intermodulation method.

4. Excessive polishing of the master was used as a means of distorting the groove and altering the shape of the recorded waves. The polishing was greater than that encountered during normal processing, but served well to bring out the injury to quality which can result if polishing is not kept to the minimum and done only with great care.

5. If the groove is improperly shaped, as by excessive polishing, the distortion is minimized by using the largest permissible tip. By "largest permissible" is meant that the tip must not ride the edges of the groove, and thus reproduce surface scratches, nor should it be so large as to result in conditions of high intermodulation distortion at minimum groove velocities, as shown in Fig. 3. Taking the normal range of velocities for 78-revolutions-per-minute records as 15 to 47 inches per second, it appears that the 2.8-mil radius would be permissible from this standpoint for the modulation levels used in the test. Loss of high-frequency response must also be expected as a result of using the larger tips.[6] This conclusion with reference to the minimizing of certain record distortions is not to be taken as advocating large- radius reproducing styli as the ideal. It is rather an expedient to which the designer of reproducing equipment (who has little control over the records which his machine may have to play) may have to resort, in spite of the sacrifice of high-frequency response and the increase of intermodulation at lower groove velocities.

6. A pickup with a worn stylus tip shows little change in playback distortion between a good record and one in which the groove contours and wave shapes are very imperfect. This may have led our predecessors to conclude that all reproducer tips should have flats so that all records will sound equally good (or poor), regardless of their groove shape or condition of wear, and may have been one of the factors (in addition to the hardening of the record) which led to the practice of mixing a little abrasive with the pressing compound, thereby making certain that a flat would be formed on the stylus tip within the first few revolutions of the turntable.

7. The close agreement between calculated and measured results encourages further theoretical study of tracing distortion. The analyses already made, confirmed by the measurements, enable us to establish much more definitely than before the desirable limits to impose with reference to minimum groove velocities, and the relation between such minimum velocities and the radius of the reproducing tip.

8. The low values of distortion found possible with optimum conditions indicate that the present-day processing methods, when properly followed, contribute little distortion, and also that pickups can be constructed which do not appreciably add to the distortion when a tip having a suitable radius is used.

[4] J. A. Pierce and F. V. Hunt, "On distortion in sound reproduction from phonograph records," *Jour. Acous. Soc. Amer.*, vol. 10, pp. 14–28; July, 1938.

[5] F. C. Barton, "High-fidelity lateral-cut disk records," *Jour. Soc. Mot. Pic. Eng.*, vol. 22, pp. 179–182; March, 1934.

[6] G. L. Beers and C. M. Sinnett, "Some recent developments in record reproducing systems," Proc. I.R.E., vol. 31, pp. 138–146; April, 1943.

A Wide-Band Transformer from an Unbalanced to a Balanced Line*

EUGENE G. FUBINI†, SENIOR MEMBER, I.R.E., AND PETER J. SUTRO‡

Summary—**The frequency characteristic of a particular type of "balun" (a transformer from an unbalanced to a balanced line) is discussed, and it is shown that by inserting a properly designed pair of quarter-wave sections to match the balun to the balanced line of higher characteristic impedance, the standing-wave ratio can be kept below 1.25 over frequency bands of the order of 4 to 1. Design parameters are given for the case of 128-ohm and 150-ohm balanced lines, for a 50-ohm unbalanced line.**

MANY WAYS of feeding a balanced load from a single-ended line have been described in the literature,[1] but very little can be found on the subject of the frequency characteristic of the corresponding transformers. Among the different types proposed, the balun represented in Fig. 1 is particularly attractive. As long as the reactance of the wire con-

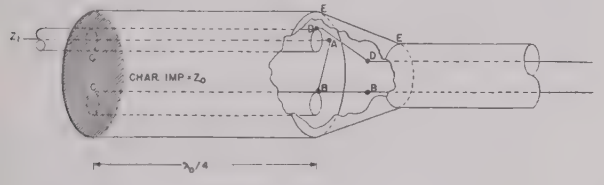

Fig. 1—Balun transformer from single-ended line to balanced line.

necting point A with point B is small compared with the reactance between the points B and C, the equivalent diagram of Fig. 2 is valid and shows that the condition for the phase is maintained for any frequency; i.e., the voltage between B and E and the voltage between

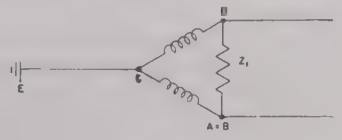

Fig. 2—Equivalent diagram of balun.

D and E are 180 degrees out of phase. When the length of the line between C and B is a quarter-wave, there is perfect matching (except for losses) between a single-ended line of characteristic impedance Z_1 and a double-ended line of the same characteristic impedance $Z_4 = Z_1$; but at frequencies different from this, the quality of the matching decreases because the reactance between B and C and between D and C is no longer very large. For example, if the characteristic impedance Z_0 of the double line inside the balun is 200 ohms, and the characteristic impedance Z_1 of the single-ended line is 50 ohms, the standing-wave ratio on the 50-ohm balanced line will be less than 1.25 over a frequency range of 2.81 to 1. On the other hand, balanced lines of 50-ohm characteristic impedance are not practical, so that the necessity arises

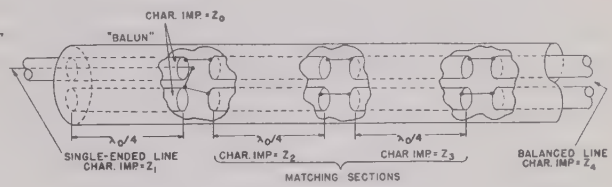

Fig. 3—Balun followed by two sections matching it to a balanced line.

of introducing some kind of transformer between the balanced terminals of the balun and the dual line. This transformer will have the function of transforming Z_1 into Z_4 (for instance, 50 ohms into 128 ohms), or vice versa.[2]

It will be shown that, if the matching section consists of two quarter-wave lines as shown in Fig. 3, the frequency band within which the standing-wave ratio is less than an assigned value can be made wider than the frequency band within which the same condition would be satisfied if the balun were terminated directly into a balanced line of the same characteristic impedance as the single-ended line ($Z_1 = Z_4 = Z_2 = Z_3$). This rather interesting fact is due to the particular frequency characteristic of the ideal load[3] (see Fig. 4) of two quarter-wave sections in cascade. A pair of quarter-wave sec-

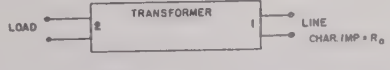

Fig. 4—Diagram defining the "ideal load" of a matching transformer.

tions designed to transform a resistance R into a resistance R_0 has an ideal load of the type shown as a solid line in Fig. 5. In this same Fig. 5 the frequency

* Decimal classification: R382.11×R117.14. Original manuscript received by the Institute, January 16, 1946; revised manuscript received, January 20, 1947.

This work was done in whole under Contract No. OEMsr-411 between the President and Fellows of Harvard College and the Office of Scientific Research and Development, which assumes no responsibility for the accuracy of the statements contained herein.

† Airborne Instruments Laboratory, Mineola, Long Island, N. Y.

‡ Columbia University, New York, N. Y.

[1] F. E. Terman, "Radio Engineers' Handbook," McGraw-Hill Book Co., New York, N. Y., 1943; page 855.

[2] Notice in this connection that, at least in the case when lossless matching transformers are used to match an ohmic resistance into another ohmic resistance, it is not necessary to specify which one of the two resistances is the load and which one the generator or the line.

[3] The "ideal load" for any transformer is that load which, applied at one end of the section, would maintain perfect matching at the other end, at any frequency; in other words, in Fig. 4, the ideal load for a section at the terminals *2* is the conjugate of the load seen from the terminals *2* looking in the direction of the terminals 1, when the resistance R_0 is connected at these latter terminals.

characteristic of the balun, as seen from the terminals BD, is also plotted for the case where $Z_0/Z_4=0.667$, and the characteristic impedance Z_1 of the single-ended line is such that $Z_1/Z_4=0.333$; e.g., $Z_4=150$ ohms, $Z_1=50$ ohms, and $Z_0=100$ ohms. The resistance and reactance are plotted relative to the characteristic impedance of the balanced line; 150 ohms in the case shown. It appears clear from Fig. 5 that the reactance of the balun near the center frequency (dashed line in Fig. 5) approximates the reactance of the "ideal load" (solid line) more nearly than a reactance which is zero throughout the whole frequency range (line of ordinate 0); this explains why the frequency band of a balun

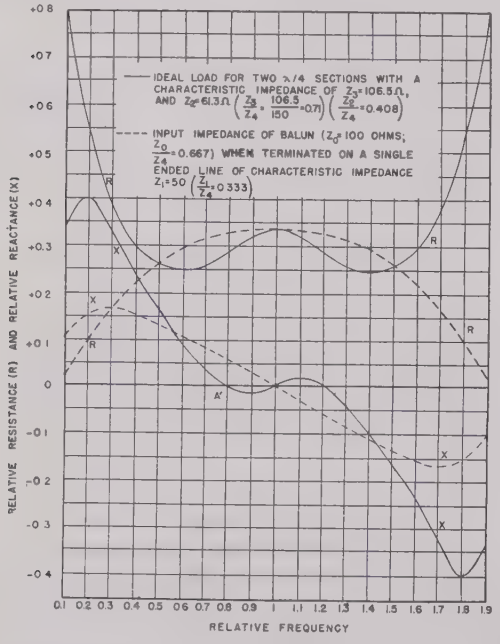

Fig. 5—Comparison of input impedance of the balun of Fig. 1

$$\left(\frac{Z_1}{Z_4}=0.333;\frac{Z_0}{Z_4}=0.667\right)$$

with the ideal load of two particular quarter-wave sections in cascade. Note: The frequencies are measured in terms of the frequency f_0 at which the sections are $\lambda/4$ long. The impedances are measured in terms of the impedance of the balanced line (150 ohms).

followed by two quarter-wave sections is better than the frequency band of the balun by itself.

In the design of a complete matching transformer of this type there are three parameters the values of which can be chosen in such a way as to get the best result: (a) the characteristic impedance Z_0 of the quarter-wave line inside the balun, and (b) the characteristic impedances Z_2 and Z_3 of the two quarter-wave sections.

The best values for these three quantities could be obtained by means of an analytic procedure. The value of Z_0 fixes the frequency characteristic of the input impedance of the balun; the values of Z_2 and Z_3 fix the shape of the ideal load of the matching sections. By means of the least-mean-squares method, it is possible to determine the values of Z_0, Z_2, and Z_3 which give a minimum standing-wave ratio in the frequency range of interest. It is much simpler, however, to follow a shorter, half theoretical, half cut-and-try process. Calculations have been carried out for two particularly important examples: the first for a transformer between a

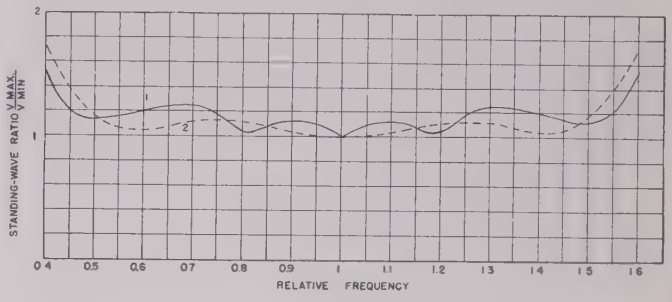

Fig. 6(a)—Standing-wave ratio in a 150-ohm balanced line connected by means of a balun to a 50-ohm single-ended line with two quarter-wave matching sections.

	Curve 1	Curve 2
Characteristic impedance of line inside balun	100 ohms	100 ohms
Characteristic impedance of first section (near balanced line)	$z_3=106.5$	$z_3=113.5$
Characteristic impedance of second section (near balun)	$z_2=61.3$	$z_2=66.$

balanced 150-ohm line and an unbalanced 50-ohm line (or, more generally, for the case $Z_1/Z_4=0.333$), the second between a balanced 128-ohm line and an unbalanced 50-ohm line (or $Z_1/Z_4=0.39$). The method actually used was as follows:

A value of Z_0 was chosen and the corresponding load impedance offered by the balun at its balanced end

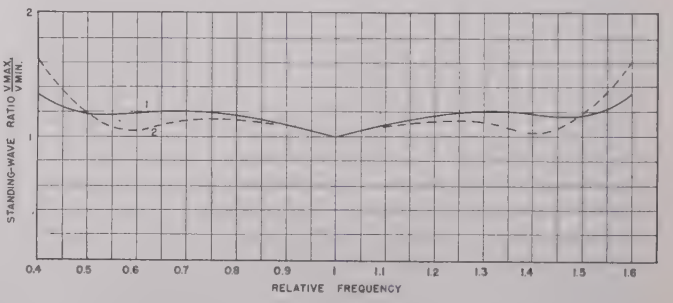

Fig. 6(b)—Standing-wave ratio in a 128-ohm balanced line connected by means of a balun to a 50-ohm single-ended line with two quarter-wave matching sections.

	Curve 1	Curve 2
Characteristic impedance of line inside balun Z_0	150 ohms	100 ohms
Characteristic impedance of first section (near balanced line)	$Z_3=95.5$	$z_3=101.3$
Characteristic impedance of second section (near balun)	$Z_2=59.7$	$z_2=63.2.$

was calculated (dashed curves in Fig. 5). Values of Z_2 and Z_3 were determined by assigning the point A' (see Fig. 5) at which the ideal load reactance crosses the zero axis, for a fixed resistance ratio $(Z_2^2/Z_3^2=Z_1/Z_4)$; then the ideal load curve for this transformer was calculated (solid curves of Fig. 5), using the standard

formulas[4] for the transformation of impedance along a section of transmission line. The ideal load was then compared with the actual load presented by the balun. For several values of Z_0/Z_4, various values of A' were tried until the optimum standing-wave ratio (as a function of frequency) appeared to have been attained (Figs. 6(a) and 6(b). The improvement obtainable over the result achieved after the first three or four trials was negligible.

It was found almost immediately that, while the best values for Z_0/Z_4 in this case are of the order of one, the exact value is not especially critical, although the transformer must be designed for the Z_0 used; that is, a value of Z_0 somewhat different from the optimum can give very nearly as good a result if the transformer is changed correspondingly. This fact permitted a considerable reduction in the number of calculations required.

The results of four such calculations (together with the corresponding values of Z_0, Z_2, Z_3) are shown in Figs. 6(a) and 6(b), in which the standing-wave ratio is plotted against relative frequency in both cases. Of the two solutions offered in each case, one maintains a standing-wave ratio below the arbitrarily assigned limit of 1.25 for a wider range of frequencies; the other, however, has the advantage that the standing-wave ratio remains lower than 1.15 over a wider frequency band.

The diagrams show that it is, therefore, possible to design matching transformers from single-ended to double-ended lines which maintain a very low standing-wave ratio (and the correct balancing condition) for frequency bands of the order of 4 to 1.

It is important to remember that all the sections should be cut so as to make them $\lambda/4$ for the arithmetic average of the frequency limits of the desired bands.[5]

These results show, in addition, the interesting fact that the transformation of a constant resistance to a constant resistance (in cases where there are no balanced-to-unbalanced devices) can be considerably improved by the addition of a parallel stub at the low-resistance end of the standard two-quarter-wave-section transformer. In effect, Fig. 2 can be considered as representing a resistance AD which is to be matched to another ohmic resistance. The results outlined in this paper show that, if the matching is achieved with two $\lambda/4$ lines, the reactance ACD (in parallel with the resistance to be matched) increases the useful frequency band.

[4] In most cases, one of the standard impedance charts based on these formulas is sufficiently accurate for the calculation.

[5] This is due to the obvious fact that any quarter-wave section transformer line acts in the same way for a frequency x per cent greater and x per cent smaller than the frequency for which it is cut.

Electrode Dissipation at Ultra-High Frequencies*

ZIGMOND W. WILCHINSKY†

Summary—**A simple method is presented for measuring the electrode dissipation in a tube operating normally in its circuit at ultra-high frequencies. Application to tube design and circuit design is indicated. Results of a typical experiment are given for a triode oscillator tube, for which values are worked out for the grid temperature distribution, required tension in grid wires, and power limitation due to grid dissipation.**

Introduction

AT ULTRA-HIGH frequencies a vacuum tube tends to operate less efficiently as the frequency increases, a considerable fraction of the loss appearing as heat in the various electrodes. Excessive electrode temperature may give rise to primary grid emission, grid buckling, change in interelectrode spacings, or high seal temperatures; any one of these difficulties may render the tube inoperable. A knowledge of the power dissipated in each electrode as a function of, say, input power, can be helpful to the circuit designer in determining the capabilities and limitations of the tube. To the tube engineer the information can be useful in designing tubes with higher power ratings.

* Decimal classification: R 252.9. Original manuscript received by the Institute, June 7, 1946.

† Formerly, Naval Research Laboratory, Washington, D. C.; now, Esso Laboratories, Standard Oil Company of New Jersey, Louisiana Division, Baton Rouge, La.

Electrode Dissipation Measurement

The schematic drawing, Fig. 1, represents a cavity oscillator using a 2C43 triode. Thermocouples were attached near the grid and plate, care being taken to keep the thermocouple leads from interfering with the high-frequency fields. A third thermocouple used for reference purposes was attached to the outer wall of the cavity.

With the oscillator operating normally, readings were recorded for rise in temperature at each thermocouple, input power (excluding heater power), high-frequency power output, and heater power. The circuit was next put into a nonoscillating condition and power was fed into the electrodes from a direct-current source in such a manner that the same combination of thermocouple temperatures was obtained. For each electrode its direct-current dissipation was, therefore, equal to its mean dissipation under oscillating conditions. Typical results obtained by this method for the oscillator operating at a frequency of 1000 megacycles are given

in Table I. The portion of the input power, thus far unaccounted for by the experiment, was lumped under the heading of miscellaneous losses, which includes experimental errors and certain types of circuit losses.

It is also possible to estimate the power dissipated in the plate and grid due to thermal radiation from the

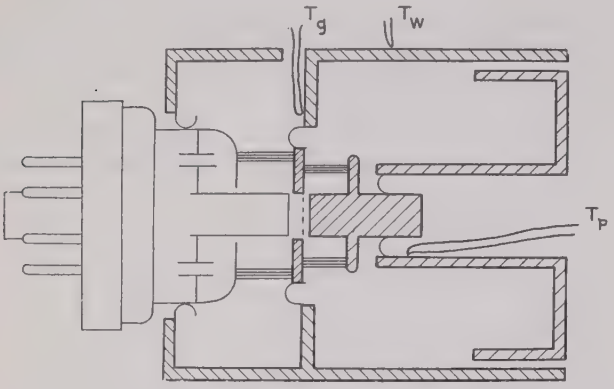

Fig. 1—Sketch of ultra-high-frequency oscillator, showing position of thermocouples. The thermocouples associated with grid, plate, and cavity wall are labeled T_g, T_p, and T_w, respectively.

cathode. Let the temperature rise at the plate, grid, and cavity-wall thermocouples be designated by T_p, T_g, and T_w, respectively. Consider the quantity T_p-T_w plotted as a function of the plate dissipation derived from the input power (see Fig. 2). Due to the resulting linear relationship[1] one can readily extrapolate the curve to $T_p-T_w=0$, the magnitude of the intercept

TABLE I
ELECTRODE DISSIPATION DATA

Measurement	Input power =3.89 watts Filament power =5.7 watts	Input power=0 Filament power =5.7 watts
High-frequency output	1.15 watts	—
Grid dissipation derived from input power	0.50 watt	—
Plate dissipation derived from input power	1.85 watts	—
Miscellaneous losses derived from input power	0.40 watt	—
Temperature rise at plate thermocouple, T_p	25.8 degrees centigrade	11.8 degrees centigrade
Temperature rise at grid thermocouple, T_g	23.5 degrees centigrade	16.2 degrees centigrade
Temperature rise at cavity-wall thermocouple, T_w	15.0 degrees centigrade	9.6 degrees centigrade

(0.5 watt) being the power radiated from cathode to plate. A similar treatment for the grid (Fig. 2) gives 1.7 watts as the power radiated from cathode to grid. Of this it is estimated that about 1.0 watt is dissipated in the wires and the remainder in the supporting structure.

A summary of the results obtained so far can be given by the following empirical equations:

Available high-frequency power = 0.30 input power (1a)
Grid dissipation = 1.0 watt + 0.13 input power (1b)
Plate dissipation = 0.5 watt + 0.47 input power (1c)
Miscellaneous losses = 4.2 watts + 0.10 input power. (1d)

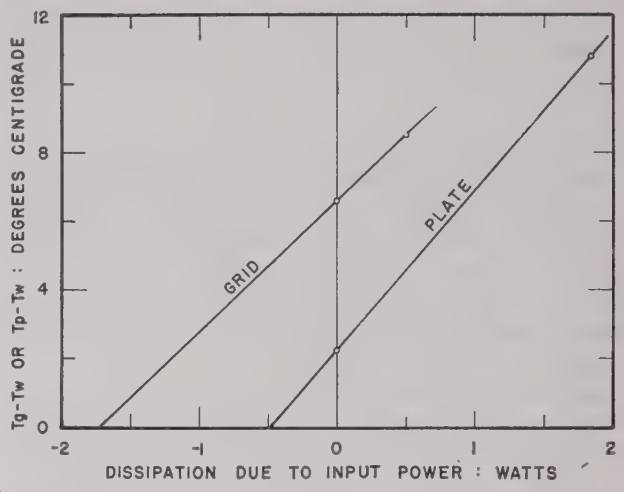

Fig. 2—Extrapolation method of finding the electrode dissipation due to radiation from cathode. Negative of intercept on axis of abscissa gives desired quantity.

APPLICATION OF RESULTS

In order to make full use of the dissipation data, one needs to know the conditions under which the circuit is to operate. However, some computations of a general nature can be made with the help of a few reasonable assumptions.

Since the grids of transmitter tubes often present considerable concern to the users of the tubes, the data obtained will be directed toward a limited analysis of some thermal properties of the grid.

Grid Temperature

The grid of the 2C43 consists of a fine square mesh stretched across a circular aperture. It can be shown that this mesh is very nearly equivalent in thermal-conduction properties to a uniform sheet of appropriate thickness. The problem then reduces to a two-dimensional radial heat-flow problem. Assuming that all the heat dissipated is eliminated by thermal conduction, the appropriate differential equation for grid temperature is

$$\nabla^2 T = \frac{\rho C}{K}\frac{\partial T}{\partial t} - \frac{p}{KD}, \tag{2}$$

the symbols used here and in subsequent equations being defined in the Appendix. If p is uniform over the grid and the periphery is held at temperature T_0, the solution to (2) is found to be

$$T-T_0=\frac{p}{4KD}(R^2-r^2) + \frac{R^2}{KD}(p_0-p)\sum_{n=1}^{\infty} a_n J_0\left(\frac{\xi_n r}{R}\right)\exp(-t/\tau_n). \tag{3}$$

[1] The relationship is practically linear if essentially no power is radiated from either the plate or grid.

This equation gives the temperature at any point on the grid mesh as a function of the distance from the center of the grid and the time t. It is assumed that for $t=0$ there exists a steady state characterized by p_0. Since the first term in the transient is the most significant, the approach to the steady state is governed chiefly by exp $(-t/\tau_1)$; hence an approximation of (3) can be written

$$T - T_0 = \frac{(R^2 - r^2)}{4KD}\left[p + (p_0 - p)\exp(-t/\tau_1)\right]. \quad (4)$$

The value of τ_1, for the 2C43 tube, was computed to be 0.045 second, indicating that the transient may become significant in certain pulsed circuit applications.

In passing it is interesting to note that the steady-state solution has the same form for any arrangement of uniform wire stretched across the aperture as for a mesh, provided that the dissipation per unit length of wire is uniform. Another observation is that, if the steady-state part of (3) is written in the form

$$T - T_0 = \frac{P}{4\pi KD}\left(1 - \frac{r^2}{R^2}\right), \quad (5)$$

it can be seen that the temperature at the center of the grid is independent of the radius of grid aperture for a given value of grid dissipation.

Grid Emission

A grid that has accumulated a coating of oxide cathode material may become a good emitter at a temperature in the neighborhood of 750 degrees centigrade. With the help of (5) one can estimate the maximum grid dissipation at which troublesome grid emission is likely to set in. The results may be translated into maximum power input or output via (1a), (1b), and (1c). For the tube under consideration, with the periphery of the grid at a temperature $T_0=200$ degrees centigrade, and the center at 750 degrees centigrade, the maximum grid dissipation allowable is computed to be 11 watts, corresponding to an input power of 85 watts and an output of 25 watts.

Required Tension in Grid Wires

If the grid wires were not stretched, thermal expansion would cause the grid to buckle as its temperature increased. Since the longest wires get hottest and expand more than the others, one can proceed by computing the thermal expansion of these wires,

$$\Delta R = \int_0^R \epsilon(T - T_0)dr = \frac{\epsilon RP}{6\pi KD}, \quad (6)$$

if ϵ is taken to be a constant. The tension at temperature T_0, necessary to just overcome the anticipated expansion, can be estimated with the help of Young's modulus

$$E = \frac{F/A}{\Delta R/R}. \quad (7)$$

Combining (6) and (7), one obtains the tension

$$F = \frac{\epsilon AEP}{6\pi KD} \quad (8)$$

which, incidentally, is independent of the grid aperture size. It is convenient to express the tension in terms of the ultimate tensile strength. Hence, for $P=11$ watts, corresponding to a maximum allowable grid temperature of 750 degrees centigrade, the required tension is 14 per cent of the ultimate tensile strength.

Discussion

For a particular use of a tube, electrode dissipation data could probably be applied much more extensively than indicated here. However, it should be pointed out that this may not always be the most economical procedure in attaining practical results. Many successful tubes and circuits have been built with only casual regard for electrode dissipation. However, some situations in which a knowledge of electrode dissipation is particularly desirable are: (a) applications where a tube is being run near its physical limits, (b) predicting suitability of a tube in applications for which circuits are not available, (c) analyzing tube difficulties suspected of being caused by electrode dissipation, and (d) as experimental data for theoretical studies of certain types of microwave generators.

Acknowledgments

The author wishes to acknowledge his indebtedness to the late Robert A. Corliss for his most capable assistance in the experimental part of this report.

Appendix: Explanation of Symbols

C = specific heat
ρ = density
K = heat conductivity
T = temperature at point on the grid
t = time
P = dissipation in grid wires due to all causes
p = power dissipated per unit area of grid aperture
p_0 = value of p prior to $t=0$
D = thickness of disk, equivalent in thermal properties to square mesh = (number of wires per unit length) × (cross-section area of one wire)
A = cross-section area of a wire
R = radius of grid aperture
r = radial distance from center of grid
ξ_n = nth zero of $J_0(x)$
$J_m(x)$ = Bessel function of x, of order m
$a_n = J_2(\xi_n)/\xi_n^2 J_1^2(\xi_n)$
$\tau_n = \rho CR^2/K\xi_n^2$
E = Young's modulus
ϵ = coefficient of thermal expansion
F = wire tension.

An Electron-Ray Tuning Indicator for Frequency Modulation*

F. M. BAILEY†, MEMBER, I.R.E.

Summary—**The design features of an electron-ray tuning indicator for frequency modulation which can be operated directly from a discriminator are described. The electrode configuration features high deflection sensitivity and a translucent fluorescent screen.**

Introduction

THE ELECTRON-ray indicator tube has received wide acceptance as a device for providing accuracy in tuning an amplitude-modulated signal in a receiving set. In this application, dial setting is accomplished by indicating a maximum voltage point. Frequency-modulation tuning is somewhat different in that it requires a device which will compare one voltage with a reference voltage and indicate when the two voltages are equal. By the use of additional tube and circuit components, a standard electron-ray tube can be made to do this, but at extra expense. The development of the ZP-601[1] was undertaken to find an electron system which would satisfy the requirements of a frequency-modulation tuning indicator. This work has made available an electronic indicator tube which, in addition to indicating a change in magnitude, compares the magnitude of two voltages, and for frequency-modulation signals indicates the direction of mistuning.

Fundamental Requirements of a Frequency-Modulation Tuning Indicator

With existing commercial discriminator circuits, the output voltage varies plus and minus 10 volts with respect to ground when the set is tuned through the signal. This gives a frequency versus voltage characteristic of approximately 10 kilocycles per volt for the standard 200-kilocycle pass band. To provide distortionless signals, the carrier should be tuned within 2 kilocycles of the center of the discriminator or within 0.2 volt. The tuning indicator must therefore be capable of detecting a voltage difference of plus or minus 0.2 volt with respect to ground. In addition, when the control voltage becomes positive the indicator should not draw an appreciable current, since the shunt resistance permitted across the discriminator for less than 1 per cent distortion is 1 megohm.

Inasmuch as the voltage produced by the discriminator is zero for both on-tune and off-channel conditions, a tuning eye which merely compares voltage would provide the same presentation for both conditions. There are two possible methods of providing a difference in on-signal presentation. One is to change the pattern by means of the negative limiter voltage developed in the grid circuit of the first limiter, and the other is to employ negative squelch voltage to alter the pattern when off channel.

Because the measurement of the discriminator voltage is a direct-current measurement, it is very desirable that the indicator be free from the thermal and contact-potential variations which are inherent in a direct-coupled system. The voltage used in the operation of the tube should not exceed 250 volts. The target or fluorescent area should be as near the front of the bulb as possible, preferably closer than in existing tuning indicators. The associated circuit should not require more than a few resistors.

The Deflection System

The mechanism of the cathode-ray tube provided the basis for the design of initial tubes. A cylindrical cathode produced a rectangular-shaped pattern, the sides of which were controlled by deflectors. One deflector was divided at the center, providing two independent electrodes on one side. Half of the pattern was then deflected with respect to the other half, forming a comparison type of presentation with one half indicating the reference voltage, and the other half the discriminator voltage.

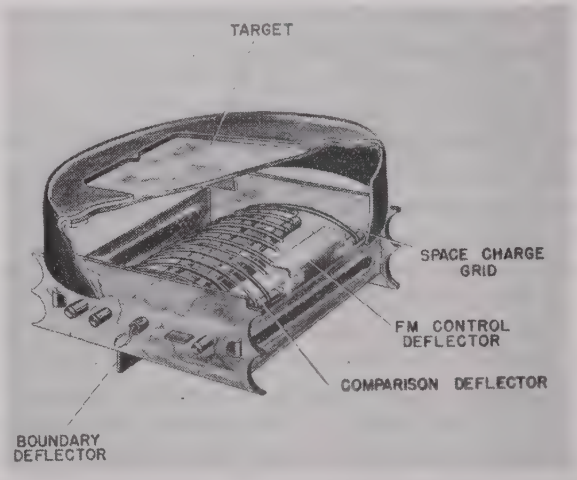

Fig. 1—Space-charge grid and deflector assembly.

By placing a space-charge grid around the cathode and deflection electrodes, the sensitivity of the deflection system was considerably increased. (See Fig. 1.) This grid provided an extensive region around the cathode in which the electrons travel at rather slow velocities and can therefore be more easily deflected by charged wires. After being deflected the electrons penetrate the space-charge grid and move in more or less rectilinear paths toward the target.

* Decimal classification: R339×R361.214. Original manuscript received by the Institute, July 21, 1946; revised manuscript received, September 24, 1946.

† General Electric Co., Schenectady, N. Y.

[1] Tubes of this type, manufactured for commercial purposes, have been assigned the RMA number 6AL7-GT.

The opacity of the space-charge grid controls the sensitivity as well as the brightness of the pattern. The grid position and pitch were adjusted to compromise these two factors to the point where the brightness was greater than 4 foot-lamberts and where the sensitivity was 10 volts for $\frac{1}{8}$ inch. This adjustment was made with the space-charge grid connected to the cathode. A plot of deflection sensitivity and brightness as a function of plate voltage for three different grid meshes is shown in Figs. 2 and 3. The sensitivity at 1/100 inch is greater than that at $\frac{1}{8}$ inch, so that it is possible to obtain a plus or minus 0.2-volt setting and maintain adequate brightness. In addition, the space-charge grid is brought out on a separate pin so that a negative bias can be applied to reduce the brightness and increase the deflection sensitivity.

The frequency-modulation deflection electrodes are mounted on one side of the cathode and give a twin deflection pattern at one edge of the target. An electrode

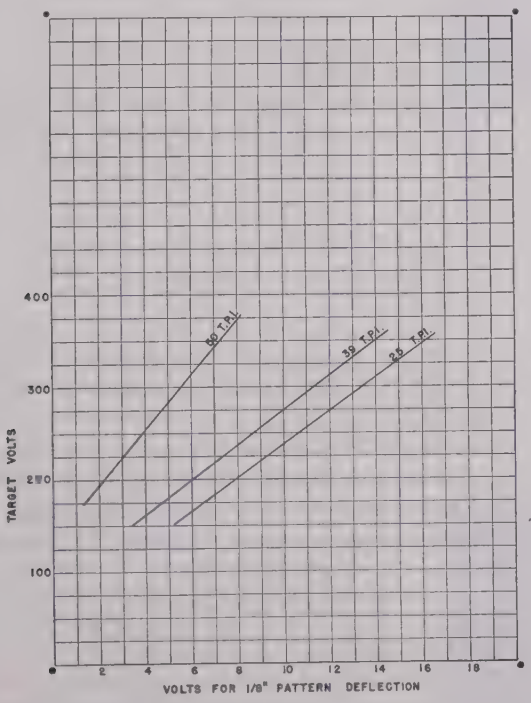

Fig. 2—Deflection sensitivity as a function of target voltage.

placed on the other side of the cathode forms a fixed boundary for that side of the pattern. This electrode may be connected to the limiter voltage in the frequency-modulation set and used to deflect that edge of the pattern when the set is on channel, thus making the pattern different when tuned on channel than when tuned off channel. For amplitude-modulation receivers the deflectors may be connected together and connected to the automatic-volume-control voltage. This causes the rectangular pattern to become narrow as the receiver is tuned to maximum signal. By placing the amplitude-modulation deflector at a greater distance from the cathode than the frequency-modulation deflector, a remote-cutoff characteristic can be obtained for the amplitude-modulation presentation and accuracy of tuning maintained for both strong and weak amplitude-modulation signals.

For a frequency-modulation receiver which has a squelch circuit for biasing the radio-frequency tubes to cutoff between stations, the squelch voltage may be applied to the space-charge grid of the tuning indicator,

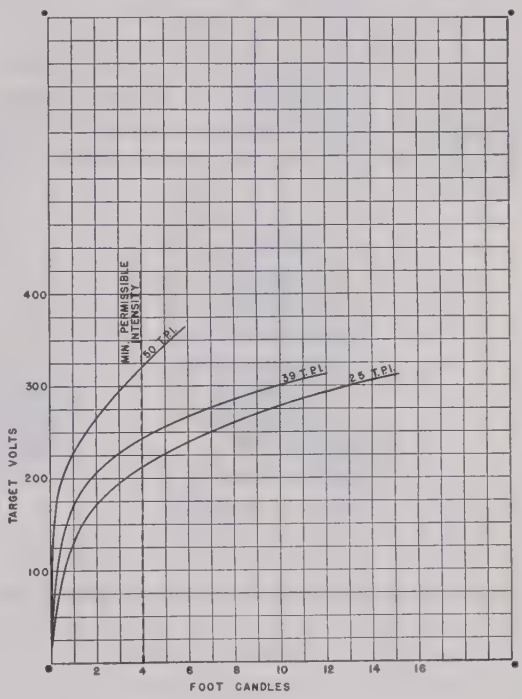

Fig. 3—Brightness as a function of target voltage.

causing the fluorescent pattern to be blanked out between channels. This provides a second scheme for making the on-channel signal different from the off-channel signal and is preferable to the system employing limiter voltage. It requires approximately 6 volts to reduce the target current of the tube to the point where the fluorescent screen cannot be seen with 315 volts applied to the target.

Deflector Design

Under the space-charge operation of deflecting wires, the deflection with positive voltage is always greater than the deflection with negative voltage. This greater sensitivity in the positive range is useless for practical purposes, since the current which the deflectors draw produces enough voltage drop in the 1-megohm filtering resistor to reduce greatly the operating voltage at the deflector.

The current drain can be diminished by utilizing fine deflection wires. From a manufacturing point of view, however, rigidity of the deflector assembly was most important. It was decided, therefore, to remove the bottom half of the space-charge grid to enable a rather large structure to be used to support the deflecting electrodes. With this arrangement it is necessary to use a cathode-bias resistor in order to place a positive potential on the cathode with respect to the deflectors so that deflection

in the positive direction may be obtained without drawing current to the deflectors.

The position of the deflectors with respect to the cathode controls the position of the boundary of the fluorescent pattern. The accuracy with which the divided deflectors are positioned controls the zero setting of the voltage-comparison arrangement.

Target Design

The fluorescent target of the ZP-601 is a translucent screen operated at low voltage. It is therefore necessary that the willemite screen be backed with a transparent electrical conductor in order to prevent charging of the

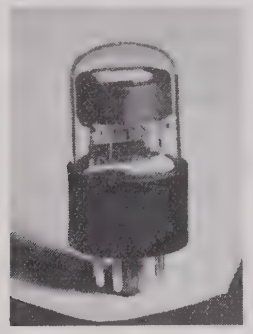

Fig. 4—Photograph of tuning-indicator tube (ZP-601).

screen for want of sufficient secondary emission. A deposit of tin chloride applied in a hot oven provided coatings of resistance between 10,000 and 40,000 ohms per square. Satisfactory operation of the target was obtained with a resistance of 200,000 ohms per square or less.

Since the brightness of the fluorescent surface must be greater than some minimum value (4 foot-lamberts), it is necessary to provide a screen with the most efficient thickness of willemite coating. If the willemite coating is too thin, insufficient light will be produced. If the coating is too thick, the opacity of the coating will be detrimental to the transmission of light through it. Furthermore, if the coating is too thick, when operating at 250 volts the ability of the conductive backing to remove charges from the screen will be impaired and the fluorescent pattern distorted or deflected completely. At 250 volts the maximum brightness occurs at a thickness corresponding to 20 per cent transmission of light, while greater thickness results in a charged screen. As a result, the tubes are made with screens coated at approximately 25 per cent.

Summary

A photograph of the final tube is shown in Fig. 4. The structure incorporates the characteristics outlined in the previous discussion, and is contained in a T-9 envelope. The tube features a translucent fluorescent target, a rectangular divided pattern, adequate sensitivity for both amplitude-modulation and frequency-modulation detectors without additional amplifiers, and a control grid for the application of squelch voltage. Circuit diagrams with corresponding tuning patterns are shown in Fig. 5.

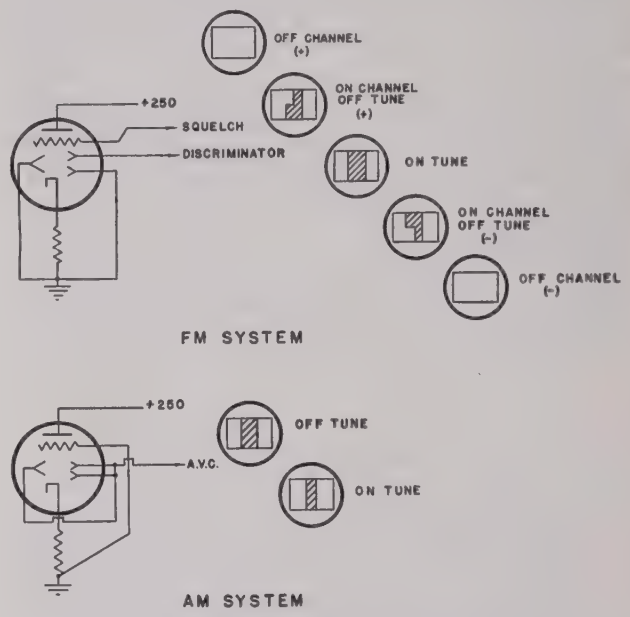

Fig. 5—Circuit diagram and tuning patterns.

Acknowledgment

The author is indebted to C. H. Bachman and D. W. Jenks for their helpful suggestions and criticisms in carrying out the development program, and to Helen C. Hertha for her part in fabricating and testing the many development samples.

Contributors to Waves and Electrons Section

F. M. Bailey was born in Yachow, China, on January 10, 1916. He was graduated from the University of Rochester with the B.S. degree in physics in 1937, and received the Ph.D. degree from Iowa State College in 1940. Since 1940, Dr. Bailey has been associated with the General Electric Company in the general engineering and electronics laboratories, working on high-frequency developments. For the past three years he has been occupied with advanced developments on receiving tubes in the electronic tube division. He is a member of the American Physical Society and of Sigma Xi.

Kenneth Bullington (A'45) was born at Guthrie, Okla., on January 11, 1913. He received the B.S. degree in electrical engineering in 1936 from the University of New Mexico, and the M.S. degree in 1937 from M.I.T. Since 1937 he has been a member of the technical staff of Bell Telephone

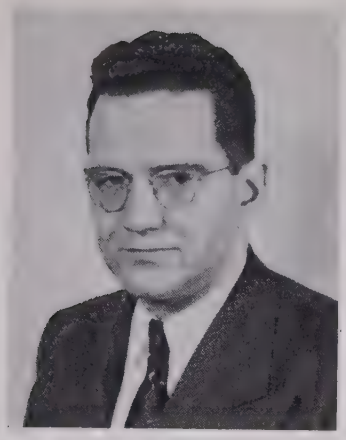

F. M. Bailey

❖

Laboratories, where he is engaged in wire and radio transmission problems.

❖

Eugene E. Fubini (A'39–SM'46) was born in Turin, Italy, in 1913. He received the Doctor of Physics degree from the university of Rome in 1933, after which he joined the National Institute of Electrotechnics at Turin, Italy, where he remained until 1938. From 1938 until 1942 he was associated with the Columbia Broadcastin System in New York City. During the years 1944 and 1945 he was technical observer in the Mediterranean Theater, in charge of radio countermeasures section of O.A.S., 8th Air Force, as consultant to Air Commander Officer, headquarters, A.A.F. He also served as research associate at the Radio Research Laboratory at Harvard during the latter part of 1945. At present Dr. Fubini is the supervising engineer of the special devices group, Airborne Instruments Laboratory, Inc., Mineola, N. Y.

❖

Thure E. Hanley (A'42) was born in 1911 in Seattle, Wash. He received the B.S. degree in physics at the University of Washington in 1936. For the last five years he has worked with the Consultants Group at the Naval Research Laboratory in Washington, D. C. At present he is with the Vacuum Tube Research Section of the Naval Research Laboratory. He is a member of the American Physical Society.

❖

Kenneth Bullington

Andrew V. Haeff (A'34–M'40–SM'43) was born in Moscow, Russia, on December 30, 1904. In 1928, he received the degree of Electrical and Mechanical Engineer from the Russian Polytechnic Institute at Harbin, China. In 1928 he majored in electrical engineering at the California Institute of Technology, where he obtained the M.S. degree in 1929 and the Ph.D. degree in 1932.

❖

Eugene E. Fubini

❖

Until the end of 1933, Dr. Haeff was a Special Research Fellow in the C.I.T., engaging in research work on ultra-high-frequency problems. From 1934 to 1941, Dr. Haeff was a member of the vacuum-tube research section of the RCA Manufacturing Company, specializing in research on u.h.f. tubes and circuits. On March 1, 1941, he joined the research staff of the Naval Re-

❖

Thure E. Hanley

❖

search Laboratory at Washington, D. C., in order to devote his full time to naval research problems particularly in connection with wartime development of radar. His present position is that of Consultant in Electronics at the Naval Research Laboratory. For a photograph of Dr. Haeff, see the November, 1946, issue of the Proceedings.

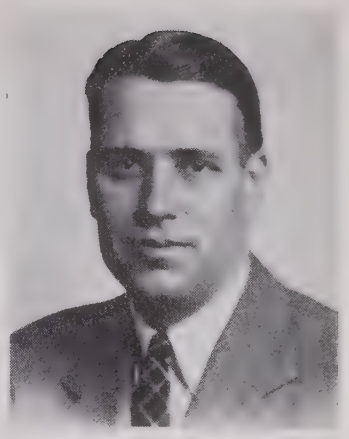

E. M. Ostlund

E. M. Ostlund (A'37–SM'44) was born October 24, 1903, in Minneapolis, Minn. He received the B.E.E. degree from the University of Minnesota in 1931. In 1924 and 1925, he was employed in the engineering test course of the General Electric Company, Schenectady, N. Y. The next two years were spent with the Brunswick-Balke-Collender Company, Chicago, Ill., as a radio receiver engineer. After additional service with G. E., and completion of college training, he was employed as a senior research engineer in the electronics laboratory of the Electro-Physical Institute, Leningrad, U.S.S.R. from 1932 to 1934. In 1934, Mr. Ostlund joined the engineering department of Federal Telegraph Company as a vacuum-tube development engineer on transmitting tubes and circuits. He was transferred in 1940 to Federal Telecommunication Laboratories, and is now serving in the Nutley laboratories as a department head in charge of development of commercial and special transmitting and receiving equipment. He is a member of the American Physical Society and the Institute of the Aeronautical Sciences.

❖

E. R. Piore (A'38–M'42–SM'43) received the B.A. and Ph.D. in physics at the University of Wisconsin in 1930 and 1935. He was assistant instructor in physics at the same university from 1935 to 1938, and in 1938 joined the Radio Corporation of

E. R. Piore

H. E. Roys

❖

America, Camden, N. J., as a research physicist. In 1942 he became engineer in charge of the television laboratories at the Columbia Broadcasting System. Since April, 1942, he has been with the Navy first as a civilian section head in the electronics division, Bureau of Ships, then as an officer in the Office of the Deputy Chief of Naval Air operations. At present Dr. Piore is director of the Physical Sciences Division, Research Group, Office of Naval Research. He is a member of the American Physical Society and Sigma Xi.

❖

H. E. Roys (A'27) was born on January 7, 1902, in Beaver Falls, Pa. He received the B.S. degree in electrical engineering from the University of Colorado in 1925. From 1925 to 1930, he was with the radio department of the General Electric Company at Schenectady. Since 1930, when he was transferred to the RCA-Victor Company in Camden, N. J., he has been associated with that company. Disk recording and reproduction problems have been his main concern for a number of years.

❖

Martin Silver (A'42) was born in New York, N. Y., on August 25, 1920. He graduated from New York University in 1941 with a bachelor degree in engineering.

Martin Silver

Upon leaving college, he entered Federal Telecommunication Laboratories and was assigned to investigate communication-type jamming equipment. Since the termination of the war he has been actively engaged in the development of frequency-modulated broadcast transmitters, monitors, links, and associated equipment.

❖

Charles B. Smith (A'43) was born in Enterprise, Miss., on August 5, 1919, and graduated from the high school in Silver Spring, Md., in June, 1937. For three

Charles B. Smith

years he worked as a radio serviceman in Washington, D. C. In 1940 he attended the Capitol Radio Engineering Institute, graduating in June, 1941. He went to work in the Consultants Group of the Naval Research Laboratory in July, 1941, where he stayed until 1945. He is now with the Vacuum Tube Research Section of the Naval Research Laboratory, Washington, D. C.

❖

Peter J. Sutro

Peter J. Sutro was born on June 20, 1921, at New York, N. Y. He received the B.A. degree in physics from Harvard University in 1942. During the war, from 1942 to 1946, he was working on radar countermeasures as a research associate at the Radio Research Laboratory of Harvard University, which was operated under a contract with the Office of Scientific Research and De-

A. R. Vallarino

❖

velopment. He has now resumed his studies in the physics department of Columbia University. He is a member of the American Physical Society.

❖

A. R. Vallarino (S'43–A'44) was born in Panama City, Panama, on August 11, 1913. He was graduated in electrical engineering from Stanford University in 1939. Transferring his studies to electrical communications, Mr. Vallarino spent the next three years in graduate and research work at Stanford University. In 1943 he joined the Federal Telecommunication Laboratories, where he is employed as a research engineer.

❖

Zigmond W. Wilchinsky was born in New York, N. Y., on August 26, 1915. He received the B.S. degree in education from Rutgers in 1937, and the M.S. degree in physics from the same institution in 1939. In 1942 he received the Ph.D. degree from the Massachusetts Institute of Technology and joined the staff of the Radiation Laboratory of M.I.T. the same year, where he was engaged in local-oscillator development. From 1943 to 1946 Dr. Wilchinsky was at the Naval Research Laboratory, working on development of circuits and tubes for triode microwave oscillators. At present, he is with the Standard Oil Company of New Jersey, engaged in petroleum research.

Zigmond W. Wilchinsky

Abstracts and References

Prepared by the National Physical Laboratory, Teddington, England, Published by Arrangement with the Department of Scientific and Industrial Research, England, and *Wireless Engineer*, London, England

The number in heavy type at the upper left of each Abstract is its Universal Decimal Classification number and is not to be confused with the Decimal Classification used by the United States National Bureau of Standards. The number in heavy type at the top right is the serial number of the Abstract.

The Annual Index to these Abstracts and References, covering those published from January, 1946, through December, 1946, may be obtained for 2s. 8d., postage included from the *Wireless Engineer*, Dorset House, Stamford St., London S. E., England.

ACOUSTICS AND AUDIO FREQUENCIES

534.13 2654
The Vibrations of Certain Coupled Systems—(*See* 2728.)

534.213(26.03) 2655
Underwater Sound Propagation—(*Tele-Tech*, vol. 6, p. 39; April, 1947.) Experimental evidence is given of the existence of sound channels at depths of 300–400 ft. in the Atlantic and 600–700 ft. in the Pacific; their depth depends on the vertical temperature gradient.

534.32:621.396.722 2656
Distortion and Acoustic Preferences—J. Moir. (Proc. I.R.E., vol. 35, p. 495; May, 1947.) Comment on 612 of April. See also 2554 of September and back reference.

534.414 2657
Properties of Simple and Multiple Cylindrical Acoustic Resonators—P. Wirz. (*Helv. Phys. Acta.*, vol. 20, pp. 3–26; February 15, 1947. In German.) The fine structure of the resonance curves of acoustic resonators observed by Zickendraht (3030 of 1942) is found to be due to interference effects. A method is described for obtaining the true resonance curves and from them evaluating the decrement, which is in good agreement with the value obtained from photographic records of the amplitude of the oscillations excited by short-time application of a stimulus of the same frequency as that of the resonator. The well known formulas for the frequency correction at the mouth of the resonator can be improved by the introduction of a term taking account of the width of the flange there. Experiments with bundles of similar tubular resonators are described and a method is given for observation of the air motion at the mouth of an excited resonator.

534.845.1 2658
Measurement of Sound Absorption by Phase-Shift Determinations—G. Sacerdote. (*Alta Frequenza*, vol. 16, pp. 98–100; April, 1947. In Italian, with English, French, and German summaries.) The absorption of an acoustic material can be found from phase difference measurements at three points in a Kundt's tube.

534.861.1 2659
Acoustical Design of Broadcast Studios—J. Peterson. (*Tele-Tech*, vol. 6, pp. 52–55, 127; March, 1947.) A discussion of modern surface treatments to eliminate echoes and other objectionable features.

534.861.1 2660
The Acoustical Design of F.M. Studios—E. J. Content. (*Tele-Tech*, vol. 6, pp. 30–34; April, 1947.) A discussion of the factors involved in the improvement of over-all frequency response and sound distribution in the studio.

534.88 2661
Sonar—The Submarine's Nemesis—McProud. (*See* 2777.)

621.395.623 2662
Sensitivity and Impedance of Electro-Acoustic Transducers—P. Vigoureux. (*Proc. Phys. Soc.*, vol. 59, pp. 19–30; January 1, 1947.) Using the method of equivalent electric circuits the output voltage is deduced in terms of the radiation resistance and the pressure. The radiation resistance can be measured by purely electrical means. The construction of impedance and admittance diagrams is explained, and it is shown how the maximum acoustic output can be obtained from electrical measurements without any acoustic measurements.

621.395.623:534.835 2663
Telephone Transmissions in Noisy Surroundings—G. Nicolle. (*Ann. Radioélec.*, vol. 2, pp. 78–86; January, 1947.) The methods adopted to improve the signal-to-noise ratio usually involve some process favoring the signal such as bringing the microphone close to the mouth of the speaker, reducing the noise by insulation, and making the apparatus as directional as possible. An alternative method proposed makes use of a differential action of two microphone elements, equally sensitive to the surrounding noise, with a directional arrangement allowing speech to affect only one of the elements. A very marked improvement in the signal-to-noise ratio is thus obtained without the use of sound insulation.

621.395.623.73 2664
Wide Range Loudspeaker Developments—H. F. Olson and J. Preston. (*RCA Rev.*, vol. 7, pp. 155–178; June, 1946.) A reprint was abstracted in 993 of May.

AERIALS AND TRANSMISSION LINES

621.315.212:621.392.029.64 2665
Guided Waves in a Coaxial Line—G. Goudet and J. Lignon. (*Onde Élec.*, vol. 27, pp. 152–159; April, 1947.) Discussion of propagation in the annular space of coaxial cables to see whether normal cables can be used for u.h.f. transmission. Coaxial cables should be designed for propagation only of the fundamental wavelength. At the higher frequencies wave guides should be used.

621.315.212:621.397.74 2666
The Provision in London to Television Channels for the B.B.C.—H. T. Mitchell. (*P.O. Elec. Eng. Jour.*, vol. 40, part 1, pp. 33–36; April, 1947.) An account of recently installed coaxial cable and the associated repeater equipment.

621.315.213.12:621.397.5 2667
Development of an Ultra Low Loss Transmission Line for Television—E. O. Johnson. (*RCA Rev.*, vol. 7, pp. 272–280; June, 1946.) A 300-ohm parallel-wire polyethylene dielectric feeder having an attenuation less than 0.8 db per 100 ft. at 50 Mc. It is weather proof and cheap to manufacture.

621.38/.39].029.64 2668
Microwave Electronics—J. C. Slater. (*Rev. Mod. Phys.*, vol. 18, pp. 441–512; October, 1946.) This comprehensive article "is essentially a set of notes for lectures delivered during the winter of 1945–46." It is written from the standpoint of a physicist and includes chapters dealing with (a) the 4-terminal network and the transmission line, (b) wave guides, (c) resonant cavities, (d) applications of the theory of resonant cavities, and (e) electronics of the reflex klystron and magnetron.

621.392.029.64 2669
On the Transmission of H. Waves in Guides of Circular Cross Section—M. Jouguet. (*Compt. Rend. Acad. Sci.* (Paris), vol. 224, pp. 998–1000; March 31, 1947.) In a straight guide the H. wave is practically stable for accidental curvatures, which on the average balance out, but its attenuation only approximates to the theoretical value if these curvatures are very small. See also 1667 of July and back references.

621.392.21 2670
Propagation Characteristics of a Uniform Line—C. Micheletta. (*Alta Frequenza*, vol. 16, pp. 47–49; February, 1947. In Italian.) Simple formulas are derived for the attenuation and phase constants using results given by Macdiarmid and Orchard (2476 of 1946).

621.392.22 2671
Non-Uniform Transmission Lines and Reflection Coefficients—L. R. Walker and N. Wax. (*Jour. Appl. Phys.*, vol. 17, pp. 1043–1045; December, 1946.) Summary in *Bell Sys. Tech. Jour.*, vol. 26, p. 393; April, 1947.) A first-order differential equation for the voltage reflection coefficient of a nonuniform line is

derived and is applied to the calculation of the resonant wavelengths of tapered lines.

621.392.4.029.58 [-621.396.67.029.58]:621.317.3 2672

The Testing of High-Frequency Aerial Systems and Transmission Lines—E. J. Wilkinson (*Proc. I.R.E.* (Australia), vol. 8, pp. 4–20; February, 1947.) A full description of the aerial arrays and transmission lines used at Shepparton, Victoria, Australia, for operation on frequencies between 6 and 22 Mc. and the theoretical considerations underlying their design. The procedure for setting up and testing the system is given in detail. A series of appendixes deal with switching and matching stubs, transmission-line unbalance, behavior of $\lambda/4$ and $\lambda/2$ lines, and evaluation of line terminations.

621.392.43:621.317.33 2673

Impedance Measurement on Transmission Lines—D. D. King. (Proc. I.R.E., vol. 35, pp. 509–514; May, 1947.) "A derivation of the formulas available for the measurement of terminal impedances on transmission lines is given in terms of hyperbolic functions. The accuracy and usefulness of a number of different methods are considered. Results are obtained in a form suitable for convenient application to practical measuring problems involving standing-wave and resonance-curve methods."

621.392.43:621.317.72.02 .56/.58] 2674

The "Micromatch"—Jones and Sontheimer (*See* 2853.)

621.396.615.141.2 : 621.314.2.029.64 : 621.315.613.7 2675

Waveguide-Output Magnetrons with Quartz Transformers—Malter and Moll (*See* 2712.)

621.396.67 2676

Recent Theories of the Aerial: Part 4—É. Roubine. (*Onde Élec.*, vol 27, pp. 160–169; April, 1947.) Conclusion of 2012 of August and 2332 of September. Outlines are given of a symbolic method for the integration of the Hallén equation and of the methods of King, Blake, and Harrison (1933 and 1934 of 1944), of Bouwkamp (2197 of 1944), of King and Middleton (1771 of 1946), and also of the modifications of Hallén's theory suggested by Miss Gray (1931 of 1944). It is impossible at present to decide which of these theories is best, owing to the difficulty of measuring input impedance accurately.

621.396.67 2677

2500-Foot Vertical Antenna—(*Electronics*, vol. 20, pp. 188, 190; May, 1947.) A German aerial system supported by an electrically driven captive helicopter.

621.396.67.029.64 2678

Microwave Omnidirectional Antennas—H. J. Riblet. (Proc. I.R.E., vol. 35, pp. 474–478; May, 1947.) Design considerations for omnidirectional 3- and 10-centimeter aerials are summarized. Elements used in the construction of aerials of this type are described.

621.396.67.029.64 2679

Parallel Plate Optics for Rapid [Aerial] Scanning—S. B. Myers. (*Jour. Appl. Phys.*, vol. 18, pp. 221–229; February, 1947.) Consideration of the problem of shaping two curved parallel plates, between which the energy feed is placed so that circular motion of the feed will produce an oscillating beam at a straight aperture. The latter serves as a line source for a bifocal reflector which facilitates the desired scanning. The method was developed to obviate rapid movement of parabolic aerials.

621.396.67:517.512.2 2680

Fourier Transforms in Aerial Theory: Part 1—J. F. Ramsay. (*Marconi Rev.*, vol. 9, pp. 139–145; October and December, 1946.) "The radiation pattern of a narrow-beam aerial can be formulated as the Fourier Transform of the aperture excitation. Examples are given of simple equiphase aperture characteristics and the evaluation of the corresponding polar diagrams. Four basic patterns are plotted, corresponding to the symmetrical, in-phase excitations known as "constant," "triangular," "cosine," and "cosine squared."

621.396.671 2681

Partially-Screened Open Aerials—R. E. Burgess. (*Wireless Eng.*, vol. 24, pp. 145–149; May, 1947.) "A simple approximate theory based on the transmission-line equations is developed for an open aerial, a portion of which is enclosed in a concentric conducting screen. The voltage and current distributions in the transmitting case are deduced. From these the effective heights of the "screened" and unscreened portions of the aerial are calculated and it is found that as the length of the unscreened portions increases so the effective height of the screen portion tends to equality with its length, as was first demonstrated experimentally by Smith-Rose and Barfield.

"The susceptance of the aerial is calculated on the assumption of no losses and it is found that the antiresonant frequencies are displaced by the presence of the screens while the resonant frequencies occur when the length of the inner conductor or of the screen is equal to an odd number of quarter-wavelengths. A simple equivalent circuit is given for an aerial which is short compared with the wavelength.

621.396.671.4 2682

Radiation Resistant of Horizontal and Vertical Aerials Carrying a Progressive Wave—E. M. Wells. (*Marconi Rev.*, vol. 9, pp. 129–137; October and December, 1946.) An extension of L. Lewin's analysis (2332 of 1939) to the case of progressive waves, using van der Pol's method.

621.396.674 2683

Design Values for Loop-Antenna Input Circuits—J. E. Browder and V. J. Young. (Proc. I.R.E., vol. 35, pp. 519—525; May, 1947.) A theoretical treatment of the problem leading up to formulas and charts for the choice of inductances, Q values and coupling coefficients of loop-aerial coupling transformers for obtaining optimum signal-to-noise ratio. The case of cable connection of the loop to the receiver is also considered.

621.396.677 2684

Aircraft Antenna Pattern Plotter—O. H. Schmitt and W. P. Peyser. (*Electronics*, vol. 20, pp. 88–91; May, 1947.) If measurements are made on a scale model of an aircraft and its aerials, the signal wavelength being proportionately reduced, the actual radiation pattern of the full-size installation can be predicted. Technical details of a system using microwaves and automatic recording are given.

621.396.677 2685

A Current Distribution for Broadside Arrays Which Optimizes the Relationship Between Beam Width and Side-Lobe Level—C. L. Dolph. (Proc. I.R.E., vol. 35, pp. 489–492; May, 1947.) Discussion of 2487 of 1946. H. J. Riblet gives a generalization of Dolph's methods which removes the limitations that (a) the spacing between radiators $\geqq\lambda/2$; (b) the beam width is characterized by the existence of a first null; (c) the current distribution is in phase; and (d) the current distribution is symmetrical about the center position of the array. In his reply Dolph shows how the calculations necessary in the application of his methods may be simplified.

621.396.677:621.396.93 2686

Various Papers on Direction-Finding—(*See* 2780 to 2783.)

621.396.677.029.64:538.566 2687

Electromagnetic Fields in a Paraboloidal Reflector.—E. Pinney. (*Jour. Math. Phys.*, vol. 26, pp. 42–55; April, 1947.) Continuation of the mathematical treatment of 1909 of 1946. The case of a radiating dipole backed by a dummy reflector, both dipoles being perpendicular to the axis of the paraboloid, is considered in detail.

621.396.679.4:621.315.24 2688

A Six-Wire Transmission-Line Application—J. C. Wadsworth. (*Proc. I.R.E.* (Australia), vol. 8, pp. 16–17, 19; March, 1947.) Comment by A. J. E. Robertson on 1686 of July and the author's reply.

621.392.029.64+621.396.67 2689

The Physical Principles of Wave-Guide Transmission and Antenna Systems [Book Review]—W. H. Watson. Oxford University Press, 207 pp., 20s. (*Wireless Eng.*, vol. 24, pp. 154–155; May, 1947.) "Its aim is to describe to physicists and engineers with theoretical interests the way in which the technique of handling radio-frequency transmission lines has been extended to deal with waveguides . . . The book can be unreservedly recommended to anyone in any way interested in waveguides."

CIRCUITS AND CIRCUIT ELEMENTS

621.314.2.015.33.029.5 2690

Electromotive Impulse Transformer—B. Lavagnino and V. Zerbini. (*Alta Frequenza*, vol. 16, pp. 31–36; February, 1947. In Italian, with English, French, and German summaries.) The heavily damped two-winding moving-coil galvanometer can transfer the time integral of an e.m.f. of short duration from one winding to the other at a constant ratio. Such a device might be used as a coupling transformer for pulse amplifiers.

621.316.722 2691

Nonlinear Limiter—E. R. Brill. (*Electronics*, vol. 20, pp. 198–202; May, 1947.) A limiter using germanium crystal rectifiers whose current versus potential characteristic follows a cube-root law. When the limiter is used in combination with a cathode-ray screen with a cube law a linear over-all transfer characteristic is obtained.

621.316.935 2692

Negative Resistance Effects in Saturable Reactor Circuits—J. M. Manley and E. Peterson. (*Trans. A.I.E.E.* (*Elec. Eng.*, December Supplement, 1946.) vol. 65, pp. 870–881; December Supplement, 1946.) General properties of oscillations produced; three types distinguished, incommensurable, subharmonic, and harmonic. Experimental data are in general agreement with theory.

621.318.323.2.042.15 2693

Iron-Dust Cores—Gleadle. (*See* 2816.)

621.318.33.042.029.3 2694

Magnetic Parameters in the Calculation of Reactors and Transformers for Audio-Frequency—G. Monti-Guarnieri. (*Alta Frequenza*, vol. 16, pp. 3–30; February, 1947. In Italian, with English, French, and German summaries.) Methods of calculation involve three dimension ratios, defining the shape of the laminations and core, and also a "parallel-harmonic" permeability depending on the ratio $B:H$. Nonlinear distortion is discussed and corrections are applied in the calculation of polarized and nonpolarized reactors to account for distortion limitation. An appendix describes apparatus and methods for determining the magnetic parameters and graphs used.

621.318.572 2695

Electronic Counters—I. E. Grosdoff. (*RCA Rev.*, vol. 7, pp. 438–447; September, 1946.) The use of resistance-coupled multivibrators in ring-chain and series-chain counters is described; gate and switching problems are discussed and applications suggested.

621.318.7 2696

Insertion Loss and Insertion Phase Shift of Multi-Section Zobel Filters with Equal Image Impedances—W. Saraga. (*P.O. Elec. Eng. Jour.*, vol. 39, part 4, pp. 167–172; January, 1947.) The method given in 1045 of 1943 (Stanesby, Broad, and Corke) can be applied to any given filter network which possesses a lattice equivalent. To simplify the derivation of these lattice equivalents for multisection Zobel filters with equal image impedances, the reactance versus frequency functions of a large number of such filters are tabulated.

621.318.74 2697

Narrow Band-Pass Filter Using Modulation—N. F. Barber. (*Wireless Eng.*, vol. 24, pp. 132–134; May, 1947.) The signal is modulated in two channels by equal voltages in phase quadrature, and the products are passed through low-pass filters, then further modulated by quadrature voltages and recombined. The final frequency is the same as that of the original signal and phase changes are preserved.

621.319.5.015.33 2698

Generation of Pulse Voltages—L. Vallese. (*Alta Frequenza*, vol. 16, pp. 68–86; April, 1947. In Italian, with English, French, and German summaries.) Fundamental principles, with typical circuits and some experimental results.

621.392.5 2699

Minimum Phase-Shift Networks—L. A. Zadeh. (*Wireless Eng.*, vol. 24, p. 157; May, 1947.) Discusses briefly the suggestion that such networks should be termed "minimum net phase-shift networks," where "net phase-shift" is defined as the total angle swept by G (the complex gain of the network) in the G-plane when ω varies from zero to the value in question.

621.392.5.016.24/.25 2700

On the Calculation of the Active and Reactive Power of Certain Electrical Networks—M. Parodi. (*Gén. Élec. Rev.*, vol. 56, pp. 143–144; March, 1947.) Expressions for the active and reactive power of a dissipative network, in terms of its input reactance and of the constants characterizing the losses, are derived from a relation due to N. I. Korman (738 of 1945.)

621.392.52:621.396.611.21 2701

Crystal Filters—I. Edvin. (*Elektrotechnika* (Budapest), vol. 39, pp. 41–47; March, 1947.) In Hungarian, with English, French, and German summaries.) The behavior of lattice and other types of filter sections s described and results obtained for band-, low-, and high-pass filters are discussed. Methods of soldering connecting wires to nodal points of the crystal are described. Balls of solder may be used on the supporting wires to create artificial reflection points.

621.396.611.1 2702

An RC Circuit Giving Over Unity Gain [at a Particular Frequency]—C. L. Longmire. (*Tele-Tech*, vol. 6, pp. 40–41, 112; April, 1947.) Applications are discussed.

621.396.611.21+537.228.1 2703

Quartz Oscillators—P. Vigoureux. (*Jour. Brit. I.R.E.*, vol. 7, pp. 46–62; March and April, 1947.) General review of subject; methods of cutting nature of equivalent circuit, oscillator characteristics, application to frequency multiplication and division, clocks, and filters.

621.396.611.21:621.316.726 2704

Stability of Crystal Oscillators—A. J. Zink, Jr. (*Electronics*, vol. 20, pp. 127–129; May, 1947.) Discussion of factors affecting crystal oscillator frequency drift and methods of minimizing it.

621.396.611.3 2705

On a Formula Relative to the Reflection of Waves—P. Marié. (*Compt. Rend. Acad. Sci.* (Paris), vol. 224, pp. 379–381; February 10, 1947.) The interpretation of a formula derivable from the papers noted in 1376 and 1377 of June.

621.396.611.4:537.533 2706

Cavity Resonators and Electron Beams—J. H. Owen Harries. (*Wireless Eng.*, vol. 24, pp. 71–80, 109–118, and 135–142; March and May, 1947.) General theoretical treatment of fundamental principles and limitations in radio-tube technique using a modulated electron beam supplying power to a load through a resonator. Energy transfer and power output conditions are analyzed; it is shown that the maximum theoretical conversion efficiency η_1 is 43 per cent, attained when the small-signal transit angle is about $\pi/2$ and the ratio of the peak voltage in the resonator along the beam to the steady voltage at entry is rather greater than unity. The over-all efficiency is $\eta_1\eta_c$ where η_c is the efficiency of transfer from resonator to load. In a given system the adjustable parameters are the beam current and the resonator-load coupling, and the criteria for obtaining maximum over-all efficiency are discussed.

The influence of wavelength on the efficiency and power output given by present electron-stream-resonator technique is considered in detail; it is concluded that this technique is only useful down to wavelengths of about 1 centimeter. Application of the theory is exemplified by considering specific shapes of resonator. Techniques for measurement of Q and of electric field and field integrals at microwavelengths and the use of models are discussed.

621.396.615:621.316.726 2707

Frequency Instability of Self Oscillators—E. Green. (*Marconi Rev.*, vol. 9, pp. 151–158; October and December, 1946.) The conditions for single-frequency operation are analyzed for an oscillator connected through a long line to an unmatched load.

621.396.615.14 2708

Improving Stability of U.H.F. Oscillators—C. A. Helber. (*Electronics*, vol. 20, pp. 103–105; May, 1947.) Mathematical analysis of the factors governing frequency stability during load-impedance changes, and a method of reducing frequency variations in a 1000-Mc. oscillator by means of a series capacitor in the anode circuit.

621.396.615.14 2709

Microwave Oscillators Using Disk-Seal Tubes—A. M. Gurewitsch and J. R. Whinnery. (Proc. I.R.E., vol. 35, pp. 462–473; May, 1947.) Typical design and performance data are given for oscillators using three disk-seal tubes now on the market. "A general small-signal oscillator theory is presented and applied to the re-entrant disk-sea -tube microwave oscillator. It is shown how information on frequency of oscillation, tuning, and frequency stability can be obtained."

621.396.615.14 2710

Generating Microwaves—S. Freedman. (*Radio News*, vol. 37, pp. 35–37, 128; March, 1947.) A general account of the various methods employed, from the Barkhausen-Kurz stage onwards, with a table in which these methods are compared as regards the energy interchange, output, energy losses, ease of adjustment, frequency flexibility, and cost. A short description is also given of the Fonda-Freedman method, which uses ordinary tubes with special circuit arrangements.

621.396.615.14.012.2 2711

***Q* Circles—A Means of Analysis of Resonant Microwave Systems: Part 2**—W. Altar. (Proc. I.R.E., vol. 35, pp. 478–484; May, 1947.) Mathematical proof of the relationships on which are based the circle diagrams described in part 1 (2360 of September).

621.396.615.141.2:621.314.2.029.64:621.315.613.7 2712

Waveguide-Output Magnetrons with Quartz Transformers—L. Malter and J. L. Moll. *RCA Rev.*, vol. 7, pp. 414–421; September, 1946.) Tests at a wavelength of 1.25 centimeters show that quartz dielectric wave guide, or parallel plate transmission-line transformers give performance substantially identical with that obtained with vacuum transformers. The use of quartz increases transformer width and reduces the length.

621.396.619.13:621.396.622 2713

Applying the 1N34 as Discriminator for F.M.—N. L. Chalfin. (*Radio News*, vol. 37, pp. 55, 150; March, 1947.) The germanium 1N34 crystal provides greater output with less residual hum than a conventional 6H6 tube. A discriminator circuit is given which uses two 1N34 units or a single 1N35. The latter consists of two matched 1N34.

621.396.619.16 2714

A Note on a Phase Modulator Principle—R. A. Wooding, Jr. (*Proc. I.R.E.* (Australia), vol. 5, pp. 13–16, 24; April, 1945.) A practical circuit for producing quasi-phase modulation.

621.396.645 2715

Design for a High-Quality Amplifier—D. T. N. Williamson. (*Wireless World*, vol. 53, pp. 118–121 and 161–163; April and May, 1947.) Discussion of the basic requirements, the design of the push-pull output stage, the output transformer and phase-splitter and driver stages. A practical circuit is shown using tetrode output tubes connected as triodes and details of the performance and effect of feedback are given.

621.396.645 2716

Design of Transmission Line Tank Circuits—W. C. Hollis. (*Electronics*, vol. 20, pp. 130–134; May, 1947.) A discussion of tank efficiency, condition for resonance, selectivity, impedance of tank circuit, and conditions for maximum impedance, with graphical design procedure.

621.396.645:518.3 2717

Cathode Followers Nomograph—M. B. Kline. (*Electronics*, vol. 20, p. 136; May, 1947.) Relates gain, amplification factor, and ratio of cathode-load resistance to tube-anode resistance.

621.396.645:621.396.822.08 2718

Linearity Range of Noise-Measuring Amplifiers—R. L. Bell. (*Wireless Eng.*, vol. 24, pp. 119–122; April, 1947.) In the amplification of noise voltages there is a finite probability of the occurrence of any peak value of voltage, however large, and all those greater than a certain value will produce overloading of the amplifier.

The errors in mean and mean-square output voltages resulting from an assumption of linear amplification are calculated in the two cases of amplifiers with resistive and selective output loads.

621.396.645.36 2719

Cancellation of Even Harmonic Distortion in Push-Pull Operation—G. F. Craven and

G. R. O. Vermeir. (*Proc. I.R.E.* (Australia), vol. 5, pp. 12–19; January, 1945.) Analysis for class, *A*, *AB*, *B*, and *C* amplifiers.

621.396.662.21 2720
Universal Coil Design—A. W. Simon. (*Radio*, vol. 31, pp. 16–17; February and March, 1947.) Simple formulas for coil winding.

621.396.69+621.396.621 2721
Machine for Receiver Manufacture—(*Toute la Radio*, vol. 14, pp. 163–164; May, 1947.) A short account of the equipment described in 1913 of July (Sargrove).

621.396.69:06.064 2722
Component Design Trends—(*Wireless World*, vol. 53, pp. 177–181; May, 1947.) A review of the Radio Component Manufacturers' Federation exhibition held in March, 1947.

517.432.1 2723
Heaviside's Operational Calculus Made Easy. [Book Review]—Turney. (*See* 2831.)

621.38.012 2724
Drafting for Electronics [Book Review]—L. F. B. Carini. McGraw-Hill Publishing Co., London, 211 pp., 12s.6d. (*Elec. Rev.* (London), vol. 140, p. 586; April 11, 1947.) Deals essentially with the production of circuit diagrams for radio receivers and transmitters, c.r.t., and the various industrial applications of electronics.

GENERAL PHYSICS

53"1946" 2725
Physics in 1946—P. Morrison. (*Jour. Appl. Phys.*, vol. 18, pp. 133–152; February, 1947.) A review of various experiments and techniques in the fields of superconductivity, microwaves, atomic physics, and atomic energy.

530.145 2726
On the Nonlinear Wave Equations of the Quantum Theory of the Electron—B. Kwal. (*Compt. Rend. Acad. Sci.* (Paris), vol. 224, pp. 1099–1100; April 14, 1947.)

531.18:531.15 2727
Is Rotation Relative or Absolute?—G. Stedman. (*Wireless Eng.*, vol. 24, p. 156; May, 1947.) Comment on 1727 of July.

534.13 2728
The Vibrations of Certain Coupled Systems—T. Vogel. (*Rev. Sci.* (Paris), vol. 84, pp. 515–522; November 15, 1946.) If each degree of freedom of a system S_1 is coupled to one and only one degree of freedom of a system S_2 and conversely, the coupling between S_1 and S_2 is termed monovalent. The theory of such systems is given and applied to the case of a rectangular window, formed by two parallel plates, in an infinite rigid wall. The equations of motion are solved and expressions found for the natural frequencies and for the transparency of the combination with loose and with tight coupling. Experiments with plates of aluminum and of rubber, forming a window in one wall of a sound-proof room, confirm the theory.

535.13:538.566 2729
Refraction Between Absorbing Media—L. Pincherle. (*Nuovo Cim.*, vol. 3, pp. 328–337; October 1, 1946. In Italian, with English summary.) Theory of a plane electromagnetic wave refracted at the plane boundary between two absorbing dielectrics. A discontinuity is found in the reflected and transmitted fields under conditions in which the average flow of energy through the boundary is zero.

535.341+621.317.33.011.5[:537.226.029.64 2730
Extension of the Measurements of Dispersion and Absorption by Liquids, to the Region of Centimetric Radio-Electric Waves—P. Abadie. (*Trans. Faraday Soc.*, vol. 42A, pp. 143–149; 1946. Discussion, pp. 155–170.)

535.343.32.029.6:541.135 2731
The Radio-Frequency Absorption Spectra of Solutions of Electrolytes—J. Forman and D. J. Crip. (*Trans. Faraday Soc.*, vol. 42A, pp. 186–193; 1946.) The absorption of several binary electrolytes in aqueous solutions of various concentrations was measured at frequencies between 25 and 375 Mc.

537.122:538.122 2732
The Radiation of Fast Electrons in the Magnetic Field—L. Arzimovich and I. Pomeranchuk. (*Jour. Phys.* (U.S.S.R.), vol. 9, no. 4, pp. 267–276; 1945.) The spectral and angular distribution is investigated.

537.2 6+621.315.6+621.317 2733
A General Discussion on Dielectrics—(*See* 2808.)

537.226 2734
Dipolar Interaction—H. Fröhlich. (*Trans. Farady Soc.*, vol. 42A, pp. 3–7; 1946. Discussion, pp. 36–40.)

537.226 2735
The Influence of Hindered Molecular Rotation on the Dielectric Polarization of Polar Liquids—J. G. Kirkwood. (*Trans. Faraday Soc.*, vol. 42A, pp. 7–12; 1946. Discussion, pp. 36–40.)

537.226 2736
Theory of the Crystalline Field in Solid and Liquid Polar Dielectrics—E. Bauer and D. Massignon. (*Trans. Faraday Soc.*, vol. 42A, pp. 12–15; 1946. Discussion, pp. 36–40.)

537.226 2737
A Contribution to the Theory of the Internal Electrical Field [in a Dielectric]—C. J. F. Böttcher. (*Trans. Faraday Soc.*, vol. 42A, pp. 16–19; 1946. Discussion, pp. 36–40.)

537.226 2738
A Comparison of Debye's and Onsager's Theories of the Dielectric Constants of Concentrated Polar Media—F. C. Frank. (*Trans. Faraday Soc.*, vol. 42A, pp. 19–24; 1946. Discussion, pp. 36–40.) "It is concluded that Debye's theory may be inaccurate but Onsager's certainly is. Arguments indicating that Debye's theory is very far wrong are refuted."

537.226 2739
Some Mathematical Models Representing Polar Molecules in Crystals—F. C. Frank. (*Trans. Faraday Soc.*, vol. 42A, pp. 24–35; 1946. Discussion, pp. 36–40.) The discussion predicts a dependence of the degree of dielectric polarization on temperature which agrees to some extent with observation.

537.226 2740
Molecular Freedom in Solid Dielectrics—C. P. Smyth. (*Trans. Faraday Soc.*, vol. 42A, pp. 175–180; 1946.)

537.226:001.8 2741
A Note on the Analysis of Dielectric Measurements—S. Whitehead. (*Trans. Faraday Soc.*, vol. 42A, pp. 66–75; 1946. Discussion, pp. 75–78.) A survey of dielectric theory in its bearing on research.

537.226.2 2742
The Dielectric Relaxation of Mixtures of Dipolar Liquids—A. Schallamach. (*Trans. Faraday Soc.*, vol. 42A, pp. 180–186; 1946. Discussion, pp. 193–194.)

537.226.2:538.56.569 2743
On the Frequency Dependence of the Dielectric Constant in Dipolar Solids—R. A. Sack. (*Trans. Faraday Soc.*, vol. 42A, pp. 61–66; 1946. Discussion, pp. 75–78.) An extension to variable fields of the work of Ising (*Zeit. für Phys.*, vol. 31, pp. 253–258; 1925), who used Debye's original theory based on the Clausius-Mosotti assumption of the internal field.

537.226.8 2744
Note on the Comparison of Entropy and Energy Changes in Diffusion and Dielectric Relaxation Processes—D. L. Levi. (*Trans. Faraday Soc.*, vol. 42A, pp. 152–155; 1946. Discussion, pp. 155–170.)

537.291 2745
Exchange of Energy Between an Electron Beam and an Electromagnetic Field of Feeble Intensity—Guénard. (*See* 2969.)

537.313 2746
On the Probability of Electron Conduction Motions—C. Budeanu. (*Compt. Rend. Acad. Sci.* (Paris), vol. 224, pp. 1054–1056; April 9, 1947.) Consideration of the probability that an electron at the junction of two resistors will traverse either of them, leads approximately to Kirchhoff's law if a sufficiently great time is considered.

537.525:538.551.25 2747
On the Theory of Electron-Plasma Oscillations—F. Borgnis. (*Helv. Phys. Acta*, vol. 20, pp. 207–221; April 30, 1947. In German.) The theory of short-wave electron oscillations in a gas-discharge plasma is generalized. The treatment of the plane problem by Langmuir and Tonks (1929 Abstracts, p. 273) must be extended to account for the occurrence of independent stationary oscillations in a plasma. The frequency of such oscillations, which can be excited between the limits of the discharge path, is not, in general, identical with the Langmuir frequency.

537.525:539.16.08 2748
Development of the Discharge in Counter Tubes with Alcohol Vapour—F. Alder, E. Baldinger, P. Huber, and F. Metzger. (*Helv. Phys. Acta*, vol. 20, pp. 73–95; February 15, 1947. In German.) The velocity of spreading of the discharge in a tube with 64 mm. Hg argon and 16 mm. Hg alcohol vapor and a potential of 1100 volts was 8.35×10^6 centimeters per second. With a given pressure ratio of alcohol to argon, the velocity increases almost linearly with the potential. With constant potential, the velocity decreases if this pressure ratio is increased.

537.525.72 2749
Low-Pressure Electrical Discharges—E. W. B. Gill and A. von Engel. (*Nature* (London), vol. 159, pp. 404–405; March 22, 1947.) High frequency discharges in a glass bulb can be initiated with low uniform gradients if the pressure is of the order of 0.01 to 0.001 mm. Hg. Maximum wavelength in meters is about four times the diameter of the bulb in centimeters; starting potential is independent of the nature of the gas.

537.533.8:546.3 2750
Rediffused Component of Secondary Electron Emission of Metals—P. Palluel. (*Compt. Rend. Acad. Sci.* (Paris), vol. 224, pp. 1492–1494; May 28, 1947.) As the primary velocity increases, the coefficient of rediffusion (or nonelastic reflection) for all the metals considered approaches asymptotically a constant value which increases with atomic number and is reached at lower primary velocities for the lighter metals.

538.122 2751
The Lines of Force Through Neutral Points in a Magnetic Field—D. Owen. (*Proc. Phys. Soc.*, vol. 59, pp. 14–18; January 1, 1947.) Continuation of 3405 of 1945. A method is given for drawing the lines of force, and the

field near a neutral point is considered geometrically.

538.2:621.365.5 2752

Theory of the Heating of Ferromagnetic Materials by Eddy Currents and by Hysteresis—M. Jouguet. (*L'Onde Élec.*, vol. 27, pp. 138–151; April, 1947.) General equations are developed for the case of a solid of revolution, without hysteresis or saturation. The effects of hysteresis and magnetizing field are then considered and formulas derived for the power dissipated by eddy currents and by hysteresis and for the total power dissipation. Discussion shows that hysteresis reduces the eddy-current heating but increases the total heating. The results are applied to the induction furnace; a form factor is introduced and current penetration and skin thickness are discussed. Hysteresis increases the skin thickness but reduces the penetration depth. The choice of the optimum frequency depends on the permeability of the material. The power absorption of an infinitely long cylinder is compared with that of a sphere; the case of an ellipsoid is also considered.

538.311+621.316.97].083:621.385.833 2753

Measurement of Feeble Magnetic Fields and of the Effects of Shielding. Applications to the Electron Microscope—D. Charles. (*Ann. Radioélec.*, vol. 2, pp. 75–77; January, 1947.) The method uses a small coil connected by a screened lead to an amplifier with a voltage gain of about 1000 for frequencies from 50 to 1000 cycles. Results are given showing the effect of single and of double cylindrical shields, with and without side holes. The results have been applied to the design of efficient shields for the C.S.F. electron microscope to eliminate the effects of parasitic fields.

538.312 2754

Electromagnetic Radiation—J. Greig. (*Wireless Eng.*, vol. 24, pp. 143–144; May, 1947.) On the assumption of a finite velocity of propagation of electric and magnetic fields, the main phenomena of electromagnetic radiation can be simply explained.

538.313 2755

The Helical Motion of Particles in a Constant Uniform Magnetic Field—F. Ehrenhaft. (*Compt. Rend. Acad. Sci.* (Paris), vol. 224, pp. 1151–1152; April 21, 1947.) Particles of Fe, Ni, Ma, Cr, Sb, etc., describe helical paths between the poles of an electromagnet. Photographs are given.

538.56:535.13 2756

The Reflection of an Electromagnetic Plane Wave by an Infinite Set of Plates: Part 1—J. F. Carlson and A. E. Heins. (*Quart. Appl. Math.*, vol. 4, pp. 313–329; January, 1947.) This problem may be formulated as a single inhomogeneous Wiener-Hopf integral equation, and as such it may be solved rigorously using the method of Fourier transformation. The functional form of the various surface-current densities, as well as the electric field, is determined. It is shown how some of the results obtained may be interpreted in a simple physical manner, and the relation to ordinary grating theory is pointed out.

538.569.4.029.64 2757

Thermal and Acoustic Effects Attending Absorption of Microwaves by Gases—W. D. Hershberger, E. T. Bush, and G. W. Leck, (*RCA Rev.*, vol. 7, pp. 422–431; September, 1946.) 15 substances, gaseous at normal temperature and pressure, strongly absorb microwaves, the absorbed energy appearing as heat or sound. Methods of measurement are described and the results are tabulated and discussed.

GEOPHYSICAL AND EXTRATERRESTRIAL PHENOMENA

523.16:621.396.822
551.510.535
551.594.6 2758

Reports on the International Conference of U.R.S.I. (International Radio-Scientific Union)—Y. Rocard. (*Rev. Sci.* (Paris), vol. 84, pp. 500–501; November 1, 1946.)

(a) Ionosphere. M. Nicolet discusses the formation of the various regions, and criticizes the conclusions of Kiepenheuer (*Annales d'Astrophysique*, vol. 8, p. 210; 1945.)

(b) Extraterrestrial electromagnetic noise. Work referred to in 323 of 1946 (Appleton), 1825 of 1946 (Hey: Stratton), and 3599 of January (Hey, Parsons, and Phillips) is considered; see also 402 of March (Appleton).

(c) Atmospherics. Discussion of the work of F. A. Baerson and S. Petersen on the geographic distribution in winter of the disturbance centers and their relation to air mass and front distribution. Summer conditions which were studied by C. K. M. Douglas are much more complex, and it is difficult to draw definite conclusions from them.

523.323:621.396.812 2759

Effect of the Moon on Radio Wave Propagation—(*See* 2903.)

523.746"1947.03" 2760

A Giant Sunspot—(*Nature* (London), vol. 159, p. 396; March 22, 1947.) The sunspot group of March 3–17, 1947, was unusually large but was not accompanied by exceptional geomagnetic disturbances.

523.78"1946.11.23":621.396.822.029.63 2761

Micro-Wave Solar Noise Observations during the Partial Eclipse of November 23, 1946—A. E. Covington. (*Nature* (London), vol. 159, pp. 405–406; March 22, 1947.) Results on 2800 Mc. from Ottawa, Canada; equivalent temperature of noise-generating region (2.20 per cent of projected area and containing sunspot group) is 1.5×10^{6}°K in excess of the average surface temperature of 5.6×10^{4}°K.

537.591 2762

Non-Primary Cosmic-Ray Electrons above the Earth's Atmosphere—G. J. Perlow and J. D. Shipman, Jr. (*Phys. Rev.*, vol. 71, pp. 325–326; March 1, 1947.) Summary of data obtained from a V-2 rocket experiment on the presence of electrons of energy $<5\times10^{8}$ e.v. above the earth's atmosphere.

537.591 2763

Highly Ionizing Particles in the Cosmic Radiation—V. Veksler, N. Dobrotin, and V. Khvoles. (*Jour. Phys.* (U.S.S.R.), vol. 9, no. 4, pp. 277–279; 1945.)

537.591.15 2764

Presence of a Penetrating Component in Extensive Showers in the Atmosphere—A. Mura, G. Salvini, and G. Tagliaferri. (*Nature* (London), vol. 159, pp. 367–369; March 15, 1947.) Confirmation by an improved experimental technique.

537.591.15 2765

The Lateral Extension of Auger Showers—D. V. Skobeltzy, G. T. Zatsepin, and V. V. Miller. (*Phys. Rev.*, vol. 71, pp. 315–317; March 1, 1947.)

537.591.15 2766

Cosmic-Ray Bursts in an Unshielded Chamber and Under One Inch of Lead at Different Altitudes—H. Bridge and B. Rossi. (*Phys. Rev.*, vol. 71, pp. 379–380; March 15, 1947.)

538.71(479.22) 2767

100 Years of Magnetic Observations at Tbilis [Tiflis]—M. Z. Nodia. (*Viestnik Akad. Nauk* (S.S.S.R.), no. 7, pp. 47–53; 1946. In Russian.)

550.384.3(68) 2768

The Earth's Magnetic Field in Southern Africa at the Epoch, July 1, 1930—E. N. Grindley. (*Phil. Trans.*, vol. 240, pp. 251–294; April 29, 1947.) Analysis of a large number of observations to determine the secular variation in the magnetic intensity, declination and inclination. Probable "normal" values are shown by maps with isomagnetic lines.

551.510.52:621.396.812.029.64 2769

Radar Reflections from the Lower Atmosphere—H. T. Friis. (Proc. I.R.E., vol. 35, pp. 494–495; May, 1947.) Using a 3-centimeter radar transmitter and a double-detection receiver, each with a shielded-lens aerial pointing upwards, echoes apparently from stratifications in the lower atmosphere have been received on clear, calm nights. During the day and on windy nights such echoes are usually unobtainable.

551.510.535 2770

Note on the [Extent and Density of the] Sporadic-E Layer—O. P. Ferrell. (Proc. I.R.E., vol. 35, pp. 493–494; May, 1947.)

551.510.535:551.506.2(51) 2771

Ionosphere Reflections and Weather Forecasting for Eastern China—E. Gherzi. (*Bull. Amer. Met. Soc.*, vol. 27, pp. 114–116; March, 1946.) Day-time investigations at Zi Ka Wei observatory, using 20-watt aerial power on a frequency of 6 Mc. show that when the Pacific trade wind is dominating the weather, *E*-layer reflections are obtained. When the Siberian air mass is predominant, reflections come from the *F*-layer. In general, F_2-layer reflections are found when tropical air is predominant. With approaching typhoons, the *E*-layer echo becomes very strong. It is suggested that similar effects might be observed in the eastern parts of the United States.

551.510.535:621.396.11 2772

The Application of Ionospheric Data to Radio Communication Problems: Part 2—Appleton and Beynon. (*See* 2895.)

551.510.535:621.396.11 2773

Oblique Radio Transmission in the Ionosphere, and the Lorentz Polarisation Term—Beynon. (*See* 2896.)

551.510.535:621.396.6 2774

Ionosphere Equipment for Field Use—Musselman. (*See* 2929.)

551.57:621.396.82:629.135
551.57:621.319.74:629.135 2775

Electrostatic Ills and Cures of Aircraft: Parts 1 and 2—Beach. (*See* 2916.)

551.593.9(54) 2776

Measurements of the Intensity of the Night Sky Light at Calcutta—S. N. Ghosh. (*Indian Jour. Phys.*, vol. 20, pp. 205–213; December, 1946.) Measurements on 50 nights during 1943–1945 show that on undisturbed nights the intensity decreased to a minimum about local midnight and then increased. On disturbed nights accompanied by magnetic disturbance, the intensity variation followed generally that of maximum ionization of the *F* region. Other nights, when the night-sky intensity varied abnormally but did not follow the electron density of the *F* region, were free from magnetic disturbance.

LOCATION AND AIDS TO NAVIGATION

534.88 2777

Sonar—The Submarine's Nemesis—C. G. McProud. (*Radio News*, vol. 37, pp. 47–49, 141; March, 1947.) Describes, with photographs and block diagrams, the RCA QCQ-2 and the Submarine Signal Co. WCA-2 equip-

ments and their operational principles. See also 1750, 1946, and 3605 of January.

621.396.674:621.396.62 2778
A Portable Direction Finding Receiver—J. M. S. Watson. (*R.S.G.B. Bull.*, vol. 22, pp. 161–164; April, 1947.) Equipment for operation in the 1.7-Mc. band.

621.396.93:551.594.6 2779
The Location of Thunderstorms by Radio Direction-Finding—F. Adcock and C. Clarke. (*Jour. I.E.E.* (London), part III, vol. 94, pp. 118–125; March, 1947. Discussion, pp. 133–140.) Polarization error due to the presence of ionospheric reflections is the main source of inaccuracy in the crossed-loop cathode-ray direction finders now used. Various systems (including time-delay methods) for improving the accuracy of location are considered and compared. Details are given of an experimental 10-30 kc. twin-channel cathode-ray direction finder, using brilliance modulation to eliminate ionospheric components of the lightning pulse and errors due to overloading; this direction finder has crossed-loop aerials but may be adapted for the spaced-loop or Adcock types. A summary was noted in 2126 of August; see also 1786 of July.

621.396.93:621.396.677 2780
The Development and Study of a Practical Spaced-Loop Radio Direction-Finder for High Frequencies—W. Ross. (*Jour. I.E.E.* (London), part III, vol. 94, pp. 99–107; March, 1947. Discussion, pp. 133–140.) The instrument is of the rotating type and uses two single-turn 1-meter square vertical coaxial screened loops 3 meters apart. The field strength required for an arc of silence of $\pm 5°$ varies from 1.5 to 4 microvolts per meter for a vertically polarized ground wave between 3 and 15 Mc. The instrument is particularly useful for taking bearings on steeply incident ionospheric waves, where Adcock direction finders are very inaccurate. The polarization error which may be introduced by the essentially nonuniform current distribution along loops is analyzed and discussed. Examples of site errors reducing the accuracy of the instrument are given. See also 2783.

621.396.93:621.396.677 2781
The Use of Earth Mats to Reduce the Polarization Error of *U*-Type Adcock Direction-Finders—R. L. Smith-Rose and W. Ross. (*Jour. I.E.E.* (London), part III, vol. 94, pp. 91–98; March, 1947. Discussion, pp. 133–140.) Polarization errors introduced by the buried horizontal feeders of a 4-aerial *U*-type Adcock direction finder were found to be greatly reduced between 3 and 10 Mc. by an earthed wire mat of 0.6-meter square mesh 31 meters in diameter (about 5 times the aerial spacing) laid symmetrically around the aerial system on or near the ground. Earthing the mat was found to be essential; on high-conductivity ground direct earth connections could be used, but on low-conductivity ground it was necessary to connect sets of radial-wire extensions of various lengths to the mat, each set resonating roughly independently of the others to provide a low-impedance path to earth for the periphery of the mat at various frequencies between 3 and 10 Mc. Provided that the feeders were not too large in diameter and were bounded to the mat, it was found unnecessary to bury them. The polarization error, besides being considerably reduced, should be more independent of weather conditions and therefore more accurately predictable.

621.396.93:621.396.677.029.58 2782
Site and Path Errors in Short-Wave Direction-Finding—W. Ross. (*Jour. I.E.E.* (London), Part III, vol. 94, pp. 108–114; March, 1947. Discussion, pp. 133–140.) Measurements made with 4-aerial Adcock and portable rotating H-type direction finders on sites chosen by visual inspection as good, (i.e., flat and open over at least 1 km.²) showed that the site or path errors varied with the transmitter bearing, frequency (6–15 Mc.) and distance (50–600 meters and 3–16 km.) in an entirely random manner through $\pm 3°$ and more for the distant transmitters. Ground-wave propagation was assumed throughout. Explanations are given, and it is concluded that a local calibration for supplying a detailed correction curve to observed bearings is not, in general, possible in the short-wave band, but may still be useful when assessing the over-all reliability of a particular installation.

621.396.93:621.396.677.029.62 2783
An Experimental Spaced-Loop Direction-Finder for Very High Frequencies—F. Horner. (*Jour. I.E.E.* (London), part III, vol. 94, pp. 126–133; March, 1947. Discussion, pp. 133–140.) This direction finder uses two single-turn 28-centimeter square vertical-coaxial-screened loops 146 centimeters apart, and the field strength required for an arc of silence of $\pm 5°$ is 20 microvolts per meter for a vertically polarized ground wave between 30 and 100 Mc. For high-angle waves, (e.g., from aircraft) it appears to be more accurate than the rotating-H Adcock type provided that care is taken to eliminate errors due to loop resonances. A similar instrument using 92-centimeter loops 220 centimeters apart to give increased sensitivity (4 μV/m) at 30 Mc. is described briefly. The polarization errors introduced by calibrating with an elevated transmitter, so close that the wave from it has appreciable curvature, is evaluated and discussed. See also 2780.

621.396.93:621.396.677.029.63 2784
Some Experiments on Conducting Screens for a U-Type Spaced-Aerial Radio Direction-Finder in the Frequency Range 600:1200 Mc/s—R. R. Pearce. (*Jour. I.E.E.* (London), part III, vol. 94, pp. 115–117; March, 1947. Discussion, pp. 133–140.) A simple direction finder was used to investigate the effect of large earth screens. A metal plate (or a $\lambda/12$ mesh of wire) not less than 4λ in diameter was required to reduce the polarization error of the direction finder to about 1°.

621.396.96:535.37 2785
Luminescence and Tenebrescence as Applied in Radar—Leverenz. (*See* 2796.)

621.396.96:621.385.832 2786
A Survey of Cathode-Ray-Tube Problems in Service Applications, with Special Reference to Radar—Bradfield, Bartlett, and Watson. (*See* 2984.)

621.396.96:621.385.832 2787
War-Time Developments in Cathode-Ray Tubes for Radar—Jesty, Moss, and Puleston. (*See* 2983.)

621.396.96:621.396.1 2788
Radar Allocations—J. Markus. (*Electronics*, vol. 20, p. 150; May, 1947.) A note on the allocation of the frequency bands 3000–3246 Mc., 9320–9500 Mc. and 5460–5650 Mc. for shipborne radar by the Federal Communications Commission.

621.396.96:621.396.812 2789
A Theory of the Performance of Radar on Ship Targets—Wilkes and Ramsay. (*See* 2904.)

621.396.96:621.396.82 2790
The War in the Ether—E. B. Addison. (*Jour. Roy. Aero. Soc.*, vol. 51, pp. 425–436; May, 1947. Discussion, pp. 436–439.) A lecture dealing mainly with the use of radio as a weapon, and the tactics evolved to use it in the defence of Britain and in the protection of our bombers when attacking targets in enemy territory.

621.396.96.029.64:531.55 2791
Centimetre Radar for Precision Gun-Laying—H. A. M. Clark. (*Proc. R.S.G.B.*, no. 1, pp. 7, 15; Spring, 1947.) Discussion of applications of radar to naval gunnery with emphasis on close-range sets. A 3-centimeter autofollowing set of this type is described in some detail.

621.396.96 2792
Principles of Radar. [Book Review]—Staff of Radar School, Massachusetts Institute of Technology. McGraw-Hill Publishing Co., London, second edition, 25s. (*Wireless Eng.*, vol. 24, p. 155; May, 1947.) "It deals with each aspect of the whole, wide field of radar with equal thoroughness and specialized knowledge, while achieving a remarkable consistency of treatment and organic unity."

MATERIALS AND SUBSIDIARY TECHNIQUES

533.5:539.163.2.08:620.191.33 2793
High-Vacuum Leak Testing with the Mass Spectrometer—W. G. Worcester and E. G. Doughty. (*Trans. A.I.E.E.* (*Elec. Eng.*, December Supplement, 1946) vol. 65, pp. 946–955; December Supplement, 1946.) Discussion, p. 1170.) See also 2441 of September.

533.5:539.163.2.08:620.191.33 2794
Spectrometer Vacuum Leak Detector—G. A. Doxey. (*Electronics*, vol. 20, pp. 142, 194; May, 1947.) Cracks are detected in high-vacuum systems by measuring leakage of helium into the system with a mass spectrometer. See also 2441 of September.

535.37 2795
Luminescent Materials—S. György. (*Elektrotechnika* (Budapest), vol. 39, pp. 70–73 and 81–86; April and May, 1947. In Hungarian, with English, French, and German summaries.) A review of the more important luminescent materials, with an account of investigations by the author and E. Nagy of the band structure and temperature dependence of the luminescence of manganese-activated zinc silicate and zinc-beryllium silicate phosphors. A relation is found between the temperature dependence of the luminescence and that of the electrical conductivity.

535.37:621.396.96 2796
Luminescence and Tenebrescence [i.e., opposite of luminescence] as Applied in Radar—H. W. Leverenz. (*RCA Rev.*, vol. 7, pp. 199–239; June, 1946.) A comprehensive description of the properties of phosphors and "scotophors" [i.e., opposite of phosphors] developed during the war for delay screens for c.r.t. Examples of typical radar displays are given; operating voltages were usually limited to 5 kilovolts and trace persistences were required up to 30 seconds. The energy imparted per signal pulse for typical p.p.i. operation is calculated for different screens and radar images are discussed in relation to the properties of the human eye. Methods are listed for converting cathode rays into visible radiation; only cathode luminescence and cathode tenebrescence have found practical application in radar. Ideal and real performances of phosphors and "scotophors" are contrasted and an idealized picture given of the mechanism of luminescence and tenebrescence.

Cascade screens comprising stratified layers of different phosphors which give an increase in phosphorescence and a decrease in initial luminescence largely overcame the difficulty of low penetration of the cathode rays due to the 5 kv. voltage limitation. They are operated at low luminescence by using the enhanced sensitivity of the dark-adapted human eye.

Long persistent images were produced having dark traces on a bright field using (a) negative modulation of luminescence ("c.r. burn" method), and (b) tenebrescent screens of "scotophors." Tabular summaries of some of the more useful c.r.t. screens are given as an aid

to radar indicator designers and there is an extensive bibliography.

535.377 2797

The Thermoluminescence and Conductivity of Phosphors—R. C. Herman and C. F. Meyer. (*Jour. Appl. Phys.*, vol. 18, pp. 258–259; February, 1947.) Correction and addendum to 743 of April.

537.226.8 2798

Power Factor and Temperature Coefficient of Solid (Amorphous) Dielectrics—M. Gevers and F. K. du Pré. (*Trans. Faraday Soc.*, vol. 42A. pp. 47–55; 1946. Discussion, pp. 75–78.) In amorphous dielectrics, including those consisting of a crystalline mass containing many lattice irregularities and impurities, the dielectric constant and the power factor are, in general almost independent of frequency and the ratio of the temperature coefficient of the dielectric constant to the power factor is nearly constant. An explanation of these properties is based on the peculiar structure of such solids.

537.226.8 2799

The Distribution of Relaxation Times in Dielectrics—C. G. Garton. (*Trans. Faraday Soc.*, vol. 42A, pp. 56–60; 1946. Discussion, pp. 75–78.) The variation of loss angle with frequency in dielectrics is explained by the existence of a distribution of relaxation times due to the presence of elements—dipoles or ions—which oscillate between "wells" of varying potential depth whose distribution is determined by considerations of temperature and viscosity.

537.228.1 2800

Effect of Foreign Ions on the Properties of Rochelle-Type Crytsals—B. Matthias and W. Merz. (*Helv. Phys. Acta*, vol. 19, pp. 227–229; July 31, 1946. In German.) All Rochelle-type crystals have a maximum in the resonance-frequency temperature curve at a point about 80° K above the Curie temperature. Addition of Tl to KH_2PO_4 raises both the maximum and the Curie temperature by an amount approximately proportional to the Tl concentration. The alkali ions produce the opposite effect.

537.533:[546.26-1+546.28 2801

Measurement of the Thermo-Electron Emission from Graphite, Silicon and Silicon Carbide—A. Braun and G. Busch. (*Helv. Phys. Acta*, vol. 20, pp. 33–66; February 15, 1947. In German.) A new method was used, the inner wall of the heating chamber serving as anode for the emitted electrons. For graphite the constants in the emission formula $I = AT^2e^{-\phi/KT}$ were found to be $\phi = 4.39$ e.v., $A = 15$ A/cm.^{2} (°K)^2. The corresponding values for silicon were 3.59 e.v. and 8 A/cm.^{2} (°K)^2. The results for single crystals of silicon carbide varied widely depending on the surface layer. The results are shown graphically.

538.221 2802

A New Magnetic Material of High Permeability—O. L. Boothby and R. M. Bozorth. (*Jour. Appl. Phys.*, vol. 18, pp. 173–176; February, 1947.) A description of the preparation, heat treatment, and properties of "supermalloy," a magnetic alloy of iron, nickel, and molybdenum. As 0.001-inch insulated tape in transformer cores, it has an initial permeability of 50,000–120,000, and permits a threefold increase in the frequency range transmitted.

538.221:621.317.41.029.63 2803

A Method to Measure Complex Permeabilities of Metals at U.H.F.—Johnson, Rado, and Maloof. (*See* 2852.)

538.23:669.157.82 2804

Demagnetizing Coefficients and Hysteresis Losses of Rectangular Iron-Silicon Strips—E. H. Sondheimer. (*Proc. Camb. Phil. Soc.*, vol. 43, part 2, pp. 254–261; April, 1947.) Investigation of the variation of the demagnetization coefficient N with the dimensions of the specimen and its intensity of magnetization. Hysteresis loss is approximately independent of N.

546.431.821:548.3 2805

Crystal Structure of Barium Titanium Oxide and Other Double Oxides of the Perovskite Type—H. D. Megaw. (*Trans. Faraday Soc.*, vol. 42A, pp. 224–231; 1946.) Compounds of the perovskite type having the empirical formula $A^{2+}B^{4+}O^3$ show distortion from the ideal structure, depending on the size of the A^{2+} cation.

546.431.821:621.315.611.011.5 2806

The Permittivity of Polycrystals of the Perovskite Type—D. F. Rushman and M. A. Strivens. (*Trans. Faraday Soc.*, vol. 42A, pp. 231–238; 1946.) The main features of the dielectric-polarization phenomena occurring in barium titanate and the mixed Ba/Pb/Sr titanates are discussed. The behavior of these compounds can be explained by a displacement of the equilibrium position of the titanium ion in the crystal structure.

62"1946" 2807

Progress in Engineering Knowledge during 1946—Alger, Stokley, Faust, Robinson, Tugman, Kuyper, and Haylon. (*See* 2996.)

621.315.6+537.226+621.317 2808

A General Discussion on Dielectrics—(*Trans. Faraday Soc.*, vol. 42A; 1946.) A special number incorporating papers and discussions at the conference at Bristol University, April 24–26, 1946. For abstracts of selected individual papers, see Materials, General Physics, and Measurements sections.

621.315.611.015.5+537.529 2809

Electric Breakdown of Solid Dielectrics—A. von Hippel. (*Trans. Faraday Soc.*, vol. 42A, pp. 78–87; 1946. Discussion, pp. 87–90.) The experimental facts are described for both crystalline and amorphous solids and the theory is propounded that excess electrons, accelerated in the applied field, produce impact ionization, avalanche formation, and breakdown. In the author's opinion in the absence of an applied field, these electrons are stopped by a friction barrier of lattice vibrations in the material. In the discussion various alternative theories are put forward.

621.315.612.015.5 2810

The Electrical Performance of Ceramic Dielectrics at Elevated Temperatures—H. A. Frey and J. M. Jesatko. (*Trans. A.I.E.E.* (*Elec. Eng.*, December Supplement, 1946), vol. 65, pp. 911–920; December Supplement, 1946. Discussion, pp. 1126–1128.) Data on the variation of resistivity with temperature of porcelain, steatite, glass, and zircon compositions; the effect of voltage gradient is also stated, and a method given for determining approximately the conditions for breakdown.

621.315.612.3.029.5 2811

Steatite for High Frequency Insulation—J. M. Gleason. (*Proc. I.R.E.* (Australia), vol. 5, pp. 2–12; April, 1945.) A detailed account of the physical and electrical properties of steatite and steatitic ceramics, with a short discussion of production methods and insulator design.

621.315.616.9.011.5+541.64 2812

The Dielectric Properties of High Polymers—R. B. Richards. (*Trans. Faraday Soc.*, vol. 42A, pp. 194–197; 1946.)

621.315.616.9.011.5.029.5 2813

The Dielectric Properties of Chlorinated Polythenes at Radio Frequencies—W. G. Oakes and R. B. Richards. (*Trans. Faraday Soc.*, vol. 42A, pp. 197–205; 1946.) Measurements over the range 10^4–10^8 cycles. Increase of the average dipole orientation relaxation time with increase of chlorine content is in accord with the change from a flexible or rubbery to a rigid state.

621.315.616.9.011.5.029.5 2814

Dipole Orientation in Solutions of Esters in Polyisobutene and Polythene—K. W. Plessner and R. B. Richards. (*Trans. Faraday Soc.*, vol. 42A, pp. 206–213; 1946.) Power factor and frequency curves are given for the range 10^4–10^8 cycles and are discussed with reference to relaxation times and dipole orientation.

621.315.616.9.029.5:678:621.317.1.011.5 2815

Dielectric Dispersion and Absorption in Natural Rubber, Neoprene, Butaprene NM and Butaprene S, Gum, and Thread Stocks—W. C. Carter, M. Magat, W. C. Schneider, and C. P. Smyth. (*Trans. Faraday Soc.*, vol. 42A, pp. 213–220; 1946.) The dielectric constants of various elastomers, gums and treads were measured over a wide range of frequency. The results obtained show reasonable agreement with predictions from the Fuoss-Kirkwood theory. The abnormally high losses of tread stocks are due to a superposition of Debye effect, Maxwell-Wagner effect, and d.c. conductance.

621.318.323.2.042.15 2816

Iron-Dust Cores—G. H. M. Gleadle. (*Wireless Eng.*, vol. 24, pp. 156–157; May, 1947.) Results are given of measurements on Ferrocart rings. See also 1692 and 1693 of July.

621.396.611.21+537.228.1 2817

Quartz Oscillators—Vigoureux. (*See* 2703.)

621.775.7:6 1.396 2818

Powder Metallurgy and Its Application to Radio Engineering—N. Fetherston and L. W. Cranch. (*Proc. I.R.E.* (Australia), vol. 5, pp. 3–14; May, 1945.) Applications of powder metallurgy include the production of self-lubricating bearings, porous metal filters, Alnico permanent magnets, tungsten rods for wire drawing, silver-graphite and silver-tungsten contacts, iron-dust cores, etc. The methods used for obtaining powdered copper and iron, sintering processes, and the manufacture of iron-dust cores are described. The selection of the grade of magnetic material best suited for a specified frequency application is discussed, and practical applications of iron-dust cores of various types are given.

666.1:621.385 2819

Glass in the Radio Industry—F. Violet, A. Danzin, and A. Commin. (*Ann. Radioélec.*, vol. 2, pp. 24–74; January, 1947.) An account of the development of glass technique in tube manufacturing, showing how research on glass composition, expansion coefficients, the physics of glass-to-metal seals, etc., has led to a progressive replacement of empirical by scientific processes. A detailed description is given of modern mass-production methods of manufacturing tube feet with projecting pins.

669.152.5 2820

New Magnetic Alloy—(*Elec. Times*, vol. III, p. 437; April 17, 1947.) "Hiperco," consisting of 35 per cent cobalt, 64 per cent iron, and 1 per cent chromium gives the highest saturation point of any magnetic material yet known.

669.198.1:669.5 2821

A New Zinc-Base Finish for Steel Parts—J. A. Williams. (*Materials and Methods*, vol. 25, pp. 95–96; March, 1947.) Method of zinc plating which gives a hard, long-wearing surface with the appearance of chromium plating and has greater corrosion resistance than tin finishes formerly used.

669.45.778:621.315.22 2822

F_3 Lead Alloy—An Improved Cable Sheathing—L. F. Hickernell and C. J. Snyder. (*Trans. A.I.E.E.* (*Elec. Eng.*, December Supplement, 1946) vol. 65, pp. 1136–1141.) Discussion on 3647 of 1946.

621.318.22:669 2823

Magnet Steels and High Performance Mag-

net Alloys [Book Review]—W. Jessop and Sons, Sheffield. (*Overseas Eng.*, vol. 20, p. 278; March, 1947.) Gives information on metallurgical aspects of the manufacture of permanent magnets, with a résumé of the theory of magnetization, demagnetization, and artificial aging. The properties and treatment of various alloys are tabulated.

679.5 2824
Plastics for Production [Book Review]—P. I. Smith. Chapman and Hall, London, 216 pp., 15s. (*Elec. Rev.* (London), vol. 140, p. 586; April 11, 1947.)

MATHEMATICS

517.512.2:621.396.67 2825
Fourier Transforms in Aerial Theory: Part 1—Ramsay. (*See* 2680.)

518.2 2826
Table of the Integral $(2/\pi)\int_0^x(1/t)\tanh^{-1}t\,dt$—M. S. Corrington. (*RCA Rev.*, vol. 7, pp. 432–437; September, 1946.) A 5-figure table for the range $x=0$ to 1, with detailed explanation of the methods of computation and checking.

518.5 2827
Analysis of Problems in Dynamics by Electronic Circuits—J. R. Ragazzini, R. H. Randall, and F. A. Russell. (Proc. I.R.E., vol. 35, pp. 444–452; May, 1947.) A method of solving integro-differential equations of physical systems by the use of an electronic system, the basic component of which is a stabilized feedback amplifier which, by external changes in connections, may be used as integrator, differentiator, or sign changer. The application of such amplifiers in systems for the solution of linear first-degree equations, simultaneous integro-differential equations, and equations with variable coefficients is considered.

518.5 2828
Mercury Memory Tanks in New EDVAC [Electronic Discrete Variable] Computer—(*Electronics*, vol. 20, pp. 168–176; May, 1947.) A tube containing mercury has an X-cut quartz crystal at each end in intimate contact with the mercury. Electrical pulses, spaced 1 μs. apart, are converted by one crystal into ultrasonic pulses which travel relatively slowly through the mercury. These are reconverted to electrical pulses by the second crystal, amplified and fed back into the first crystal producing a closed cycle of stored pulses. Multiple electronic switch or gate circuits introduce or withdraw any pulse as required so that a low-loss storage device is provided capable of storing eight 10-digit numbers and referring to any one in an average time of 200 μs.

519.28:52/59 2829
Choice of a 'Reality Index' for Suspected Cyclic Variations—W. O. Kermack and W. Gleissberg. (*Nature* (London), vol. 159, pp. 305–306; March 1, 1947.) A criticism of Gleissberg's application of his "reality index" to data concerning sunspot maxima (1496 of June).

538.566:621.396.677.029.64 2830
Electromagnetic Fields in a Paraboloidal Reflector—E. Pinney. (*See* 2687.)

517.432.1 2831
Heaviside's Operational Calculus Made Easy [Book Review]—T. H. Turney. Chapman and Hall, London, 2nd ed., 1947, 102 pp., 10s. 6d. (*Distrib. Elec.*, vol. 19, p. 242; April, 1947.) Embodies some additional information and, in some instances, more detailed explanations. For review of first edition see 1253 of 1945.

MEASUREMENTS AND TEST GEAR

621.317+621.315.6+537.226 2832
A General Discussion on Dielectrics—(*See* 2808.)

621.317.081.3+53.081.3 2833
International Committee of Weights and Measures—(*Nature* (London), vol. 159, pp. 325–326; March 8, 1947.) Includes a recommendation that absolute electrical units based on the m.k.s. or c.g.s. system should be substituted for the present international electrical units based on the mercury ohm and the silver voltameter. The ratios accepted by the Committee are:

1 mean international ohm = 1.00049 ohm (absolute)
1 mean international volt = 1.00034 volt (absolute).

621.317.081.3+53.081.3 2834
Absolute Electrical Units—(*Elec. Rev.* (London), vol. 141, p. 94; July 18, 1947.) In accordance with decisions taken by the International Committee of Weights and Measures (2832 above) the system of electrical units employed at the National Physical Laboratory will be changed on January 1, 1948, from "international" to "absolute" units. The conditions to be satisfied for the issue of N.P.L. certificates after this date are stated.

621.317.1:621.396.621.029.62 2835
The Testing Procedure for F.M. V.H.F. Receivers—Fanker and Ratcliffe. (*See* 2912.)

621.317.32:621.396.81:621.396.97 2836
BC [Broadcasting] Field Intensity Measurements—(*Tele-Tech*, vol. 6, pp. 64–65; April, 1947.) A portable set covering the frequency range 200–7000 kc. in four bands and with an intensity range from 20 μV. per meter to 10 volts per meter.

621.317.33:621.392.43 2837
Impedance Measurement on Transmission Lines—King. (*See* 2673.)

621.317.33.011.5+535.341]:537.226.029.64 2838
Extension of the Measurements of Dispersion and Absorption by Liquids, to the Region of Centimetric Radio-Electric Waves—Abadie. (*See* 2730.)

621.317.33.011.5+535.341]:537.226.2.029.64 2839
Wave Guide Measurements of Dielectric Absorption of Solutions of Polar Substances in Non-Polar Solvents—H. W. Hall, I. G. Halliday, W. A. Johnson, and S. Walker. (*Trans. Faraday Soc.*, vol. 42A, pp. 136–143; 1946. Discussion, pp. 155–170.) Variation of dielectric absorption with viscosity at 10^{-10} c.p.s.

621.317.33.011.5+535.341]:621.315.615.029.64 2840
Some Measurements on the Absorption of Centimetric Waves by Liquid Dielectrics—F. J. Cripwell and G. B. B. M. Sutherland. (*Trans. Faraday Soc.*, vol. 42A, pp. 149–152; 1946. Discussion, pp. 155–170.)

621.317.33.011.5+535.341]:[621.315.615.2.029 5/.6 2841
Dielectric Absorption in Benzene and Liquid Paraffin Solutions at Ultra High Frequencies—W. Jackson and J. G. Powles. (*Trans. Faraday Soc.*, vol. 42A, pp. 101–108; 1946. Discussion, pp. 155–170.) The variation of loss angle with frequency conforms to the original Debye theory. Experimental arrangements are described.

621.317.33.011.5+535.341]:621.315.615.9.029.64 2842
Measurements on the Absorption of Microwaves: Parts 1 and 2—D. H. Whiffen and H. W. Thompson. (*Trans. Faraday Soc.*, vol. 42A, pp. 114–129; 1946. Discussion, pp. 155–170.) The results of measurements of the absorption of 1.27 centimeter- and 3.26 centimeter-waves and of absorption by temperature variations in a number of liquid hydrocarbons are presented and discussed in relation to relaxation phenomena.

621.317.33.011.5.029.64:537.226.8 2843
The Representation of Dielectric Properties and the Principles Underlying Their Measurement at Centimeter Wavelengths—W. Jackson. (*Trans. Faraday Soc.*, vol. 42A, pp. 91–101; 1946. Discussion, pp. 155–170.) The representation of the electrical properties of dielectric media is explained and resonance methods of measuring them are compared with the standing-wave method. It is stressed that very great care is necessary in the designing of the standing-wave detector system.

621.317.33.011.5.029.64:546.212 2844
Dielectric Properties of Water—C. H. Collie, D. M. Ritson, and J. B. Hasted. (*Trans. Faraday Soc.*, vol. 42A, pp. 129–136; 1946. Discussion, pp. 155–170.) Description of the apparatus used in measurements at wavelengths of 10.0 and 1.25 centimeters, over the temperature range 0 degrees to 100 degrees centigrade. Experimental results are given and briefly discussed.

621.317.33.011.5.029.64:546.212-16 2845
Measurements of the Dielectric Properties of Ice—J. Lamb. (*Trans. Faraday Soc.*, vol. 42A, pp. 238–244; 1946.) Measurements were made (a) at a frequency of 10^{10} c.p.s. over the temperature range 0 to -40 degrees centigrade; and (b) at a temperature of -5 degrees centigrade, over the frequency range 8×10^8 -1.25×10^6 c.p.s. The loss-factor temperature curve for 10^{10} c.p.s. shows a sharp elbow at about -5 degrees centigrade, above which temperature the loss factor increases rapidly. Possible explanations of this are suggested.

621.317.33.011.5.029.64:621.315.611 2846
Some Measurements of the Permittivity and Power Factor of Low Loss Solids at 25000 Mc/s Frequency—R. P. Penroe. (*Trans. Faraday Soc.*, vol. 42A, pp. 108–114; 1946. Discussion, pp. 155–170.) Dielectric properties were investigated by using a flat circular disk of dielectric inserted at one end of an H_0-mode cylindrical cavity resonator and measuring the consequent variation in resonant length. The derivation of permittivity and power factor is explained and the experimental accuracy discussed.

621.317.333:621.319.53 2847
A $2\frac{1}{2}$-Million Volt Surge Generator—(*Engineer* (London), vol. 183, p. 273; March 28, 1947.) For testing cables and insulating materials.

621.317.333.82:620.179.1:621.315.2 2848
The Henley 1,200,000 Volt Impulse Testing Plant: Part 1: The Basic Principles for Cable Testing—T. R. P. Harrison. (*Distrib. Elec.*, vol. 19, pp. 224–227; April, 1947.) The basic circuit and operation of many stages in cascade are described and waveform control and the effect of the circuit inductance discussed. For voltage measurement a c.r.o. is used with a capacitor-type potential divider.

621.317.361+531.761 2849
WWV Schedules—(*Electronics*, vol. 20, p. 87; May, 1947.) A summary of the standard frequency transmissions from the National Bureau of Standards, Washington, D. C.

621.317.382.029.6 2850
Microwave Power Measurement—T. Moreno and O. C. Lundstrom. (Proc. I.R.E., vol. 35, pp. 514–518; May, 1947.) "Possible methods of microwave power measurement are reviewed. The design requirements for bolometric wattmeters are outlined, and examples are given of bolometer elements that have been developed to meet these requirements. A recently developed bolometer element that may be used over an exceedingly wide band of fre-

quencies is included. The results of experiments to investigate sources of error and to determine the accuracy of these wattmeters are summarized. These experiments indicate that, although serious errors are possible, proper usage will hold errors to within a few per cent."

621.317.39:531.76:621.3.015.33 2851
Pulse Width Measuring Method—(*Tele-Tech*, vol. 6, p. 57; April, 1947.) An instrument with an accuracy of one-fourth μs. for pulse widths of 3 to 12 μs. independent of repetition frequency.

621.317.41.029.63:538.221 2852
A Method to Measure Complex Permeabilities of Metals at U.H.F.—M. H. Johnson, G. T. Rado, and M. Maloof. (*Phys. Rev.*, vol. 71, p. 472; April 1, 1947.) Summary of American Physical Society paper. The method involves measurement of the changes in Q and in the resonant frequency when a metal is substituted for the ferromagnetic center conductor in a coaxial resonator.

621.317.72.029.56/.58:621.392.43 2853
The "Micromatch"—M. C. Jones and C. Sontheimer. (*QST*, vol. 31, pp. 15–20; April, 1947.) A meter for direct measurement of the standing wave ratio of transmission lines and r.f. power. It operates over the frequency range 3 to 30 Mc. and for line impedances of 70 to 300 Ω and, as a power meter at maximum sensitivity, has a full scale deflection corresponding to approximately 10 watts or 40 watts with a 70-Ω or 300-Ω line respectively.

621.317.733 2854
Considerations on the Equations of Balance of an A.C. Wheatstone Bridge—M. Romanowski and G. Leclerc. (*Gen. Élec. Rev.*, vol. 56, pp. 129–132; March, 1947.) Discussion of the classical methods for reducing the effects of parasitic capacitance and an account of a method, due to J. Carvallo, of eliminating the effect of the capacitances localized at the corners of the bridge. The case where an intermediate point on one of the arms has appreciable capacitance to earth is also considered.

621.317.75.029.64 2855
Microwave Spectrum Analyzers—H. R. Traver and F. L. Burroughs. (*Tele-Tech*, vol. 6, pp. 35–38; April, 1947.) Details of sharply tuned superheterodyne receivers whose frequency of reception is made to sweep across the frequency spectrum at a rate slow compared with the pulse repetition frequency of the oscillator being studied. Details are given of an analyzer for 9300 Mc. using a reflex klystron as local oscillator.

621.317.761.087 2856
Direct Frequency Measurement—L. M. Berman. (*Electronics*, vol. 20, pp. 202–208; May, 1947.) Summary of 2504 of September.

621.317.79:621.396.611 2857
Automatic [Circuit] Testing Machine—(*Toute la Radio*, vol. 14, pp. 144–145; May, 1947.) A short account of the principles and operation of the apparatus described by Williams, Marshall, Bissmire, and Crawley (2181 of August).

621.396.615.12:621.317.79 2858
Standard Frequency Generator—S. J. Haefner and R. H. Smith. (*Tele-Tech*, vol. 6, pp. 58–59; April, 1947.) Push-button operation gives frequencies from 40 kc. to 1000 kc. in steps of 40 kc. With an interpolation oscillator continuously variable from 10 kc. to 50 kc. any frequency in the above range is obtained.

621.396.615.17:621.396.822 2859
Noise Signal Generator—W. P. Dolphin. (*R.S.G.B. Bull.*, vol. 22, pp. 158–160; April, 1947.) The noise factor is defined and it is shown that a noise generator gives a true value for the signal-to-noise ratio independent of the bandwidth of the receiver. The generator consists of a saturated diode with a resistive load, the noise output being controlled by varying the filament current. A practical account of the technique for frequencies up to 100 Mc. is given and other uses of the generator are indicated.

OTHER APPLICATIONS OF RADIO AND ELECTRONICS

535.61-15:621.317.755:535.33 2860
An Infra-Red Spectroscope with Cathode-Ray Presentation—E. F. Daly and G. B. B. M. Sutherland. (*Proc. Phys. Soc.*, vol. 59, pp. 77–87; January 1, 1947.) An instrument by means of which a range of 2.5 to 3.58, anywhere between 1 and 16μ, can be scanned in 14 seconds. See also 3373 of 1946.

535.61-15:621.383.001.8 2861
An Infrared Image Tube and Its Military Applications—G. A. Morton and L. E. Flory. (*RCA Rev.*, vol. 7, pp. 385–413; September, 1946.) Description of components of infrared electron telescope, comprising image tube, objective for forming infrared image on photocathode and optical system for viewing reproduced image.

535.61-15:621.389 2862
Infra-Red Ray Development—(*Electrician*, vol. 138, pp. 933–934; April 11, 1947.) British equipment, perfected in 1941, consists fundamentally of a small vacuum container with two flat parallel sides, spaced about 0.5 centimeter apart, lying at right angles to the axis of a telescope. One side supports a caesium-silver infrared-sensitive photocathode, while the other is coated with fluorescent material and is electrically conducting. A d.c. potential of 3–4 kv., derived from a small Zamboni pile, is maintained between the photocathode and the anode. Radiation from an infrared source, after filtering out any visible component, is focused on the photocathode, the electrons from which give an image on the fluorescent screen. With infrared headlights and binoculars the system was largely used for night driving. The smallest British receiver, a single eyepiece model, weighs only one and one quarter pounds, compared with 16 pounds for the German equivalent. See also 2207 of August.

536.48 2863
Possible Use of Thermal Noise for Low Temperature Thermometry—E. Gerjuoy and A. T. Forrester. (*Phys. Rev.*, vol. 71, pp. 375–376; March 15, 1947.) Further comment on 483 of March: see also 2185 of August. It is shown, theoretically, that the minimum measurable temperature, under given conditions, is about 2 degrees Kelvin.

537.531 2864
The Physical Properties of Super-Voltage X Rays—H. Miller. (*Radiography*, vol. 13, pp. 37–41; April, 1947.) A general account, with special reference to voltages ranging up to 20 mv., whose use for X-ray therapy gives promise of valuable new possibilities.

539.16.08 2865
Spread of Discharge in Geiger Counters—J. D. Craggs and A. A. Jaffe. (*Nature* (London), vol. 159, pp. 369–370; March 15, 1947.

539.16.08 2866
Simplified Spark Counter—H. Greinacher. (*Helv. Phys. Acta*, vol. 20, pp. 222–224; April 30, 1947. In German.) Uses a symmetrical spark gap with small platinum-ball electrodes sealed in a glass bulb. This is connected in series with a 0.5-M Ω resistor shunted by a small capacitor, a neon lamp, a telephone earpiece, and the secondary of a transformer giving about 2200 volts. A tube with a thin end is sealed into the glass bulb to allow the counter to be used for α-particles. Telephone clicks, though weak, are quite audible and the glow tube is bright enough for photographic recording of α, β, or γ rays on a moving film, using a narrow slit.

539.16.08 2867
A Method for Measuring the Velocity of the Ion Transfer in Rapid Counter Tubes—P. Huber, F. Alder, and E. Baldinger. (*Helv. Phys. Acta*, vol. 19, pp. 204–206; July 31, 1946. In German.)

539.16.08:621.318.572.015.33 2868
On the Pulse Shape in Rapid Counter Tubes—P. Huber, F. Alder, E. Baldinger, and F. Metzger. (*Helv. Phys. Acta*, vol. 19, p. 207–211; July 31, 1946. In German.)

539.16.08:621.383 2869
The Multiplier as a Counter for Elementary Particles—K. P. Meyer. (*Helv. Phys. Acta*, vol. 19, pp. 211–214; July 31, 1946. In German.)

621.317.39:531.719.27 2870
Rate-of-Change Meter—R. W. Treharne, J. A. Kammerer, and R. Hofstadter. (*Electronics*, vol. 20, pp. 106–107; May, 1947.) "Varistor-compensated circuit converts nonlinear voltage variables into linear voltage variables. Application in radio altimeters shows rate of climb directly, with short time lag."

621.317.39:621.396.645:539.4 2871
Carrier-Type Amplifier for Electric Gages—H. C. Roberts. (*Electronics*, vol. 20, pp. 92–95; May, 1947.) An RC-coupled amplifier for use with various types of electrical gauge circuits in static and dynamic tests on strains, pressures, etc., in railway rolling stock, bridges, and tracks.

621.317.39.083.7:629.13 2872
Radio Telemetering for [Dynamic] Testing [of] Aircraft in Flight—C. L. Frederick. (*Trans. A.I.E.E.* (*Elec. Eng.*, December Supplement, 1946.) vol. 65, pp. 861–870.) Description of stabilized oscillators modulated by metering equipment; regulated power supplies; f.m. transmitter; automatic frequency-controlled receiver; and heterodyne analyzer used by the United States Navy in 1945.

621.357.8:537.533.73 2873
Electron Diffraction Examination of Electrolytically Polished Surfaces—J. J. Trillat. (*Compt. Rend. Acad. Sci.* (Paris), vol. 224, pp. 1102–1103; April 14, 1947.) Tests carried out on samples of pure iron, aluminum, and copper show that electrolytic polishing causes the Beilby layer to disappear to an extent depending upon the duration of the operation. The nature of the bath appears to play an important part in the case of aluminum, a metal easily oxidized.

621.365.5+621.365.92 2874
Industrial Applications of High Frequency—M. Descarsin. (*L'Onde Élec.*, vol. 27, pp. 121–137; April, 1947.) Basic principles, historical development, and numerous applications of both induction and dielectric heating.

621.365.5:538.2 2875
Theory of the Heating of Ferromagnetic Materials by Eddy Currents and by Hysteresis—Jouguet. (*See* 2752.)

621.365.52 2876
Design of Induction Heating Coils for Cylindrical Magnetic Loads.—J. T. Vaughan and J. W. Williamson. (*Trans. A.I.E.E.* (*Elec. Eng.* December Supplement, 1946), vol. 65, pp. 887–892. Discussion, pp. 1165–1166.) Extension of previous paper (148 and 2271 of 1946) to design of coils for magnetic loads. Variation in impedance of coil circuit with changing temperature necessitates special design of circuit to absorb maximum power. See also 2271 of 1946.

621.365.92.072.8 2877
High Frequency Heating—J. F. Capper. (*Elec. Times*, vol. 111, pp. 417–421; April 17, 1947.) Discussion of methods and advantages of automatic loading control.

621.369.2 2878
Some Applications of Infra-Red Lamp Radiation to Treatment [of Materials], Drying [of leather, etc.] and Baking [of Paints and Varnishes]—M. Déribéré. (*Gén. Élec. Rev.*, vol. 56, pp. 71–74; February, 1947.)

621.38.001.8 2879
The Elecgrical Engineer in the Service of Other Industries—H. C. Turner and G. M. Tomlin. (*Beama Jour.*, vol. 54, pp. 57–64; February, 1947.) Abridgment of I.E.E. Measurement Section paper. A description of various electronic instruments used in test processes, including a magnetic sorting bridge for indicating variations in purity, heat treatment, hardness, and depth of carburization in steels. Two types of vibration analyzer are described and details given of the use of supersonic equipment in metal testing and measurement of thickness of metallic films.

621.38.001.8:621.317 2880
Valves and Their Industrial Low-Current Applications—F. Fanchamps. (*Bull. Sci. Ass. Inst. Electrotech.* (Montefiore), vol. 60, pp. 11–34; January, 1947.) Describes the basic principles of tube methods of measurement of various quantities, with applications in engineering and automatic control.

621.383.4 2881
High-Sensitivity Photoconductive Cell—Hewlett. (*See* 2972.)

621.384.6.07 2882
Stabilizing Linear Particle Accelerators by Means of Grid Lenses—D. Gabor. (*Nature* (London), vol. 159, pp. 303–304; March 1, 1947.) The mode of action of grid lenses is outlined, and their advantages described. "Grid lenses may well compete with beryllium foils in the stabilization of linear accelerators for extreme energies."

621.385.833:[538.311+621.316.97].083 2883
Measurement of Feeble Magnetic Fields and of the Effects of Shielding. Application to the Electron Microscope—Charles. (*See* 2753.)

621.386.1:544 2884
Apparatus and Techniques for Practical Chemical Identification by X-Ray Diffraction—C. S. Smith and R. L. Barrett. (*Jour. Appl. Phys.*, vol. 18, pp. 117–191; February, 1947.)

621.398:621.397.6 2885
Miniature Airborne Television Equipment—Kell and Sziklai. (*See* 2961.)

621.398:629.13 2886
Guide-Beam Control Technic for V-2 Rockets—G. Hausz. (*Tele-Tech*, vol. 6, pp. 76–80; March, 1947.) The Leitstrahl (Ls) system operated on frequencies in the range 42–64 Mc. and used two narrow beams from a transmitter 5 to 10 miles behind the launching point and on the line from there to the target. The beams were directed at angles of 0.4 degree on either side of this line, that on the left being modulated at 5 kc. and the other at 7 kc. The two beams were switched on alternately for 0.01 second. In the missile, equal amplitude signals were only received when on course. Deviations gave rise to an error voltage which was applied to control circuits to correct the deviations. The high accuracy obtained was largely due to the aerial assembly, which consisted of two horizontal $\lambda/2$ dipoles, 220 yards apart, giving a system of very narrow beams, only two of which were used. A capacitor switching system was employed. Details of the transmitter-wagon and missile-borne equipments are given, with block diagrams. See also 2512 of September.

621.398:629.13:621.397.6 2887
Flying Torpedo with an Electric Eye—Zworykin. (*See* 2962.)

621.398:629.135.52 2888
Radio Control of Model Flying Boats—V. Welge. (Proc. I.R.E., vol. 35, pp. 526–530; May, 1947.) Control is effected by variations in amplitude of seven audio modulating tones on a carrier in the frequency band 116.0 to 118.5 Mc.

PROPAGATION OF WAVES

621.396.11 2889
On the Field of Radio Waves Between Two Semiconducting [Imperfectly Conducting] Surfaces—P. A. Ryazin and L. M. Brekhovskikh. (*Bull. Acad. Sci.* (U.R.S.S.), *sér. phys.*, vol. 10, no. 3, pp. 285–305; 1946. In Russian.) Starting from Maxwell's equations and boundary conditions (2) the case is discussed where the field is excited by a vertical dipole located in the intermediate non-conducting space at any arbitrary height above the lower medium. The boundary surfaces of the media are assumed to be flat and parallel (Fig. 1). The problem is thus similar to that of the propagation of radio wave between the surface of the earth and the ionosphere if the above assumptions can be applied to the latter case.

The main results obtained are: (a) At large distances the waves in the intermediate air layer are of the surface type as distinct from the space type. (b) The variation of the intensity and phase of radio waves near the earth surface is calculated. Sommerfeld's solution taking into account only one boundary surface is a particular case of the more general theory developed in this paper. (c) The phase velocity of waves, at least of the longer wavelengths, exceeds the velocity of light. (d) It is confirmed that the attenuation factor in Austin's and other empirical formulas is of exponential form.

621.396.11 2890
On the Propagation and Dispersion of Radio Waves—V. A. Fock. (*Viestnik Akad. Nauk* (S.S.S.R.), no. 3, pp. 23–34; 1946. In Russian.) A general elementary survey introducing methods developed by the author.

621.396.11:538.566 2891
Diffraction of Radio Waves Around the Earth's Surface—V. Fock. (*Jour. Phys.* (U.S.S.R.), vol. 9, no. 4, pp. 255–266; 1945.) Full paper, of which a summary was noted in 160 of 1946.

621.396.11:551.5 2892
The Mode Theory of Tropospheric Refraction and Its Relation to Wave-Guides and Diffraction—H. G. Booker and W. Walkinshaw. (*Physical Society Special Report on Meteorological Factors in Radio-Wave Propagation*, pp. 80–127.) The bearing of the theory of waveguides upon refraction, particularly of radio waves, in the troposphere and upon diffraction beyond the horizon is explained in detail. Propagation curves suitable at any rate for a qualitative description of the effects of tropospheric radio refraction are given. Atmospheric propagation may be described in terms of a series of characteristic E- or H-waves similar to those which can travel between parallel metal sheets. The lower edge of the track of these waves often, but not always, coincides with the earth's surface. The height of the upper edge depends on the distribution of refractive index with height and upon the order of the mode involved.

Beyond the horizon the E_1- or H_1-wave becomes predominant. Normally all the characteristic waves leak copiously from the tops of their tracks, but under conditions of superrefraction the degree of this leakage is reduced and may even be entirely suppressed for the first mode at meter wavelengths and below. This wave can then produce at long range a remarkably high field strength within its track.

621.396.11:551.5 2893
A Variational Method for Determining Eigen-Values of the Wave Equation Applied to Tropospheric Refraction—G. G. Macfarlane. (*Proc. Camb. Phil. Soc.*, vol. 43, Part 2, pp. 213–219; April, 1947.) A general method of solution for both real and complex eigen-values corresponding to any type of atmospheric refractive index profile. There existed previously two methods of analysis for problems on the tropospheric refraction of radio waves, the perturbation method applicable to cases where energy leaks considerably from an atmospheric duct, and Rayleigh's method, which may be applied in the case of real eigen-values, or trapped modes of propagation. The present work may be considered as an extension of Rayleigh method to the case of complex eigen-values. An example is given of the use of the method when the refractive index varies with height according to a power law. See 2894 and 2892.

621.396.11:551.5 2894
A Method for Deducing the Refractive-Index Profile of a Stratified Atmosphere from Radio Observations—G. G. Macfarlane. (*Physical Society Special Report on Meteorological Factors in Radio-Wave Propagation*, pp. 250–252.) A profile of refractive index can be obtained either from one set of radio height-gain measurements at a fixed range and a few measurements of field strength at a constant height, or from two sets of height-gain measurements at different wavelengths. Such a profile may be more reliable for predicting radio field strengths than one obtained from a single meteorological sounding. See also 2893 above.

621.396.11:551.510.535 2895
The Application of Ionospheric Data to Radio Communication Problems: Part 2—E. V. Appleton and W. J. G. Beynon. (*Proc. Phys. Soc.*, vol. 59, pp. 58–76; January 1, 1947.) "Graphs are given from which may be estimated the maximum usable frequency of radio waves reflected by an ionospheric layer in oblique incidence transmission. The curves based on the theory given in part 1 of the paper are drawn for such ranges of layer thickness and layer height as are met with in practice. The limitations in the accuracy and applicability of the theory in practice are briefly discussed. Attension is also drawn to the occurrence of abnormal transmission conditions under which long-distance communication via the ionosphere is possible on frequencies exceeding the normally predicted values." For part 1 see 3290 of 1940.

621.396.11:551.510.535 2896
Oblique Radio Transmission in the Ionosphere, and the Lorentz Polarization Term—W. J. G. Beynon. (*Proc. Phys. Soc.*, vol. 59, pp. 97–107; January 1, 1947.) The work of Ratcliffe (15 of 1940) upon the appropriateness of the Sellmeyer or Lorentz dispersion formulas in this connection is extended and shown to be consistent with that of Newbern Smith (1586 of 1941). The analysis is applied to a large number of experimental results.

The maximum usable frequencies over distances of 1000 kilometers and 700 kilometers were found to depart from the values calculated using the Sellmeyer formula by only 0.2 and 0.03 respectively of the amount that would be expected if the Lorentz formula applied.

These experimental results are thus in agreement with the theoretical conclusion of Darwin (1934 Abstracts, p. 606) that the Sellmeyer type of formula is applicable to the case of the refraction of radio waves in the ionosphere.

621.396.11:551.510.535 2897
Gyro Interaction of Radio Waves—L. G. H. Huxley, H. G. Foster, and C. C. Newton. (*Na-*

ture (London), vol. 159, pp. 300–301; March 1, 1947.) An outline of preliminary experimental data and discussion of results. For the tests, the modulation introduced by two suitably situated transmitters operating near the gyro-frequency, on 200 kc. signals from Droitwich, was observed. Certain of the main features of Bailey's theory were confirmed quantitatively. The practical implications of the results are mentioned. For Bailey's theory see 1934 Abstracts, p. 606, and 840 of 1937.

621.396.11:551.510.535 2898
Predicting Amateur "Conditions"—N. A. Atwood. (*QST*, vol. 31, pp. 21–25, 120; April, 1947.) A new method for quick determination of the best "working area" from a given position using Central Radio Propagation Laboratory maximum usable frequency charts.

621.396.11.029.62:551.510.535 2899
Six-Metre Transatlantic Signals—R. Naismith. (*Wireless World*, vol. 53, p. 186; May, 1947.) The recent reception of these signals coincided with a high value of vertical-incidence critical frequency for region F2 and a theoretical maximum frequency for transmission by the tangential ray of 48.9 Mc. Alternative modes of propagation are considered and rejected. This therefore is the first proved case of highly efficient transmission over 6000 kilometers involving only one reflection.

621.396.11.029.64 2900
Wave Theoretical Interpretation of Propagation of 10-Centimeter and 3-Centimeter Waves in Low-Level Ocean Ducts—C. L. Pekeris. (PROC. I.R.E., vol. 35, pp. 453–462; May, 1947.) An analysis of results obtained in the West Indies. "Below the horizon, the 10-centimeter wave was found to propagate by the first normal mode with a theoretical decrement of 1 decibel per nautical mile, as against an observed value of about 0.8 decibel per nautical mile in the first 80 miles from transmitter. Theory verified the observed constancy of decrement with height for this wavelength. Beyond 80 miles the observed rate of attenuation dropped to a low value of 0.2 decibel per nautical mile. This change of slope in the intensity curve is probably due to the emergence of scattered radiation after the direct diffracted beam had been depleted." With the exception of one point there is quantitative agreement between the observed and theoretical distribution of intensity with height for the 10-centimeter wave.

"The 3-centimeter wave was found to propagate below the horizon by the first and second modes, with theoretical decrements of zero and 0.5 decibel per nautical mile, respectively. The latter agrees with the observed values at high elevations, but near the surface, where theoretically attenuation should be negligible, the observed rate of attenuation exceeds the theoretical value by about 0.3 decibel per nautical mile. This is probably due to attenuation by scattering from horizontal inhomogeneities in the distribution of refractive index, and from the rough surface. Theory verifies the observed increase of decrement and decrease of intensity with height above about 10 feet for the 3-centimeter band."

621.396.4.029.62 2901
A Multi-Channel V.H.F. Radio Communications System—Knox and Brereton. (*See* 2927.)

621.396.41.029.64 2902
On the Calculation of Multiplex Radio-Telephone Links on Ultra-Short Waves—H. Chireix. (*Ann. Radioélec.*, vol. 2, pp. 3–12; January, 1947.) Reprint of 1559 of June.

621.396.812:523.323 2903
Effect of the Moon on Radio Wave Propagation—(*Nature* (London), vol. 159, p. 396; March 22, 1947.) P. A. de G. Howell claims to have observed during 1938–39 and 1944–45 a correlation between long distance transmission conditions and the moon's phase. High signal level, low noise, and little fading are associated with full moon and the reverse with new moon.

621.396.812:621.396.96 2904
A Theory of the Performance of Radar on Ship Targets—M. V. Wilkes and J. A. Ramsay. (*Proc. Camb. Phil. Soc.*, vol. 43, pp. 220–231; April, 1947.) An expression is derived for the power returned to the receiver of a radar installation from a ship surface. Conditions of superrefraction are not considered; under normal conditions, provided a suitable value of effective earth radius is taken, good agreement with experimental results on the variation of signal strength with range is obtained. Measurements using a balloon-borne metallized sphere are also described.

621.396.812.029.64:551.510.52 2905
Radar Reflections from the Lower Atmosphere—Friis. (*See* 2769.)

621.396.11:551.5 2906
Meteorological Factors in Radio-Wave Propagation—[Book Notice]—Physical Society, London, 325 pp., 24s. Report of a Conference held on April 8, 1946, by the Physical Society and the Royal Meteorological Society. Individual papers will be abstracted in due course.

RECEPTION

621.396.619.11/.13 2907
Laboratory Tests of Weak Signal Narrow-Band F.M.—O. G. Villard, Jr. (*CQ*, vol. 3, pp. 21–26, 72; April, 1947.) When an a.m. receiver is used for the reception of a.m. transmissions and also of f.m. transmissions by distuning, narrow-band f.m. gives better results for the same carrier power on strong signals, but poorer results on weak signals not much above the background noise level.

621.396.619.13.029.62:621.396.933 2908
Comparing F.M. with A.M. for Aircraft Communications—(*Tele-Tech*, vol. 6, pp. 52–56, 111; April, 1947.) "For military [v.h.f.] operations [narrow-band] f.m. has capabilities for greater range and noise suppression, is less critical as to tuning, less susceptible to jamming."

621.396.621+621.396.69 2909
Machine for Receiver Manufacture—(*Toute la Radio*, vol. 14, pp. 163–164; May, 1947.) A short account of the equipment described in 1913 of July (Sargrove).

621.396.621 2910
High-Fidelity Receiver—R. Gondry. (*Toute la Radio*, vol. 14, pp. 136–143; May, 1947.) A detailed description, with complete circuit diagram and performance curves, of a receiver with variable selectivity, low and high tone control, adjustable expansion, a switch for speech or music, and a high-power output amplifier.

621.396.621:621.396.61 2911
Technical Characteristics of Transmitters, E. Aisberg. (*Toute la Radio*, vol. 14, pp. 132–134; May, 1947.) Stresses the importance, in the design of receivers, of detailed knowledge of the frequency and modulation characteristics, intensity ratios, etc., of the transmission to be received.

621.396.621.029.62:621.317.1 2912
The Testing Procedure for F.M. V.H.F. Receivers—E. M. Fanker and R. A. Ratcliffe. (*Proc. I.R.E.* (Australia), vol. 8, pp. 4–12; March, 1947. Discussion, pp. 12–16.) The fundamental operating principles are discussed when they differ from these of a.m. circuits. The alignment procedure and methods for measuring the receiver characteristics are described and values given for typical equipment.

621.396.621.076.2.029.62/.63 2913
Very High Precision Tunable Receiver for V.H.F.—S. Y. White. (*Tele-Tech*, vol. 6, pp. 48–51, 107; April, 1947.) Description of a receiver with permeability tuning and plug-in tank circuits for use between 60 and 600 Mc.

621.396.621.078] 2914
Automatic Controls in Modern Receivers—F. Juster. (*Toute la Radio*, vol. 14, pp. 150–153; May, 1947.) A concise account of delayed automatic volume control, the Lamb system for parasitic suppression and automatic frequency control. The latter is strongly recommended.

621.396.722:534.32 2915
Distortion and Acoustic Preferences—Moir (*See* 2656.)

621.396.82:551.57:629.135
621.319.74:551.57:629.135 2916
Electrostatic Ills and Cures of Aircraft: Parts 1 and 2—R. Beach. (*Elec. Eng.*, vol. 66, pp. 325–334 and 453–462; April and May, 1947.) In part 1, "the process by which electrification is accumulated [by aircraft in flight] and the mechanism by which radio interference is produced are described." In part 2 various methods for dissipating static charges on aircraft are given. Experimental results show the effectiveness of metallic bristles, with chemically etched points, for suppressing static interference.

621.396.822:621.396.615.17 2917
Noise Signal Generator—Dolphin. (*See* 2859.)

621.396.822:621.396.621.53 2918
Noise-Figure Reduction in Mixer Stages—M. J. O. Strutt. (PROC. I.R.E., vol. 35, p. 496; May, 1947.) Corrections to 1573 of June.

621.396.822:621.396.645 2919
Noise Factor: Part 3—L. A. Moxon. (*Wireless World*, vol. 53, pp. 171–176; May, 1947.) Discussion of: noise sources in an r.f. amplifier and the circuit quantities which determine their effect; the meaning of equivalent noise resistance as applied to tube shot noise; formulas for the noise factor; and the use of grounded-grid and neutralized triodes as the first tubes in v.h.f. receivers. For parts 1 and 2 see 864 of April and 1196 of May.

621.396.822.029.63:523.78"1946.11.23" 2920
Micro-Wave Solar Noise Observations During the Partial Eclipse of November 23, 1946—Covington. (*See* 2761.)

621.396.822.08:621.396.645 2921
Linearity Range of Noise-Measuring Amplifiers—Bell. (*See* 2718.)

621.396.828 2922
The Suppression of Radio Interference from Electrical Appliances—S. F. Pearce. (*Beama Jour.*, vol. 54, pp. 40–47; February, 1947.) A description of a number of circuits for efficient suppression in a wide range of appliances. The components requiring careful design are the capacitor for earthed appliances and the line inductor for those which are not earthed. For satisfactory performance at frequencies above 30 Mc. a "bushing type" capacitor is necessary in which the current-carrying conductor passes through the body of the capacitor. Design particulars are given for filters having an insertion loss of about 80 db in the range 5 to 100 Mc., with a formula for calculating the lowest frequency at which the required attenuation is obtained.

STATIONS AND COMMUNICATION SYSTEMS

621.394.14 2923
Table of Q-Code—(*Radio* (Moscow), no.

3, p. 51; June, 1946. In Russian.) With meanings and Russian equivalents.

621.395.44.029.6 2924
2000 Telegrams per Minute by Microwave—J. Z. Millar. (*Tele-Tech*, vol. 6, pp. 36–40; March, 1947.) A description of the equipment of the New York-Philadelphia link. See also 1578 of June.

621.396(675)"1939/1945" 2925
Development of Telecommunications in the Belgian Congo During the War—J. G. Jonlet. (*Bull. Sci. Ass. Inst. Électrotech.* (Montefiore), vol. 60, pp. 43–63; February, 1947.) Historical, with some details of the 50-kw. short-wave transmitter put into service in 1943. See also 870 of April.

621.396.1:621.396.96 2926
Radar Allocations—Markus. (*See* 2788.)

621.396.4.029.62 2927
A Multi-Channel V.H.F. Radio Communications System—J. B. Knox and C. H. Brereton. (*RCA Rev.*, vol. 7, pp. 179–198; June, 1946.) A description of the installation of an f.m. network (42 to 50 Mc.) on the Canadian Pacific Coast. The results of propagation tests are discussed and land profiles of test and operative links are given. The aerial systems and equipment are briefly described and a statistical analysis of recorded field strengths for various stations is shown graphically.

621.396.41.029.64 2928
On the Calculation of Multiplex Radio-Telephone Links on Ultra-Short Waves—Chireix. (*See* 2902.)

621.396.6:551.510.535 2929
Ionosphere Equipment for Field Use—G. H. Musselman. (*Electronics*, vol. 20, pp. 112–116; May, 1947.) The requirements of field equipment are listed and modern pulsed measurement systems briefly described. Details are given of a simplified technique with an automatic motor-tuned receiver and a variable-frequency (1.5 to 4.0 Mc.) transmitter half a mile distant. Recording is automatic.

621.396.61/.62].029.64 2930
Dishing Out the Milliwatts on 10 kMc/s—Correction to 1931 of July. The last phrase should read "using a Hallicrafter S-29 portable receiver as i.f. to a.f. amplifier."

621.396.619.13:621.397.5(94) 2931
Frequency Modulation and Television—N. S. Gilmour. *Proc. I.R.E.* (Australia), vol. 5, pp. 3–8; July, 1944.) Discusses modern developments with particular reference to post-war application in Australia.

621.396.619.13.029.62:621.396.933 2932
Comparing F.M. with A.M. for Aircraft Communications—(*See* 2908.)

621.396.619.16 2933
Pulse Modulation and Demodulation Theory—M. M. Levy. (*Jour. Brit. I.R.E.*, vol. 7, pp. 64–83; March and April, 1947.) Modulation is accomplished by shifting in time the position of a periodic train of pulses by an amount proportional to the modulating signal; in demodulation the position of one edge of each pulse is moved in time in synchronism with the modulated pulse, so giving a train of variable-width pulses which after detection yield the modulating signal. The nature of the distortion produced by these processes is studied and it is shown that a distortionless pulse communication system can be evolved by following certain simple rules.

621.396.65 2934
Radio Relays for Telegraphy—F. B. Bramhall. (*Telegr. Teleph. Age*, vol. 65, pp. 10, 12–32; April, 1947.) Beamed microwaves of frequencies about 3000 Mc. used for communication in the U.S.A. See also 876 of April and 1578 of June, U.D.C. of which should more properly be 621.396.65.

621.396.65 2935
Development of Radio Relay Systems—C. W. Hansell. (*RCA Rev.*, vol. 7, pp. 367–384; September, 1946.) Survey of development and requirements. Suggested signal-to-noise ratios for printer telegraph, 18 db; for on-off-keyed printer telegraph, 21 db; for ordinary telephone, 40 db; for broadcast, facsimile, and television, 50 db; and for high-quality music, 60 db. The bandwidth occupied by a phase modulated multichannel relay system is $2B+2Bd/\sqrt{3}$, where B is the modulation frequency band and d is the peak phase deviation.

621.396.65.029.62:621.396.93 2936
Frequency Modulation Mobile Radiotelephone Services—H. B. Martin. (*RCA Rev.*, vol. 7, pp. 240–252; June, 1946.) A discussion of the proposed use of frequencies in the ranges 30 to 44 Mc. and 152 to 162 Mc. for common-carrier mobile radio-telephone communication for motor vehicles and surface vessels.

621.396.712.029.58(945) 2937
Melbourne Division Visits "Radio Australia"—(*Proc. I.R.E.* (Australia), vol. 8, pp. 22–23; February, 1947.) A brief description of the lay-out of the h.f. broadcasting station at Shepparton, Victoria, Australia. See also 2672 above.

621.396.712(489) 2938
Broadcasting Equipment—(*Overseas Eng.*, vol. 20, p. 279; March, 1947.) A short account of the new equipment and studio arrangements at Radio House, Copenhagen.

621.396.712.3(944) 2939
Broadcasting Studio Equipment—L. N. Schultz. (*Proc. I.R.E.* (Australia), vol. 5, pp. 3–17; October, 1944.) Specification of the complete equipment for station 2GB, Sydney.

621.396.73 2940
Emergency Broadcast Pickup Techniques—G. Riley. (*Electronics*, vol. 20, pp. 108–111; May, 1947.) Methods and equipment used for emergency outdoor broadcasts by radio station WOR, New York.

621.396.828.029.56.62 2941
The Staggering Band Theorem—L. E. Rapp. (*QST*, vol. 31, pp. 60–61, 136; April, 1947.) A plan to eliminate interference in the amateur frequency bands by devoting particular bands to c.w. transmissions and telephone transmissions during alternate 24-hour periods.

621.396.931 2942
The Development of a Radio Communication Network for the South African Railways—G. D. Walker. (*Trans. S. Afr. I.E.E.* vol. 37, pp. 283–305; December, 1946. Discussion, pp. 305–307.) Sections 1, 2, and 3 give, respectively, details of the extent of the radio network, the requirements of the service, and the equipment now in use. Eighteen spot frequencies within the band 4 to 14 Mc. are used and telephonic as well as telegraphic facilities are provided.

Section 4 deals with aerial design; a stack of three aerials supported between a single pair of towers is used, each aerial consisting of a 2-fold half-wave dipole.

Section 5 deals with the arrangements for matching the aerial to the 600Ω feeder at more than one frequency; a novel form of compound stub is described.

Section 6 describes some pulse transmissions under conditions of oblique incidence on the ionospheric layers.

SUBSIDIARY APPARATUS

621.313.2 2943
The "Electrotor"—(*Elec. Rev.* (London), vol. 140, pp. 663–664; April 25, 1947.) Miniature low-voltage (1.5–6 volts) d.c. motor of novel design; ring-shaped permanent magnet stator, gap-ring wound rotor with brushes bearing directly upon bared edges of winding. Manufactured in several sizes, the smallest weighing 1 Geiger-Muller and being one-half centimeter in diameter and length, speed 7000 r.p.m. and voltage 1.5.

621.314.12:621.394/.396].66 2944
The Amplidyne—E. C. Barwick. (*Elec. Times*, vol. 111, pp. 449–453 and 485–488; April 24 and May 1, 1947.) A description of a quick response d.c. generator requiring an exceptionally low field power for excitation. Some typical control circuits are described in part 1. Part 2 describes the application of amplidyne control to such equipment as winding gear, cable laying machinery, and synchronous motors. See also 3765 of 1946.

621.314.653 2945
Characteristics of Resistance Ignitors—D. E. Marshall and W. W. Rigrod. (*Electronics*, vol. 20, pp. 122–126; May, 1947.) The magnitude of variations of current, voltage, and firing time with operating conditions are presented as a guide to designers.

621.316.54 2946
Fundamental Properties of the Vacuum Switch—R. Koller. (*Trans. A.I.E.E.* (*Elec. Eng.*, August and September, 1946.) vol. 65, pp. 597–604. Discussion, *ibid.*, December Supplement, vol. 65, pp. 1141–1142; 1946.) Summary noted in 2021 of 1946.

621.316.728 2947
Design of Electronically Regulated Power Supplies—B. A. Penners and W. Davis. (*Radio* vol. 31, pp. 9–15; February and March, 1947.) A comprehensive theoretical discussion presenting complete design data.

621.352.8 2948
Novel Batteries—(*Elec. Rev.* (London), vol. 140, p. 571; April 11, 1947.) Development of a new type of battery, based on the electrochemical catalysis of oxygen and hydrogen gases, is now proceeding on behalf of the British Electrical and Allied Industries Research Association at Cambridge University. A small type of silver–silver chloride–magnesium dry cell manufactured during the war by the Burgess Battery Co., Antioch, U.S.A., delivers a large output at low voltage for a short time. Such a cell 1 and three-eighths inches in diameter and 3 and five-eighths inches long gave 100A at a peak of 1.4 volts for 1 and one-half minutes when activated by water. For a full account of these cells, see Reprint 90-33 of the Electrochemical Society of America. See also 901 of April; in this, U.D.C. should read as above.

621.385.832.087.5 2949
Recording Oscilloscope Images—(*Tele-Tech*, vol. 6, pp. 45–46; April, 1947.) A beam splitter in the camera for radar oscilloscopes reflects blue light to the camera lens and transmits orange-yellow light for the operator's vision, thus permitting simultaneous inspection and photography.

621.398 2950
Magslip Transmission—(*Engineer* (London), vol. 183, pp. 317–319; April 11, 1947.) A brief outline of the principles of Magslip transmission and its application to gunnery work. The rapid development of Magslip production during the war is described and the construction of a typical transmitter unit is shown. The rigorous tests necessary to maintain the

high standard of mechanical and electrical precision are stressed. See also 2585 of September.

TELEVISION AND PHOTOTELEGRAPHY

621.397:38 2951

Commercial Applications for Picture Telegraphy—R. C. Walker. (*Electronic Eng.*, vol. 19, pp. 44–45; February, 1947.) An account of methods of facsimile transmission using "Teledeltos," a dry recording paper needing no processing. The system is used for telegraphy and transmission of drawings.

621.397:621.357.087 2952

Electro-Chemical Recording—C. P. Fagan. (*Marconi Rev.*, vol. 9, pp. 146–150; October and December, 1946.) Methods used for facsimile work, etc., are briefly described, with special attention to azo-dye recording.

621.397.5:6 2953

Television System for Industrial Applications—(*Electronics*, vol. 20, pp. 138–156; May, 1947.) A television system for visual inspection of operations on a factory production line from a remote point.

621.397.5:621.315.213.12 2954

Development of an Ultra-Low-Loss Transmission Line for Television—Johnson. (*See* 2667.)

621.397.5:621.396.67 2955

Television Antennas for Apartments—(*Electronics*, vol. 20, pp. 96–102; May, 1947.) The possibility of installing master aerials feeding many receivers is discussed. Existing systems in the U.S.A. for broadcast and short-wave signal reception are described and the difficulties to be overcome in an u.h.f. system are stated. The aerials would probably consist of separate dipoles and reflectors for each local television station, tuned and orientated for optimum reception, and each channel would require a wide-band booster amplifier. Typical proposed designs, both with and without amplifiers, are described and the requirements of the amplifiers and methods of matching to the customer's feeder-line are discussed.

621.397.5(94):621.396.619.13 2956

Frequency Modulation and Television—Gilmour. (*See* 2931.)

621.397.6 2957

A New Type of the Mosaic for the Television Pick Up Tubes—G. Braude. (*Jour. Phys.* (U.S.S.R.), vol. 9, no. 4, pp. 348–350; 1945.) The mosaic covers both sides of a thin dielectric plate which has a certain amount of leakage between the two faces.

621.397.6 2958

An Experimental Color Television System—R. D. Kell, G. L. Fredendall, A. C. Schroeder, and R. C. Webb. (*RCA Rev.*, vol. 7, pp. 141–154; June, 1946.) A description of a demonstration apparatus. Three-color scanning in sequence is obtained by rotating color filters synchronized to the frequency of the mains. Three-dimensional color is obtained by a stereo-attachment for the camera used in conjunction with polarizing material on the rotating color filters and polarizing spectacles worn by the viewer. The sound channel is transmitted during a portion of the horizontal blanking period.

621.397.6:621.383.8 2959

Mimo-Miniature Image Orthicon—P. K. Weimer, H. B. Law, and S. V. Forgue. (*RCA Rev.*, vol. 7, pp. 358–366; September, 1946.) For use in airborne television equipment; over-all length 9 inches and diameter 1 and one-half inches.

621.397.6:621.398 2960

Naval Airborne Television Reconnaissance System—R. E. Shelby, F. J. Somers, and L. R. Moffett. (*RCA Rev.*, vol. 7, pp. 303–337; September, 1946.) High fidelity long-range airborne television reconnaissance system developed by U.S. Navy Department; 20 frames per second, 40 fields per second, 567 lines per frame interlaced and 5 Mc. bandwidth are used. With peak power of 1400 watts, maximum plane-to-ground range was 200 miles. Satisfactory definition obtained at altitudes from 5000 to 10,000 feet.

621.397.6:621.398 2961

Miniature Airborne Television Equipment—R. D. Kell and G. C. Sziklai. (*RCA Rev.*, vol. 7, pp. 338–357; September, 1946.) "A developmental television camera, designed especially for airborne applications and using the image orthicon, is described. This camera is part of a complete airborne television transmitter system weighing 50 pounds. The transmitter has a power output of eight watts in the 260-to-380 megacycle range. Experimental results in guiding a medium-angle bomb with the aid of the miniature equipment are given."

621.397.6:621.398:629.13 2962

Flying Torpedo with an Electric Eye—V. K. Zworykin. (*RCA Rev.*, vol. 7, pp. 293–302; September, 1946.) Memorandum prepared as early as 1934 giving suggestion for controlling guided missiles by television.

621.397.62 2963

Philco Projection TV Receiver—(*Tele-Tech*, vol. 6, pp. 41, 127; March, 1947.) An instrument using a modified Schmidt optical system with a 4-inch 20-kV projection tube to give a 15 by 20 inch picture, of great brightness and contrast.

621.397.62:621.396.828 2964

On the Reduction of Noise [Souffle] in Certain Television Analysers Using Slow Electrons—R. Barthélemy. (*Compt. Rend. Acad. Sci.* (Paris), vol. 224, pp. 977–978; March 31, 1947.) Certain American receivers make use of electron multipliers in the analyzers. The modulated fraction of the beam entering the multiplier is very small, about 5 to 10 per cent of the mean intensity. Improved performance can be achieved by filtration of the beam, either by deviation or by a suitably polarized grid, so that only the useful part of the current passes forward into the multiplier.

621.397.74:621.315.212 2965

The Provision in London of Television Channels for the B.B.C.—Mitchell. (*See* 2666.)

621.397.62 2966

Television Receiving Equipment [Book Review]—W. T. Cocking. Iliffe and Sons, 2nd ed., 354 pp., 12s. 6d. (*Jour. Brit. I.R.E.*, vol. 7, p. 63; March and April, 1947.) Covers many of the improvements in technique which have been effected in late years and is recommended for the use of students. For review of first edition see 3503 of 1940.

TRANSMISSION

621.396.61:621.396.621 2967

Technical Characteristics of Transmitters—Aisberg. (*See* 2911.)

621.396.61.029.62 2968

A Complete 10-Meter Mobile Station—C. T. Haist. (*CQ*, vol. 3, pp. 15–19, 76; April, 1947.) Circuits and description of 50-watt equipment operated from a 12-volt car battery. An 829B h.f. transmitting tube is used in the power amplifier.

VACUUM TUBES AND THERMIONICS

537.291 2969

Exchange of Energy Between an Electron Beam and an Electromagnetic Field of Feeble Intensity—P. Guénard. (*Compt. Rend. Acad. Sci.* (Paris), vol. 224, pp. 898–900; March 24, 1947.) An expression is derived for the ratio of the mean power, given up by the beam while traversing the field, to the beam power where it enters the field, for the particular case of small signals.

621.38/.39].029.64 2970

Microwave Electronics—Slater. (*See* 2668).

621.383:535.215.2 2971

Fatigue of Ag-Cs_2O, Ag-Cs Photoelectric Surfaces—S. Pakswer. (*Jour. Appl. Phys.*, vol. 18, pp. 203–206; February, 1947.) Description of fatigue phenomena for red and blue light. Theory suggests a change in selective absorption caused by polarization of the Cs atoms.

621.383.4 2972

High-Sensitivity Photoconductive Cell—C. W. Hewlett. (*Gen. Elec. Rev.*, vol. 50, pp. 22–25; April, 1947.) Construction, performance, and applications of a thallous sulphide semiconductor cell developed by General Electric Company.

621.385:666.1 2973

Glass in the Radio Industry—Violet, Danzin, and Commin. (*See* 2819.)

621.385.029.63/.64 2974

Tentative Theory of the Travelling-Wave Valve—J. Bernier. (*Ann. Radioélec.*, vol. 2, pp. 87–101; January, 1947.) The traveling-wave tube is considered as made up of a transmission line (or wave guide) of low phase propagation velocity, closed at each end by its characteristic impedance, with uniformly distributed sources of field, these sources being due to the effect of the electron beam. The gain of such tubes is calculated; it increases with the current and the length of the line. In general the bandwidth decreases as the gain increases. The traveling-wave tube is somewhat analogous to a cascade of triode coupled by Lecher lines. Modifications of the theory are indicated when the transmission line has many modes of propagation and the case is discussed where the line consists of a wave guide filled with a dielectric of high refractive index.

621.385.032.7+621.32.032.7]:001.4 2975

Nomenclature System for Glass Bulbs—A. Brann. (*Electronics*, vol. 20, pp. 184–188; May, 1947.) American system for bulbs used in electric lamp and tube manufacture.

621.385.1+621.396.694 2976

Tube Registry—(*Electronics*, vol. 20, pp. 254–259; May, 1947.) Summary of tube information furnished by the R.M.A. Data Bureau. Types listed are: 5549. Forced-air-cooled triode. Directly heated, 12.6 volts. Anode dissipation 4 kw. 5559 (revised). Indirectly heated, mercury thyratron triode. Ionization time 10 μs. Deionization time 1 ms. 5557. Same as 5559 (revised) except directly heated. For 6C23, 8C22 and other tubes not listed above, see 2288 of August.

621.385.1.012(4) 2977

Radio Valves: Western European Valves—K. I. Drozdoff. (*Radio* (Moscow), no. 3, pp. 32–61; June, 1946. In Russian.) Definitions of continental code, and diagrams of tube bases for the E-11 and U-11 series.

621.385.1.012(4) 2978

Radio Valves: Mains Valves in the [Continental] Alphabetic Series—K. I. Drozdoff. (*Radio* (Moscow), nos. 4, 5 and 6, 7, pp. 51–60 and 53–62; July, August, and September, October, 1946. In Russian.) Tables of data, with possible equivalents.

621.385.1.032.216 2979

Oxide Cathodes. Their Experimental, Theoretical and Technical Development—O. Weinreich. (*Gén. Élec. Rev.*, vol. 56, pp. 75–

90; February, 1947.) An account of progress from 1904 to 1944. Several theories of electronic emission processes are outlined. Developments associated with the construction of magnetrons are described. Experimental studies of the mechanism of emission by means of X rays, electron diffraction, and pulse voltages are discussed. Pulse technique opens up a wide field for new investigations which may lead to an adequate theory.

621.385.1.072.2 2980

Characteristics of Certain Voltage-Regulator Tubes—G. M. Kirkpatrick. (PROC. I.R.E., vol. 35, pp. 485–489; May, 1947.) Characteristics and stability of a number of tubes of types VR75, VR105, and VR150 are examined and an equivalent circuit determined. The results are of value when VR tubes are used to provide reference potentials in electronic stabilizers.

621.385.3:621.396.813 2981

The Reduction of Microphonics in Triodes—A. H. Waynick. (*Jour. Appl. Phys.*, vol. 18, pp. 239–245; February, 1947.) An analysis of the effect of grid displacement on the anode current of a planar triode.

621.385.3.029.63.015.33 2982

Development of Pulse Triodes and Circuit to Give One Megawatt at 600 Megacycles—R. R. Law, D. G. Burnside, R. P. Stone, and W. B. Whalley. (*RCA Rev.*, vol. 7, pp. 253–264; June, 1946.) A description of the development of the air-cooled A-2231 tube and its use in a push-pull oscillator circuit tuning over the range 560 to 640 Mc.

621.385.832:621.396.96 2983

War-Time Developments in Cathode-Ray Tubes for Radar—L. C. Jesty, H Moss, and R. Puleston. (*Jour. I.E.E.* (London), part IIIA, vol. 93, no. 1, pp. 149–166; 1946.) A review of the war-time history from the design point of view. For technical reasons, most of the tubes used for radar were electrostatic, little use being made of magnetic deflection. Progress in the design of tube envelopes, electron guns, bases, screens, and deflection systems, is discussed, with special reference to afterglow screens, rigidity, and uniformity of construction, ability to withstand shock and vibration, and semi-mass-production methods. Testing procedures and tubes for particular applications are described, with illustrations of intensity-modulated and deflection-modulated displays and a comprehensive list of tube types.

621.385.832:621.396.96 2984

A Survey of Cathode-Ray-Tube Problems in Service Applications with Special Reference to Radar—G. Bradfield, J. G. Bartlett, and D. S. Watson. (*Jour. I.E.E.* (London), part IIIA, vol. 93, no. 1, pp. 128–148; 1946.) R.A.F., Army and R.N. problems are considered separately. The special requirements associated with radar displays for air interception, air navigation, precision fire control, and the plane position indication of ships, aircraft, towns, and shell splashes are reviewed. The need for large projected displays and for the dark-trace tube is discussed, with photography and visibility problems, which have an important bearing upon the choice of tube for a particular purpose. A number of practical applications are described and illustrated.

621.386.032.22 2985

Operations in the Production of Electronic Tube Components—(*Machinery*, vol. 53, pp. 160–164; February, 1947.) Production methods are described for the rotating anode assembly for certain X-ray tubes.

621.396.615.141.2 2986

Theory of the Magnetron as Microwave Generator—F. Lüdi. (*Helv. Phys. Acta*, vol. 19, pp. 1–20; February 20, 1946. In German.) For previous work see 3338 of 1943 and 3531 of 1945. This article gives theory and experimental results for the multisegment type of magnetron only.

621.396.615.141.2 2987

A Tunable Squirrel-Cage Magnetron—The Donutron—F. H. Crawford and M. D. Hare. (PROC. I.R.E., vol. 35, pp. 361–369; April, 1947.) The donutron is an all-metal multisegment magnetron with a single resonant cavity. "It is tuned by the relative axial displacement of alternate anode segments, through flexure of one wall of the cavity in which the anode structure is supported." The best of 60 models tested can be tuned over a 1.5 to 1 frequency range (in the 6–12 centimeter wave band) with a single value of voltage and magnetic field. An efficiency of 40–50 per cent was obtained with a power output of about 50 watts which was constant to 3 db. over the tuning range. The various possible modes of operation and methods of suppressing or enhancing them are described.

621.396.615.141.2 2988

Technical Problems in the Manufacture of Cavity Magnetrons—G. H. Bézy. (*Gén. Élec. Rev.*, vol. 56, pp. 68–71; February, 1947.) Discusses the conditions which should be satisfied by anode, cathode, and coupling system, and describes methods of overcoming certain difficulties in their construction and final assembly.

621.396.615.141.2 2989

Space Charge Frequency Dependence of Magnetron Cavity—W. E. Lamb, Jr. and M. Phillips. (*Jour. Appl. Phys.*, vol. 18, pp. 230–238; February, 1947.) A theoretical investigation of the effect produced on the resonant frequencies of a magnetron cavity by the presence of a thin layer of charge surrounding the cathode.

621.396.615.142 2990

On the Conversion Efficiency of Velocity-Modulation Tubes of the Reflex Type—J. Bernier. (*Ann. Radioélec.*, vol. 1, pp. 359–382; October, 1946.) For satisfactory efficiency the h.f. voltage should neither be so low that the electrons are not sufficiently checked on their return, nor so high that too much energy is required to control the forward beam. A quantitative study of the effects is made assuming that space-charge effects are negligible, electron trajectories rectilinear and the h.f. field uniform and well defined, though of finite magnitude. The conversion efficiency is calculated (a) for different values of the h.f. field supposing all electrons are reflected by the mirror, and (b) when only half the electrons are reflected by a mirror at the potential of the cathode and the h.f. field is infinitely narrow.

621.396.615.142.2 2991

Practical Limitations of the Power and Efficiency of Two-Cavity Klystrons—P. Guénard. (*Ann. Radioélec.*, vol. 2, pp. 13–23; January, 1947.) A discussion with certain simplifying assumptions. For this type of tube the efficiency decreases rapidly with increase of frequency from about 30 per cent for the longer waves to zero for millimeter wavelengths. The h.f. power can exceed 1 kw. at wavelengths above 10 centimeters but decreases rapidly with increase of frequency and is only a few watts for a wavelength of 3 centimeters.

621.396.615.142.2 2992

Practical Limitations of the Power and Efficiency of Two-Cavity Klystrons—P. Guénard. (*Onde Élec.*, vol. 27, pp. 94–103; March, 1947.) See 2991 above. The present paper gives a fuller discussion and includes appendices on (a) the efficiency of tubes without grids, and (b) the effects of space charge on longitudinal debunching.

621.396.615.142.2 2993

The Maximum Efficiency of Reflex-Klystron Oscillators—E. G. Linder and R. L. Sproull. (PROC. I.R.E., vol. 35, pp. 241–248; March, 1947.) "The theory of reflex-klystron oscillators is given in detail. It includes a discussion of relations in a loaded oscillator. It is shown that maximum efficiency for small amplitudes is given by $\eta_0 = 0.169M^2i_1/G_eV_0$, where M is the coefficient of modulation of the gap, i_1 is the effective current, G_e is the shunt conductance of the unloaded resonator, and V_0 is the beam voltage. Possibilities of increasing efficiency are considered, including effects of grid transmission on effective current and on space charge, and effects of multiple electron transits."

621.396.645:621.396.822 2994

Noise Factor: Part 3—Moxon. (*See* 2919.)

MISCELLANEOUS

001.4:[621.32.032.7+621.385.032.7 2995

Nomenclature System for Glass Bulbs—Brann. (*See* 2975.)

62"1946" 2996

Progress in Engineering Knowledge During 1946—P. L. Alger, J. Stokley, F. H. Faust, E. L. Robinson, J. L. Tugman, W. W. Kuyper, and W. D. Haylon. (*Gen. Elec. Rev.*, vol. 50, pp. 12–55; March, 1947.) A survey of developments in materials, techniques, and design and application engineering, with an extensive bibliography.

620.1.05 2997

Ingenious New Testing Machine—(*Overseas Eng.*, vol. 20, p. 320; April–May, 1947.) For tensile, compression, beam, shear, and bending tests and also suitable for many precision pressing operations. Maximum load capacity 25 tons.

621.396 de Forest 2998

Lee de Forest—(*Radio Craft*, vol. 18, pp. 17–57, 130; January, 1947.) A collection of papers describing the work of de Forest, with appreciations from prominent scientists and radio engineers, specially written to mark the 40th anniversary of his invention of the audion.

621.396 Tesla 2999

Nikola Tesla (1856–1943)—F. Bedeau. (*Onde Élec.*, vol. 27, p. 75; February, 1947.) A short account of his work on rotating fields and h.f. alternators and oscillators.

621.396.621(100.2) 3000

Density of Radio Receivers Throughout World—(*Tele-Tech*, vol. 6, p. 92; March, 1947.) A table giving the number of receiving sets per 100 population in 85 countries. See also 1588 of June.